

DOCKETED
USNRC

*82 JAN -7 AIC :02

OFFICE OF SECRETARY
DOCKETING & SERVICE
BRANCH

CONTAINMENT LOADS REPORT (CLR)

MARK III CONTAINMENT

Approved: *F. Reuter*
F. Reuter, Manager
Mark III Containment Design

Approved: *P. P. Stancavage*
P. P. Stancavage, Manager
Containment Engineering

Approved: *P. W. Ianni*
P. W. Ianni, Manager
Containment Design

NUCLEAR ENERGY ENGINEERING DIVISION • GENERAL ELECTRIC COMPANY
SAN JOSE, CALIFORNIA 95125



A DISCLAIMER OF RESPONSIBILITY

This document is being made available by General Electric Company without consideration in the interest of promoting the spread of technical knowledge. Neither General Electric Company nor the individual authors:

- A. Make any warranty or representation, expressed or implied, with respect to the accuracy, completeness, or usefulness of the information contained in this document, or that the use of any information disclosed in this document may not infringe privately owned rights;*

- B. Assume any responsibility for liability or damage which may result from the use of any information disclosed in this document; or*

- C. Imply that a plant designed in accordance with the recommendations found in this document will be licensed by the United States Nuclear Regulatory Commission or that it will comply with Federal, State or local regulations.*

TABLE OF CONTENTS

	<u>Page</u>
1. INTRODUCTION	1-1
1.1 Confirmatory Testing	1-2
1.2 Definition of LOCA	1-2
1.3 Design Margins	1-3
2. REVIEW OF PHENOMENA	2-1
2.1 Design Basis Accident (DBA)	2-1
2.2 Intermediate Break Accident (IBA)	2-5
2.3 Small Break Accident (SBA)	2-5
2.4 Safety Relief Valve Actuation	2-7
2.5 Other Considerations	2-8
3. DYNAMIC LOAD TABLE	3-1
4. DRYWELL STRUCTURE	4-1
4.1 Drywell Loads During a Large Break Accident	4-1
4.1.1 Sonic Wave	4-1
4.1.2 Drywell Pressure	4-1
4.1.3 Hydrostatic Pressure	4-2
4.1.4 Loads on the Drywell Wall During Pool Swell	4-2
4.1.5 Condensation Oscillation Loads	4-3
4.1.6 Fall Back Loads	4-3a
4.1.7 Negative Load During ECCS Flooding	4-4
4.1.8 Chugging	4-4
4.1.9 Loads Due To Chugging	4-5
4.1.9.1 Chugging Loads Applied to Top Vent	4-5a
4.1.9.2 Pool Boundary Chugging Loads	4-5a
4.2 Drywell Loads During Intermediate Break Accident	4-6
4.3 Drywell During a Small Break Accident	4-6
4.3.1 Drywell Temperature	4-6
4.3.2 Drywell Pressure	4-7
4.3.3 Chugging	4-8
4.4 Safety Relief Valve Actuation	4-8
4.5 Drywell Environmental Envelope	4-8
4.6 Top Vent Temperature (Cycling Profile During Chugging)	4-8
4.7 Drywell Multicell Effects	4-8a

TABLE OF CONTENTS (Continued)

	Page
5. WEIR WALL	5-1
5.1 Weir Wall Loads During a Design Basis Accident	5-1
5.1.1 Sonic Wave	5-1
5.1.2 Outward Load During Vent Clearing	5-1
5.1.3 Outward Load Due to Vent Flow	5-1
5.1.4 Chugging Loads	5-1
5.1.5 Inward Load Due to Negative Drywell Pressure	5-3
5.1.6 Suppression Pool Fallback Loads	5-4
5.1.7 Hydrostatic Pressure	5-4
5.1.8 Safety Relief Valve Loads	5-4
5.1.9 Condensation	5-4
5.2 Weir Wall Loads During An Intermediate Break Accident	5-4
5.3 Weir Wall Loads During a Small Break Accident	5-5
5.4 Weir Wall Environment Envelope	5-5
5.5 Weir Annulus Multicell Effects	5-5
6. CONTAINMENT	6-1
6.1 Containment Loads During a Large Steam Line Break (DBA)	6-1
6.1.1 Compressive Wave Loading	6-1
6.1.2 Water Jet Loads	6-1
6.1.3 Initial Bubble Pressure	6-2
6.1.4 Hydrostatic Pressure	6-2
6.1.5 Local Containment Loads Resulting from the Structures at or Near the Pool Surface	6-3
6.1.6 Containment Load Due to Pool Swell at the HCU Floor Wetwell Pressurization	6-3
6.1.7 Fall Back Loads	6-4
6.1.8 Post Pool Swell Wave	6-4
6.1.9 Condensation Oscillation Loads	6-5
6.1.10 Chugging	6-5
6.1.11 Long-Term Transient	6-5
6.1.12 Containment Environmental Envelope	6-6
6.2 Containment Loads During an Intermediate Break Accident	6-6
6.3 Containment Loads During a Small Break Accident	6-6
6.4 Safety Relief Valve Loads	6-7
6.5 Suppression Pool Thermal Stratification	6-7
6.6 Containment Wall Multicell Effects	6-7

TABLE OF CONTENTS (Continued)

	Page
7. SUPPRESSION POOL BASEMAT LOADS	7-1
8. LOADS ON STRUCTURES IN THE SUPPRESSION POOL	8-1
8.1 Design Basis Accident	8-1
8.1.1 Vent Clearing Jet Load	8-1
8.1.2 Drywell Bubble Pressure and Drag Loads Due to Pool Swell	8-1
8.1.3 Fall Back Loads	8-2
8.1.4 Condensation Loads	8-2
8.1.5 Chugging	8-2
8.1.6 Compressive Wave Loading	8-3
8.1.7 Safety Relief Valve Actuation	8-3
9. LOADS ON STRUCTURES AT THE POOL SURFACE	9-1
10. LOADS ON STRUCTURES BETWEEN THE POOL SURFACE AND THE HCU FLOORS	10-1
10.1 Impact Loads	10-1
10.2 Drag Loads	10-3
10.3 Fall Back Loads	10-3
11. LOADS ON EXPANSIVE STRUCTURES AT THE HCU FLOOR ELEVATION	11-1
12. LOADS ON SMALL STRUCTURES AT AND ABOVE THE HCU FLOOR ELEVATION	12-1
REFERENCES	R-1
ATTACHMENT A - SAFETY RELIEF VALVE LOADS (QUENCHER)	A-1
ATTACHMENT B - SUPPRESSION POOL SEISMIC INDUCED LOADS	B-1
ATTACHMENT C - WEIR ANNULUS BLOCKAGE	C-1
ATTACHMENT D - DRYWELL PRESSURE DISTRIBUTION	D-1

TABLE OF CONTENTS (Continued)

	<u>Page</u>
ATTACHMENT E - DRYWELL NEGATIVE PRESSURE CALCULATIONS	E-1
ATTACHMENT F - WETWELL ASYMMETRIC PRESSURES	F-1
ATTACHMENT G - SUBMERGED STRUCTURE LOADS DUE TO LOCA AND SRV ACUATIONS	G-1
ATTACHMENT H - WEIR WALL LOADS DURING DRYWELL DEPRESSURIZATION	H-1
ATTACHMENT I - POOL SWELL VELOCITY	I-1
ATTACHMENT J - SCALING ANALYSES AND SMALL STRUCTURE POOL SWELL DYNAMIC LOADS	J-1
ATTACHMENT K - DELETED	K-1
ATTACHMENT L - CONTAINMENT ASYMMETRIC LOADS	L-1
ATTACHMENT M - MULTIPLE SAFETY/RELIEF VALVE ACTUATION FORCING FUNCTION METHODS	M-1
ATTACHMENT N - SUPPRESSION POOL THERMAL STRATIFICATION	N-1
ATTACHMENT O - DIGITIZATION OF FORCING FUNCTION FOR CONDENSATION OSCILLATION	O-1

LIST OF ILLUSTRATIONS

<u>Figure</u>	<u>Title</u>	<u>Page</u>
2.1	Loss-of-Coolant Accident Chronology (DBA)	2-9
2.2-1	Schematic of the Mark III Pool Swell Phenomenon	2-10
2.2-2	Typical Suppression Pool Cross Section 238 Plant	2-11
2.2-3	Plan at Elevation 11 ft 0 in.	2-12
2.2-4	Containment Floor Drain Sump 238 Plant	2-13
2.2-5	Containment Equipment Drain Sump 238 Plant	2-14
2.2-6	Plan at Elevation (-) 5 ft 3 in.	2-15
2.3	Idealized Quencher Bubble Pressure Oscillation in Suppression Pool	2-16
4.1	Drywell-Loading Chart for DBA	4-9
4.2	Drywell-Loading Chart for SBA	4-10
4.3	Drywell-Loading Chart for IBA	4-11
4.4	Short Term Drywell and Containment Pressure Response to a Large Steam Line Break (DBA)	4-12
4.5	PSTF Test Results - Vent Static Pressure Differential	4-13
4.5a	PSTF Test Results - Vent Static Pressure Differential	4-14
4.6	Typical Drywell Pressure Traces During Condensation, Run 23, Test 5807	4-15
4.6a	Condensation Oscillation Load Spatial Distribution on Drywell Wall, Containment and Basemat	4-16
4.6b	Condensation Oscillation Forcing Function on the Drywell Wall O.D. Adjacent to the Top Vent	4-17
4.7	Typical Top Vent Pressure Trace During Chugging, Run 19	4-18
4.7a	Peak Pressure Pulse Train in Top Vent During Chugging	4-19
4.7b	Peak Force Pulse Train in Top Vent During Chugging	4-19a
4.7c	Average Force Pulse Train in Top Vent During Chugging	4-19b
4.7d	Average Pressure Pulse Train in Top Vent During Chugging	4-19c
4.8	Typical Containment Pressure Trace During Chugging, Run 11 (Ref. Test 5707)	4-20
4.8a	Typical Pressure Time-History on the Pool Boundary During Chugging	4-21
4.8b	Suppression Pool Chugging Normalized Peak Underpressure Attenuation	4-21a
4.8c	Suppression Pool Chugging Normalized Mean Underpressure Attenuation	4-21b

LIST OF ILLUSTRATIONS (Continued)

Figure	Title	Page
4.8d	Suppression Pool Chugging Normalized Spike Attenuation	4-21c
4.8e	Suppression Pool Chugging Spike Duration "d" as a Function of Location in the Pool	4-21d
4.8f	Suppression Pool Chugging Normalized Peak Post Chug Oscillations	4-21e
4.8g	Circumferential Underpressure Amplitude Attenuation	4-21f
4.8h	Circumferential Post Chug Oscillation Amplitude Attenuation	4-21g
4.8i	Suppression Pool Chugging Normalized Post Chug Oscillation Attenuation	4-21h
4.8j	Chugging Pressure Time-History on the Drywell Wall Adjacent to Vert	4-21i
4.9	Drywell - Containment Pressure Differential During Chugging	4-22
4.10	Maximum Design Drywell Atmosphere Bulk Temperature and Pressure Envelope	4-24
4.11	Drywell Top Vent Cyclic Temperature Profile and Area of Application During Chugging	4-25
5.1	Weir Wall-Loading Chart for DBA	5-6
5.2	Weir Wall-Loading Chart for SBA	5-7
5.3	Weir Wall-Loading Chart for IBA	5-8
5.4	Typical Weir Wall Chugging Time History - Test Series 5707, Run 1	5-9
5.4a	Typical Pressure Time-History for Weir Annulus During Chugging	5-10
5.5	Underpressure Distribution on the Weir Wall and Drywell I.D. Wall During Chugging	5-10a
5.5a	Peak Pressure Pulse Train on the Weir Wall and Drywell I.D. Wall During Chugging	5-10b
5.5b	Mean Pressure Pulse Train on the Weir Wall and Drywell I.D. Wall During Chugging	5-11
5.6	Normalized Weir Annulus Pressure Pulse Attenuation	5-11
5.7	Pressure Transient in Drywell Initiated by Vessel Reflood Line Break Level 238	5-12
5.8	Vent Backflow Weir Annulus Water Surge Velocity Vs. Height Above Weir Wall	5-13
5.9	Mean Pressure Pulse Train on the Weir Wall and Drywell I.D. Wall During Chugging With Superposition of Adjacent Spikes	5-14
6.1	Containment-Loading Chart for DBA	6-8
6.2	Containment-Loading Chart for IBA	6-9
6.3	Containment-Loading Chart for SBA	6-10
6.4	Observed Bubble Pressure During Pool Swell Test Series 5706, Run 4	6-11

LIST OF ILLUSTRATIONS (Continued)

<u>Figure</u>	<u>Title</u>	<u>Page</u>
6.5	Dynamic Loads Associated with Initial Bubble Formation in the Pool	6-12
6.6	Containment Pressure Differential During Bubble Formation	6-13
6.7	Deleted	6-14
6.8	Drag Loads on Protruding Structures Due to Pool Swell	6-15
6.9	Containment Loading Due to Flow ΔP Across HCU Floor	6-16
6.10	Typical Containment Wall and Basemat Pressure Traces During Condensation, Run 23 (Ref. Test 5807)	6-17
6.11	Containment Wall and Basemat Pressure Time Histories, Test 5807, Run 11	6-18
6.12	Containment Wall Chugging Pressure Time History, Test 5707, Run 9	6-19
6.13	Basemat Chugging Pressure Time History, Test 5707, Run 9	6-20
6.14	Calculated Atmosphere Bulk Temperature and Pressure Design Envelope for all Breaks	6-21
6.15	Long Term Containment Pressure Following a DBA	6-22
6.16	HCU Floor ΔP vs HCU Floor Open Area	6-23
6.17	Suppression Pool Temperature Profile for the Large Breaks	6-24
7.1	Pool Boundary Loads During Bubble Formation	7-2
8.1	Structures Within Suppression Pool-Loading Chart for DBA	8-4
8.2	Deleted	8-5
8.3	Deleted	8-6
9.1	Structures at the Pool Surface-Loading Chart During DBA	9-2
10.1	Small Structures Between the Pool Surface and the HCU Floor-Loading Chart During DBA	10-4
10.2	Profile of Impact Loads on Small Structures Within 18 ft of the Pool Surface	10-5
10.3	Pressure Drop Due to Flow Across Grating Within 18 ft of the Pool Surface	10-6
10.4	Drag Load on Solid Structures within 18 ft of the Pool Surface	10-7
10.5	Drag Loads for Various Geometries (slug flow)	10-8

LIST OF ILLUSTRATIONS (Continued)

<u>Figure</u>	<u>Title</u>	<u>Page</u>
10-6	Summary of Pool Swell Loading Specifications for Small Structures in the Containment Annulus (Not Applicable to the Steam Tunnel or Expansive HCU Floors)	10-9
11-1	Expansive Structures at HCU Elevation - Loading During DBA	11-3
12.1	Small Structures at the HCU Floor Elevation - Loading Chart During DBA	12-3
12.2	Loads at HCU Floor Elevation Due to Pool Swell Froth Impact and Two-Phase Flow	12-4

LIST OF TABLES

<u>Table</u>	<u>Title</u>	<u>Page</u>
1.1.1	Summary of PSTF Tests	1-4
1.3.1	Summary of Specified and Realistic Design Values	1-6
3.1.1	Summary of Postulated Accidents Affecting Mark III Structures	3-1
4.1	Chugging Loads	4-8b

ABSTRACT

This technical report provides numerical information for thermal hydraulic dynamic loading conditions in GE Mark III Reference Plant pressure suppression containment system during a loss-of-coolant accident, safety relief valve discharge and related dynamic events. Information and guidance has been provided to assist the containment designer in evaluating the design conditions for the various structures which form the containment system. Confirmatory tests are completed. Observed test data or calculations upon which the loads are based, are discussed. A Class III supplement to this report (22A4365AB) includes additional proprietary information in support of the load definition.

1. INTRODUCTION

The information in this document represents the General Electric Company recommendation for containment loads. Loss of coolant accident (LOCA) and safety relief valve (SRV) dynamic loads, based upon pressure suppression and safety relief valve test programs, are included. General Electric has concluded the confirmatory test program for the Mark III containment configuration. These tests support and confirm the pressure suppression loads that result from the postulated LOCA and from SRV operation. The confirmatory program includes a series of scaled multivent tests that demonstrate no significant vent interaction effects for the LOCA process. The Caorso tests, also included, demonstrate the conservative SRV loads.

General Electric will use the design load values specified herein as the basis for the 238 GESSAR license application. Other load values or smaller margins than those provided in this document may be used if the architect engineer is willing to defend them through the licensing process.

The architect engineer is responsible for the definition of load combinations, which include loads of the type described in this document, as well as more normal loads such as deadweight, seismic, wind, missile impact, jet impingement, etc. The architect engineer is also responsible for determining the effect of the above loads and load combinations on the structures and equipment. Thus, the architect engineer is responsible for project unique containment analyses.

During a loss-of-coolant accident and events such as safety/relief valve actuation, the structures forming the containment system and other structures within the Reactor Building experience dynamic phenomena. This report provides numerical information on the dynamic loads that these phenomena impose on the Mark III containment system structures.

The loading information is based on either observed test data or conservatively calculated peak values. The LOCA loading combinations are presented in the form of bar charts for each of the containment system structures. In addition to defining the timing of the LOCA related loads, the bar charts identify

other loading conditions such as seismic accelerations, dead-weight, etc. For each bar on the chart, reference is made to the section where specific discussion of the load is presented.

To provide a better understanding of the various dynamic loads and their inter-relationships, Section 2 contains a qualitative description of sequential events for a wide range of postulated accidents. The air clearing loading phenomena associated with the actuation of a safety relief valve is also described.

1.1 CONFIRMATORY TESTING

Impact and impingement load specifications for small structures affected by suppression pool swell, are based on the results of the PSTF air tests conducted in March 1974 and reported in Reference 9. The intent of these tests was to provide conservative design data. It was recognized that the data base would require extension beyond that provided by the air tests and to achieve this, additional impact tests for both small and large structures were included in the PSTF schedule. These tests involved measurement of pool swell impact forces on a variety of targets representative of small structures found in the Mark III containment annulus, and are discussed in Attachment J.

This document relies on a large experimental test data base from the PSTF program. See Table 1.1.1 for a summary of these tests. The scaling of the large scale and 1/3 area scale PSTF precludes direct application to the prototype Mark III. Conservative interpretation of these tests results, employing dimensional similitude scaling relationship, is used to arrive at specified design loads for Mark III. (See Attachment J.)

Evaluation of full scale Caorso SRV tests is included in Attachment A. The evaluation shows that the test result loads are significantly lower than the current design loads and the use of reduced design loads are justified.

1.2 DEFINITION OF LOCA

A loss-of-coolant accident (LOCA) is the sudden break of a high energy pipe in the reactor coolant pressure boundary of the nuclear steam supply system. The largest postulated break could be either the break of a main steam or a recirculation line. This loss-of-coolant accident (LOCA) is the design basis accident (DBA). Other small line breaks result in loss-of-coolant accidents, and although their energy release does not result in large dynamic loadings, their thermal effects may control the design of structures. The intermediate break accident (IBA) and small break accident (SBA) fall into this category. The size of the SBA is defined as that which will not cause automatic depressurization of the reactor. The SBA is of concern because it imposes the most severe temperature condition inside the drywell.

1.3 DESIGN MARGINS

Table 1.3.1 summarizes the loads due to a LOCA for the containment structures. Reasonable design margins are clearly shown by comparing the magnitude of the values between the conservatively specified design values and the realistic expected loads. The Mark III loads presented in this document should be interpreted as rigid wall loads. A similar case for showing the conservatism in the loads specified for relief valve actuation is given in Attachment A.

It is shown in this report that the W II dynamic loading phenomena has been conservatively bounded and the PS test data is conservatively interpreted. Parameter simulation has justified the application of the test data to MK III designs with adequate design conservatism added. Any further margin considerations cannot be technically envisioned. In fact, where possible, the containment designer may chose to justify more realistic design values.

Table 1.1.1
SUMMARY OF PSTF TESTS

<u>Test Series</u>	<u>Number of Blowdowns</u>	<u>Venturi Range (inch)</u>	<u>Top Vent Submergence Range (feet)</u>	<u>Initial Pressure (psia)</u>	<u>Blowdown Type</u>	<u>Number of Vents</u>	<u>Area Pool/Vent Scaling</u>	<u>Primary Objectives*</u>	<u>Reference Report</u>
5701	21	2 1/8-3 5/8	2.0 - 15.5	1050	Saturated Steam	1	Full	1. Vent Clearing 2. Full Scale Condensation Demo 3. Drywell Pressure	4
5702	17	2 1/8-3 5/8	1.93 - 11.97	1050	Saturated Steam	2	Full	1. Vent Clearing	4
5703	3	2 1/2-3 5/8	6.77 - 11.05	1050	Saturated Steam	3	Full	1. Vent Clearing	4
5705	4	1 - 4 1/4	6.0 - 8.0	1065	Air	2	Full	1. Pool Swell Scoping	7
5706	7	4 1/4	6.0 - 10.0	1065	Air	2	Full	1. Pool Swell 2. Impact Loading	7
5707	22	2 1/8 - 3	7.5	1050	Air and Steam	3	Full	1. Chugging	16
5801	19	2 1/8-3	5.0 - 10.0	1050	Saturated Steam	3	1/3	1. 1/3 Scale Demonstration 2. Pool Swell 3. Roof Density and ΔP	11
5802	3	2 1/8-3	6.0	1050	Saturated Steam	3	1/3	1. Pool Swell	11

22A4365
Rev. 2

101678

1-4

Table 1.1.1 (Continued)

Test Series	Number of Blowdowns	Venturi Range (inch)	Top Vent ϕ Submergence Range (feet)	Initial Pressure (psia)	Blowdown Type	Number of Vents	Area Pool/Vent Scaling	Primary Objectives*	Reference Report
5803	2	2 1/8-3	5.0 - 7.5	1050	Saturated Liquid	3	1/3	1. 1/3 Scale Demo 2. Liquid Blowdown	11
5804	5	2 1/8-3	5.0	1050	Saturated Steam	3	1/3	1. Roof Density and ΔP Repeatability	11
5805	52	1 - 3	5.0 - 10.0	1050	Saturated Steam	3	1/3	1. Pool Swell Impact	12
5806	12	2 1/2-4 1/4	5.0 - 7.5	1065	Air	3	1/3	1. Pool Swell	13
5807	20	1 - 3	7.5	1050	Saturated Steam and Liquid	3	1/3	1. Steam Condensation	15
6002	14	2-1/8 - 3	5 - 10	1050	Steam	9	1/9	1. Pool Swell Multivalent Effects	17
6003	12	2-1/2	7.5	1050	Steam	9	1/9	1. Steam Condensation Multivalent Effects	18

*In general tests are not direct prototype simulations, but parametric studies to be used in analytic model evaluations.

Table 1.3.1

SUMMARY OF SPECIFIED AND REALISTIC DESIGN VALUES

<u>Load</u>	<u>Specified for Design</u>	<u>Engr'g Estimate</u>	<u>Design Basis</u>		<u>Section</u>	<u>Comments</u>
			<u>Analysis</u>	<u>Test</u>		
<u>STRUCTURE: Drywell</u>						
<u>BREAK SIZE: Large</u>						
Drywell Pressurization	30 psig	18 psig	Model (Ref. 1) plus margin		4.1.2	Peak calculated 21.8 psig
Hydrostatic Pressure	ρH	ρH	Standard analytical techniques		4.1.3	
Bubble Formation	0 + 21.8 psid	18 psid	Max pressure equal D.W. pressure		4.1.4	
Wetwell Pressurization	11 psid	3-5 psid	Model in Supplement 1 to Ref. 1	5801, 5802 5803, 5804	12.1	Test shows pressure differential in the 3 to 5 psi range
<u>Pool Swell</u>						
Slug impact load	115 psi	60 psi		5706, 5801 5802, 5805	12.1	Applies to small flat structures attached to D.W. (see Fig. 10.6). See Attachment J.
Froth impingement load	15 psi	15 psi		5706, 5801 5802, 5805		Applies to small struc- tures attached to D.W. (see Fig. 10.6). See Attachment J.
Velocity for computing drag loads (slug flow)	40 ft/sec	30 ft/sec	Bounding calculation		9.0 10.2	See Attachment I
Condensation Oscillation Loads	± 7 psid (mean)	± 4 psid		5702, 5703 5801, 5807	4.1.5	See Fig. 4.6.a for pressure distribution
Fallback Velocity for Drag Loads	35 ft/sec	20 ft/sec	Bounding calculation		4.1.6	

22A4365
Rev. 3

090779

1-6

Table 1.3.1 (Continued)

Load	Specified for Design	Engr'g Estimate	Design Basis		Section	Comments
			Analysis	Test		
Negative Load During ECCS Flooding	-21 psid	-15 psid	Bounding calculation		4.1.7	Assumes no vacuum relief
Chugging						
Gross structure	±2 psid	±1 psid		5801, 5802 5803, 5804	4.1.8	Design pressures are +30 psig and -21 psid
Loading within top vent					4.1.9.1	
● Pre-chug under-pressure	-15.0 psid (peak) -9.0 psid (mean)	-12 psid (peak) -8 psid (mean)		5707	4.1.9.2	
● Pulse (spike)	540 psid (peak) 214 psid (mean)	500 psid (peak) 180 psid (mean)		5707		Local and global pulse train specified
● Net force	250 kips (peak) 91 kips (mean)	250 kips (peak) 75 kips (mean)		5707		Local and global net upward vertical load
Loading on drywell I.D.					5.1.4	Same as weir wall specification
Loading on drywell O.D.				5707	4.1.9.2	See Table 4.1 for duration and frequency
● Pre-chug under-pressure	-5.8 psid (peak) -2.65 psid (mean)	-4.0 psid (peak) -1.0 psid (mean)				
● Pulse (spike)	100 psid (peak) 24 psid (mean)	75 psid (peak) 20 psid (mean)				

22A4365
Rev. 3

1-7

090779

Table 1.3.1 (Continued)

<u>Load</u>	<u>Specified for Design</u>	<u>Engr'g Estimate</u>	<u>Design Basis</u>		<u>Section</u>	<u>Comments</u>
			<u>Analysis</u>	<u>Test</u>		
• Post-chug oscillation	±6.5 psid (peak) ±2.2 psid (mean)	±4.0 psid (peak) ±1.1 psid (mean)				
<u>STRUCTURE: Drywell</u>	<u>BREAK SIZE: Intermediate</u>					
ADS					4.2	See Attachment A
Chugging					4.1.8- 4.1.9.2	Same as large break specification
<u>STRUCTURE: Drywell</u>	<u>BREAK SIZE: Small</u>					
Temperature	330°F/310°F	330°F/ 310°F	Bounding calculation		4.3.1	3 hr at 330°F initially, next 3 hr at 310°F
Chugging					4.1.8- 4.1.9.2	Same as large break specification

22A4365
Rev. 2

Table 1.3.1 (Continued)

Load	Specified for Design	Engr'g Estimate	Design Basis		Section	Comments
			Analysis	Test		
<u>STRUCTURE: Weir Wall</u>						
<u>BREAK SIZE: Large**</u>						
Outward Load Due to Vent Clearing	10 psig	5 psig	Model in Ref. 1		5.1.2 5.1.3	First 30 sec of blowdown
Chugging				5707	5.1.4	Local and global loading specified
• Pre-chug under-pressure	-2.15 psid (peak) -0.98 psid (mean)	-2.0 psid (peak) -0.5 psid (mean)				
• Peak spike of pulse train	43 psid (peak) 15 psid (mean)	35 psid (peak) 13 psid (mean)				
Inward Load Due to Negative Drywell Pressure Differential	12,800 lb _f /vent	8000 lb _f (top vent) 6000 lb _f (mid) 4000 lb _f (bottom)	Bounding calculation		5.1.5	Attachment H
Hydrostatic Pressure	ρH	ρH	Standard analytical techniques		5.1.7	
<u>STRUCTURE: Weir Wall</u>						
<u>BREAK SIZE: Intermediate**</u>						
ADS						Attachment A
<u>STRUCTURE: Weir Wall</u>						
<u>BREAK SIZE: Small**</u>						
Temperature	330°F/310°F		Bounding calculation		5.4	330°F for 3 hr initially 310°F for next 3 hr

**Chugging Loads on Weir Wall are the same for large, intermediate and small break accidents.

090779

22A4365
Rev. 3

1-9

Table 1.3.1 (Continued)

Load	Specified for Design	Engr'g Estimate	Design Basis		Section	Comments
			Analysis	Test		
STRUCTURE: Containment	BREAK SIZE: Large					
Water Jet	<1 psig	0 psig	Attachment G	5706	6.1.2	Measured pressure is small and is obscured by bubble pressure
Bubble Formation	10 psid	8 psid		5701, 5702 5703, 5705 5706	6.1.3	
Hydrostatic Pressure	ρH	ρH	Standard analytical techniques		6.1.4	
Pool Swell Loads for Attached Structures at Pool Surface	10 psid (bubble)	8 psid	D.W. bubble pressure		6.1.5	Only large structures see bubble pressure
	40 ft/sec (drag velocity)	30 ft/sec	Bounding calculation		6.1.5	See Attachment I
Pool Swell at HCU Floor	15 psi (froth impingement)	10 psi		5706	6.1.6	
	11 psi (flow ΔP)	3-5 psi	Model in Ref. 1	5801, 5802 5803, 5804	6.1.6	Test shows pressure differential in the 3 to 5 psi range
Fallback Velocity for Drag Loads	35 ft/sec	20 ft/sec	Bounding calculation		6.1.7	
Post Pool Swell Waves	2 ft	2 ft		PSTF Tests	6.1.8	Negligible load
Condensation Oscillation Loads	± 1 psid (mean)	± 0.6		5807, 5701 5702	6.1.9	See Figure 4.6a
Chugging				5707	4.1.9.2	See Table 4.1 for dura- tion and frequency
• Pre-chug-under- pressure	-1.3 psid (peak) -1.0 psid (mean)	-0.8 psid (peak) -0.3 psid (mean)				

22A4365
Rev. 3

1-10

Table 1.3.1 (Continued)

<u>Load</u>	<u>Specified for Design</u>	<u>Engr'g Estimate</u>	<u>Design Basis</u>		<u>Section</u>	<u>Comments</u>
			<u>Analysis</u>	<u>Test</u>		
● Pulse (spike)	3.0 psid (peak) 0.7 psid (mean)	2.2 psid (peak) 0.6 psid (mean)				
● Post-chug oscillation	±1.7 psid (peak) ±1.0 psid (mean)	±1.5 psid (peak) ±0.5 psid (mean)				
Pressurization	15 psig	5 psig	Model (Ref. 1) plus margin		6.1.11	Peak calculated value is 9.8 psig
Temperature	185°F*	<150°F	Supplement 1 to Ref. 1		6.1.11	Conservative calculated peak temperature is 176°F
<u>STRUCTURE: Containment</u>	<u>BREAK SIZE: Intermediate</u>					
Pressurization	15 psig	5 psig	Bounding calculation		6.2	
ADS					6.2	See Attachment A
Chugging					4.1.8- 4.1.9.2	Same as large break specification
<u>STRUCTURE: Containment</u>	<u>BREAK SIZE: Small</u>					
Temperature Stratification (Dome)	220°F	185°F	Bounding calculation		6.3	Local temperatures of 300/250°F are possible in the event of reactor steam/liquid blowdowns to containment.
Pressure	2 psig	1 psig	Bounding calculation		6.3	Typical value
Chugging					4.1.8- 4.1.9.2	Same as large break specification

22A4365
Rev. 4

1-11

*See paragraph 6.1.11

Table 1.3.1 (Continued)

<u>Load</u>	<u>Specified for Design</u>	<u>Engr'g Estimate</u>	<u>Design Basis</u>		<u>Section</u>	<u>Comments</u>
			<u>Analysis</u>	<u>Test</u>		
STRUCTURE: Basemat	BREAK SIZE: Large					
Hydrostatic	ρH	ρH	Standard analytical techniques			
Bubble Formation	10 → 21.8 psid	18 psid	Peak equal to D.W. pressure	5706/4	7.0	10 psi over 1/2 pool assumed to increase linearly to 21.8 psi. See Figs. 7.1 and 6.6
Condensation Oscillation Load	±1.7 psid	±1.0 psid		5807, 5702, 5701	7.0	See Figure 4.6a
Chugging				5707	4.1.9.2	See Table 4.1 for duration and frequency
• Pre-chug under-pressure	-1.8 psid (peak) -1.34 psid (mean)	-1.5 psid (peak) -0.7 psid (mean)				See Figures 4.8b through 4.8f for basemat attenuation
• Pulse (spike)	10 psid (peak) 2.4 psid (mean)	7.5 psid (peak) 2 psid (mean)				
• Post-chug oscillation	±2.1 psid (peak) ±1.3 psid (mean)	±2.0 psid (peak) ±1.0 psid (mean)				
STRUCTURE: Basemat	BREAK SIZE: Intermediate					
ADS					7.0	See Attachment A
Chugging					4.1.9.2	Same as large break specification
STRUCTURE: Basemat	BREAK SIZE: Small					
Chugg [†]					4.1.9.2	Same as large break specification

22A4365
Rev. 3

1-12

090779

Table 1.3.1 (Continued)

Load	Specified for Design	Estimate	Design Basis		Section	Comments
			Analysis	Test		
<u>STRUCTURE: Submerged Structures</u>						
<u>BREAK SIZE: Large*</u>						
LOCA Water Jet Loads					G2.2	Load is bounded by LOCA air bubble load
LOCA Air Bubble Load		8.2 psid*	Attachment G		G2.3	Load is on a sample structure 4 ft from the top vent axis
Velocity for Computing Drag Loads	40 ft/sec	30 ft/sec	Bounding Calculation			See Attachment I
Fall Back Velocity for Drag Loads	35 ft/sec	20 ft/sec	Bounding Calculation		G2.4	
LOCA Condensation Oscillation Loads		0.7 psid	Attachment G		G2.5	Frequency 2.+3.5 Hz - Load is on a sample structure 4 ft from the vent exit
LOCA Chugging Loads		1.9 psid	Attachment G		G2.6	Load is on a sample structure 4 ft from the top vent exit
X-Quencher Water Jet Load		Negligible	Attachment G		G3.1	Load is negligible outside a sphere circumscribed by the quencher arms
X-Quencher Air Bubble Load		0.5 psid	Attachment G		G3.2	Load is on a sample structure 9 ft from Quencher center
<u>STRUCTURE: Submerged Structures</u>						
<u>BREAK SIZE: Intermediate*</u>						
ADS						
<u>STRUCTURE: Submerged Structures</u>						
<u>BREAK SIZE: Small*</u>						
No Additional loads generated						

*Chugging loads are the same for large, intermediate and small break accidents.

Table 1.3.1 (Continued)

<u>Load</u>	<u>Specified for Design</u>	<u>Engr'g Estimate</u>	<u>Design Basis</u>		<u>Section</u>	<u>Comments</u>
			<u>Analysis</u>	<u>Test</u>		
STRUCTURE: Structures at Pool Surface	<u>BREAK SIZE: Large</u>					
Bubble Formation						
Drywell	21.8 psid	18 psi	Equal to D.W. pressure		9.0	Large structures only
Containment	10.0 psid		Attenuated D.W. pressure			
Velocity for Computing Drag Loads	40 ft/sec	30 ft/sec	Bounding calculation		9.0	
Fallback Velocity for Drag Loads	35 ft/sec	20 ft/sec	Bounding calculation		4.1.6	
STRUCTURE: Structures at Pool Surface	<u>BREAK SIZE: Intermediate</u>					
ADS						See Attachment A
STRUCTURE: Structures at Pool Surface	<u>BREAK SIZE: Small</u>					
No additional loads generated						(See large break tabulation)

22A4365
Rev. 3

Table 1.3.1 (Continued)

Load	Specified for Design	Engr'g Estimate	Design Basis		Section	Comments
			Analysis	Test		
<u>STRUCTURE: Structures Between Pool Surface and HCU Floor</u>						
<u>BREAK SIZE: Large</u>						
Slug Impact Loads						
Small flat structures	115 psi	60 psi		5801, 5802 5805, 5706	10.1	See Attachment J
Piping	60 psi	30 psi		5801, 5802 5805, 5706	10.1	See Attachment J
Froth Impingement Loads	15 psi	15 psi		5706	10.1	See Attachment J and Figure 10.6
Velocity for Computing Drag Loads	40 ft/sec	30 ft/sec	Bounding calculation		10.2	See Attachment I. See Figure 10.3 for grating loads
Fallback Velocity for Drag Loads	35 ft/sec	20 ft/sec	Bounding calculation		10.3	
<u>STRUCTURE: Structures Between Pool Surface and HCU Floor</u>						
<u>BREAK SIZE: Intermediate</u>						
No additional loads generated						(See large break tabulation)
<u>STRUCTURE: Structures Between Pool Surface and HCU Floor</u>						
<u>BREAK SIZE: Small</u>						
No additional loads generated						(See large break tabulation)

22A4365
Rev. 2

101678

1-15

Table 1.3.1 (Continued)

Load	Specified for Design	Engr'g Estimate	Design Basis		Section	Comments
			Analysis	Test		
STRUCTURE: Expansive Structures at HCU Floor Elevation						
<u>BREAK SIZE: Large</u>						
Wetwell Pressurization	11 psig (3-4 sec)	3-5 psig (1-2 sec)	Model in Ref. 1	5801, 5802 5803, 5804	11.0	
Froth Impingement	15 psig (100 ms)	10 psig (100 ms)		5801, 5802 5805, 5706	11.0	See Attachment J discussion
Flow Pressure Differential	11 psig	3-5 psig	Model in Ref. 1	5801, 5802 5803, 5804	12.0	Test shows pressure differential of 3 to 5 psi
Fallback and Water Accumulation	1 psi	0.5 psi	Bounding calculation		12.0	Based on water flow through HCU floor
STRUCTURE: Expansive Structures at HCU Floor Elevation						
<u>BREAK SIZE: Intermediate</u>						
No additional loads generated						See large break tabulation
STRUCTURE: Expansive Structures at HCU Floor Elevation						
<u>BREAK SIZE: Small</u>						
No additional loads generated						See large break tabulation

GENERAL NOTES TO TABLE 1.3.1

1. Where S/R valve loads are specified in the applicable bar charts, refer to Attachment A, Section A5.6 for margin discussion.
2. Not all loads for IBA and SBA are tabulated. Generally the large break load condition will govern.

22A4365
Rev. 2

Table 1.3.1 (Continued)

<u>Load</u>	<u>Specified for Design</u>	<u>Engr'g Estimate</u>	<u>Design Basis</u>		<u>Section</u>	<u>Comments</u>
			<u>Analysis</u>	<u>Test</u>		
STRUCTURE: Small Structures at HCU Elevation						
Froth Impingement	15 psid	10 psid		5801, 5802 5805, 5706	12.0	See Attachment J discussion
Flow Pressure Differential	11 psid	3-5 psid	Model in Ref. 1	5801, 5802 5803, 5804	12.0	Test shows pressure differential of 3 to 5 psi
Fallback and Water Accumulation	1 psid	0.5 psid	Bounding Calculation		12.0	Based on water flow through HCU floor

22A4365
Rev. 3

2. REVIEW OF PHENOMENA

The purpose of this section of the report is to qualitatively review the sequence of events that could occur during the course of the design basis accident (DBA), an intermediate break accident (IBA), a small break accident (SBA) and during safety relief valve actuation. The objective of this review is to provide an understanding of the various pool dynamic loads and their inter-relationships, and to define the dynamic loading terminology. Specific design load values are provided in subsequent sections.

2.1 DESIGN BASIS ACCIDENT (DBA)

The Figure 2.1 chart shows the events occurring during a DBA and the potential loading conditions associated with these events.

With the instantaneous rupture of a steam or recirculation line a theoretical sonic wave exits the broken primary system pipe and expands into the drywell atmosphere. At the break exit point, the wave amplitude theoretically is reactor operating pressure (1000 psia). However, there is rapid attenuation as the wave front expands spherically outward into the drywell at sonic velocity.

As the drywell pressure increases, the water initially standing in the vent system accelerates into the pool and the vents are cleared of water. During this vent clearing process, the water leaving the horizontal vents forms jets in the suppression pool and causes water jet impingement loads on the structures within the suppression pool and on the containment wall opposite the vents. During the vent clearing transient, the drywell is subjected to a pressure differential and the weir wall experiences a vent clearing reaction force.

Immediately following vent clearing, an air and steam bubble forms at the exit of the vents. The bubble pressure initially is assumed equal to the current drywell pressure (peak calculated is 21.8 psig). This bubble theoretically transmits a pressure wave through the suppression pool water and results in loading on the suppression pool boundaries and on equipment located in the suppression pool.

As air and steam flow from the drywell becomes established in the vent system, the initial vent exit bubble expands to suppression pool hydrostatic pressure. GE Large Scale Pressure Suppression Test Facility (PSTF) Tests (Ref 4) show that the steam fraction of the flow is condensed but continued injection of drywell air and expansion of the air bubble results in a rise in the suppression pool surface. During the early stages of this process, the pool swells in a bulk mode (i.e., a slug of solid water is accelerated upward by the air). During this phase of pool swell, structures close to the pool surface will experience loads as the rising pool surface impacts the lower surface of the structure. See Figures 2.2-4, 2.2-5, and 2.2-6. In addition to these initial impact loads, these same structures will experience drag loads as water flows past them. Equipment in the suppression pool will also experience drag loads.

Data from PSTF air tests (5706) indicates that after the pool surface has risen approximately 1.6 times the initial submergence of the top vent, the water ligament thickness has decreased to two feet or less and the impact loads are significantly reduced. This phase is referred to as incipient breakthrough; i.e., ligament begins to break up.

Ligament thickness continues to decrease until complete breakthrough is reached and the air bubble can vent to the containment free space. The breakthrough process results in formation of an air/water froth.

Continued injection of drywell air into the suppression pool results in a period of froth pool swell. This froth swell impinges on structures it encounters but the two phase nature of the fluid results in loads that are very much less than the impact loads associated with bulk pool swell.

When the froth reaches the elevation of the floors on which the Hydraulic Control Units for the Control Rod Drives are located, approximately 20 feet above pool level, the froth encounters a flow restriction; at this elevation, there is approximately 25% open area. See Figures 2.2-2 and 2.2-3. The froth pool swell experiences a two phase pressure drop as it is forced to flow through the available open areas. This pressure differential represents a load on both the floor structures themselves and on the adjacent containment and drywell. The result is a discontinuous pressure loading at this elevation.

Figure 2.2-1 is a diagram that summarizes the various phases of pool swell and the nature of the dynamic loading conditions that occur. It should be emphasized that the pool swell elevation information presented on Figure 2.2-1 is based on an assessment of the PSTF air tests. As such it is considered conservative since the PSTF air test data have been interpreted and used in a conservative manner.

The pool swell impact and impingement target data presented in Section 10 of this document is applicable to small structures. This restriction on the application of the impact test data is necessary since the basic tests involved targets with a width of 20 inches. For this size target, only the suppression pool water in the immediate vicinity of the target has to be re-directed by the impact impulse, thus, the impact loads are not dependent upon the pool swell water ligament thickness. Attachment J discussed application of PSTF impact data to small structures.

For floors that are expansive enough to decelerate a large sector of the pool rather than a small region of the pool in the vicinity of the target, the impulsive loading on the floor is dependent upon the momentum of the entire slug and is related to slug thickness.

As drywell air flow through the horizontal vent system decreases and the air/water suppression pool mixture experiences gravity induced phase separation, pool upward movement stops and the "fallback" process starts. During this process, floors and other flat structures experience downward loading and the containment wall theoretically can be subjected to a small pressure increase. However, this pressure increase has not been observed experimentally.

The pool swell transient associated with drywell air venting to the pool typically lasts 3 to 5 seconds. Following this, there is a long period of high steam flow rate through the vent system; data indicates that this steam will be entirely condensed in a region right at the vent exits. For the DBA reactor blowdown, steam condensation lasts for a period of approximately one minute. Potential structural loadings during the steam condensation phase of the accident have been observed, are relatively small, and are included in the containment loading specification.

As the reactor blowdown proceeds the primary system is depleted of high energy fluid inventory and the steam flow rate to the vent system decreases. This reduced steam flow rate leads to a reduction in the drywell/containment pressure differential which in turn results in a sequential recovering of the horizontal vents. Suppression pool recovering of a particular vent row occurs when the vent stagnation differential pressure corresponds to the suppression pool hydrostatic pressure at the row of vents.

Toward the end of the reactor blowdown, the top row of vents is capable of condensing the reduced blowdown flow and the two lower rows will be totally recovered. As the blowdown steam flow decreases to very low values, the water in the top row of vents starts to oscillate back and forth causing what has become known as vent "chugging." This action results in dynamic loads on the top vents and on the weir wall opposite the upper row of vents. In addition an oscillatory pressure loading condition can occur on the drywell and containment, but is insignificant. Since this phenomenon is steam mass flux dependent (the chugging threshold appears to be in the range of 10 lb/sec/ft²) it is present for all break sizes. For smaller breaks, it is the only mode of condensation that the vent system will experience.

Shortly after a DBA, the Emergency Core Cooling System (ECCS) pumps automatically start up and pump condensate water and/or suppression pool water into the reactor pressure vessel. This water floods the reactor core and then starts to cascade into the drywell from the break; the time at which this occurs depends upon break size and location. Because the drywell is full of steam at the time of vessel flooding, the sudden introduction of cool water causes rapid steam condensation and drywell depressurization. When the drywell pressure falls below the containment pressure, the drywell vacuum relief system is activated and air from the containment enters the drywell. Eventually sufficient air returns to equalize the drywell and containment pressures; however, during this drywell depressurization transient, there is a period of negative pressure on the drywell structure; a conservative negative load condition is therefore specified for drywell design.

Following vessel flooding and drywell/containment pressure equalization, suppression pool water is continuously recirculated through the core by the ECCS

pumps. The energy associated with the core decay heat results in a slow heat up of the suppression pool. To control suppression pool temperature, operators will activate the RHR heat exchangers. After several hours, the heat exchangers control and limit the suppression pool temperature increase. The suppression pool is conservatively calculated to reach a peak temperature of 176°F and with long term containment spray operation the peak temperature can approach 185°F. The increase in air and water vapor pressure at these temperatures results in a pressure loading of the containment.

The post DBA containment heatup and pressurization transient is terminated when the RHR heat exchangers reduce the pool temperature and containment pressure to nominal values.

2.2 INTERMEDIATE BREAK ACCIDENT (IBA)

An intermediate size break is defined as a break that is less than the DBA but is of sufficient magnitude to automatically depressurize the primary system due to loss of fluid and/or automatic initiation of the ECCS systems. In practice, this means liquid breaks greater than 0.05 ft² and steam breaks greater than 0.4 ft² as determined by analysis.

In general, the magnitude of dynamic loading conditions associated with a loss of coolant accident decrease with decreasing break size. However, the intermediate break is examined because the Automatic Depressurization System (ADS) may be involved. Simultaneous actuation of the multiple safety/relief valves committed to this system introduces significant containment system loads, as discussed in Section 2.4.

2.3 SMALL BREAK ACCIDENT (SBA)

Small breaks are defined as breaks not large enough to automatically depressurize the reactor. Accident termination is dependent upon operator action and the duration of the accident is determined by operator response. The dynamic loads produced by this class of accident are small. However, there are certain conditions associated with smaller reactor system breaks that must be considered during the design process. Specifically, the drywell and weir wall must be

designed for the thermal loading conditions that can be generated by a small steam break (SBA). For a definition of the design conditions, the following sequence of events is postulated.

With the reactor and containment operating at maximum normal conditions, a small break occurs allowing blowdown of reactor steam to the drywell. The resulting drywell pressure increase leads to a high drywell pressure signal that scrams the reactor and activates the containment isolation system. Drywell pressure continues to increase at a rate dependent on the size of the assumed steam leak. This pressure increase to 3 psig depresses the water level in the weir annulus until the level reaches the top of the upper row of vents. At this time, air and steam enter the suppression pool. Steam is condensed and the air passes to the containment free space. The latter results in gradual pressurization of the containment at a rate dependent upon the air carryover. Eventually, entrainment of the drywell air in the steam flow through the vents results in all the drywell air being carried over to the containment. At this time, containment pressurization ceases. The drywell is now full of steam and has a positive pressure differential sufficient to keep the weir annulus water level depressed to the top vents and chugging can occur. Continued reactor blowdown steam is condensed in the suppression pool.

The thermodynamic process associated with blowdown of primary system fluid is one of constant enthalpy. If the primary system break is below the RPV water level, blowdown flow consists of reactor water. Upon depressurizing from reactor pressure to drywell pressure, approximately one-third of this water flashes to steam, two-thirds remain as liquid, and both phases will be in a saturated condition at drywell pressure. Thus, if the drywell is at atmospheric pressure, the steam-and-liquid blowdown will have a temperature of 212°F.

If the primary system rupture is located so that the blowdown flow consists of reactor steam, the resultant steam temperature in the drywell is significantly higher than the saturated temperature associated with liquid blowdown. This is because a constant enthalpy decompression of high pressure saturated steam results in a superheat condition. For example, decompression of 1,000 psia saturated steam to atmospheric pressure results in 298°F superheated steam (86°F of superheat).

Reactor operators are alerted to the SBA incident by the leak detection system, or high drywell-pressure signal, and reactor scram. For the degraded accident evaluation, rapid depressurization is assumed to be manually initiated at 10 minutes to terminate the event. For the purpose of evaluating the duration of the superheat condition in the drywell, it is assumed that operator response to the small break is to shut the reactor down in an orderly manner using selected relief valves and with the RHR heat exchangers controlling the suppression pool temperature. (This assumes the main condenser is not available and the operators must use the suppression pool for an energy sink. In all probability, the condenser would be available and the suppression pool would not be involved in the shutdown.) Reactor cooldown rate is assumed to be started 30 minutes after the break and at 100°F/hr. Using these procedures, leads to a reactor cool-down in approximately three to six hours. At that time, the RHR system (in the shutdown mode) maintains the reactor at 212°F or less and the blowdown flow rate is terminated. It should be noted that the end-of-blowdown chugging phenomenon discussed in Section 2.1 will also occur during a small break accident and will last the duration of reactor depressurization.

2.4 SAFETY RELIEF VALVE ACTUATION

In addition to loads on the valves and discharge piping, actuation of the safety/relief (S/R) valves causes pressure disturbances in the suppression pool water which results in dynamic loads on the suppression pool floor, the weir wall, the drywell and the containment adjacent to the pool. Structures in the pool also experience this loading. Relief valve actuation can be initiated either automatically by a reactor pressure increase to the valve setpoints or by an active system such as ADS.

The phenomena which cause these loads is as follows. Prior to actuation, the S/R discharge lines contain air at atmospheric pressure and a column of water in the submerged section. Following S/R valve actuation, the pressure builds up inside the piping and expels the water column. The air follows the water through the holes in the quencher arms and forms a large number of small bubbles. Once in the pool, the bubbles expand, coalesce and form four large bubbles. Each of the four bubbles expands analogous to a spring and accelerates the surrounding pool of water. The momentum of the accelerated water causes the bubble to over-expand and the bubble pressure becomes negative. This negative pressure slows down and finally reverses the motion of the water leading to compression

of the bubble. This sequence of expansion and contraction is repeated with a mean frequency of about 8 Hz until the bubble reaches the pool surface.

The bubble oscillation causes oscillating pressures throughout the pool. The magnitude of the pressure amplitude decreases with time and with distance from the bubble. The duration of this load is less than 1 second (See Figure 2.3). SRV steam condensation during valve discharge to the pool also occurs. This phenomenon results in low amplitude pressure fluctuations.

In evaluating the Mark III structural loads and containment/drywell capability it is necessary to properly account for the hypothetical accident related loads and their sequence of occurrence. In defining the loads for this evaluation, this report addresses the design basis accident (pipe break) and the loads associated with the hypothetical concurrent earthquake, pool dynamics, and static loading. The ability of the design to accommodate these loadings, when properly sequenced, constitutes the design basis of the structure. This design basis includes the single failure criterion; i.e., any single component may fail to act when called upon during loss-of-coolant accidents

This report also addresses an additional consideration namely the inadvertent opening of a single S/R valve. The opening of a single valve is not a direct result of the LOCA and, furthermore, is not an expected occurrence during the accident sequence. However, the loading chart figures show the loads associated with a single safety/relief valve actuation as an additional load for demonstrating additional capability.

Safety relief valve loading data is discussed in Attachment A.

2.5 OTHER CONSIDERATIONS

In addition to the LOCA and S/R valve dynamic loads that have been identified in the preceding sections, other loads must be considered during the design process (deadweight, seismic accelerations, etc.) These loads are included in the loading diagrams contained in this report.

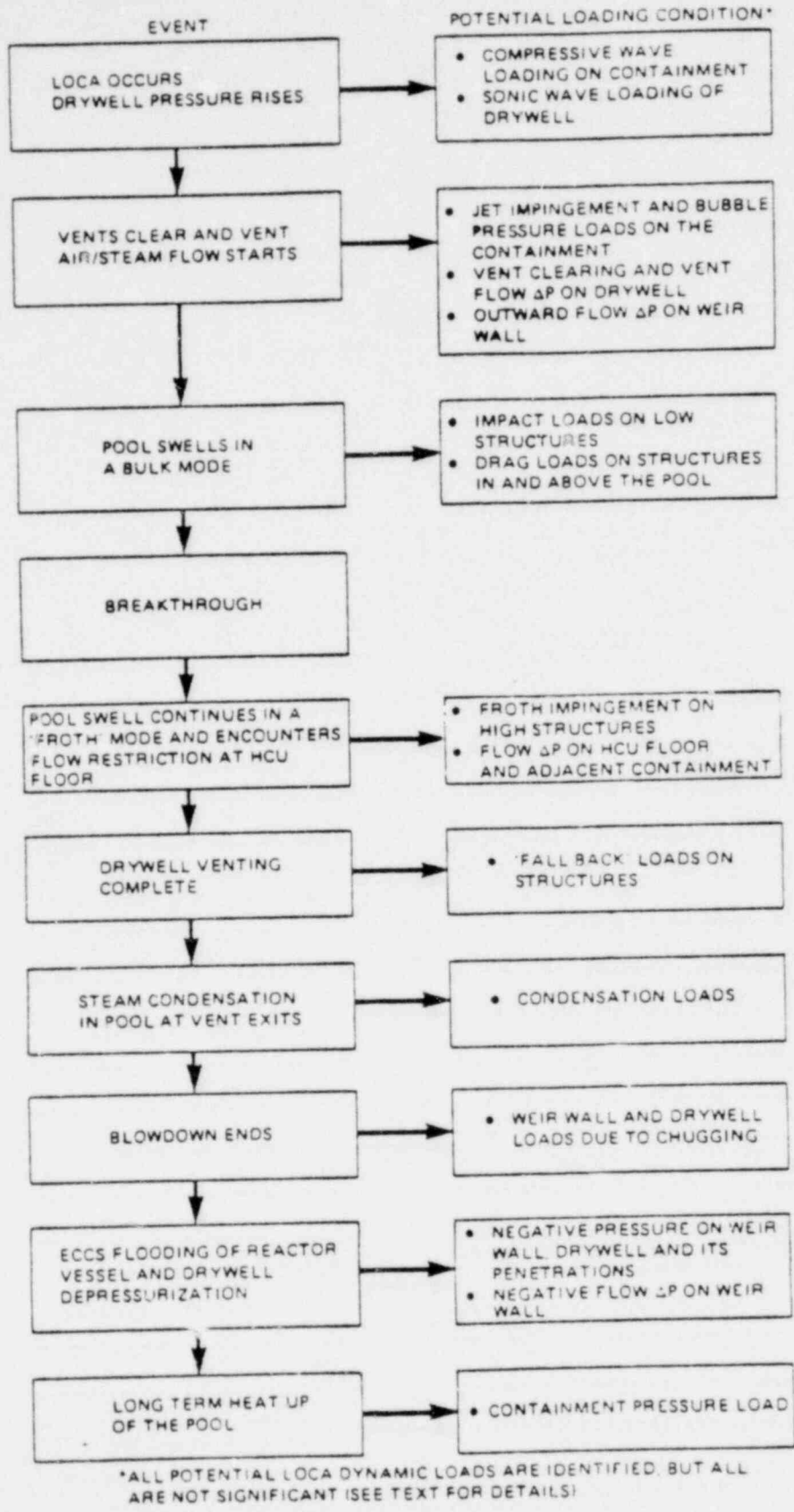


Figure 2.1. Loss-of-Coolant Accident Chronology (DBA)

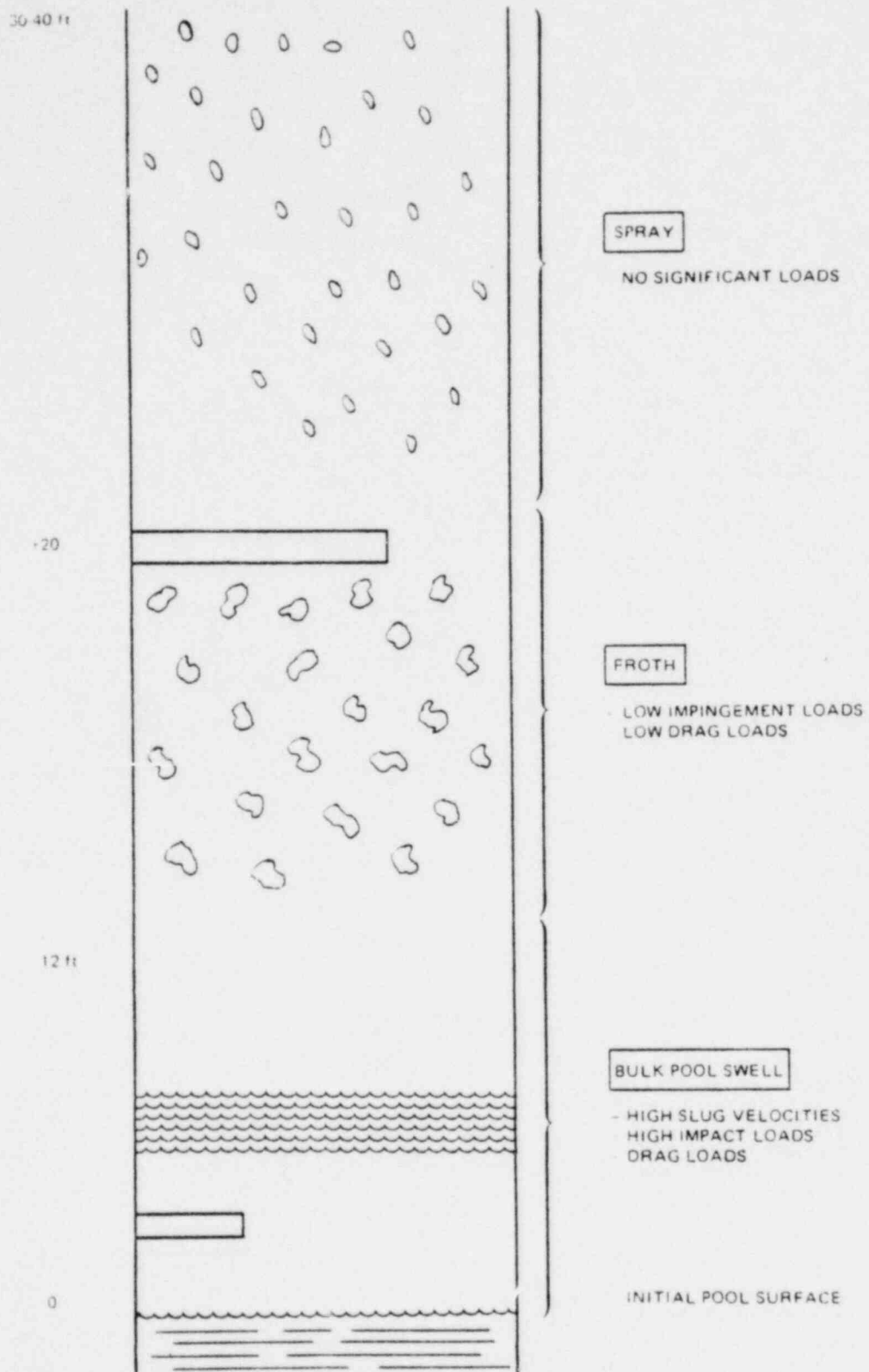


Figure 2.2-1. Schematic of the Mark III Pool Swell Phenomenon

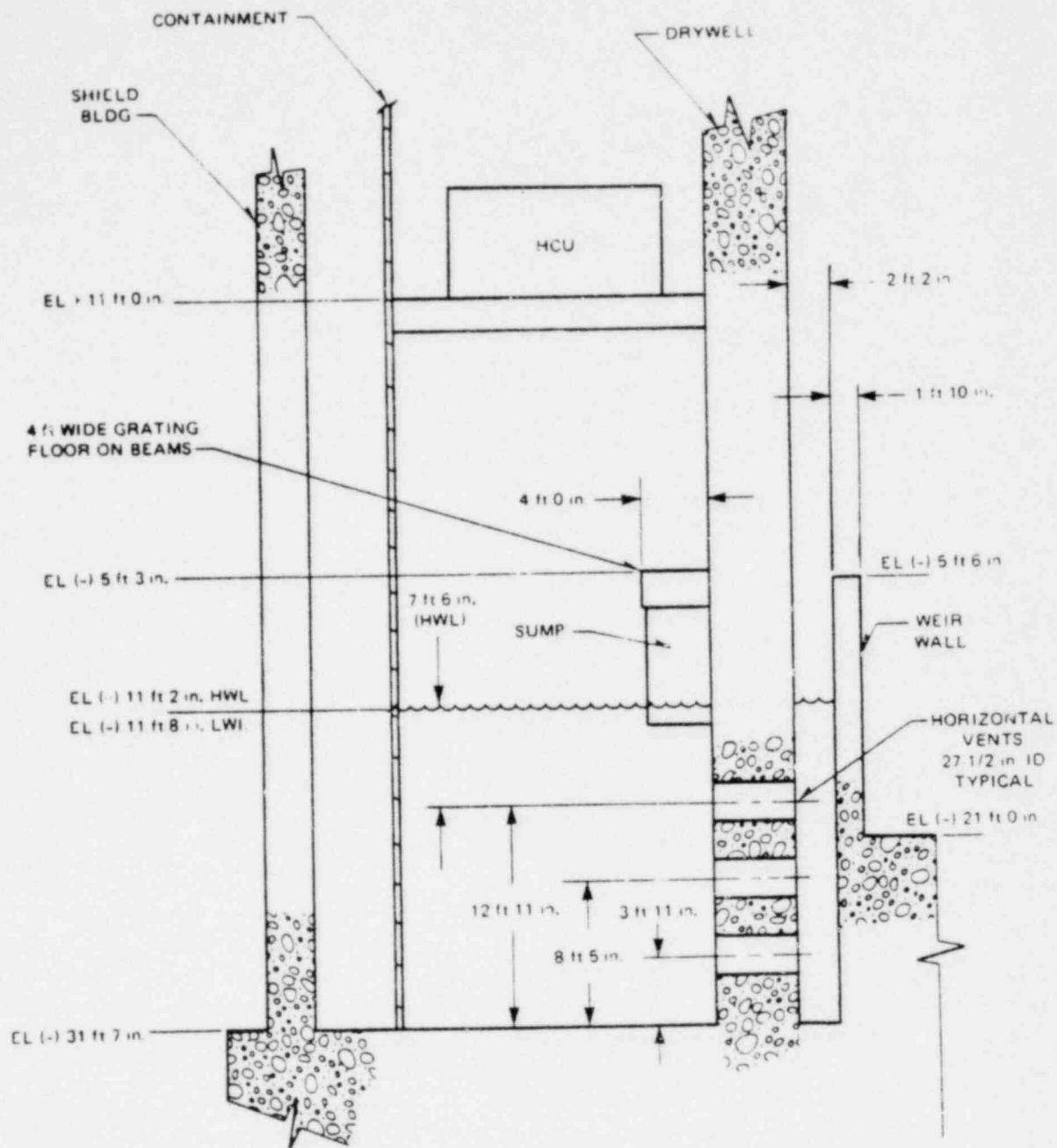


Figure 2.2-2. Typical Suppression Pool Cross Section 238 Plant

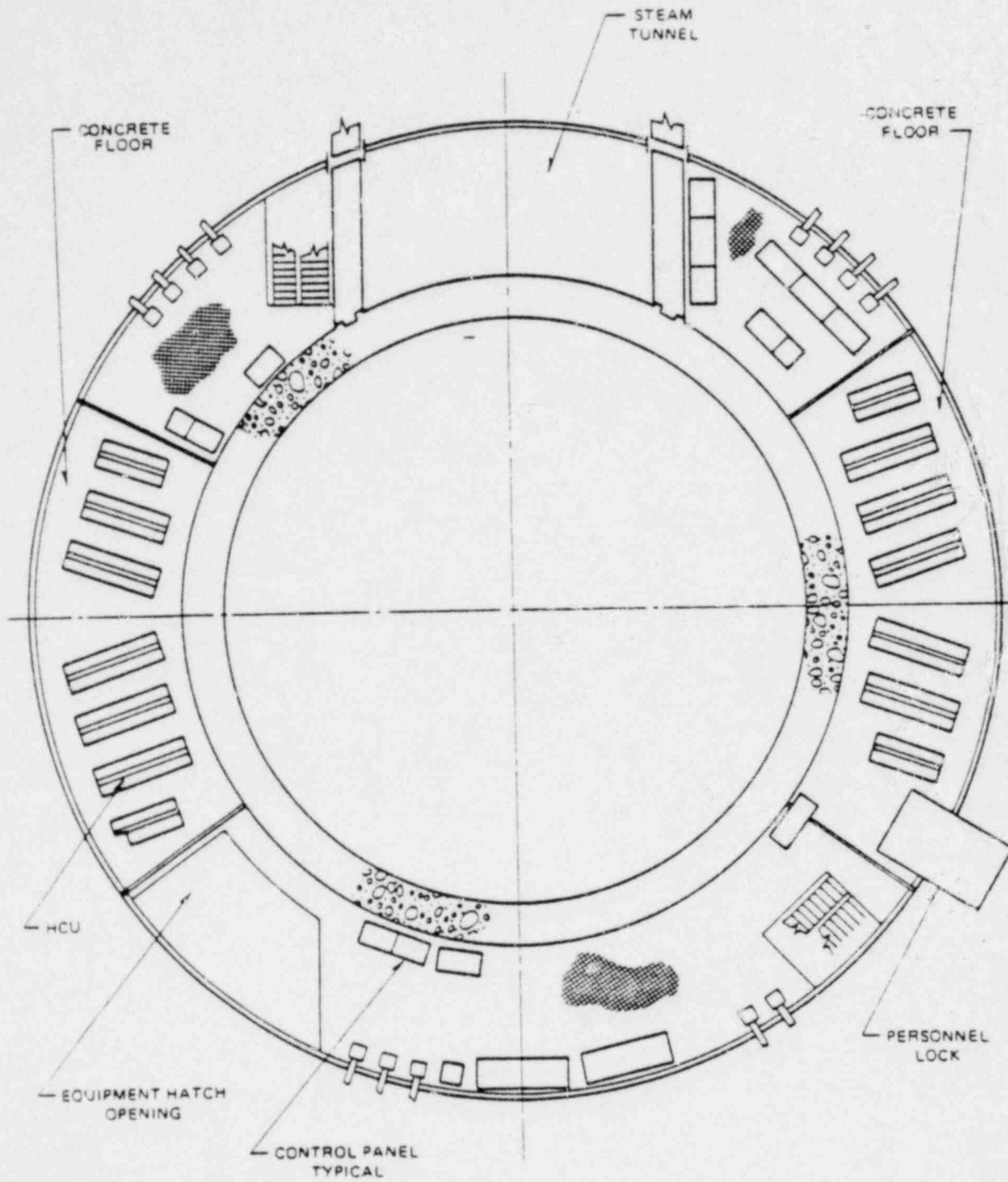


Figure 2.2-3. Plan At Elevation 11 ft 0 in.

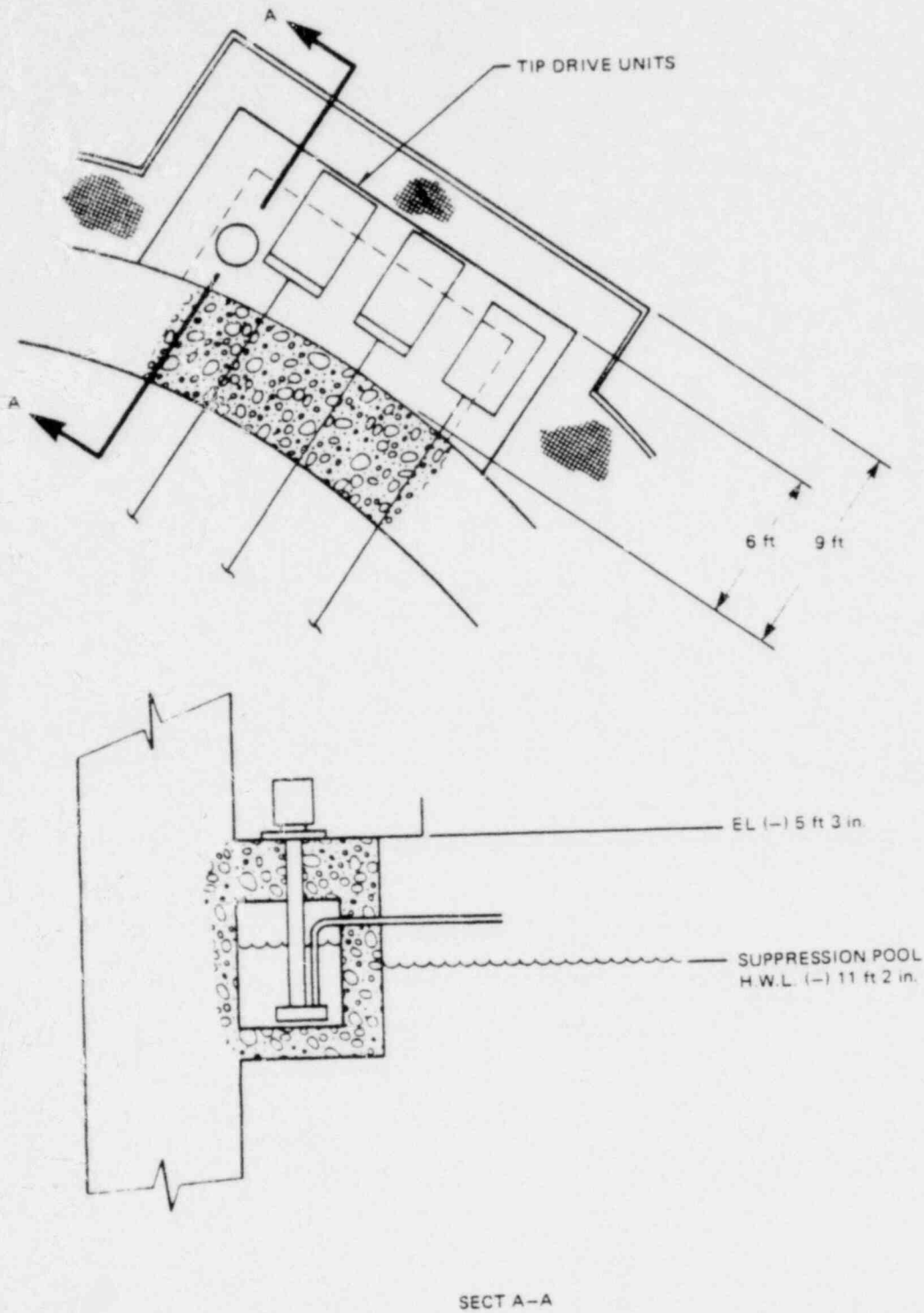


Figure 2.2-4. Containment Floor Drain Sump 238 Plant

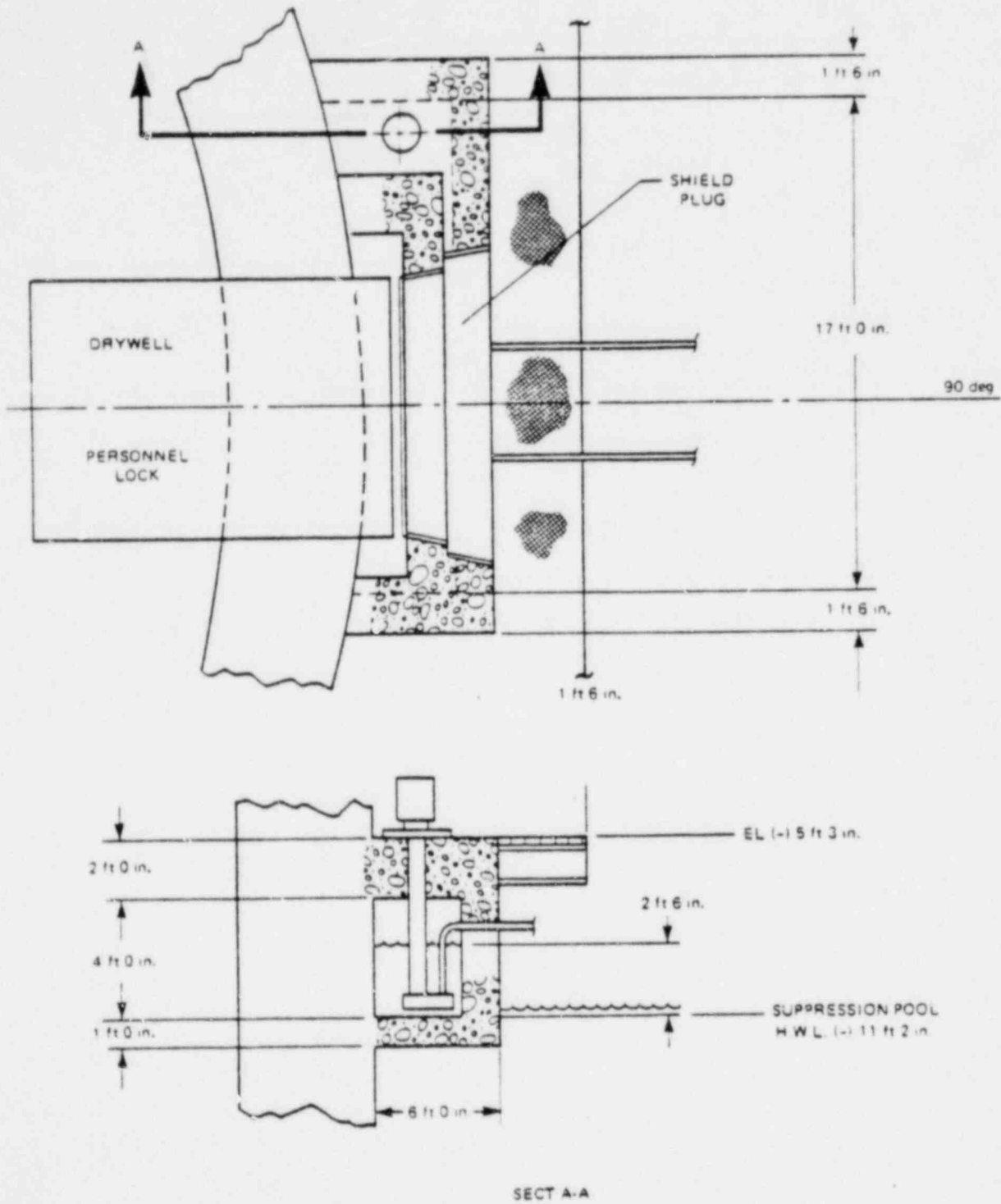


Figure 2.2-5. Containment Equipment Drain Sump 238 Plant

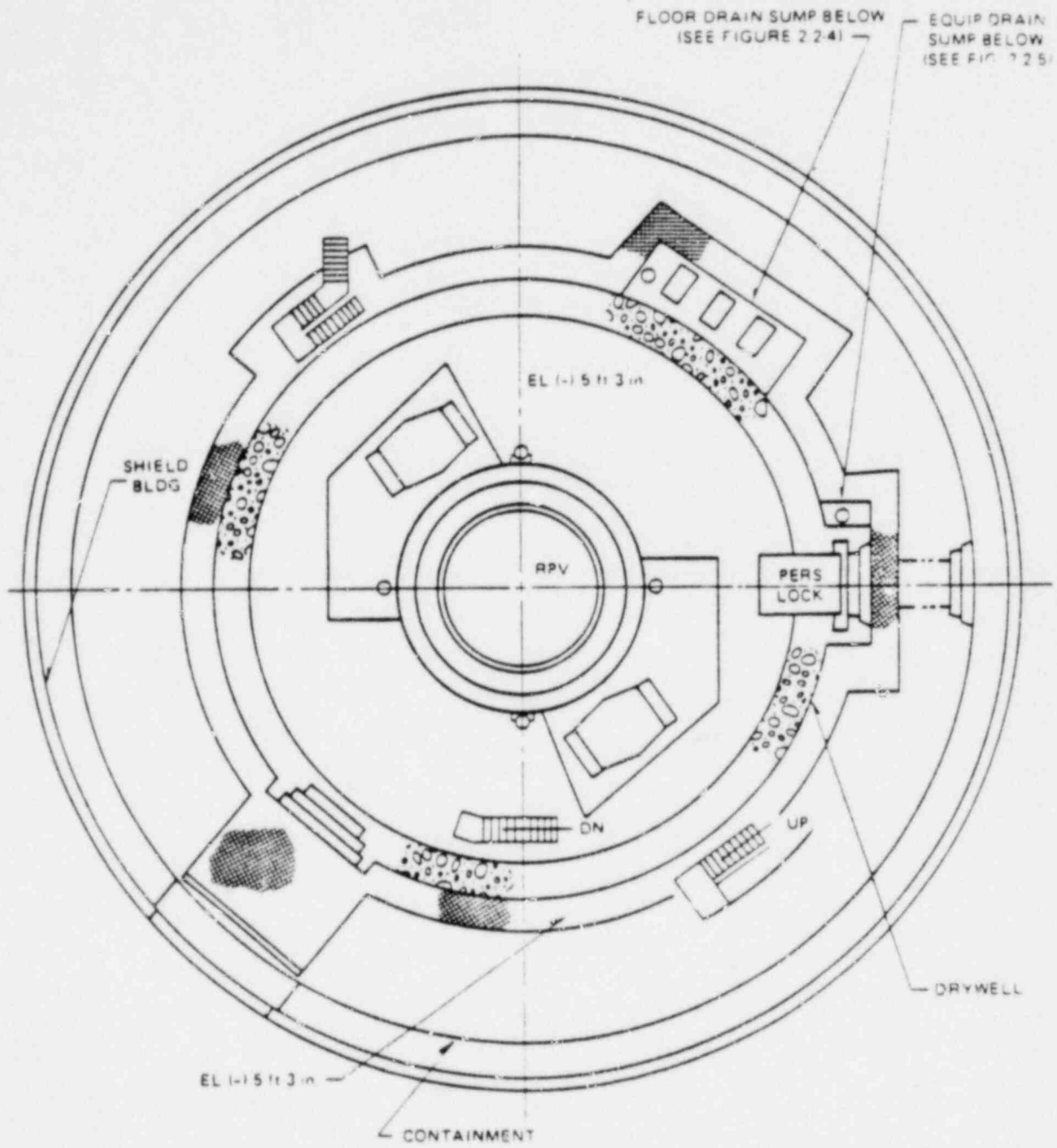


Figure 2.2-6. Plan At Elevation (-) 5 ft 3 in.

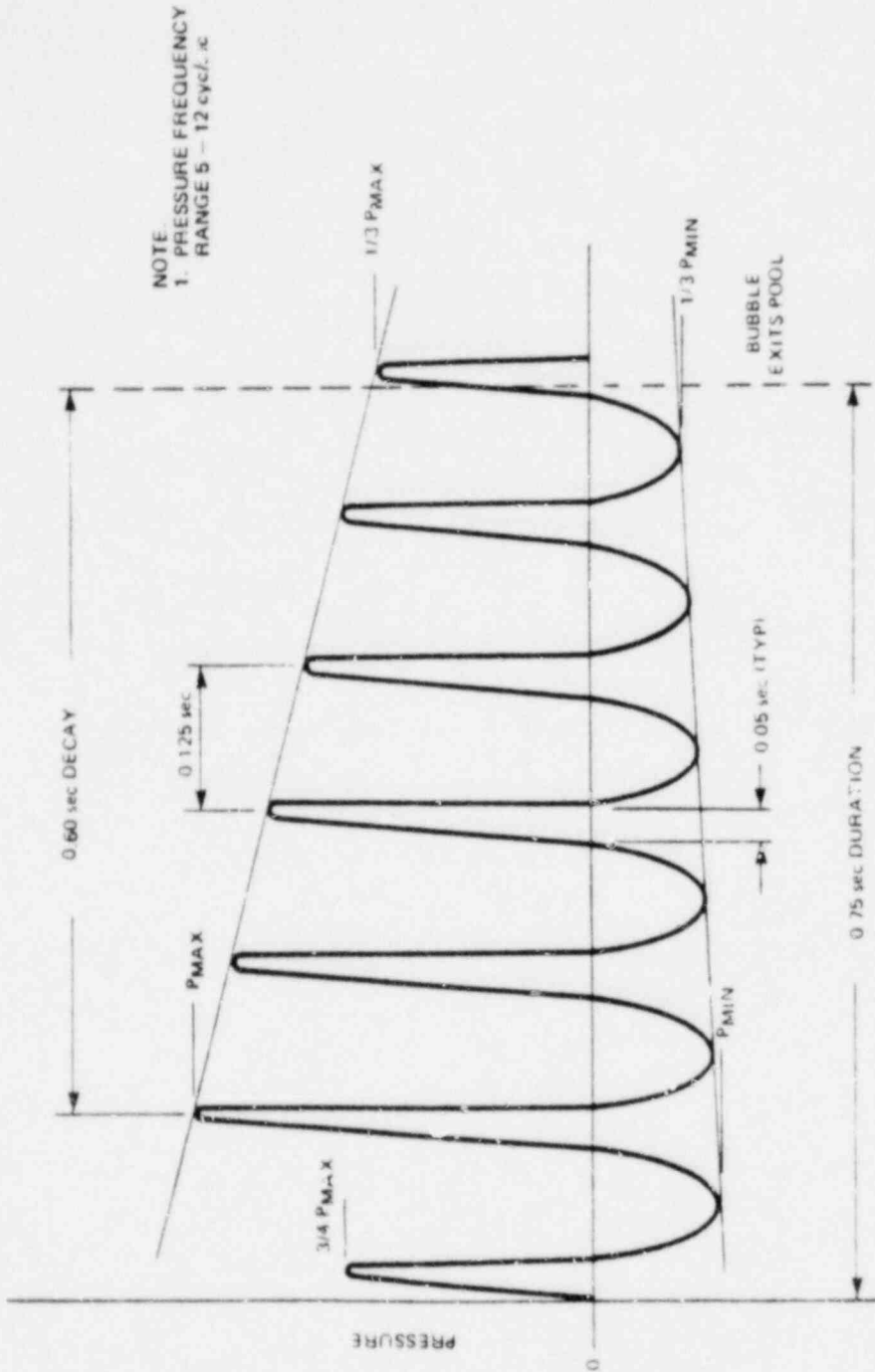


Figure 2.3. Idealized Quencher Bubble Pressure Oscillation In Suppression Pool

3. DYNAMIC LOAD TABLE

The dynamic loading information for the Mark III containment system is presented in the subsequent sections of this report. The data is presented in bar chart form and shows the temporal distribution of loading sequences for the various structures. At any given time on a bar chart it is assumed that the particular structure being considered experiences all the loading conditions in those "boxes" which span the given time unless a specific exception is indicated.

Each chart has applicable loading information references. Table 3.1.1 summarizes the accidents that influence the design of various structures.

Table 3.1.1
Summary of Postulated Accidents Affecting Mark III Structures

<u>Structure</u>	<u>(DBA) Large Break</u>	<u>(IBA) Intermediate Break</u>	<u>(SBA) Small Break</u>
Drywell	X	X	X
Weir Wall	X	X	X
Containment	X	X	X
Suppression Pool Floor	X	X	-
Structures in Suppression Pool	X	X	-
Structures at the Suppression Pool Surface	X	X	-
Structures Between the Pool Surface and the HCU Floor	X	-	-
Structures at the HCU Floor Elevation	X	-	-

Notes:

1. X indicates accident with significant loading conditions
2. For concurrent S/R valve events, see appropriate bar charts

4. DRYWELL STRUCTURE

The drywell structure experiences loads during both the design basis loss-of-coolant accident and during a small steam break accident. Loads occurring during an intermediate break accident are less severe than those associated with the large and small break. The designer should consider other dynamic loads that are not included in this report. These are pipe whip, jet impingement, missile, etc.

4.1 DRYWELL LOADS DURING A LARGE BREAK ACCIDENT

Figure 4.1 is the loading bar chart for the drywell structure during a large steam line break. A discussion of the loading conditions follows:

4.1.1 Sonic Wave

Theoretically, a sonic compressive wave is initiated in the drywell atmosphere following the postulated instantaneous rupture of a large primary system pipe. This phenomenon is not considered in the drywell design conditions on the basis that the finite opening time of a real break coupled with the rapid attenuation with distance and short duration does not produce any significant loading in the drywell.

4.1.2 Drywell Pressure

During the vent clearing process, the drywell reaches a peak calculated differential pressure of 21.8 psid. During the subsequent vent flow phase of the blowdown, the peak pressure differential is less than 21.8 psid due to the wetwell pressurization from the two-phase pool swell flow reaching the containment annulus restriction at the HCU floor (see Figure 4.4). This wetwell pressurization is a localized load that acts on the Drywell O.D. below the HCU floor. Interaction between pool swell and the limited number of structures at or near the pool surface does not adversely affect the drywell pressure.

Figure 4.4 shows the drywell pressure during the DBA. It includes the HCU floor pool swell interference effects. The analytical model presented in Ref. 1 was used to calculate these values.

Blockage of the weir annulus flow area by equipment located above the annulus entrance has the potential for increasing the real drywell pressure differential. Attachment C presents data which show no potential pressure increase for blockages up to 30 percent of the total area.

During the blowdown process, the drywell is subjected to differential pressures between levels because of flow restrictions. This value varies with the size of the restriction, but a bounding value for a 25 percent restriction is 0.5 psi as discussed in Attachment D. On the basis of this bounding calculation, it has been concluded that differential pressures within the drywell during the DBA will be small and as such, need not be included in the drywell loading specifications.

4.1.3 Hydrostatic Pressure

During the period of vent flow, the water normally standing in the weir annulus is expelled into the main suppression pool and the lower regions of the drywell experience an inward load due to the hydrostatic pressure associated with the pool water. If it is assumed that an earthquake is occurring at this time, the horizontal and vertical accelerations of the building can influence the hydrostatic pressure calculations. See Attachment B.

4.1.4 Loads On The Drywell Wall During Pool Swell

During bubble formation, the outside of the drywell wall in the pool will be subject to varying pressures. A bounding range of 0 to 21.8 psid is specified on those sections of the drywell wall below the suppression pool surface. The basis for this specification is the knowledge that the minimum pressure increase is 0 psi and the maximum bubble pressure can never exceed the peak drywell pressure of 21.8 psid. Above the nominal suppression pool surface, the pressure linearly decreases from 21.8 psid to 0 psid over 18.0 feet (see Figure 6.5).

Any structures in the containment annulus that are within approximately 20 feet of the initial suppression pool surface will experience upward loads during

pool swell (see Figure 12.2). If these structures are attached to the drywell wall, then the upward loads will be transmitted into drywell structure. In addition, the region of the drywell below the HCU floors will experience the wetwell pressurization transient during pool swell froth at the HCU floor, as shown in Figure 4.4.

Sections 9, 10, 11 and 12 discuss applied loads for equipment, floors, etc. that are located in the containment annulus.

4.1.5 Condensation Oscillation Loads

Following the initial pool swell transient (during a LOCA) when the drywell air is vented to the containment free space, there is a period of 0.05 to 1.5 minutes (depending upon break size and location) when high steam mass flows through the top vents and condensation oscillation occurs. Vent steam mass fluxes of up to 25 lbm/sec/ft² occur as a result of either a main steam or recirculation line break. Steam and liquid blowdown tests with various blowdown orifice sizes have been performed in the PSTF facility.

Some pressure oscillations have been observed on the drywell wall. Figures 4.5 and 4.5a give a summary of the magnitude of the top vent exit pressure fluctuations observed during PSTF steam tests. The data has been plotted against vent submergence and is independent of this parameter.

Additional instrumentation was located on the drywell wall above the top vent in PSTF Series 5807. Typical test data traces are shown in Figure 4.6 and show the localized nature of the condensation loads. Maximum pressure amplitude decreases from approximately ±10 psid to approximately ±2 psid in two feet.

The condensation oscillation forcing function to be used for design is defined as a summation of four harmonically related sine waves developed from a regression analysis of the data obtained in test series 5807 (Reference 15):

$$P(\tau) = \frac{A(\tau)}{2} \{ 0.8 \sin (2\pi \times \tau \times f(\tau)) \\ + 0.3 \sin (4\pi \times \tau \times f(\tau)) \\ + 0.15 \sin (6\pi \times \tau \times f(\tau)) \\ + 0.2 \sin (8\pi \times \tau \times f(\tau)) \} \text{ (psid)}$$

(Eq. 4-1)

where:

$P(\tau)$ = pressure amplitude (psid) for consecutive cycles beginning at time $t = 3$ sec. and ending at T_{P_n}

$A(t)$ = peak-to-peak pressure amplitude variation with time, (psid)
 $= 5.5 \{ 3.395 - 0.106t + 1.15 \log t - 7.987 (\log t)^2 + 7.688 (\log t)^3 - 1.344 (\log t)^4 \}$ Eqn (4.2)*

$f(t)$ = fundamental frequency variation with time, (Hz)
 $= 0.8 \{ 2.495 - 0.225 t - 0.742 \log t + 10.514 (\log t)^2 - 9.271 (\log t)^3 + 3.208 (\log t)^4 \}$ Eqn (4.3)*

*Log terms shown in Equations 4.2 and 4.3 are log to base 10.

t = time (sec), $3 \leq t \leq 30$, time from initiation of LOCA blowdown

τ = time increment for successive periods $T_{P_i} < \tau < T_{P_n}$,
 $T_{P_1} = \frac{1}{f(3)}$; where n is number of cycles between 3 and 30 sec.

$$T_{P_n} = \frac{1}{f(3 + T_{P_1} + T_{P_2} + \dots + T_{P_{n-1}})}$$

$P(\tau)$ from Eqn (4.1) has been calculated for 4 cycles and is shown in Figure 4.6b. Eqn (4.1) has been calculated and digitized in Attachment 0 of this report. The spatial distribution of the forcing function amplitude over the wetted surface of the suppression pool is shown in Figure 4.6a. The amplitudes shown are the maximum values determined from Eqn (4.1) normalized to 1.0 at the top vent centerline.

4.1.6 Fall Back Loads

In general, the data generated in the PSTF indicates that no significant loading conditions on the drywell wall occur during pool fall back. Figure 6.4 shows that suppression pool wall pressures following bubble breakthrough return to their initial pre-LOCA values during the 1.5 to 5 second period when the pool level is subsiding. Therefore, fall back pressure loads are not specified for Mark III drywell.

Structures attached to the drywell wall experience drag loads as the water level subsides to its initial level. These structures could experience drag forces associated with water flowing at 35 ft/sec; typical drag coefficients are shown on Figure 10.5. This is the terminal velocity for a 20 ft. free fall and is a conservative bounding number.

4.1.7 Negative Load During ECCS Flooding

Somewhere between 100 and 600 seconds following a LOCA (the time is dependent on break location and size) the ECCS system will refill the reactor pressure vessel. Subsequently, cool suppression pool water will cascade from the break to the drywell and start condensing the steam in the drywell. The rapid drywell depressurization produced by this condensation will draw non-condensable gas from the containment free space via the drywell vacuum breakers. It is during this drywell depressurization transient that the maximum drywell negative pressure occurs. However, for design purposes a conservative bounding end point calculation was performed which assumes that drywell depressurization occurs before a significant quantity of air can return to the drywell via the vacuum relief system. This theoretical conservative calculation yields a drywell to containment negative pressure differential of 21 psi (see Attachment E).

4.1.8 Chugging

During vent chugging, drywell pressure fluctuations result if significant quantities of suppression pool water are splashed into the drywell when the returning water impacts the weir wall. This can result in a pressure differential between the drywell and containment as shown in Figure 4.9. The maximum values of this load (+2.0, -0.7 psid) are negligible when compared to the peak positive drywell pressure used for drywell design and the negative pressure discussed in Attachment E (Peak Negative Drywell Pressure). Chugging is an oscillatory phenomenon having a period of 1 to 5 seconds.

The PSTF data shown on Figure 4.9 from the 5801, 5802, 5803 and 5804 series of 1/3 scale PSTF tests. The data has been plotted against top vent submergence with no obvious correlation. Because volumes and areas of the 1/3 scale tests are correctly scaled, the tests are more appropriate as a source of chugging

induced drywell pressure data than large scale tests 5701, 5702, and 5703 discussed in Reference 4. The large scale PSTF configuration had a drywell volume to vent area ratio only one-third of either the full scale Mark III or the 1/3 scale PSTF configuration. Drywell pressure variations during chugging result from a combination of fluctuating steam condensation rates at the vent exit and water splashing into the drywell. The undersized drywell of the large scale PSTF would tend to exaggerate the drywell pressure response.

4.1.9 Loads Due to Chugging

In addition to the bulk drywell pressure fluctuations, high amplitude pressure pulses are observed when the steam bubbles collapse in the vents during chugging. The dominant pressure response to the top vent during chugging is of the pulse train type with the peak amplitude of the pulses varying randomly from chug to chug. The pressure pulse train associated with a chug consists of a sequence of four pulses with exponentially decreasing amplitude as shown in the typical pressure trace in Figure 4.7.

The dominant pressure responses in the suppression pool during chugging is characterized by a prechug underpressure, an impulse (pressure spike), and a post chug oscillation as shown in the data trace in Figure 4.8.

The chugging process as observed in PSTF tests has a random amplitude and frequency. Although it is expected that chugging will occur randomly among the vents, synchronous chugging in all top vents is assumed. Each vent is expected to be periodically exposed to the peak observed pressure spike. The pool boundary load definition considers that the chugging loads transmitted to the drywell wall, weir wall, basemat and containment are the result of several vents chugging simultaneously at different amplitudes.

The potential for asymmetric chugging loads is discussed in Attachment L.

4.1.9.1 Chugging Loads Applied To Top Vent

Within the top vent, the peak pressure pulse train shown in Figure 4.7a is applied for local or independent evaluation of vents. Although some variation is observed in the pressure distribution from the top to the bottom of the vent, it is conservatively assumed that during the chugging event the entire top vent wall is simultaneously exposed to spatially uniform pressure pulses. Because some net unbalance in the pressure distribution gives rise to a vertical load, the peak force pulse train shown in Figure 4.7b is applied vertically upward over the projected vent area concurrently with the peak pressure pulse train to evaluate local effects at one vent. For global effects, the average force pulse train shown in Figure 4.7c is applied vertically over the projected area of all top vents concurrently with the average pressure pulse train within the vent shown in Figure 4.7d.

As can be seen in Figure 4.7, the underpressure preceding the pressure pulse train within the top vent is very small compared to the peak (spike) overpressure. The mean measured pressure (results from tests) was -9 psid with a standard deviation of ± 3 psid. On this basis, the specified design value is -15 psid.

4.1.9.2 Pool Boundary Chugging Loads

The chugging load applied to the pool boundary (drywell, basemat and containment) is described by the typical forcing function shown in Figure 4.8a. The forcing function consists of a pre-chug underpressure defined as a half sine wave, a triangular pulse (pressure spike) loading characterized by a time duration "d" and a post-chug oscillation described by a damped sinusoid. The pulse is at its maximum magnitude and duration near the top vent on the drywell wall due to the localized nature of the phenomena. The amplitude of the pre-chug underpressure and the post-chug oscillation are also maximum at this location.

For local load considerations on the pool boundary:

- Pre-chug underpressure
 - peak amplitude - Table 4.1
 - distribution - Figure 4.8b

- Pulse (spike)
 - peak amplitude - Table 4.1
 - distribution - Figure 4.8d
 - duration - Figure 4.8e

- Post-chug oscillation
 - peak amplitude - Table 4.1
 - distribution - Figure 4.8f

Local chugging loads should be used to evaluate local effects such as pool liner buckling and vent liner stresses. Local chugging loads shall not be combined with other loads.

For distribution in the horizontal (circumferential) direction, the pre-chug underpressure attenuates on the drywell, basemat and containment, as shown in Figure 4.8g. The pulse attenuation is the same as the lower portion of the vertical attenuation shown in Figure 4.8d, except that the peak is at the vent centerline, and the post-chug oscillation attenuates on the drywell, basemat and containment, as shown in Figure 4.8h. The profiles in Figures 4.8g and 4.8h represent the peak observed value at one vent, with the other vents chugging at the mean value.

For global load considerations on the pool boundary:

- Pre-chug underpressure
 - mean amplitude - Table 4.1
 - distribution - Figure 4.8c

- Pulse (spike)
 - mean amplitude - Table 4.1
 - distribution - Figure 4.8d
 - duration - Figure 4.8e

- Post-chug oscillation
 - mean amplitude - Table 4.1
 - distribution - Figure 4.8i

- No horizontal attenuation for this loading

Global loads should be used for load combinations and for piping and equipment response calculations.

4.2 DRYWELL LOADS DURING INTERMEDIATE BREAK ACCIDENT

The loading conditions caused by an intermediate break are less than those in a DBA or small break; however, they are examined because actuation of the ADS can be involved. (See Attachment A) Figure 4.3 is a bar chart for this condition.

4.3 DRYWELL DURING A SMALL BREAK ACCIDENT

A small steam break can lead to high atmospheric temperature conditions in the drywell. Figure 4.2 is the bar chart for this accident.

4.3.1 Drywell Temperature

For drywell design purposes, it is assumed that the operator reaction to the small break is to initiate a normal shutdown. Under these circumstances, the blowdown of reactor steam can last for a 3 to 6-hour period. The corresponding design temperature is defined by finding the combination of primary system pressure and drywell pressure which produces the maximum superheat temperature. Steam tables show that the maximum drywell steam temperature occurs when the primary system is at approximately 450 psia and the containment pressure is at a maximum.

During an SBA the continuing blowdown of reactor steam will cause all the air initially in the drywell to be purged to the containment free space. The peak superheat temperature is 330°F. This temperature condition exists until the RHR shutdown cooling is completed in approximately three hours. At this time, after three hours, the pressure in the reactor pressure vessel is 150 psia and the corresponding superheat temperature is 310°F. This may exist for three hours. These superheat temperatures correspond to drywell atmosphere only; separate analyses are required to determine transient response of the drywell wall to the elevated steam temperatures. See Section 4.5 for additional environmental information.

4.3.2 Drywell Pressure

With the reactor and containment operating at maximum normal conditions, a small break occurs allowing blowdown of reactor steam to the drywell. The resulting drywell pressure increase leads to a high drywell pressure signal that scrams the reactor and activates the containment isolation system. Drywell pressure continues to increase at a rate dependent on the size of the assumed steam leak. This pressure increase to 3 psig depresses the water level in the weir annulus until the level reaches the top of the upper row of vents. At this time, air and steam enter the suppression pool. Steam is condensed and the air passes to the containment free space. The latter results in gradual pressurization of the containment at a rate dependent upon the air carryover rate. Eventually, entrainment of the drywell air in the steam flow through the vents results in all drywell air being carried over to the containment. The drywell is now full of steam and a positive pressure differential sufficient to keep the weir annulus water level depressed to the top vents is maintained. Continued reactor blowdown steam is condensed in the suppression pool.

4.3.3 Chugging

During a small break accident there will be chugging in the top vents. Applicable chugging loads on the drywell and vents are discussed in Sections 4.1.8 and 4.1.9. The Mark III drywell design does not require the combination of the SBA thermal loading condition with the 21.0 psi negative pressure load.

4.4 SAFETY RELIEF VALVE ACTUATION

Relief valve operation can be initiated as a result of either a single failure, ADS operation, or by a rise in reactor pressure to the valve set points. In addition, the drywell can be exposed to S/R valve actuation loads any time the operator elects to open a valve or valves, as during an isolated cooldown. The loads generated by S/R valve actuation are discussed in Attachment A.

4.5 DRYWELL ENVIRONMENTAL ENVELOPE

Figure 4.10 shows the design envelope of drywell atmospheric pressures and temperatures for the spectrum of postulated loss-of-coolant accidents. Figure 4.10 defines only the drywell atmospheric condition; separate analyses are required to evaluate the transient structural response to these conditions. The high pressure and the high temperature conditions shown for the first 45 seconds cannot occur simultaneously and need not be considered in combination.

4.6 TOP VENT TEMPERATURE (CYCLING) PROFILE DURING CHUGGING

Full scale test results (Reference 16) indicate that during chugging the water level in the weir annulus fluctuates over a 4 foot band centered at about the top vent centerline. The weir wall and the inside drywell wall then are subjected to steam temperature (230°F) above the top vent and cold pool temperature (100°F) near the lower vents, with a transition region in-between, where the temperature fluctuates due to the chugging process.

For weir annulus thermal stratification, the most severe design condition results from imposing the maximum drywell temperature (330°F) concurrent with the initial suppression pool temperature (see Section 4.3.1).

For evaluation of local effects, the cyclic temperature profile during chugging is shown in Figure 4.11. The cycling temperature ranges from 100°F to 230°F; and the period is equal to the chugging period, which randomly varies from 1 to 5 seconds. The areas of application are:

- 4 foot horizontal band on the weir wall and inside drywell,
- the upper inside vent surface,
- and an area of the outside drywell wall just above each top vent, as shown on Figure 4.11.

The duration of the thermal cycling is identical to the duration of chugging (see bar charts, Figure 4.3). As the event proceeds, the ΔT reduces in amplitude due to bulk pool temperature increase. As part of the design calculation, this bulk pool temperature should be considered and is shown in Figure 6.17. The long and short term thermal gradients are discussed in Attachment N.

4.7 DRYWELL MULTICELL EFFECTS

Chugging is conservatively considered to be synchronous for the Mark III load definitions. The typical pressure time history is shown on Figure 4.8a. Superimposed chugging spikes from adjacent vents, as confirmed by multi-cell tests (ref. 18), are minor and considered to be insignificant. On Figure 4.8; these spikes are superimposed to indicate the typical magnitude.

Table 4-1
CHUGGING LOADS

	PRE-CHUG UNDERPRESSURES AND DURATION		PULSE (SPIKE) AND DURATION 'd'		POST-CHUG OSCILLATION AND FREQUENCY	
	PEAK (A)	MEAN (A)	PLA _{pk}	PLA _d	PEAK (B)	MEAN (B)
DRYWELL WALL	-5.8 PSID 125 MS	-2.65 PSID 125 MS	100 PSID 8 MS	24 PSID 8 MS	6.50 PSID 10-12 HZ	2.2 PSID 10-12 HZ
CONTAINMENT	-1.3 PSID 125 MS	-1.0 PSID 125 MS	3 PSID 2 MS	0.7 PSID 2 MS	1.7 PSID 10-12 HZ	1.00 PSID 10-12 HZ
BASEMAT	-1.8 to -1.3 PSID 125 MS	-1.34 to -1.0 PSID 125 MS	10 to 3 PSID 4 to 2 MS	2.4 to 0.7 PSID 4 to 2 MS	2.1 to 1.7 PSID 10-12 HZ	1.29 to 1.0 PSID 10-12 HZ

STRUCTURE: DRYWELL
 ACCIDENT: LARGE STEAM LINE BREAK (DBA)

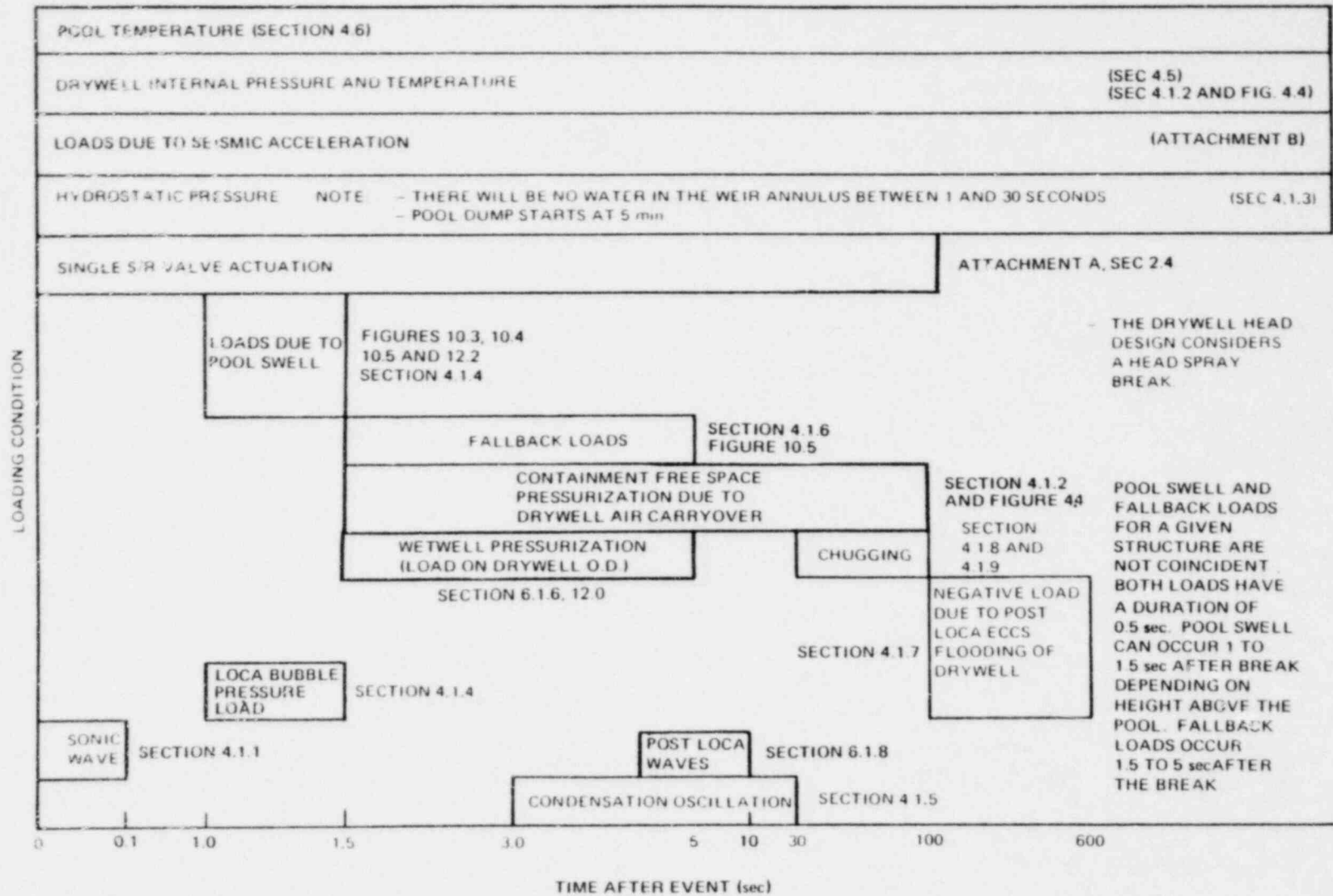
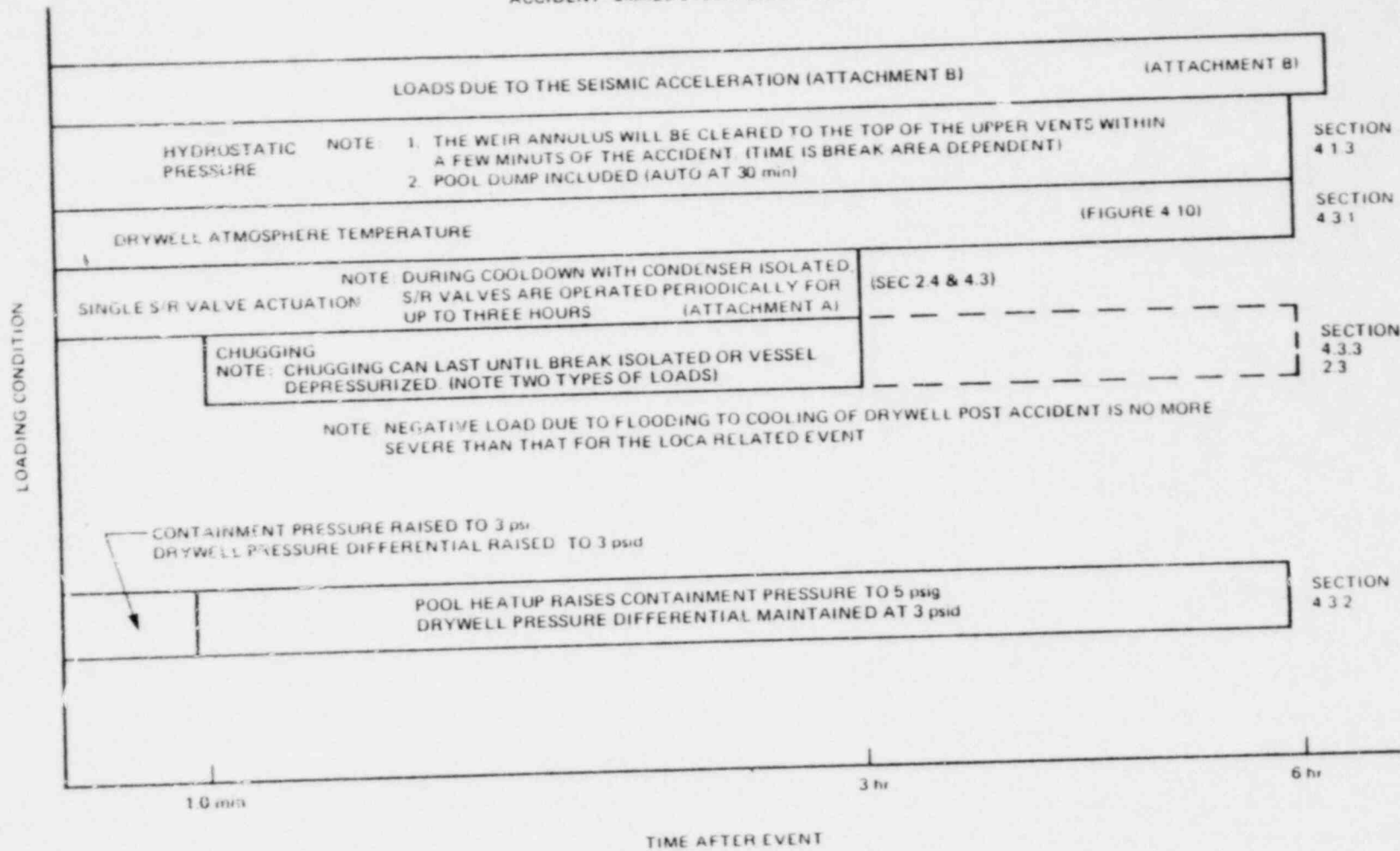


Figure 4.1. Drywell-Loading Chart for DBA

018810

22A4365
 Rev. 4

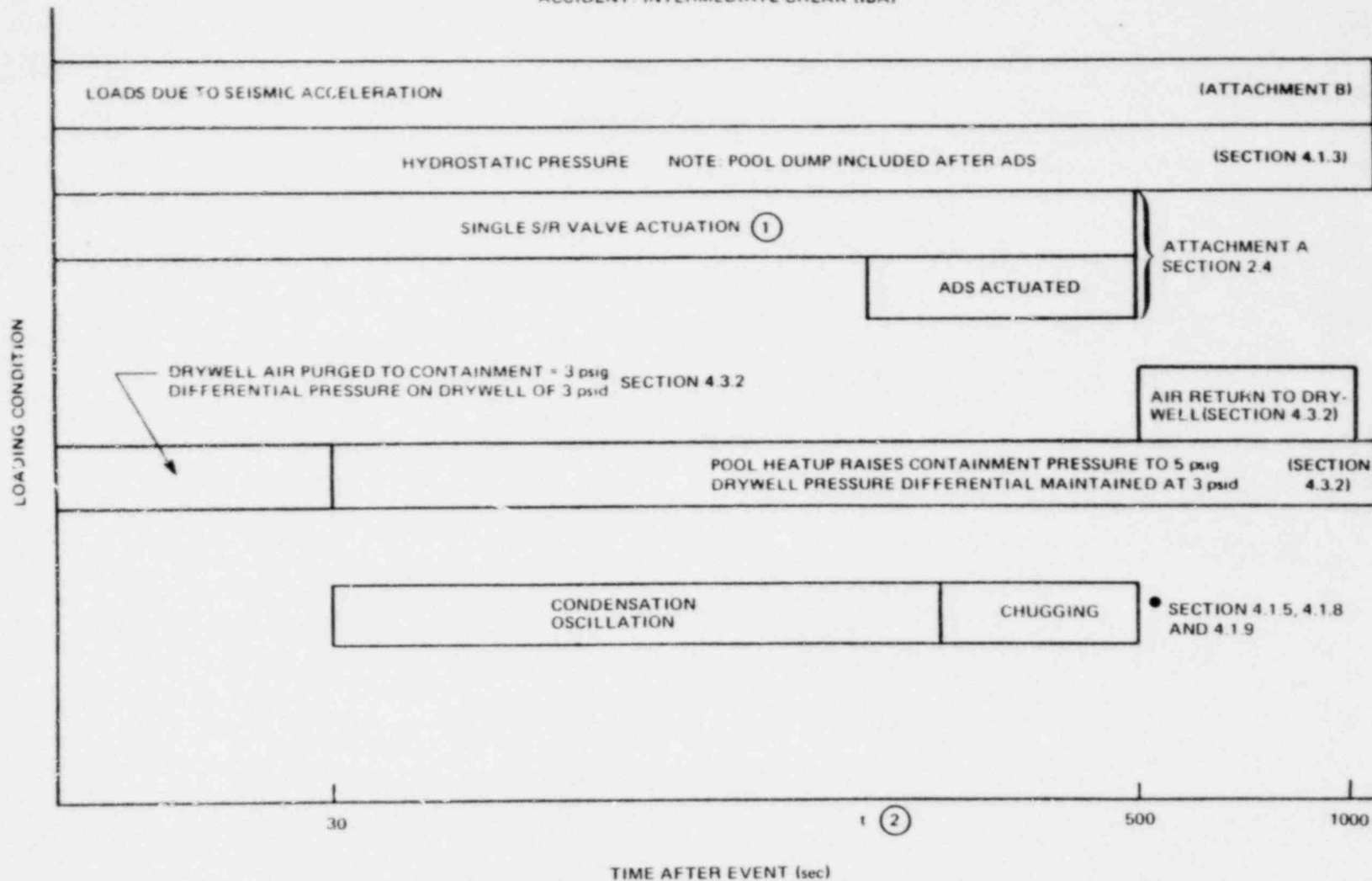
STRUCTURE DRYWELL
ACCIDENT SMALL STEAM BREAK (SBA)



22A4365
Rev. 4

Figure 4.2. Drywell-Loading Chart for SBA

STRUCTURE: DRYWELL
 ACCIDENT: INTERMEDIATE BREAK (IBA)



- ① SINGLE SRV LOADS DO NOT COMBINE WITH OTHER SRV LOADS
- ② TIME SCALE DEPENDENT UPON BREAK SIZE, MINIMUM VALUE OF $t \approx 2$ min

Figure 4.3. Drywell-Loading Chart for IBA

011880

22A4365
 Rev. 4

4-11

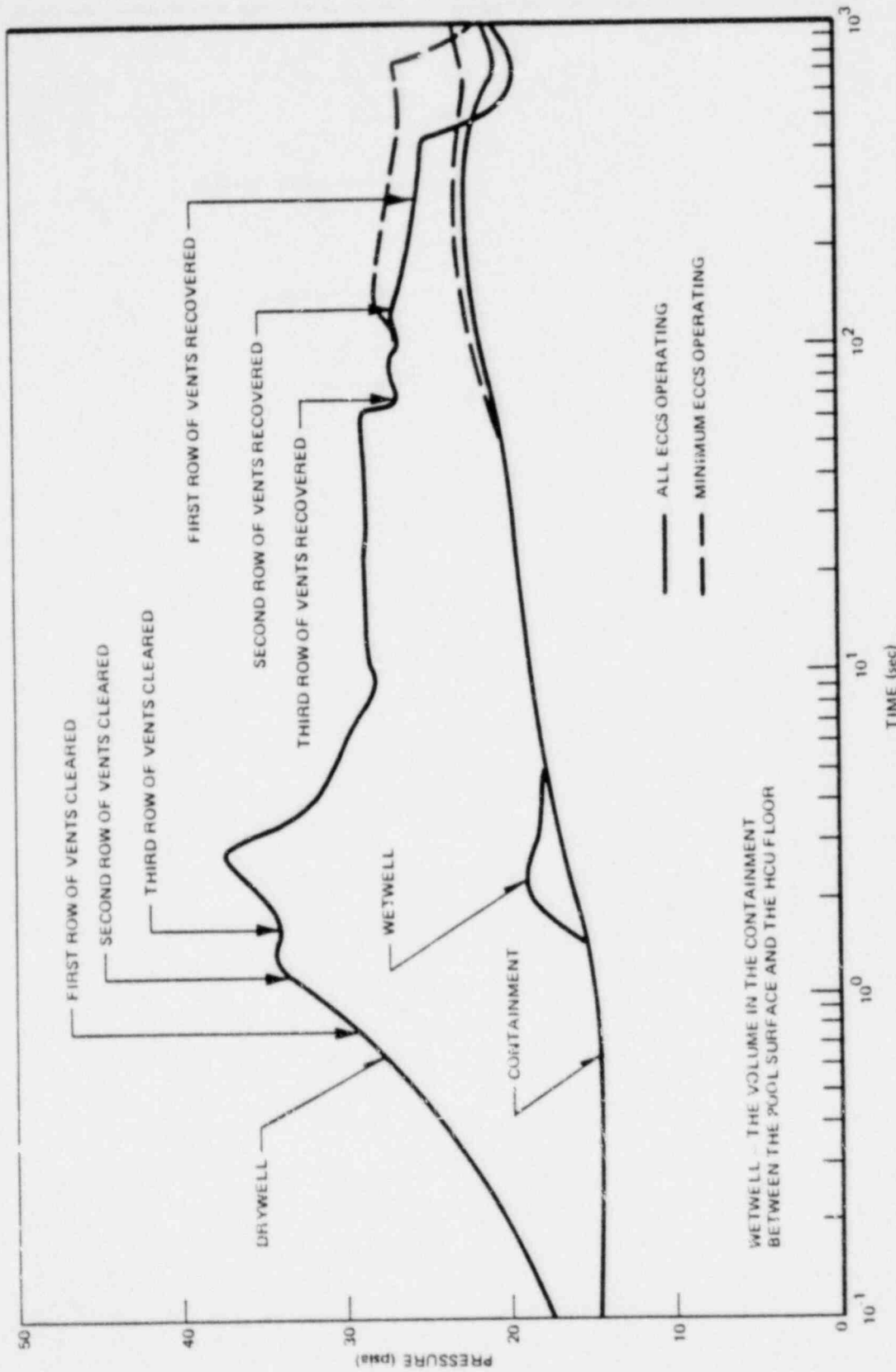


Figure 4.4. Short Term Drywell and Containment Pressure Response to a Large Steam Line Break (DBA)

This figure is PROPRIETARY and is provided under separate cover.

Figure 4.5. PSTF Test Results - Vent Static Pressure Differential

This figure is PROPRIETARY and is provided under separate cover.

Figure 4.5a. PSTF Test Results - Vent Static Pressure Differential

This figure is PROPRIETARY and is provided under separate cover.

Figure 4.6. Typical Drywell Wall Pressure Traces During Condensation,
Run 23, Test 5807

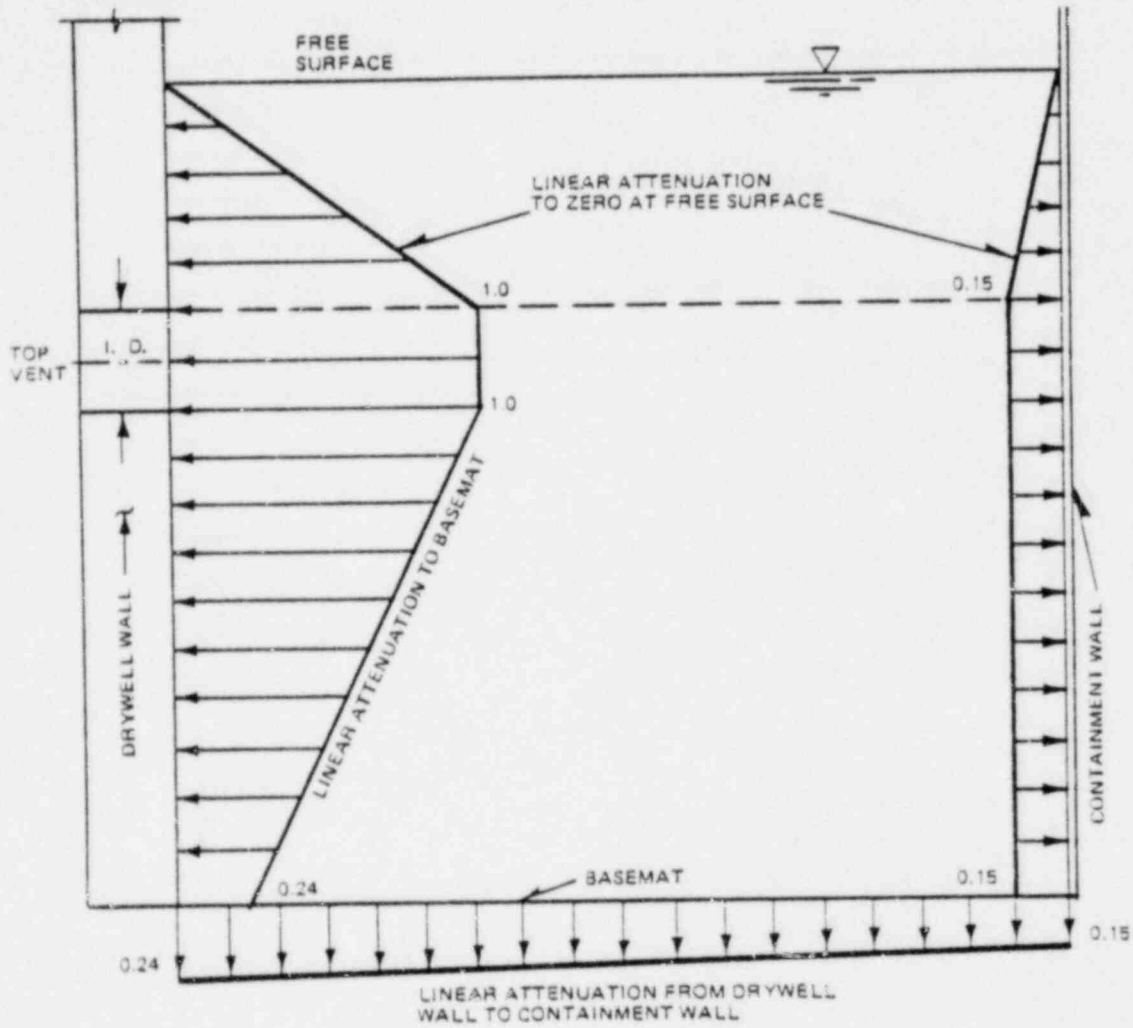
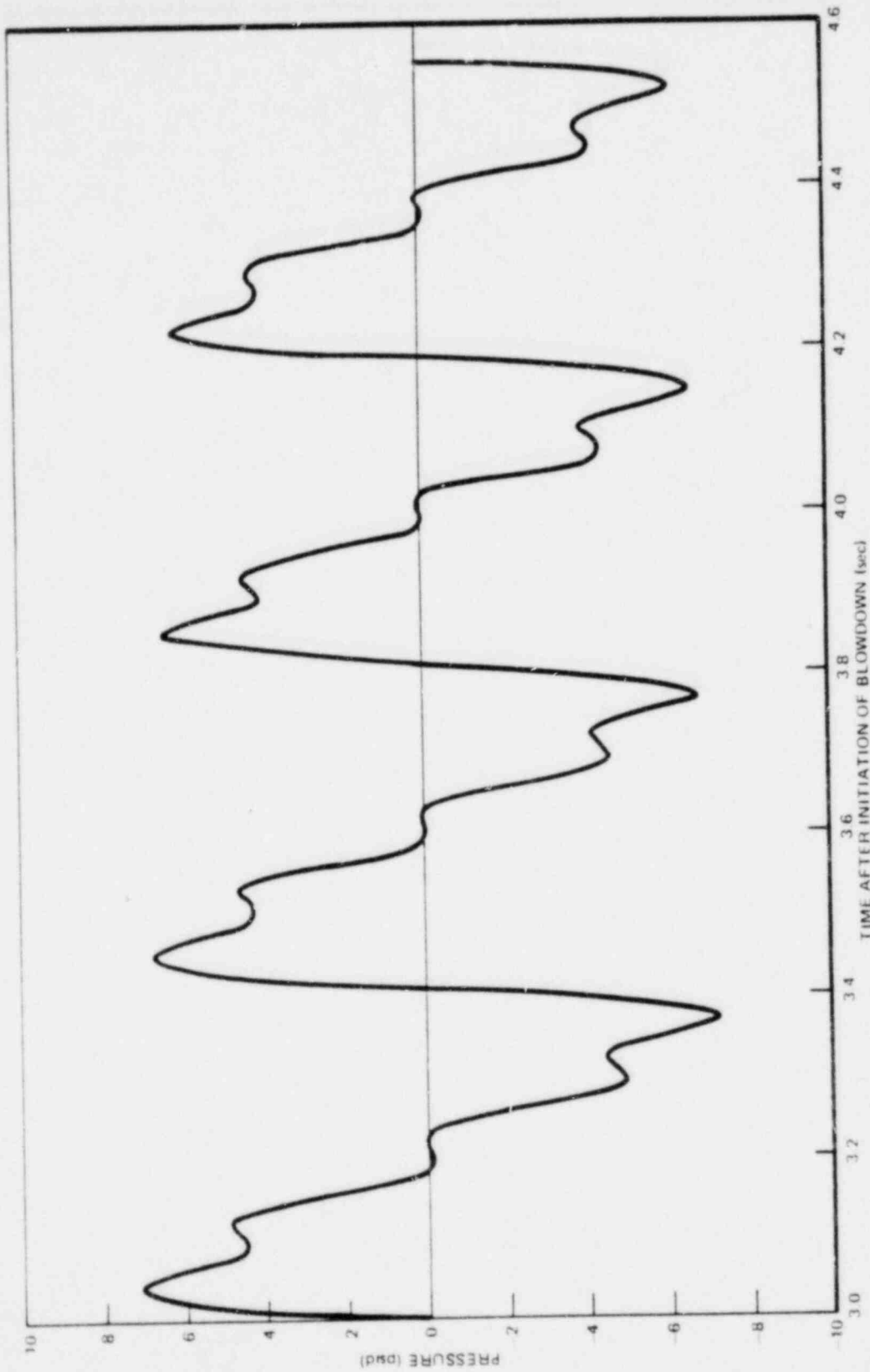


Figure 4.6a. Condensation Oscillation Load Spatial Distribution on the Drywell Wall, Containment Wall and Basemat



NOTE: THE CO FORCING FUNCTION PRESENTED IN ATTACHMENT 0 AS A FUNCTION OF TIME SHOULD BE USED FOR DESIGN

Figure 4.6b. Condensation Oscillation Forcing Function on the Drywell Wall 0.D.
Adjacent the Top Vent

This figure is PROPRIETARY and is provided under separate cover.

Figure 4.7. Typical Top Vent Pressure Trace During Chugging, Run 19

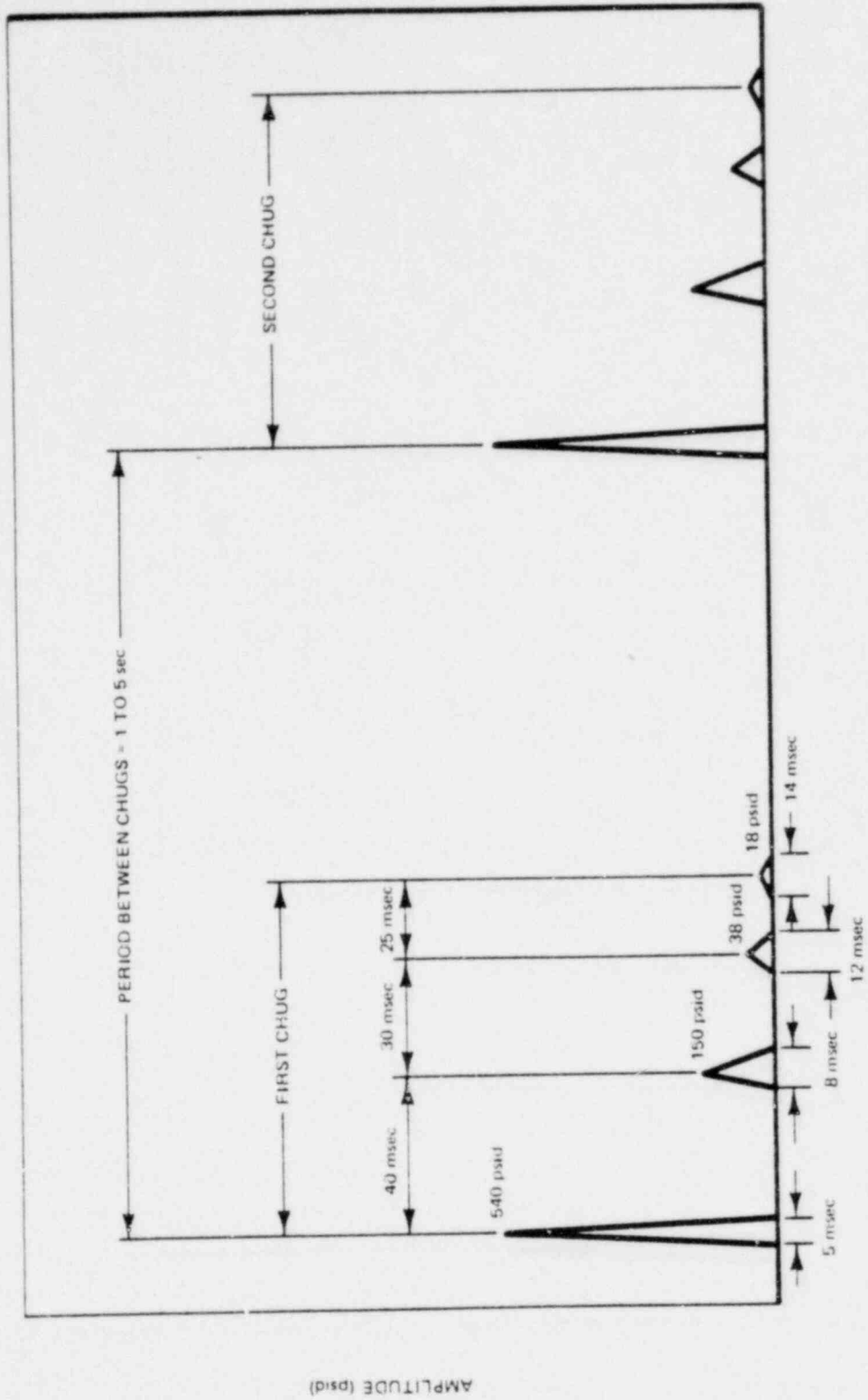


Figure 4.7a. Peak Pressure Pulse Train in Top Vent During Chugging

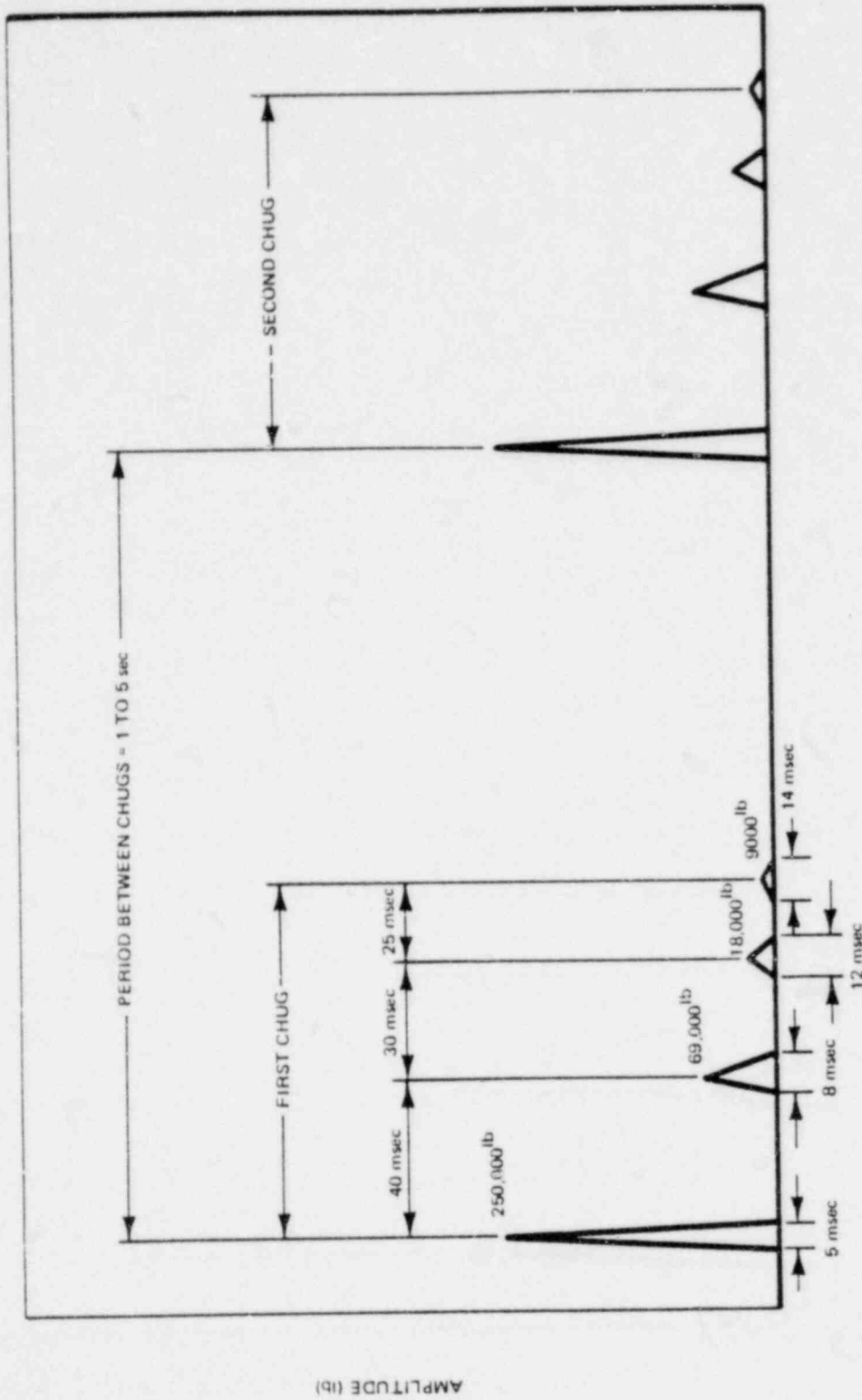


Figure 4.7b. Peak Force Pulse Train in Top Vent During Chugging

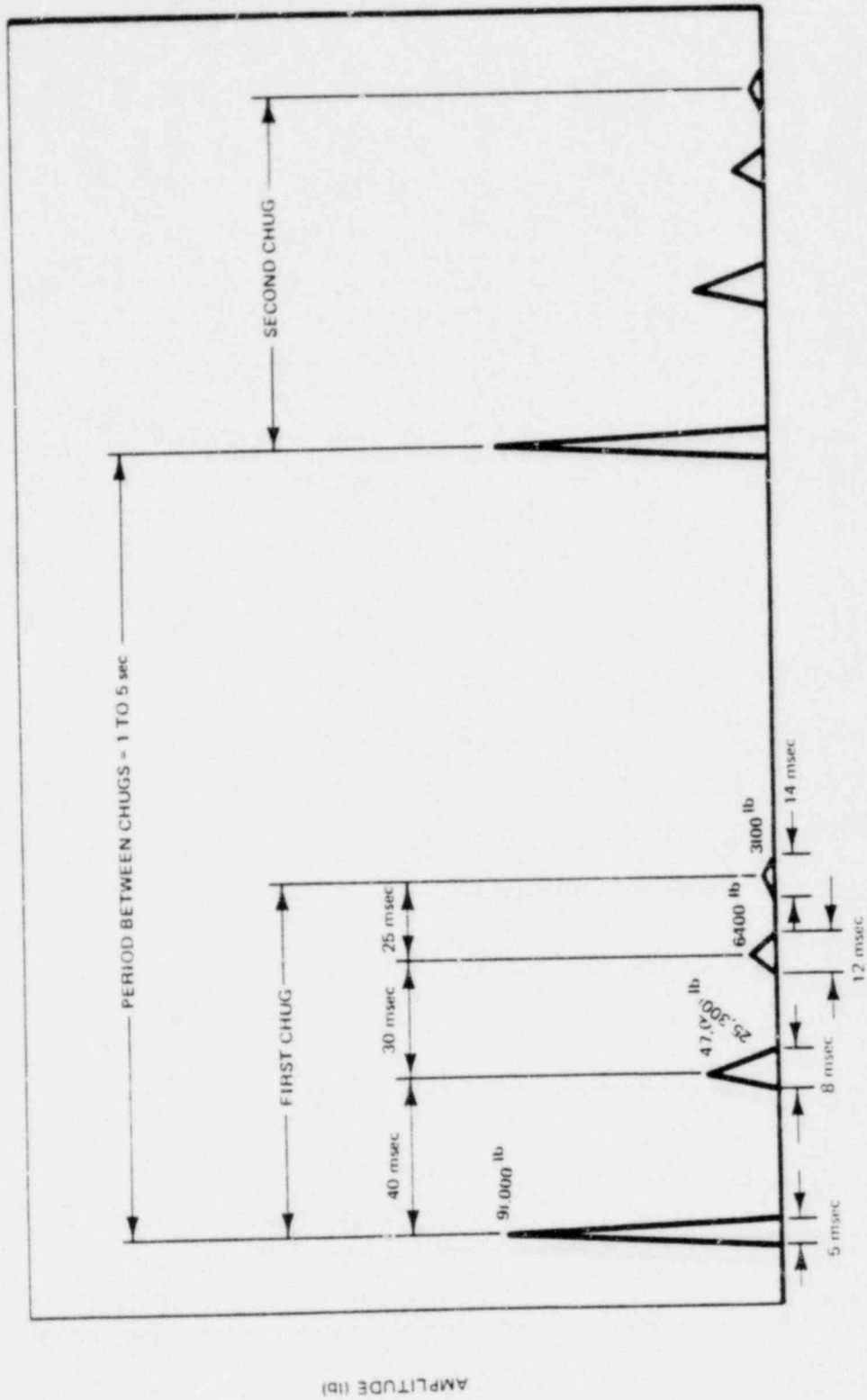


Figure 4.7c. Average Force Pulse Train in Top Vent During Chugging

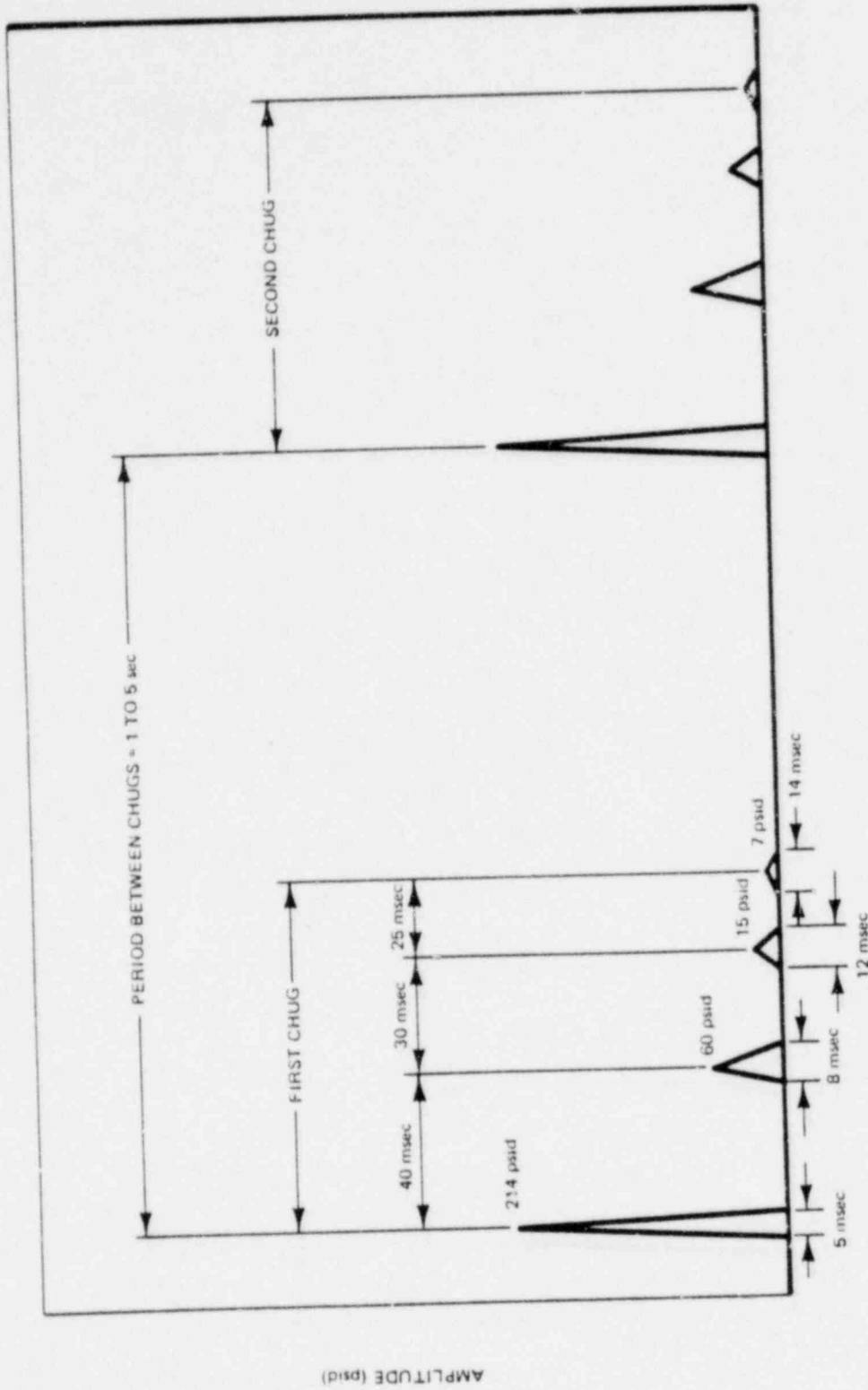


Figure 4.7d. Average Pressure Pulse Train in Top Vent During Chugging

This figure is PROPRIETARY and is provided under separate cover.

Figure 4.8. Containment Wall Pressure Trace During Chugging, Run 11
(Ref. Test 5707)

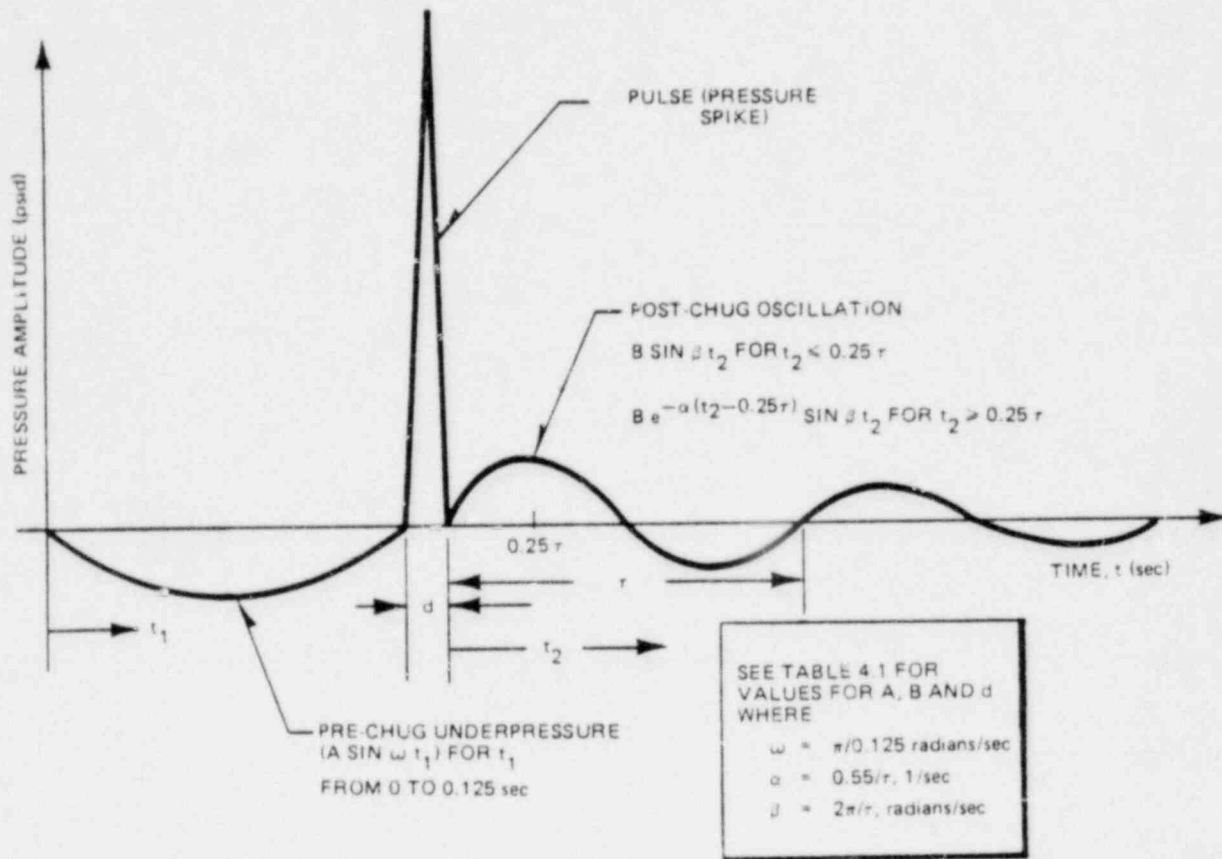


Figure 4.8a. Typical Pressure Time-History on the Pool Boundary During Chugging

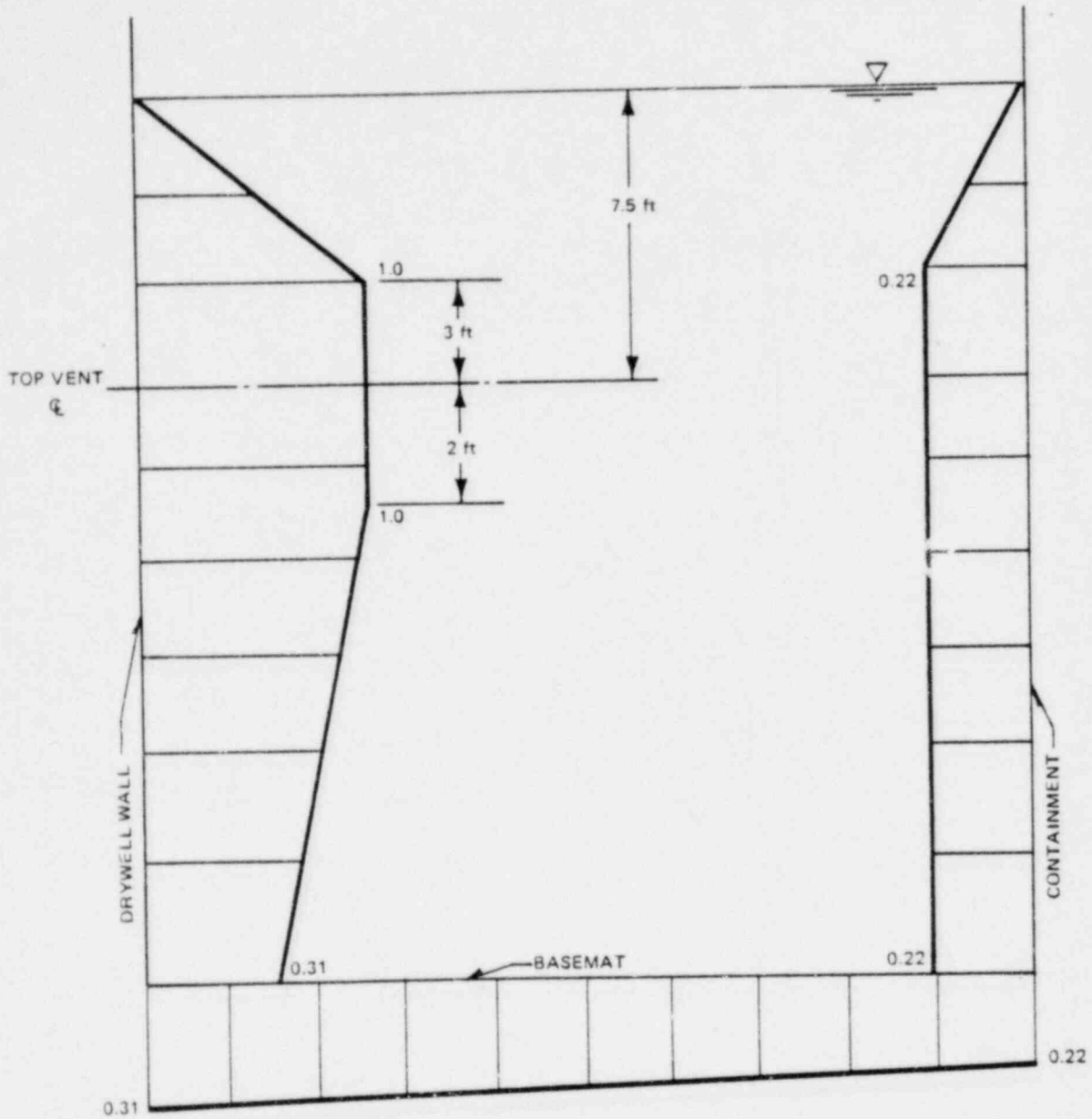


Figure 4.8b. Suppression Pool Chugging Normalized Peak Underpressure Attenuation

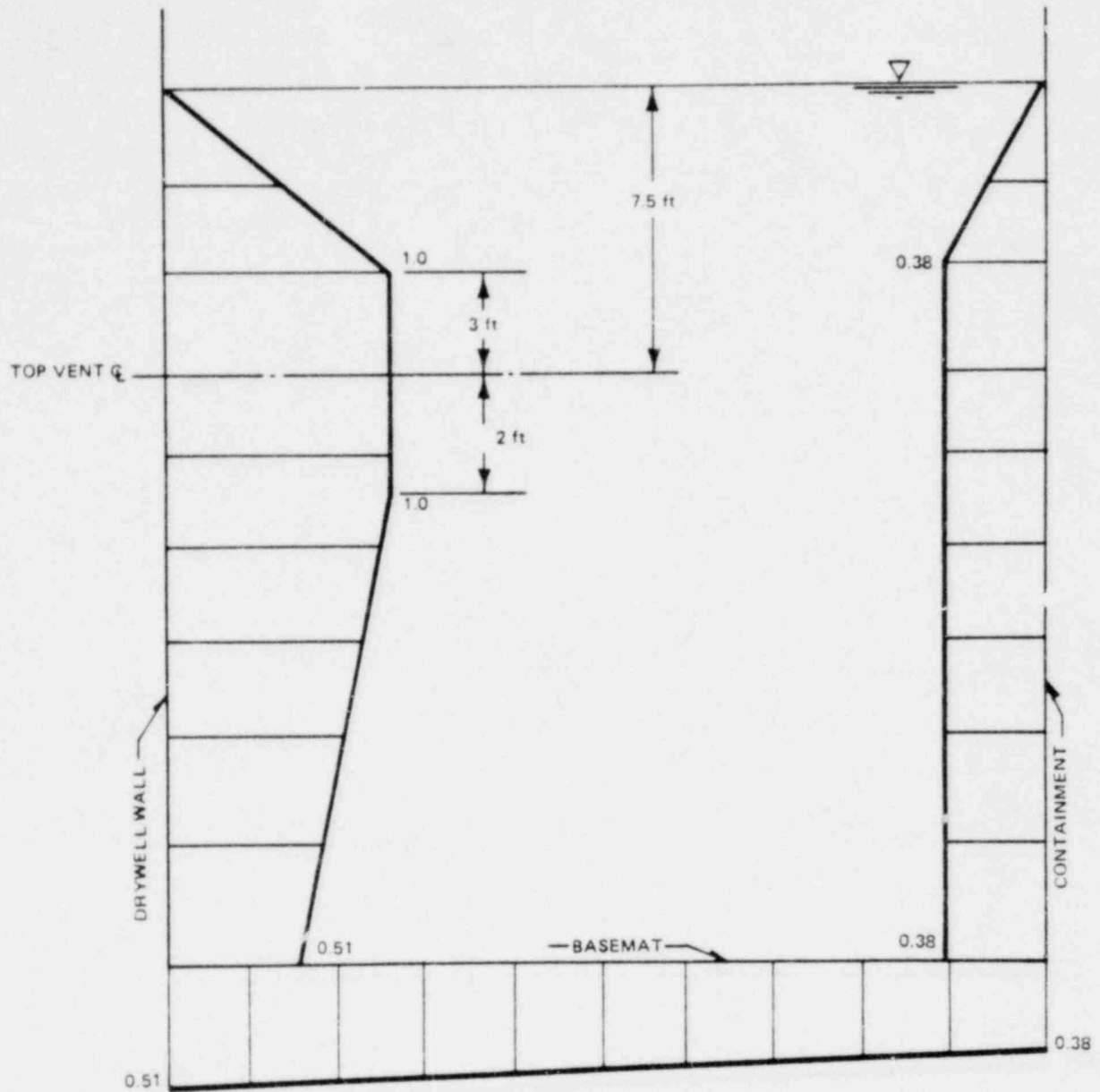


Figure 4.8c. Suppression Pool Chugging Normalized Mean Underpressure Attenuation

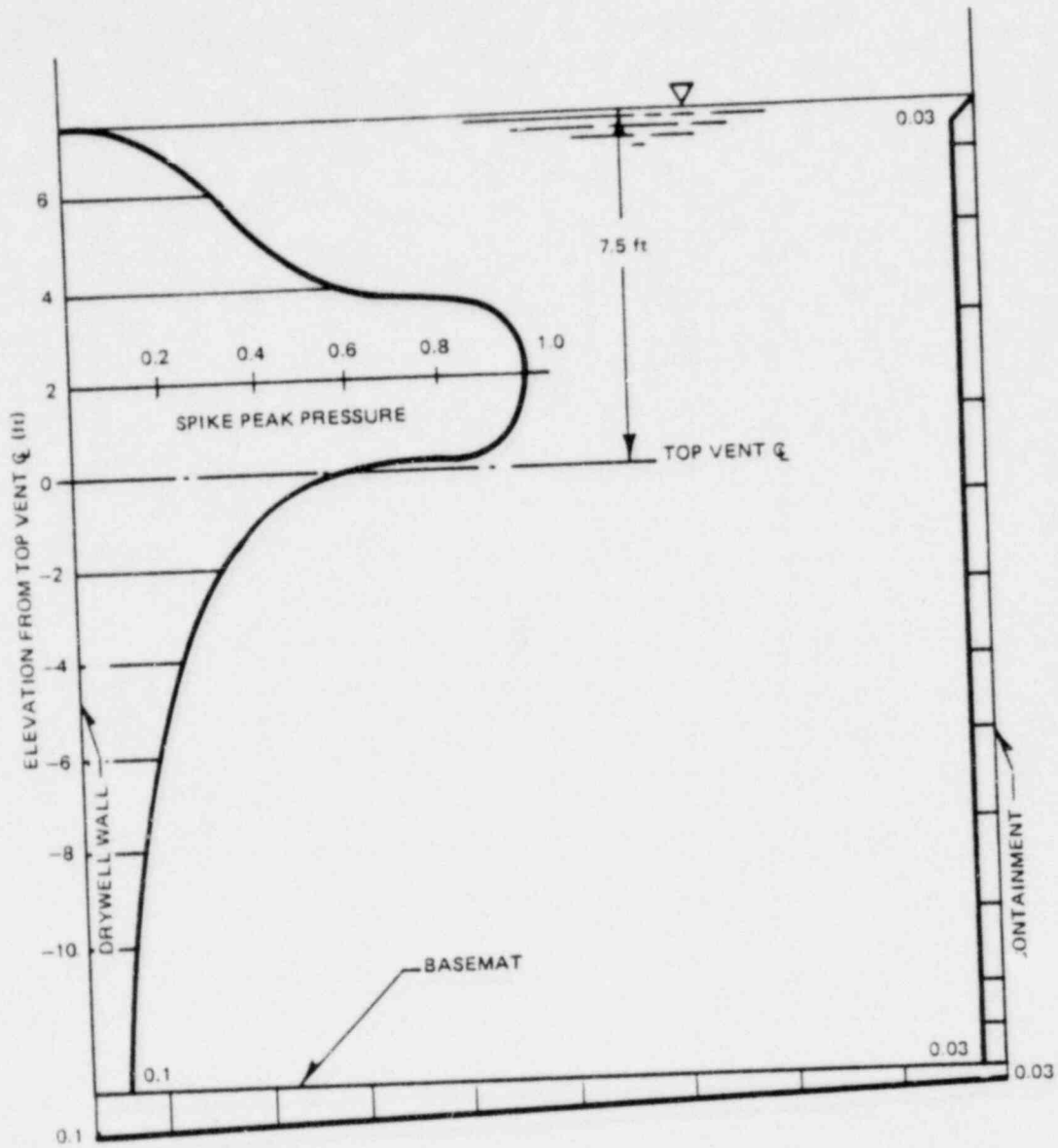


Figure 4.8d. Suppression Pool Chugging Normalized Spike Attenuation

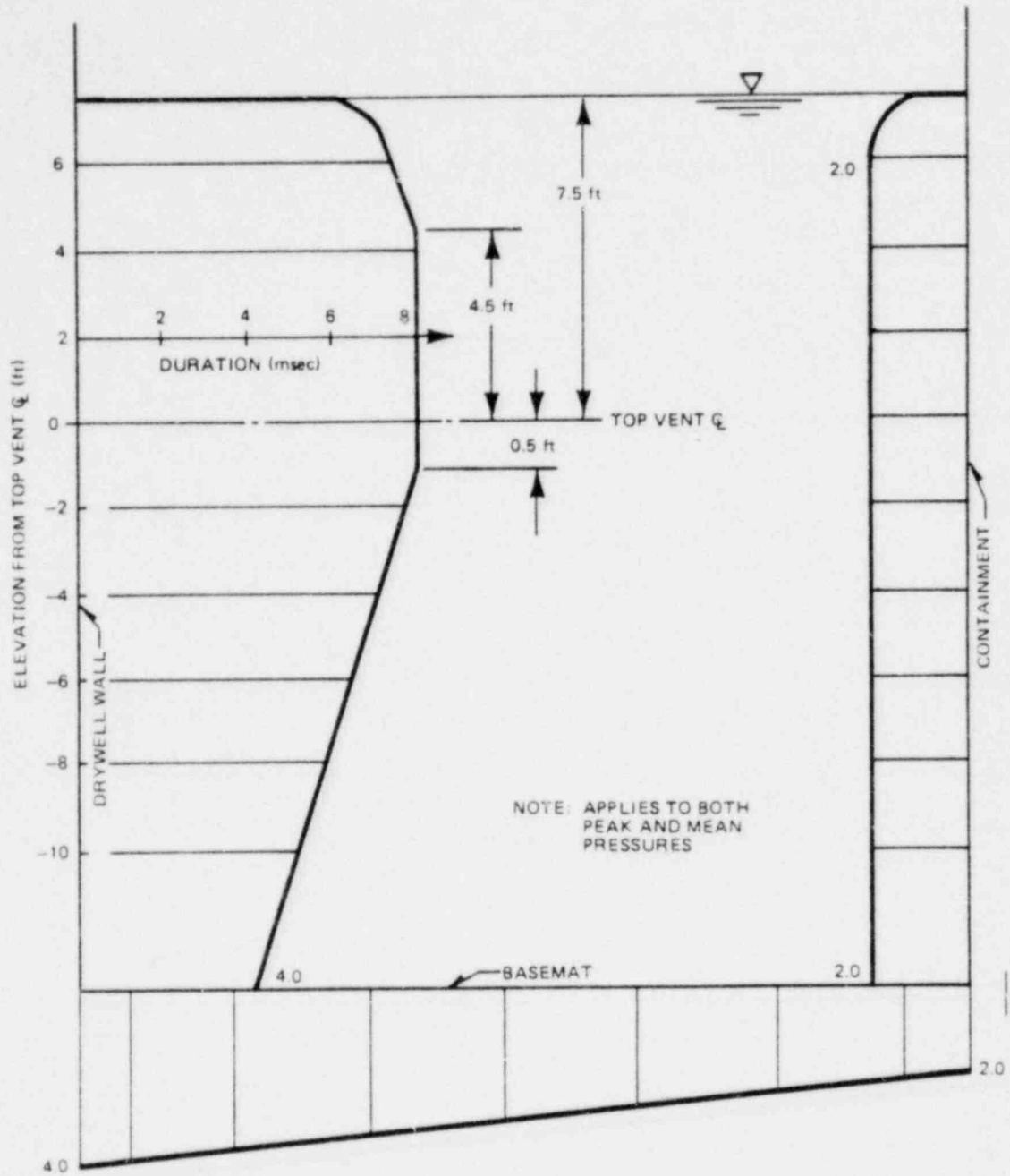


Figure 4.8e. Suppression Pool Chugging Spike Duration "d" as a Function of Location in the Pool

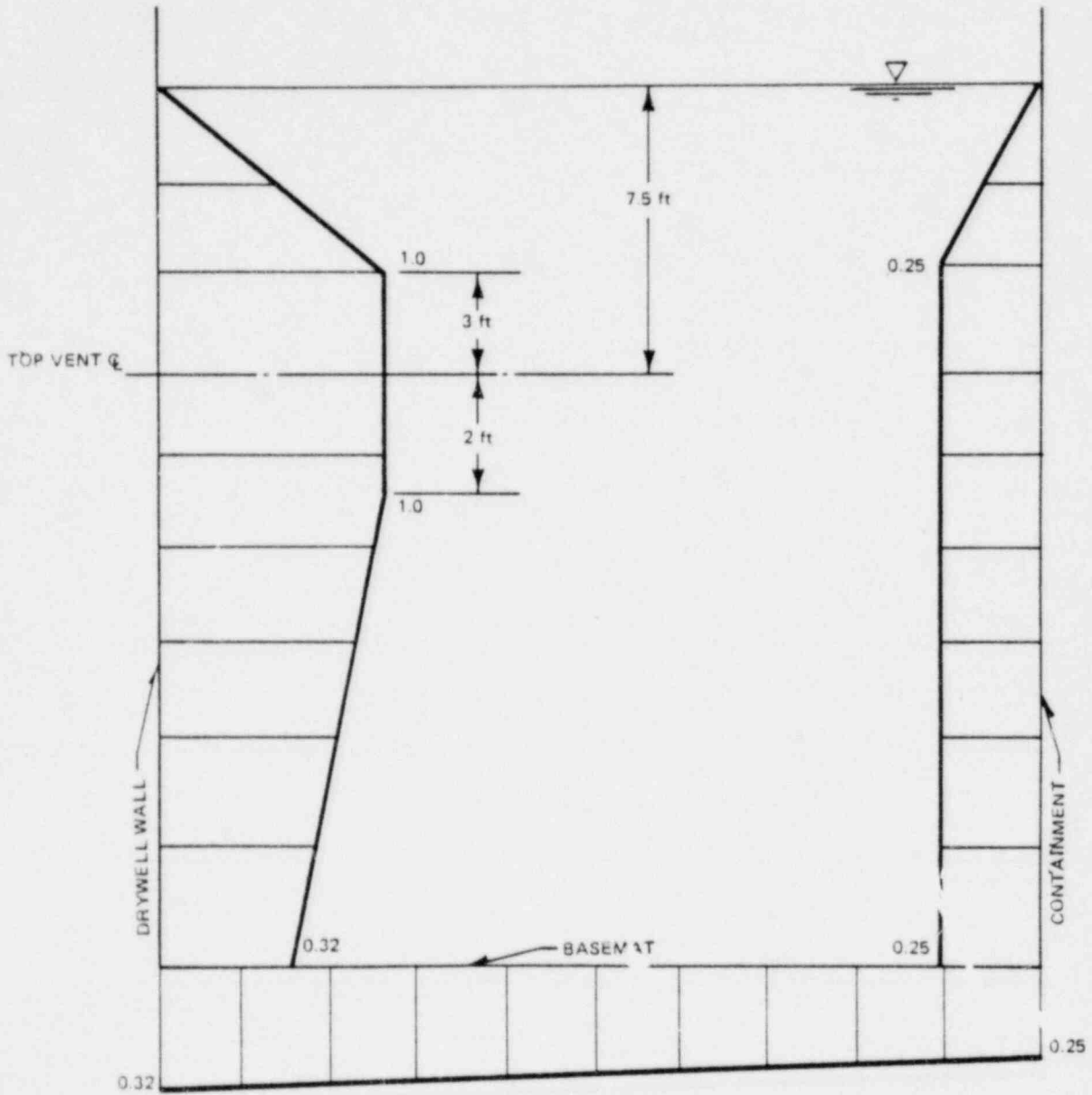


Figure 4.8f. Suppression Pool Chugging Normalized Peak Post Chug Oscillations

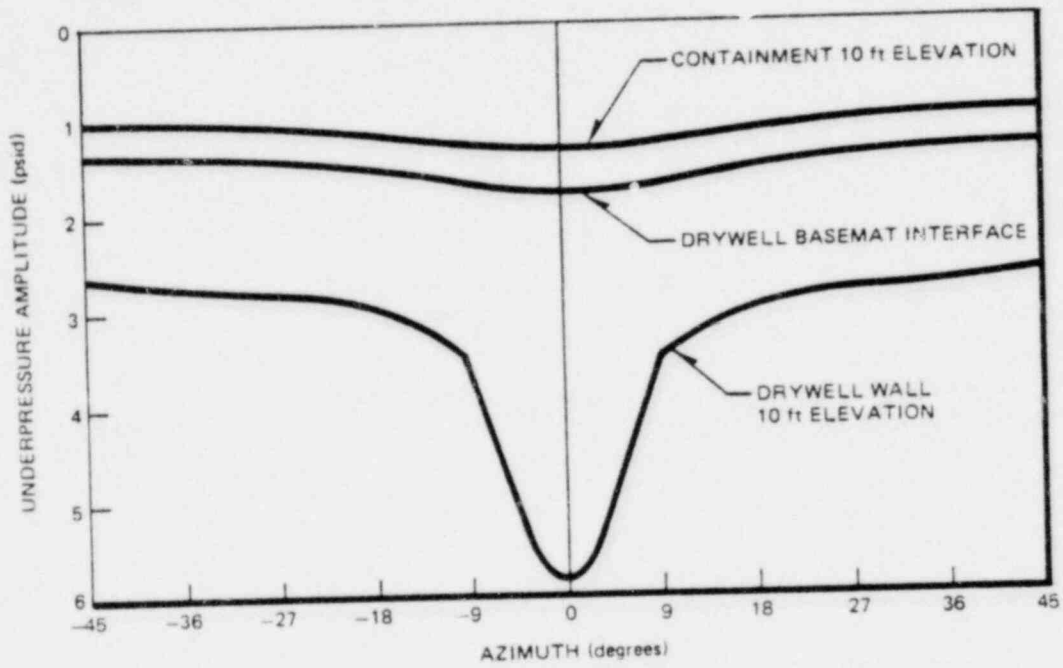


Figure 4.8g. Circumferential Underpressure Amplitude Attenuation

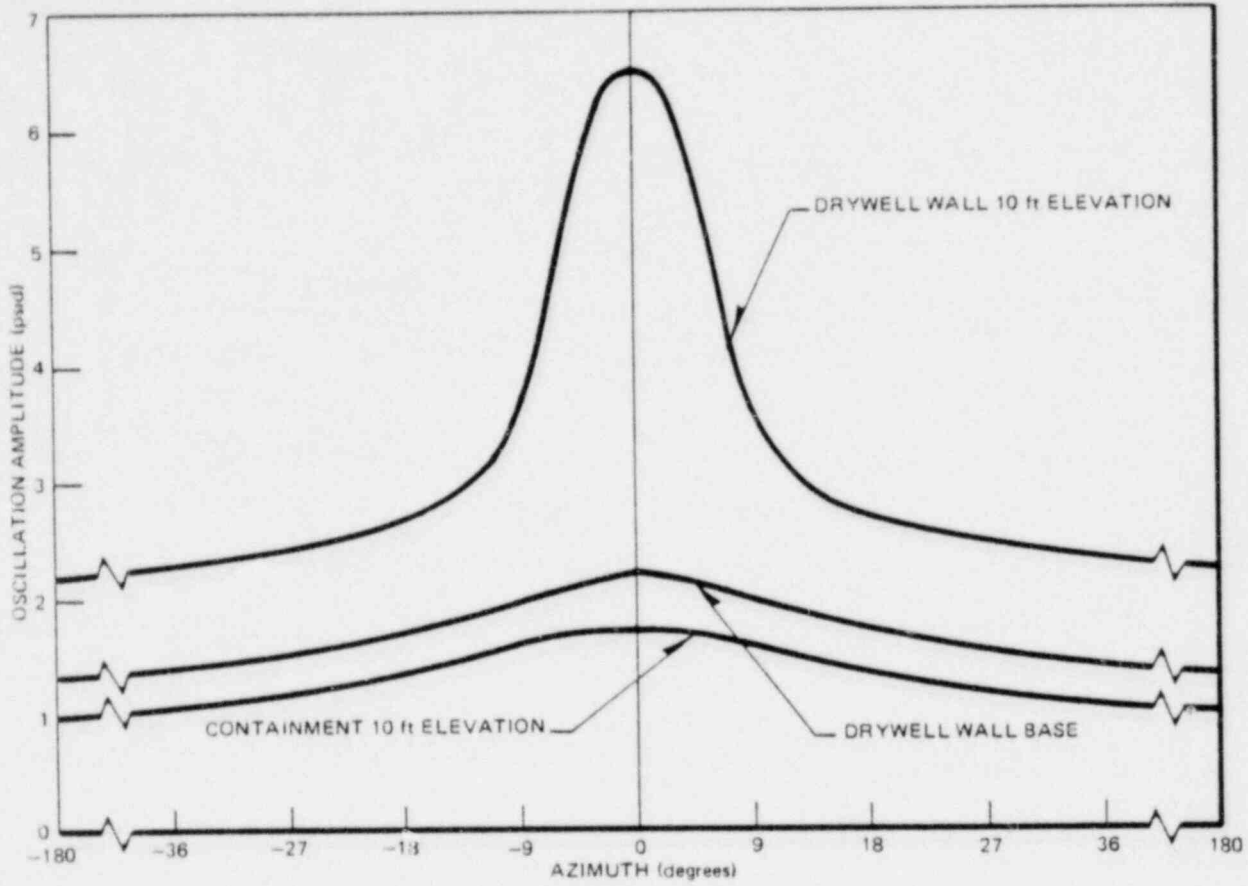


Figure 4.8h. Circumferential Post Chug Oscillation Amplitude Attenuation

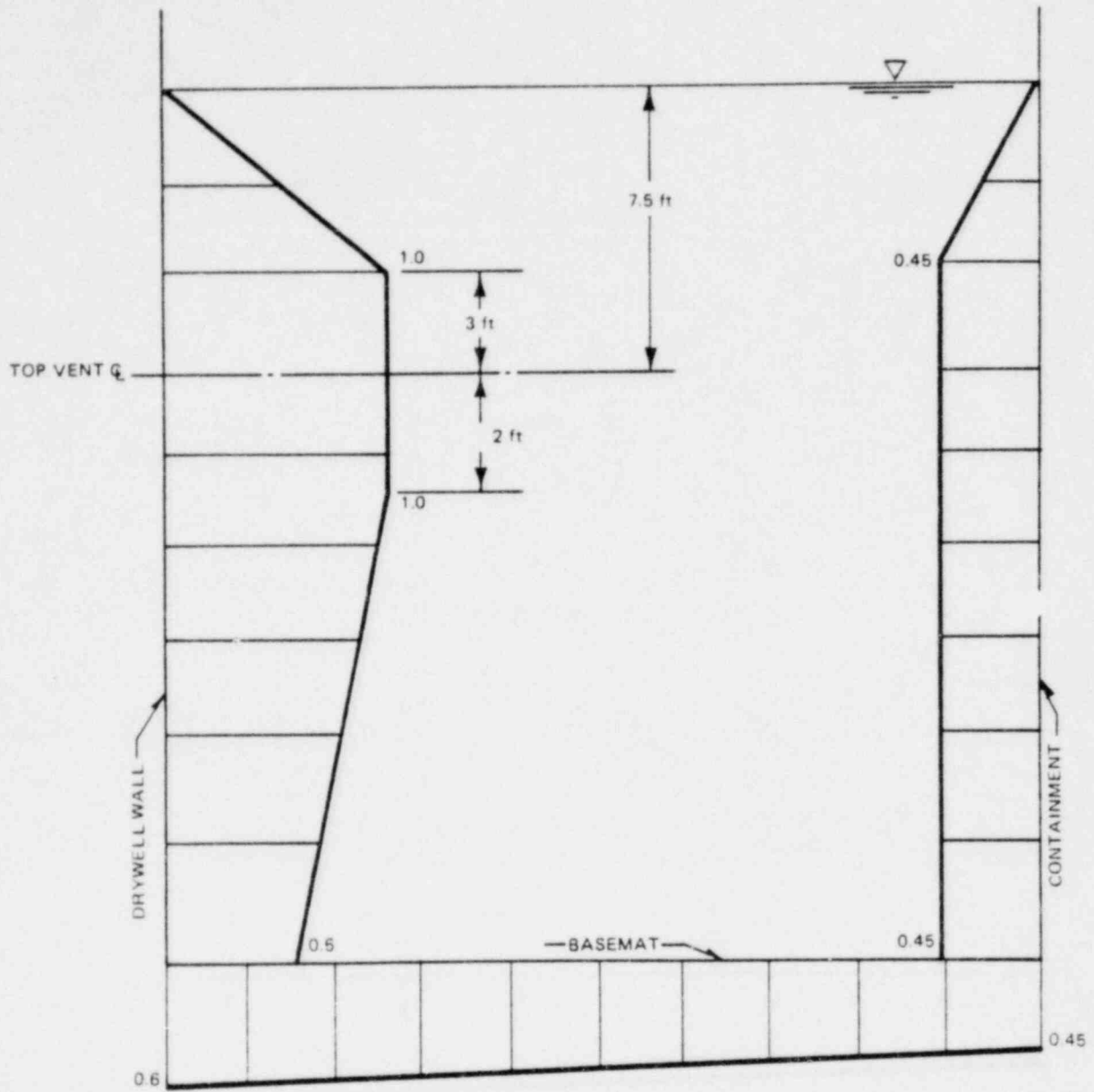
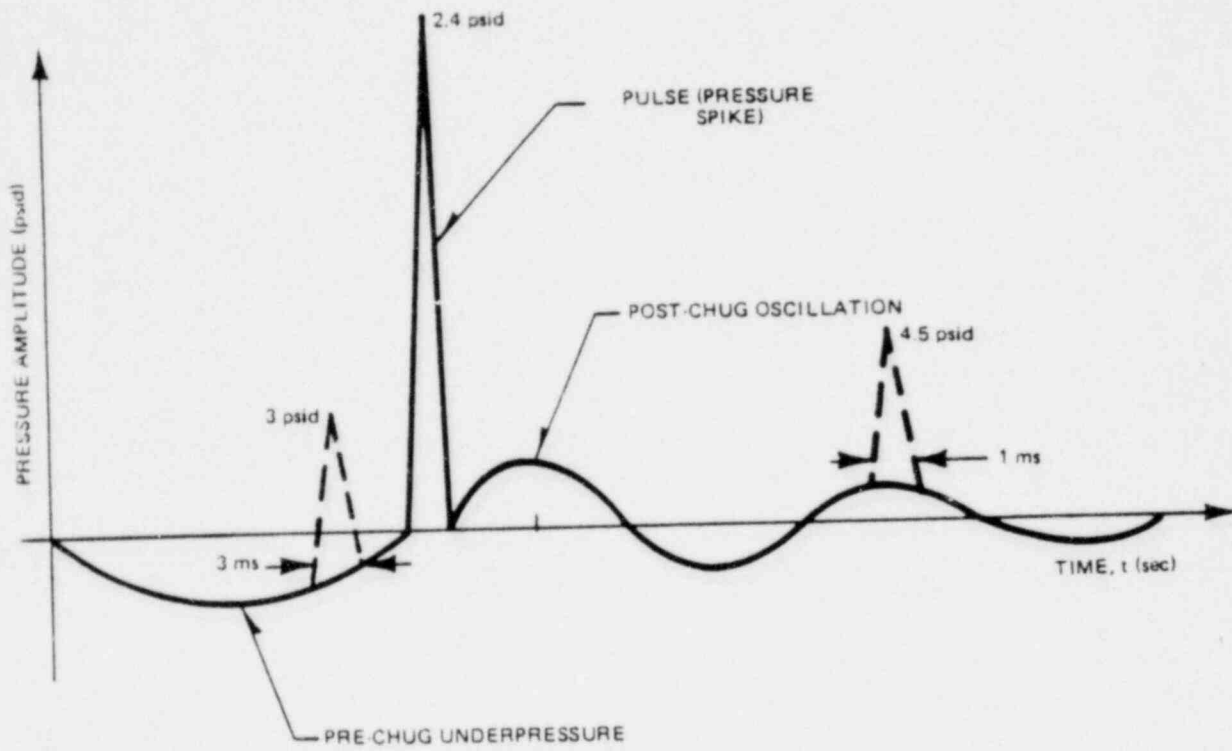


Figure 4.8i. Suppression Pool Chugging Normalized Post Chug Oscillations Attenuation



NOTE: FORCING FUNCTION FROM FIGURE 4.8a

Figure 4.8j. Chugging Pressure Time-History on the Drywell Wall Adjacent to Vent

This figure is PROPRIETARY and is provided under separate cover.

Figure 4.9. Drywell - Containment Pressure Differential During Chugging

Deleted

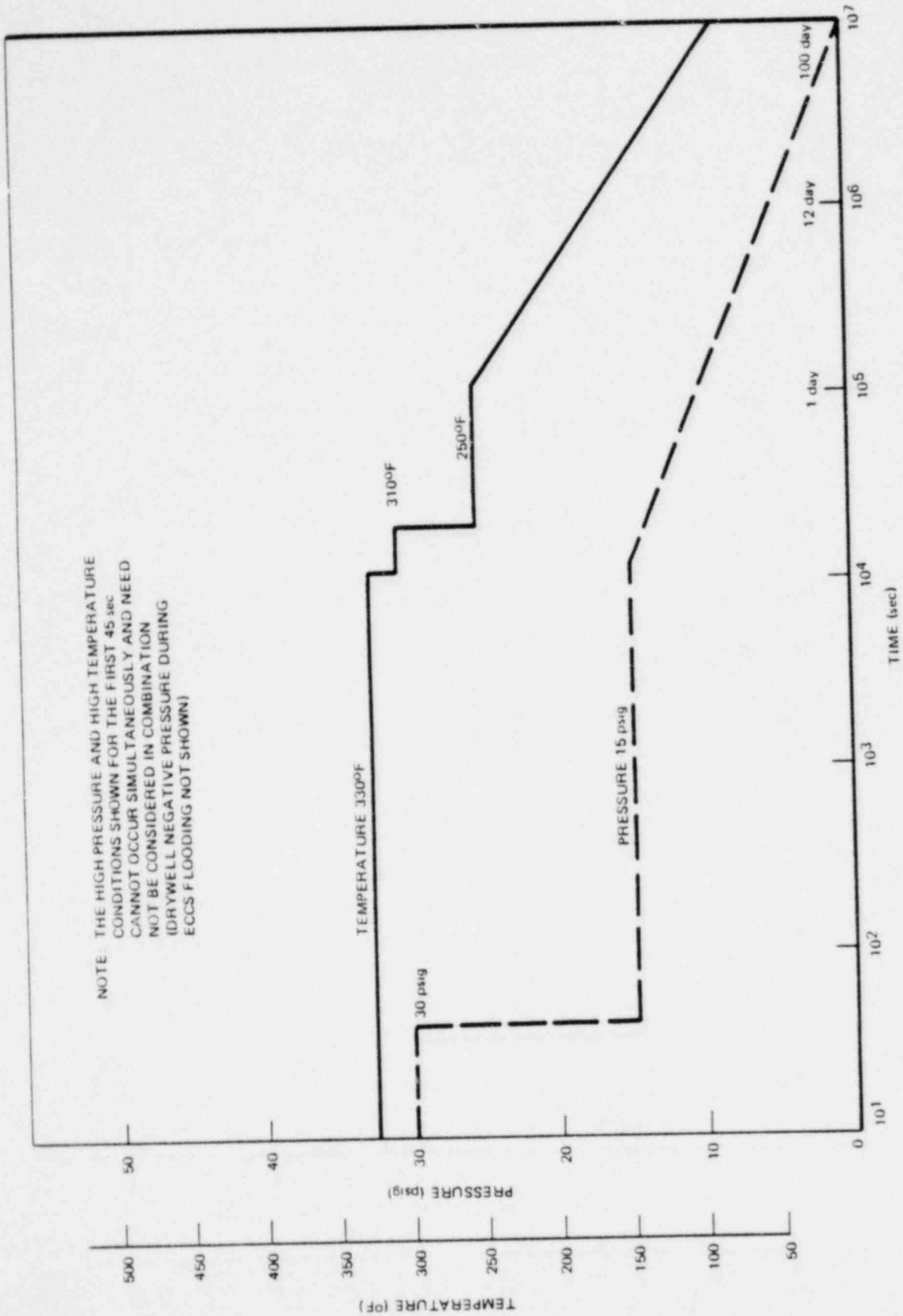


Figure 4.10. Maximum Design Drywell Atmosphere Bulk Temperature and Pressure Envelope

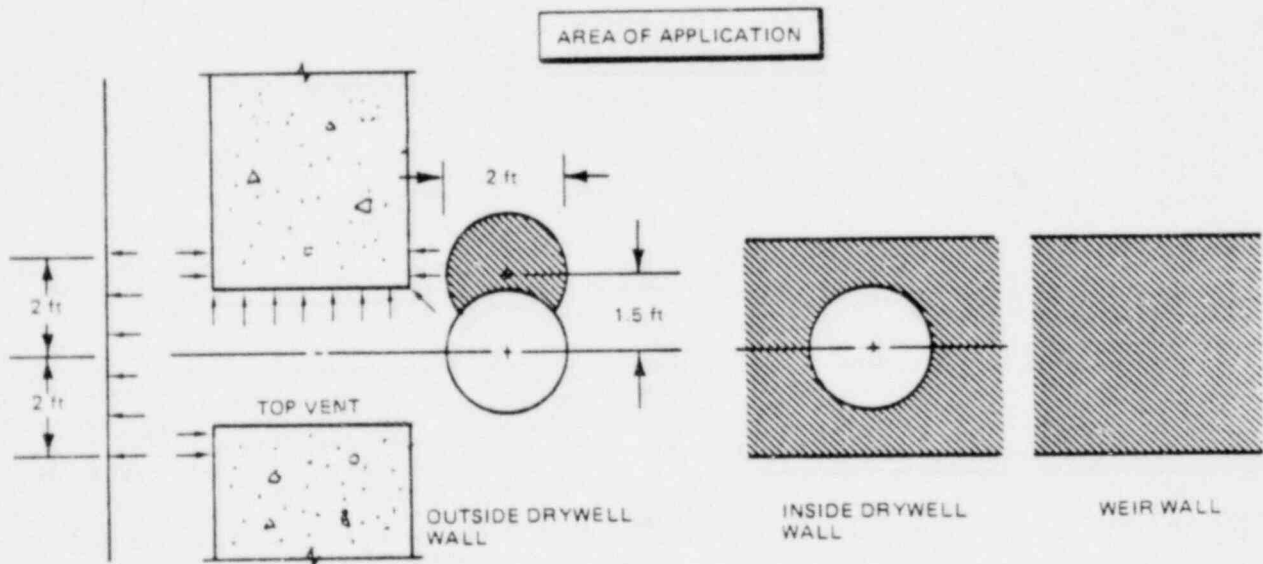
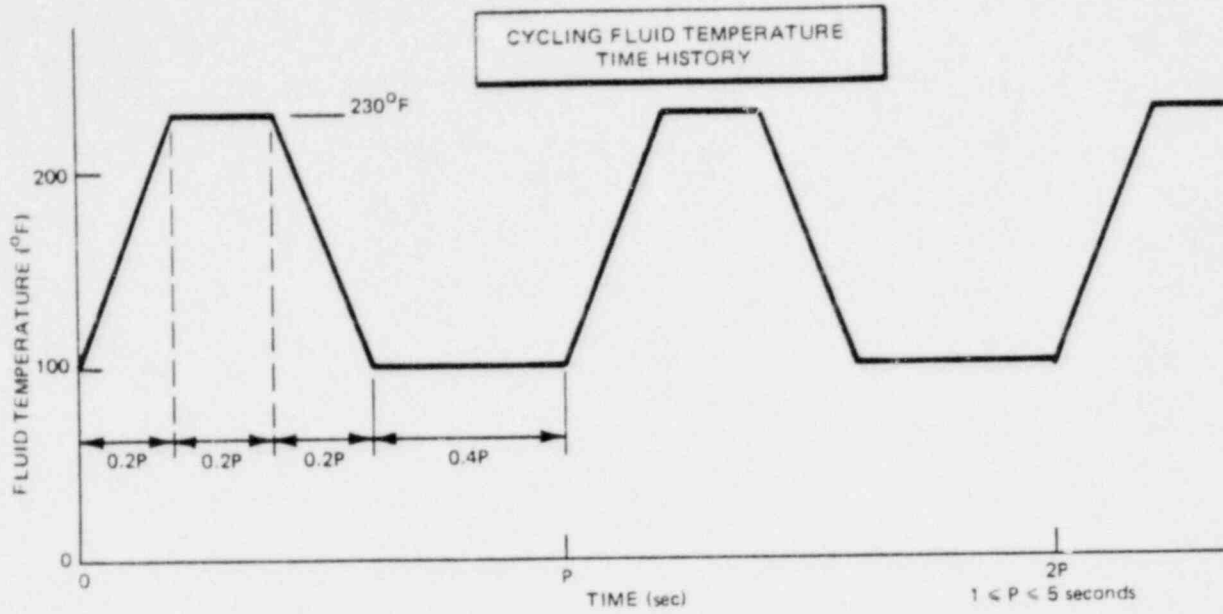


Figure 4.11. Drywell Top Vent Cyclic Temperature Profile and Area of Application During Chugging

5. WEIR WALL

The weir wall experiences loading conditions during both the design basis accident and during a small steam break accident. Figures 5.1 and 5.2 are the bar charts for these two cases. The intermediate break loads are less severe than those associated with the large and small break. Figure 5.3 is the bar chart for this case.

5.1 WEIR WALL LOADS DURING A DESIGN BASIS ACCIDENT

5.1.1 Sonic Wave

For the reasons discussed in 4.1.1, this phenomenon is not included in the weir wall design conditions. A sonic compressive wave does not produce a design load condition in the drywell.

5.1.2 Outward Load During Vent Clearing

The pressure drop at any point on the weir wall due to the acceleration of water during vent clearing is less than the local hydrostatic pressure. Therefore, there is no net outward load on the weir wall due to vent clearing. This conclusion is based on the predictions of the analytical model presented in Reference 1.

5.1.3 Outward Load Due to Vent Flow

Once flow of air, steam and water droplets has been established in the vent system, there will be a static pressure reduction in the weir annulus that leads to approximately a 10 psi uniform outward pressure on the weir wall. This loading was calculated with the vent flow model described in Reference 1 and for design purposes is assumed to exist during the first 30 seconds of blowdown.

5.1.4 Chugging Loads

The pressure pulses generated inside the top vents during chugging (see Section 4.1.9) propagate toward the weir annulus. A typical trace of the

pressure pulses on the weir wall is shown in Figure 5.4. The dominant pressure response in the weir annulus during chugging is characterized by a pre-chug underpressure followed by a pressure pulse train, as shown in Figure 5.4a. The load applied to the weir annulus (weir wall, basemat and inside drywell wall) is described by a pre-chug underpressure, defined as a half sine wave as shown in Figure 5.5, followed by the pressure pulse train shown in Figures 5.5a or 5.5b. For local load considerations the peak amplitudes are applied, and for global considerations the mean amplitudes are applied.

Vertical attenuation of the weir underpressure is very small; for design evaluation, no attenuation should be assumed. For the pressure pulse train, the attenuation on the weir wall and drywell ID wall in the vertical direction is shown in Figure 5.6. For all global loads, there is no attenuation in the circumferential direction.

5.1.5 Inward Load Due to Negative Drywell Pressure

Due to negative drywell pressure discussed in Section 4.1.7, reverse water flow in the horizontal vents will lead to inward acting impingement loads on the weir wall. A simple, steady-state flow analysis leads to flow velocities approaching 40 ft/sec if it is assumed that a 21 psi negative differential exists between the drywell and containment.

This leads to a total impingement force on the weir wall of 12,800 lb. per vent applied over the projected area of the vents as shown in Attachment H. This number is based on a simple jet impingement analysis which assumes that the force on the weir wall corresponds to a change of the horizontal momentum of the water flowing through the vents.

This same negative drywell condition can theoretically result in the flow of water over the weir wall into the drywell. Using the nominal predicted drywell depressurization time history shown in Figure 5.7, a peak velocity of 30 feet/sec can be calculated at the top of the weir wall. This velocity is decreased due to the effects of gravity with elevation and the spreading of the flow field so that the maximum elevation reached is 14 feet above the top of the weir wall as shown in Figure 5.8. Structures in the path of the water are designed for drag loads using the following equation:

$$F = \frac{C_D A \rho V^2}{2g_c}$$

where:

- F = Drag Load Force, lbf
- C_D = Drag coefficient
- A = Area Normal to Flow, Ft²
- ρ = Density of Water, 62.4 lbm/ft³
- g_c = Newton's constant, 32.2 lbm-ft/lbf-sec²
- V = Velocity of fluid, ft/sec.

5.1.6 Suppression Pool Fallback Loads

For the reasons presented in 4.1.6 and since the weir annulus pressure is controlled by vent flow during the period of interest, no suppression pool fallback pressure loads are specified for the weir wall.

5.1.7 Hydrostatic Pressure

During the first second after the DBA, the water in the annulus is depressed to the bottom vent; therefore, there is no inward hydrostatic pressure load on the weir wall. Post LOCA hydrostatic load is an outward load due to the difference between the water within the weir wall and the level in the suppression pool. The influence of seismic accelerations on hydrostatic pressure distribution is discussed in Attachment B.

5.1.8 Safety Relief Valve Loads

In the event of safety relief valve actuation, the hydrodynamic pressure oscillations associated with the pipe air clearing transient can reach the weir wall through the vents. Attachment A provides loading information. The S/R valve load is applied to the projected vent hole area on the weir wall.

5.1.9 Condensation

There will be no loads induced on the weir during condensation, as shown by lack of transducer response in the tests.

5.2 WEIR WALL LOADS DURING AN INTERMEDIATE BREAK ACCIDENT

Figure 5-3 shows the bar chart for the weir wall during the IBA. The safety relief loads associated with ADS activation are discussed in Attachment A. The LOCA induced pressure differential across the weir wall will be small.

5.3 WEIR WALL LOADS DURING A SMALL BREAK ACCIDENT

The loading sequence for the weir wall during a small steam line break is essentially the same as for the drywell wall with the exception that there will be no pressure differential across the weir wall other than hydrostatic pressure. Apart from that, the information in Section 4.3 applies.

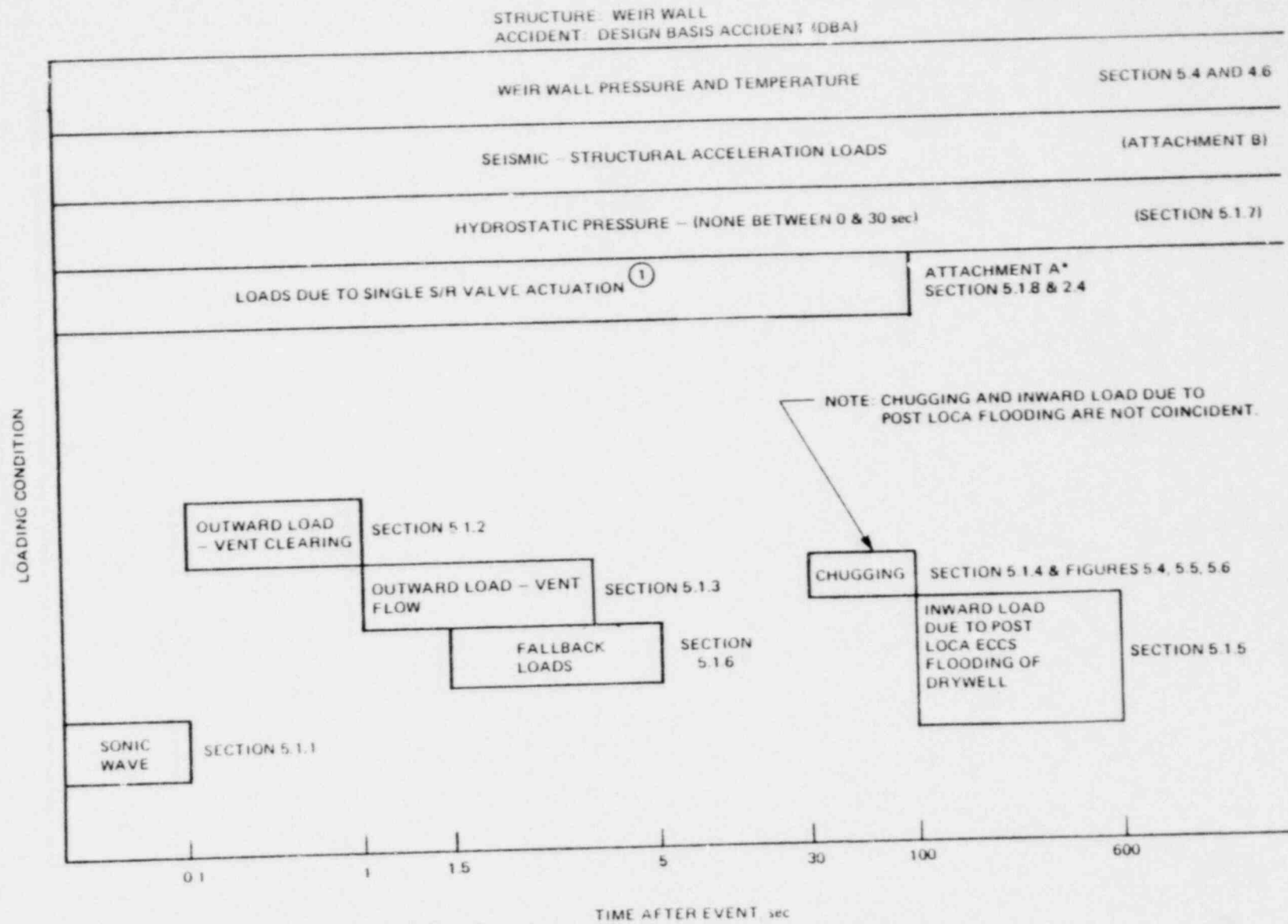
5.4 WEIR WALL ENVIRONMENT ENVELOPE

The temperature and pressure for the drywell envelope data (Figure 4-10) applies to the weir wall with the exception of the temperature of that part of the outside face which is below the elevation of the upper vents. This region will remain submerged and will be maintained at suppression pool temperature. It should be noted that the weir wall structure is totally within the drywell and effects of environmental conditions should be examined on this basis, including the thermal cycling during chugging (see Section 4.6).

The first 6 hours of the environmental conditions defined on Figure 4.10 are based on a small steam break. Faster shutdown by operator can reduce the duration of the small break to 3 hrs. For a large break, the free volume inside the weir wall is flooded and environmental temperature conditions will correspond to the water temperature in this volume. This is less severe than the conditions of Figure 4.10.

5.5 WEIR ANNULUS MULTICELL EFFECTS

Chugging is conservatively considered to be synchronous for the Mark III load definitions. The typical pressure time history is shown on Figure 5.4a. Superimposed chugging spikes from adjacent vents, as confirmed by multicell tests (ref. 18), are minor and considered to be insignificant. On Figure 5.9 these spikes are superimposed to indicate the typical magnitude.

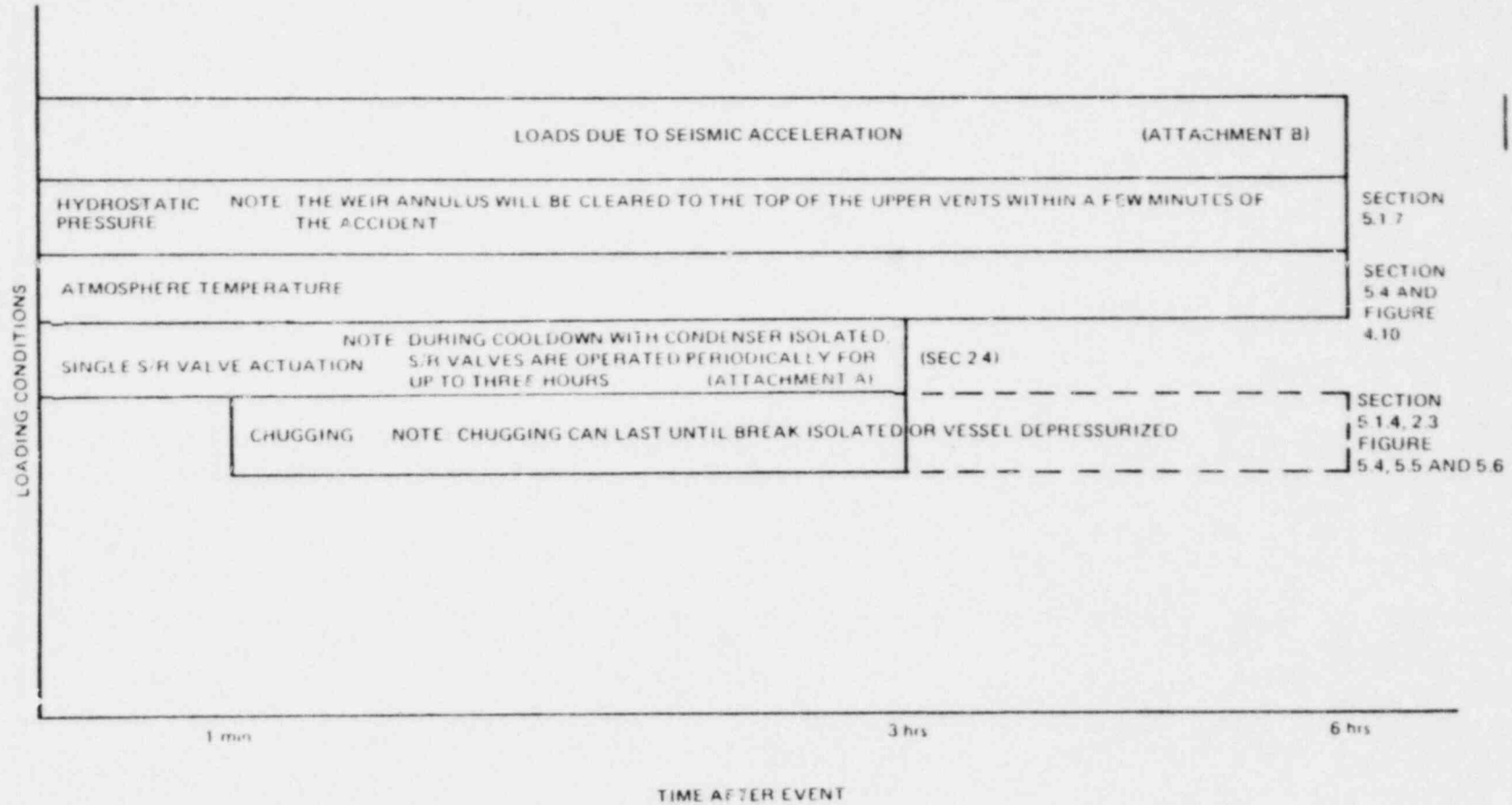


*ADD S/R DYNAMIC LOAD TO STATIC LOAD DUE TO DRYWELL AIR PURGED TO CONTAINMENT. VAPOR PRESSURE AT 140 F.

^① APPLIES TO BOTTOM 2 VENTS ONLY

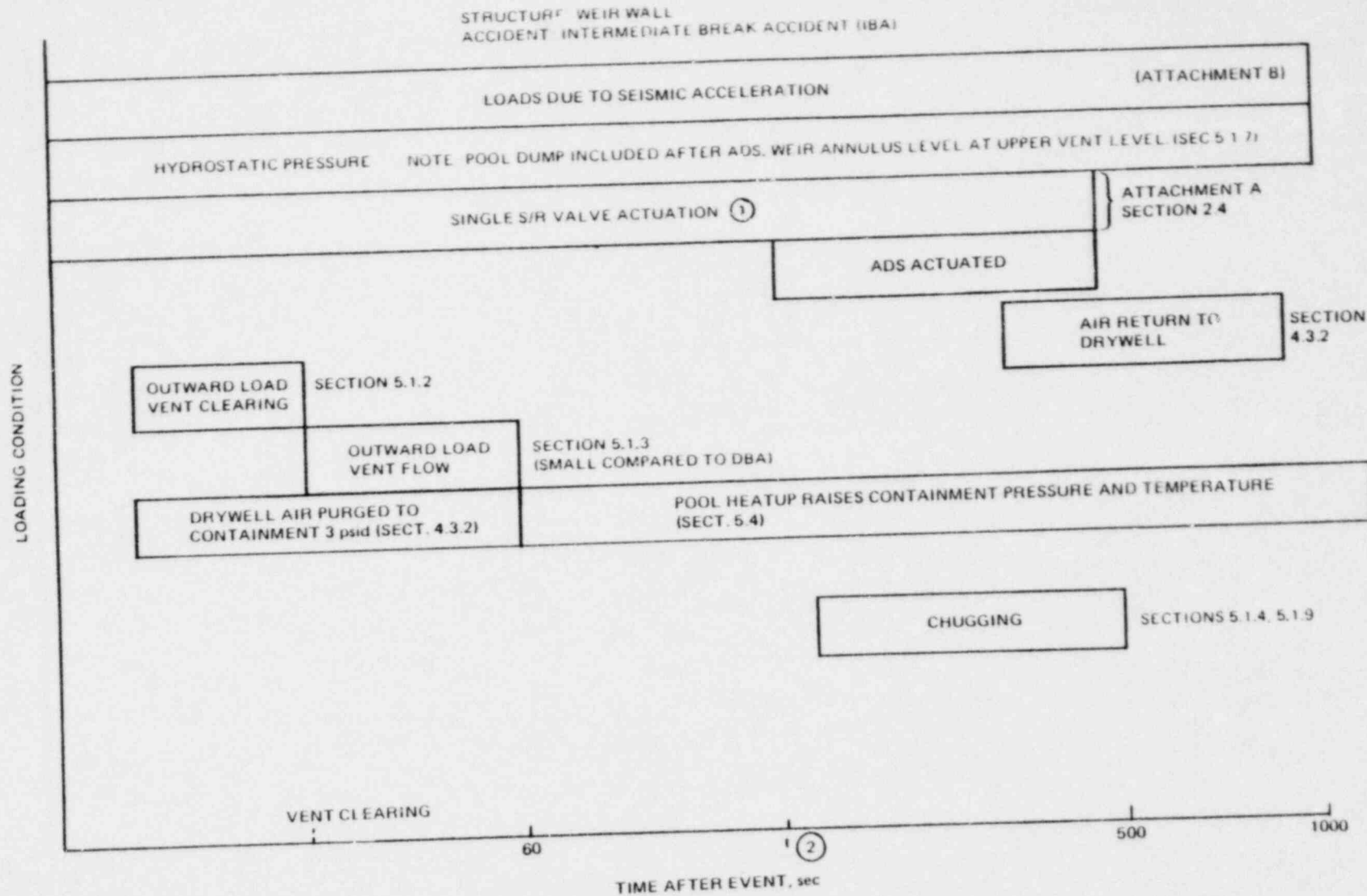
Figure 5-1. Weir Wall-Loading Chart for DBA

STRUCTURE WEIR WALL
ACCIDENT SMALL BREAK ACCIDENT (SBA)



22A4365
REV. 4

Figure 5-2. Weir Wall-Loading Chart for SBA



22A4365
Rev. 4

- ① SINGLE SRV LOADS DO NOT COMBINE WITH OTHER SRV LOADS
- ② TIME SCALE DEPENDENT UPON BREAK SIZE, MINIMUM VALUE OF $t = 20$ min

Figure 5-3. Weir Wall-Loading Chart for IBA

088T10

5-8

This figure is PROPRIETARY and is provided under separate cover.

Figure 5.4. Typical Weir Wall Chugging Pressure Time History - Test Series 5707, Run 1.

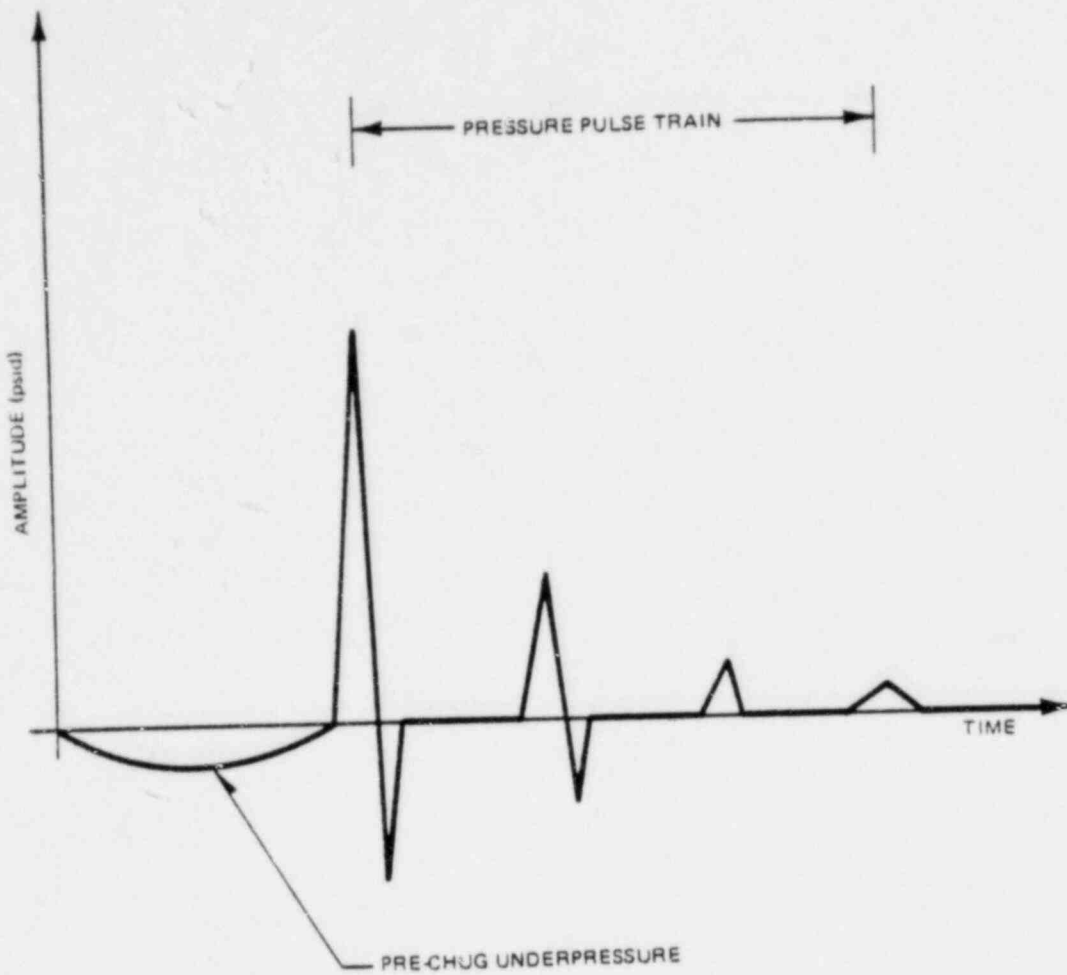


Figure 5.4a. Typical Pressure Time-History for Weir Annulus During Chugging

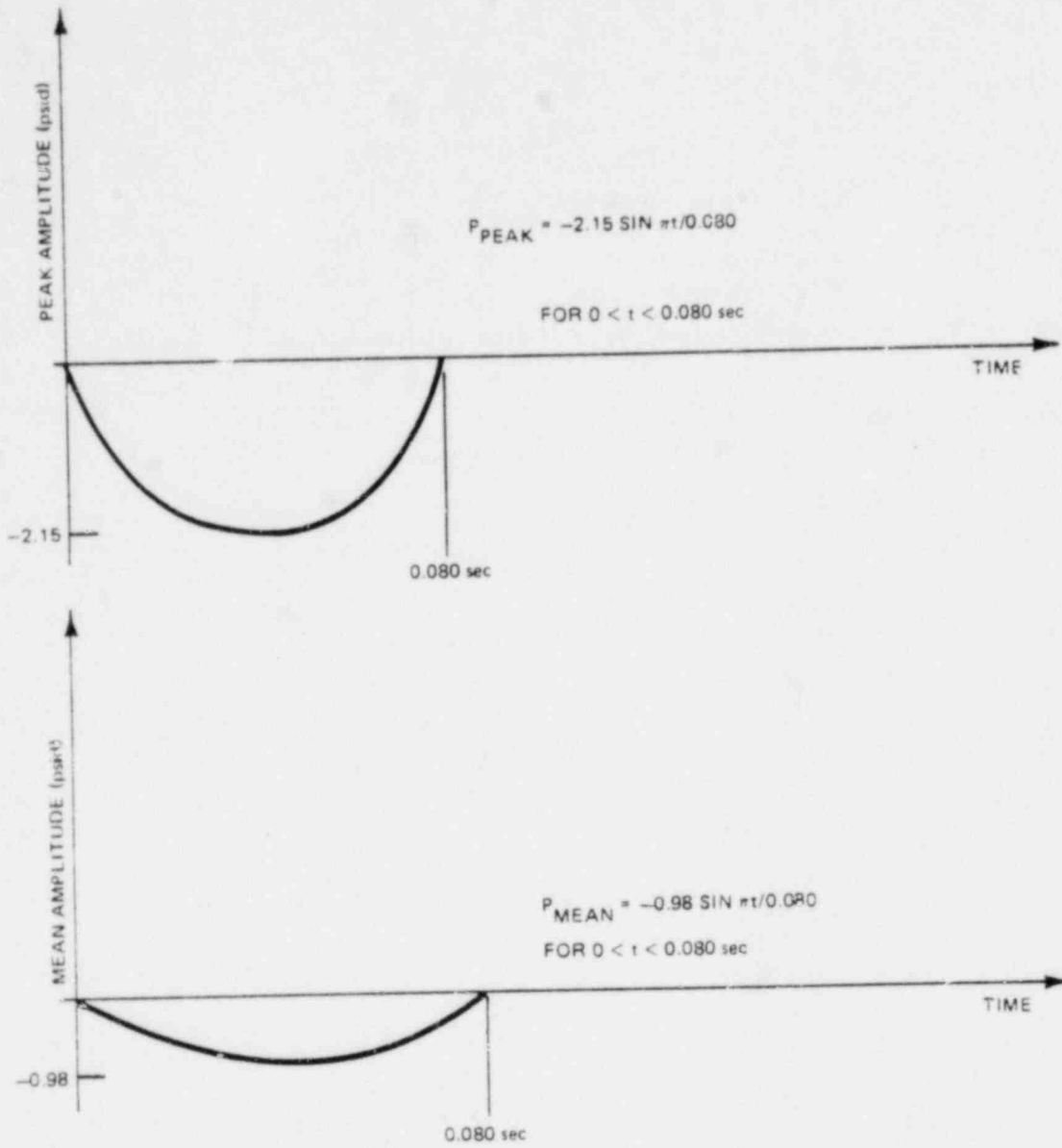


Figure 5.5. Underpressure Distribution on the Weir Wall and Drywell I.D. Wall During Chugging

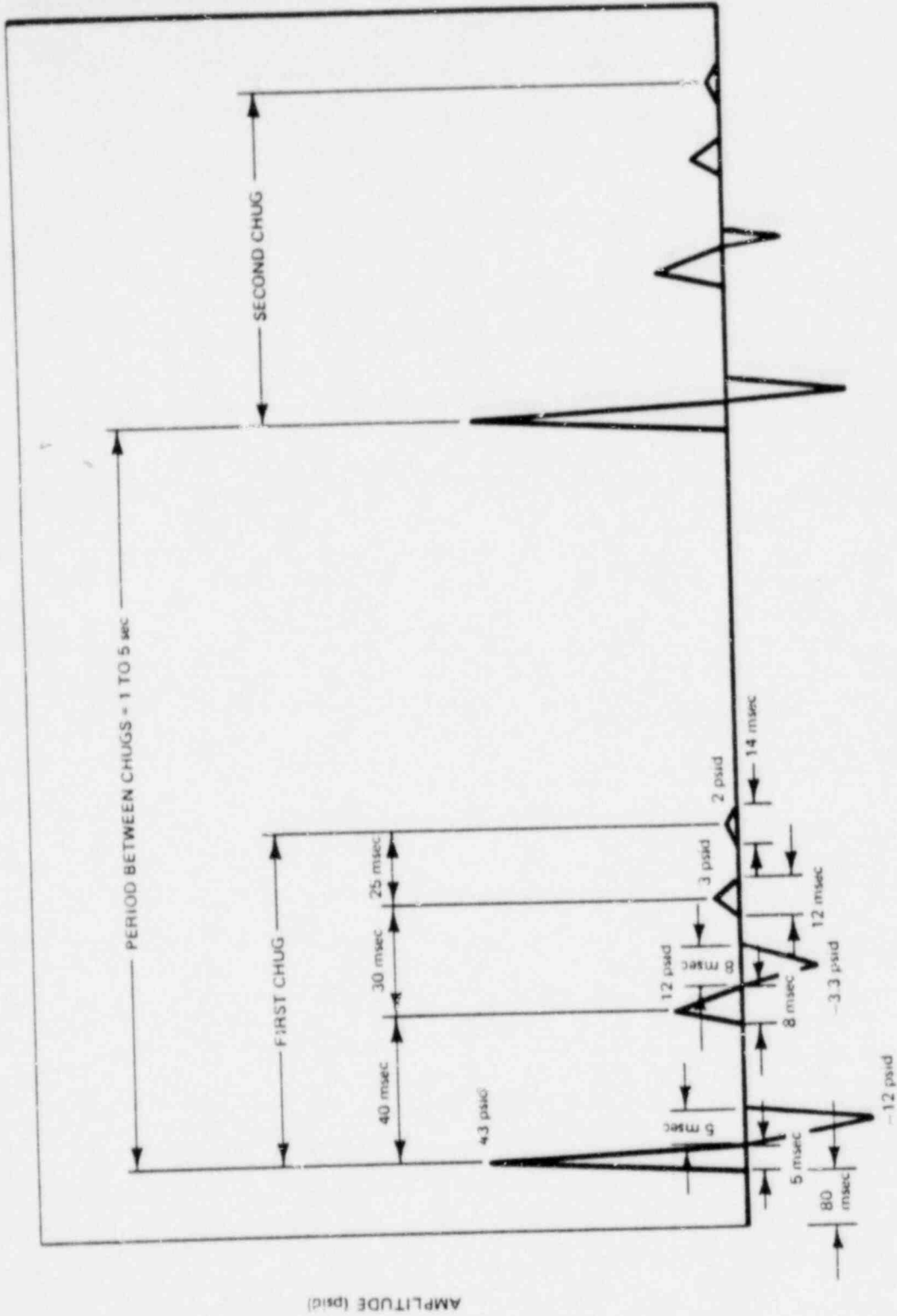


Figure 5.5a. Peak Pressure Pulse Train on the Weir Wall and Drywell I.D. Wall During Chugging

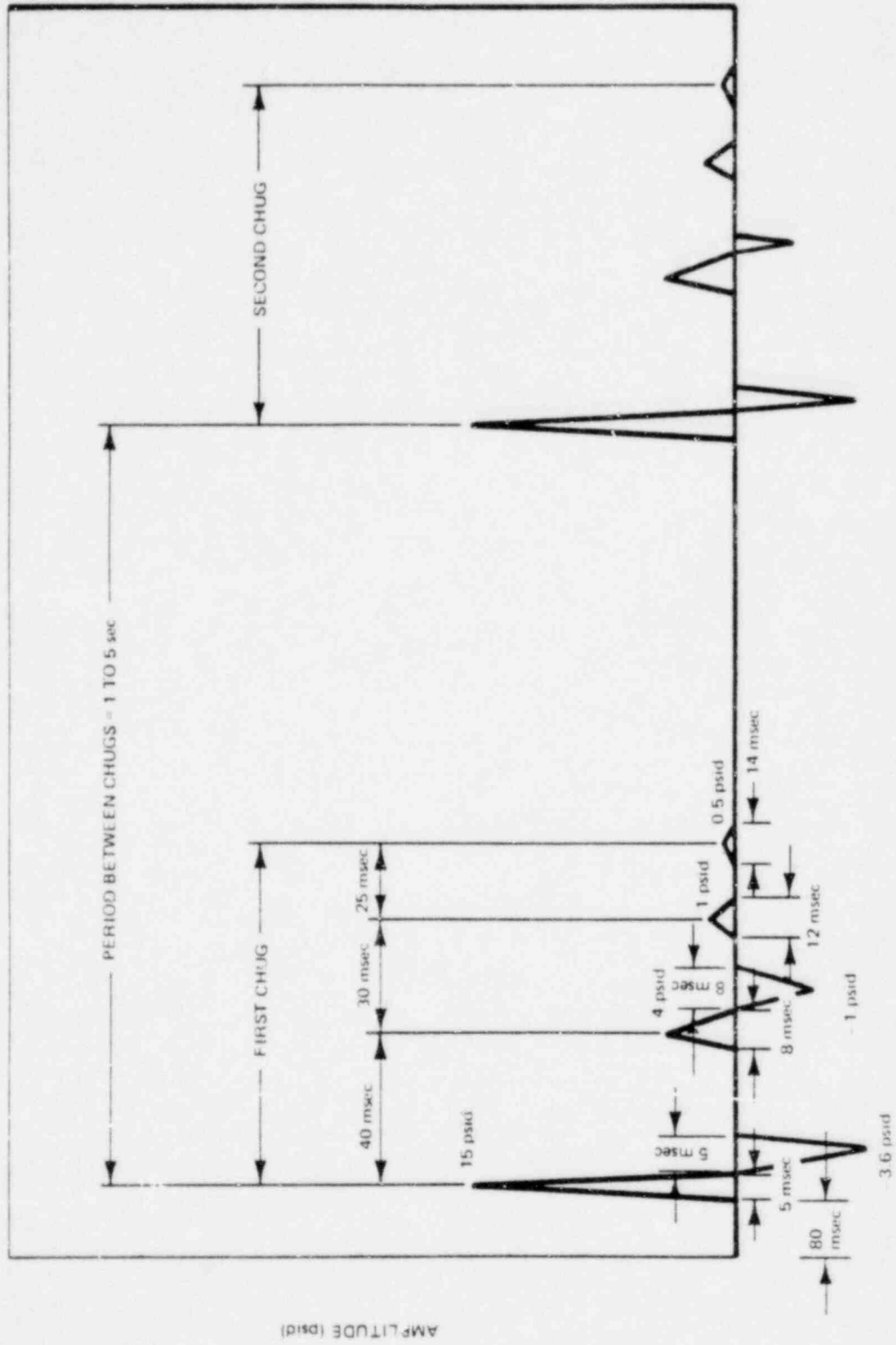


Figure 5.5b. Mean Pressure Pulse Train on the Weir Wall and Drywell 1.D. Wall During Chugging

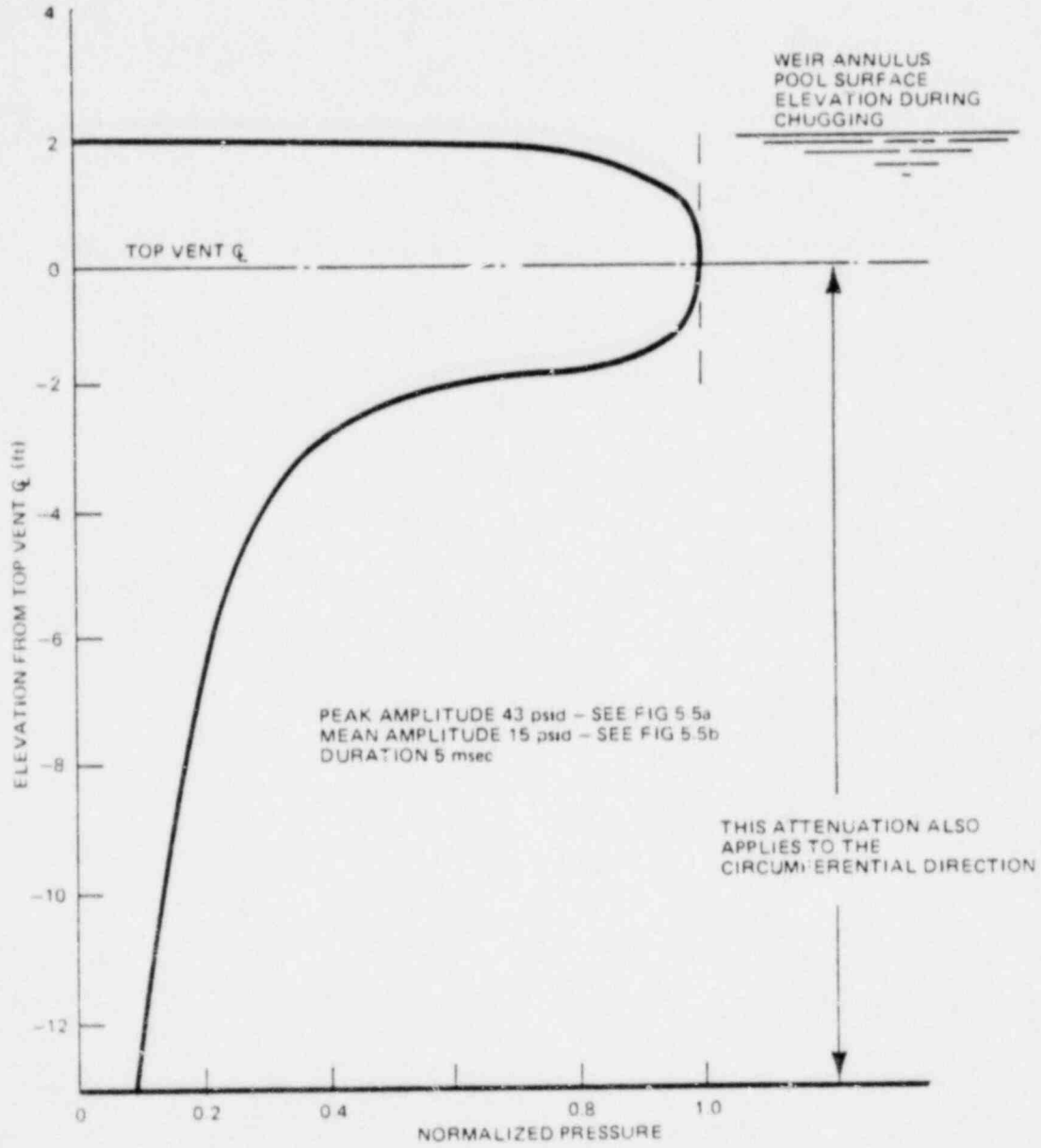


Figure 5.6. Normalized Weir Annulus Pressure Pulse Attenuation

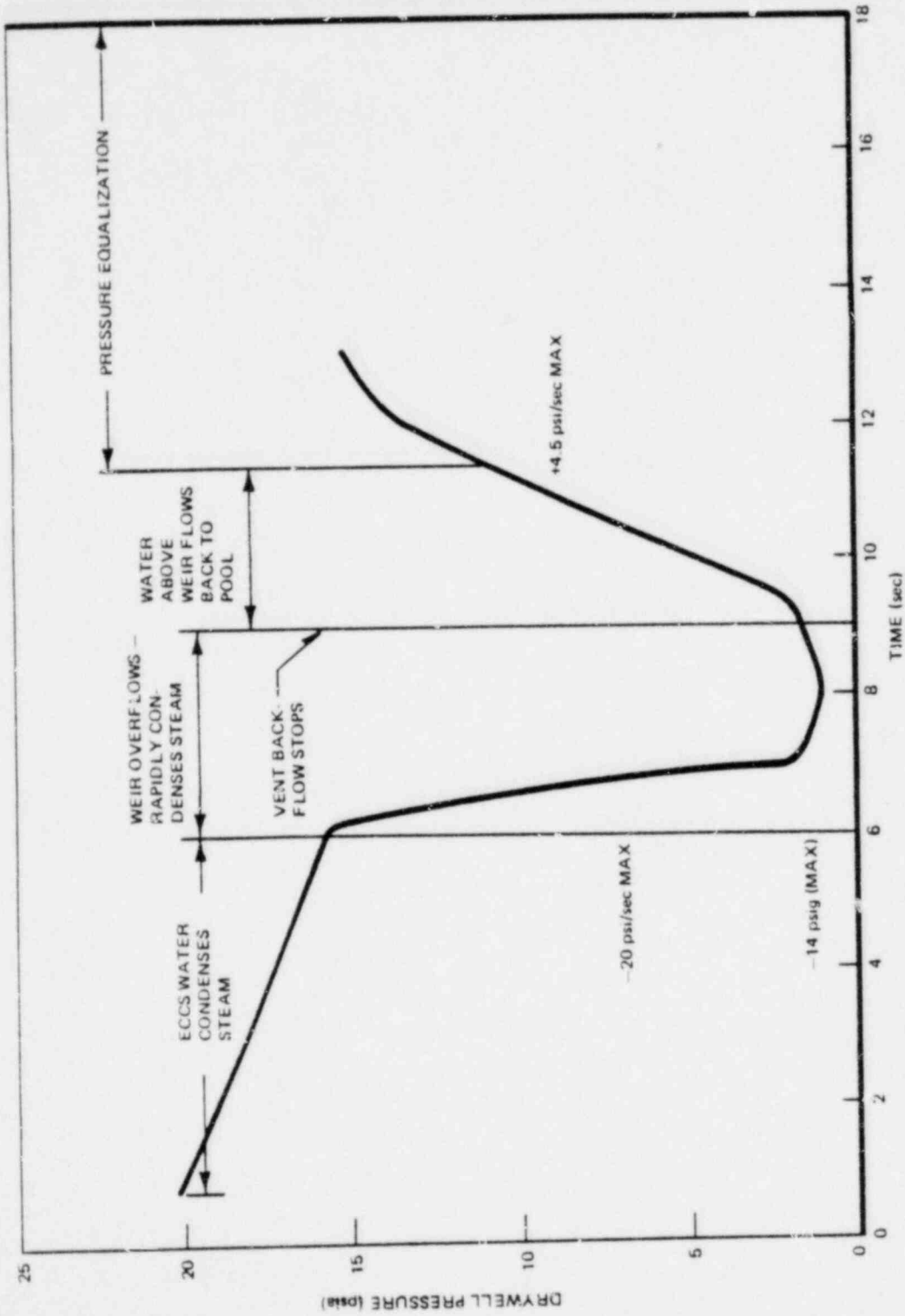


Figure 5.7. Pressure Transient in Drywell Initiated by Vessel Reflood to Line Break Level-238 Standard Plant

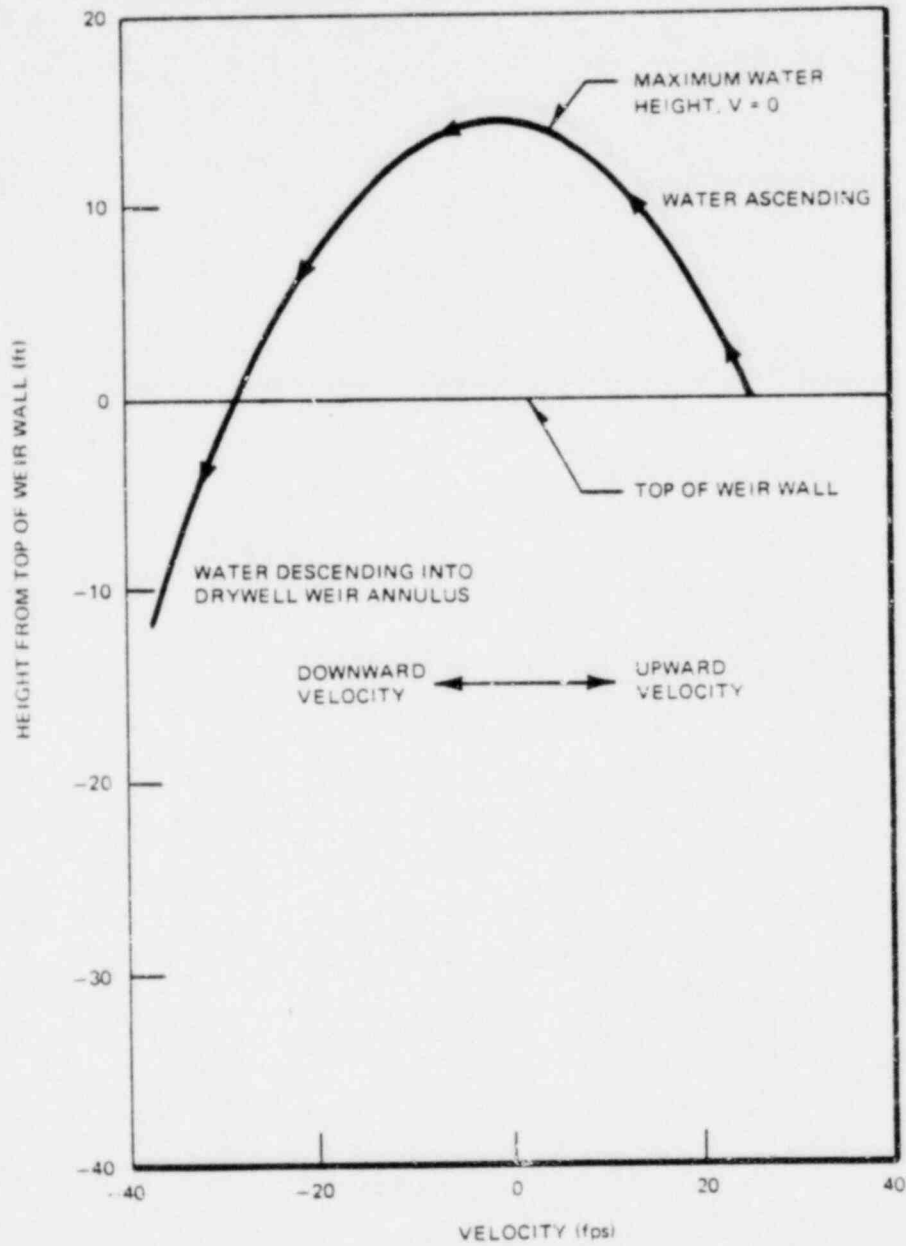


Figure 5.8. Vent Backflow Weir Annulus Water Surge Velocity Vs. Height Above Weir Wall

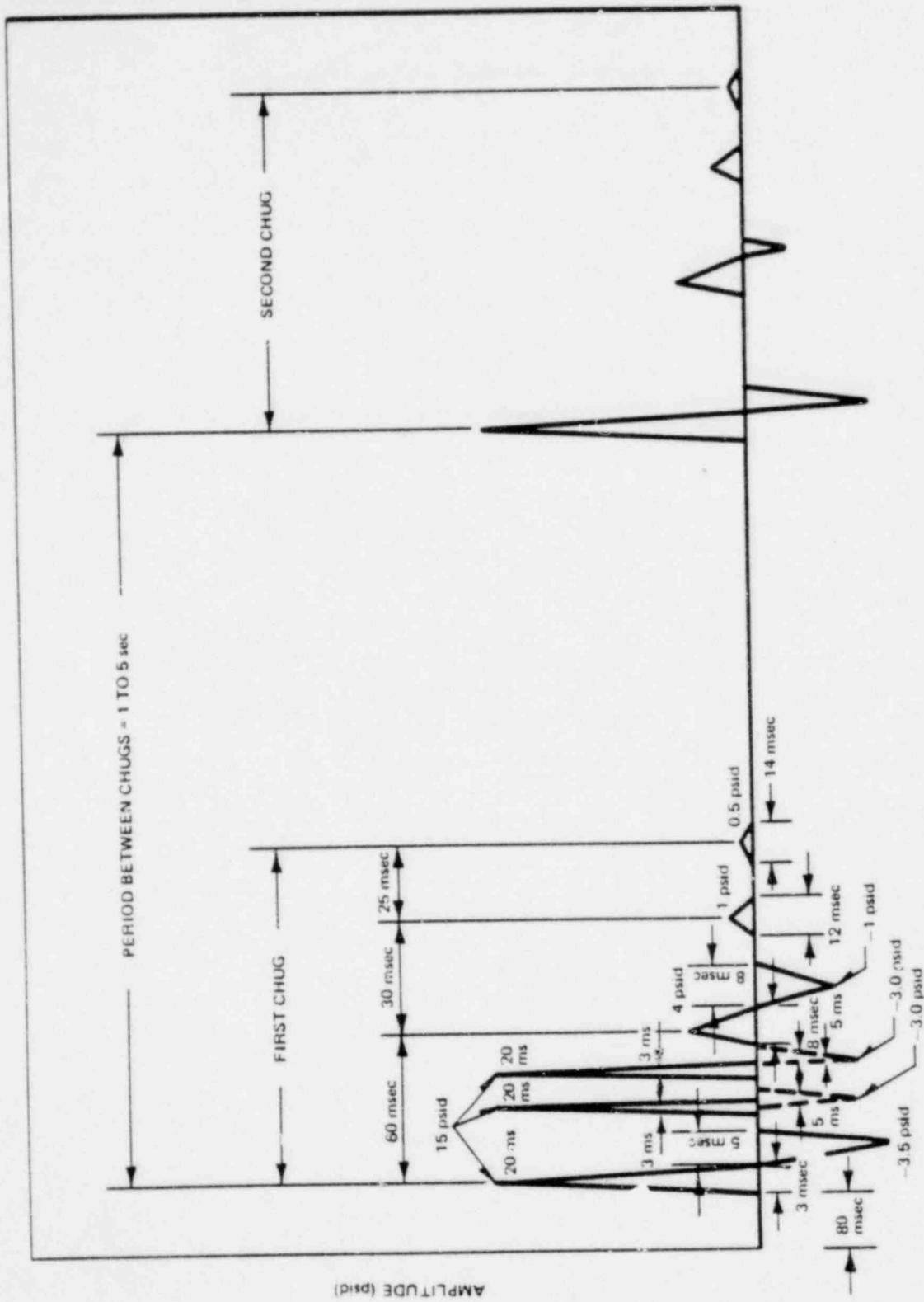


Figure 5.9. Mean Pressure Pulse Train on the Weir Wall and Drywell I.D. Wall During Chugging with Superposition of Adjacent Spikes

6. CONTAINMENT

The containment experiences dynamic loadings during all three classes of loss-of-coolant accidents. The containment designer should consider other containment loads such as negative pressures during containment spray activation, pipe whip, shield building loads, jet impingement etc. that are not included in this report.

6.1 CONTAINMENT LOADS DURING A LARGE STEAM LINE BREAK (DBA)

Figure 6-1 is the bar chart showing the loading conditions that the containment structure may experience during the DBA LOCA. Design loads for the various structures in the containment annulus are presented in Sections 7 thru 12. Figures 2.2-2 through 2.2-6 show typical structures above the suppression pool in the standard plant arrangements.

6.1.1 Compressive Wave Loading

Very rapid compression of the drywell air could, theoretically, result in a compressive wave being generated in the weir annulus water. This wave could then travel down the weir annulus, through the vents and across the pool to the containment wall. This phenomenon is not specifically included in the containment design conditions on the basis that the approximately 20 psi per second pressure rate in the drywell is not sufficiently rapid to generate a compressive wave in the water. In addition, even if a 20 psi/sec wave were generated at the weir annulus surface, the very significant attenuation as the wave crosses the 18.5 ft. wide suppression pool would lead to insignificant containment wall loads. This phenomena has never been observed in any GE Pressure Suppression test.

6.1.2 Water Jet Loads

Examination of applicable PSTF data shown in Figure 6.4, indicates some evidence of a loading of the containment wall due to the water jet associated with the vent clearing process (i.e., less than 1 psid), as indicated by the small spike at 0.8 sec. Water jet loads are negligible when compared to the subsequent air bubble pressure discussed in Section 6.1.3 and are not specifically included as a containment design load.

6.1.3 Initial Bubble Pressure

The PSTF air test data for runs 3 and 4 (Ref. 7) has been examined for evidence of bubble pressure loading of the suppression pool wall opposite the vents. These tests were chosen because the drywell pressure at the time of vent clearing is comparable to that expected in a full scale Mark III (i.e., approximately 20 psid and because the vent air flow rates and associated pool dynamics would be more representative than the large scale steam blowdown tests. The maximum bubble pressure load on the containment observed during PSTF testing was 10 psid as shown in Figure 6.4. Figure 6.6 is a summary of all the peak containment wall pressure observed in PSTF tests during the bubble formation phase of the blowdown. The Mark III design load which is based on these tests, is shown in Figure 6.5.

The magnitude of the containment pressure increase following vent clearing is dependent upon the rate at which the drywell air bubble accelerates the suppression pool water. Circumferential variations in the air flow rate may occur due to drywell air/steam mixture variations but it results in negligible variations in the containment bubble pressure load. (See Attachment L).

The conservative asymmetric condition assumes that all air is vented on half of the drywell periphery and steam is vented on the other half.

The large scale PSTF test data is the basis for specifying the maximum asymmetric load of 10 psid. Figure 6-6 is a summary of all the peak containment wall pressures observed in PSTF tests during the bubble formation phase of the blowdown. Figure 6.4 shows a typical transient. A maximum increase of 10 psid on the containment wall was observed in the PSTF at the Mark III drywell peak calculated pressure of 36.2 psid. Figure 6-6 shows the maximum increase close to zero. Thus, use of a 10 psid asymmetric pressure condition applied in a worst case distribution is a bounding specification will be used for containment evaluation.

6.1.4 Hydrostatic Pressure

In addition to the hydrostatic load due to the suppression pool water, the data presented in Attachment B is used to determine the hydrostatic pressure loads on

the containment during an earthquake. During periods of horizontal accelerations there will be an asymmetric distribution around the circumference of the containment. The maximum pool level above the pool bottom in the suppression pool is 22 feet and is 26 feet for the drywell and weir annulus.

6.1.5 Local Containment Loads Resulting from the Structures at or Near the Pool Surface

Any structures in the containment annulus that are at or near the suppression pool surface experience upward loads during pool swell. If these structures are attached to the containment wall, then the upward loads are transmitted into the containment wall. Sections 9 and 10 discuss the types of loads that will be transmitted.

Localized loads on the containment wall resulting from the pressure losses associated with water flow past a body are depicted in Figure 6-8. The data presented in this figure is based on drag type calculations and assumes that the affected structures have design features which preclude impact type loads from occurring.

6.1.6 Containment Load Due to Pool Swell at the HCU Floor (Wetwell Pressurization)

This structure is approximately 20 ft. above the pool surface and is 8 feet above the point where breakthrough begins. Froth will reach the HCU floor approximately 1/2 second after top vent clearing and will generate both impingement loads on the structures and a flow pressure differential as it passes through the restricted annulus area at this elevation.

The impingement will result in vertical loads on the containment wall from any structures attached to it and the flow pressure differential will result in an outward pressure loading on the containment wall at this location. The impingement loads will be 15 psi and the froth pressure drop across the HCU floor has been calculated to be 11 psi; the containment wall will see an

11 psi discontinuous pressure loading at this elevation. Figure 6-9 shows details of the 11 psi pressure loading. The bases for both the impingement and flow pressure loading are discussed in Section 11 and 12.

When evaluating the containment response to the pressure differential at the HCU floor, any additional loads transmitted to the containment via HCU floor supports (beam seats, etc.) must be assumed to occur simultaneously. These loads are based on the assumption that there is approximately 1500 ft² of vent area reasonably distributed around the annulus at this elevation. For plant configurations with HCU flow vent area other than 1500 ft² (see Figure 6-16 for the froth pressure drop). The question of circumferential variations in the pressure underneath the HCU floor is addressed in Section 12, and Attachment F.

6.1.7 Fall Back Loads

No significant pressure loads are indicated from the data generated by the PSTF during the period when suppression pool water is subsiding to its original level following pool swell. Figure 6-4 shows that during the 2 to 5 seconds suppression pool fall back is occurring, the pool wall pressure probes show no evidence of pressures higher than the initial static pressure.

Structures within the containment annulus below the HCU floor will experience fall back induced drag loads as the water level subsides to its initial level. For design purposes, it is assumed that these structures will experience drag forces associated with water flowing at 35 ft/sec; typical drag coefficients are shown on Figure 10-5. This is the terminal velocity for a 20 ft. free fall and is a conservative, bounding number.

6.1.8 Post Pool Swell Waves

Visual observations of PSTF tests indicate that following pool swell, the surface of the suppression pool is agitated with random wave action having peak to peak amplitudes of less than 2 ft. These waves do not generate significant containment loading conditions.

6.1.9 Condensation Oscillation Loads

During the condensation phase of the blowdown, there have been some pressure oscillations measured on the containment wall in PSTF tests. Figures 6.10 and 6.11 show typical traces of the containment wall pressure fluctuations observed during the condensation phase of the $1\sqrt{3}$ scale PSTF tests.

The forcing function to be used for design is described in section 4.1.5. The magnitude of the load on the containment wall is shown in Figures 4.6a and 4.6b.

6.1.10 Chugging

Examination of the PSTF data shows that attenuated vent system pressure fluctuations associated with the chugging phenomenon is transmitted across the suppression pool. Figures 6.12 and 6.13 show typical containment wall and basemat pressures from full scale PSTF tests. Chugging loads on the containment are defined in subsection 4.1.9.2.

6.1.11 Long-Term Transient

Following the blowdown, the Mark III containment system will experience a long term suppression pool temperature increase as a result of the continuing core decay heat. The operators will activate the RHR system to control the temperature increase, but there will be a period of containment pressurization before the transient is terminated. Figure 6.14 shows the envelope of containment atmospheric pressure and temperature for all postulated breaks. The Figure defines only the containment atmospheric condition. Separate analyses are required to evaluate the transient structural response to these conditions. Peak design containment pressure is 15 psig and peak design containment temperature is 185°F.

The model used to simulate the long term post LOCA containment heat up transient is described in supplement 1 to Reference 1.

6.1.12 Containment Environmental Envelope

Figure 6.14 is a diagram showing the maximum design containment pressure and temperature envelope for any size of credible primary system rupture. The long term containment pressure following a DBA is shown on Figure 6.15.

6.2 CONTAINMENT LOADS DURING AN INTERMEDIATE BREAK ACCIDENT

Figure 6.2 is the bar chart for the containment during an intermediate break that is of sufficient size to involve the ADS system. Since these breaks are typically quite small and because there is a two minute timer delay on the ADS system, all the drywell air will have been purged to the containment prior to the time the ADS relief valves open. Thus, the containment will experience the loads from multiple relief valve actuation coupled with the 5 psi, pressure increase produced by the drywell air purge and pool heatup. Since the former are pressure oscillations whose magnitude is not dependent upon the datum level, these loads are additive. Attachment A defines the loading magnitudes which are assumed for the S/R valve discharge.

The seismic induced increase in suppression pool hydrostatic pressure as a result of horizontal accelerations is asymmetric. This loading sequence is discussed in more detail in Attachment B.

6.3 CONTAINMENT LOADS DURING A SMALL BREAK ACCIDENT

No containment loads will be generated by a small break in the drywell that are any more severe than the loads associated with the intermediate or DBA break. Figure 6.3 is the bar chart for this case.

There are unguarded RWCU lines in the containment that can release steam to the containment free space in the event of a rupture. The RWCU isolation

valves and flow limiter for this system are designed to terminate the blow-down before significant containment pressurization can occur. Typically a 2 psi pressure increase may occur.

Steam released by a pipe break in the containment may stratify and form a pocket of steam in the upper region of the containment. The steam temperature will be at approximately 220°F whereas the air temperature will be at approximately its initial pre-break temperature. This temperature stratification should be accounted for in the design.

Local temperatures of 330/250°F are possible in the event of reactor steam/liquid blowdowns to the containment.

6.4 SAFETY RELIEF VALVE LOADS

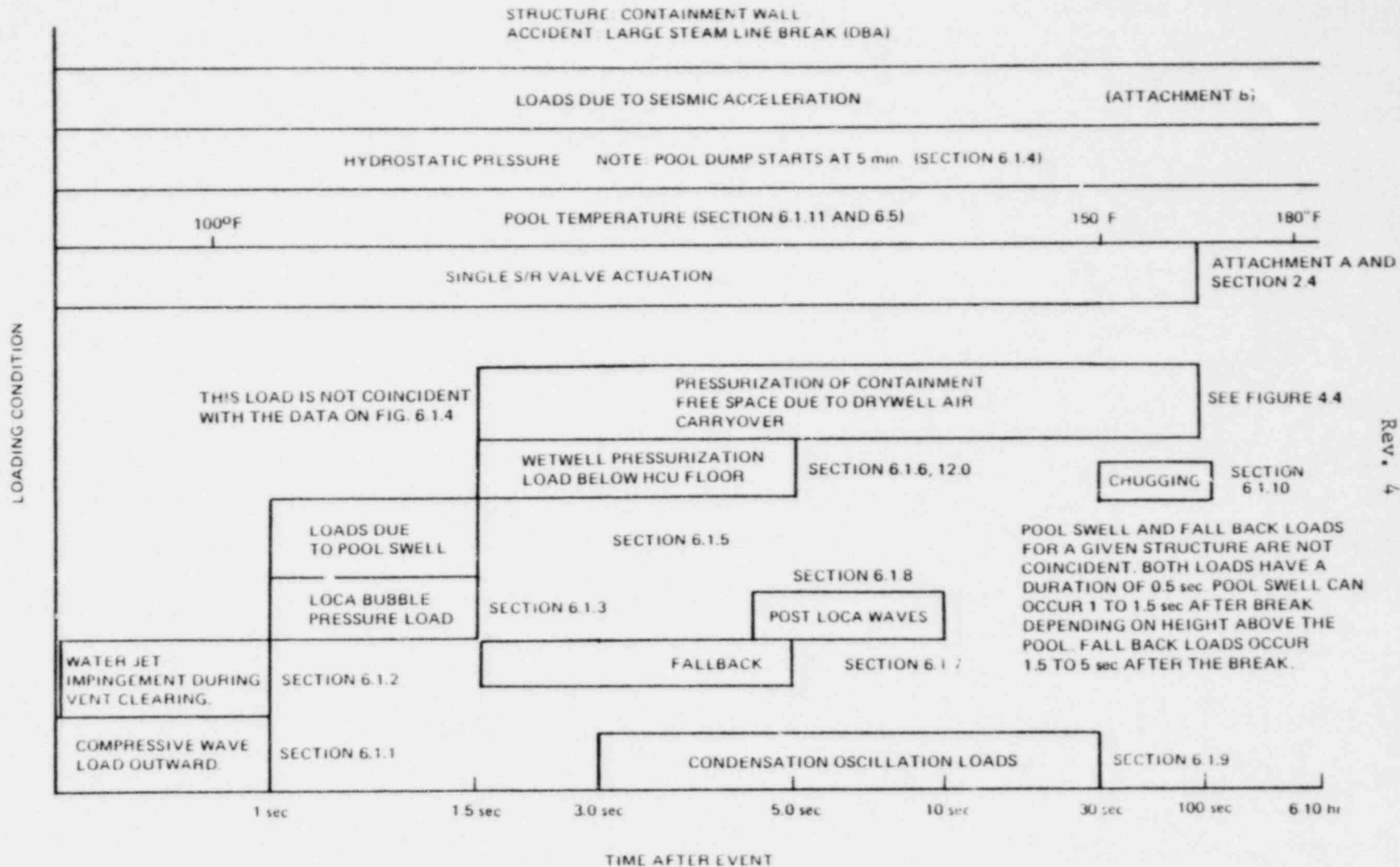
Relief valve operation can be initiated as a result of either a single failure, ADS operation, or a rise in reactor pressure to the valve set points. In addition, the containment can be exposed to S/R valve actuation loads any time the operator elects to open a valve or valves as during an isolated cooldown. The loads generated by S/R valve actuation are discussed in Attachment A.

6.5 SUPPRESSION POOL THERMAL STRATIFICATION

During the period of steam condensation in the suppression pool, the pool water in the immediate vicinity of the vents is heated. For the Mark III configuration, most of the condensing steam mass and energy are released to the pool through the top vents. By natural convection the hot water rises, and the cold water is displaced towards the bottom of the pool. The vertical temperature gradient resulting from this effect is known as thermal stratification and is discussed in Attachment N. The momentary thermal stratification for large break accident used in containment evaluation is shown in Figure 6.17.

6.6 CONTAINMENT WALL MULTICELL EFFECTS

No multicell effects on the containment wall were observed for pool swell or condensation phenomena during multicell testing (ref 17 and 18).



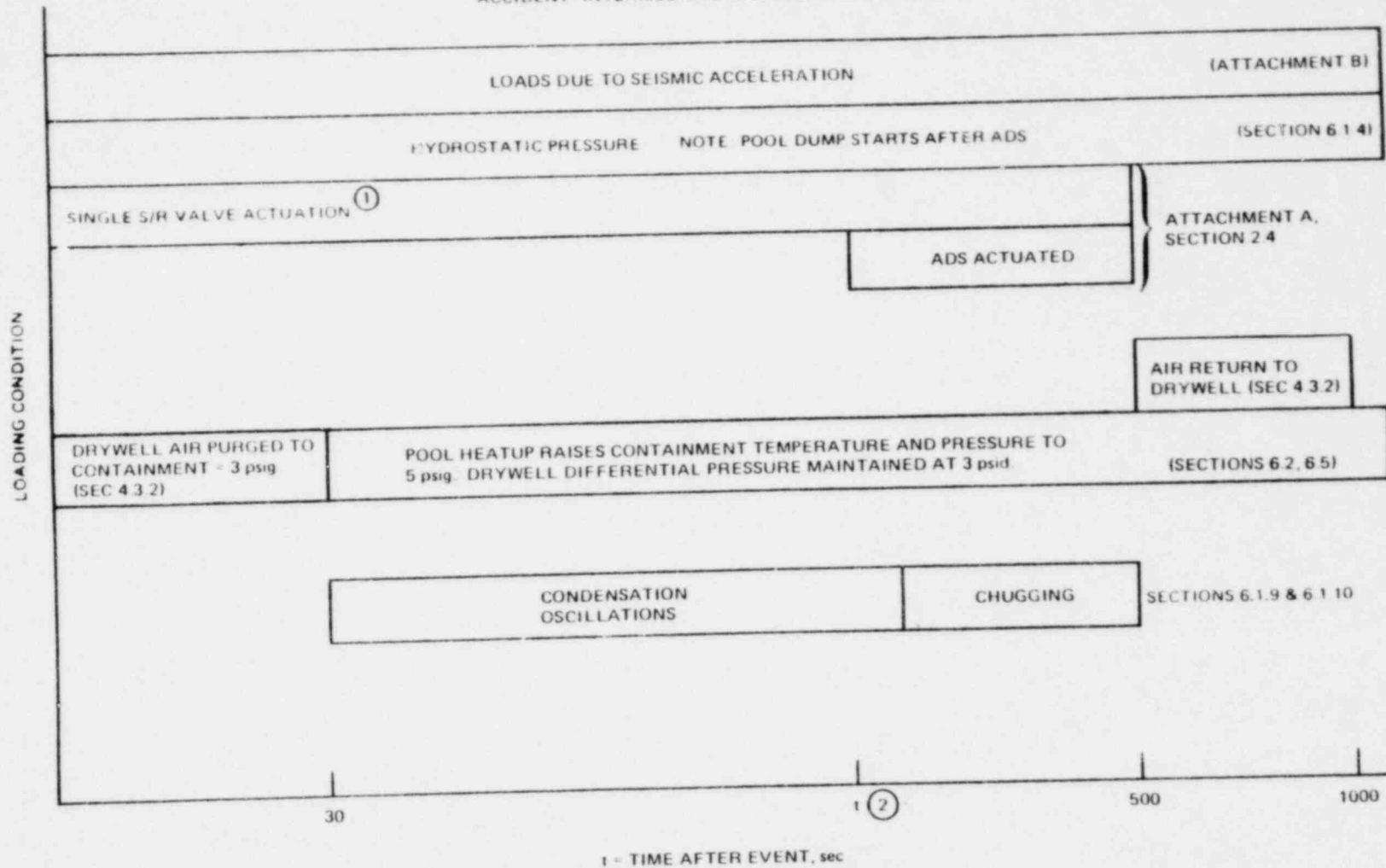
22A4365
Rev. 4

Figure 6.1. Containment-Loading Chart for DBA

011880

6-8

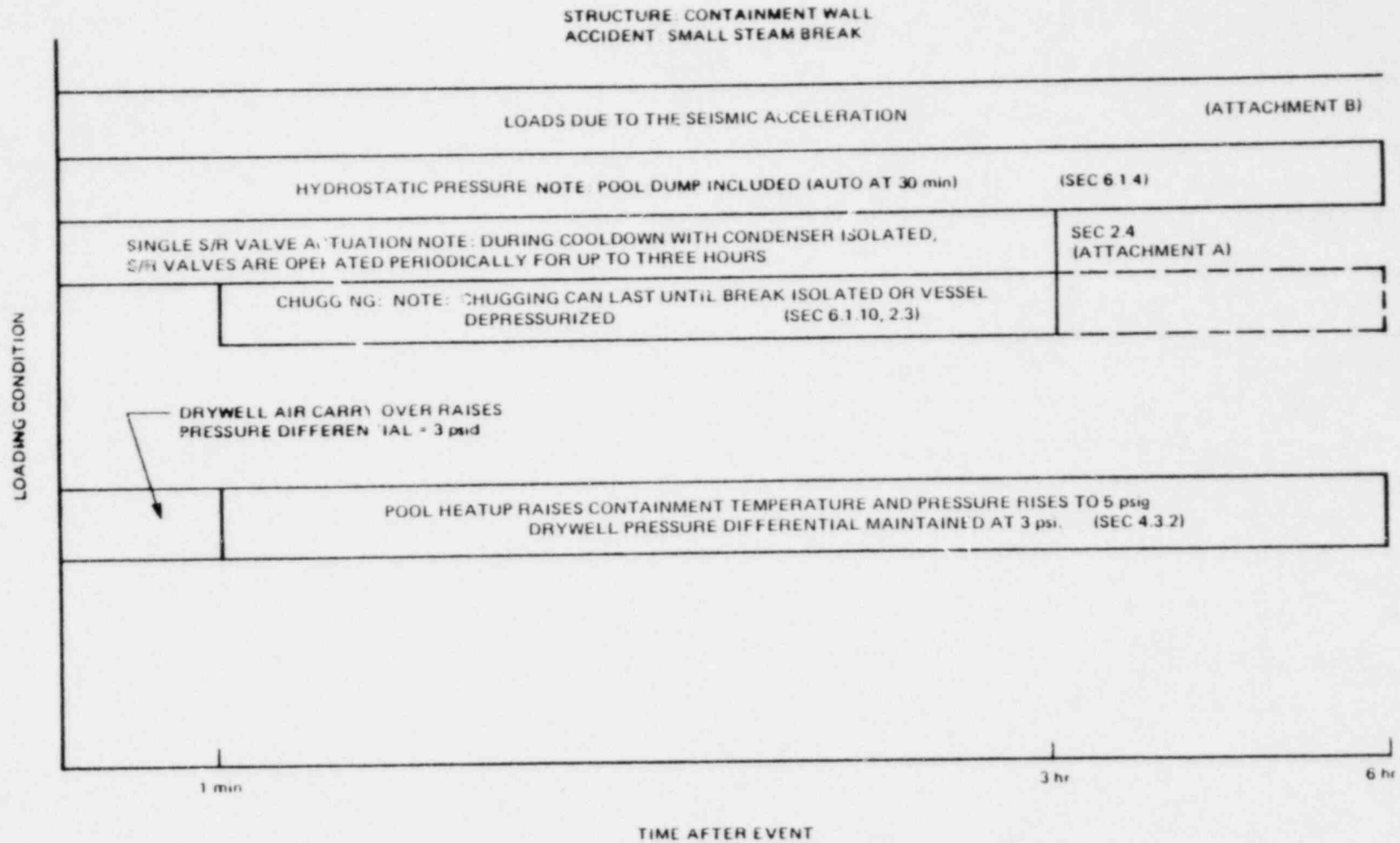
STRUCTURE CONTAINMENT WALL
ACCIDENT INTERMEDIATE STEAM LINE BREAK (IBA)



22A4365
Rev. 4

- (1) SINGLE SRV LOADS DO NOT COMBINE WITH OTHER SRV LOADS
- (2) TIME SCALE DEPENDENT UPON BREAK SIZE, MINIMUM VALUE OF $t = 2$ min

Figure 6.2. Containment-Loading Chart for IBA

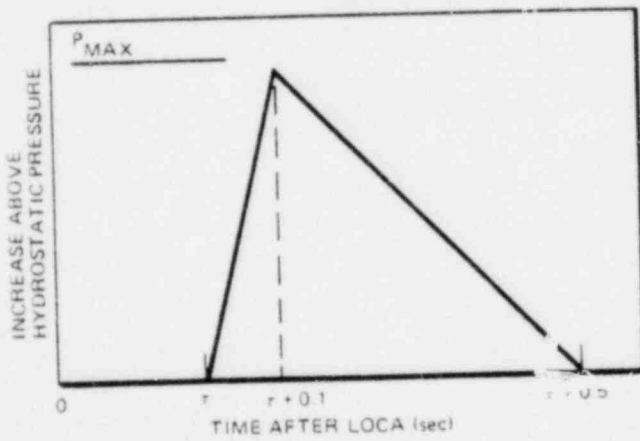
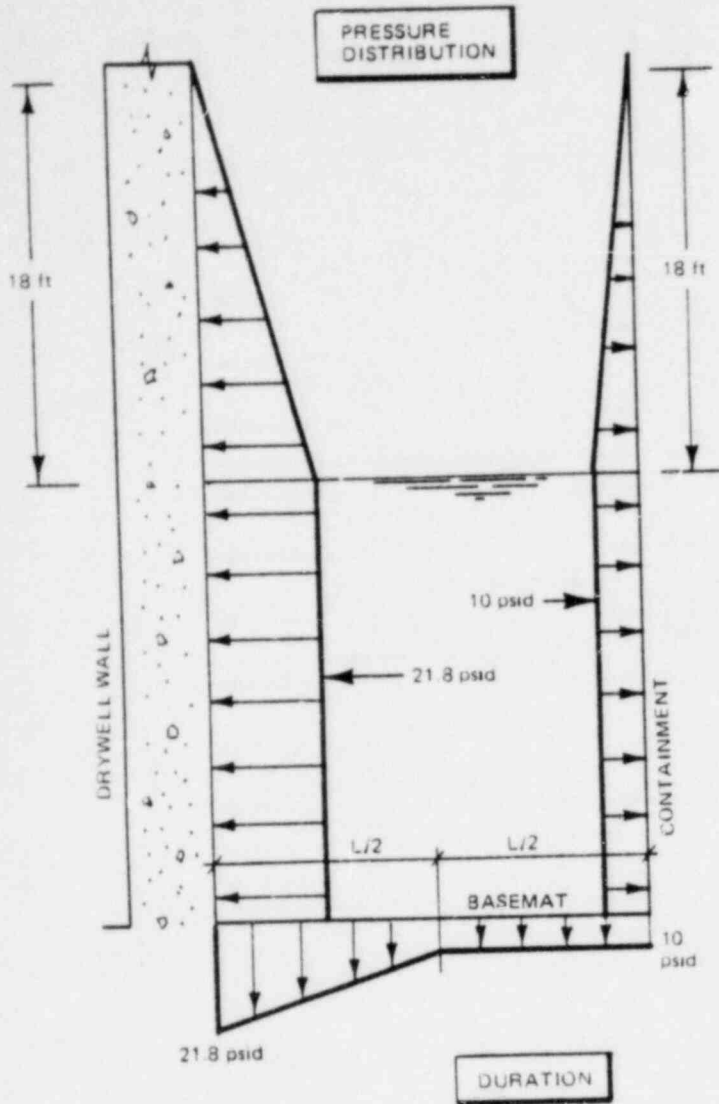


22A4365
REV. 4

Figure 6.3. Containment-Loading Chart for SBA

This figure is PROPRIETARY and is provided under separate cover.

Figure 6.4. Observed Bubble Pressure During Pool Swell -
Test Series 5706 Run 4



FOR $y < y_0$, $\tau = 1.0$ sec
 FOR $y > y_0$, $\tau = 1.0 + (y - y_0)/40$ (sec)

WHERE

- τ = DELAY DUE TO FINITE POOL SWELL VELOCITY
- y = HEIGHT ABOVE BASEMAT, ft
- y_0 = INITIAL POOL DEPTH, ft (BASED UPON 40 fps POOL SWELL VELOCITY)
- $y_{MAX} = y_0 + 18$ ft

Figure 6.5. Dynamic Loads Associated with Initial Bubble Formation in the Pool

This figure is PROPRIETARY and is provided under separate cover.

Figure 6.6. Containment Pressure Differential During Bubble Formation

This page intentionally deleted

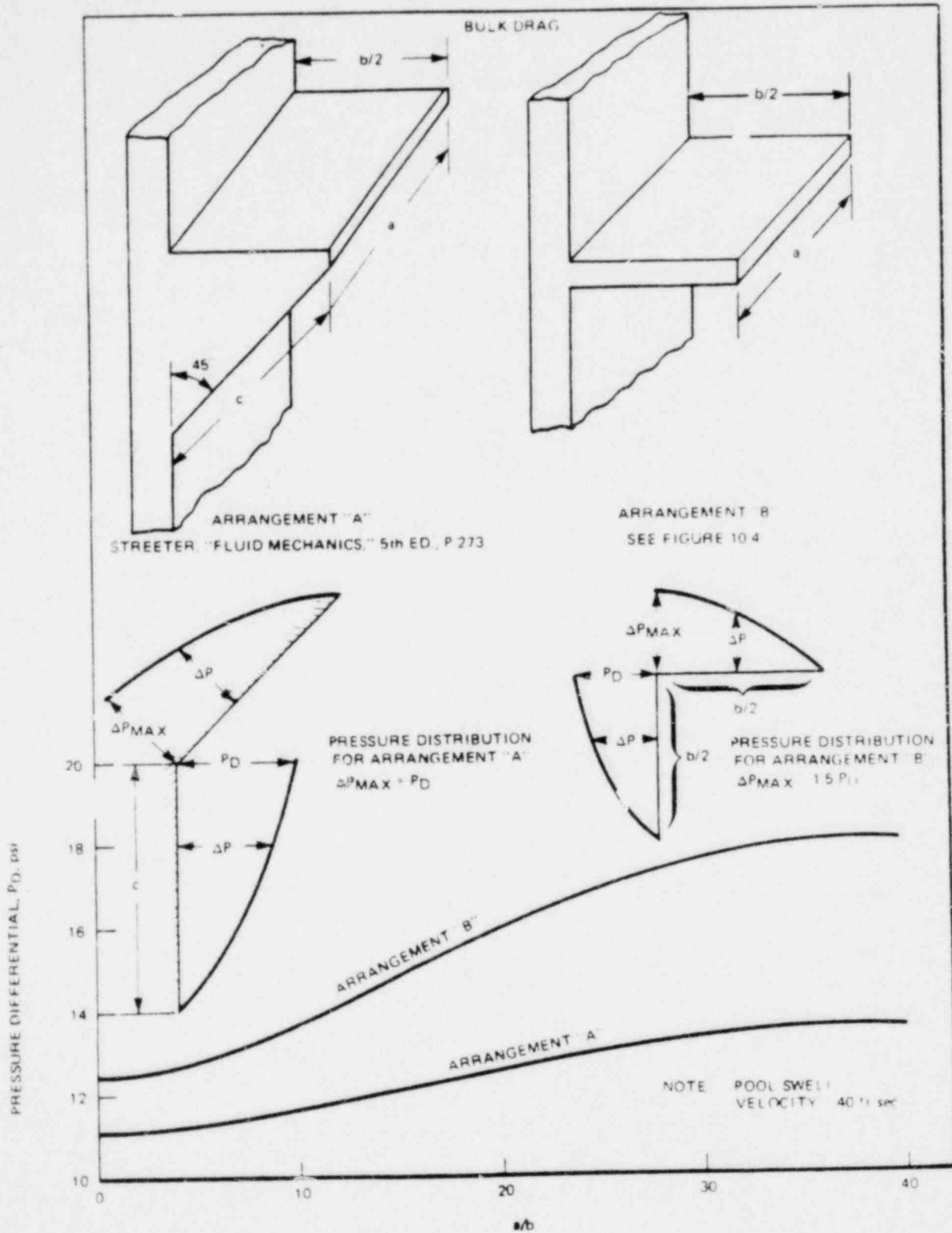


Figure 6.8. Drag Loads on Protruding Structures Due to Pool Swell

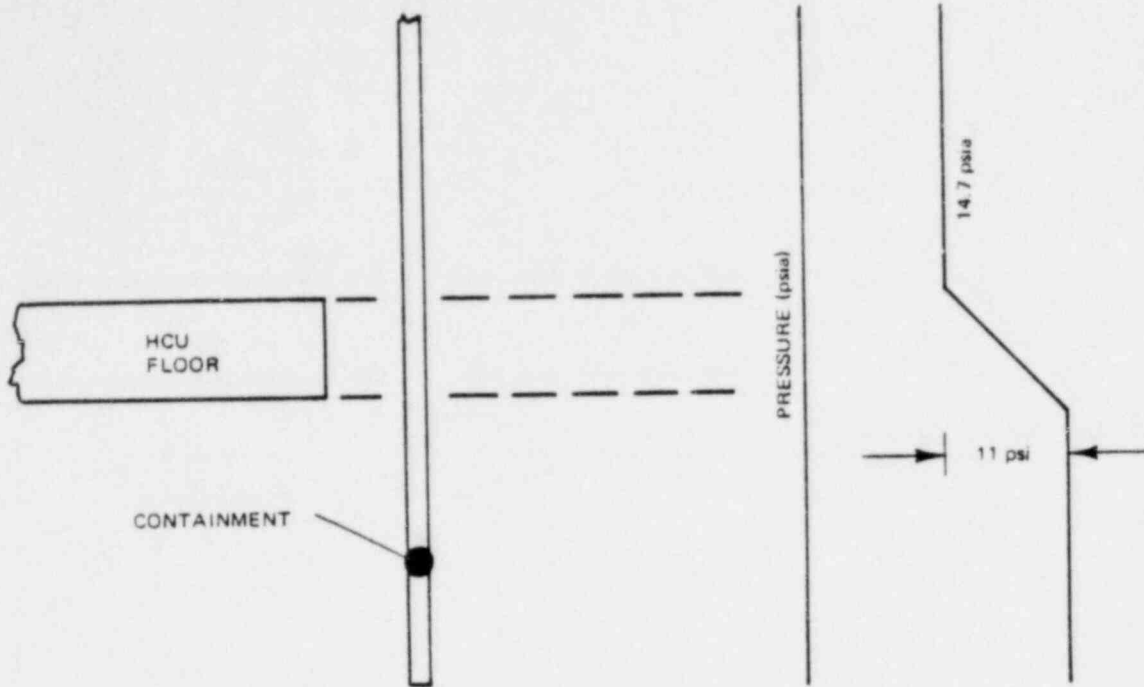


Figure 6.9. Containment Loading Due to Flow ΔP ACROSS HCU FLOOR

This figure is PROPRIETARY and is provided under separate cover.

Figure 6.10. Typical Containment Wall and Basemat Pressure Traces During
Condensation, Run 23 (Ref. Test 5807)

This figure is PROPRIETARY and is provided under separate cover.

Figure 6.11. Containment Wall and Basemat Pressure Time Histories,
Test 5807, Run 11

This figure is PROPRIETARY and is provided under separate cover.

Figure 6.12. Containment Wall Chugging Pressure Time History
Test Series 5707 Run 9

This figure is PROPRIETARY and will be provided under separate cover.

Figure 6.13. Basemat Chugging Pressure Time History,
Test Series 5707 Run 9

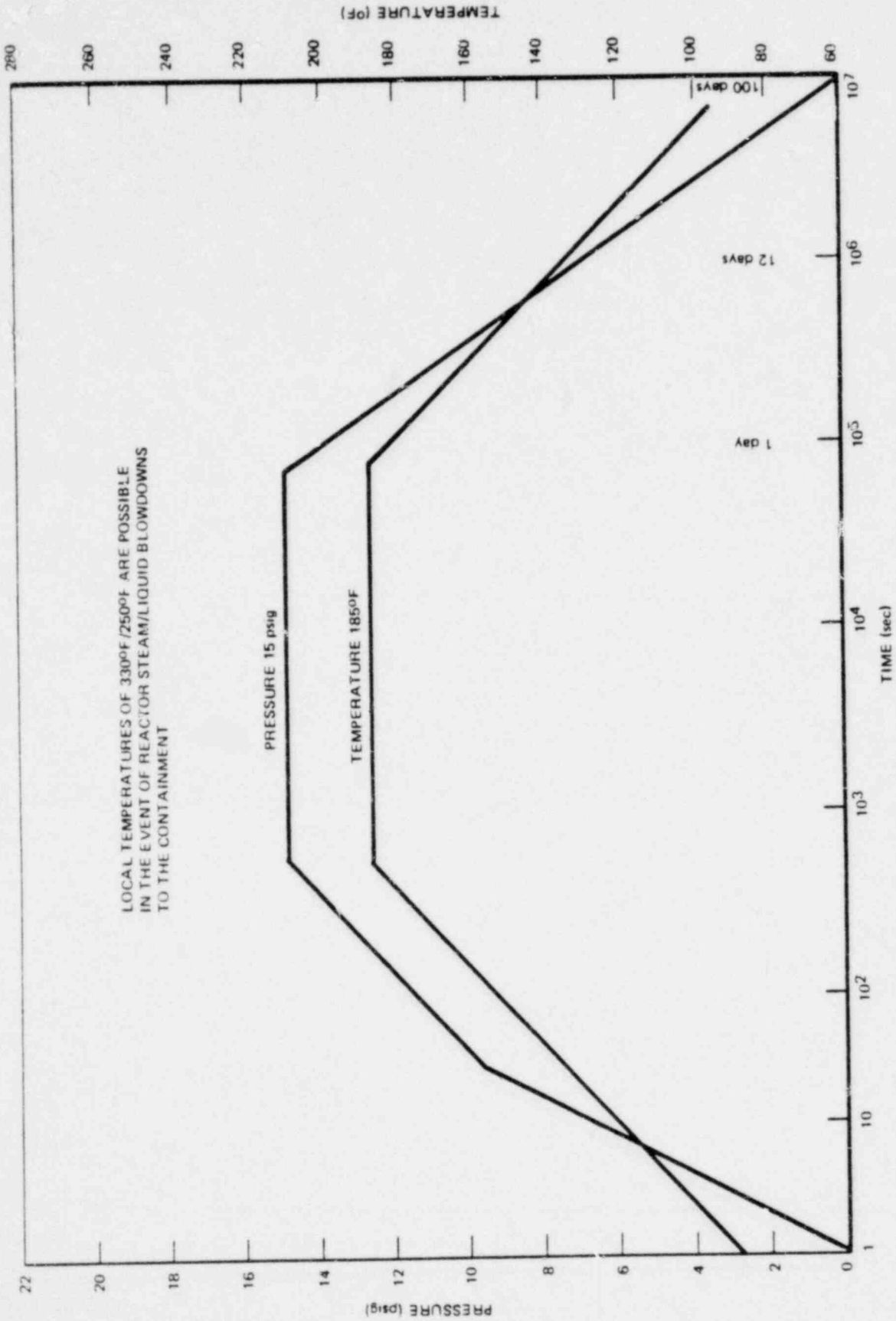


Figure 6.14. Containment Atmosphere Bulk Temperature and Pressure Design Envelope for All Breaks

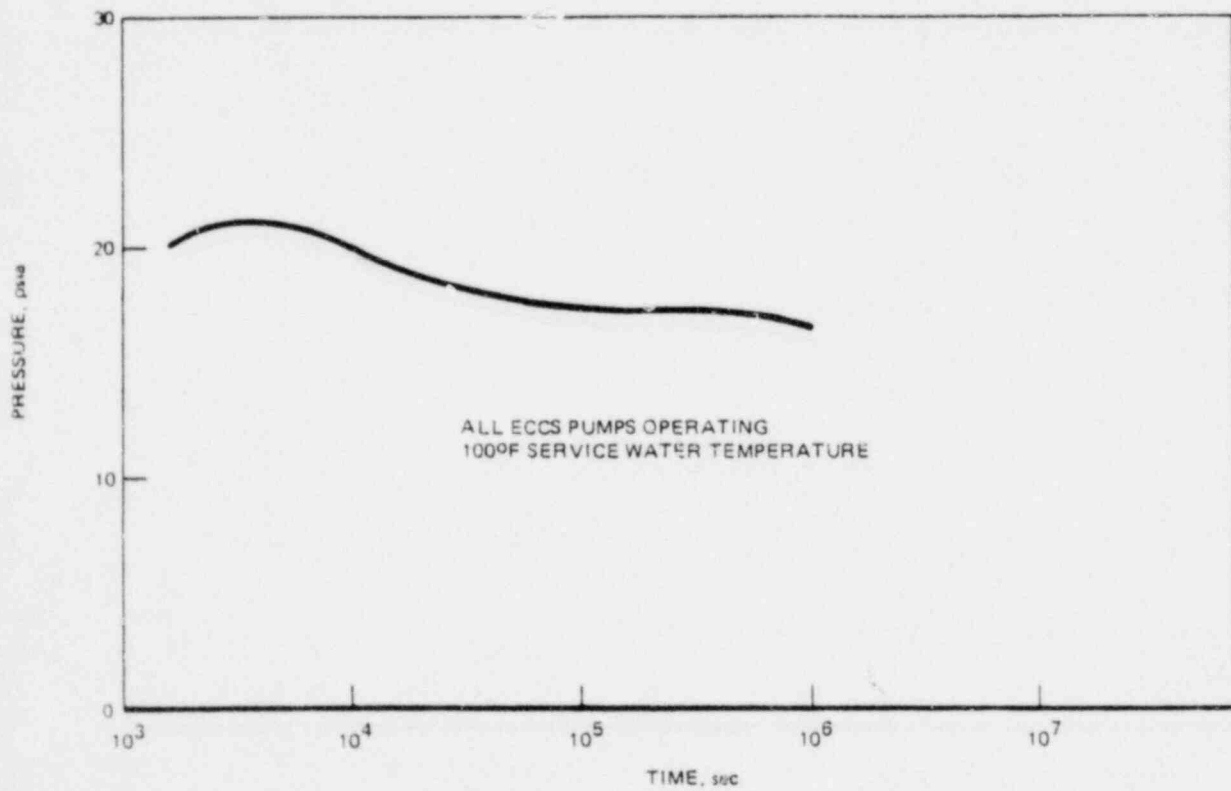
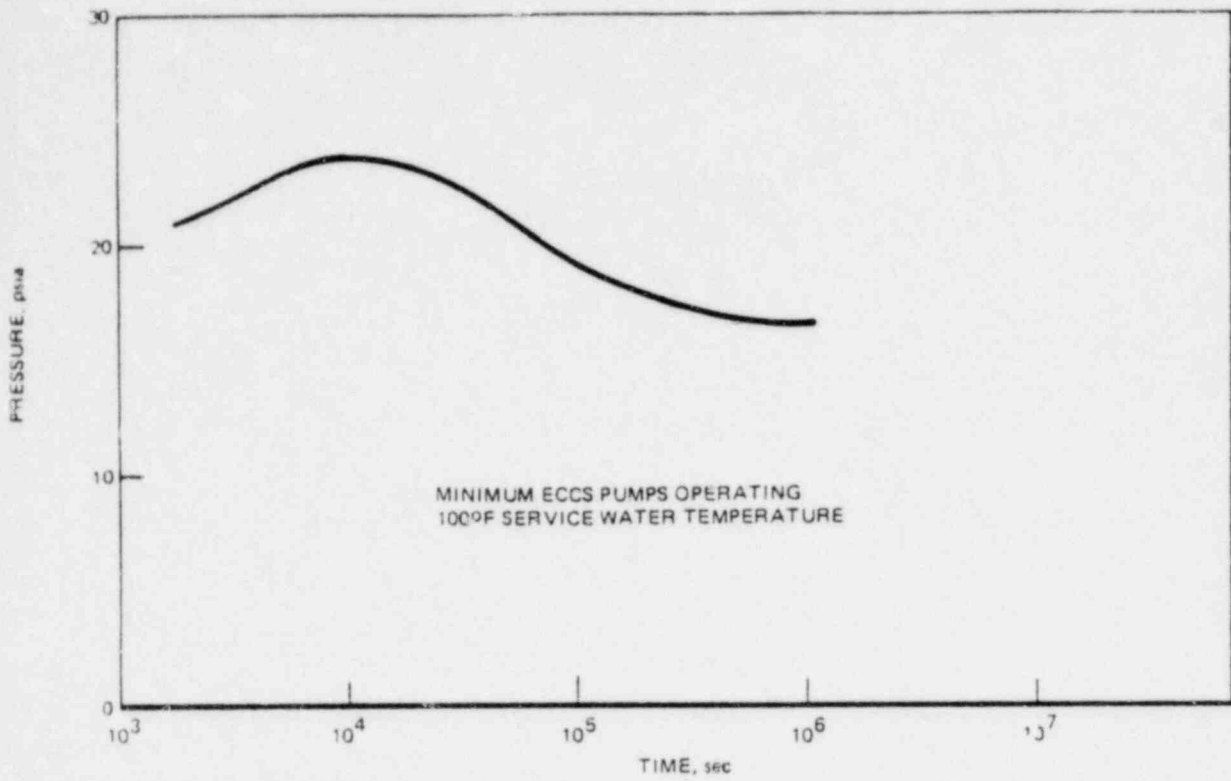


Figure 6.15. Long Term Containment Pressure Following a DBA

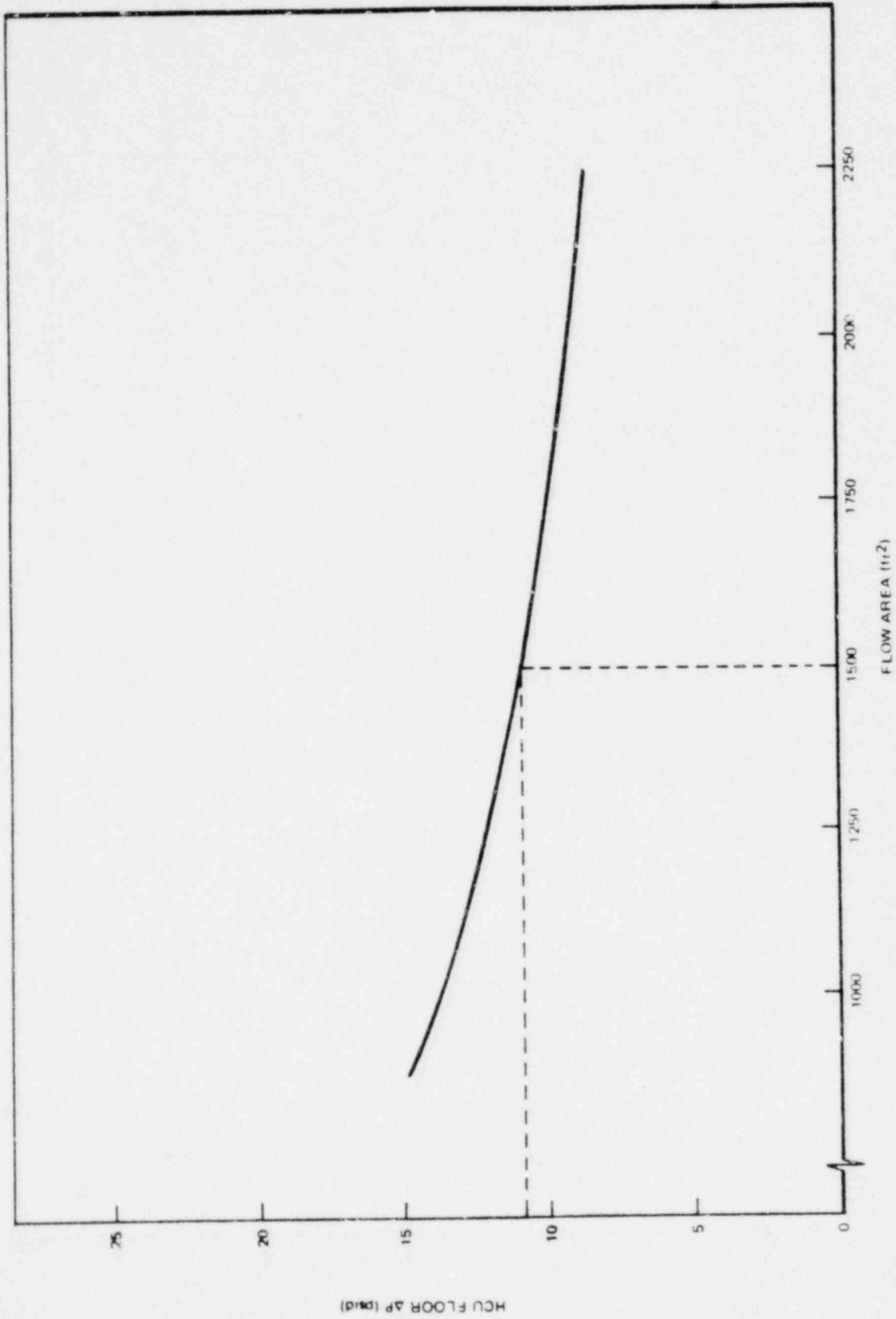


Figure 6.16. HCU Floor ΔP vs HCU Floor Open Area

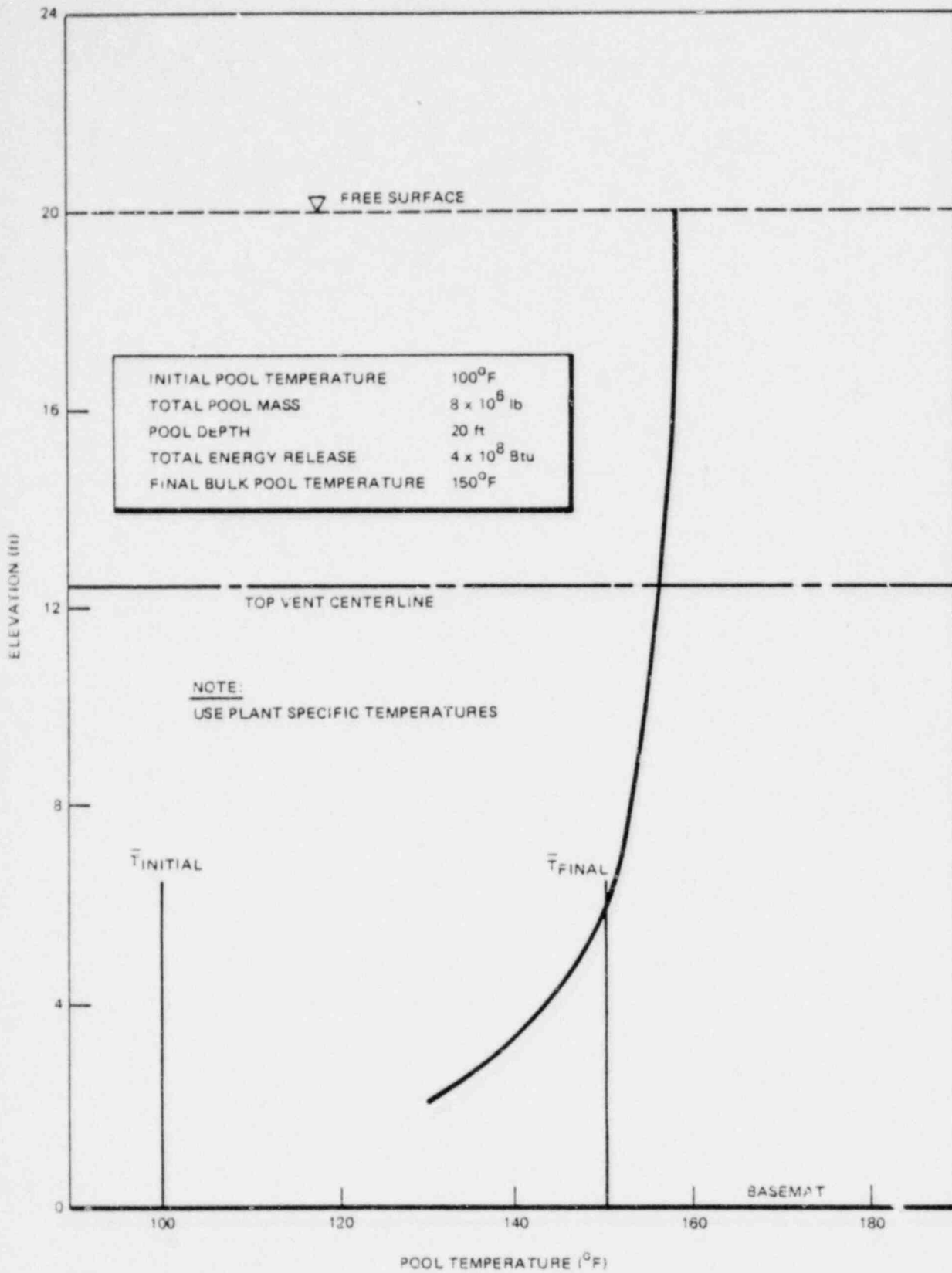


Figure 6.17. Suppression Pool Temperature Profile for Large Breaks

7. SUPPRESSION POOL BASEMAT LOADS

In addition to the normal, seismic, deadweight and hydrostatic pressure loadings, that section of the basemat which forms the bottom of the suppression pool also experiences dynamic LOCA loads and oscillatory loads during safety/relief valve actuation. The safety/relief valve loads are discussed in Attachment A.

The outer half of suppression pool floor will experience a 10 psi bulk pressure load associated with initial air bubble formation as discussed in Section 6.1.3. This pressure rise above hydrostatic is assumed to increase to 21.8 psi at the drywell wall - with the increase from 10 psi to 21.8 psi to be assumed linear and distributed over 50% of the pool width as indicated in Figure 7.1. This specification is based on the observation that the maximum pressure that the initial bubble can ever have is the maximum drywell pressure during the accident. Data trace no. 1 shown on Figure 6.4 indicates that the pressure increase is no greater than 10 psi at a point halfway across the suppression pool. Thus the specification that the pressure increases linearly between this point and the drywell wall will bound the actual pressure distribution. During the condensation and chugging phases of the postulated LOCA blowdown, the loading on the basemat is the same as that on the containment. See Sections 6.1.9 and 6.1.10.

The containment pressure increases to 3 psi due to drywell air carryover and the long term pressure and temperature increases as shown on Figure 6.15. The time history of these pressure transients is as shown on Figures 6.1, 6.2 and 6.3.

Safety/relief valve oscillating loads are defined in Attachment A. The net loading on the suppression pool liner will reverse during the negative pressure phase of the oscillation, and this lifting load on the liner needs to be considered during the design process. Where ground water level is a concern, this pressure should also be considered in the basemat liner design.

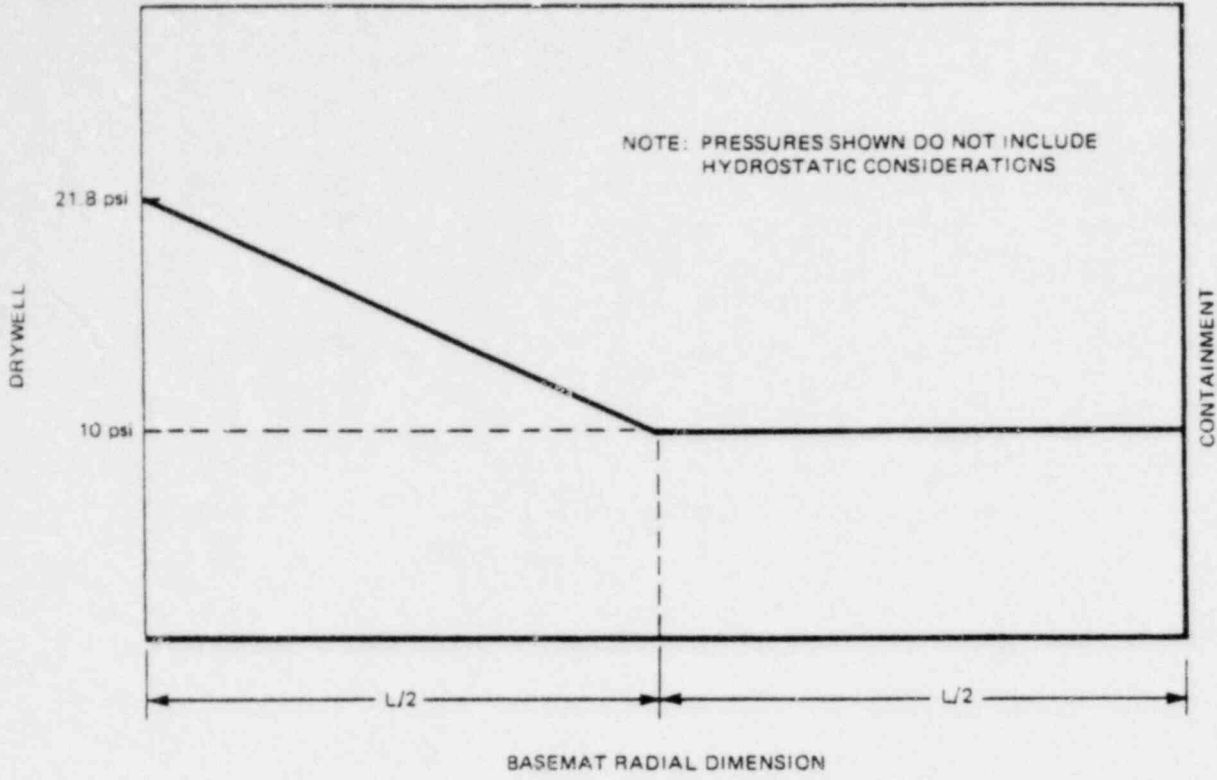


Figure 7.1. Pool Boundary Loads During Bubble Formation

8. LOADS ON STRUCTURES IN THE SUPPRESSION POOL

There are certain structures within the suppression pool which will experience dynamic loads during both loss-of-coolant accidents and/or safety/relief valve actuation.

8.1 DESIGN BASIS ACCIDENT

Figure 8.1 is the bar chart that defines the loads that structures in the suppression pool experience during the LOCA.

8.1.1 Vent Clearing Jet Load

During the initial phase of the DBA, the Drywell air space is pressurized and the water in the weir annulus vents is expelled to the pool and induces a flow field in the suppression pool. This induced flow field creates a dynamic load on structures submerged in the pool. However, this dynamic load is less (see attachment G) than the load induced by the LOCA air bubble which forms after the water is expelled. Since the air bubble dynamic load is bounding, this load is conservatively used in place of the water jet load. The air bubble load is discussed in Section 8.1.2 and attachment G.2.2.

8.1.2 Drywell Bubble Pressure and Drag Loads Due to Pool Swell

During the initial phase of the DBA, pressurized drywell air is purged into the suppression pool through the submerged vents. After vent clearing, a single bubble is formed around each top vent. It is during the bubble growth period that unsteady fluid motion is created within the suppression pool. During this period all submerged structures below the pool surface will be exposed to transient hydrodynamic loads.

The methodology and calculation procedures for determining submerged structures drag loads are discussed in attachment G.2.3.

Structures in the suppression pool should be designed conservatively for the LOCA drywell bubble pressure (see Figure 7.1) and acceleration drag (attachment G). This applies to small submerged structures, e.g., pipes.

8.1.3 Fail Back Loads

There is no pressure increase in the suppression pool boundary during pool fall back as discussed in Section 4.1.6. Structures within the containment suppression pool that are above the bottom vent elevation will experience drag loads as the water level subsides to its initial level. For design purposes, it is assumed that these structures will experience drag forces associated with water flowing at 35 ft/sec; that is the terminal velocity for a 20 ft free fall and is a conservative, bounding number. Free fall height is limited by the HCU Floor.

8.1.4 Condensation Loads

Steam condensation begins after the vent is cleared of water and the drywell air has been carried over into the wetwell. Condensation oscillation phase is vibratory in nature and induces a bulk water motion and therefore creates drag forces on structures submerged in the pool. This condensation oscillation continues until pressure in the drywell decays.

The methodology and calculation procedures for determining condensation loads on submerged structures are discussed in attachment G.2.5.

8.1.5 Chugging

Following the condensation oscillation phase of the blowdown the vent mass flux falls below a critical value and a random collapse of the steam bubbles occurs. This pressure suppression phase is called chugging and causes a high pressure wave (spike) on structures submerged in the pool.

The methodology and calculation procedures for determining chugging loads on submerged structures are discussed in attachment G.2.6.

8.1.6 Compressive Wave Loading

As discussed in Section 6.1.1, the very rapid compression of the drywell air theoretically generates a compressive wave. But as pointed out in Sections 6.1.1 and 6.1.2, there were no loads recorded on the containment wall in PSTF for this phenomena. From this, it can be concluded that compression wave loads on structures in the suppression pool are significantly smaller than loads caused by the water jet, for structures close to drywell. For structures near the containment, neither compressive or jet loads are significant.

8.1.7 Safety Relief Valve Actuation

Loads on submerged structures due to safety relief valve actuation are discussed on Attachment G.

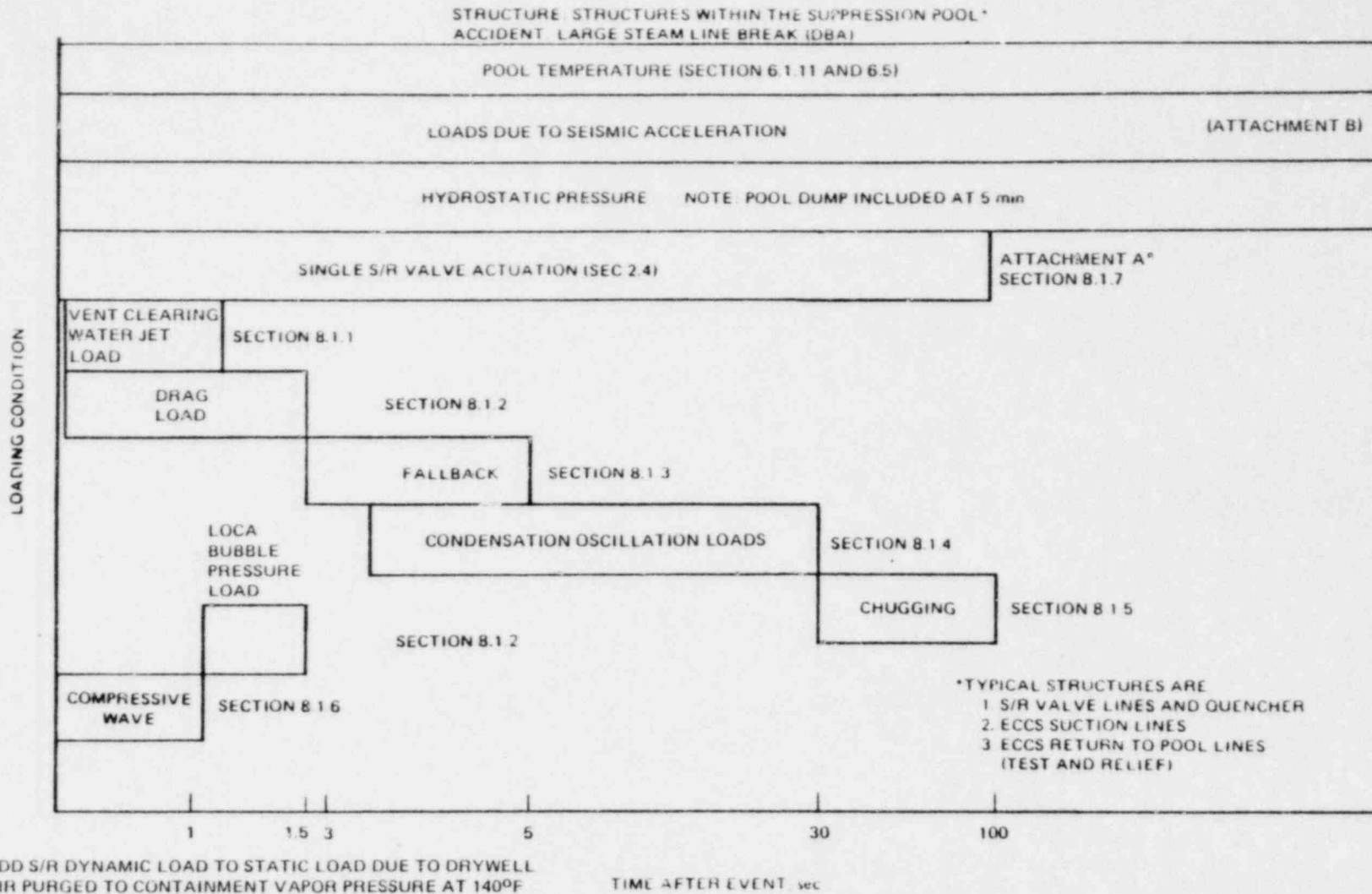


Figure 8-1. Structures within Suppression Pool-Loading Chart for DBA

011880

22A4365
Rev. 4

22A4365
Rev. 3

8-5

Deleted
Sh 8-5

090779

Deleted
Sh 8-6

9. LOADS ON STRUCTURES AT THE POOL SURFACE

Some structures have their lower surfaces either right at the suppression pool surface or slightly submerged. This location means that these structures do not experience the high pool swell impact loads discussed in Section 10. However, they experience pool swell drag loads and LOCA induced bubble loads. Relief valve loads must also be considered. These are:

- (a) Pool swell drag loads produced by water flowing vertically past the structures at 40 ft/sec. (See Section 8.1.2 and Attachment I).
- (b) Pressure loads generated by formation of the vent exit air bubble immediately following LOCA vent clearing. This type of load will result when the structure is expansive enough to restrict pool swell and cause the bubble pressure to be transmitted through the pool to the under side of the structures. For the GE reference design, the TIP and drywell personnel lock platforms and the sump tanks below are the only structures in this category. All are located on the drywell wall. The maximum upward floor pressure specified for this design is equal to the maximum drywell pressure 21.8 psid (see Figure 4.4). Similar structures located on the containment wall would be designed for a maximum upward floor pressure of 10.0 psid (see Figure 7-1). This is conservative because the bubble pressure can never exceed the drywell pressure, and no credit is taken for the attenuation of pressure associated with the head of water above the bubble. These structures should be designed conservatively for the combined loads specified above (i.e., drag loads and bubble pressure).
- (c) Loads due to the safety/relief valve actuation. See Attachment A. Only structures with surfaces in the suppression pool will experience the S/R valve bubble loads.

Pool fall back loads are as discussed in Section 4.1.6.

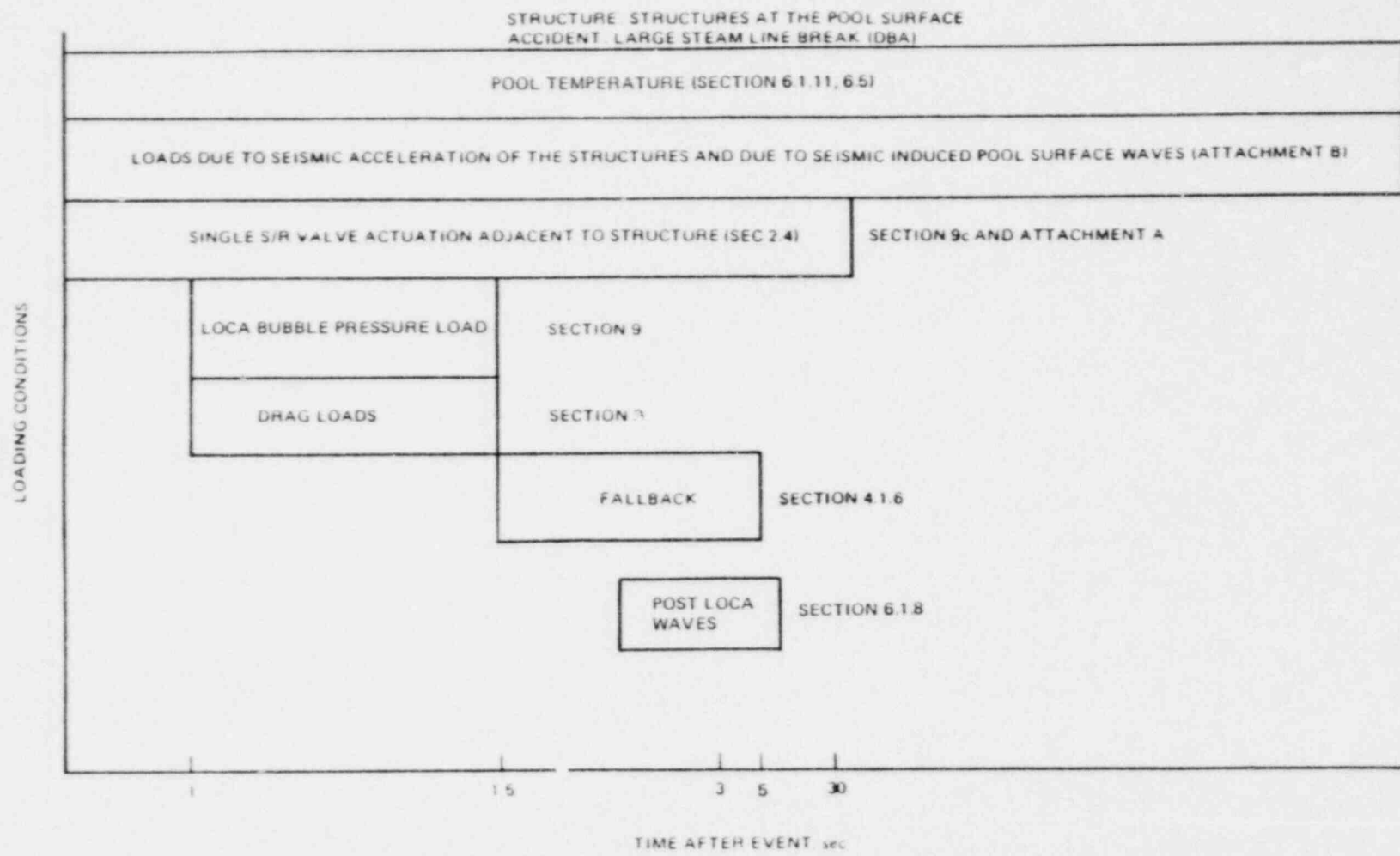


Figure 9-1. Structures at the Pool Surface-Loading Chart During DBA

090779

22A4365
Rev. 3

10. LOADS ON STRUCTURES BETWEEN THE POOL SURFACE AND THE HCU FLOORS

Equipment and platforms located in the containment annulus region, between the pool surface and the HCU platform, experience pool swell induced dynamic loads whose magnitude is dependent upon both location and the geometry of the structure. The pool swell phenomenon can be considered as occurring in two phases, i.e., bulk pool swell followed by froth pool swell. The pool swell dynamic loading conditions on a particular structure in the containment annulus are dependent upon the type of pool swell that the structure experiences. In addition to location, the size of the structure is also important. Large platforms or floors will completely stop the rising pool, and thus incur larger loadings whereas small pieces of equipment and structural items will only influence the flow of a limited amount of water in the immediate vicinity of the structure. The steam tunnel and HCU floors are the only structures that could be categorized as expansive. Section 11 discusses these structures.

The remainder of this section deals with relatively small structures defined as approximately 20 inches wide. Figure 10-1 is the loading bar chart for these structures. Structures at this elevation will be subjected to vertical loads only. Horizontal loading mechanisms are not identified and 1/3 scale impact tests verify this conclusion.

10.1 IMPACT LOADS

Figure 10-2 shows the impact loading profile that is applicable to small structures which are exposed to bulk pool swell. The PSTF air test data shows that after the pool has risen approximately 1.6 times vent submergence (i.e., 12 ft.) the ligament thickness has decreased to 2 ft or less and the impact loads are then significantly reduced. However, bulk pool swell impact loading is applied uniformly to any structures within 18 ft of the pool surface as shown on Figure 10-2. For evaluating the time at which impact occurs at various elevations in the containment annulus, a water surface velocity of 40 ft/sec is assumed. Bulk pool swell would start 1 sec after LOCA.

The basis for the loading specification is the PSTF air test impact data discussed in Reference 7. Specifically, test Series 5706 run number 4 is used. These tests involved charging the reactor simulator with 1000 psia air and blowing down through a 4.25 inch orifice. Fully instrumented targets located over the pool provided the impact data.

Additional tests have been conducted which provide impact data for typical structures that experience bulk pool swell. Data from these tests (Series 5805) indicates that the specified design load is conservative.

It should be noted that impact loads are not specified for gratings. The width of the grating surfaces (typically 1/4 inch) do not sustain an impact load. This has been verified in the one third scale PSTF test Series 5805. Figure 10.3 should be used for calculating grating drag loads.

For structures above the 19 ft elevation but below the HCU floors, the froth impingement data portion shown in Figure 12.2 should be used. Again, this impingement load is applied uniformly to all small structures with the time history shown.

For structures between 18 and 19 feet above the suppression pool design loads and duration are linearly interpolated from the values shown on Figures 12.2 and 10.2.

Figure 10.6 is a summary of the loading specifications for small structures in the containment annulus as a function of height above the pool.

The influence of seismic induced submergence variations on the pool swell transient and resulting impact loads has been considered. It has been concluded that the effect on the magnitude pool swell impact load is not significant. This conclusion is based on a consideration of the influence of submergence on swell velocity and the significant load attenuation which will result from the pool surface distortions. The very significant margins between the specified loads and the expected loads (see Attachment J) provides confidence

that any local increase in swell velocities will not result in loads in excess of design values.

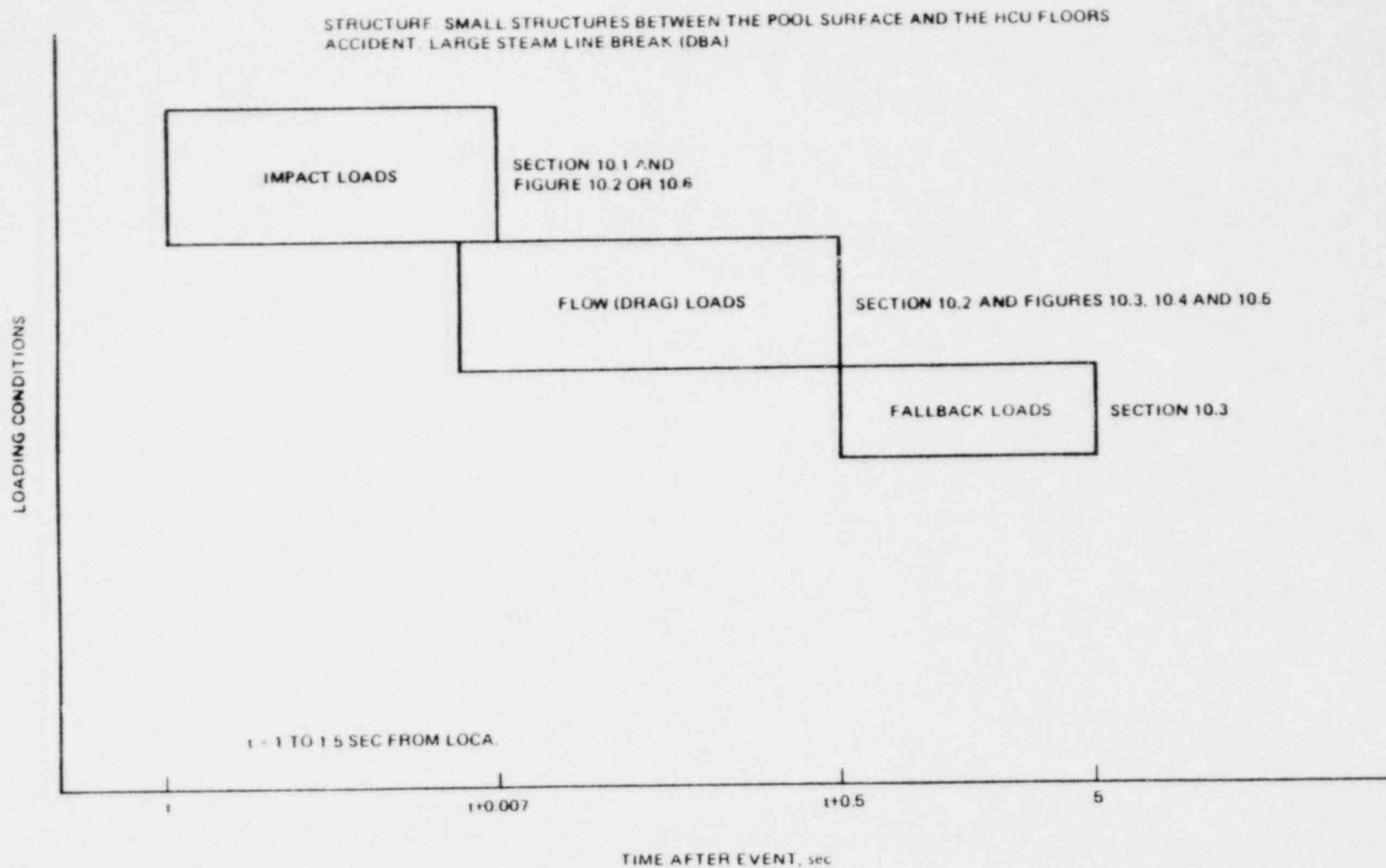
The conservatism in these load definitions are illustrated in Attachment J.

10.2 DRAG LOADS

In addition to the impact loads, structures that experience bulk pool swell are also subject to drag loads as the pool water flows past them with velocities as high as 40 ft/sec. Figures 10-3, 10-4 and 10-5 provide drag load information for geometrical shapes. Data is applied to all small structures in the containment annulus between the pool surface and the HCU floors.

10.3 FALL BACK LOADS

Fall back loads are discussed in Sections 4.1.6, 6.1.7, and 8.1.3.

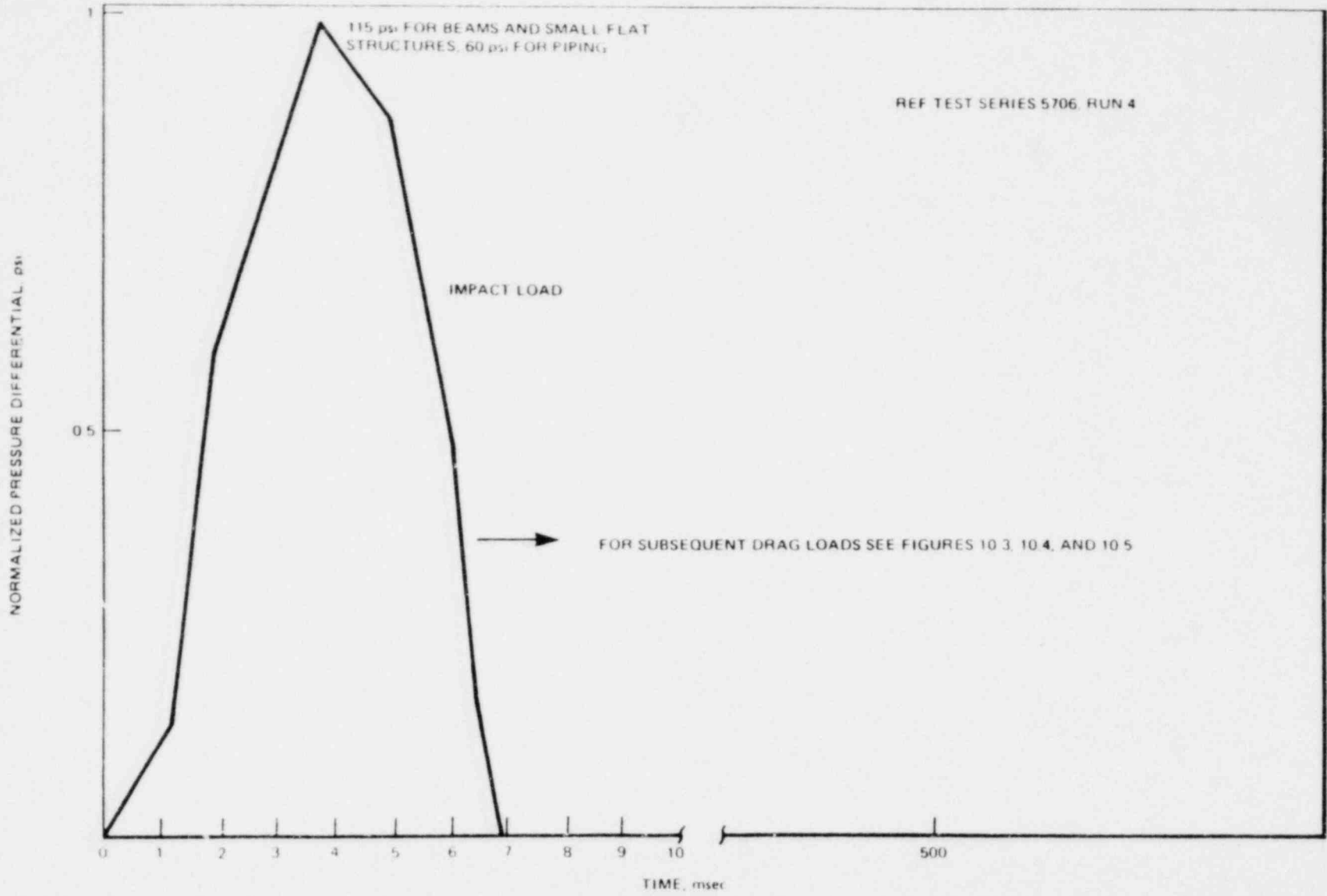


22A4365
Rev. 3

090779

10-4

Figure 10-1. Small Structures Between the Pool Surface and the HCU Floor-Loading Chart During DBA



042178

22A4365
Rev. 2

10-5

Figure 10-2. Profile of Impact Loads on Small Structures Within 18 ft of the Pool Surface

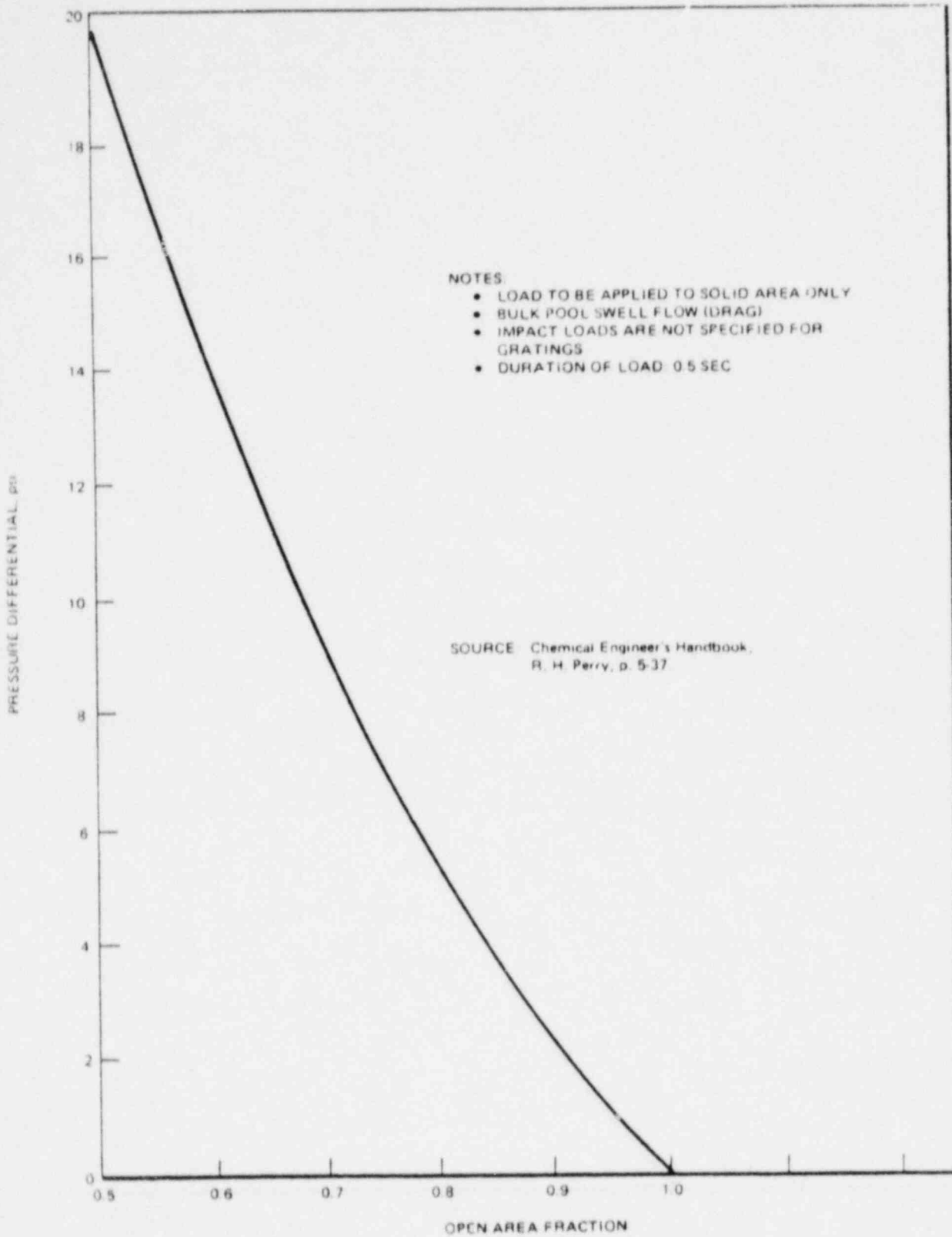


Figure 10-3. Pressure Drop Due to Flow Across Grating Within 18 ft of the Pool Surface

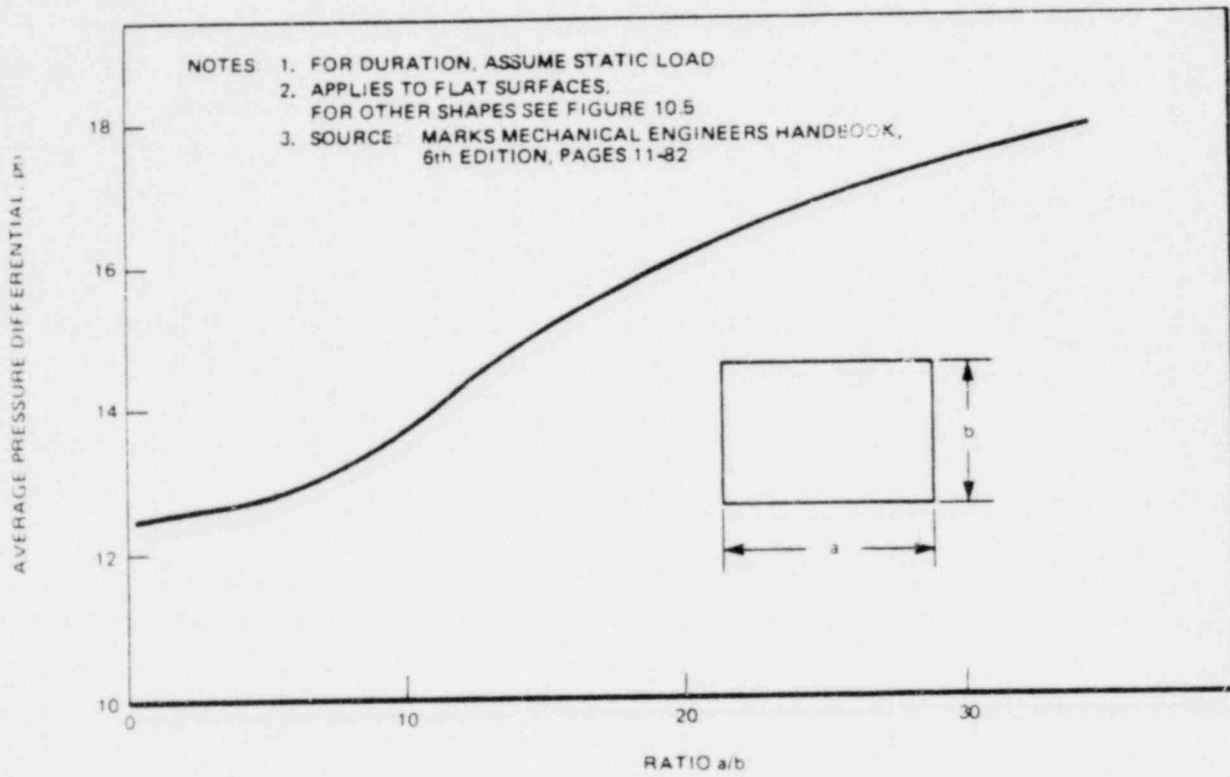


Figure 10-4. Drag Load on Solid Structures within 18 ft of the Pool Surface

(REF: FLUID MECHANICS, VICTOR L. STREETER, 5th ED. MC GRAW HILL)

BODY SHAPE	DRAG COEFFICIENT* C_D			BASED ON $V = 40$ fps PRESSURE DIFFERENTIAL (psi)	BASED ON $V = 35$ fps PRESSURE DIFFERENTIAL (psi)
CIRCULAR CYLINDER	1.2			13	10
ELLIPTICAL CYLINDER	0.6		2:1	7	5
ELLIPTICAL CYLINDER	0.32		4:1	4	3
ELLIPTICAL CYLINDER	0.29		8:1	3	2
SQUARE	2.0			22	17
TRIANGLE	2.0		120°	22	17
TRIANGLE	1.72		120°	19	14
TRIANGLE	2.15		90°	23	18
TRIANGLE	1.60		90°	17	13
TRIANGLE	2.20		60°	24	18
TRIANGLE	1.39		60°	15	12
TRIANGLE	1.8		30°	19	15
TRIANGLE	1.0		30°	11	8
SEMITUBULAR	2.3			25	19
SEMITUBULAR	1.12			12	9

*These drag coefficients are conservative because they are for low Reynold's Number flow conditions ($10^4 - 10^5$ Range). Use of lower values may be used if its applicability can be demonstrated.

Figure 10-5. Drag Loads for Various Geometries (slug flow)

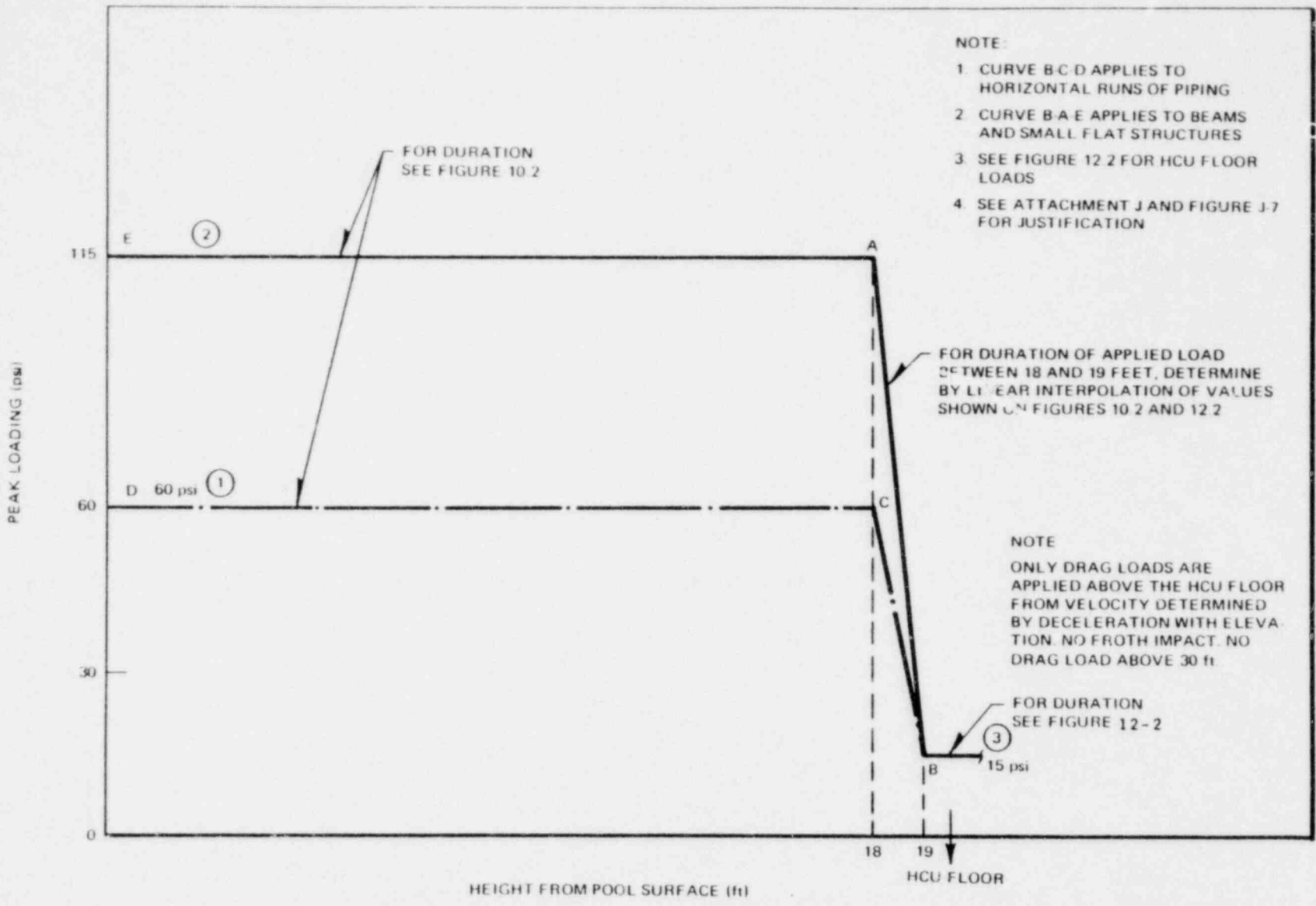


Figure 10-6. Summary of Pool Swell Loading Specifications for Small Structures in the Containment Annulus (Not Applicable to the Steam Tunnel or Expansive HCU Floors)

101678

22A4365
Rev. 2

10-9

11. LOADS ON EXPANSIVE STRUCTURES AT THE HCU FLOOR ELEVATION

At the HCU floor elevation there are portions of the floor which are comprised of beams and grating and other portions that are solid expansive structures. The bottom of the steam tunnel is at approximately the same elevation (19 ft-6 in.). The small structure portion (beams and grating) of the HCU floor is discussed in Section 12.

The expansive structures at this elevation experience an impulsive loading followed by an 11 psi pressure differential. The impulsive load is due to the momentum of the froth which is decelerated by the expansive structure. The 11 psi pressure differential is based on an analysis of the transient pressure in the space between the pool surface and the HCU floor resulting from the froth flow through the 1500 ft² vent area at this elevation (see Section 6.1.6). Figure 11-1 shows the loading sequences and Figure 12-2 shows the loading history.

PSTF test Series 5706 is the basis for the froth impingement load of 15 psi lasting for 100 msec (see Reference 9). Representative tests of the expected Mark III froth conditions at the HCU floor are the 5 ft submergence tests of Series 5801, 5802, 5803 and 5804. These tests confirmed the adequacy of the 15 psi impingement load.

The 11 psi froth flow pressure differential lasting for 3 sec is based on an analysis of the transient pressure in the space between the pool surface and the HCU floor. The value of 11 psi is from an analysis that assumes that the density of the flow through the annulus restriction is the homogeneous mixture of the top 9 ft of the suppression pool (i.e., 18.8 lbm/ft³). Supplement 1 to Reference 1 describes the analytical model used to simulate the HCU floor flow pressure differential and presents a comparison of model predictions with test data. This is a conservative density assumption confirmed by the PSTF 1/3 scale tests which show average densities of approximately 10 lbm/ft³. Reference 11 indicates the HCU floor pressure differential is in the 3 to 5 psi range.

The potential for circumferential variations in the pressure transient in the wetwell region beneath the HCU floor have been examined and on the basis of bounding calculations it is concluded that the pressure variation will be less than 0.5 psid (see Attachment F).

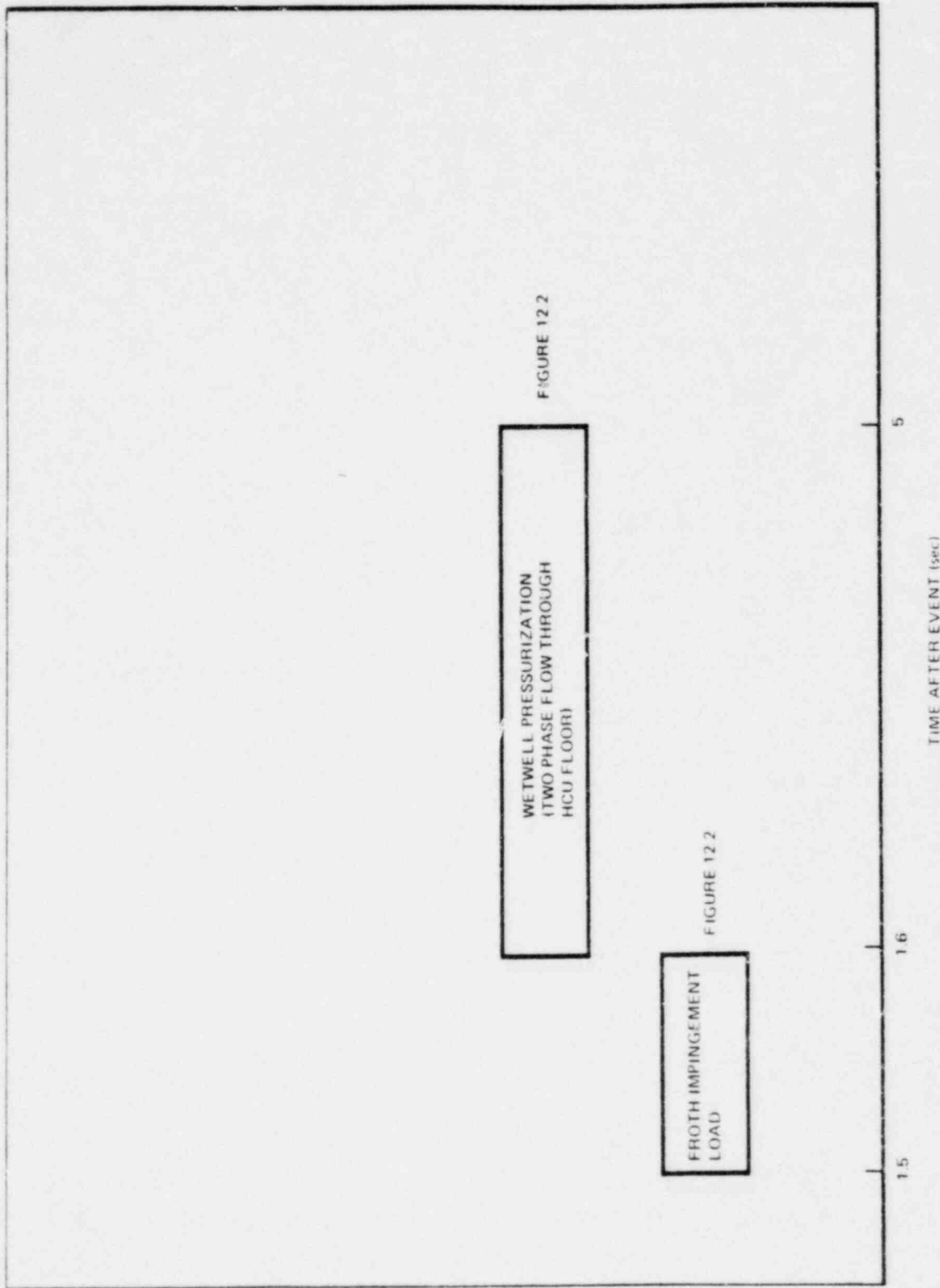


Figure 11-1. Expansive Structures at HCU Elevation - Loading During DBA

12. LOADS ON SMALL STRUCTURES AT AND ABOVE THE HCU FLOOR ELEVATION

Structures at the HCU floor elevation experience "froth" pool swell which involves both impingement and drag type forces. Figure 12.1 shows the loading sequences. Only structures in the line of sight of the pool will experience froth pool swell loads.

PSTF air tests show that the structures experience a froth impingement load of 15 psi lasting for 100 milliseconds (Reference 9). The impingement data is shown on Figure 12.2. Structures must be designed for this short term dynamic impingement load; grating structures are not subjected to this impingement load (Reference 12).

As discussed in Section 6.1.6, following the initial froth impingement there is a period of froth flow through the annulus restriction at this elevation.

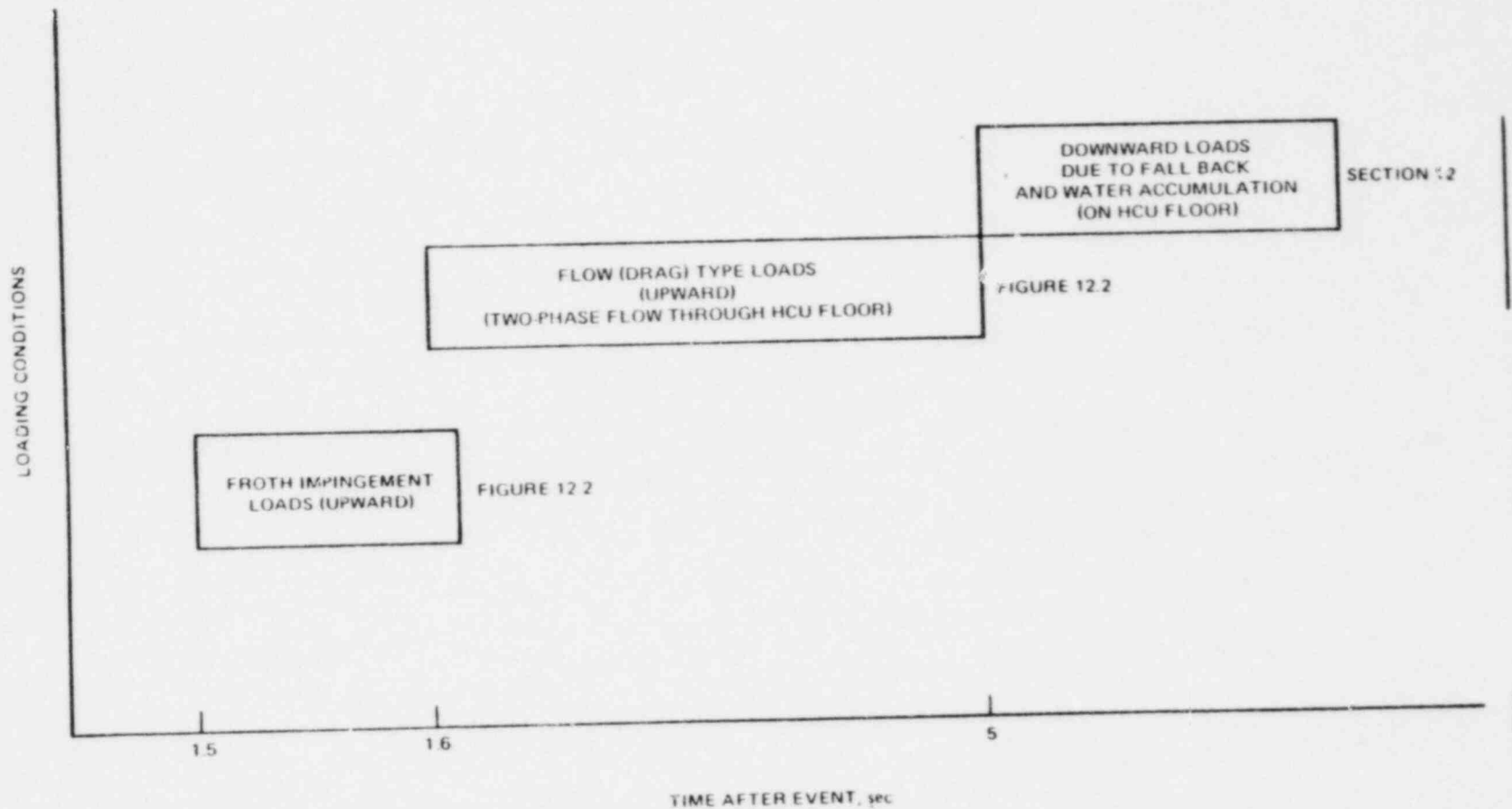
The froth flow pressure differential load (i.e., drag type force) specification of Figure 12.2 is based on an analysis of the transient pressure in the space between the pool surface and the HCU floor. The value of 11 psi is from an analysis that assumes that the density of the flow through the annulus restriction is the homogeneous mixture of the top 9 ft of the suppression pool water and the free air between the HCU floor and the pool (i.e., $18.8 \text{ lb}_m/\text{ft}^3$). This is a conservative density assumption confirmed by the PSTF 1/3 scale tests which show an average density of approximately $10 \text{ lb}_m/\text{ft}^3$. Representative tests of the expected Mark III froth conditions at the HCU floor are the 5 ft submergence tests of Series 5801, 5802, 5803, and 5804. Reference 11 indicates the HCU floor pressure differential during these tests was in the 3 to 5 psi range (Drag load on HCU floor).

Those small structures above the HCU floor that could be exposed to pool swell froth may be exposed to a drag load. The drag load is determined for the geometric shape of the structure (reference Figure 10.5) using a froth density of $18.8 \text{ lb}_m/\text{ft}^3$ as in the HCU floor ΔP calculation and the velocity of the froth at the elevation of the structure. The velocity used is 50 ft/sec at 19-1/2 ft above the suppression pool and is decelerated by the effects of gravity. The velocity of 50 ft/sec is a bound of the available data (Reference 13). No pool swell is assumed for structures more than 30 ft above the suppression pool.

The potential for circumferential variations in the pressure transient in the wetwell region beneath the HCU floor have been examined and on the basis of bounding calculations it is concluded that the pressure variation will be less than 0.5 psid. (See Attachment F.)

Since the air tests were performed, additional PSTF tests have been conducted with the specific objective of providing further data on the interaction of pool swell with the HCU floors. The test results are in Reference 11. Supplement 1 to Reference 1 describes the analytical model used to simulate the HCU floor floor pressure differential and presents a comparison of model predictions with test data. The model is shown to be conservative.

STRUCTURE STRUCTURES AT THE HCU FLOOR ELEVATION
ACCIDENT LARGE STEAM LINE BREAK (DBA)



22A4365
Rev. 3

Figure 12.1. Small Structures at the HCU Floor Elevation - Loading Chart During DBA

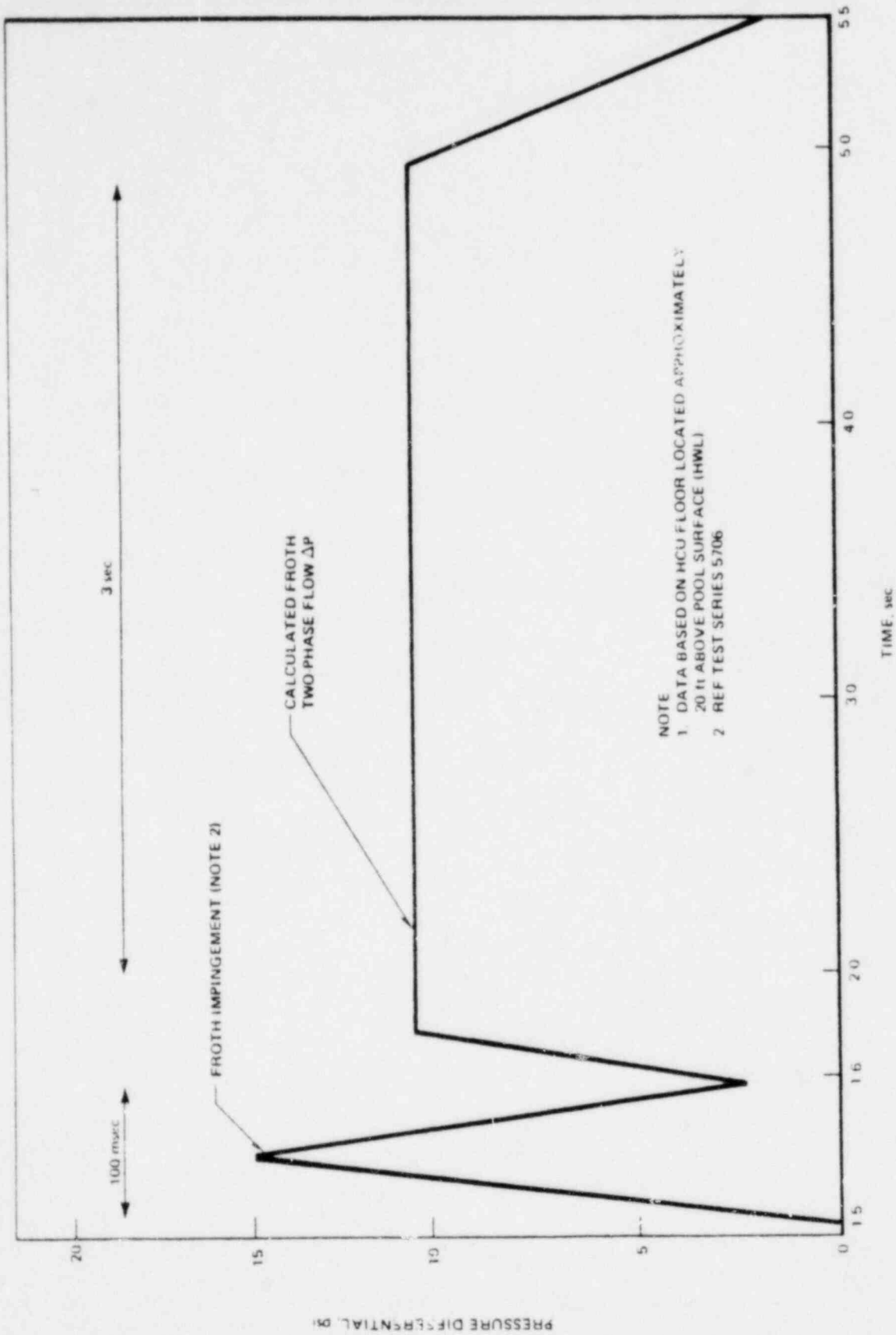


Figure 12.2. Loads at HCU Floor Elevation Due to Pool Swell Froth Impact and Two-Phase Flow

REFERENCES

NOT ALL THE REFERENCES APPEAR IN THE TEXT. THE FIRST 11 REFERENCES REPRESENT A COMPREHENSIVE BIBLIOGRAPHY OF REPORTS RELATED TO GE'S PSTF PROGRAM.

1. Bilanin, W. J., The General Electric Mark III Pressure Suppression Containment System Analytical Model, NEDO-20533, June 1974 and Supplement 1, August 1975.
2. Mark III Confirmatory Test Program Progress Report, April 1973. NEDM-10848 (Proprietary Report).
3. Mark III Analytical Investigation of Small-Scale Tests Progress Report, August 1973. NEDO-10976.
4. Mark III Confirmatory Test Program Phase 1 - Large Scale Demonstration Tests, October 1974, NEDM-13377 (Proprietary Report).
5. Third Quarterly Progress Report: Mark III Confirmatory Test Program, NEDO-20210, December 1973 (Proprietary Report).
6. Fourth Quarterly Progress Report: Mark III Confirmatory Test Program, NEDO-20345, April 1974 Supplement 1 (Proprietary Report).
7. Fifth Quarterly Progress Report: Mark III Confirmatory Test Program, NEDO-20550, July 1974 Supplement 1 (Proprietary Report).
8. Sixth Quarterly Progress Report: October 1974. (Letter Transmittal to NRC Staff.) (Proprietary Data Attached.)
9. Seventh Quarterly Progress Report: Mark III Confirmatory Test Program, NEDO-20732-P, December 1974 (Proprietary Report).
10. Eighth Quarterly Progress Report: Mark III Confirmatory Test Program, NEDO-20853-P, April 1975 (Proprietary Report).
11. Mark III Confirmatory Test Program 1/3 Scale Three Vent Tests, NEDO-13407, April 1975 (Proprietary Report).
12. Mark III Confirmatory Test Program 1/3 Scale Pool Swell Impact Tests - Test Series 5805, NEDE-13426-P, August 1975 (Proprietary Report).
13. Mark III Confirmatory Test Program 1/3 Scale Three Vent Air Tests - Test Series 5806, NEDE-13435-P, November 1975 (Proprietary Report).
14. Test Results Employed by GE for BWR Containment and Vertical Vent Loads, NEDE-21078P, October 1975 (Proprietary Report).
15. Mark III Confirmatory Test Program - $1/\sqrt{3}$ Scale Condensation and Stratification Phenomena - Test Series 5807, NEDE-21596-P, March 1977 (Proprietary Report).

16. Mark III Confirmatory Test Program - Full Scale Condensation and Stratification Phenomena - Test Series 5707, NEDE-21853-P, August 1978 (Proprietary Report).
17. Mark III Confirmatory Test Program - 1/9 Area Scale Multivalent Pool Swell Tests - Test Series 6002, NEDE-24648P, September 1979 (Proprietary Report)
18. Mark III Confirmatory Test Program, 1/9 Area Scale Condensation and Stratification Phenomena, Test Series 6003, NEDE-24720-P, November 1979 (Proprietary Report)

ATTACHMENT A
SAFETY RELIEF VALVE LOADS (QUENCHER)

	Page
A1.0 INTRODUCTION	A-5
A2.0 SUMMARY & CONCLUSIONS	A-6
A2.1 Load Reduction	A-6
A3.0 DESCRIPTION OF PHENOMENA	A-7
A4.0 ARRANGEMENT	A-10
A4.1 Distribution in Pool (Quencher Arrangement)	A-10
A4.2 SRV/DL Line Routing	A-11
A4.2.1 Line Lengths and Volume	A-11
A4.2.2 Drywell Penetration Sleeve	A-12
A4.2.3 SRV/DL Vacuum Breaker	A-13
A5.0 QUENCHER LOADS ON POOL BOUNDARY	A-28
A5.1 Pressures on Drywell, Basemat, and Containment	A-28
A5.1.1 Single S/R Valve Loads	A-29
A5.1.2 Two Adjacent S/R Valve Loads	A-29
A5.1.3 Ten S/R Valve Loads	A-29
A5.1.4 Eight S/R Valve Loads (ADS)	A-30
A5.1.5 All (19) S/R Valve Loads	A-30
A5.2 Loads on Weir Wall	A-30
A5.3 Loads on Submerged Structures	A-30
A5.4 Normalized Pressure - Time History (Theoretical Raleigh Bubble)	A-33
A5.5 Representative Pressure Time History	A-33
A5.6 Estimated Margins	A-33
A5.6.1 Peak Bubble Pressures	A-33
A5.6.2 95%-95% Confidence	A-34
A5.6.3 Margin	A-34
A6.0 OTHER LOADS ON STRUCTURES IN THE POOL	A-66
A6.1 LOCA and Pool Swell	A-66
A6.1.1 Forces on Pipes Due to Vent Clearing--Pool Swell and Fallback	A-66
A6.2 Thermal Expansion Loads	A-66
A6.3 Seismic Loads by A.E.	A-66
A6.4 Seismic Slosh Loads by A.E.	A-66

	<u>Page</u>
A7.0 QUENCHER ANCHOR LOADS	A-69
A7.1 Quencher Arm Loads and Quencher Loading Application	A-69
A7.2 Quencher Design Information	A-70
A7.2.1 Codes and Standards	A-70
A7.2.2 Design Pressures, Temperature, Loads, Configuration, and Performance	A-71
A7.2.2.1 Component Data	A-71
A7.2.2.2 SRVDL Geometry	A-71
A7.2.2.3 Quencher Design Criteria	A-72
A7.2.2.4 Quencher Configuration and Location	A-72
A8.0 S/R LOAD COMBINATIONS	A-81
A8.1 Symmetric and Asymmetric Load Cases	A-82
A8.2 SSE and OBE Considerations	A-83
A8.3 LOCA Considerations	A-83
A8.3.1 DBA with M.S. Line Break	A-84
A8.3.2 DBA with Recirculation Line Break	A-84
A8.3.3 Other SRV Conditions	A-84
A8.4 Recommended Design Load Summation	A-85
A9.0 FATIGUE CYCLES	A-87
A10.0 RECOMMENDED CALCULATION PROCEDURES FOR MARK III USERS	A-90
A10.1 Constraints	A-90
A10.2 Determine SRVDL Design	A-91
A10.3 S/R Valve Air Clearing Loads Mark III 238 Standard Plant	A-93
A10.3.1 Absolute Pressure on Basemat and Walls	A-93
A10.3.2 How to Find the Attenuated Pressure on the Drywell Wall, Basemat and Containment Wall	A-94
A11.0 PARAMETRIC STUDIES	A-104
A12.0 BASIS AND JUSTIFICATION FOR DEVELOPMENT QUENCHER LOADS	A-106
A12.1 Introduction	A-106
A12.2 Test Data Application for Mark III Containment	A-107
A12.2.1 Miniscale Test Observations	A-107
A12.2.2 Small-Scale Test Observations	A-107
A12.2.3 Large-Scale Test Observations	A-107
A12.3 Physical Parameters	A-108

	<u>Page</u>
A12.4 Correlation of Positive and Negative Pressure Peaks	A-118
A12.5 Development of Design Value Calculation Method	A-140
A12.6 Application	A-173
A12.7 SRV Load Reduction	A-209a
A12.8 References (for A12)	A-210

A1.0 INTRODUCTION

General Electric has determined that the quencher is a desirable alternative feature to minimize suppression pool boundary loads resulting from the air clearing phenomena in the Safety Relief Valve Discharge Line (SRVDL). The quencher device will be specified for the standard 238 Mark III design and is recommended for BWR-6, Mark III application.

This attachment provides the following:

- a. Recommended quencher arrangement.
- b. Recommended quencher distribution in the pool.
- c. Calculation of pool boundary loads for 238 Standard Mark III application.
- d. Definition of other loads including quencher anchor loads.
- e. S/R valve combination design load cases and estimated valve cycles.
- f. Procedures for calculating pool boundary loads for other Mark III plants.
- g. Justification and basis for quencher loads.

It should be emphasized that the specific pool boundary loads identified herein are for a particular SRVDL configuration are used for example only, and should not be used arbitrarily by other designers. Since the calculation of the quencher loads is highly sensitive to and dependent upon the SRVDL design, procedures in this attachment A are provided to obtain plant unique pool boundary loadings for other SRVDL and pool designs.

A2.0 SUMMARY AND CONCLUSIONS

Once the SRVDL routing is established the detailed calculation of the pool boundary loads resulting from the quencher air clearing transient is performed. The line air volume is the critical parameter and for the Mark III design a series combination of both 10" Schedule 40 and 12" Schedule 40 pipe is utilized in the line design. The SRVDL peak pressure is limited to 625 psid (S/R valve back pressure limit).

Table A4.3 lists the SRVDL air leg information for the 238 Standard Plant. The maximum air volume is 56.13 ft³. With this design, the maximum quencher bubble pressures are tabulated in Table A4.4. See Section A10 for clarification. This design procedure is based on single and multiple or consecutive actuation considerations at 95-95% confidence.

To assure that the initial water leg ($L_{\text{water}} \leq 18$ feet) is not exceeded following the initial actuation, vacuum breakers are used on the SRVDL. The water leg limit is a design objective for the standard 238 Mark III containment.

The design procedure requires an optimization of the SRVDL air volume to assure the 625 psid peak pressure limit is not exceeded with a minimum air volume.

Table A4.2 summarizes the SRVDL design requirements and objectives necessary to obtain the S/R valve pressure loads for the 238 Mark III containment identified in this attachment.

A.2.1 LOAD REDUCTION

The GESSAR PDA quencher design bubble pressures summarized in Table A.4.4 have been shown to be conservative based on applicable plant test results. The analyses of test results provide the load reduction shown in Table A.4.5. The reduced design quencher bubble pressures for design controlling loads are based on a 90-90 percent confidence level of the CAORSO data. Load reduction justification is discussed in Section A.12.7.

A3.0 DESCRIPTION OF THE PHENOMENA

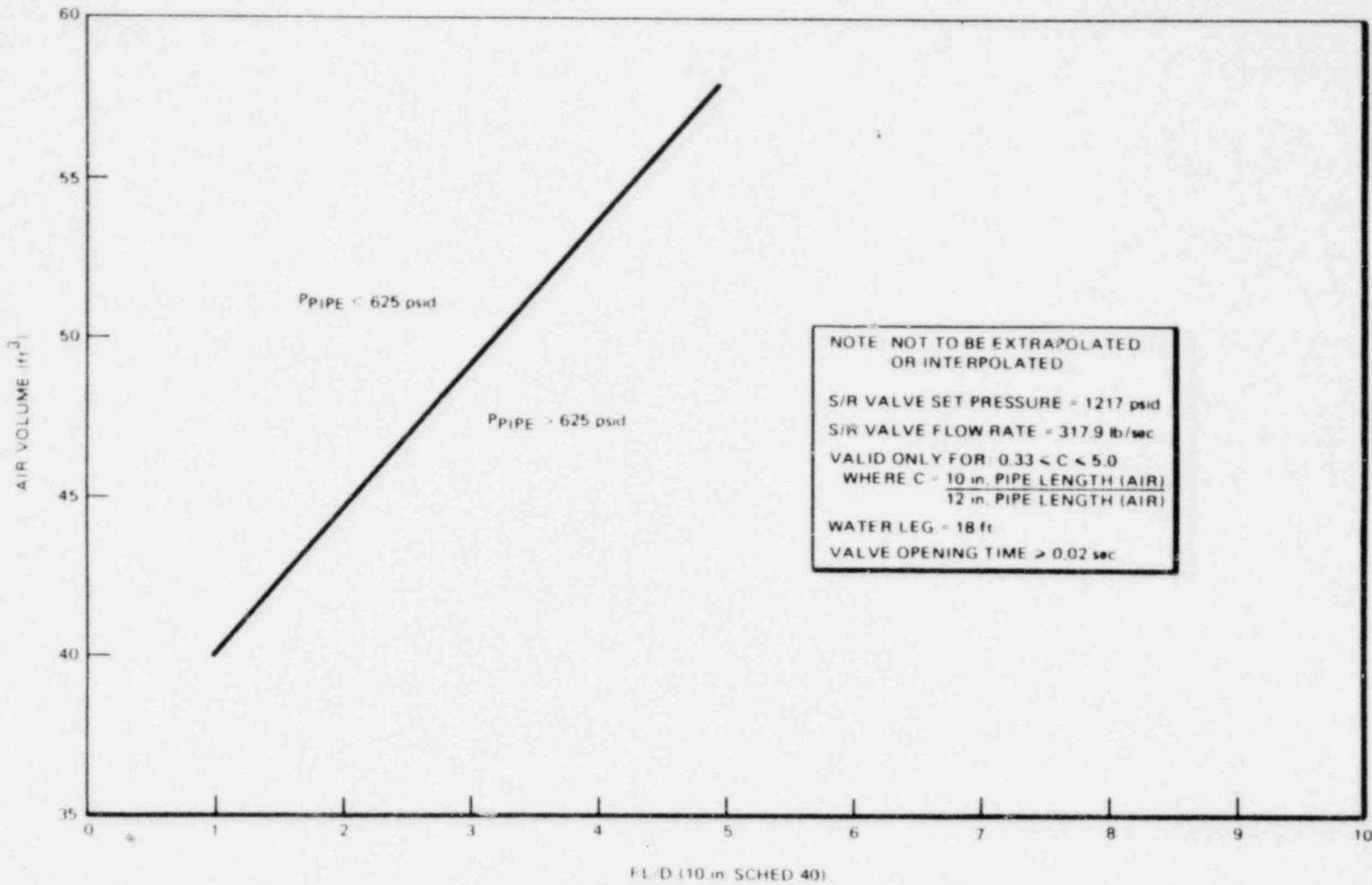
Prior to the lifting of a pressure relief valve, the downstream piping between the S/RV discharge and the water surface is filled with air at drywell pressure and temperature conditions. The discharge piping terminates at some pre-determined submerged depth in the suppression pool with the water level inside the pipe at the same level as the water level in the suppression pool.

When a relief valve lifts, the effluent reactor steam causes a rapid pressure build up in the discharge pipe. This rapid compression of the column of air in the pipe causes a subsequent acceleration of the water slug in the submerged portion of the pipe. During this blowout process the pressure in the pipe builds to a peak as the last of the water is expelled. The compressed cushion of air between the water slug and the effluent vapor exits the quencher and forms four clouds of small bubbles that begin to expand to the lower pool pressure. This expansion leads to coalescence of the bubble cloud into four bubbles. The four bubbles continue to oscillate, displacing the water and propagating a pressure disturbance throughout the suppression pool. The dynamics of the submerged bubbles of air are manifested in pressure oscillations (similar to that of a spring-mass system) arising from the bubble expansion coupled with inertial effects of the moving water mass. The sequence of expansion and contraction is repeated with an identifiable frequency until the bubbles reach the pool surface.

The magnitude of the pressure disturbance in the suppression pool decreases with increasing distance from the point of discharge, resulting in a damped oscillatory load at every point on structures below the water surface.

From an air-clearing standpoint, a decrease in the volume of air initially in the discharge pipe will result in a decrease in the containment loads due to relief valve discharge. Since the design limit of the safety/relief valve is 625 psid,* the discharge pipe volume must be sized so this limit will not be exceeded. There is a balance that must be reached; pool boundary loads are optimized while the safety/relief valve line pressures are not exceeded. Figure A3.1 demonstrates the effect of discharge pipe air volume on the peak pipe pressure. This figure was developed for the specific parameters listed on the figure. The pipe pressures were calculated for first actuations or opening of a safety/relief valve.

*Based on back pressure specifications to which valves are purchased



22A4365
 Rev. 4

Figure A3.1. SRVDE Air Volume Versus FL/D with 625 psid Constraint during Air Clearing

011880

A4.0 ARRANGEMENT

A4.1 DISTRIBUTION IN POOL (QUENCHER ARRANGEMENT)

Figures A4.1 and A4.2 show the elevation and plan views of the standard quencher arrangement. For the 238 Standard Plant the quencher arm is located at 6.5 feet above the basemat and the inclined penetration is 45° . This results in a water leg length of ≈ 18 ft.

This arrangement meets the following objectives:

1. Minimize drywell structural interference.
2. Permit water circulation through top and bottom of the drywell sleeve penetration.
3. Locate quencher arms at an elevation between vent holes to minimize vent discharge loads on the quencher during LOCA.

Figure A4.1 shows two support methods. The alternate position is the designer's option. An advantage to the side anchor arrangement is that it eliminates containment liner penetration for anchor requirements.

Figure A4.3 shows the recommended quencher azimuthal locations in the standard 238 pool. As shown in this figure the low, intermediate and high pressure-switch set valves are uniformly distributed around the pool to preclude concurrent adjacent valves operation.

Table A4.1 identifies the figures for S/R valve location, quencher elevation and plan view for the Mark III 238, 218 and 251 plants.

As shown in Figures A4.1, A4.6 and A4.8, the elevation of the quencher arms from basemat, varies for the various Mark III plant configuration to satisfy the arrangement objectives cited above. The recommended quencher arm elevations for the three plant sizes are:

Standard Plant 238 6.5 ft above basemat

Standard Plant 218 5.5 ft above basemat

Standard Plant 251 5.0 ft above basemat

A4.2 SRVDL ROUTING

The SRVDL is routed by the Architectural Engineer from the first pipe anchor point just below the S/R valve using 10", 12", and 14" Schedule 40 pipe to the drywell and 10" Schedule 80 through the drywell wall to and including the quencher. The SRVDL should have a sufficient slope in the air leg section routing to prevent condensation accumulation in the line. Figure A10.2 is a typical layout of the SRVDL Routing.

A4.2.1 Line Lengths and Volume

Line lengths and volumes are based on the layout shown in Figure A10.2 and the S/R valve constraint of 625 psid. These lengths and volumes are shown in Table A4.3. The layout design does not represent an optimized layout with respect to pipe air volume. It is possible to reduce the air volume within the 625 psid pipe pressure constraint and thus reduce pool boundary loads.

The SRVDL pipe size and line lengths shown are optimized to satisfy a S/R valve back pressure constraint of 550 psid rather than 625 psid, and at the same time minimize the air volume in the lines to obtain the pressures on the suppression pool walls. The design loads for pool boundaries and for support of the quencher device are sensitive to and dependent on the design of the Safety Relief Valve Discharge Line (SRVDL). The design requirements for SRVDL are discussed in Section A10.2 and A11.0.

The SRVDL from the 45° elbow just above the pool to the quencher is a 10" Schedule 80 pipe. (See Figure A4.1.) The increase to Schedule 80 pipe is to provide for corrosion allowance. The corrosion allowance for Carbon Steel is 0.125"/40 years/side and stainless steel is 0.002"/40 years/side.

A4.2.2 Drywell Penetration Sleeve

The Drywell Penetration Sleeve is a 14" Schedule 80 pipe at 45° which acts as a conduit for the SRVDL. The sleeve is shown in Figure A4.1 with the lower lip of the upper end just below the pool level and extending down to the top level of the top drywell vent. The sleeve may be extended as shown by dotted line, if needed for support.

A.4.2.2.1 Thermal Consideration

Studies indicate that the 14" Schedule 80 pipe sleeve to concrete interface does not exceed the 200°F limit for normal S/R valve operation. The design temperature criteria from the ASME boiler and pressure code subsection CC-3440, concrete temperature, Section III, Division 2 is:

- "a. The following temperature limitations are for normal operation or any other long term period. The temperatures shall not exceed 150°F except for local areas, such as around a penetration, which are allowed to have increased temperatures not to exceed 200°F.
- b. The temperature limitations for accident or any other short term period shall not exceed 350°F for the interior surface. However.

local areas are allowed to reach 650°F from steam or water jets in the event of a pipe failure."

A4.2.3 SRVDL Vacuum Breaker

Vacuum breakers are provided for each of the S/R valve discharge lines to prevent excessive water rise in the SRVDL pipe above normal S/R pool level following valve actuations.

At the time of initial opening of the S/R valve, the water level in the S/R Valve Discharge Line (SRVDL) is at the normal suppression pool level. After the S/R valve closes, the steam remaining in the line condenses, creating a vacuum which draws the water to a higher than normal pool water level in the line. Higher SRVDL peak pressure and thrust load will occur if the SRV opens when the water is above the normal pool level. The purpose of the discharge line vacuum breakers is to prevent the water from rising substantially above its normal level when a subsequent S/R valve opening occurs, and thus, the SRVDL peak pressure is about the same as for the first opening.

The SRV vacuum breakers are located in the drywell above the expected level of water rise in the line subsequent to SRV closure. This eliminates the possibility of wetwell pressurization in the event of a stuck open vacuum breaker and ensures proper functioning of the vacuum breaker during the reflood transient.

The following parameters will yield satisfactory performance for most SRVDL geometries and is recommended to satisfy the above requirements. However, plant specific analysis for vacuum breaker design should be performed by the design engineer to confirm this.

- a. The vacuum breaker effective area, $(A/\sqrt{K})^*$ is equal to or greater than 0.30 ft².
- b. The vacuum breaker shall open (fully closed to fully open) in 0.2 second or less when an instantaneous ΔP of 0.5 PSID is applied across it.
- c. The minimum opening differential pressure to start the vacuum breaker to open is equal to or less than 0.2 PSID.

- d. The vacuum breaker must be fully open when pressure difference is equal to or less than 0.5 PSID.
- e. The vacuum breaker should be located in the drywell at an elevation above the maximum water level rise in the line following a SRV closure.

* $\frac{A}{\sqrt{K}}$ is used to calculate flow through the vacuum breaker as follows:

$$w = \sqrt{\Delta P (2\rho g_c) (144)} \frac{A}{\sqrt{K}}$$

where

w = Flowrate through vacuum breaker in lbm/sec

ΔP = Pressure differential across the vacuum breaker (PSID)

ρ = Air or steam density in lbm/ft³

$$g_c = 32.2 \frac{\text{lbm} \cdot \text{ft.}}{\text{lbf} \cdot \text{sec}^2}$$

$\frac{A}{\sqrt{K}}$ = Effective area of valve in ft²

Table A4.1
QUENCHER ARRANGEMENT

<u>Mark III Plants</u>	<u>S/R Valve Location</u>	<u>Quencher Elevation/Plan View</u>
238-732 STD.	Figure A4.3	Figure A4.1/Figure A4.2
238-615	Figure A4.4	Figure A4.1/ *
218-592	Figure A4.5	Figure A4.6/ *
251-784	Figure A4.7	Figure A4.8/ *
251-848	Figure A4.9	Figure A4.8/ *

*Typical plan view similar to Figure A4.2.

Table A4.2
SRVDL DESIGN REQUIREMENTS AND OBJECTIVES

SRVDL DESIGN REQUIREMENTS

- (a) Maximum SRVDL Pipe Pressure \leq 625 psid. (Coordinates of (fL/D) and (SRVDL Air Volume) must be \leq 625 psid as plotted on Figure A3.1)

- (b) Two vacuum breakers are required in the drywell.

SRVDL DESIGN OBJECTIVES

1. Water leg \leq 18 ft.

2. Safety-relief valve opening time \geq 0.02 sec.

3. Minimize the SRVDL air leg volume.

4. Minimize length of longest SRVDL.

5. Minimize the contribution of fL/D to the first half of the discharge line.

6. Start 12" S/40 or 14" S/40 pipe just below the first anchor point to meet objective (5).

7. The ratio of the air legs (length of 10" S/40 pipe/length of 12" S/40 pipe = C) should be $0.33 \leq C \leq 5.0$.

8. Slope lines down toward pool to avoid condensate-water accumulation in line (no horizontal runs).

9. SRVDL vacuum breakers should be 10" size. One \geq 10 ft. above the weir wall and the other just below the seismic restraint at the SRV.

Table A.4.3
SRVDL MARK III 238 STANDARD PLANT

S/R Valve	Total Length	Air Leg Length			Volume (ft ³)	Max. fL/D	
		10" S/40	12" S/40	14" S/40		(a)	(b)
V-1	79'-8"	30'-5"	49'-3"	-	54.9	2.09	4.21
V-2	80'-2"	26'-11"	53'-3"	-	56.13	2.46	4.95
V-3	73'-7"	33'-7"	3'-9"	36'-3"	55.36	2.41	4.85
V-4	77'-2"	20'-5"	56'-9"	-	55.29	2.30	4.63
V-5	76'-11"	19'-5"	57'-6"	-	55.32	2.31	4.65
V-6	77'-1"	20'-0"	57'-1"	-	55.30	2.31	4.65
V-7	77'-4"	20'-8"	56'-8"	-	55.40	2.31	4.65
V-8	77'-2"	19'-11"	57'-3"	-	55.4	2.31	4.65
V-9	77'-1"	19'-7"	57'-6"	-	55.4	2.31	4.65
V-10	77'-5"	20'-1"	57'-4"	-	55.55	2.31	4.65
V-11	76'-11"	19'-4"	57'-7"	-	55.34	2.31	4.65
V-12	77'-8"	20'-11"	56'-9"	-	55.56	2.31	4.65
V-13	77'-3"	20'-5"	56'-10"	-	55.36	2.31	4.65
V-14	76'-5"	29'-11"	26'-9"	19'-9"	55.72	2.41	4.85
V-15	76'-11"	19'-5"	57'-6"	-	55.32	2.31	4.65
V-16	77'-4"	20'-4"	57'-0"	-	55.5	2.31	4.65
V-17	72'-9"	32'-6"	3'-9"	36'-6"	55.0	2.22	4.47
V-18	79'-5"	28'-7"	50'-10"	-	55.16	2.27	4.57
V-19	81'-0"	33'-5"	47'-7"	-	55.3	2.27	4.57

Note:

1. $f = 0.015$
2. (a) is normalized to 10" schedule 40 pipe
3. (b) is normalized to 12" schedule 40 pipe
4. Design constraints are listed in Table A.4.2.
5. The values are based on Figure A.10.2 (Safety/relief valve discharge piping arrangement). (These line designs have not been optimized to take advantage of the maximum pipe pressure of 625 psid).

Table A.4.4
QUENCHER BUBBLE PRESSURE MARK III, 238 STANDARD PLANT
95-95% CONFIDENCE LEVEL.

Case Description	Design Value-Bottom Maximum Pressure (psid)		Containment Normalized Factor @ Point 10 ^a	Containment Peak Pressure @ Point 10 (psid) ^a	
	P _B (+)	P _B (-)		P _B ⁺	P _B ⁻
<u>Single Valve First Actuation, at 100°F Pool Temperature</u>	13.5	-8.1	0.711	9.6	-5.8
<u>Single Valve Subsequent Actuation, at 120°F Pool Temperature</u>	28.2	-12.0	0.711	20.1	-8.5
<u>Two Adjacent Valves First Actuation at 100°F Pool Temperature</u>	13.5	-8.1	0.856	11.6	-6.9
<u>10 Valves (One Low Set and Nine Next Level Low Set) First Actuation at 100°F Pool Temperature</u>	16.7	-9.3	0.916	15.3	-8.5
<u>19 Valves (All Valve Case) First Actuation, at 100°F Pool Temperature</u>	18.6	-9.9	1.0	18.6	-9.9
<u>8 ADS Valves First Actuation at 120°F Pool Temperature</u>	17.4	-10.4	0.821	14.3	-8.5

^aPoint 10 on Containments is Peak Pressure.

Table A.4.5

REDUCED ^①QUENCHER BUBBLE PRESSURE MARK III, 238 STANDARD PLANT

Case Description	Design Value-Bottom Maximum Pressure (psid)		Containment Normalized Factor @ Point 10 ^a	Containment Peak Pressure @ Point 10 (ps.) ^a	
	P _B (+)	P _B (-)		P ⁺	P ⁻
Single Valve <u>First Actuation</u> , at 100°F Pool Temperature	10.8	-6.5	0.711	7.7	-4.6
Single Valve <u>Subsequent Actuation</u> , at 120°F Pool Temperature	18.3	-7.8	0.711	13.0	-5.5
Two Adjacent Valves <u>First Actuation</u> at 100°F Pool Temperature	10.8	-6.5	0.856	9.2	-5.5
10 Valves (One Low Set and Nine Next Level Low Set) <u>First Actuation</u> at 100°F Pool Temperature			(Not Used for Design)		
19 Valves (All Valve Case) <u>First Actuation</u> , at 100°F Pool Temperature	12.1	-6.4	1.0	12.1	-6.4
8 ADS Valves <u>First Actuation</u> at 120°F Pool Temperature	11.3	-6.8	0.821	9.3	-5.5

^aPoint 10 on Containments is Peak Pressure.

①Based on 90-90% confidence level of Caorso data.

22A4365
Rev. 4

A-18a

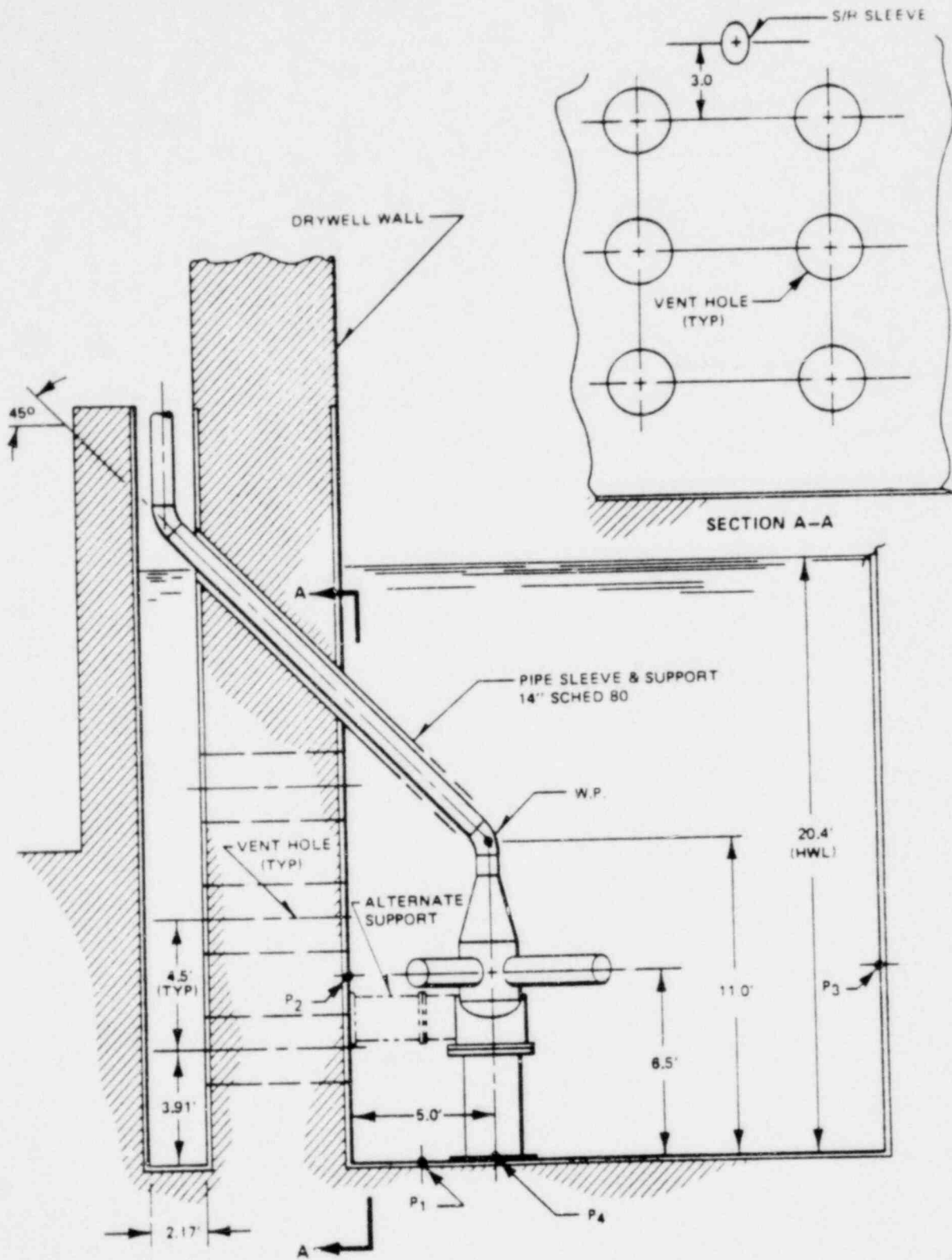


Figure A4.1. 238 Standard Mark III Quencher Arrangement Elevation

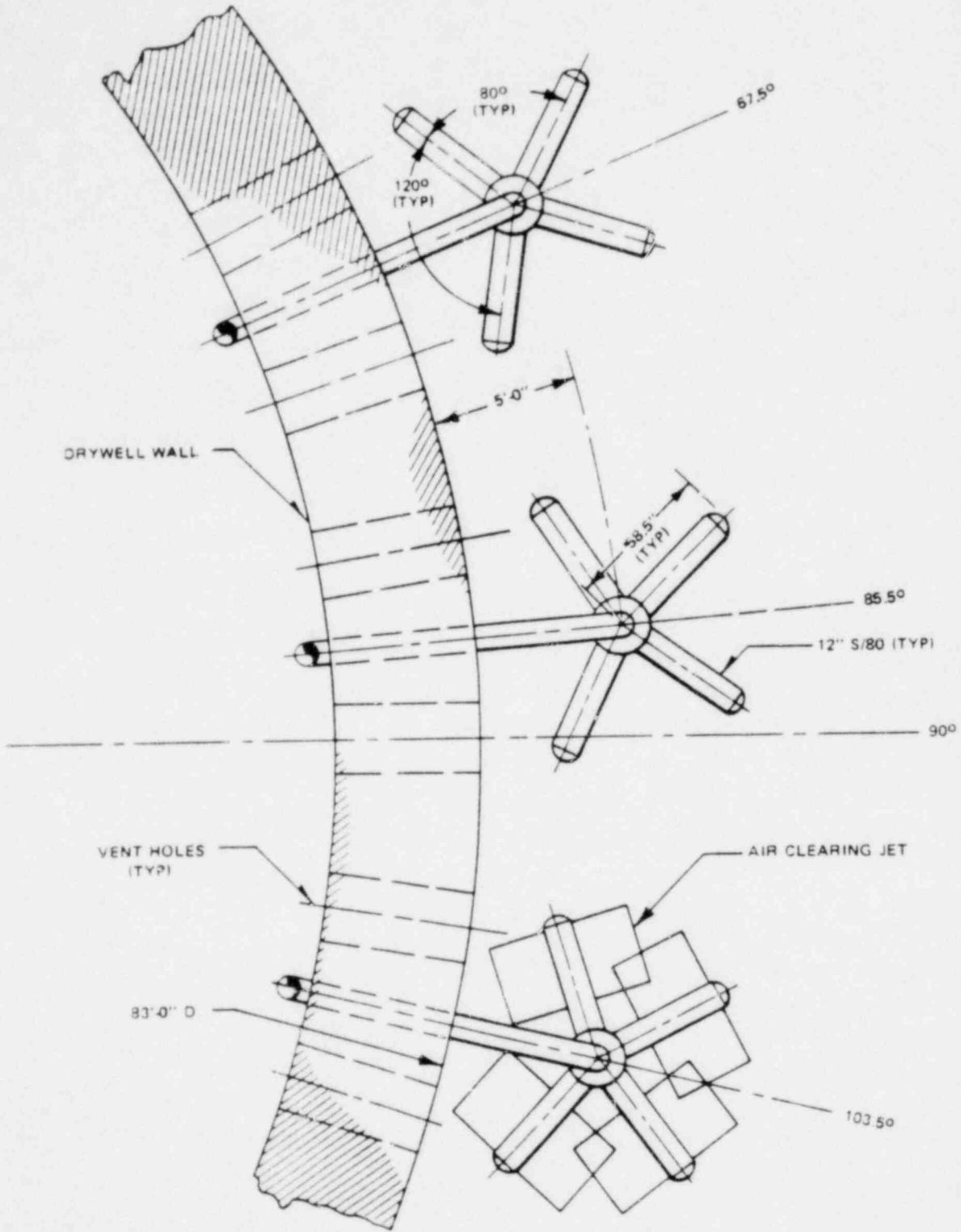
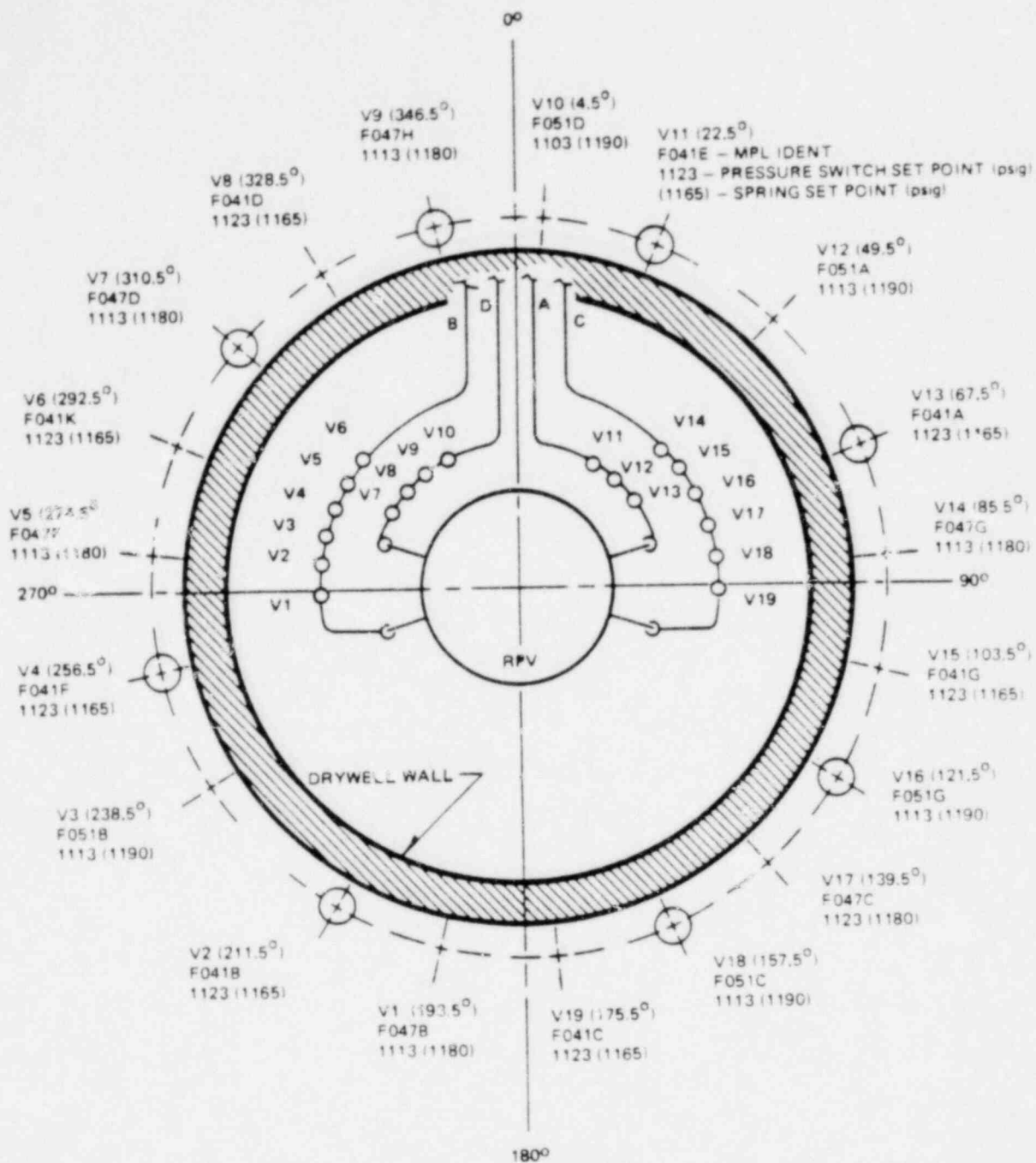


Figure A4.2. Mark III Quencher Plan View (Typ.) 238 Plant Arrangement Shown



LEGEND ADS = ○
NOTES: 19 S/R VALVES

Figure A4.3. S/R Valve Discharge Locations for 238-748 Standard Plant

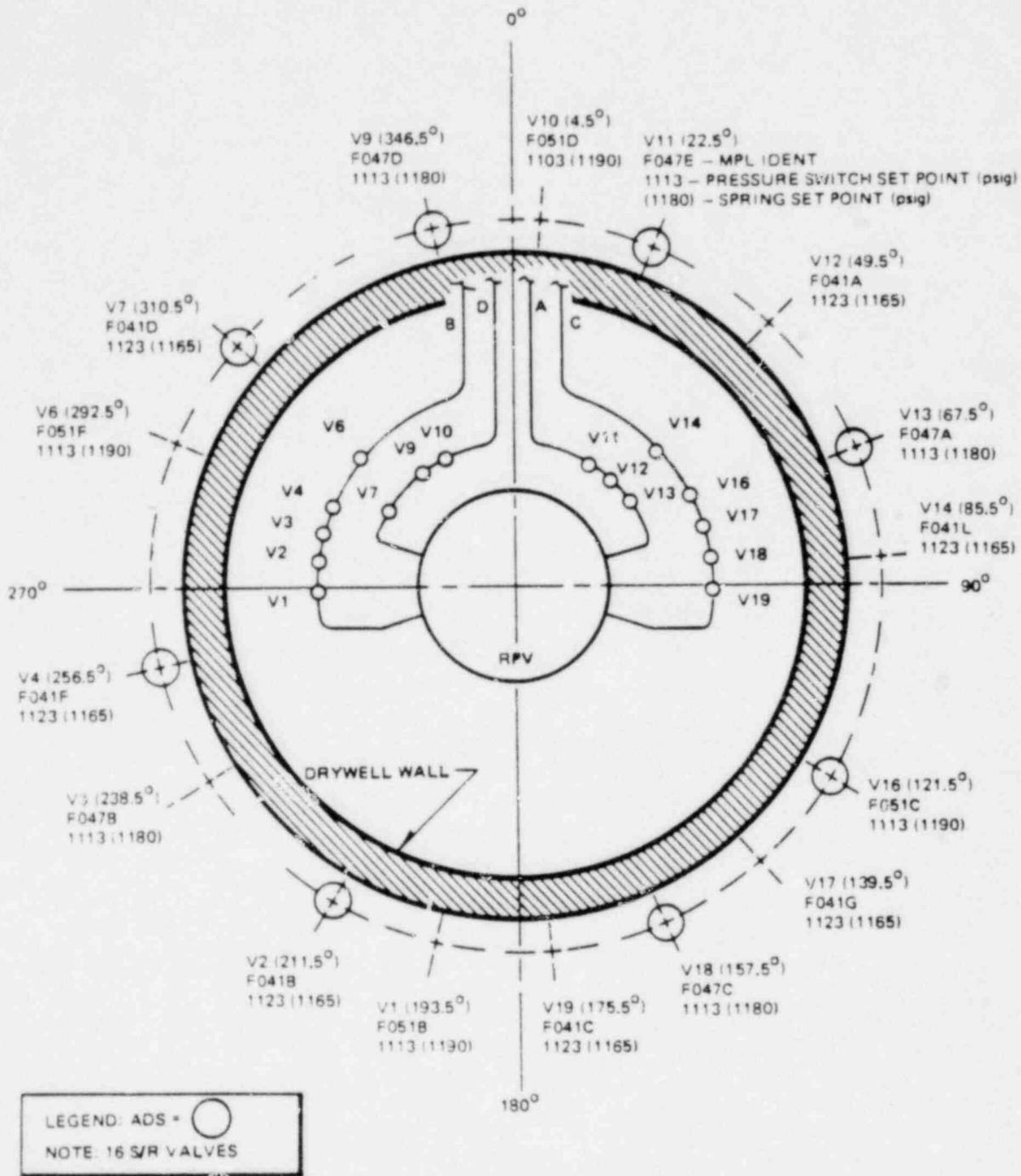
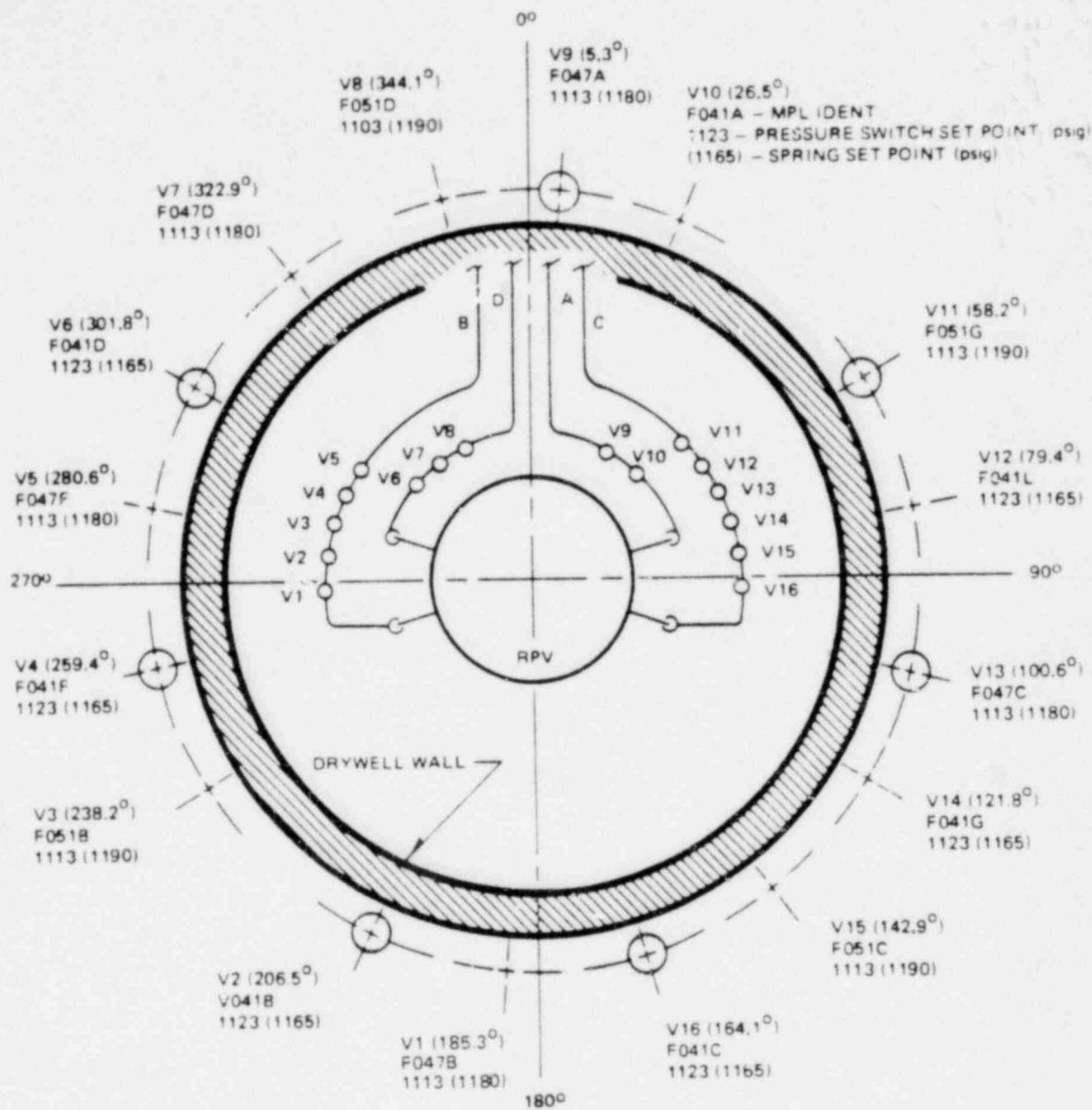


Figure A4.4. S/R Valve Discharge Locations for 238-648 Standard Plant



LEGEND: ADS = ○
NOTES: 16 S/R VALVES

Figure A4.5. S/R Valve Discharge Locations for 218-624 Plant

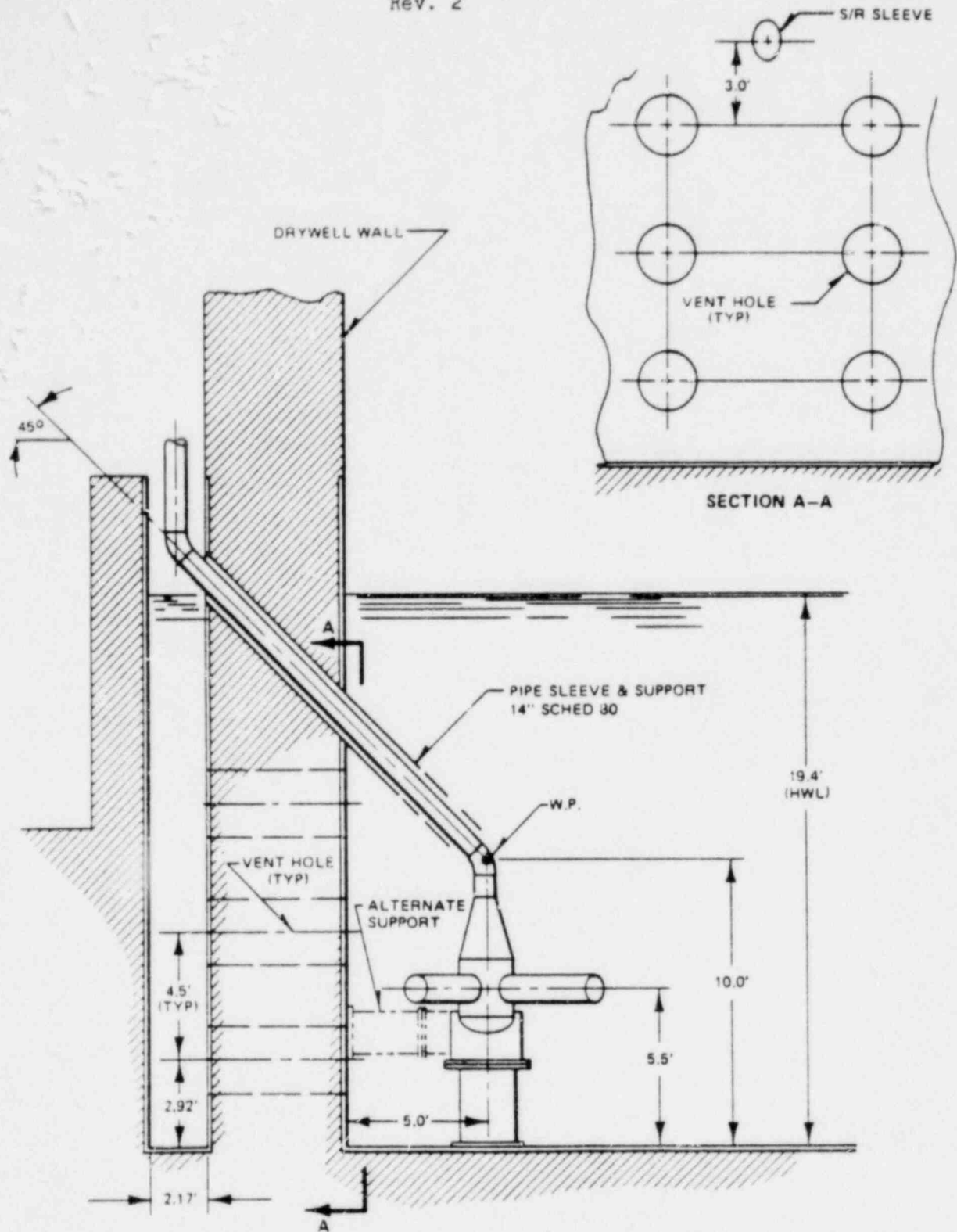


Figure A4.6. 218 Standard Plant Mark III Quencher Arrangement Elevation

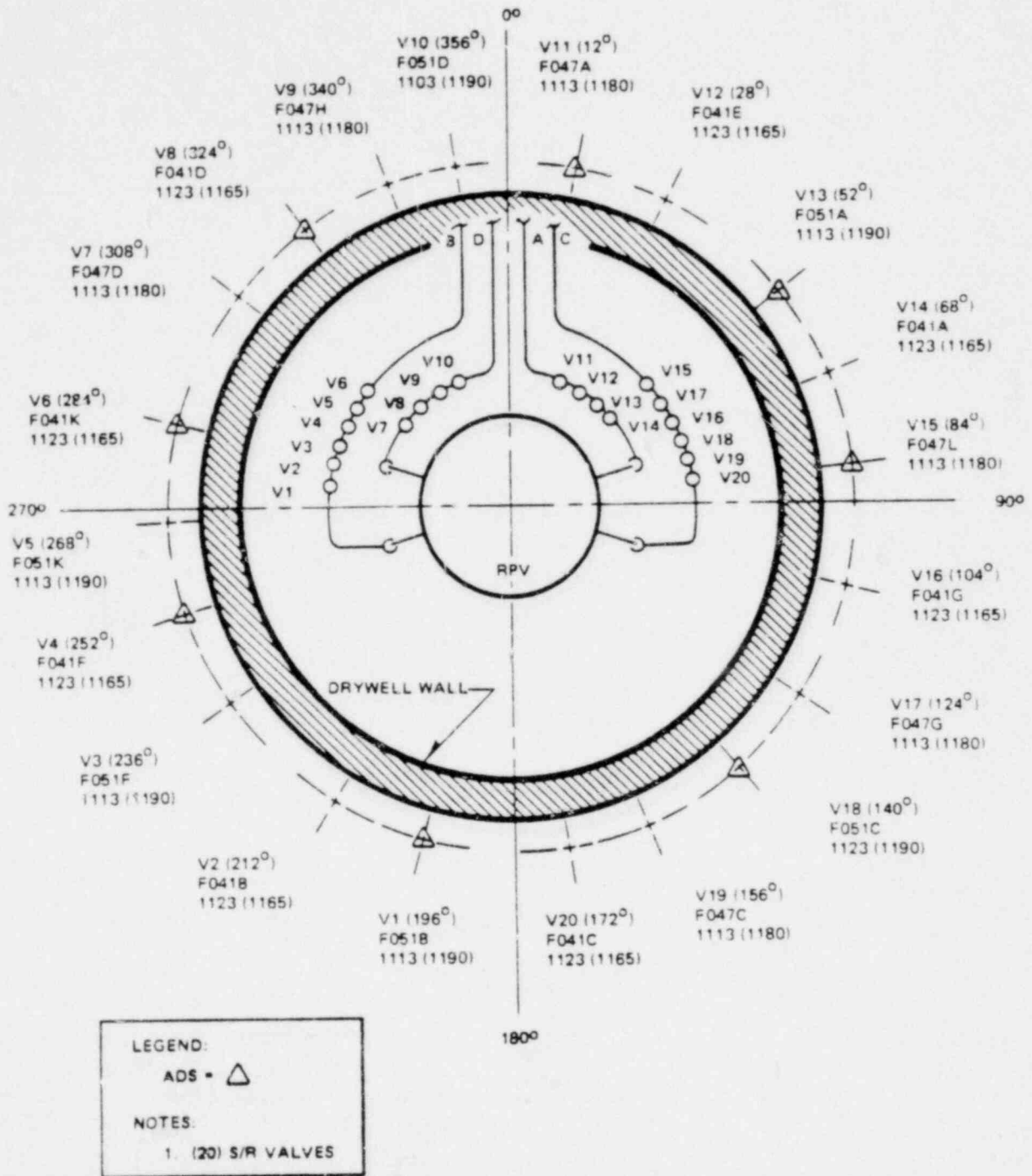


Figure A4.7. S/R Valve Discharge Locations for 251-800 Plant

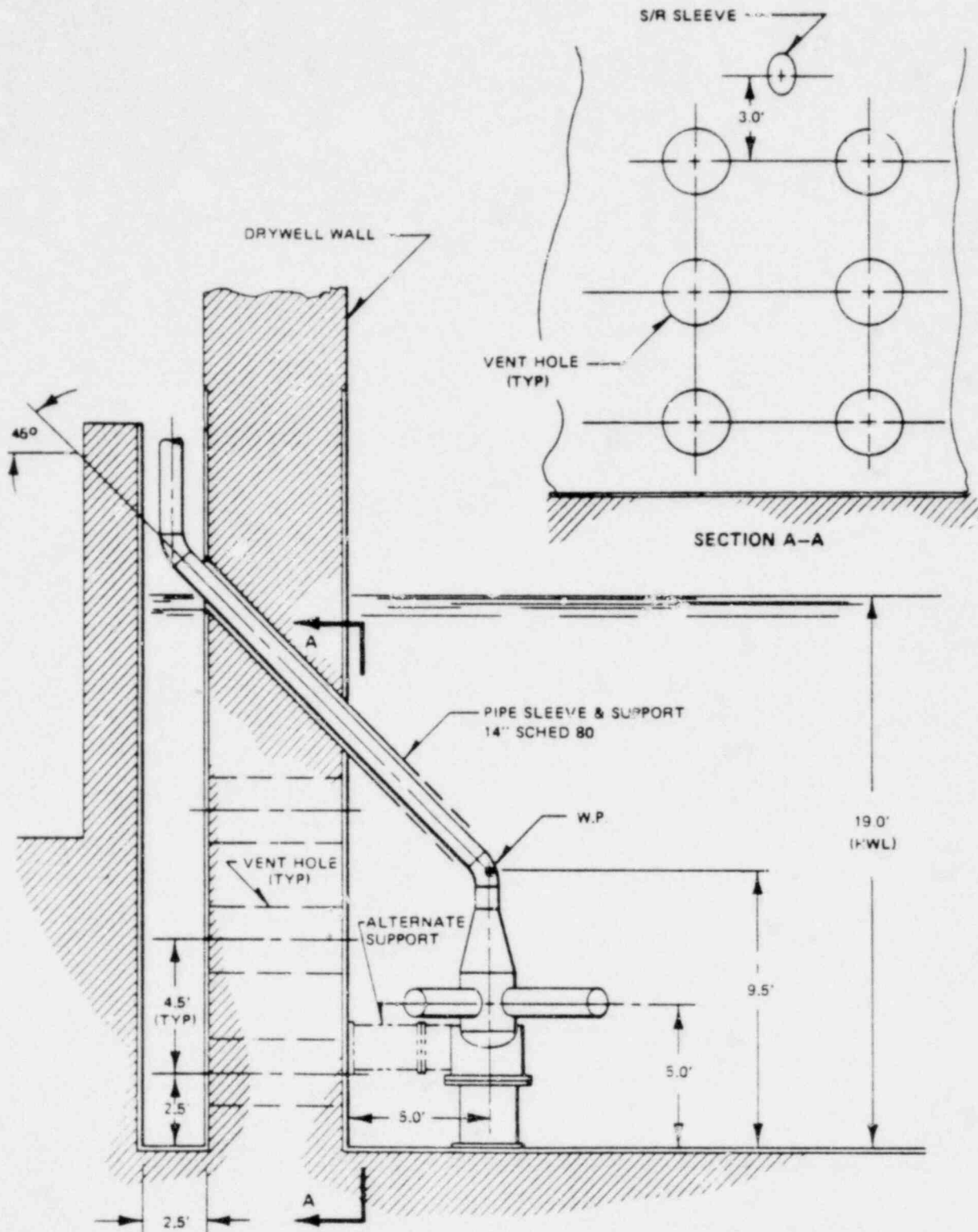
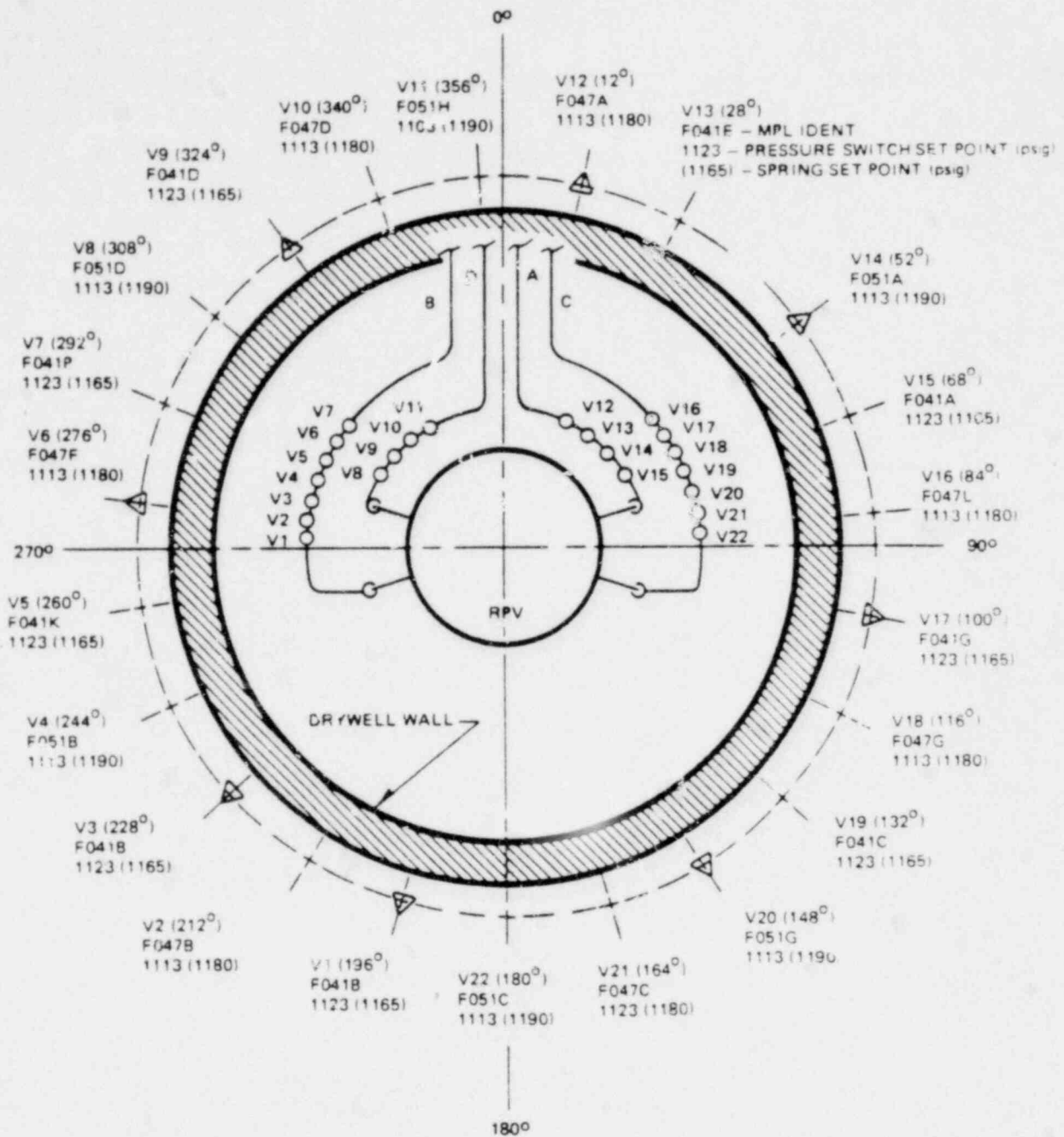


Figure A4.8. 251 Standard Plant Mark III Quencer Arrangement Elevation



LEGEND: ADS = \triangle
NOTES: 1. 22 S/R VALVES

Figure A4.9. S/R Valve Discharge Locations for 251-848 Plant

A5.0 QUENCHER LOAD ON POOL BOUNDARY

A5.1 PRESSURES ON DRYWELL, BASEMAT AND CONTAINMENT

Drywell wall, basemat and S/R Valve Loads are calculated as discussed in Section A10.0. For the 238 Standard Plant, the maximum and minimum bubble pressure below the quencher just after air clearing are shown in Table A4.4. actuations (psid).

The absolute pressure on the pool walls can be calculated by the following equation:

$$P_{(a)} = P_{\text{containment}} + \frac{\rho h(a)}{144} + \Delta P(r)$$

where:

$P_{(a)}$ = Absolute pressure at point (a) (psia)

r = Distance from center of quencher to point (a) (ft)

$P_{\text{containment}}$ = Absolute pressure of containment atmosphere (psia)

$h(a)$ = Head of water acting at point (a) (ft)

ρ = Density of pool water ≈ 62.4 (lb/ft³)

$\Delta P(r)$ = Bubble pressure attenuated by distance, r to point (a),
for multiple S/R valve actuations (psid).

The pressure decays with time and this is discussed in Section A5.4.

The following paragraphs discuss the dynamic pressure fields, at radial and circumferential locations of the pool for the 238 standard plant (Figure A4.3 and Table A10.2). The pressure fields are based on P_{Bmax} normalized to 1 psid. These dynamic peak pressure fields can be used to reflect the changes in the maximum and/or minimum bubble pressure. If for example $P_{Bmax} = 25$ psid for another SRVDL layout, the normalized values of Tables A5.1 through A5.5 would be multiplied by 25 to obtain the design pressures.

A5.1.1 Single S/R Valve Loads

The normalized dynamic peak pressures $\Delta P(r)$ for a single S/R Valve Discharge valve are given in Table A5.1 and the normalized radial and circumferential peak values are shown in Figures A5.1, A5.2, and A5.2a. (The values given presume an air leg volume of 56.13 ft^3 for all SRVDS's).

This is the base case and this pressure field is used to develop any other S/R Valve combination as described in Section A10.0.

A5.1.2 Two Adjacent S/R Valve Loads

The normalized dynamic peak pressures $\Delta P(r)$ are given in Table A5.2 and the normalized radial and circumferential peak values are plotted in Figures A5.3, A5.4, and A5.4a for the two adjacent S/R Valves V-8 and V-9.

A5.1.3 Ten S/R Valve Loads

Normalized $\Delta P(r)$ loads are given in Table A5.3 and the normalized values are shown in Figures A5.5, A5.6, and A5.6a for the ten (1103 and 1113 psi low set point) valves V-10, V-12, V-14, V-16, V-18, V-1, V-3, V-5, V-7 and V-9.

A5.1.4 Eight S/R Valve Loads (ADS)

Normalized $\Delta P_{(r)}$ loads are given in Table A5.4 and the normalized values are shown in Figures A5.7, A5.8, and A5.8a for the eight S/R valves, V-11, V-13, V-16, V-18, V-2, V-4, V-7 and V-9.

A5.1.5 All (19) S/R Valve Loads

Normalized $\Delta P_{(r)}$ loads are given in Table A5.5 and the normalized values are shown in Figures A5.9, A5.10, and A5.10a for all (19) valves V-1 to V-19.

A5.2 LOAD ON WEIR WALL

The S/R valve loads on the weir wall are the same as those on the drywell wall except they only act on the projected area through the drywell wall vents.

A5.3 LOADS ON SUBMERGED STRUCTURE

For submerged structures, the loads are specified in Section G3 of Attachment G.

THESE PAGES ARE INTENTIONALLY DELETED

A5.4 NORMALIZED PRESSURE TIME HISTORY (Theoretical Raleigh Bubble)

The ideal pressure is normalized for the maximum $\Delta P(r)$ positive value as shown in Figure A5.11. The frequency is 5 to 12 Hz as derived from the test data shown on Figure A5.12, and the total time of oscillation is 0.75 sec. (i.e., the time for the air bubbles to rise to the surface of the pool, or attenuation has dropped the amplitude to negligible values). Figure A5.11 is used by the designer for determining pressure amplitudes with time and the number of pressure cycles (see Section A9.0 fatigue cycles).

It should be noted that bubble pressure decays to $1/3 P_{max}$ occur in 5 cycles for any frequency between 5 and 12 Hz. For this linear attenuation rule it is observed that the pressure amplitude is fully decayed ($P = 0$ psig) in 7.5 pressure cycles after the peak. The justification for this application is from examination of full scale plant data where most traces were observed to decay to a small fraction of their peak value in 2 or 3 cycles.

A5.5 REPRESENTATIVE PRESSURE TIME HISTORY

Figure A5.12 depicts a representative pressure time history at points P₁ through P₄ as shown on Figure A4.1. These curves provide the designer a realistic picture of the pressure oscillations as opposed to the idealized Raleigh bubbles.

A5.6 ESTIMATED MARGINS

A5.6.1 Peak Bubble Pressures

For the examples shown in this document, the maximum loads on any structure resulting from the S/R valve air clearing phenomena are governed by the peak quencher bubble load. For the Mark III Standard 238 plant these values are shown on the next page.

A5.6.2 Peak Bubble Pressure Load Reduction

See Section A12.7 for information that supports use of reduced bubble pressure design values.

Generalized Bottom Pressure
Load Case^a

	<u>A</u>	<u>B</u>	<u>C</u>	<u>D</u>
1. Predicted Maximum Bubble Pressure, psid (+/-)	+8.8/-6.2	+12.3/-7.7	+11.5/-7.9	+16.1/-9.1
2. Specified for Standard 238 Design, psid (+/-)	+13.5/-8.1	+18.6/-9.9	+17.4/-10.4	+28.2/-12.0
3. Pressure Margin	4.7/1.9	6.3/2.2	5.9/2.5	12.1/2.9
4. % Margin (Based on Predicted Maximum Bubble Pressure)	35/23	34/22	34/24	43/24

^aSee Section A12.5.1 for load case description.

A5.6.2 95%-95% Confidence

95%-95% means that there is 95% confidence that 95% of any new data obtained will fall within the maximum levels of the current data base. See Section A12.5.1.2 for additional discussion.

A5.6.3 Margin

The apparent margin in the specified containment design based on quencher bubble pressure is calculated as 20 to 45%.

Table A5.1

MARK III 238-732 STANDARD PLANT DYNAMIC PRESSURE FIELD FOR ONE S/R VALVE

TIME = 0.15 sec (Positive Pressure psid) ΔP (r)
0.08 sec (Negative Pressure psid) ΔP (r)

S/R Valves Angle (degrees) Reference Point	V-10												
	283.5	292.5	301.5	310.5	319.5	328.5	337.5	346.5	355.5	4.5	4.5	13.5	
1	0	0	0	0	0	0	0	0	0	0	0	0	
2	0	0.274	0.334	0.423	0.566	0.805	0.984	0.805	0.805	0.984	0.805	0.805	
3	0	0.280	0.345	0.449	0.632	1.0	1.0	1.0	1.0	1.0	1.0	1.0	
4	0	0.282	0.348	0.453	0.645	1.0	1.0	1.0	1.0	1.0	1.0	1.0	
5	0	0	0.277	0.339	0.435	0.598	0.902	1.0	0.902	1.0	0.902	0.902	
6	0	0.198	0.227	0.268	0.328	0.427	0.605	0.994	1.0	0.994	1.0	0.994	
7	0.168	0.188	0.216	0.254	0.311	0.406	0.566	0.902	1.0	0.902	1.0	0.902	
8	0	0.159	0.178	0.203	0.239	0.290	0.372	0.494	0.716	0.885	0.716	0.716	
9	0.137	0.151	0.169	0.192	0.224	0.269	0.337	0.431	0.563	0.645	0.563	0.563	
10	0.138	0.152	0.170	0.194	0.227	0.274	0.345	0.449	0.605	0.711	0.605	0.605	
11	0.138	0.152	0.169	0.193	0.225	0.272	0.343	0.445	0.594	0.691	0.594	0.594	
12	0.137	0.151	0.168	0.191	0.224	0.266	0.331	0.420	0.535	0.605	0.535	0.535	
13	0	0	0	0	0	0	0	0	0	0	0	0	

Table A5.2
MARK 111 238-732 STANDARD PLANT DYNAMIC PEAK PRESSURE FIELD FOR TWO ADJACENT S/R VALVES

TIME = 0.15 sec (Positive Pressure) ΔP (r)
= 0.08 sec (Negative Pressure) ΔP (r)

S/R Valves Angle (degrees) Reference Point	265.5	274.5	283.5	292.5	301.5	310.5	319.5	328.5	337.5	346.5	355.5	V-9	V-10
1			0	0	0	0	0	0	0	0	0	0	0
2			0.274	0.334	0.504	0.657	0.910	1.0	1.0	1.0	1.0	1.0	1.0
3			0.280	0.345	0.529	0.721	1.0	1.0	1.0	1.0	1.0	1.0	1.0
4			0.282	0.348	0.533	0.733	1.0	1.0	1.0	1.0	1.0	1.0	1.0
5			0.277	0.339	0.515	0.687	1.0	1.0	1.0	1.0	1.0	1.0	1.0
6	0	0	0.198	0.227	0.333	0.399	0.504	0.688	1.0	1.0	1.0	1.0	1.0
7	0	0.168	0.188	0.274	0.316	0.379	0.479	0.646	0.989	1.0	1.0	1.0	1.0
8	0	0.159	0.178	0.258	0.298	0.354	0.442	0.573	0.807	1.0	1.0	1.0	1.0
9	0.137	0.151	0.218	0.245	0.280	0.331	0.405	0.508	0.656	0.766	0.796	0.776	0.776
10	0.138	0.152	0.219	0.247	0.283	0.335	0.413	0.526	0.697	0.841	0.856	0.841	0.841
11	0.138	0.152	0.218	0.246	0.282	0.334	0.410	0.521	0.686	0.822	0.840	0.822	0.822
12	0.137	0.151	0.216	0.244	0.278	0.328	0.399	0.497	0.629	0.736	0.757	0.736	0.736
13	0	0	0	0	0	0	0	0	0	0	0	0	0

Table A5.3

MARK III 238-732 STANDARD PLANT DYNAC-C PEAK PRESSURE FIELD FOR 10 S/R VALVES

TIME = 0.15 sec (Positive Pressure psid) ΔP (r)
 = 0.08 sec (Negative Pressure psid) ΔP (r)

S/R Valves Angle (Degrees) Reference Point	V-10			V-12			V-14					
	4.5	13.5	22.5	31.5	40.5	49.5	58.5	67.5	76.5	85.5	94.5	103.5
1	0	0	0	0	0	0	0	0	0	0	0	0
2	1.0	0.969	0.782	0.758	0.913	1.0	0.910	0.801	0.950	1.0	0.950	0.801
3	1.0	1.0	0.849	0.825	1.0	1.0	1.0	0.894	1.0	1.0	1.0	0.894
4	1.0	1.0	0.862	0.837	1.0	1.0	1.0	0.912	1.0	1.0	1.0	0.912
5	1.0	1.0	0.813	0.789	1.0	1.0	1.0	0.845	1.0	1.0	1.0	0.845
6	1.0	1.0	0.834	0.820	1.0	1.0	1.0	0.907	1.0	1.0	1.0	0.914
7	1.0	1.0	0.804	0.772	1.0	1.0	1.0	0.850	1.0	1.0	1.0	0.857
8	1.0	0.890	0.724	0.694	0.834	0.991	0.866	0.750	0.857	0.989	0.860	0.756
9	0.841	0.745	0.651	0.637	0.704	0.768	0.720	0.675	0.723	0.776	0.714	0.667
10	0.903	0.782	0.669	0.655	0.741	0.827	0.758	0.699	0.761	0.835	0.752	0.692
11	0.884	0.772	0.664	0.650	0.731	0.809	0.748	0.693	0.750	0.817	0.742	0.686
12	0.804	0.720	0.638	0.625	0.680	0.733	0.695	0.660	0.698	0.741	0.688	0.652
13	0	0	0	0	0	0	0	0	0	0	0	0

Table A5.3 (Continued)

S/R Valves Angle (Degrees) Reference Point	V-16				V-18				V-1			
	<u>112.5</u>	<u>121.5</u>	<u>130.5</u>	<u>139.5</u>	<u>148.5</u>	<u>157.5</u>	<u>166.5</u>	<u>175.5</u>	<u>184.5</u>	<u>193.5</u>	<u>202.5</u>	<u>211.5</u>
1	0	0	0	0	0	0	0	0	0	0	0	0
2	0.950	1.0	0.950	0.801	0.950	1.0	0.950	0.801	0.910	1.0	0.913	0.707
3	1.0	1.0	1.0	0.894	1.0	1.0	1.0	0.894	1.0	1.0	1.0	0.776
4	1.0	1.0	1.0	0.912	1.0	1.0	1.0	0.912	1.0	1.0	1.0	0.788
5	1.0	1.0	1.0	0.845	1.0	1.0	1.0	0.845	1.0	1.0	1.0	0.739
6	1.0	1.0	1.0	0.914	1.0	1.0	1.0	0.907	1.0	1.0	1.0	0.860
7	1.0	1.0	1.0	0.857	1.0	1.0	1.0	0.850	1.0	1.0	1.0	0.753
8	0.860	1.0	0.860	0.756	0.860	0.989	0.857	0.750	0.851	0.975	0.824	0.675
9	0.727	0.779	0.727	0.667	0.714	0.776	0.723	0.661	0.704	0.762	0.694	0.604
10	0.764	0.838	0.764	0.692	0.752	0.835	0.761	0.685	0.743	0.821	0.731	0.622
11	0.754	0.819	0.754	0.686	0.742	0.817	0.750	0.679	0.732	0.803	0.721	0.618
12	0.702	0.744	0.702	0.652	0.688	0.741	0.698	0.646	0.679	0.726	0.669	0.592
13	0	0	0	0	0	0	0	0	0	0	0	0

22A4365
Rev. 2

Table A5.3 (Cont Inued)

S/R Valves Angle (degrees) Reference Point	V3	V5	V7	V9												
	220.5	229.5	238.5	247.5	256.5	265.5	274.5	283.5	292.5	301.5	310.5	319.5	328.5	337.5	346.5	355.5
1	0	0	0	0	0	0	0	0	0	0	0	0	0	0	0	0
2	0.707	0.913	1.0	0.910	0.801	0.950	1.0	0.950	0.801	0.950	1.0	0.988	0.868	1.0	1.0	1.0
3	0.776	1.0	1.0	1.0	0.894	1.0	1.0	1.0	0.894	1.0	1.0	1.0	0.959	1.0	1.0	1.0
4	0.778	1.0	1.0	1.0	0.912	1.0	1.0	1.0	0.912	1.0	1.0	1.0	0.976	1.0	1.0	1.0
5	0.739	1.0	1.0	1.0	0.845	1.0	1.0	1.0	0.845	1.0	1.0	1.0	0.911	1.0	1.0	1.0
6	0.800	1.0	1.0	1.0	0.907	1.0	1.0	1.0	0.914	1.0	1.0	1.0	0.944	1.0	1.0	1.0
7	0.753	1.0	1.0	1.0	0.850	1.0	1.0	1.0	0.873	1.0	1.0	1.0	0.886	1.0	1.0	1.0
8	0.675	0.824	0.975	0.851	0.750	0.857	0.989	0.860	0.773	0.879	1.0	0.875	0.784	0.920	1.0	1.0
9	0.604	0.694	0.762	0.704	0.661	0.723	0.776	0.727	0.684	0.733	0.788	0.741	0.707	0.772	0.852	0.860
10	0.622	0.731	0.821	0.743	0.685	0.761	0.835	0.764	0.708	0.771	0.846	0.779	0.731	0.810	0.913	0.916
11	0.618	0.721	0.803	0.732	0.679	0.750	0.817	0.754	0.702	0.761	0.828	0.769	0.725	0.800	0.895	0.901
15	0	0	0	0	0	0	0	0	0	0	0	0	0	0	0	0

Table A5.4
 MARK 111 238-732 STANDARD PLANT DYNAMIC PEAK PRESSURE FIELD FOR EIGHT (8) S/R VALVES

TIME = 0.15 sec (Positive Pressure) ΔP (r)
 TIME = 0.08 sec (Negative Pressure) ΔP (r)

S/R Valves Angle (degrees) Reference Point	V-11													V-13			
	4.5	13.5	22.5	31.5	40.5	49.5	58.5	67.5	76.5	85.5	94.5	103.5	0	0	0	0	
1	0	0	0	0	0	0	0	0	0	0	0	0	0	0	0	0	
2	0.801	0.910	1.0	0.913	0.707	0.707	0.871	1.0	0.850	0.657	0.599	0.657	0.850	0.657	0.599	0.657	
3	0.894	1.0	1.0	1.0	0.776	0.776	1.0	1.0	1.0	0.721	0.635	0.721	1.0	0.721	0.635	0.721	
4	0.912	1.0	1.0	1.0	0.788	0.788	1.0	1.0	1.0	0.733	0.641	0.733	1.0	0.733	0.641	0.733	
5	0.845	1.0	1.0	1.0	0.739	0.739	0.964	1.0	0.943	0.687	0.615	0.687	1.0	0.687	0.615	0.687	
6	0.907	1.0	1.0	1.0	0.775	0.767	1.0	1.0	1.0	0.716	0.636	0.725	1.0	0.716	0.636	0.725	
7	0.850	1.0	1.0	0.987	0.729	0.741	0.987	1.0	0.962	0.694	0.627	0.681	1.0	0.694	0.627	0.681	
8	0.750	0.851	0.975	0.809	0.651	0.663	0.809	0.939	0.782	0.621	0.578	0.608	1.0	0.621	0.578	0.608	
9	0.661	0.707	0.749	0.677	0.596	0.592	0.664	0.722	0.650	0.556	0.528	0.560	1.0	0.556	0.528	0.560	
10	0.685	0.743	0.809	0.715	0.614	0.611	0.702	0.783	0.688	0.573	0.539	0.577	1.0	0.573	0.539	0.577	
11	0.679	0.735	0.791	0.705	0.610	0.606	0.692	0.764	0.678	0.569	0.536	0.573	1.0	0.569	0.536	0.573	
12	0.646	0.679	0.713	0.652	0.584	0.580	0.639	0.686	0.625	0.546	0.520	0.550	1.0	0.625	0.546	0.550	
13	0	0	0	0	0	0	0	0	0	0	0	0	0	0	0	0	

Table A5.4 (Continued)

S/R Valves Angle (degrees) Reference Point	V-16				V-18				V-2			
	112.5	121.5	130.5	139.5	148.5	157.5	166.5	175.5	184.5	193.5	202.5	211.5
1	0	0	0	0	0	0	0	0	0	0	0	0
2	0.893	1.0	0.910	0.801	0.910	1.0	0.893	0.657	0.599	0.657	0.850	1.0
3	1.0	1.0	1.0	0.894	1.0	1.0	1.0	0.721	0.635	0.721	1.0	1.0
4	1.0	1.0	1.0	0.912	1.0	1.0	1.0	0.733	0.641	0.733	1.0	1.0
5	0.983	1.0	1.0	0.845	1.0	1.0	0.983	0.687	0.615	0.687	0.943	1.0
6	1.0	1.0	1.0	0.856	1.0	1.0	1.0	0.725	0.636	0.716	1.0	1.0
7	0.971	1.0	1.0	0.835	1.0	1.0	0.971	0.681	0.627	0.694	0.962	1.0
8	0.792	0.954	0.826	0.735	0.826	0.954	0.792	0.608	0.578	0.621	0.782	0.939
9	0.646	0.725	0.691	0.646	0.691	0.725	0.646	0.560	0.528	0.556	0.650	0.709
10	0.685	0.786	0.730	0.670	0.730	0.786	0.685	0.577	0.539	0.573	0.688	0.771
11	0.674	0.767	0.720	0.665	0.720	0.767	0.674	0.573	0.536	0.569	0.678	0.752
12	0.620	0.688	0.666	0.628	0.666	0.688	0.620	0.550	0.520	0.546	0.625	0.672
13	0	0	0	0	0	0	0	0	0	0	0	0

Table A5.4 (Continued)

S/R Valves Angle (degrees) Reference Point	V-4							V-7				
	<u>220.5</u>	<u>229.5</u>	<u>238.5</u>	<u>247.5</u>	<u>256.5</u>	<u>265.5</u>	<u>274.5</u>	<u>283.5</u>	<u>292.5</u>	<u>301.5</u>	<u>310.5</u>	<u>319.5</u>
1	0	0	0	0	0	0	0	0	0	0	0	0
2	0.871	0.707	0.707	0.871	1.0	0.850	0.657	0.599	0.657	0.893	1.0	0.910
3	1.0	0.776	0.776	1.0	1.0	1.0	0.721	0.635	0.721	1.0	1.0	1.0
4	1.0	0.788	0.788	1.0	1.0	1.0	0.733	0.641	0.733	1.0	1.0	1.0
5	0.964	0.739	0.739	0.964	1.0	0.943	0.687	0.615	0.687	0.983	1.0	1.0
6	1.0	0.741	0.741	1.0	1.0	1.0	0.716	0.636	0.725	1.0	1.0	1.0
7	0.972	0.717	0.717	0.972	1.0	0.962	0.694	0.627	0.681	0.971	1.0	1.0
8	0.793	0.639	0.639	0.793	0.939	0.782	0.621	0.578	0.608	0.792	0.967	0.845
9	0.646	0.584	0.584	0.646	0.709	0.650	0.556	0.528	0.560	0.660	0.740	0.716
10	0.685	0.602	0.602	0.685	0.771	0.688	0.573	0.539	0.577	0.698	0.801	0.737
11	0.675	0.598	0.598	0.675	0.752	0.678	0.569	0.536	0.573	0.688	0.782	0.726
12	0.621	0.572	0.598	0.621	0.672	0.625	0.546	0.520	0.550	0.635	0.704	0.673
13	0	0	0	0	0	0	0	0	0	0	0	0

22A4365
REV. 2

Table A5.4 (Continued)

S/R Valves Angle (degrees) <u>Reference Point</u>	V-9			
	<u>328.5</u>	<u>337.5</u>	<u>346.5</u>	<u>355.5</u>
1	0	0	0	0
2	0.801	0.950	1.0	0.950
3	0.894	1.0	1.0	1.0
4	0.912	1.0	1.0	1.0
5	0.845	1.0	1.0	1.0
6	0.885	1.0	1.0	1.0
7	0.846	1.0	1.0	1.0
8	0.745	0.842	0.976	0.856
9	0.657	0.707	0.761	0.710
10	0.681	0.745	0.821	0.748
11	0.675	0.735	0.803	0.738
12	0.642	0.681	0.726	0.684
13	0	0	0	0

Table A5.5 (Continued)

S/R Valves Angle (degrees) Reference Point	V-16	V-17	V-18	V-19	V-1	V-2
1	112.5	130.5	148.5	175.5	193.5	211.5
2	0	0	0	0	0	0
3	1.0	1.0	1.0	1.0	1.0	1.0
4	1.0	1.0	1.0	1.0	1.0	1.0
5	1.0	1.0	1.0	1.0	1.0	1.0
6	1.0	1.0	1.0	1.0	1.0	1.0
7	1.0	1.0	1.0	1.0	1.0	1.0
8	1.0	1.0	1.0	1.0	1.0	1.0
9	1.0	1.0	1.0	1.0	1.0	0.989 0.972
10	1.0	1.0	1.0	1.0	1.0	1.0
11	1.0	1.0	1.0	1.0	1.0	1.0
11	0.983	0.989	0.983	0.983	0.974	0.953 0.937
13	0	0	0	0	0	0

Table A5.5 (Continued)

S/R Valves Angle (degrees) <u>Reference Point</u>	V-8		V-9	
	<u>328.5</u>	<u>337.5</u>	<u>346.5</u>	<u>355.5</u>
1	0	0	0	0
2	1.0	1.0	1.0	1.0
3	1.0	1.0	1.0	1.0
4	1.0	1.0	1.0	1.0
5	1.0	1.0	1.0	1.0
6	1.0	1.0	1.0	1.0
7	1.0	1.0	1.0	1.0
8	1.0	1.0	1.0	1.0
9	1.0	1.0	1.0	1.0
10	1.0	1.0	1.0	1.0
11	1.0	1.0	1.0	1.0
12	0.987	0.980	0.983	0.974
13	0	0	0	0

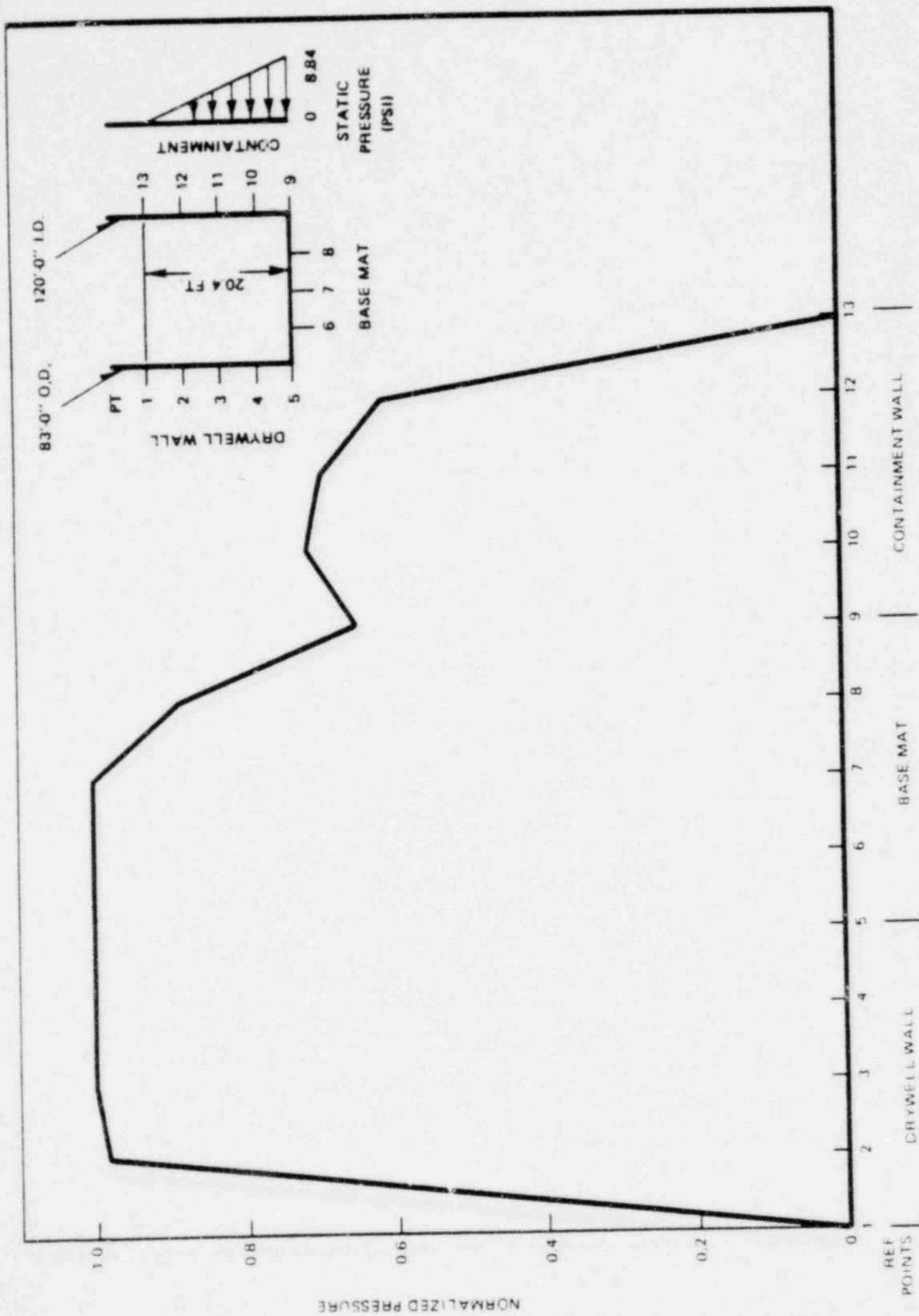


Figure A5.1. Mark III 238-732 Standard Plant One S/R Valve Normalized Wall Pressure at 4.5°

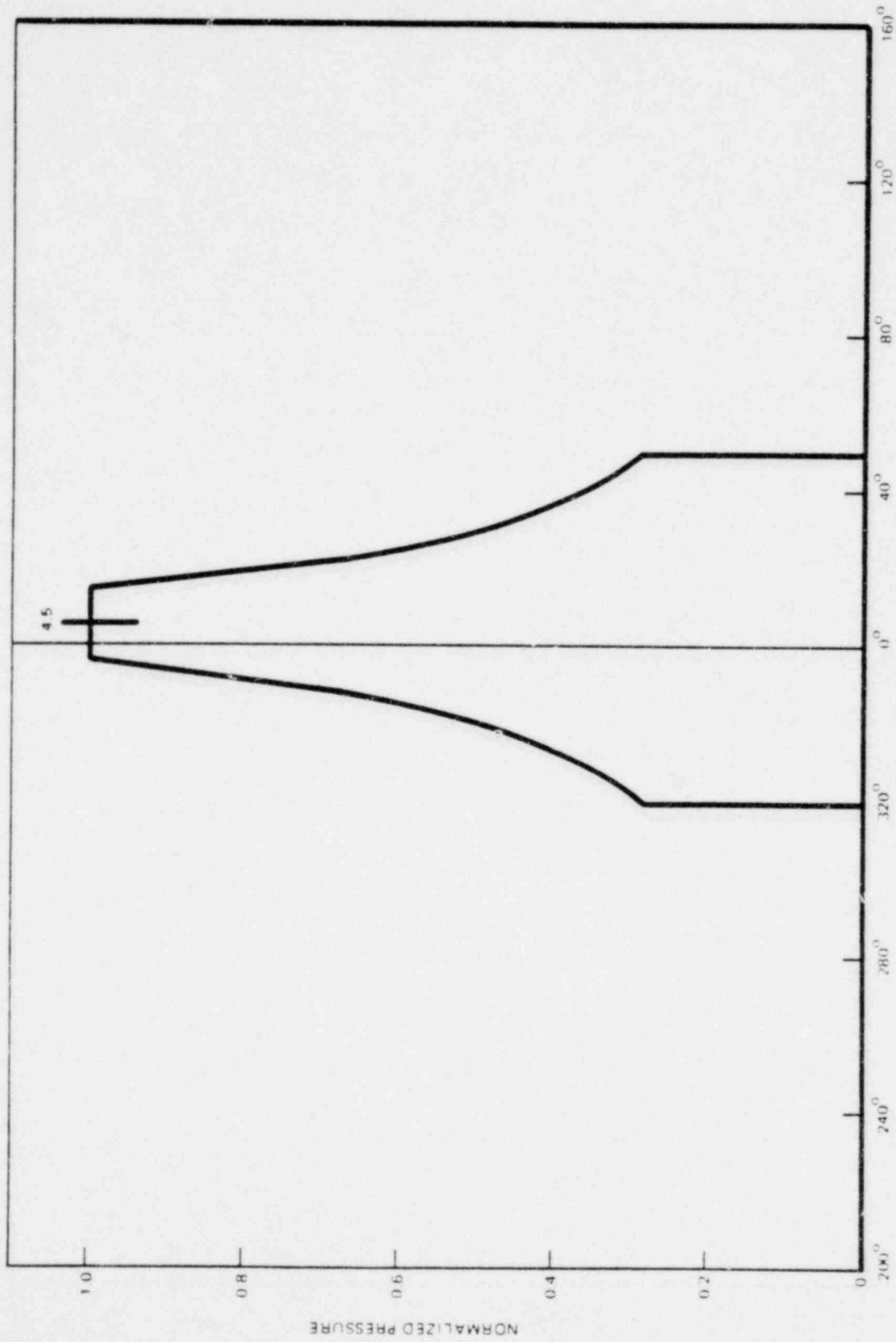


Figure A5.2. Single S/R Valve Reference Point 4 (Circumferential Distribution)

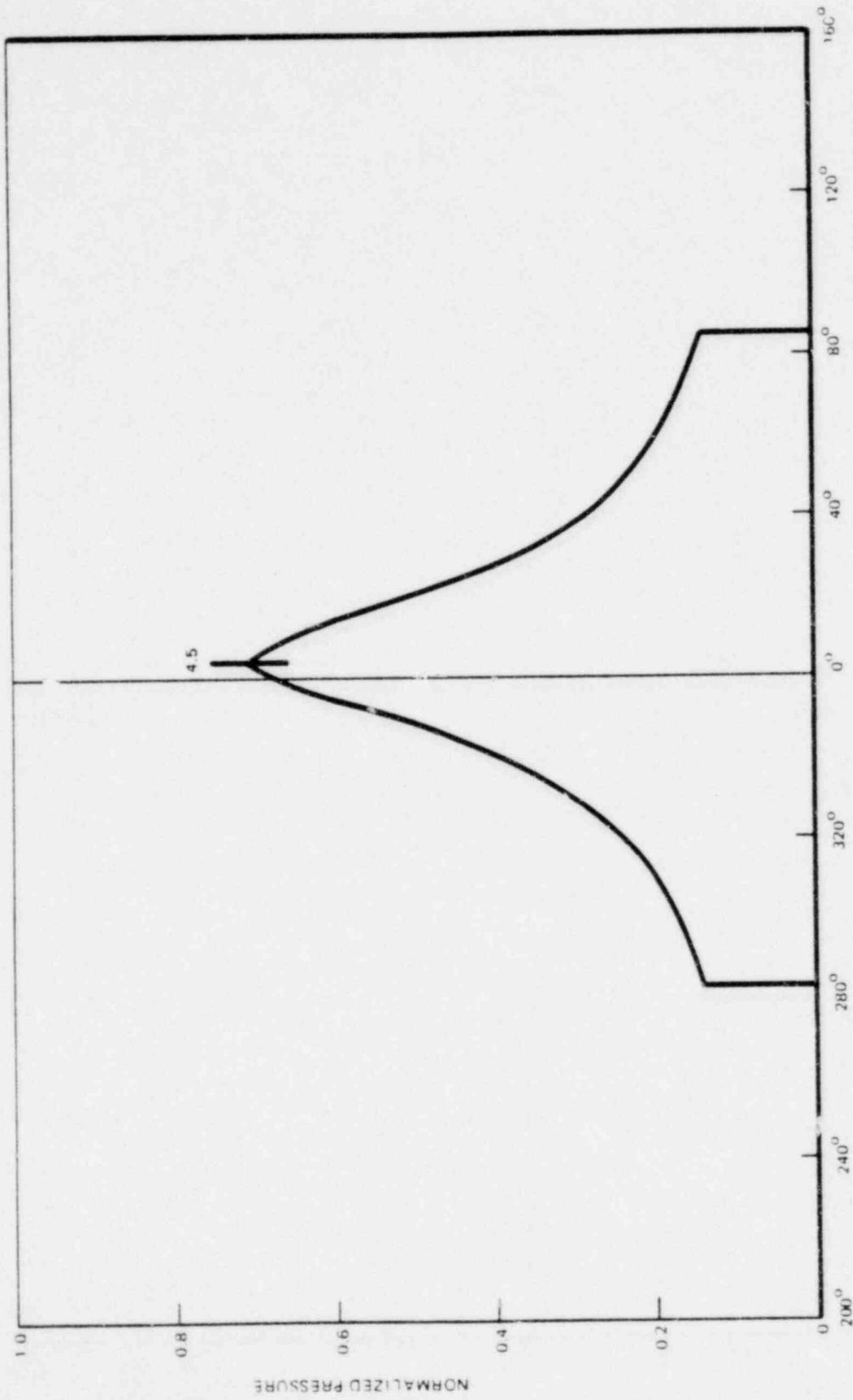


Figure A5.2a. Single S/R Valve Reference Point 10 (Circumferential Distribution)

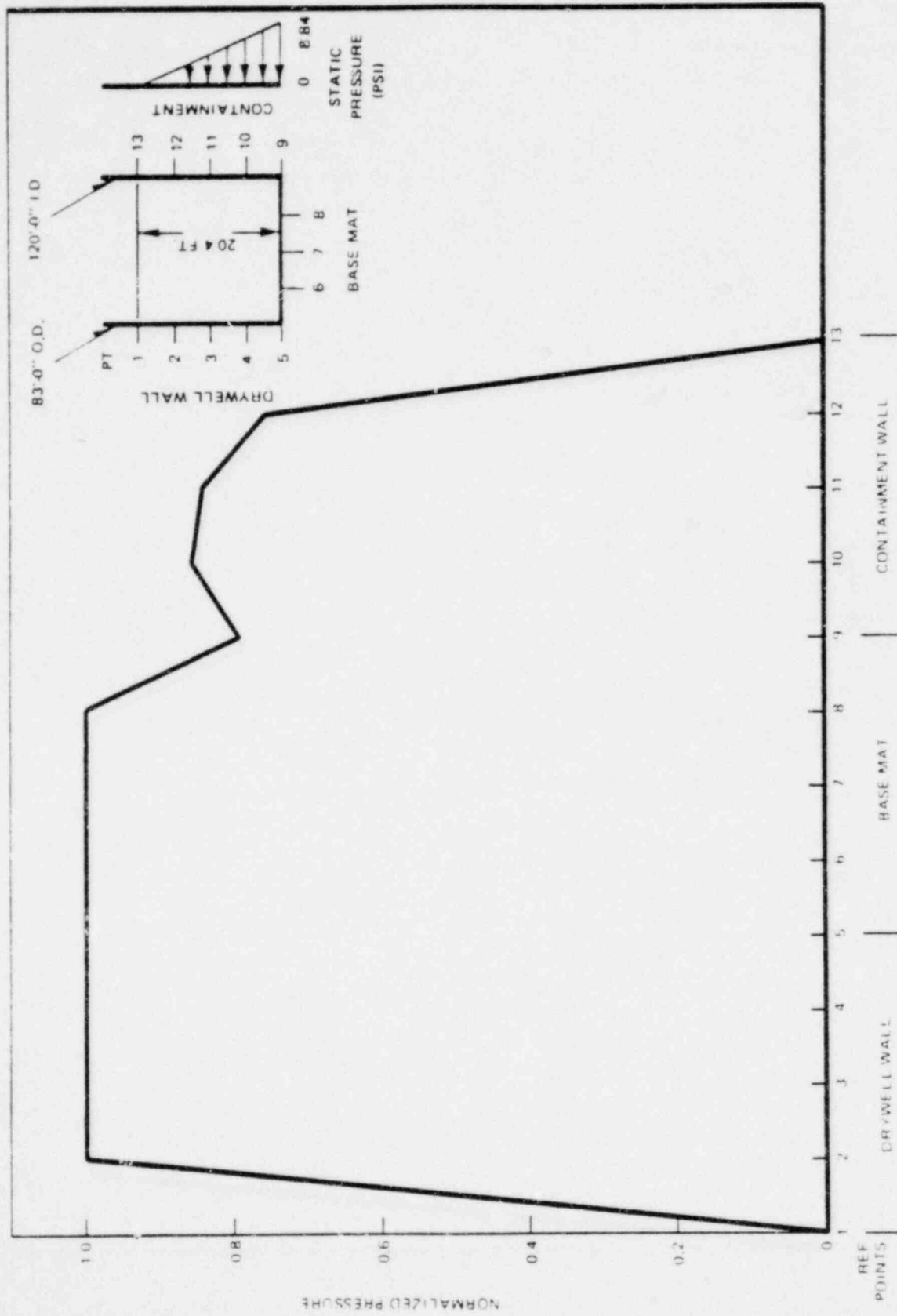


Figure A5.3. Mark III 238-783 Standard Plant 2 S/R Valve Normalized Wall Pressure at 355.5°

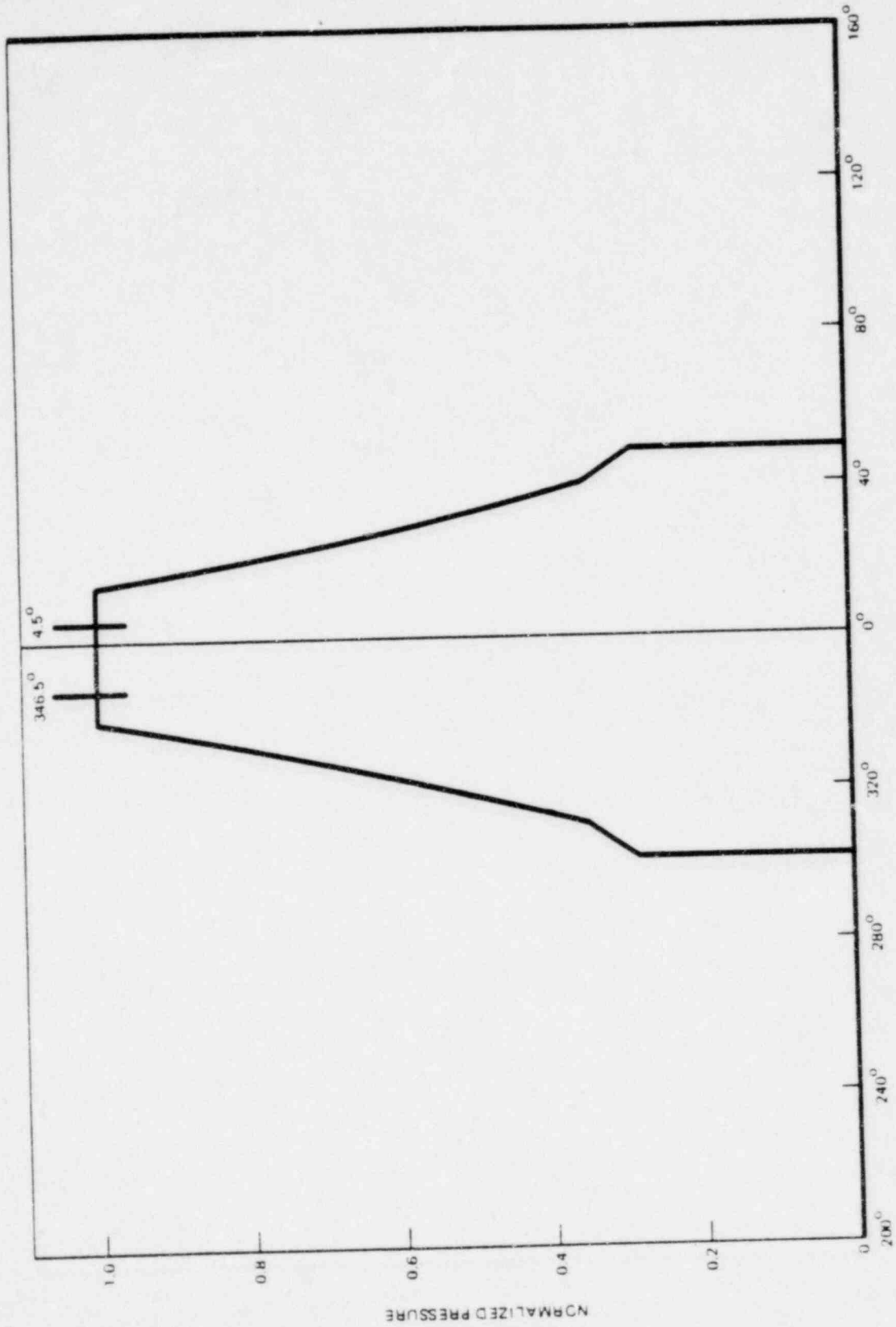


Figure A5.4. Two S/R Valves Reference Point 4 (Circumferential Distribution)

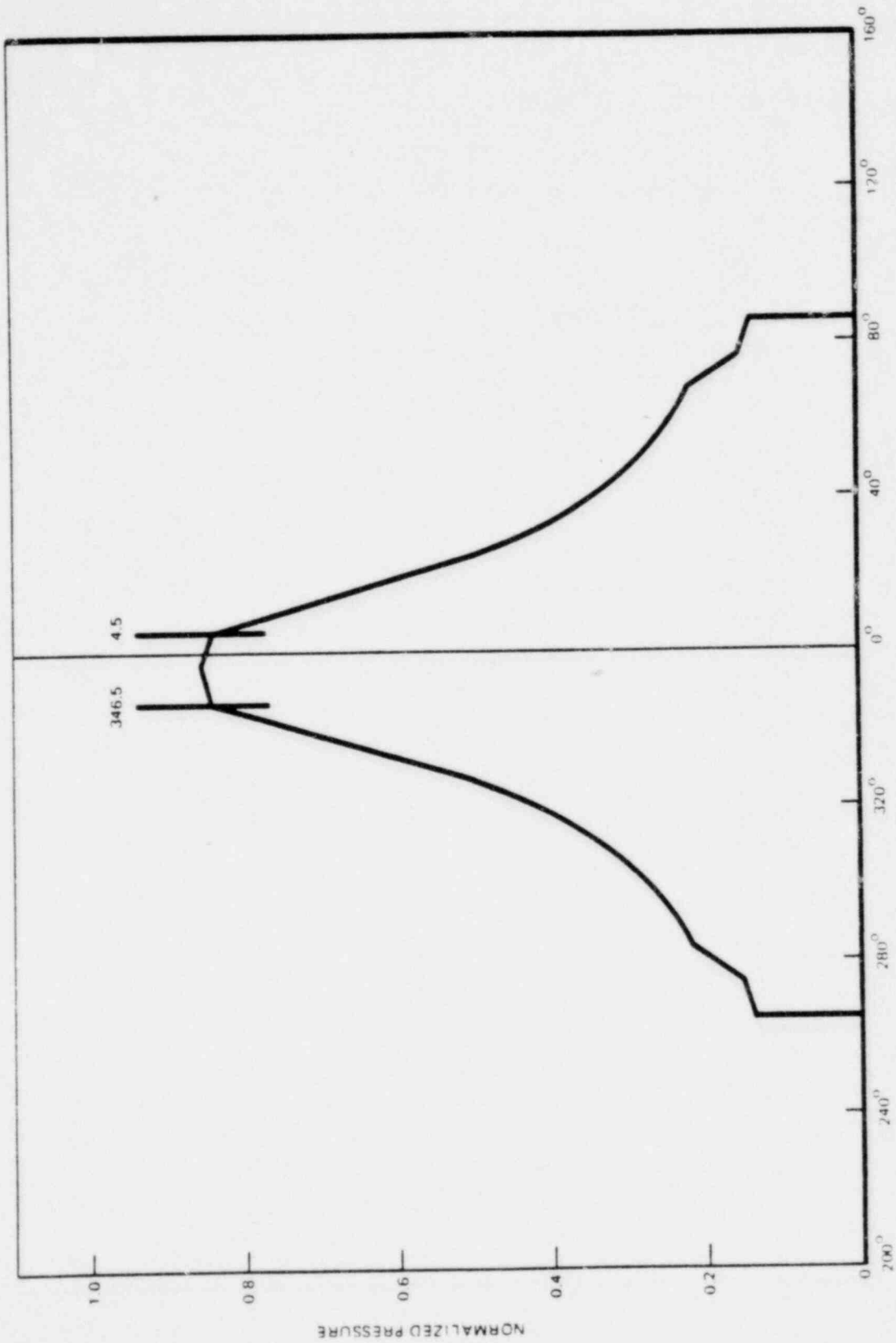


Figure A5.4.a. Two S/R Valves Reference Point 10 (Circumferential Distribution)

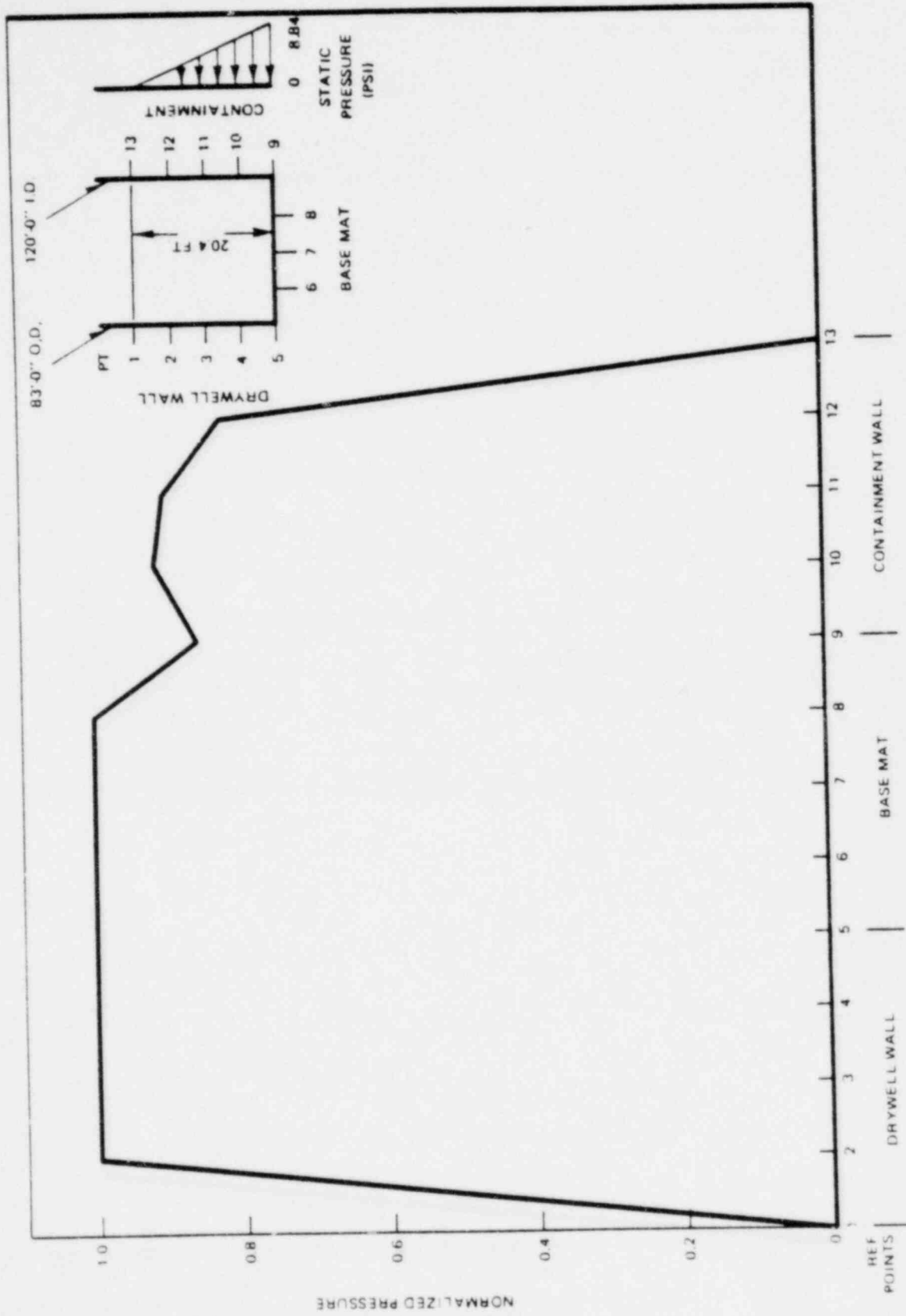


Figure A5.5. Mark III 238-732 Standard Plant 10 S/R Valves Wall Pressure at 355.5°

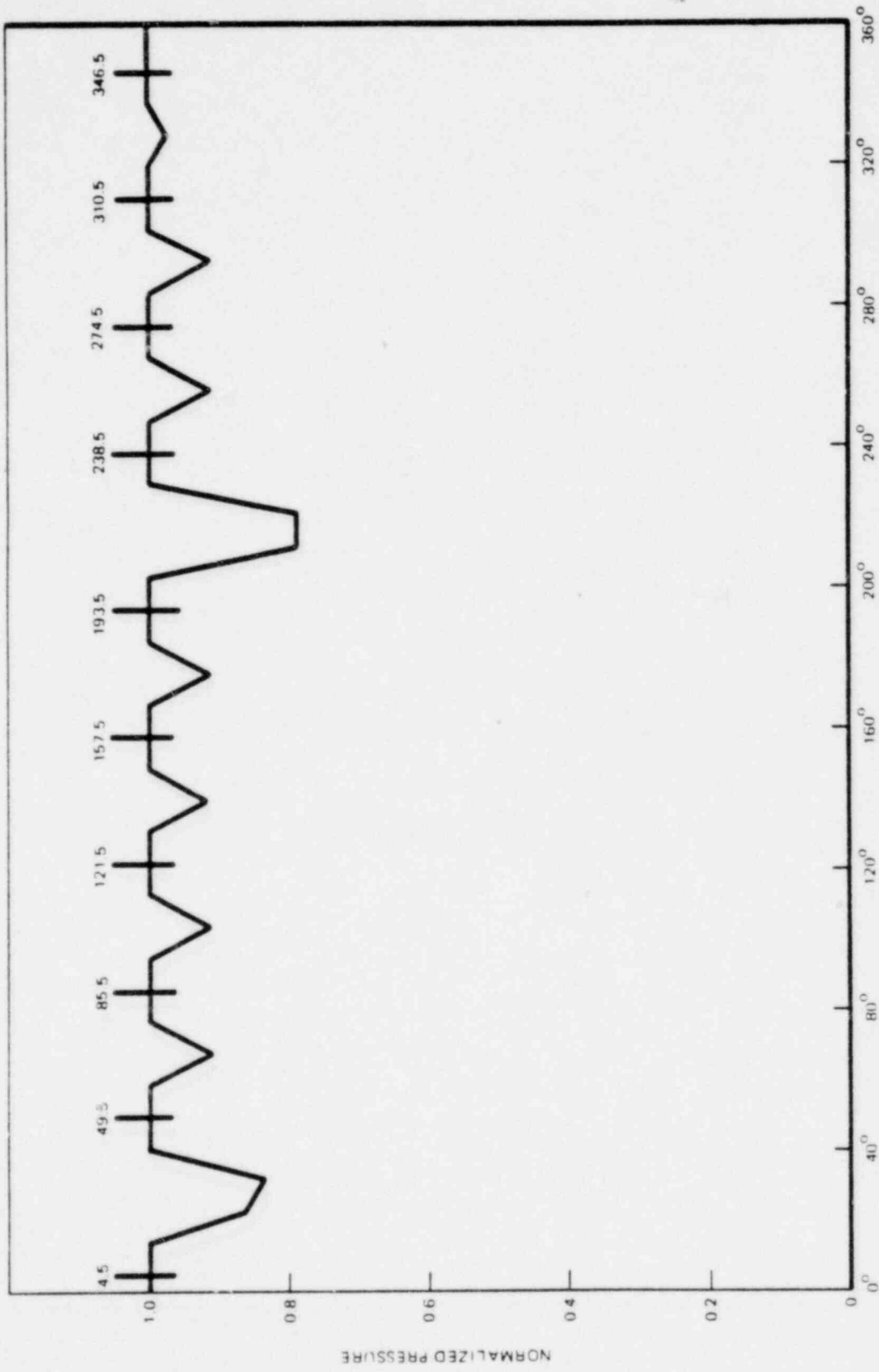


Figure A5.6. Ten Safety/Relief Valves Point 4 (Circumferential Distribution)

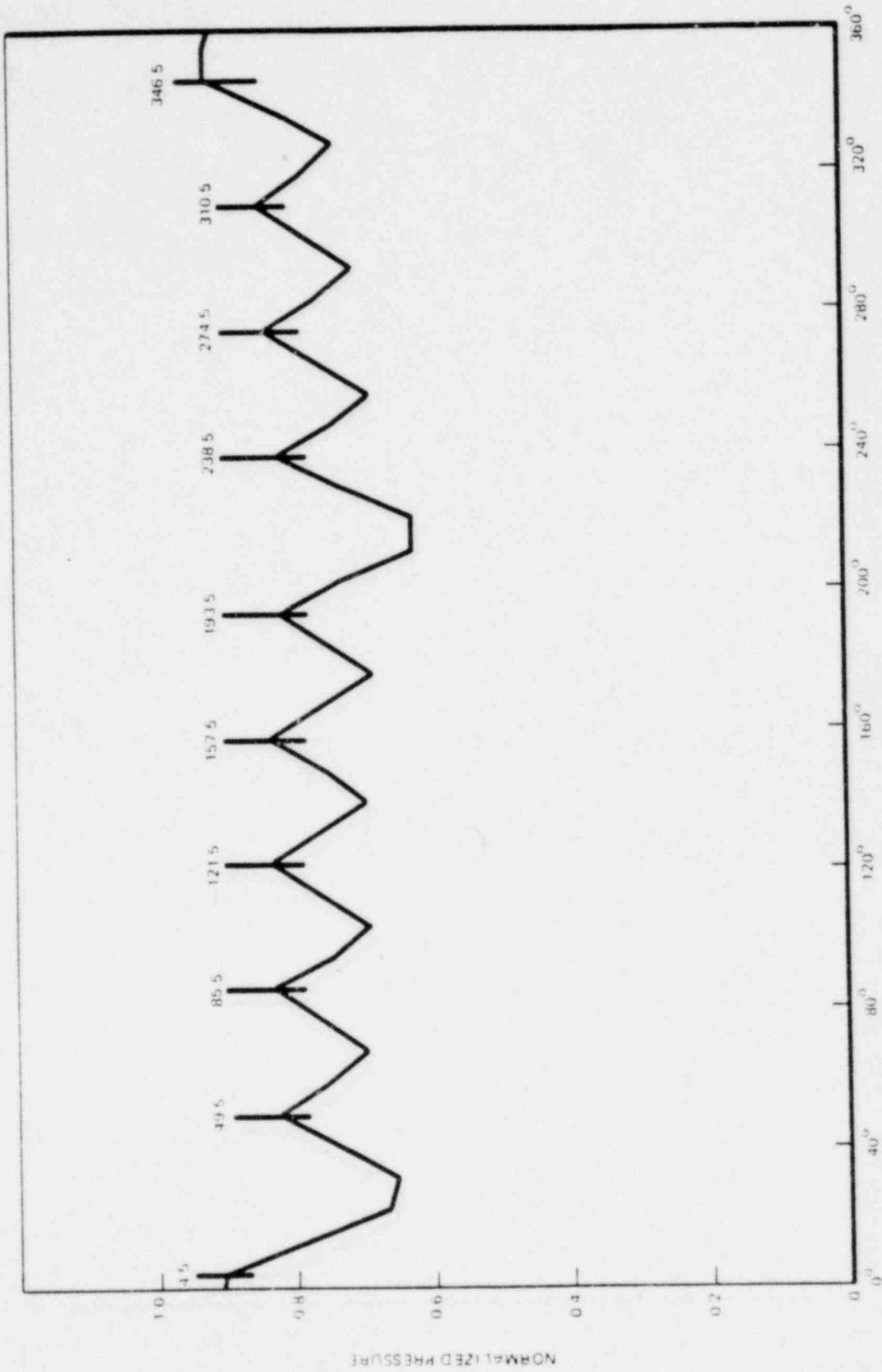


Figure A5.6(a). Ten Safety/Relief Valves Reference Point 10 (Circumferential Distribution)

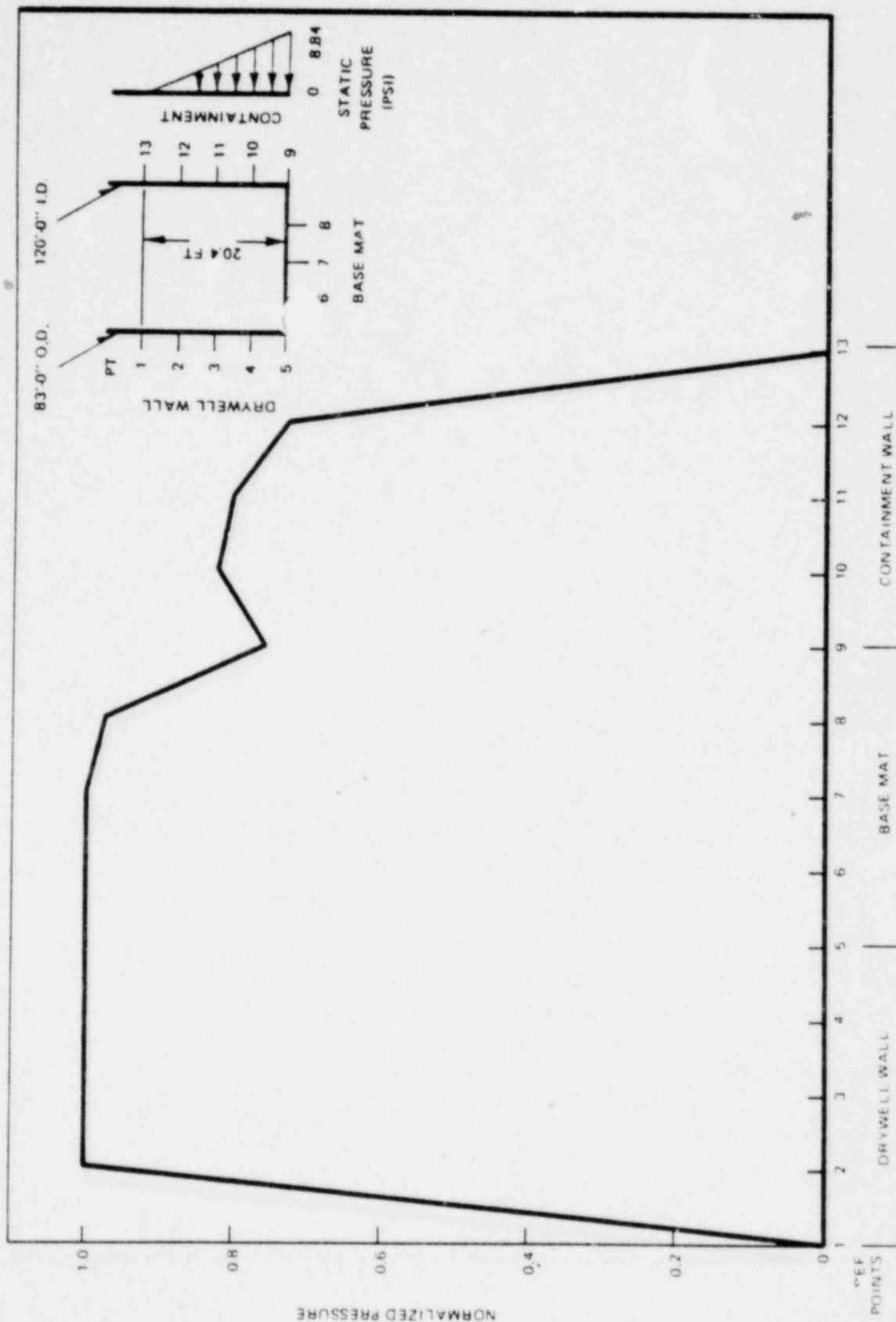


Figure A5.7. Mark III 238-732 Standard Plant, 8 S/R Valves Wall Pressure at 346.5°

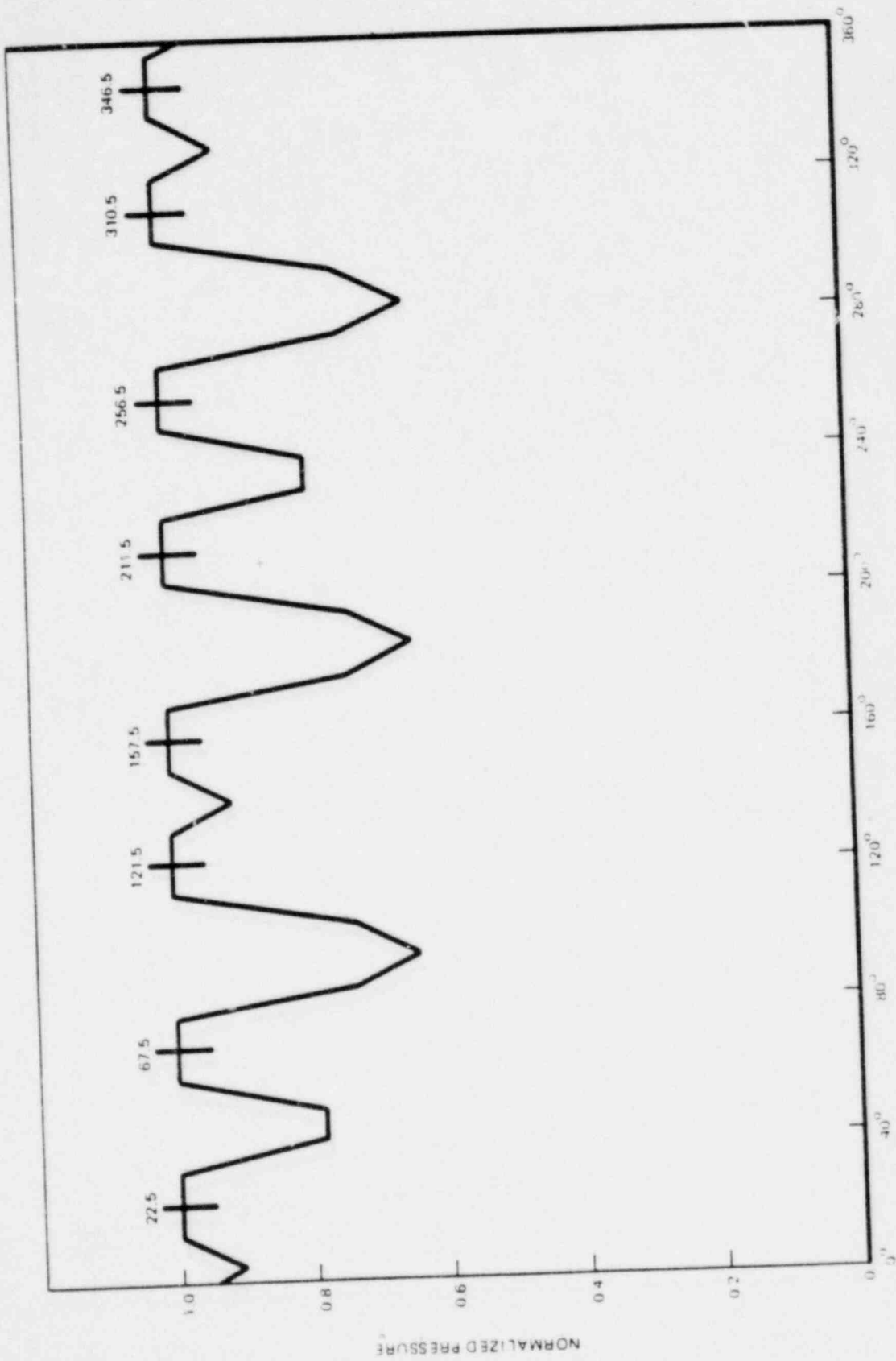


Figure A5.8. Eight Safety/Relief Valves Point 4 (Circumferential Distribution)

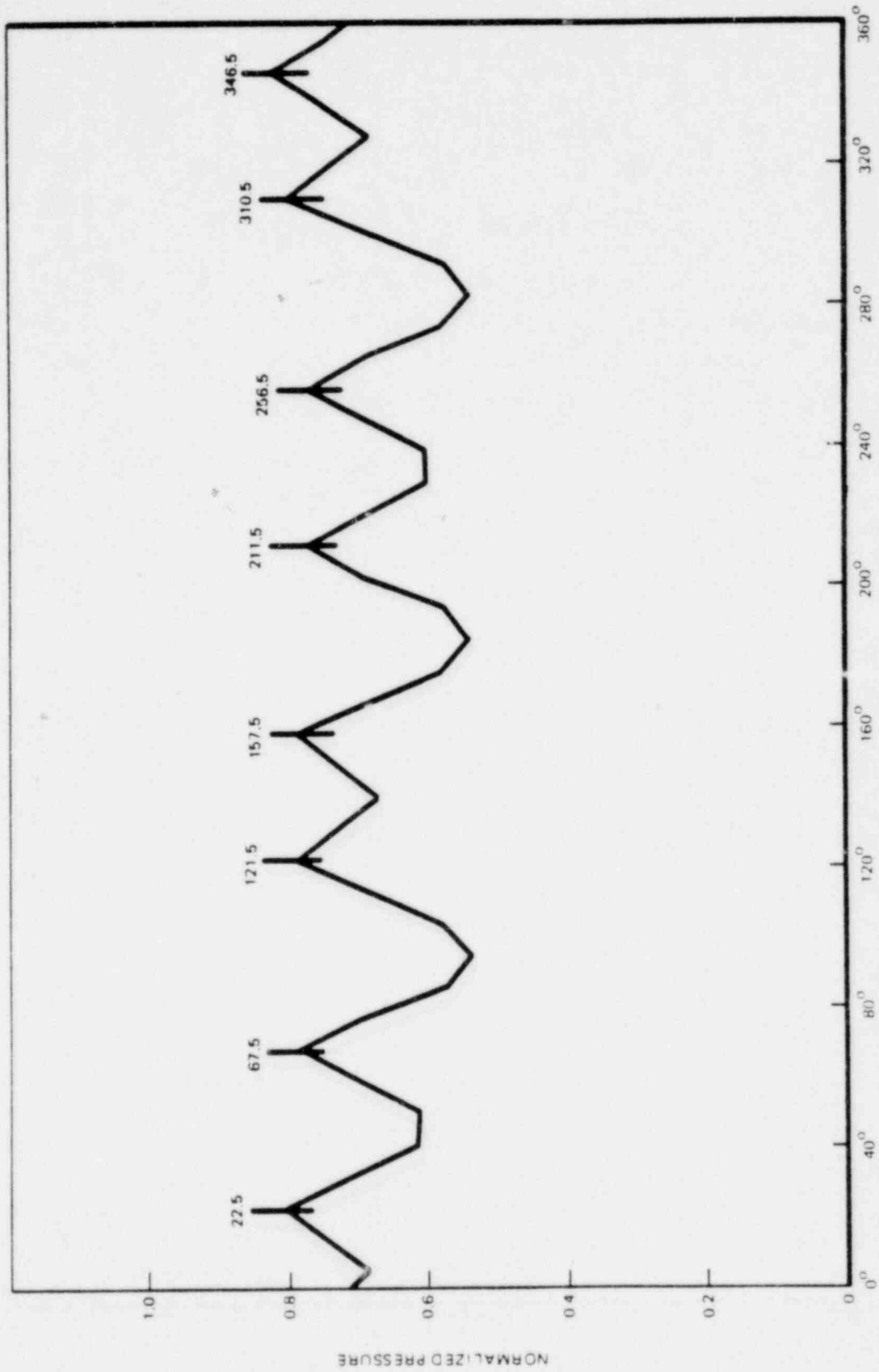


Figure A5.8a. Eight Safety/Relief Valves Reference Point 10 (Circumferential Distribution)

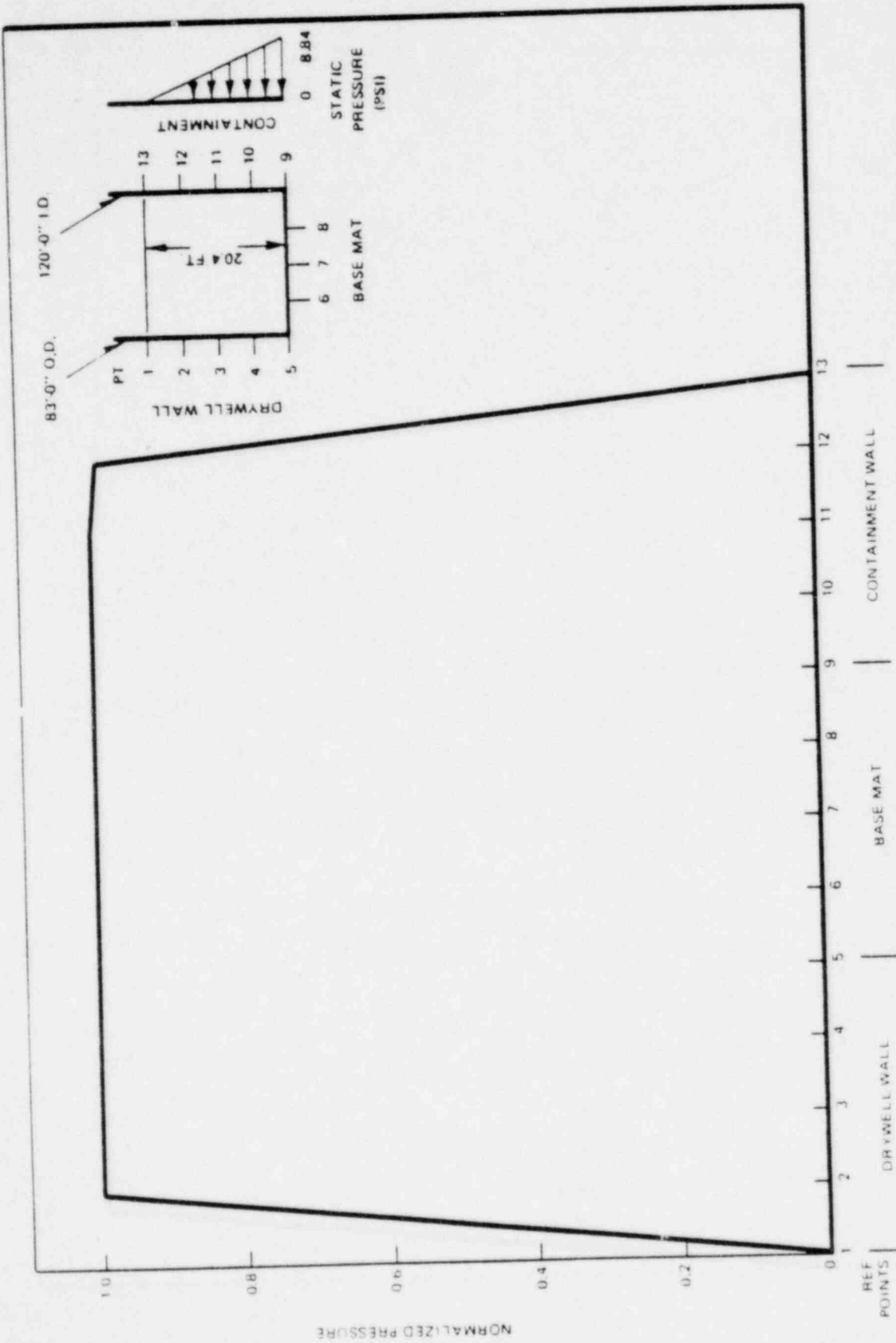


Figure A5.9. Mark III 238-782 Standard Plant 19 S/R Valve Wall Pressure at 130.5° Azimuth

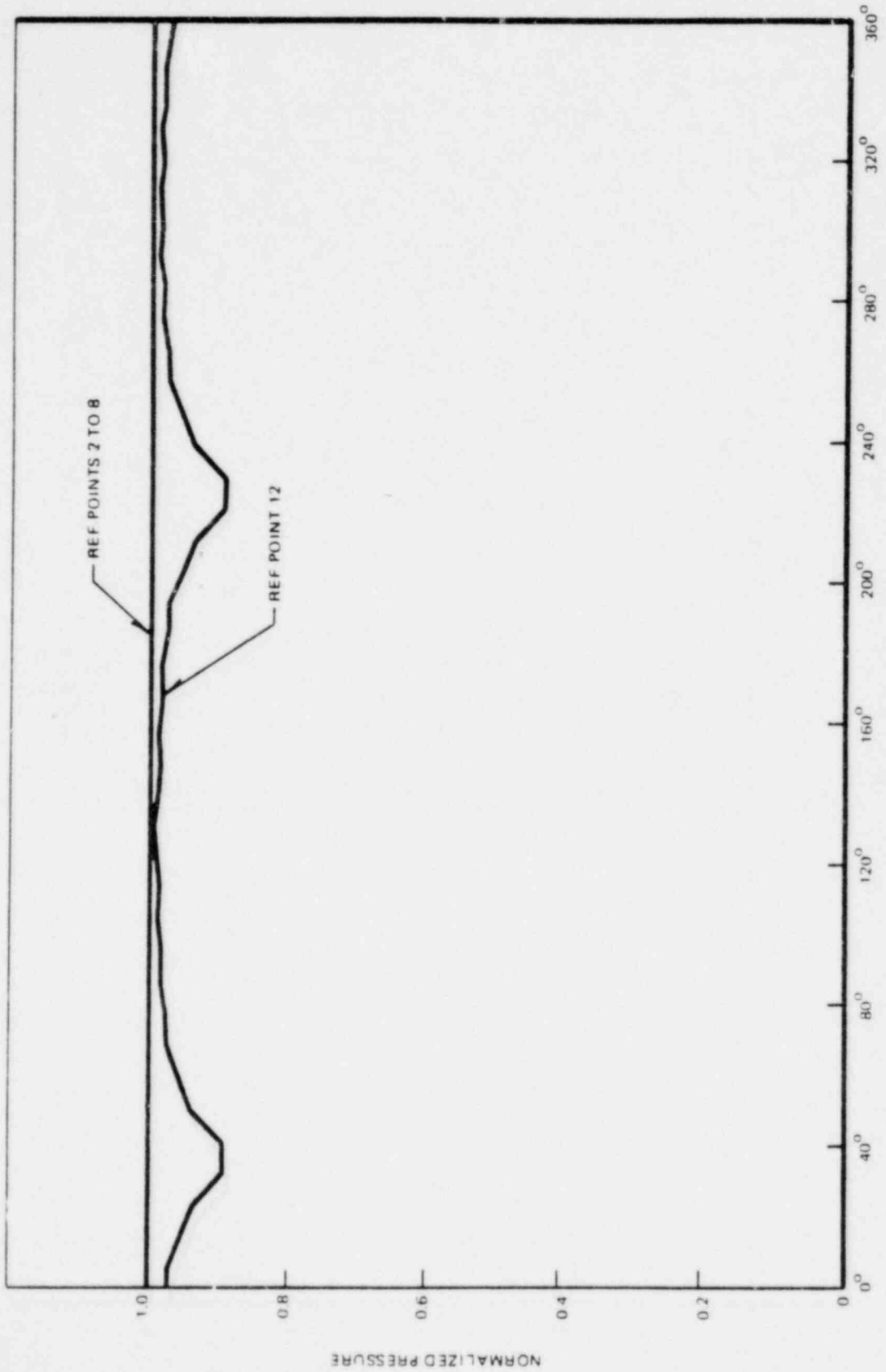


Figure A5.10. Nineteen Safety/Relief Valves (Circumferential Distribution)

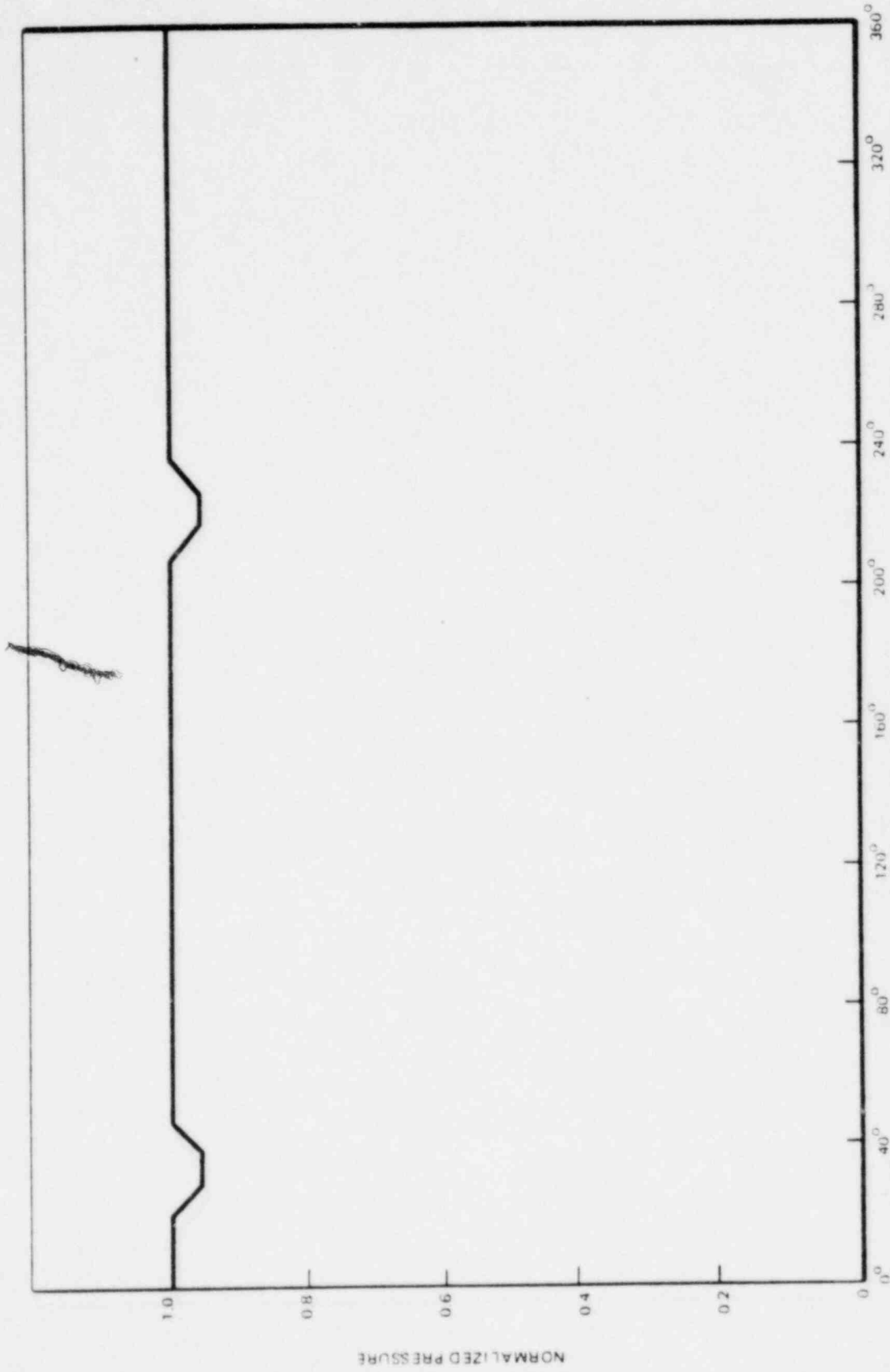
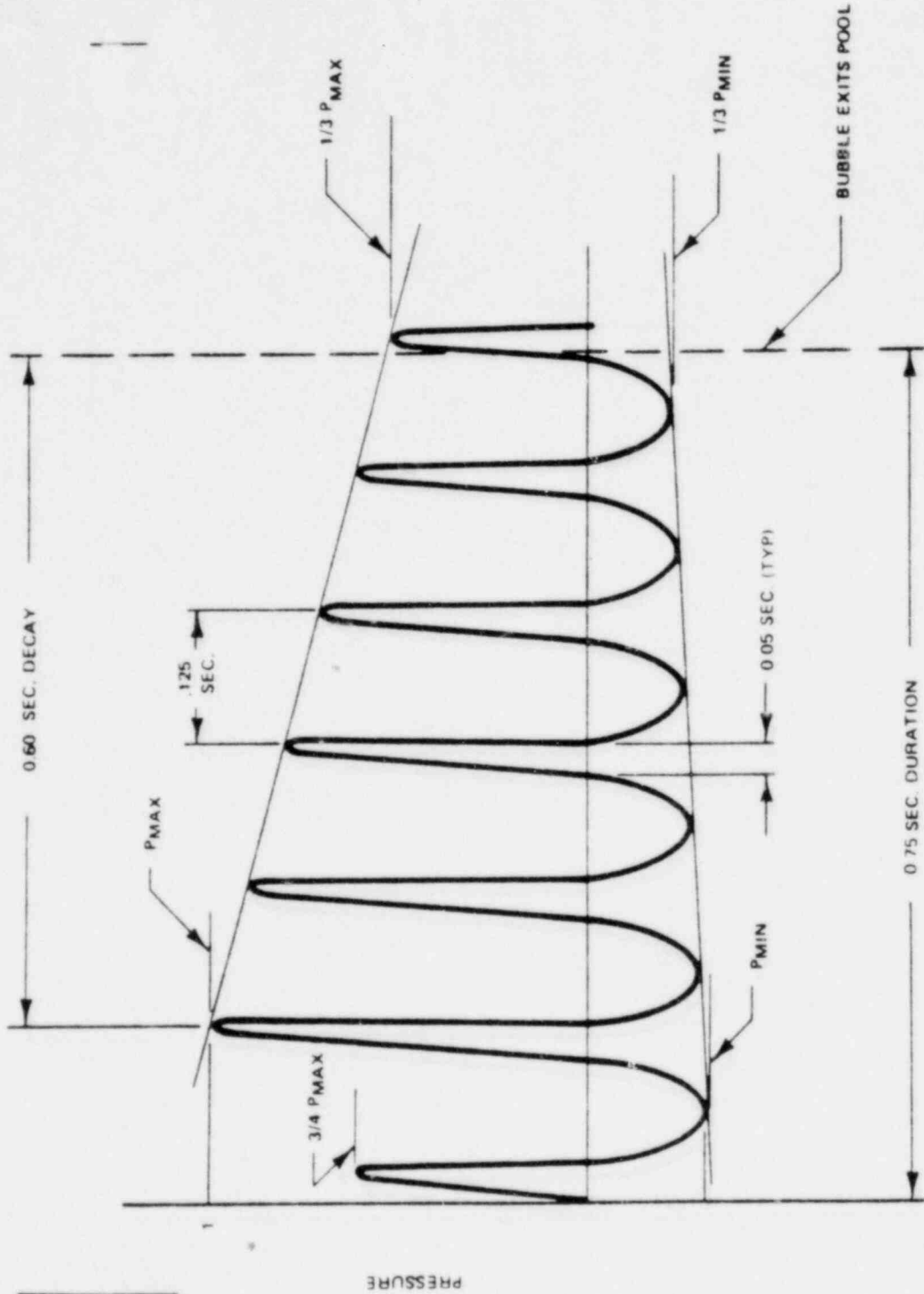


Figure A5.10a. Nineteen S/R Valves Reference Point 10 (Circumferential Distribution)



NOTE
1. PRESSURE
FREQUENCY
RANGE 5 - 12
CYC/SEC.

Figure A5.11. Idealized Quencher Bubble Pressure Oscillation in Suppression Pool

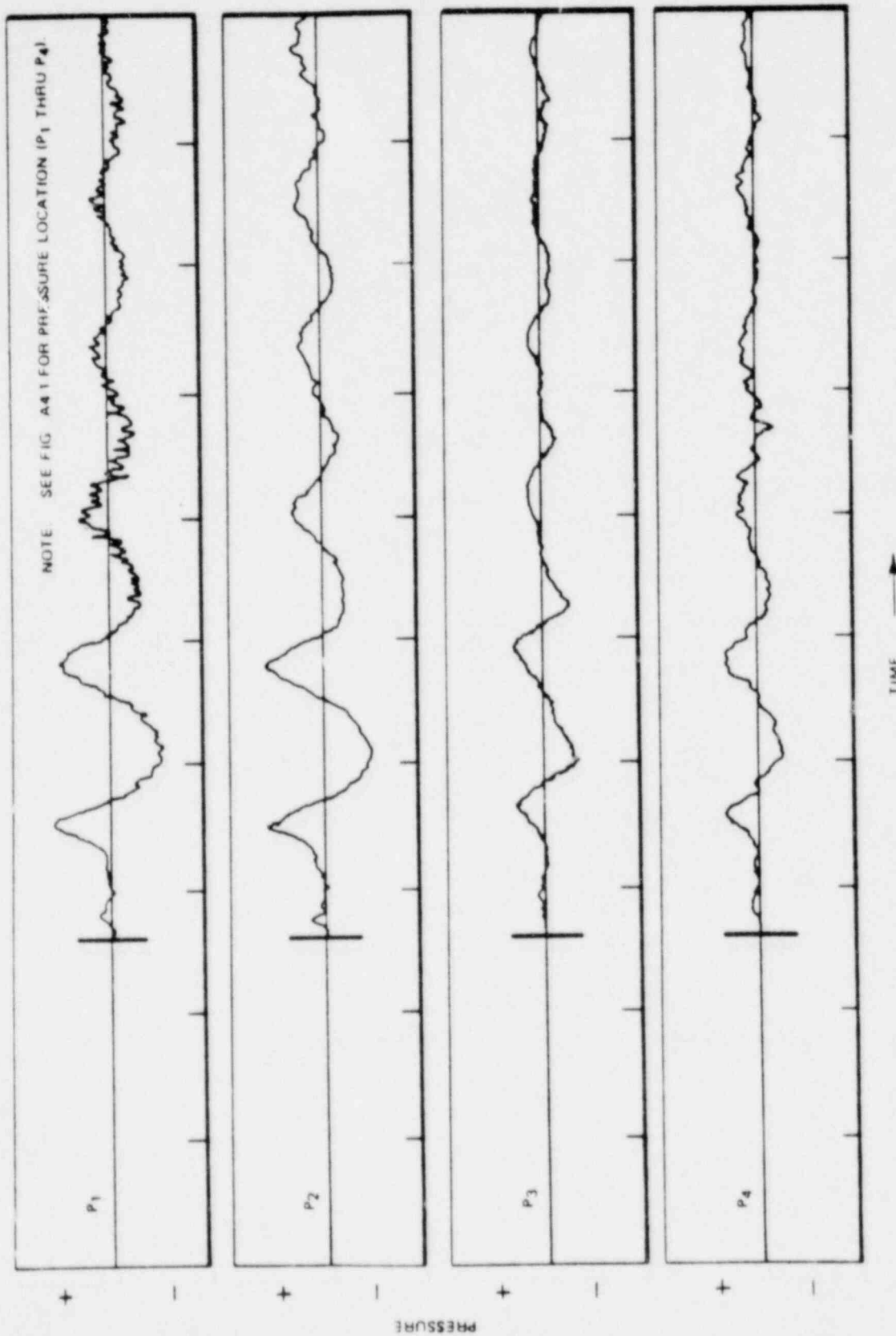


Figure A5.12. Representative Pressure Time History for Quencher Dynamic Load

THIS FIGURE IS INTENTIONALLY DELETED.

A6.0 OTHER LOADS ON STRUCTURES IN THE POOL

A6.1 LOCA AND POOL SWELL

See Section 2.

A6.1.1 Forces on Pipes Due to Vent Clearing Pool Swell and Fallback

The loadings are given for the quencher and reduced to effective pressure on a pipe in Table A6.1. The effective pressures of Table A6.1 can be applied normal to the projected SRVDL or sleeve areas to obtain the maximum design forces. These loads are included in the quencher anchor loads in Section A7.0.

A6.2 THERMAL EXPANSION LOADS

Figure A6.1 gives the pressure and corresponding temperature for the SRVDL as a function of fL/D . The temperature can then be applied to the SRVDL for determining thermal expansion loads.

A6.3 SEISMIC LOADS (BY ARCHITECT-ENGINEER)

The seismic loads are to be applied by the plant designer. These are included in Quencher Anchor Loads, Section A7.0.

A6.4 SEISMIC SLOSH LOADS (BY ARCHITECT-ENGINEER)

See Attachment B.

Table A6.1
LOCA LOADS ON PIPES

<u>Event</u>	<u>Time (sec)</u>	<u>F[*]_p Force On Quencher (lbf)</u>	<u>Water Velocity (ft/sec)</u>	<u>Ref</u>
Water Clearing	0.1 to 0.7		30	Sec. 8.1.1 and Fig. G-3
Pool Swell	0.7 to 3		40	Sec. 8.1.2
Fall Back	3 to 6		35	Sec. 8.1.3

$$*F_p = \frac{C_D \rho V^2}{2g (144)} A$$

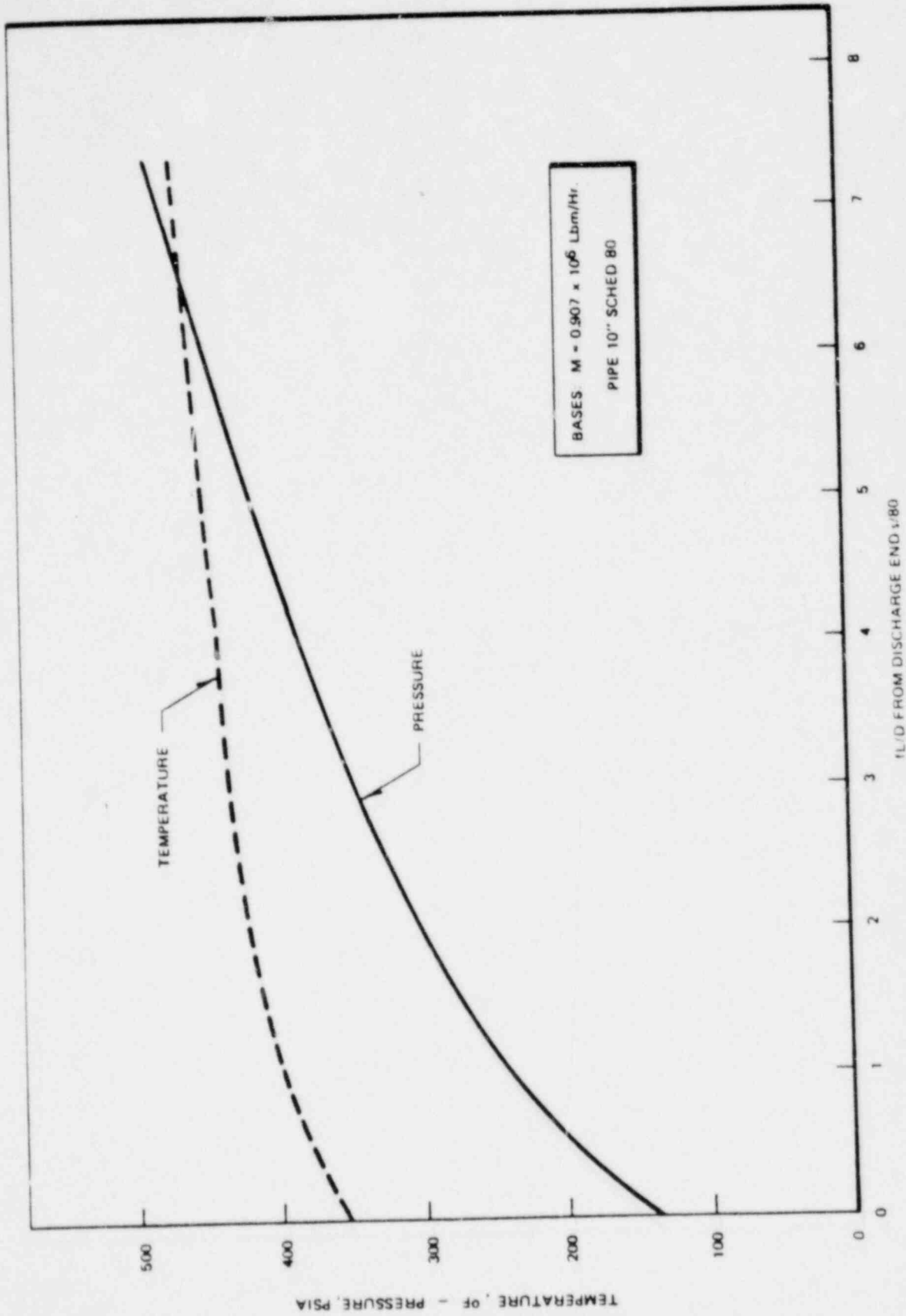


Figure A6.1 Calculated Pressure and Temperature Along S/R Piping During Steady Design Flow

A7.0 QUENCHER ANCHOR LOADS

Figures A4.1, A4.2, A4.6 and A4.8 show the general arrangement of the quencher in the pool. GE has estimated anchor loads for a bottom quencher attachment and these are defined in Tables A7.1 and A7.2 and Figures A7.1 through A7.3, for the 238 Standard Plant. Both air clearing and water clearing load cases were evaluated, as they do not occur simultaneously.

As shown in Figure A7.2 the anchor loads are specified at the base of the quencher and need to be translated to the basemat for embedment design. An additional adapting pedestal is required from the quencher bottom flange to basemat.

There may be advantages to side pedestal anchorage to the drywell. These decisions and investigations are left to the Architect Engineer.

The designer should evaluate the optimum location for anchorage of the RVDL to the drywell sleeve. The analyses should consider line thermal expansion. The designer should also evaluate the drywell penetration sleeve to assure that the drywell concrete local temperature limit is not exceeded. Preliminary thermal calculations for the 238 Standard Plant drywell sleeve show that concrete temperatures for normal operation do not exceed 200°F and 14" Schedule 80 sleeve is acceptable. Designers should perform independent calculations to assure these findings.

A7.1 QUENCHER ARM LOADS AND QUENCHER LOADING APPLICATION

Table A7.1 lists maximum forces exerted on the sparger arms. Corresponding points of force application are illustrated in Figure A7.1. In design of the sparger all of these forces shall be considered as acting simultaneously in directions presenting a maximum loading condition.

Table A7.2 lists typical design loads for the Mark III quencher configuration. These loads consist of allowable inlet line loads, typical operating loads resulting from water clearing, air clearing, LOCA, and safe shutdown earthquake loads. The resultant of these forces, which are considered to act simultaneously in a maximum loading condition, are expressed as base reaction loads illustrated by F_L , F_V , M_L and M_V in Figure A7.2. These are typical design loads for the quencher supporting structure.

Interface loads for plant unique conditions must be calculated and incorporated into the overall plant design.

A7.2 QUENCHER DESIGN INFORMATION

Figures A4.1, A4.2 and A4.3 show the quencher side elevation, top elevation and elevation and angular locations in the suppression pool. The following information is given to assist the designer in the design of a quencher.

A7.2.1 Codes and Standards

- a. American Society of Mechanical Engineers (ASME) Boiler and Pressure Code.
 - (1) ASME Section III, Nuclear Power Plant Components
- b. American National Standards Institute (ANSI)
 - (1) ANSI B16.25, Butt Welding Ends for Pipe, Valves, Flanges, and Fittings.
- c. American Institute of Steel Construction (AISC).

A7.2.2 Design Pressures, Temperatures, Loads, Configuration, and Performance

A7.2.2.1 Component Data

Safety/Relief Valve, Discharge Piping and Quencher:

- | | | |
|----|--|--|
| a. | Design Pressure | 570 psig |
| b. | Design Temperature | 470°F |
| c. | Maximum Pressure | 625 psig |
| d. | Maximum Temperature | sat. steam |
| e. | Maximum Flow
at 1190 psig | 520 metric tons/hr |
| f. | Maximum Steady State
Back Pressure | 40% of safety/relief valve inlet pressure
at rated ASME flow. |
| g. | S/R valve Minimum
Disc. Stroke Time | 0.020 sec |
| h. | Minimum Ambient
Service Temperature | 60°F |

A7.2.2.2 SRVDL Geometry

(See Section A10.)

A7.2.2.3 Quencher Design Criteria

- a. Forces See Figures A7.1, A7.2, A7.3 and
Tables A7.1 and A7.2
- b. Fatigue See Section A9.0 and Figure A5.11
- c. Cycles of operation See Section A9.0 and Figure A5.11

A7.2.2.4 Quencher Configuration and Location

- a. PROPRIETARY, Provided under separate cover
- b. PROPRIETARY, Provided under separate cover
- c. PROPRIETARY, Provided under separate cover
- d. PROPRIETARY, Provided under separate cover
- e. Quencher arm length 58.5 in.
to C_L Quencher
- f. Quencher pipe size/
schedule 12 in./Sched 80 (suggested)
- g. Internal Quencher 101.6 sq in.
pipe area
- h. Min clearance between ≥ 5 ft
 C_L Quencher and pool
floor/basement

- | | | |
|----|---|---|
| i. | Plane of 4 Quencher legs | Horizontal |
| j. | Angle between Quencher legs for greatest installation flexibility | 80°, 80°
80°, 120° |
| k. | Corrosion allowance: | |
| | carbon | 0.240 in. (0.120 per wetted side) |
| | stainless | 0.0048 in. (0.0024 per wetted side) |
| l. | Min submergence to C _L Quencher | 2/3 of min water level or 6 ft min whichever is greater |
| m. | Design rating | 625 psig |
| n. | Minimum clearance between Quencher and CCCS suction | 117 inches |

Table A7.1
QUENCHER ARM LOADS
(Reference Figure A7.1)

<u>Load Description</u>	<u>Mark III</u>
Air clearing - (lbs) (Location F_a , any direction normal to arm centerline)	<u>+16,460*</u>
Adjacent S/R - (lbs) (Location F_b - horizontal direction)	<u>+974</u>
LOCA vent - (lbs) (Location F_b , horizontal direction)	1,866
Arm weight - (lbs) (Location F_c , downward direction)	390
Earthquake load, 1.25g - (lbs) at SSE (Location F_c , vertical direction)	<u>+488</u>
Earthquake load, 1.0g - (lbs) at SSE (Location F_b , horizontal direction)	<u>+390</u>

*Due to single valve subsequent actuation.

Table A7.2
MARK III QUENCHER ANCHOR LOADS
(Reference Figure A7.2)

	<u>Air Clearing</u>	<u>Water Clearing</u>
Lateral Loads - (lbs)		
F_b - Air and water clearing	28,510	8,553
LOCA vent water clearing	10,240	10,240
F_c - SSE Earthquake load (1.0g) quencher mass	3,940	3,940
- SSE Earthquake load (1.0g), water mass	1,680	1,680
F_i - Inlet line load	<u>10,855</u>	<u>10,855</u>
<hr/> $*F_{\lambda}$ - Total base lateral reaction load	<hr/> 53,545	<hr/> 35,268
Vertical Loads - (lbs)		
F_a - Air clearing	<u>+11,344</u>	<u>+4,651</u>
Transient wave	<u>+9,000</u>	-3,700
	-15,000	+2,400
Pool swell	-14,742	-14,742
Quencher weight	+3,940	+3,940
SSE Earthquake load (1.25g)	<u>+4,925</u>	<u>+6,425</u>
F_i - Inlet line load	<u>+10,855</u>	<u>+10,855</u>
Water clearing		+150,000/-2,000
	<hr/> 40,064	<hr/> 178,271
<hr/> $*F_v$ - Total base vertical reaction load	<hr/> -56,866	<hr/> -37,722

Table A7.2 (Continued)

	<u>Air Clearing</u>	<u>Water Clearing</u>
Lateral Moments Transferred to Base Plate - (ft-lbs)		
M_a - Air and water clearing	37,524	11,257
Pool swell	17,751	17,751
Moments resulting from lateral loads -		
2.64 x [F_b (air clearing) + LOCA vent clearing]	102,300	49,614
2.32 x F_c (earthquake, quencher mass)	9,141	9,141
6.67 x F_i (inlet line)	72,402	72,402
3.00 x F_w (earthquake, water mass)	_____	<u>5,040</u>
$*M_l$ - Total base lateral reaction moment	239,118	165,205
Vertical Moments Transferred to Base Plate - (ft-lbs)		
M_b - Air clearing	105,618	31,685
Multiple valve actuation	0	0
LOCA vent clearing	8,047	8,047
M_i - Inlet line moment	<u>25,836</u>	<u>25,836</u>
$*M_v$ - Total base vertical reaction moment	139,501	65,568

*Quencher bottom flange anchor loads. (Individual loads are time dependent and peak values are conservatively combined.)

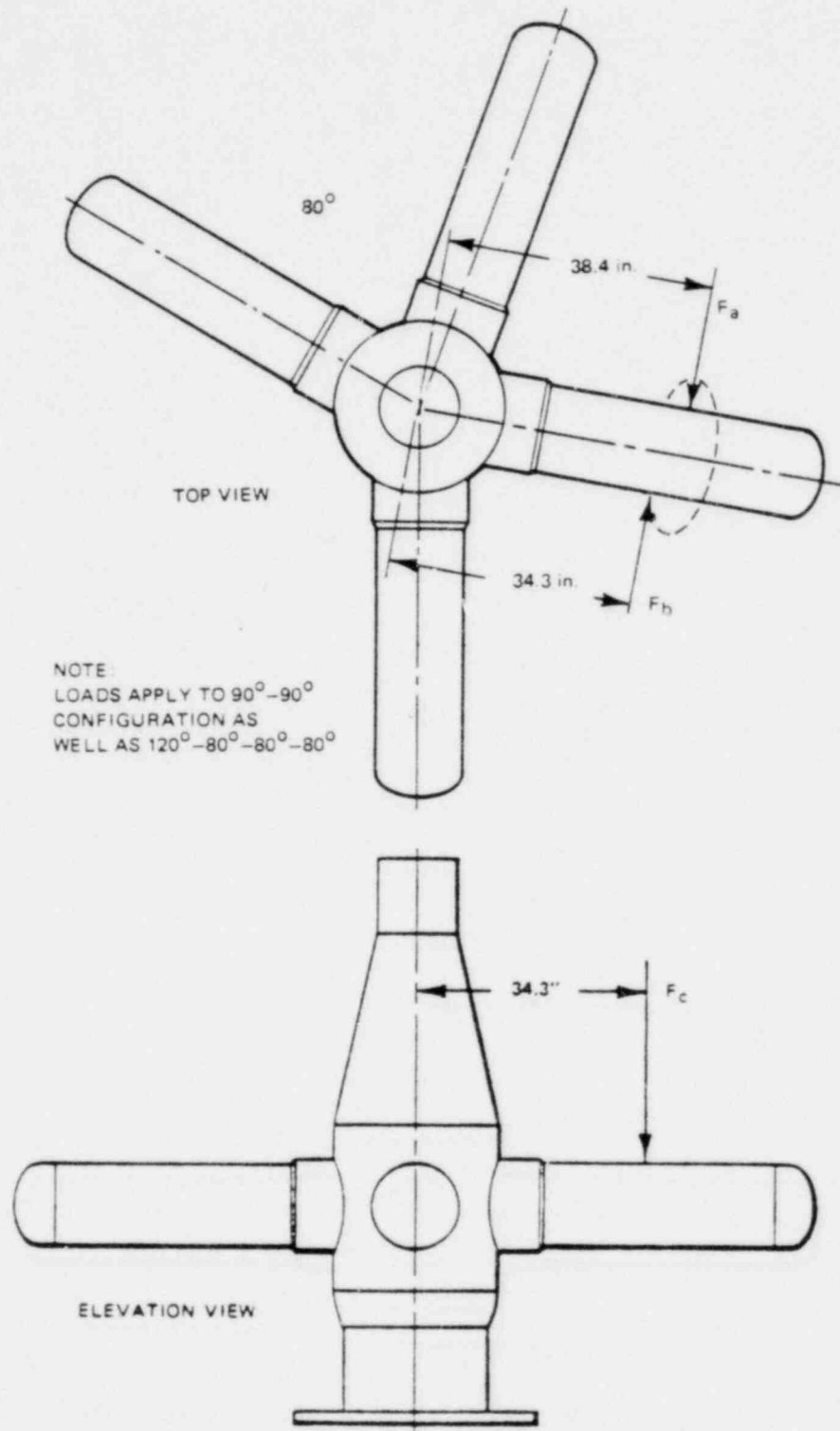


Figure A7.1. Quencher Arm Loads

ORTHOGONAL INLET LINE LOADS F_i
AND M_i FOLLOW THE RELATIONSHIP:

$$\left| \frac{F_i}{F_o} \right| + \left| \frac{M_i}{M_o} \right| \leq 1$$

WHERE: $F_o = 10,855 \text{ lb}$
 $M_o = 25,836 \text{ ft-lb}$

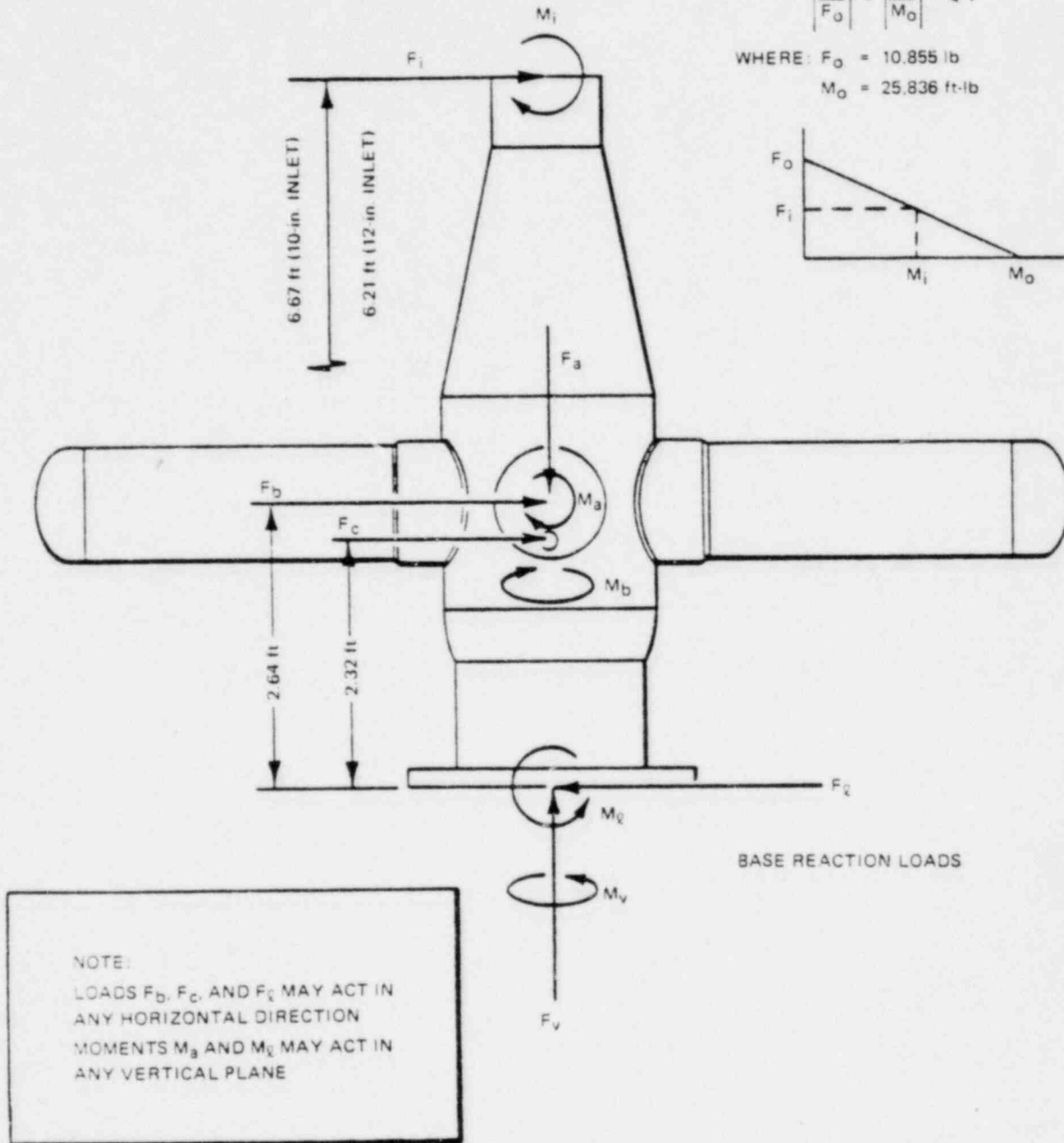
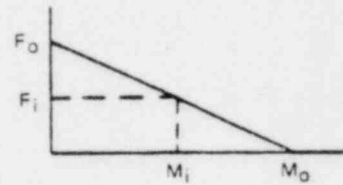


Figure A7.2. Quencher Load Diagram

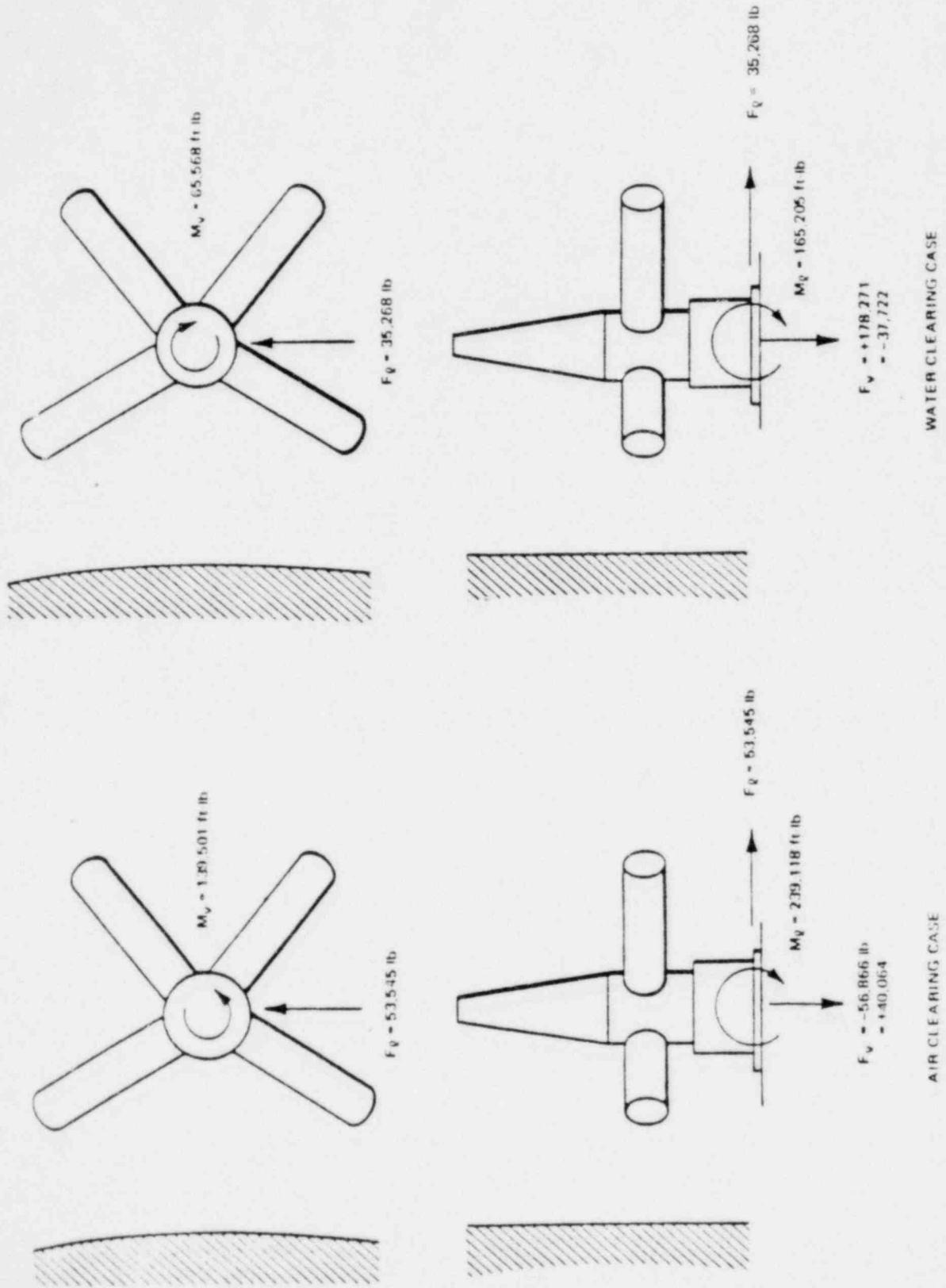


Figure A7.3. Quencher Anchor Load Summary

This figure is PROPRIETARY and is
provided under separate cover.

Figure A7.4. Sectional View of Quencher Leg (Typical Each Side)

A8.0 S/R VALVE LOAD COMBINATIONS

Safety/relief valve discharge piping routed to the suppression pool is arranged so that the points of discharge within the pool are uniformly distributed. (See Figure A4.3.) The location of valve discharge around the pool is for distribution of air clearing loads as well as for considerations of pool thermal mixing.

The number of S/R valves that can open at one time is dependent on many variables. The following table shows several discrete cases where various numbers of open valves can be postulated for the 238 Standard Plant:

Case	Number of Valves	
(1)	1	Single active failure, normal function or operator action. (First or subsequent actuation)
(2)	2 (adjacent)	1 normal plus single active failure of adjacent valve (First actuation)
(3)	10	All ≤ 1113 psi set point valves (First actuation)
(4)	8	ADS Activation (First actuation)
(5)	19 (All)	Vessel pressure ≥ 1123 psi. (First actuation)

The number of S/R valves that will open during a reactor vessel pressure transient could be from 1 to 19 valves. This can be shown for situations where various reactor power levels are assumed when the transient event is initiated. Therefore, the containment must be able to withstand any

number of valves discharging at a given moment. Since the discharge points for valves with various setpoints, or those associated with ADS, are distributed around the suppression pool, the discharge of one or two valves represents an asymmetric load on the containment.

A8.1 SYMMETRIC AND ASYMMETRIC LOAD CASES

The following selected cases represent the asymmetric cases for containment loads:

- A. 1 S/R Valve - This situation can occur due to an operator action or a single active failure. Subsequent actuation of a SRV after an initial pressure transient would be limited to the single 1103 psi set point valve.

- B. 2 Adjacent S/R Valves - This situation can occur due to a pressure transient at low power, which would lift one valve. Concurrent with this the single active failure of an adjacent valve is assumed.

The probability of the precise combination of two adjacent valves would be very low, since common set point valve discharge points are uniformly distributed around the pool. However, if the containment structural design requirements are satisfied under this asymmetric condition, subsequent analysis need not be performed for the multitude of other more probable asymmetric load cases.

The following selected cases represent the symmetric cases for containment loads:

- C. 8 ADS Valves - This situation can occur with an intermediate break where the ADS system is activated.

- D. 10 Valves - This event can occur due to a low power isolation transient.
- E. 19 (All) Valves - This event can occur due to a high power isolation transient.

For structural evaluation the 5 load cases listed above are recommended. From observation of Figures A5.2a, A5.4a, A5.6a, A5.8a, and A5.10a the 1 or 2 valve load case is the governing case for asymmetrical considerations, and the 19 valve load case for maximum symmetrical consideration. The final selection of valve combinations is the designer's (A.E.) responsibility.

A8.2 SSE AND OBE CONSIDERATIONS

Whatever asymmetric or symmetric load cases are evaluated for design, these should be combined with OBE and SSE seismic levels. The seismic combination which yields the controlling stress condition, may be either (OBE or SSE) since allowables and load factors are different for the two conditions.

A8.3 LOCA CONSIDERATIONS

In evaluating the Mark III structural loads and containment/drywell capability it is necessary to properly account for the hypothetical accident related loads and their sequence of occurrence. In defining the loads for this evaluation, this report addresses the design basis accident (pipe break) and the loads associated with the hypothetical concurrent earthquake, pool dynamics, and static loading. The ability of the design to accommodate these loadings, when properly sequenced, constitutes the design basis of the structure. This design basis includes the single failure criterion; i.e., any single component may fail to act when called upon.

This report also addresses an additional consideration namely the inadvertent opening of a single S/R valve. The opening of a single valve is not a direct result of the LOCA and, furthermore, is not an expected occurrence during the accident sequence. However, the loading chart figures show the loads associated with a single safety/relief valve actuation as an additional load for demonstrating additional capability.

A8.3.1 DBA With M.S. Line Break

For the DBA, with M.S. line break no valve will lift due to rapid vessel depressurization (Figure 4.1).

A8.3.2 DBA With Recirculation Line Break

For the DBA, recirculation line break, no valves will lift due to rapid vessel depressurization (Figure 4.1).

A8.3.3 Other SRV Conditions

Other SRV conditions have also been analyzed at the forcing function level and their effect (except for SRV steam condensation) were found to be less controlling than the base case (GESSAR PDA) SRV loads. These other conditions result from a detailed analysis of pressure traces from Caorso SRV Quencher plant tests and the postulation of an SRV discharge under LOCA conditions. These other SRV conditions are:

1. A water clearing spike which precedes the air bubble pressure oscillation for the SRV quencher discharge
2. A leaking SRV discharge
3. SRV steam condensation
4. An SRV discharge for the LOCA related conditions is postulated with a pressurized drywell and wetwell.

The conditions are identified since the forcing function frequency range was generally broader but with much lower pressure amplitude than the normal SRV base cases described in A8.0 and A8.1. Analyses showed that the effects from these additional cases were generally less than the major bubble effects from the base cases even when load reduction factors of Section A12.7 are considered. Comparisons are discussed in the following sections.

A8.3.3.1 Water Clearing Pressure Spike For One SRV, First Actuation, Normal Operating Conditions

During Caorso SRV testing, a high frequency (15 to 30 Hz) pressure spike was observed just prior to the air bubble oscillation as shown in the typical trace on Figure A8.3-1. This spike occurs during the water clearing portion of the SRV blowdown. Multipliers were applied to the predicted bubble pressure amplitude such that the Caorso data, including the spike, would be bounded at a 90-90 one-sided statistical tolerance limit and account for Mark III design conditions.

A comparison was then made of Amplified Response Spectra (ARS) for the forcing function including the water spike and the GESSAR PDA currently specified waveform (Figure A5.11). The results show that the ARS for the GESSAR specified SRV discharge waveform bounds the ARS for the waveform which includes a water spike. In summary, the water spike observed in the Caorso data is not significant due to its short duration and limited number of cycles (one to three) and its effect is bounded by the waveform of Figure A5.11.

A8.3.3.2 First Actuation of One SRV With a Pressurized Containment

For the case of an SRV actuation under small break accident LOCA conditions, when the drywell and containment are pressurized, the initial water level in the SRVDL is depressed below normal water level. This lower water level is due to pressurization of the SRV line through the SRV vacuum breaker. Using a simplified model, the predicted bubble pressure forcing function results in water spike pressures which are lower than predicted for normal operating conditions, and air bubble pressures which are slightly higher due to an increase in air mass from the pressurized drywell condition. This case was

also found to be bounded by the waveform of Figure A5.11 for single valve, first actuation loads when a comparison was made of the amplified response spectra generated from the bubble pressure forcing functions.

A8.3.3.3 Water Clearing Pressure Spike for One SRV, Second Actuation, Normal Operating Conditions

Second Actuation, normal operating condition SRV blowdowns are also characterized by a high frequency water spike followed by lower magnitude, lower frequency air clearing loads as shown in Figure A8.3.2. Second actuations occur with higher initial SRV discharge line (SRVDL) temperature, higher pool temperature, and lower air mass in the SRVDL. Second actuation forcing functions were obtained by applying multipliers to the predicted bubble pressure amplitude such that the Caorso data, including water spike, would be bounded at the 90-90 one-sided statistical tolerance limit and account for Mark III design conditions. Comparison of ARS for this pressure load to the waveform of Figure A5.11 for one SRV, second actuation, showed the GESSAR PDA specification to be bounding.

A8.3.3.4 Second Actuation of One SRV With a Pressurized Containment

Subsequent actuation of SRV's under accident (LOCA) conditions are not predicted to occur; thus no load specifications are required.

A8.3.3.5 First Actuation of One SRV, Leaking Valve Condition

During the Caorso test series one SRV was found to be leaking. Several tests were conducted with this valve to determine the effect on bubble pressure. Results showed the typical water spike followed by low amplitude high frequency (20 to 30 Hz) random oscillatory behavior which was atypical of normal air bubble response. This trace is provided in Figure A8.3.3. An evaluation of this effect was performed using a typical leaking SRV data trace from Caorso. The pressure amplitude was increased to account for design operating conditions. A comparison of amplified response spectra was made for this leaking valve trace and the Figure A5.11 waveform for one SRV, subsequent actuation. The Figure A5.11 waveform was found to be bounding.

The probability of leaky SRV actuation in combination with LOCA is sufficiently small such that the leaky SRV is not specified in combination with LOCA loads (C.O. and Chugging).

A8.3.3.6 Steam Condensation, One SRV

During the Caorso testing of the SRV blowdown, steam condensation effects were observed after the air bubble oscillation phase. Boundary pressure amplitudes of 0.5 to 3.3 psid with typical mean values about ± 2.0 psid, and frequency content of 40 to 110 Hz were noted. These values also apply to Mark III. An evaluation of the effect of these steam condensation loads was made by selecting a Caorso data trace with the highest RMS pressure value. The steam condensation trace with the highest RMS pressure value is shown in Figure A8.3.4. This case was compared to the Figure A5.11 waveform by an evaluation of amplified response spectra. The case was bounded by the GESSAR PDA specification for one SRV subsequent actuation. For load cases in which first actuation SRV loads are significant to design, the SRV steam condensation trace shown in Figure A8.3-4 should be evaluated in series with the waveform of Figure A5-11 for first actuation.

(GE COMPANY PROPRIETARY INFORMATION PROVIDED UNDER SEPARATE COVER)

Figure A8.3-1. SRV Quencher Bubble Pressure - First Actuation |

(GE COMPANY PROPRIETARY INFORMATION PROVIDED UNDER SEPARATE COVER)

Figure A8.3-2. SRV Quencher Bubble Pressure - Second Actuation |

(GE COMPANY PROPRIETARY INFORMATION PROVIDED UNDER SEPARATE COVER)

Figure A8.3-3. SRV Quencher Bubble Pressure - Leaking Valve
First Actuation

(GE COMPANY PROPRIETARY INFORMATION PROVIDED UNDER SEPARATE COVER)

Figure A8.3-4. Pool Boundary Pressure Time-History for One Second
of SRV Condensation

A8.4 RECOMMENDED DESIGN LOAD SUMMATION

The design loads on MK III structures are comprised of static (dead loads, live loads, hydro, etc.) and alternating dynamic loads (seismic and S/R valve loads, etc.).

For postulated simultaneous occurrence of S/R valve loads and SSE, the method recommended by the Task Group on Dynamic Analysis (TGDA) of the ASME Code committee for combining loads will be adopted:

$$R = \sum_{i=1}^n (DC)_i \pm \left\{ \sum_{i=1}^n (AC)_i^2 \right\}^{1/2}$$

where

R = resultant response of the structure, e.g., displacement, acceleration, load or stress.

DC = slowly varying or non-alternating component of the dynamic response.

AC = alternating component of response defined as maximum response value minus its corresponding DC component.

i = 1, 2, . . . number of time varying events for which the resultant response is calculated.

The use of this method is justified by the fact that earthquake excitation is a random process with amplitude increasing to a peak and then decaying and the fact that the amplitude of the S/R valve loads also rise to a peak and then decay. Therefore, considering that the dynamic responses of

such loads possess varying frequencies, amplitudes and random phase relationship with respect to each other, this method is adequate for calculating the design loads.

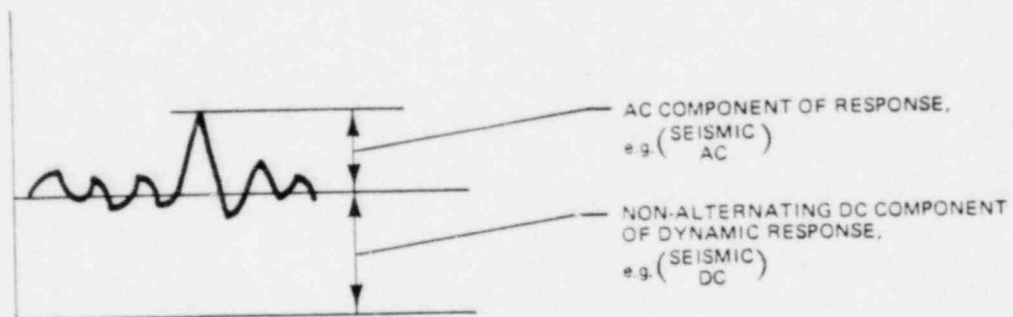
More simply, the above equation with respect to loads or stresses, etc., may be represented by:

$$EF = D.L. + L.L. + Hydro + \left[\begin{array}{c} SRV \\ DC \end{array} \right] + \left[\begin{array}{c} Seismic \\ DC \end{array} \right] + \sqrt{\left[\begin{array}{c} SRV \\ AC \end{array} \right]^2 + \left[\begin{array}{c} Seismic \\ AC \end{array} \right]^2}$$

where:

- D.L., L.L., Hydro = Static Loads
- $\left[\begin{array}{c} SRV \\ DC \end{array} \right]$, $\left[\begin{array}{c} Seismic \\ DC \end{array} \right]$ = Slowly varying or non-alternating component (DC) of the dynamic response
- $\left[\begin{array}{c} SRV \\ AC \end{array} \right]$, $\left[\begin{array}{c} Seismic \\ AC \end{array} \right]$ = Alternating component of response defined as the maximum response value minus the corresponding DC component.

This is simply represented as follows:



when the alternating component has no DC component, the DC terms drop out.

A9.0 FATIGUE CYCLES

A number of safety relief valve (SRV) discharge events may occur during the 40-year plant life. An analysis, based on many years of BWR plant operations, was performed to determine the mean frequency of occurrence of these potential events. Results of the study are summarized in Table A9.1.

Transients which result in containment isolation are identified in the table. During isolation events the decay heat is initially removed from the reactor vessel via the SRV's. As shown in the table, half to all of the valves are initially actuated. Subsequently, the low-low set valve cycles until the RHR steam condensing mode is established or the main condenser becomes available. The total actuations of the low-low set valve during an isolation event is 15 per event. The valve nominally remains open 80-90 seconds following each opening actuation.

The non-isolation transients are also listed in Table A9.1. These events typically result in a single opening actuation of several or all SRV's, but the low-low set SRV does not cycle. When all valves are actuated, the open duration is 5-10 seconds.

Considering 15 actuations for each isolation event and all of the non-isolation events, the total number of SRV actuations is approximately 1800. Each actuation results in certain pressure pulses in the suppression pool which are transmitted to the containment as discussed throughout attachment A. For fatigue evaluation purposes the most significant forcing function on the containment due to SRV actuation is the SRV bubble pressure.

The normal bubble frequency range and duration are provided in Figure A5.11. Using this figure in conjunction with the SRV actuations provides the number of cycles affecting the containment due to the SRV air bubbles.

The SRV steam condensation pressure oscillation frequency is nominally specified as 80 CPS. This value is based upon the pressure trace shown in Figure A8.3-4. Utilizing this frequency, the noted durations per actuation, and the number of actuations provides the cycles in the event this load has significant stress

affect on the containment. The phenomenon creates a relatively high number of cycles but the lower pressure amplitude forcing function typically results in low stress intensities. Hence, the containment fatigue factor due to this load is minor compared to the normal bubble effect.

The discussed events, actuations, frequencies and durations are applicable to all BWR6 plants as low-low set logic has been incorporated. However, specific fatigue usage factors due to the various SRV forcing functions will vary as the factors are dependent on the unique stress analyses applicable to a given plant. The SRV loading fatigue effects should be considered by the containment designer.

Table A9.1
SAFETY/RELIEF VALVE ACTUATION

<u>Events</u>	<u>Mean Frequency/ 40 Years</u>	<u>Number of Valves Open for Initial Blow</u>			<u>Isolation Type Event</u>
		<u>(All 2/3)</u>	<u>(1/2- 2/3)</u>	<u>(1/3 -0)</u>	
Turbine Trip (w/BP)	53	x			No
Load Rejection (w/BP)	30	x			No
Pressure Regulator Failure	26		x		Yes
Feedwater Controller Failure	20		x		No
Trip of Both Recircu- lation Pumps	13		x		No
Recirculation Con- troller Failure	13		x		No
Loss of Feedwater Flow	30			x	No
Loss of Auxiliary Power	15	x			Yes
Closure of all MSIV's	40	x			Yes
Loss of Condenser Vacuum	26	x			Yes
Inadvertent Relief Valve Opening	4.0			x	No
Turbine Trip (w/o BP)	0.5	x			Yes
Load Rejection (w/o BP)	0.5	x			Yes

This page deleted intentionally.

A10.0 RECOMMENDED CALCULATION PROCEDURES FOR MARK III DESIGNERS

The following information provides the procedures for predicting loads on the drywell wall, basemat, and containment wall associated with the air clearing transient following the opening of a safety-relief valve for the 238 standard MARK III plant. The numbers are applicable for those plants having a quencher of the standard design installed on the discharge end of the pipe. The given bubble pressures are based on information in Section A12.0. For design purposes, a statistical evaluation of the data was used. Design values represent a 95%-95% tolerance statement relative to that data. The bubble pressures are predicted for the first opening and consecutive opening cases.

A10.1 CONSTRAINTS

The following constraints are not to be exceeded for the design of the RVDL.

- (1) Peak Pipe Pressure ≤ 25 psid.
- (2) $\frac{FL}{D}$ cannot exceed those values given in Figure A3.1 at the corresponding pipe volume.
- (3) Water Leg ≤ 17.8 ft.

Constraints on routing the safety/relief valve discharge line are:

1. No more than one 90° long radius bend coming off the relief valve, and two 45° long radius bends entering the quencher in the 10" schd 80 piping. The remaining bends should be in the

12" schd 40 piping as far down stream as possible such that no more than 50% of the total fL/D of the system is in the first half of the length of the discharge line.

2. The initial length of 10" schd 40 pipe be kept to a minimum.

A10.2 DETERMINE SRVDL DESIGN

The following steps are recommended for designing the SRVDL within the above constraints and the design requirements in Table A4.2.

- (1) Layout Preparation for SRVDL Routing
The designer will prepare a layout drawing similar to Figure A10.2 and later detail the SRVDL. The longest line will be evaluated first.
- (2) From the longest SRVDL length the air volume and fL/D values are calculated and plotted on Figure A3.1. This is an iterative process where a balance of 10, 12, and 14-inch SCH 40 piping is adjusted to the minimum total air volume and fL/D for the 625 psi pipe pressure constraint. It is important to insure that all the SRVDL air volume and fL/D from the SRV to the free water surface is included. Figure A10.1 shows the portion of SRVDL from the SRV to the first anchor.
- (3) For the portion of the SRVDL shown in Figure A10.1, the loss coefficients, K, for each of the three flexible joints are shown on the figure. The line lengths for each plant size is given in Tables A10.1, A10.2 and A10.3.
- (4) Repeat the iterative process of (2) for each of the other SRVDL.

(5) fL/D

The corresponding maximum values of fL/D are calculated in reference to the 10" pipe velocities as shown below. Pipe friction losses should be considered from the S/R valve to the surface of the water.

(a) For reference to 10" pipe velocities:

$$fL/D)_{\text{Ref } 10''} = \left[K_{\text{Total } 10''} + K_{\text{Total } 12''} \left(\frac{A_{10''}}{A_{12''}} \right)^2 + K_{\text{Total } 14''} \left(\frac{A_{10''}}{A_{14''}} \right)^2 + \dots \right]$$

where:

$$K_{\text{Total } 10''} = fL/D_{10''} + K_{\text{Losses } 10''} S/40$$

$$K_{\text{Total } 12''} = fL/D_{12''} + K_{\text{Losses } 12''} S/40$$

$$K_{\text{Total } 14''} = fL/D_{14''} + K_{\text{Losses } 14''} S/40$$

$$A_{10''} = \text{Hydraulic area of 10" schd 40 pipe (ft}^2\text{)}$$

$$A_{12''} = \text{Hydraulic area of 12" schd 40 pipe (ft}^2\text{)}$$

$$A_{14''} = \text{Hydraulic area of 14" schd 40 pipe (ft}^2\text{)}$$

$$D_{10''} = \text{Diameter of 10" schd 40 pipe (ft)}$$

$$D_{12''} = \text{Diameter of 12" schd 40 pipe (ft)}$$

$$D_{14''} = \text{Diameter of 14" schd 40 pipe (ft)}$$

The friction factor "f" in the above equations should be calculated based on the pipe diameter, relative roughness of the pipe, and the Reynolds number. A Reynold's number of approximately 3×10^6 is appropriate. Based on this Reynold's number and the pipe of a commercial steel a typical value of "f" is 0.015.

Using the system fL/D calculated above enter Figure A3.1 with corresponding air volume. The intersection must fall on or above the 625 psid curve.

- (6) Determine the quencher bubble pressure using the actual air volume in the RVDL, see Section A12.6.

A10.3 S/R VALVE AIR CLEARING LOADS MARK III 238 STANDARD PLANT

After the quencher bubble pressure has been obtained, Section A12.6, the next step is to calculate wall pressures based on the peak bubble value (+ and -).

A10.3.1 Absolute Pressure on Basemat and Walls

The absolute pressure anywhere on the drywell wall, basemat, and containment wall in the wetwell region can be calculated by the equation:

$$P(a) = P_{\text{containment}} + \frac{\rho h(a)}{144} + \Delta P(r) \quad (1)$$

where

$P(a)$ = absolute pressure at arbitrary point "a" (psia)

r = distance from quencher center to point "a" (ft)

$P_{\text{containment}}$ = absolute pressure of containment atmosphere (psia)

$h(a)$ = water head acting at point "a" (ft)

ρ = water density (approx. 62.4 lbm/ft³)

$\Delta P(r)$ = bubble pressure attenuated by distance (r) to point "a".

The attenuated bubble pressure for one S/RV, $\Delta P(r)$, can be calculated from the bubble pressure, ΔP_B , [which is obtained from Section A12.6] using the following equations:

$$\Delta P(r) = 2 \times \Delta P_B \left(\frac{r_0}{r} \right) \text{ for } r > 2r_0 \quad (2)$$

$$\Delta P(r) = \Delta P_B \text{ for } r \leq 2r_0 \quad (3)$$

where,

r_0 = quencher radius = 4.875 ft.

A10.3.2 How to Find the Attenuated Pressure on the Drywell Wall, Basemat, and Containment Wall.

A10.3.2.1 Develop grid to determine values of (r)

1. Make a scaled layout of the pool with quencher (Figure A10.3).
2. Divide wall distances by four (4).

3. Arc distance by $360^\circ \div (\text{vent stations})$ (Table A10.4).
4. Draw line (Figure A10.3) from bubble cloud extremity (i.e., quencher radius) tangent to drywell wall and project to containment. This gives the area of pressure influence for this quencher.
5. The point (a) is then selected and the distance (r) to (a) is obtained from the layout.

A10.3.2.2 Wall Pressure at Point (a) Single S/R Valve.

The wall pressures are obtained from A10.3.1 equation (2) and (3).

A10.3.2.3 Wall Pressure at Point (a) for Multiple S/R Valve.

In the event of multiple S/RV actuation the attenuated bubble pressure, ΔP_B , must be calculated using the following equations:

$$\Delta P(r) = \left[\sum_{n=1}^n \Delta P_n^2 \right]^{1/2}$$

where,

$$\Delta P_n = 2\Delta P_B \left(\frac{r_0}{r_n} \right) \quad \text{for } r_n > 2r_0$$

$$\Delta P_n = \Delta P_B \quad \text{for } r_n \leq 2r_0$$

If the calculated $\Delta P(r) > \Delta P_B$, set $\Delta P(r) = \Delta P_B$. Note that r_n = the distance from the center of the quencher to point a.

For the cases where multiple valves are discharged due to a pressure transient, the valves in each set point group (1103, 1113, and 1123 psi) are assumed to discharge simultaneously. The setpoint groups, however, will discharge at different times depending on the rate of reactor pressure increase associated with the event under consideration. The most severe pressure transient is the postulated "generator load rejection with failure of the turbine bypass valve" event which results in a calculated 132 psi per second pressure increase at the beginning of the transient. This results in a 0.075 second difference in time of discharge due to the 10 psi difference in pressure setpoints of the valve groups. Using the quencher bubble model presented in Figure A5.11, it is seen that when P_{MAX} from the 1123 psi setpoint valves occurs, the bubble pressure from the 1113 psi setpoint valves has dropped to $0.9175 P_{MAX}$, and the bubble pressure from the 1103 psi setpoint valve is $0.835 P_{MAX}$. These values are used in determining the attenuated bubble pressure at a point (a) for the multiple S/R valve cases.

For local peak containment pressure loading, there is significant reduction in pressure at certain locations when considering the time sequenced phasing approach. The most limiting position on the containment is not affected (i.e., the local peak pressure is equal to the maximum positive bubble pressure, 18.6 psid). In addition, the 95-95 confidence level statistical analysis for the individual valve is conservatively applied to the multiple valve cases without consideration of the number of valves being actuated. In reality, the 95-95 confidence total load for the 19 valve case is much lower than that used in the local pool boundary load calculation. These two factors (i.e., time phasing and the multiple valve statistical consideration) have not been included in the development of the local pressure distributions on the containment wall because they do not affect the limiting local pressure. However, these factors are important to the structural response and will be employed in the building response evaluation. Attachment M presents the method for treating these effects in determining structural response used for the equipment evaluations.

Table A10.1
218 STANDARD PLANT PIPE SPOOL DIMENSIONS

<u>Valve No.</u>	<u>Dimension A (in.)</u>	<u>Dimension B (in.)</u>	<u>Total Dimension (in.)</u>	<u>(A + B) (ft)</u>
V1	73.38	82.50	155.88	13.0
V2	73.38	82.50	155.88	13.0
V3	73.38	82.50	155.88	13.0
V5	73.38	72.12	145.50	12.12
V6	130.00	71.62	201.62	16.80
V7	118.38	71.50	189.88	15.82
V8	115.88	71.00	186.88	15.57
V9	115.88	71.00	186.88	15.57
V10	130.00	71.62	201.62	16.80
V11	73.38	72.12	145.50	12.12
V12	73.38	72.38	145.76	12.15
V13	73.38	82.50	155.88	13.0
V14	73.38	82.50	155.88	13.0
V15	73.38	82.50	155.88	13.0
V16	73.38	82.50	155.88	13.0

The valve numbers shown on the table above are the same valve numbers on Figure A4.5.

Table A10.2
238 STANDARD PLANT PIPE SPOOL DIMENSIONS

<u>Valve No.</u>	<u>Dimension A (in.)</u>	<u>Dimension B (in.)</u>	<u>Total Dimension (in.)</u>	<u>(A + B) (ft)</u>
V1	75.00	82.25	157.25	13.10
V2	75.00	82.25	157.25	13.10
V3	75.00	82.25	157.25	13.10
V4	75.00	82.25	157.25	13.10
V5	75.00	72.00	147.00	12.25
V6	75.00	71.62	146.62	12.22
V7	137.62	71.38	209.00	17.42
V8	126.75	71.12	197.87	16.50
V9	120.25	70.88	191.13	15.93
V10	119.88	70.62	190.50	15.88
V11	119.88	70.62	190.50	15.88
V12	120.25	70.88	191.13	15.93
V13	137.62	71.38	209.00	17.42
V14	75.00	71.62	146.62	12.22
V15	75.00	72.00	147.00	12.25
V16	75.00	82.25	157.25	13.10
V17	75.00	82.25	157.25	13.10
V18	75.00	82.25	157.25	13.10
V19	75.00	82.25	157.25	13.10

The valve numbers shown on the table above are the same valve numbers on Figure A4.3.

Table A10.3
251 STANDARD PLANT PIPE SPOOL DIMENSIONS

<u>Valve No.</u>	<u>Dimension A (in.)</u>	<u>Dimension B (in.)</u>	<u>Total Dimension (in.)</u>	<u>(A + B) (ft)</u>
V1	73.38	82.62	156.0	13.0
V2	73.38	32.62	156.0	13.0
V3	73.38	82.62	156.0	13.0
V4	73.38	82.62	156.0	13.0
V5	73.38	72.62	146.0	12.17
V6	73.38	72.25	145.63	12.14
V7	73.38	72.00	145.38	12.12
V8	144.75	71.12	216.50	18.04
V9	133.50	70.88	205.13	17.09
V10	128.38	70.62	199.75	16.65
V11	128.00	70.38	199.13	16.60
V12	128.38	70.75	199.13	16.60
V13	128.75	71.00	199.75	16.65
V14	133.88	71.25	205.13	17.09
V15	145.00	71.50	216.50	18.04
V16	73.38	72.00	145.38	12.12
V17	73.38	72.25	145.63	12.14
V18	73.38	72.62	146.0	12.17
V19	73.38	82.62	156.0	13.0
V20	73.38	82.62	156.0	13.0
V21	73.38	82.62	156.0	13.0
V22	73.38	82.62	156.0	13.0

The valve numbers shown on the table above are the same as valve numbers on Figure A4.9.

22A4365
Rev. 2

Table A10.4
DRYWELL AND SUPPRESSION POOL GEOMETRY

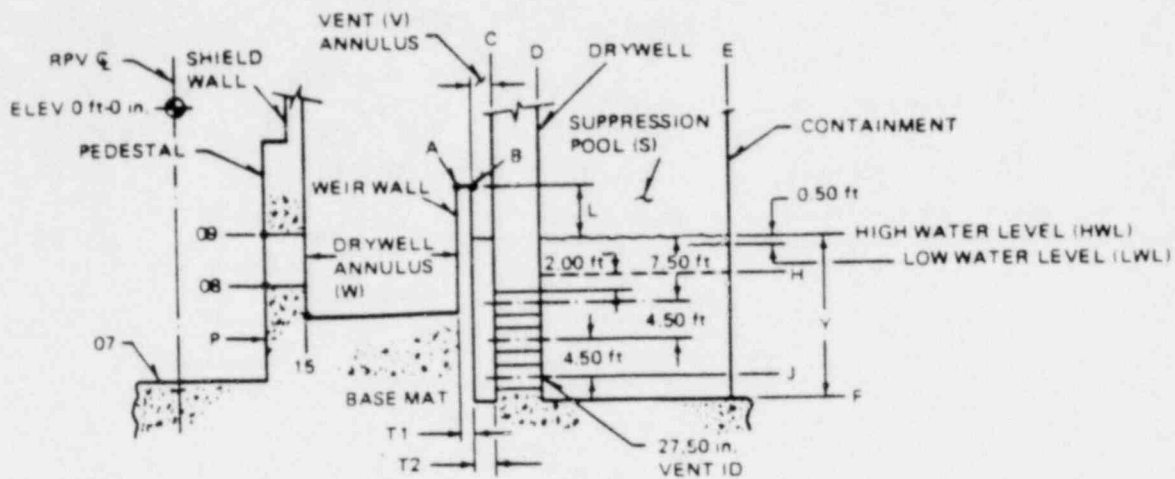


TABLE 1

PLT SIZE/CNTMT DIA OR NO. OF FUEL BUNDLE					DESCRIPTIONS	
218/114	*218/120	*238	251/800	*251/864		
(-) 8.33	(-) 8.33	(-) 5.50	(-) 7.08	(-) 7.08	A	ELEV TOP OF WEIR WALL
455	455	482	570	570	V	VENT ANNULUS AREA (ft ²)
5760	6863	6382	8170	8170	V+S	TOTAL AREA (ft ²)
(-) 12.58	(-) 12.58	(-) 11.16	(-) 13.00	(-) 13.00	HWL	HIGH WATER LEVEL ELEV
4.25	4.25	5.67	5.92	5.92	L	MIN FREEBOARD (ft)
(-) 16.92	(-) 16.92	(-) 15.50	(-) 17.33	(-) 17.33	H	DRAWDOWN LEVEL ELEV
19.42	19.42	20.42	19.00	19.00	Y	POOL DEPTH (ft)
111.00	131.90	129.60	153.90	153.90		POOL VOL (1,000 ft ³) AT LWL
21.80	17.31	34.15	30.03	30.03		DRAWDOWN MAKEUP VOL (1000 ft ³)
(-) 29.08	(-) 29.08	(-) 27.67	(-) 29.50	(-) 29.50	J	¢ OF BOTTOM VENTS ELEV
(-) 32.00	(-) 32.00	(-) 31.58	(-) 32.00	(-) 32.00	F	ELEV TOP OF BASE MAT
102	102	120	135	135		NUMBER OF VENTS
34	34	40	45	45		VENT STATIONS
420	420	495	557	557		GROSS VENT AREA (ft ²)
2100	2100	2475	2785	2785		VENT VOLUME (ft ³)
16	16	19	20	22		NUMBER OF SAFETY RELIEF VALVE
6.38	6.38	5.75	5.25	5.25		CIRCUMFERENTIAL VENT SPC'G DW ID
2223	2223	2535	2688	2688	W	AREA (ft ²)
27.84	27.84	39.29	39.82	38.75	W	VOLUME (1000 ft ³)
267.6	267.60	301.10	351.90	351.90	P	AREA (ft ²)
5525	5525	6948	7477	7477	P	VOLUME (ft ³)
(-) 28.98	(-) 28.98	(-) 28.58	(-) 28.33	(-) 28.33	07	RSO PT ELEV (REF)
(-) 19.35	(-) 19.35	(-) 19.46	(-) 18.71	(-) 19.21	08	RSO PT ELEV (REF)
(-) 12.35	(-) 12.35	(-) 12.46	(-) 11.71	(-) 12.21	09	RSO PT ELEV (REF)
(-) 20.85	(-) 20.85	(-) 20.98	(-) 21.50	(-) 21.90	15	RSO PT ELEV (REF)
118.00	118.00	145.50	165.60	(LTR)	110°F	REQD POOL VOL (1000 ft ³)
102.40	102.40	124.20	141.90	(LTR)	100°F	VS SVCE WATER TEMP
87.60	87.60	108.50	123.20	(LTR)	90°F	

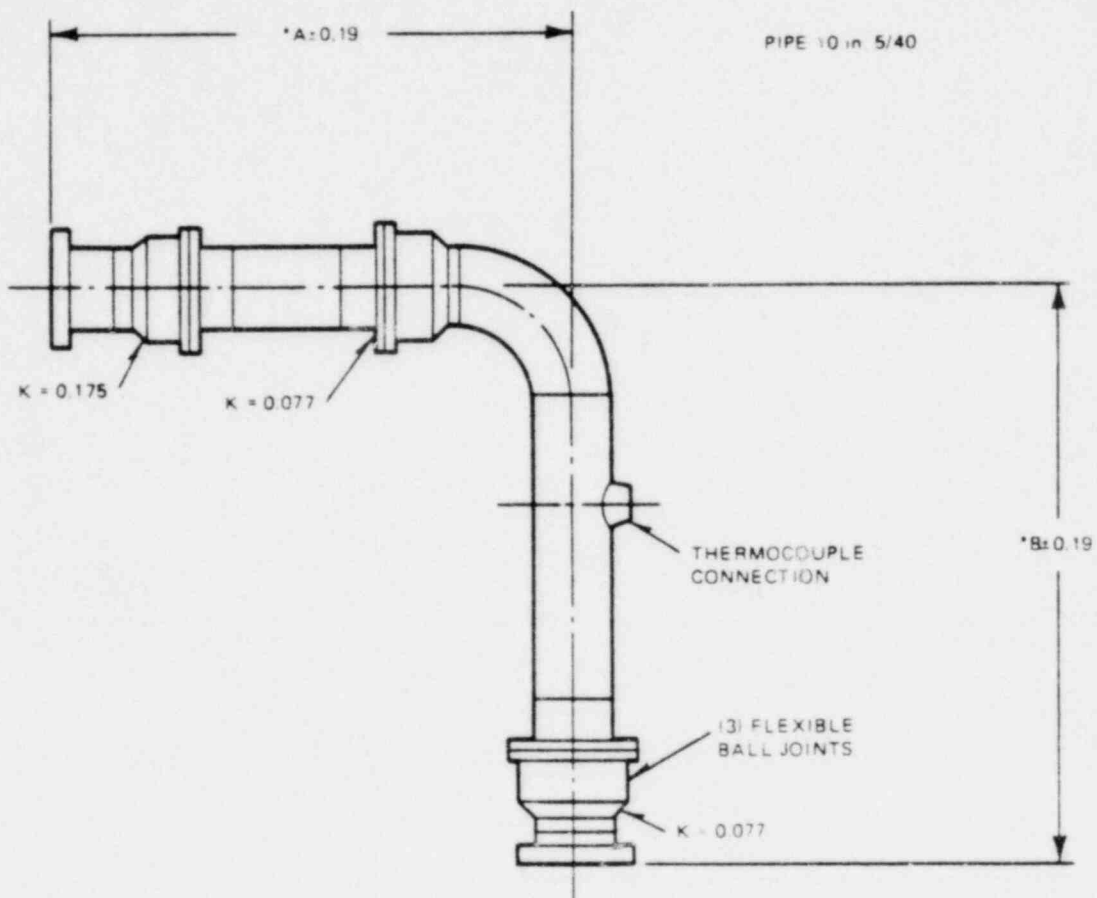
TABLE 2

PLT SIZE		08 (REF)	15 (REF)	A	B	C	D	E	T ₁	T ₂
218	DIA	18.42	29.83	61	64.67	69	79	114	1.83	2.17
	RAD	9.21	14.91	30.50	32.33	34.50	39.50	57		
218*	DIA	18.42	29.83	61	64.67	69	79	120	1.83	2.17
	RAD	9.21	14.91	30.50	32.33	34.50	39.50	60		
238*	DIA	19.58	31.58	65	68.67	73	83	120	1.83	2.17
	RAD	9.79	15.79	32.50	34.33	36.50	41.50	60		
251*	DIA	21.17	32.67	67	70	75	85	130	1.50	2.50
	RAD	10.58	16.33	33.50	35	37.50	42.50	65		

NOTES

- PLANTS IDENTIFIED WITH (*)
ASTERISK ARE STANDARD PLANTS

22A4365
Rev. 2

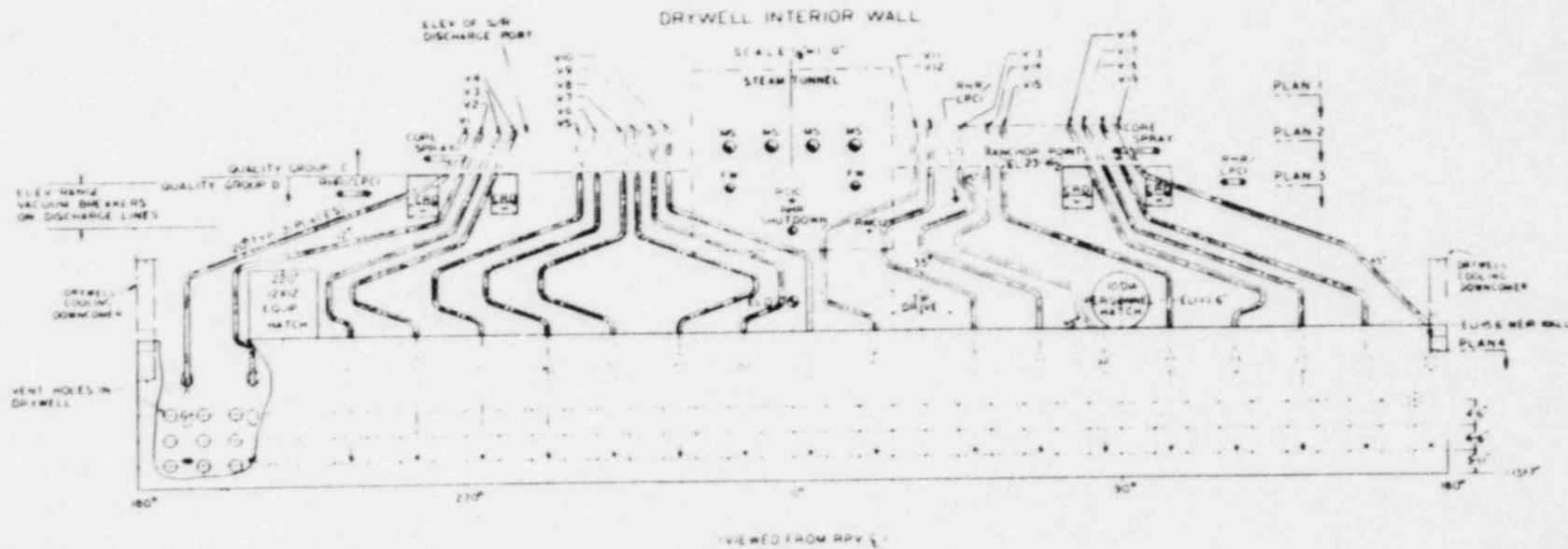


*SEE TABLE A10.1, A10.2 AND A10.3
FOR VALUES OF A AND B FOR THE
21B, 23B AND 251 STANDARD PLANTS

Figure A10.1. Safety/Relief Discharge Piping Detail SRV to First Anchor

NOTES

1. EQUAL DISTRIBUTION OF QUENCHERS IN THE SUPPRESSION POOL IS REQUIRED FOR THE FOLLOWING FUNCTION:
 - (A) ADS VALVES
 - (B) SPRING SET POINTS
2. NON-VERTICAL LENGTHS OF DISCHARGE PIPE ARE LOCATED AS HIGH ABOVE THE SUPPRESSION POOL AS IS PRACTICAL
3. SLOPE ALL DISCHARGE PIPES TOWARD THE SUPPRESSION POOL
4. TWO VACUUM BREAKERS ARE REQUIRED. ONE IS LOCATED AT LEAST 10 FEET ABOVE THE WEIR WALL. THE OTHER IS LOCATED AS CLOSE TO THE SAFETY RELIEF VALVE AS PRACTICAL
5. VXX IDENTIFIES RELATIVE VALVE LOCATION ON MAIN STEAM LINES

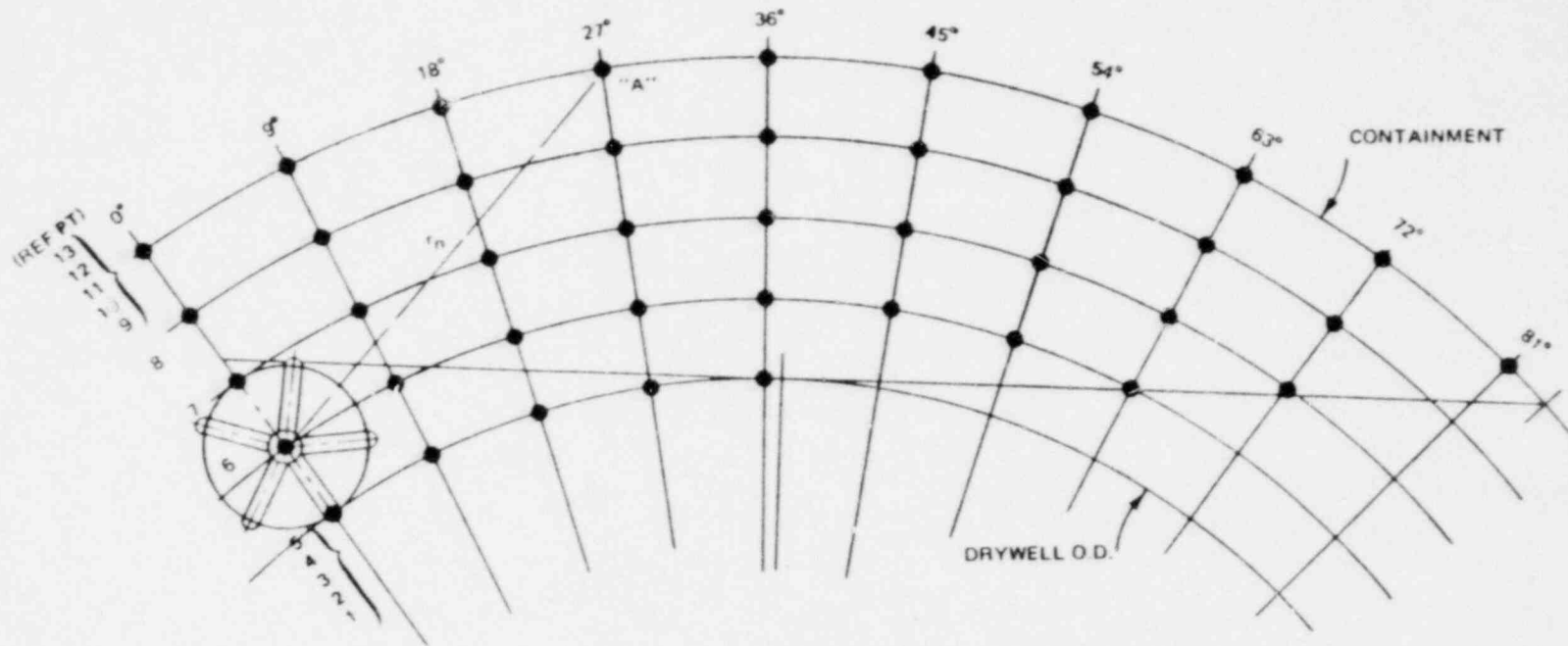


22A4765
Rev. 2

Figure A10.2. Safety/Relief Valve Discharge Piping Arrangement

042178

A-102



22A4365
Rev. 2

DISTANCE FROM CENTER OF QUENCHER (r_n) IN ft.

REFERENCE POINT/ANGLE	0°	9°	18°	27°	36°	45°	54°	63°	72°	81°
13	-	-	-	-	-	-	-	-	-	-
12	16.1	18.2	23.2	29.4	36.6	43.9	50.9	58.1	64.6	71.1
11	14.1	16.4	21.9	28.4	35.8	43.2	50.4	57.5	64.1	70.7
10	13.7	16.1	21.7	28.2	35.6	43.0	50.2	57.4	64.0	70.6
9	15.1	17.3	22.6	28.9	36.2	43.5	50.7	57.7	64.3	70.9
8	11.0	13.6	19.7	26.2	33.6	40.7	47.9	54.6	61.1	-
7	7.8	10.8	17.2	24.0	31.3	38.3	45.1	51.8	57.9	-
6	6.5	9.8	16.1	22.8	29.7	36.4	42.9	49.2	-	-
5	8.2	10.8	16.3	22.4	28.7	35.2	-	-	-	-
4	5.2	8.7	15.1	21.5	28.0	34.6	-	-	-	-
3	6.1	9.3	15.4	21.7	28.2	34.8	-	-	-	-
2	9.9	12.1	17.2	23.0	29.2	35.6	-	-	-	-
1	-	-	-	-	-	-	-	-	-	-

042178

Figure A10.3. 238 Standard Plant Distance from Center of Quencher to Pressure Point (ft)

A-103

All.0 PARAMETRIC STUDIES

The containment designer may choose to lay out the SRVDL such that equipment within the drywell can be accommodated somewhat differently than the GE Standard Plant. The application of the quencher data correlation allows for some flexibility in the pipe routing within the previously identified constraints. Generally speaking, the greatest flexibility exists in the routing of the air leg portion of the RVDL. Recommendations for quencher location within the pool and the drywell wall penetration location minimize the flexibility in the water leg portion of the SRVDL. To demonstrate the sensitivity of the changes to the air leg portion of the SRVDL, with all other parameters held fixed, Table All.1 has been generated.

The basic data correlation equation shown in Section A12.6 can be used by the containment designer to determine quencher design value bottom pressures for plant unique configurations. After the bubble pressures have been determined, the procedures for determining suppression pool boundary loads identified in Section A.10.3 should be utilized.

Table All.1
QUENCHER BUBBLE PRESSURE SENSITIVITY TO SRVDL AIR VOLUME

RVDL Air Volume (ft ³)	Maximum Allowable fl/D at 10" SH40 Pipe	Bubble Pressure (psid)			
		First Actuation		Subsequent Actuation	
		P+	P-	P+	P-
40	1.0	9.9	-6.7	20.9	-10.4
44	1.85	10.9	-7.1	22.9	-10.9
48	2.72	11.6	-7.4	24.2	-11.2
52	3.60	12.6	-7.8	26.4	-11.6
56	4.45	13.6	-8.3	28.4	-12.0
60	5.35	14.4	-8.6	29.7	-12.2

Standard Conditions:

Steam Flow Rate (in.) = 520 metric tons/hr

Pool Temperature (T_w) = 100°F (first actuation)
120°F (subsequent actuation)

Water Leg, WCL = 17.8 ft (5.42 m)

Valve Opening Time, VOT = 20 msec.

Quencher Submergence, SUBM = 13.92 ft. (4.24 m)

A12.0 BASIS AND JUSTIFICATION FOR DEVELOPED QUENCHER LOADS

A12.1 INTRODUCTION

To assure that the containment loads resulting from S/R valve discharge phenomena are conservatively low on Mark III containment, General Electric recommends a special discharge device in the S/R valve line discharge in the suppression pool. The device selected is called a "quencher." This device has been designed for application to pressure suppression containments based on a series of small and large scale tests. The quencher arrangement is shown in Figures A4.1 and A4.2 and has been scaled directly from the large scale prototype.

This section describes the basis for definition of the "quencher" performance in Mark III Design and Section A5 presents the resulting containment pressure loads for the standard 238 plant. Included in this report is a test description and a summary of test data upon which the quencher design and performance are based.

Full scale tests at the Caorso plant were conducted. Data evaluation shows that the SRV bubble pressures shown in Table A4.4 are very conservative and that reduced values should provide adequate design margins. See section A12.7 for further discussion. The test data is shown in References 4 and 5.

22A4365
Rev. 2

A-107 thru A-124

SECTION A12.2 CONTAINS GE COMPANY PROPRIETARY INFORMATION
PROVIDED UNDER SEPARATE COVER

042178

A12.3 PHYSICAL PARAMETERS

Due to the complexity of the phenomena associated with quencher performance, it was not feasible to conduct the quencher tests such that the effects of various parameters on maximum bubble pressure could be studied one at a time. For instance, consecutive actuation of a safety/relief valve changes the local pool temperature, pipe temperature, velocity of the water column, and mass, temperature and steam content of the air column. Each of these changes will have an effect on the peak bubble pressure, but only the combined effect can be assessed from the data. It was therefore necessary to identify the important parameters phenomenologically and then determine the influence of each parameter statistically.

The following sections explain the reasons for choosing the physical parameters that were used in the statistical analysis of the first actuation data. As far as subsequent actuations are concerned, only the maximum peak bubble pressure for any series of actuations is of concern. This maximum peak was correlated with the peak of the first actuation.

A12.3.1 Important Parameters

A complete list of parameters which might have minor effects on peak bubble pressure would be very long. It was therefore necessary to identify the most important parameters and include the rest only if they were found to be statistically significant. The selection of important parameters was done by phenomenological considerations as well as the qualitative observations discussed in Section A12.2. Figure A12.3-1 shows the interaction and interdependence of various parameters influencing quencher clearing.

A12.3.2 Overview of the Phenomenon

Since the peak pressure on the pool boundaries is the main concern, we must first look for factors that influence containment air clearing loads, i.e.:

- (1) number of quenchers discharging air simultaneously;
- (2) bubble size; and
- (3) peak bubble pressure.

Peak bubble pressure depends on the number of bubbles originally formed and their distribution in the pool. The same factors also determine the final shape of the bubble. Thus, the effects of shape of the bubble are included in the bubble pressure.

A12.3.2.1 Number of Quenchers

As discussed in Section A12.2.1, increasing the number of quenchers has the same effect on the peak boundary pressures as reducing the size of the pool. The size of the pool must be judged by the size of the quencher; therefore, pool surface area per quencher (A_W) divided by the area of the quencher (A_Q = the area of the circle that circumscribes the quencher) is an important parameter. The influence of this parameter would intuitively be expected to diminish as the value of the parameter increases.

A12.3.2.2 Bubble Size

For a given peak bubble pressure, bubble size depends on the mass and the temperature of the bubble. Since the bubble is essentially at pool temperature, one of the important parameters is pool temperature (T_W).

Assuming constant initial conditions in the discharge line, the mass of the bubble is proportional to the initial air volume in the pipe. Since the air is spread over the quencher area, the important dimension becomes the height of the bubble, which is proportional to the initial air volume (V_A)/quencher area (A_Q); hence, V_A/A_Q becomes a key parameter.

A12.3.2.3 Peak Bubble Pressure

Due to expansion and heat transfer to the wetted surface of the discharge pipe and contact with the suppression pool water, the air is essentially cooled to suppression pool temperature. Therefore, for a given air mass, the peak bubble pressure depends on:

- (1) bubble shape, and
- (2) mass flow rate.

A12.3.2.3.1 Bubble Shape

Bubble shape refers to the outline of the bubble at the completion of the air-clearing transient. For a given mass flow rate vs. time, the shape of the bubble is strongly influenced by the quencher area, the distribution of the holes on the quencher arms and the manner in which the holes are uncovered. For quenchers that are geometrically similar to the large-scale test device and have comparable air-clearing dynamics, the bubble forms a flat circular cylinder. The dynamics of a flat bubble depend strongly on the thickness of the bubble and is reflected in V_A/A_Q .

A12.3.2.3.2 Mass Flow Rate

For a given quencher, the mass flow rate of air into the pool is determined by the dynamics of the air-clearing transient, and the degree of mixing of air with water and steam. Since steam condenses almost instantly upon entering the pool, mixing of air with steam or water results in more gradual introduction of air into the pool (i.e., lower mass flow rate of air and, therefore, lower bubble pressure). However, systems of similar geometry (viz., simple discharge pipes of large L/D) have comparable degrees of mixing. Thus, for a given quencher and a given air temperature, the mass flow rate of air depends on the discharge pressure which is a function of:

- (1) the length of the water column in the discharge pipe;
- (2) air volume in the discharge pipe; and
- (3) steam flow rate from the safety/relief valve.

For a given steam flow rate, the length of the water column is the main parameter affecting the peak pipe pressure, the air discharge pressure, and the velocity of water as it clears the quencher arms. The faster the water is expelled from the quencher arms, the faster the holes become available for air flow. Since the air flow rate depends on discharge pressure and on opening area, the length of the water column is a parameter that affects the air flow rate and, therefore, the peak bubble pressure.

The air volume has already been identified as a key parameter; however, it should be pointed out that the effect of increased air volume in this case is to reduce the mass flow rate and thereby reduce the peak bubble

pressure. This is in the opposite direction of the effect of V_A/A_Q which was previously identified. In fact, as the air volume is increased, these opposing effects eventually cancel each other out.

It has been determined from the numerical solution of the air-clearing problem for various steam flow rates, that the discharge pressure is proportional to the maximum steam flow rate (\dot{m}_S) to a power of approximately 0.7.

The air flow rate (or steam flow rate) is converted into a mass flux to be suitable as a physical parameter. This is done by dividing the mass flow rate by an area such as quencher opening area (defined as the total hole area). For quenchers of similar geometry, the opening area is proportional to the quencher area (A_Q), and therefore, bubble pressure becomes a function of the mass flux across the quencher area (A_Q). To summarize, air mass flux depends on V_A , $(\dot{m}_S^{0.7})/A_Q$ and the length of the water column.

Since the maximum steam flow rate occurs only when the valve is fully open, valve opening time must also be considered as a parameter affecting peak bubble pressure. However, as long as the valve is fully open before the water column is expelled, valve opening time does not significantly affect peak bubble pressure.

A12.3.3 List of Parameters

To summarize, the following main parameters were identified as the ones that significantly affect the peak boundary loads:

- (1) Pool area per quencher/quencher area (A_V/A_Q);
- (2) Pool temperature (T_W);

22A4365
Rev. 2

- (3) Initial air volume/quencher area (V_A/A_Q);
- (4) (Steam flow rate to the power 0.7)/quencher area ($\dot{m}_s^{0.7}/A_Q$);
- (5) Valve opening time (VOT); and
- (6) Lengths of water column (WCL).

Other parameters fall in one of the following categories:

- (1) Parameters which, within the range of the data, did not seem to have any effect at all on the boundary pressures, such as initial air temperature, eccentricity of the quencher relative to a circular pool, and distance of the quencher from the bottom of the pool (with constant submergence).
- (2) Parameters which were properly scaled for all tests (except for a few miniscale runs) and held constant in GE quencher design. These include all important geometric properties of the quencher, such as arm length and diameter, size and arrangement of the holes, and quencher area.
- (3) Parameters that become important only for subsequent actuations (e.g., pipe temperature and water velocity prior to valve actuation). The combined effect of these parameters is accounted for by the use of a statistically determined multiplier applied to the first actuation loads.

A12.3.4 Effects of the Parameters

Each of the parameters identified in the previous sections affects the peak bubble pressure, sometimes in more than one way. In what follows, these parameters and their effects will be discussed in more detail.

A12.3.4.1 Pool Area Per Quencher/Quencher Area (A_w/A_Q)

This parameter begins to have an effect only when a large number of relief valves is actuated simultaneously. The role of this parameter is to empirically account for wall effects and for the combined effect of multiple relief valve actuation.

A12.3.4.2 Pool Temperature (T_w)

Part of the energy absorbed by the air column during the compression process in the discharge line is lost by heat transfer to the surroundings, and the remainder enters the bubble. The magnitude of pressure oscillations in the pool depends on the energy contained in the bubble. Therefore, for high heat transfer rates, the magnitude of the pressures will be low. The heat transfer rate depends on the pool temperature and vanishes when the air temperature becomes equal to pool temperature. The pool temperature, therefore, establishes the lower limit of the energy content of the bubble at the end of bubble formation process. In other words, pool temperature affects the so-called "bubble formation efficiency" and, thereby, the peak bubble pressure.

A12.3.4.3 Air Volume/Quencher Area (V_A/A_Q)

The effect of air volume is rather complex. On the one hand, the air column serves as a cushion to provide a low pipe-clearing pressure; on the other hand, more air means a larger bubble, more energy and higher peak bottom pressures.

The fact that very small and very large V_A both lead to negligible pressure changes on the boundaries suggests that peak bubble pressure must increase with increasing air-volume, reach a maximum and then decrease and asymptotically approach zero.

The strong influence of V_A/A_Q on the peak bubble pressure implies that the thickness of the flat quencher bubble is indeed its characteristic length. This indicates that the bubble expands and contracts mainly in the vertical direction as a one-dimensional spring-mass system.

A12.3.4.4 Steam Flow Rate and Valve Opening Time

The discharge pressure increases with steam flow rate. Since the air flow rate, which is proportional to discharge pressure, affects peak bubble pressure, the latter must also increase with steam flow rate.

Condensation of steam on the walls of the discharge line has the effect of reducing steam flux. Consecutive actuation of the valve increases the discharge pipe temperature causing a reduction in the condensation on the pipe walls. This partially explains the increase in bubble pressure with repeated actuation.

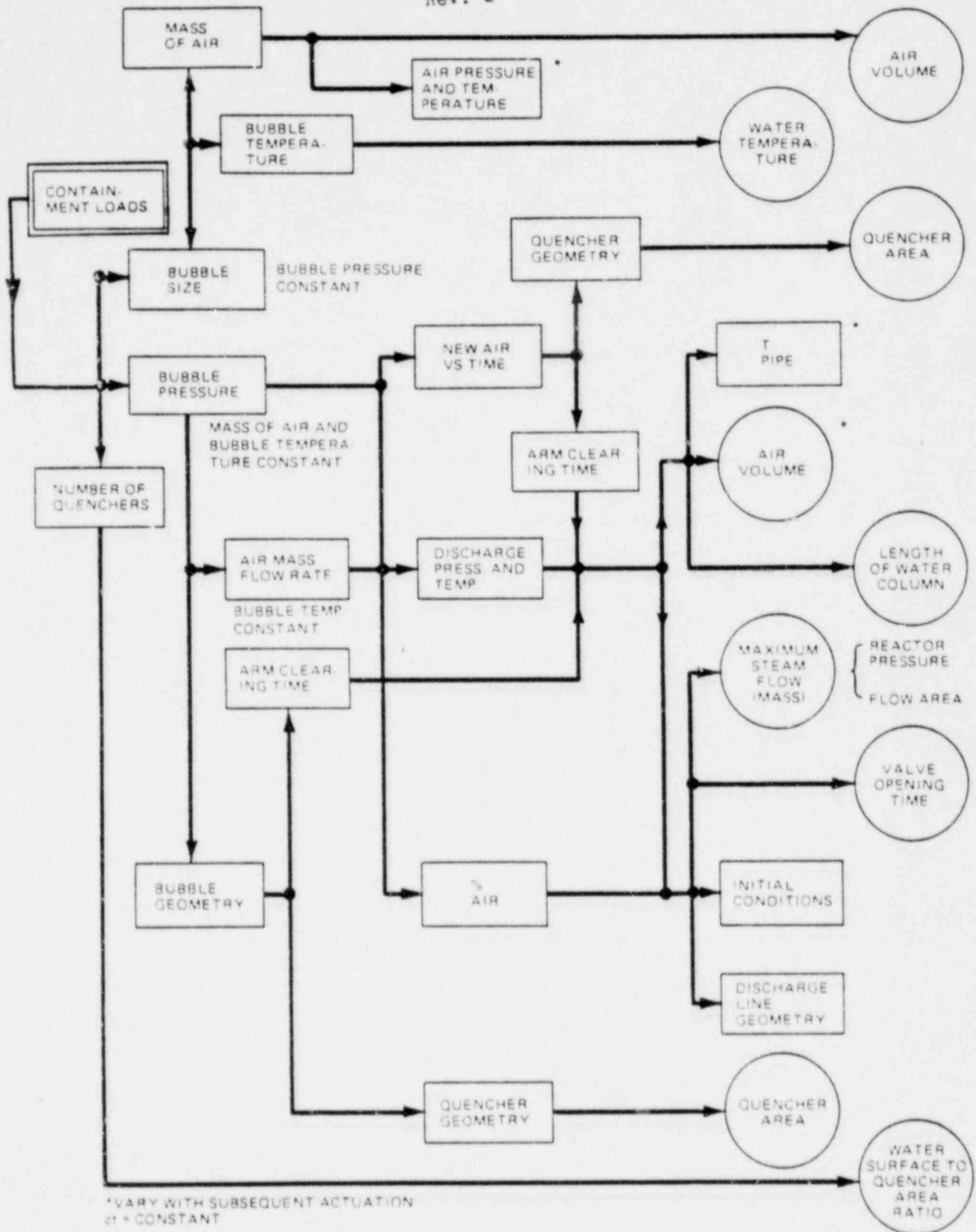
Valve opening time affects the variation of steam flow rate with time. However, once the valve is fully open, the flow rate remains essentially constant for the remainder of the air clearing transient. Because air-clearing occurs after the valve is fully open (in the range of practical values of valve opening time) valve opening time does not significantly affect the mean steam flow-rate or the peak bubble pressure.

A12.3.4.5 Length of Water Column (WCL)

The length of water column is the submerged length of pipe to the center of the quencher. The peak pipe pressure and, therefore, discharge pressure are both affected by the length of the water column due to the longer time required to accelerate and clear a large water mass compared

to a small mass. The duration of the clearing of the quencher arms depends on the volumetric flow rate of water, which also depends on water column length. The discharge pressure affects the air flow rate. Therefore, WCL affects air flow rate and, thereby, the peak bubble pressure.

Another factor which depends on WCL is the wetted pipe area available for cooling of the compressed air during air-clearing. This wetted area, of course, increases with WCL. This has the effect of reducing the energy that enters the bubble and tends to counteract the previous effect of WCL (Figure A12.2-8).



*VARY WITH SUBSEQUENT ACTUATION
if = CONSTANT

Figure A12.3-1. Relationship of Key Parameters

A12.4 CORRELATION OF POSITIVE AND NEGATIVE PRESSURE PEAKS

Despite the complexity of the bubble dynamics for the quencher, a simple correlation exists between the peak positive and the peak negative bubble pressures. This correlation is based on the principle of conservation of energy and has been verified against the test data.

The correlation provides a convenient means for determining one of the peak pressures, provided the other peak is known. Being quite general, it is applicable to bubbles of any geometry and pressure, regardless of the initial conditions in the discharge line, first or subsequent actuation of the relief valve.

A12.4.1 Development of the Correlation

Consider an air bubble of arbitrary geometry with a volume V_0 and pressure P_∞ (same as local absolute pressure) in thermodynamic equilibrium with the surrounding water. If the bubble is compressed to a pressure P_{\max} corresponding to a volume V_{\min} and then allowed to oscillate, it will act as a spring-mass system. The pressure will oscillate between P_{\max} and P_{\min} , and the volume will oscillate between V_{\min} and V_{\max} .

Conservation of energy dictates that the minimum pressure must correspond to the maximum pressure in such a way that the energy received during the compression is equal to energy transferred during the expansion, using the equilibrium state as the reference state:

$$W_{\text{comp}} = -W_{\text{exp}}$$

or

$$\int_{V_0}^{V_{\min}} \frac{1}{PdV} = - \int_{V_0}^{V_{\max}} \frac{1}{PdV} \quad (\text{A12.4-1})$$

Assuming the compression and expansion processes to be isothermal, the following relationship between P and V exists:

$$VP = P_{\infty} V_0$$

where

P_{∞} = absolute surrounding pressure;

V_0 = initial air volume at $P_{\infty} = P_0$;

P = instantaneous bubble pressure; and

V = instantaneous bubble volume.

Rearranging:

$$V = \frac{P_{\infty} V_0}{P}$$

and

$$dV = \frac{P_{\infty} V_0 dp}{P^2} \quad (\text{A12.4-2})$$

Substituting in Equation A12.4-1 we obtain:

$$\int_{P_{\infty}}^{P_{\max}} -P_{\infty} V_0 \frac{dP}{P} = - \int_{P_{\infty}}^{P_{\min}} P_{\infty} V_0 \frac{dP}{P} - P V_0 \ln \frac{P_{\max}}{P_{\infty}}$$

$$= -P_{\infty} V_0 \ln \frac{P_{\min}}{P_{\infty}} = -P_{\infty} V_0 \ln \frac{P_{\infty}}{P_{\min}}$$

which simplifies to:

$$\frac{P_{\max}}{P_{\infty}} = \frac{P_{\infty}}{P_{\min}}$$

$$\boxed{P_{\max} P_{\min} = P_{\infty}^2}$$

(A12.4-3)

For the case of interest, $P_{\text{abs}}^+ P_{\text{abs}}^- = P_{\infty}^2$

where

P_{abs}^- = minimum absolute bubble pressure, and

P_{abs}^+ = maximum absolute bubble pressure.

Notice that this relationship holds for bubbles of any shape and is not limited to spherical bubbles. Furthermore, any energy losses that will occur in the real case will tend to reduce both P_{max} and P_{min} . That the process is properly considered isothermal is demonstrated by comparison to data.

In terms of gauge pressures (P^+ and P^-), Equation A12.4-3, by simple algebra, takes the following form:

$$P^- = P^+ P_\infty / (P^+ + P_\infty) \quad (\text{A12.4-3A})$$

A12.4.3 Comparison with Test Data

Figure A12.4-1 shows a comparison of minimum absolute pressures predicted by Equation A12.4-3 and the actual measured values. Seventy data points from small-scale and large-scale tests have been plotted, covering a wide range of parameters. As can be seen, the agreement is quite good, indicating that the combined effects of irreversibilities result in actual bubble thermodynamics which are very well approximated by a reversible isothermal process.

Notice that large values of negative gauge pressure correspond to small values of P_{abs}^- . The predictions for BVR's will be in the lower end of the 45° line where the model gives conservative results.

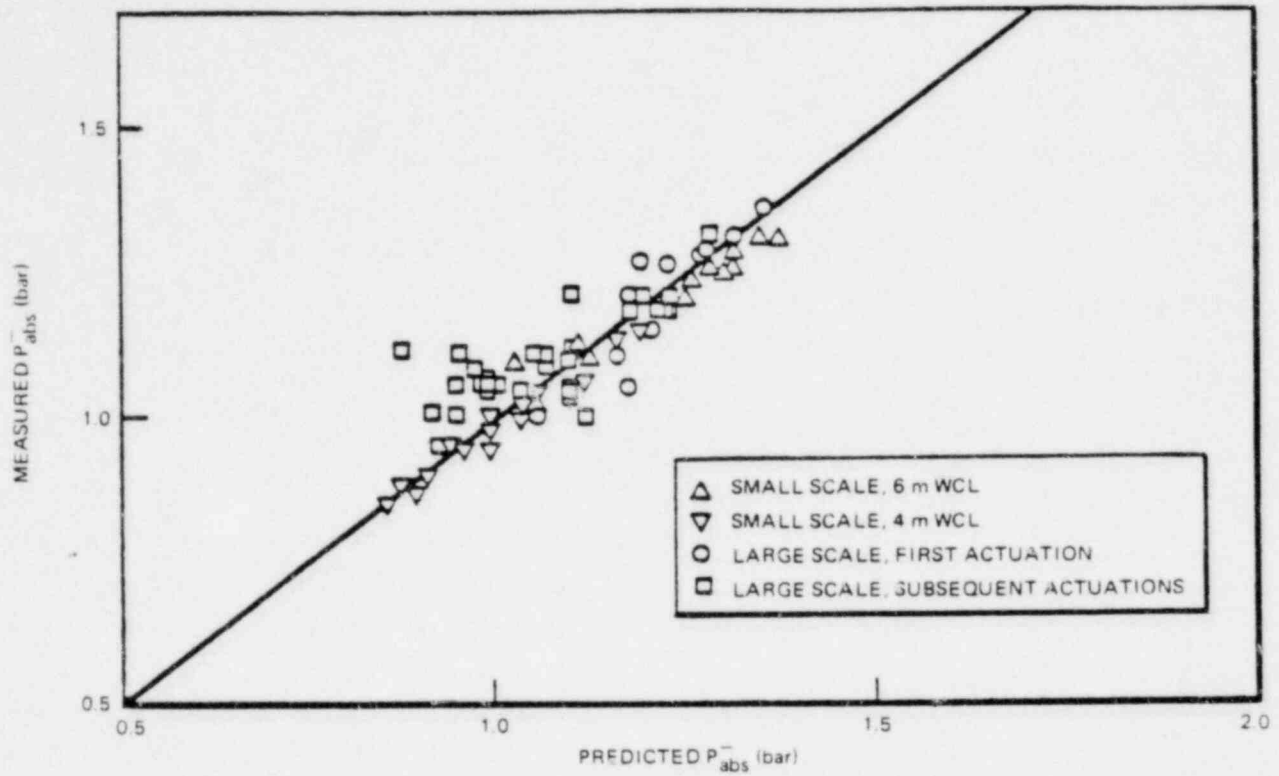


Figure A12.4-1. Comparison of Eq. (A12.4-3) Predictions with Test Data

A12.5 DEVELOPMENT OF THE DESIGN VALUE CALCULATION METHOD

A12.5.1 Introduction

It is desired that design values be calculated so that, with a high confidence, a high percentage of actual values of maximum positive pressure (MPP) and maximum negative pressure (MNP) will be less than the corresponding design values. The general form of such an equation, when based on test data, is to first calculate a predicted value, then add an amount which is the product of a confidence coefficient and a value which covers the uncertainty and variability in the test results.

It is noted in the test data that subsequent, sequential actuations had higher MPP values than first actuations. Accordingly, equations are provided for predicted values and design values for MPP, for both first and maximum subsequent actuations. An equation to obtain MNP values directly from MPP values is also provided.

A12.5.1.1 Objective

The objective of this section is to develop the method for calculating the design value of maximum positive bottom pressure (MPP) and maximum negative pressure (MNP) at the quencher and on the floor immediately beneath, in the suppression pool of a BWR plant containment, due to oscillation of the air bubble discharged immediately after safety/relief valve actuation. The pressures are maximums over the oscillations. MPP and MNP are differences above and below the absolute pressure at quencher elevation, where the absolute pressure is due to atmospheric and hydrostatic pressures. The generalized bottom pressure load cases of interest are as follows:

- (A) first actuation of one or two valves (100°F suppression pool);
- (B) first actuation of three or more adjacent valves (100°F suppression pool);

- (C) first actuation of an ADS valve (120°F suppression pool); and
- (D) subsequent actuation of a single valve (120°F suppression pool).

Water surface area ratio distinguishes generalized load cases A and B. Similarly, the effect of water surface as well as pool temperature distinguish case C. Generalized load case D must be distinguished because it was found from testing that the highest MPP and MNP occur on the second or third actuation of a valve, subsequent to the first actuation, when the valve is discharged sequentially with closure times of from 5 seconds to 1 minute. This consistent pattern for the maximum subsequent actuation is shown in Figures A12.5-1 and A12.5-2. Accordingly, design values will be found not only for the first actuation but also for the maximum of subsequent actuations.

A12.5.1.2 Criterion

The design values are to be such that there is 100_Y% confidence that at least 100(1 - α)% of actual plant MPP (or MNP) values will be less than the design values. Values for 100_Y% (confidence value) and 100(1 - α)% (the percentage of the distribution of individuals) are both 95%.

This criterion implies that, if we should have complete knowledge of the distribution of actual MPP values, we would set the design value such that 95% of actual values are less than the design value. But the criterion further recognizes that, since we have but a finite amount of data, we must estimate that upper 95% point; but we will do so in a conservative manner such that we are 95% confident (100_Y%) that the true upper 95% point lies less than the one established.

A12.5.1.3 Data Available

The development of the design value calculation method for MPP is largely empirical; that is, based on the analysis of test data. Theory was drawn upon to identify variables of potential importance in prediction, and to normalize some variables for scaling differences among the three sizes of test equipment. The design value calculation method for MNP, however, uses a relationship to MPP based on theory and confirmed empirically, as described in Section A12.4 and A12.5.14.2.

One hundred sixteen data relevant to the plant quencher configuration were chosen from testing in three sizes of equipment, as follows:

(1) First Actuations:

37 data from large-scale testing
70 data from small-scale testing
9 data from miniscale testing
116

(2) Maximum Subsequent Actuations:

10 data sequences from large-scale testing.

A12.5.1.4 Strategy of Statistical Analysis

The design value calculation method for MPP is the result of a statistical analysis of the test data, conducted according to the following strategy:

- (1) Identify the measured variables of potential importance in prediction.
- (2) Normalize some variables for scale differences among the three test configurations and for application to the plants.

- (3) Determine the sensitivity of MPP to each variable simultaneously, in a prediction equation linear in coefficients estimated by multiple linear regression (curve fitting), thus maximizing the amount of data used to estimate each coefficient. Retain only terms which make a statistically significant reduction in the variability of the observed values about the prediction surface.
- (4) Predict the first actuation MPP for the plant using a composite prediction equation comprised of the large scale mean MPP and a term for each variable which adjusts that mean from large-scale conditions to plant conditions. The coefficients were estimated on large, small- or miniscale data, depending on whether the variable was actually varied in that data. Accordingly, it is assumed that the plant quencher configuration is sufficiently similar to the configurations in the three tests that, after normalization of some variables, the sensitivity of MPP in the plants will be of the same magnitude as observed in each test. Where possible, preference was given to selecting a coefficient estimated on large scale data, because that test configuration used a quencher of physical dimensions near those of the quenchers used.
- (5) When called for by the load case, predict MPP for maximum subsequent actuations from the predicted MPP for first actuation.
- (6) To account for the uncertainty in estimates of coefficients and for the variability in individual values, find the variance of individual future values for plant conditions. There are two contributions to this variance: (1) the variance of the predicted value, and (2) the variance of individual values.

- (7) Find the design value for each bottom pressure load case. The design value equation consists of the predicted value plus a confidence coefficient times the standard deviation future values.

A12.5.1.5 Glossary

- MPP = Abbreviation for maximum positive pressure
- MNP = Abbreviation for maximum negative pressure
- MPP1 = An observed value of MPP on a first actuation
- MPPQ = An observed value of MPP on a maximum subsequent actuation
- MNP1 = An observed value of MNP on a first actuation
- MNPQ = An observed value of MNP on a maximum subsequent actuation
- PRD1 = A predicted value of MPP on a first actuation
- PRDQ = A predicted value of MPP on a maximum subsequent actuation
- PRN1 = A predicted value of MNP on a first actuation
- PRNQ = A predicted value of MNP on a maximum subsequent actuation
- MPPDV = A design value for MPP
- MNPDV = A design value for MNP

A12.5.2 Design Value Equations for Maximum Positive Pressure and Maximum Negative Pressure

Implementing the foregoing strategy, the design value equation for MPP appears in its basic form on the first line of Table A12.5.1. That table goes on to give all subordinate equations and terms, and the design value equation for MNP, together with the succeeding sections herein where each equation is derived, or each term evaluated. Thus, Table A12.5.1 serves as an index to the development of the design value equations for MPP and MNP.

A12.5.3 Derivation of Equation for MPPDV (Maximum Positive Pressure Design Value)

$$\text{MPPDV} = \text{PRED} + \text{CONF} \times \text{SIFV}$$

where

MPPDV = the MPP design value in bars difference (bar d);

PRED = predicted value (bars);

CONF = confidence coefficient; and

SIFV = standard deviation of individual future values (bars).

This equation reflects a standard statistical relationship, when a design value is to be based on a predicted value plus an allowance for statistical uncertainty and variability, implementing the design value criterion stated in subsection A12.5.1.2.

A12.5.4 Derivation of Equation for Predicted Maximum Positive Pressure (PRED)

$$PRED = CMSA \times PRD1$$

where

PRED = the predicted MPP:

CMSA = the coefficient for maximum subsequent actuation:

For first actuations, $CMSA = 1.0$ and $PRED = PRD1$.

For maximum subsequent actuations, $CMSA = 1.744$
and $PRED = PRDQ$.

PRD1 = the predicted MPP for first actuation.

The evaluation of PRD1 will be described first because of its fundamental role. There are generalized load cases which involve only the first actuation, but even for the load case which involves maximum subsequent actuation, it is necessary to first predict the first actuation, for two reasons: (1) the dependence of MPP on most variables can be determined only for the first actuation because that was the only kind of test run in the small- and miniscale experiments, and most of the large scale experiments; and (2) it was found that for the 10 large-scale data having subsequent actuations, the maximum subsequent actuation could be predicted from the first in a simple, proportional manner.

Evaluation of CMSA will be described in the succeeding section.

A12.5.5 Evaluation of Term PRD1 (Predicted First Actuation Maximum Positive Pressure)

The predicted value for first actuations for MPP is found from an equation resulting from fitting the experimental data. In Sections A12.2 and A12.3, theory was drawn upon to identify relevant variables and to normalize some variables among the three sizes of test configuration used. One-hundred sixteen data were available, 37 from large-scale testing, 70 from small-scale, and 9 from miniscale. A multiple regression (curve fitting) procedure was used on each data set separately, to estimate coefficients in an equation linear in coefficients. Not all variables were actually varied in each experiment. For some variables, both first and second degree terms were important. No terms were retained which did not make a reduction in the variability of the data about the prediction surface, significant at the 1% level or less. Special treatment was given to two variables. The MPP data for air volume ratio (VAAQ) were noted to first increase, then begin decreasing. But, for conservatism, the prediction surface was projected horizontally for higher VAAQ values, rather than decreasing, since some extrapolation to plant conditions is required. For steam mass flux (MNAQ), since the three sets of data were widely separated in this variable, the principal fit was to large-scale data; but a straight line was then used to join large and mini mean predicted values, slightly overpredicting the mean small-scale predicted value en route. Thus, in effect, MNAQ was used to provide for reprediction of all three data sets in one equation.

Finally, a single prediction equation was composited from coefficients estimated from the three sets of data. Since the large-scale configuration was closest dimensionally to that of quenchers used, coefficients estimated on that data were preferred, but use of coefficients estimated on the other two data sets was also necessary. The resulting prediction equation for MPP is shown in Table A12.5.2. Figure A12.5-24 is a comparison of observed to predicted MPP values for each of the three data sets.

A12.5.5.1 Raw and Transformed Variables

Raw and transformed variables used in the fitting are identified and described in Section A12.5.2 and A12.5.3. The transformed variables are illustrated in Figure A12.5-3.

Besides the transformed variables shown, two other variables were fitted initially. One was air temperature in the discharge pipe. This variable was found to not be significant in predicting MPP. The other was pressure upstream of the safety-relief valve prior to actuation, which, in a plant, would be reactor pressure. In the small-scale data where both reactor pressure and steam flow rate were measured, those two variables had a correlation coefficient of 0.6, a significant value; thus, normalized steam flow rate only was retained in the prediction equation.

The ranges of data from each test configuration, and values for a typical plant, for the raw and transformed variables, are illustrated in Figures A12.5-4 and A12.5-5. The data, together with predicted values, are tabulated in Table A12.5.3.

A12.5.5.2 Statistical Analysis

The statistical analysis assured that the sensitivity of MPP to each variable was governed by that sensitivity within a set of data known to be consistent, leaving the question of how to reconcile the three sets of data in one prediction equation to a separate analysis. Accordingly, the multiple linear regression procedure was used on the three sets of data separately. Least squares estimates of the coefficients were obtained. The so-called stepwise procedure was used, in backward stabilization mode, whereby variables are offered for fitting, all are fitted at the outset, but the fitting criterion is then successively made more discriminating so that in the end one is left with only those

variables which make a significant contribution to the fit. Variables were retained if they were significant at the 1% level, or less. In this procedure, as each variable is forced out, the other variables are reexamined for possibly now making a significant contribution to the fit; this is a desirable feature because the inadvertant partial correlation between some pairs of variables means that one variable can, to some extent, play the role of a second, so that whether or not the second variable is significant. There is, in general, no restriction on the form of each variable; a chosen variable in first degree, second degree (squared), first degree cross product with other variables, are all treated as separate variables in the regression procedure. Indeed, these possible forms were systematically examined for their significance, and those forms having both statistical and physical significance were retained.

Table A12.5.4 shows the data set from which a coefficient for each variable could be estimated. There is duplication in the case of only three variables: coefficients for MNAP, LNTW and VOT could be estimated from both large and small-scale data. Per subsection A12.5.1.4(4), estimates from the large-scale data would be preferred. For MNAP, the range of values from the small-scale data was so narrow as to not give a reliable estimate of the coefficients; thus, the coefficients from the large-scale data were used. For LNTW, there was little to choose between the large and small-scale coefficients; the large-scale coefficient was slightly larger, leading to a more conservative prediction at higher temperatures, and so was chosen. For VOT, the coefficient for this variable was not significant in the large-scale data and only barely significant in the small-scale data; for conservatism, the coefficient from the small-scale data was used.

It was found that second degree terms were significant for MNAP, AWAQ and WCL, reflecting curvature in the data. Such terms describe parabolas, of course, which may not be suitable for extrapolation beyond the range of the data. Accordingly, special consideration was given to VAAQ and MNAQ for which prediction outside the range of the data would be necessary. These considerations are described in detail below. The second degree terms were called MNQ2, AWQ2 and WCL2, respectively.

With all variables being fit simultaneously, in order to confirm that the term or terms for each variable are indeed filling the role called for by the data, it is helpful to see the pattern of the data points after adjustment by all terms in the prediction equation except one. These partially adjusted observed values, herein called shell residuals (in the sense that they form a shell for showing the effect on prediction of those terms), are shown in Figures A12.5-6 through A12.5-13. Also shown, by smooth curves, are the role played by the term(s) for that variable. Conformance of these curves to the shell residuals indicates that the effect of that variable on MPP has been accounted for in the term(s) used in the prediction equation.

Figure A12.5-6 shows the shell residuals for VAAQ, with respect to that variable. These are for the small-scale data, from which the coefficient for VAAQ was estimated. Also shown are two straight lines, one the horizontal continuation of the other, which show the effect of the VAAQ term in the equation. As can be seen, the shell residuals for VAAQ reach a maximum and then decrease. But rather than extrapolating this decrease, the prediction equation was modified for conservatism to provide for a horizontal projection for VAAQ values exceeding 0.255.*

*That the VAAQ values reached a maximum and began decreasing was found to be a statistically significant trend, and may be expected from physical considerations as described in Section A12.3. Thus, the horizontal projection is appropriate and conservative.

Thus, the same MPP value will be predicted for all values of VAAQ greater than 0.255, rather than decreasing values as indicated by the data.

In Figure A12.5-7 the shell residuals from the large-scale data for the MNP and MNQ2 terms are shown, together with the effect of those terms on the prediction. Because the ranges of MNAQ for the three data sets differ so much, this variable was used empirically to permit the prediction equation to predict the data in all three sets. Thus, a line tangent to the parabola at $MNAQ = 6.89$ was drawn so as to meet the predicted value of the mini scale data at $MNAQ = 60.7$. This line is shown over-predicting the mean predicted value for small scale data, an element of conservatism in the prediction equation in that the higher two mean predicted values among the three data sets were permitted to govern prediction on MNAQ.

Figures A12.5-8 and A12.5-9 show the shell residuals for LNTW for the large-scale and small-scale data, respectively. The effect of the LNTW term is also shown. The coefficient used was estimated on the large-scale data, but it can be seen that the fit to small-scale data is also satisfactory.

Figure A12.5-10 shows the shell residuals and effect of the water column length terms (WCL and WCL2) for the small-scale data.

Figures A12.5-11 and A12.5-12 show the shell residuals for VOT for the small-scale and large-scale data, respectively. The effect of the VOT term in the prediction equation is also shown; its coefficient was estimated on the small-scale data, having been found to be not significant in the large-scale data, as suggested by the shell residuals' following the 0 line.

Figure A12.5-13 shows the shell residuals for AWAQ for the miniscale data, together with the effect of the AWAQ and AWQ2 terms. The AWAQ model is probably really asymptotic, but no use is made of it for values of AWAQ greater than 20.

Terms for the several variables were brought together into the single equation shown in Table A12.5.2, which predicts MPP for the first actuations (PRD1). The structure of this equation is illustrated in general terms in Figure A12.5-14 where, in Figure A12.5-14a, an equation linear in coefficients, in standard intercept form, is illustrated. The equation is shown passing through (\bar{x}_1, \bar{y}) ; and \hat{y} , the predicted value of y at some \hat{x}_1 is also shown. But the standard intercept form is not convenient for a prediction equation composited from more than one set of data. Rather, the combination of mean-adjusted and reference-adjusted terms is used, as illustrated in Figures A12.5-14b and A12.5-14c. Figure A12.5-14b applies to those terms where the coefficients are estimated from the large-scale data, appropriate since \bar{y} is also the average observed MPP for the large-scale data. It shows the predicted y , \hat{y} , as \bar{y} adjusted by a $\Delta\hat{y}$ for \hat{x}_1 found as $a_1 (\hat{x}_1 - \bar{x}_1)$. Figure A12.5-14c describes the $\Delta\hat{y}$'s for terms with coefficients estimated on data other than large scale. Each of this type of $\Delta\hat{y}$ is found as the term $a_3 (\hat{x}_3 - x_3 \text{ ref})$. $x_3 \text{ ref}$ is the mean value of x_3 in the large-scale data, and \hat{x}_3 is the value of x_3 at which \hat{y} is being calculated. \bar{x}_3 and \bar{y} are in the data set from which a_3 was estimated.

For the 238 Standard Plant, the value of each variable is shown in Table A12.5.5. These values are entered in place of the variable names in the equation in Table A12.5.2, which are the x_1 terms in Figure A12.5-14.

The actual calculation of predicted values for first actuations (PRD1) is carried out for the load cases in connection with calculating design values, in Section A12.5.17.

A12.5.6 Evaluation of Term CMSA (Coefficient for Maximum Subsequent Actuation)

CMSA is the coefficient on PRD1 for first actuation for load cases involving maximum subsequent actuations. For load cases involving only one actuation, CMSA = 1.0.

Figure A12.5-15 shows the observed MPP values for the maximum subsequent actuations of the 10 runs versus the PRD1 values for the first actuations of those runs. The eight points without arrows are observed maximums which were, in fact, followed by lower values; the two points with arrows are third subsequent actuations where that actuation was maximum but there were no further actuations. The important observation is that observed maximum subsequent actuations tend to be proportional to predicted first actuations, rather than simply a fixed amount greater, for example. That is, a line fitted through the points was found to have a slope significantly greater than zero. Since it would be physically reasonable for the relationship to pass through the origin, the prediction line for maximum subsequent actuation from predicted first actuation was chosen passing through the origin and (\bar{x}, \bar{y}) . Therefore, for load cases involving subsequent actuations, CMSA = 1.744.

A12.5.7 Evaluation of Term CONF (Confidence Coefficient)

CONF depends on the confidence statement to be made and on the number of data on which SIFV is based. The confidence statement has the form written in subsection A12.5.1.2. A value of 37 data points (the number of large-scale data) is used for first actuations; a value of 10 data points is used for maximum subsequent actuations, the number of those data. The corresponding CONF values for the 95-95 statement are 2.15 and 2.91. These values appear in Table A12.5.5, and are taken from standard tables for "one-sided statistical tolerance limits."

The confidence statement is valid when the distribution of individual values (in this case, of residuals about the prediction surface) is normal. That this is nearly so in the observed data is shown in Figure A12.5-16, which shows residuals for large, small and miniscale first actuation predictions, and the large-scale maximum subsequent actuation predictions.

The normal distribution corresponding to the histogram of maximum subsequent actuation residuals is considerably broader than suggested by those data in Figure A12.5-16.

A12.5.8 Derivation of Equations for SIFV (Standard Deviation of Individual Future Values) and VIFV (Variance of Individual Future Values)

SIFV is the standard deviation of individual future values, and VIFV is the variance of individual future values:

$$SIFV = (VIFV)^{1/2},$$

is the usual relationship between standard deviation and variance.

$$VIFV = VPRD + VIND$$

reflects the fact that VIFV is comprised of two parts: (1) VPRD, the variance of the predicted value, and (2) VIND, the variance of individual values. This equation follows from the independence of the errors in predicted value and individual value as they appear in the usual error model in Figure A12.5-17.

A12.5.9 Derivation of Equation for VPRD (Variance of the Predicted Value)

VPRD, the variance of the predicted value, is found by propagation of errors on the predicted value:

$$\text{PRED} = \text{CMSA} \times \text{PRD1}.$$

Propagation of errors is a general procedure for finding the variance of a function when the variance of each random variable in the function is known. For any function, y , of random variables, x_i , $y = g(x_i)$, the propagation of errors equation for the variance of y , for errors independent among the x_i , is

$$\text{Var } y = \sum_i^n \left(\frac{\partial y}{\partial x_i} \right)^2 \Bigg|_{\text{at } \bar{x}_i} \times \text{Var } x_i.$$

Application of the propagation of errors equation to the equation for PRED gives the variance of the predicted value:

$$\text{VPRD} = \text{VPRI} + \text{VPRM}$$

where VPRI is the contribution of the variance of the predicted first actuation:

$$\text{VPRI} = (\text{CMSA})^2 \times \text{VVP1}$$

and VPRM is the contribution of the variance of the predicted maximum subsequent actuation (required by load case c) due to the variance in CMSA:

$$\text{VPRM} = (\text{PRD1})^2 \times \text{VVPM}.$$

A12.5.10 Evaluation of Term VVPI (Variance of the Predicted First Actuation)

VVPI is the variance of the predicted first actuation (PRD1). This variance is found by the equation shown in Figure A12.5-18, the standard expression for the variance of a predicted value from an equation found by multiple regression. In the first term, it reflects the variance in the intercept at the average of each of the independent variables (i.e., the uncertainty in the vertical location of the prediction surface). And in the sums of terms, sometimes called the "flaring" terms, the expression reflects the variance of estimate of each coefficient in the equation, and the covariances between all pairs of coefficients which are not completely independent. Each of these variances and covariances can be computed as the product of an element in the so-called c matrix* and the variance of residuals, both outputs of the multiple regression computation. The c matrix is shown in Table A12.5.7. The c value for pairs of coefficients estimated from different data sets is 0 in theory, and as confirmed by analysis. One special technique required was that the variance of residuals used to find each coefficient variance was that of the data set in which the coefficient was estimated, rather than the combined data set, taking advantage of the better precision of estimates in data sets having low residual variability. These different variances of residuals are subscripted t_i in Figure A12.5.18 and are tabulated in Table A12.5.7.

The \dot{x}_i values on Figure A12.5-18 are the values of each variable for the plant. The values of \bar{x}_i are the observed mean for variables whose coefficients were estimated on the large scale data, and the large-scale data value, x_i ref, for variables whose coefficients were estimated on other than large-scale data, just as distinguished in Figures A12.5-14b and A12.5-14c. For VAAQ, because the horizontal portion is greater than 0.255

*Inverse matrix of coefficients in the normal equations.

and does not involve the coefficient, $x' = 0.255$ was used for any cases where VAAQ is greater than 0.255. For MNAQ, because the straight-line tangent does not involve the coefficients on MNAQ and MNQ2, $x' = 6.89$ was used for any cases where MNAQ is greater than 6.89.

A12.5.11 Evaluation of Term VVPM (Variance of Coefficient for Maximum Subsequent Actuation)

VVPM is the variance of CMSA, the coefficient on the predicted first actuation to obtain the predicted maximum subsequent actuation. Referring to Figure A12.5-16, VVPM is the variance of estimate of the coefficient 1.744 for load cases involving the maximum subsequent actuation. For load cases involving only the first actuation, where CMSA = 1.0, VVPM is not applicable and VPRM = 0.

The variance of estimate of the slope of a line through the origin is found by the standard equation shown in Figure A12.5-19, and VVPM is evaluated in that figure as 0.01199.

A12.5.12 Derivation of Equation for VIND (Variance of Individual Values)

VIND is the variance of individual values:

$$VIND = (\text{PROR} \times \text{PRED})^2.$$

Because the variance of individual values about the prediction surface is required beyond the range of measurement of some of the variables, it is necessary to consider whether the standard deviation of residuals is apparently constant over all predicted values, or is in some way proportional to predicted values. From studies of possible proportionality in all data from small and large-scale tests, both as originally fit within the data sets and as repredicted by the composite prediction equation in Table A12.5-2, it was determined that the standard deviation of residuals should be regarded as proportional to the predicted value, both for first actuation and for maximum subsequent actuation, according to the prediction

line shown in Figure A12.5-20. The line is based on the maximum subsequent actuation data. The average absolute residual within each 0.1 bar cell of the predicted maximum subsequent actuation is shown plotted versus those predicted values. The proportionality of the plotted points is clear, and is used within and beyond the range of predicted values shown. The standard deviation is obtained by the equation shown on Figure A12.5-20, the 0.798 divisor being the expected value of the upper half of the normal distribution, corresponding to the average absolute residual when the residuals are normally distributed. The procedure for calculating the expected value of the upper half of a standard normal distribution is illustrated in Figure A12.5-21.

A12.5.13 Evaluation of Term PROR

PROR is the coefficient to multiply by the predicted value to obtain the standard deviation of individual values, $(VIND)^{1/2}$. Its evaluation is shown on Figure A12.5-20 as 0.229. Thus, one standard deviation of individual values (residuals) is 22.9% of the predicted value.

A12.5.14 Derivation of Equation for MNPDV (Maximum Negative Pressure, Design Value)

MNPDV is the design value for maximum negative pressure (MNP). It was derived in Section A12.4 as:

$$P^+ P^- = P_{\infty}^2 .$$

P^+ is the absolute pressure equivalent of MPP at quencher elevation, P^- is the absolute pressure equivalent of MNP, and P_{∞} is the absolute pressure

at quencher elevation (considering atmospheric pressure and hydrostatic pressure). To obtain an appropriate pressure difference value,

$$MNPDV = PINF \times MPPDV / (PINF + MPPDV).$$

MPPDV is found in Section A12.5.3.

A12.5.15 Derivation of Equation for PINF and SUBM

PINF is P_{∞} at quencher elevation, in absolute pressure units. Evaluated in bars, it is:

$$PINF = 1.014 + 0.0980 \times SUBM$$

where 1.014 is atmospheric pressure in bars (14.7/14.5); 0.098 is bars per meter of hydrostatic head; and SUBM is meters submergence at the centerline of the quencher.

The maximum negative pressure design value corresponding to any maximum positive pressure design value can be found using the above equations.

A12.5.16 Statistical Confirmation of MNPDV

The negative pressures were treated by the same statistical analysis procedure as that used for the positive pressure data discussed in this appendix. Through this analysis, it was confirmed that the predicted positive pressure can stand alone for prediction of negative pressure. The same independent variables used in positive pressure predictions were offered for fitting, together with the positive pressure, but none of these variables made a significant reduction in variability of the fit compared to the fit using positive pressure alone.

By way of further confirmation, the following two models were fitted to the maximum negative pressure (MNP) data:

$$\text{MNP} = C_1 + C_2 \times \text{MPP}, \text{ and}$$

$$P^- = C_3 + C_4 \times \left(\frac{P_\infty^2}{P^+} \right)$$

MNP and MPP are the observed maximum negative and maximum positive pressure differences, respectively; P^- and P^+ are observed maximum negative and maximum positive absolute pressures, and P_∞ is the absolute pressure at quencher elevation. Both fits were highly significant and of identical quality. Intercept C_3 was not significantly different from 0, and C_4 was not significantly different from 1.0, at even the 10% level.

In application, the predicted maximum positive pressure must, of course, be used for P^+ . Therefore, it is of interest to fit the negative pressure data using the predicted positive pressure values in place of measured positive pressures. Such fitting of both of the above equations to large and small data gave fits which were significant and of identical quality, with C_3 and C_4 again not significantly different from 0 and 1, respectively, confirming from the data the appropriateness of the relationship $P^+ P^- = P_\infty^2$.

The adequacy of $P^+ P^- = P_\infty^2$ using predicted maximum positive pressures can be confirmed visually for first actuations by comparison of the residuals for large and small-scale repredicted data in Figures A12.5-22 and A12.5-23. Since there is only one term in the equation, shell residuals are not applicable.

A12.5.17 Numerical Results for Maximum Positive and Negative Pressures

Numerical results for design value for each of the generalized bottom pressure load cases, using the values of Table A12.5.5 are given in Table A12.5.6. Figure A12.5-25 presents a graphical representation of the maximum positive pressures to show the relationship between predicted and design values.

Table A-12.5.1

DESIGN VALUE EQUATIONS WITH SUBORDINATE EQUATIONS AND TERMS

<u>Section</u>	<u>Equations</u>
A-12.5.3	$MPPDV = MPP \text{ DESIGN VALUE} = PRED + CONF \times SIFV$
A-12.5.4	$PRED = CMSA \times PRD1$
A-12.5.5	$PRD1$
A-12.5.6	$CMSA$
A-12.5.7	$CONF$
A-12.5.8	$SIFV = VIFV^{1/2}$
A-12.5.9	$VIFV = VPRD + VIND$
A-12.5.10	$VPRD = VPRI + VPRM$
A-12.5.11	$VPRI = CMSA^2 \times VVPI$
A-12.5.12	$VVPI$
A-12.5.13	$VPRM = PRD1^2 \times VVPM$
A-12.5.14	$VVPM$
A-12.5.15	$VIND = (PROR \times PRED)^2$
A-12.5.16	$PROR$
A-12.5.17	$MNPDV = MNP \text{ DESIGN VALUE} = PLNF \times MPPDY / (PLNF + MPPDY)$
A-12.5.18	$PLNF = 1.014 + 0.0980 \times SUBM$

The terms are defined and the equations are derived in the Sections shown.
The indexes are defined in Section A12.5.3.

22A4365

Rev. 2

A-163 and A-164

Table A12.5.2

EQUATION FOR PREDICTION OF PRD1, MAXIMUM POSITIVE
PRESSURE FOR FIRST ACTUATION

(GE COMPANY PROPRIETARY INFORMATION PROVIDED UNDER SEPARATE COVER)

042178

22A4365
Rev. 2

A-165 thru A-174

Table A12.5.3
DATA AND PREDICTED VALUES
(10 Sheets)

(GE COMPANY PROPRIETARY INFORMATION PROVIDED UNDER SEPARATE COVER)

042178

Table A12.5.4
VARIATION OF VARIABLES BY TEST

	<u>Large-Scale</u>	<u>Small-Scale</u>	<u>Miniscale</u>
Dependent:			
MPP	Yes	Yes	Yes
MNP	Yes	Yes	Not Reported
Independent:			
VAAQ	No	SEL	No
MVAQ	SEL*	Varied**	No
LNTW	SEL	Varied	No
SUBM	No	SEL	No
VOT	Varied	SEL	No
AWAQ	No	No	SEL

*Coefficient(s) estimated on this data set was selected for prediction equation.

**Variable was varied, but coefficient not selected.

Table A12.5.5

VALUES OF VARIABLES FOR STANDARD 238 MARK III PLANT

Generalized Bottom Pressure Load Case

<u>Parameter</u>	<u>a. First Actuation One or Two Valves (100°F Water)</u>	<u>b. First Actuation All Valves (100°F Water)</u>	<u>c. First Actuation ADS Valve (120°F Water)</u>	<u>d. Subsequent Actuation Single Valve (120°F Water)</u>
VAAQ	0.23	0.23	0.23	0.23
MNAQ	11.41	11.41	11.41	11.41
MNQ1	6.89	6.89	6.89	6.89
MNQ2	47.47	47.47	47.47	47.47
MNQJ	11.41	11.41	11.41	11.41
LNTW	3.63	3.63	3.89	3.89
WCL	5.42	5.42	5.42	5.42
WCL2	29.38	29.38	29.38	29.38
VOT	20.00	20.00	20.00	20.00
AWAQ	20.00	3.93	7.85	20.00
AWQ2	400.00	15.44	61.62	400.00
CONF	2.15	2.15	2.15	2.91
PINF	1.43	1.43	1.77	1.43

$$\begin{aligned} \text{Air Volume } (V_A) &= 1.59 \text{ m}^3 \\ \text{Quencher Area } (A_Q) &= 6.93 \text{ m}^2 \\ \text{VAAQ} = V_A/A_Q &= 0.23 \end{aligned}$$

$$\begin{aligned} \text{Maximum Steam Flow Rate (in)} &= 520 \text{ metric ton/hr} \\ \text{MNAQ} = m^{0.7}/A_Q &= 11.41 \end{aligned}$$

$$\begin{aligned} \text{Temperature of Suppression Pool } (T_W) &= 37.8^\circ\text{C } (100^\circ\text{F}) \text{ or } 48.9^\circ\text{C } (120^\circ\text{F}) \\ \text{LNTW} &= 3.63 \text{ or } 3.89 \end{aligned}$$

$$\begin{aligned} \text{Length of Water Column (WCL)} &= 5.42 \text{ m.} \\ \text{WCL2} = (\text{WCL})^2 &= 29.38 \end{aligned}$$

Table A12.5.5 (Continued)

Valve Opening Time (VOT) = 20 msec.

Effective Water Surface Area (A_w) = 548.05 m² (single valve)
 54.79 m² (ADS valves)
 27.20 m² (all valves)

Water Surface Ratio (AWAQ) = A_w/A_Q = 20.00 (single valve)
 = 7.85 (ADS valves)
 = 3.93 (all valves)

MNQ1 = MNAQ if MNAQ \leq 6.89

MNQ1 = 6.89 if MNAQ > 6.89

MNQ2 = (MNQ1)²

MNQJ = MNAQ

Quencher Submergence to Centerline (SUBM) = 4.24 m

Containment Pressure = 14.7 psia (19.7 psia for ADS only)
 = 1.0135 bar (1.358 bar for ADS only)

PINF = Containment Pressure + Hydrostatic Pressure

Hydrostatic Pressure = 0.098 x SUBM

= 1.0135 + 0.4158 = 1.43 bar

= 1.358 + 0.4158 = 1.77 bar (for ADS only)

Table A12.5.6
VALUES FOR A STANDARD 238 MARK III PLANT

<u>Generalized Bottom Pressure Load Case</u>	<u>a</u>	<u>b</u>	<u>c</u>	<u>d</u>
MPPDV (psid)	13.44	18.73	17.40	28.13
MPPDV (bar d)	0.927	1.29	1.20	1.94
PRED	0.603	0.851	0.790	1.11
PRD1	0.603	0.851	0.790	0.639
CMSA	1.0	1.0	1.0	1.74
CONF	2.15	2.15	2.15	2.91
SIFV	0.151	0.205	0.191	0.284
VIFV	0.0227	0.0421	0.0364	0.0805
VPRD	0.00357	0.00407	0.00363	0.0154
VPR1	0.00357	0.00407	0.00363	0.0105
VVF1	0.00357	0.00407	0.00363	0.00345
VPRM	0.	0.	0.	0.00490
VVPM	NA*	NA	NA	0.0120
VIND	0.0191	0.0380	0.0327	0.0651
PROR	0.229	0.229	0.229	0.229
MNPDV (psid)	8.15	9.84	10.38	11.93
MNPDV (bar d)	0.562	0.679	0.716	0.823
PINP	1.43	1.43	1.77	1.43
SUBM	4.24	4.24	4.24	4.24

*NA = Not Applicable.

Table A12.5.7
c MATRIX VALUES* (Page 1 of 2)

c_{i1}	3.08E-02				
c_{i2}	-8.91E-04	2.75E-05			
c_{i3}	0	0	2.52E-01		
c_{i4}	0	0	-6.47E-02	2.42E-01	
c_{i5}	0	0	3.23E-02	-2.93E-02	3.67E-03
c_{i6}	0	0	0	0	0
c_{i7}	0	0	-3.48E-04	-5.30E-06	1.624E-07
c_{i8}	0	0	0	0	0
c_{i9}	0	0	0	0	0
	c_{1j}	c_{2j}	c_{3j}	c_{4j}	c_{5j}
c_{i6}	2.86E-01				
c_{i7}	0.	4.22E-07			
c_{i8}	1.09E-02	0.	2.37E-01		
c_{i9}	8.12E-04	0.	-1.953E-02	1.653E-03	
	c_{6j}	c_{7j}	c_{8j}	c_{9j}	
1	AWAQ	estimated on miniscale data			
2	AWQ2	estimated on miniscale data			
3	VAAQ	estimated on small-scale data			
4	WCL	estimated on small-scale data			
5	WCL2	estimated on small-scale data			
6	LNTW	estimated on large-scale data			
7	VOT	estimated on small-scale data			
8	YNAQ	estimated on large-scale data			
9	YVQ2	estimated on large-scale data			

$$c_{ij} = c_{ji}$$

c_{ij} for coefficients estimated on different data sets = 0

*Inverse matrix of coefficients in the normal equations. (See Figure A12.5-18.)

Table A12.5.7 (Continued)

	<u>Mean (bar d)</u>	<u>Residuals (MPP)</u>	
		<u>Variance</u>	<u>Standard Deviation</u>
First Actuations			
37 Large-Scale Data	-0.01070*	0.00938**	0.0969
70 Small-Scale Data	0.00325	0.00927**	0.0938
9 Miniscale Data	0.000832	0.000493**	0.0222
Maximum Subsequent Actuations			
10 Large-Scale Data	0	0.01188	0.1090

	<u>Mean (bar d)</u>	<u>Residuals (MNP)</u>	
		<u>Variance</u>	<u>Standard Deviation</u>
First Actuations			
37 Large-Scale Data	0.00479	0.00892	0.0945
70 Small-Scale Data	0.0187	0.00214	0.0463

*In least squares fitting, the mean of residuals = 0. These are not exactly 0, due to use of an equation involving coefficients estimated on sets of data other than on line shown.

**VRESID_{ti} in Figure A12.5-18.

(GE COMPANY PROPRIETARY INFORMATION PROVIDED UNDER SEPARATE COVER)

Figure A12.5-1. MPP for First and Subsequent Actuations Positive--
Large Scale

(GE COMPANY PROPRIETARY INFORMATION PROVIDED UNDER SEPARATE COVER)

Figure A12.5-2. MNP for First and Subsequent Actuations Negative--
Large Scale

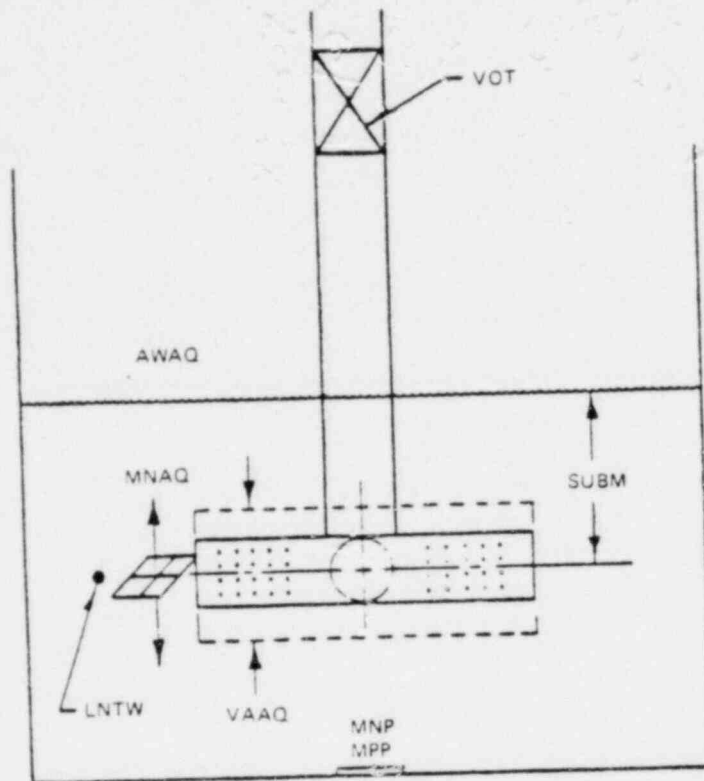


Figure A12.5-3. Quencher Diagram Illustrating Dependent and Independent Variables

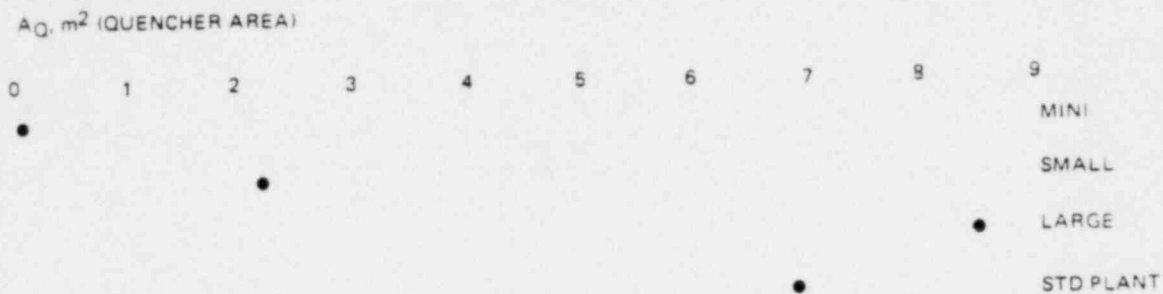


Figure A12.5-4. Ranges of Values/ Raw and Transformed Independent Variables
(Page 1 of 4)

22A4365
Rev. 2

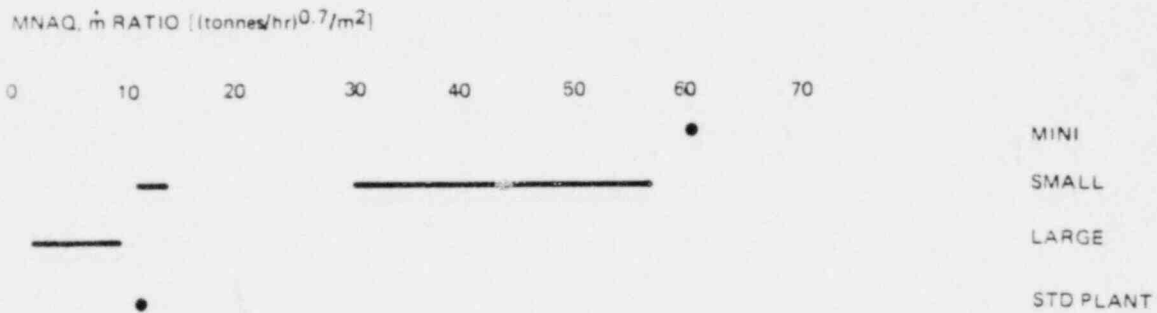
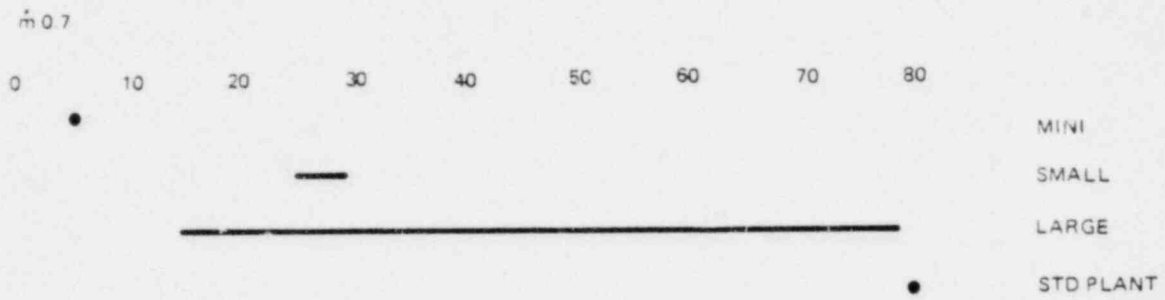
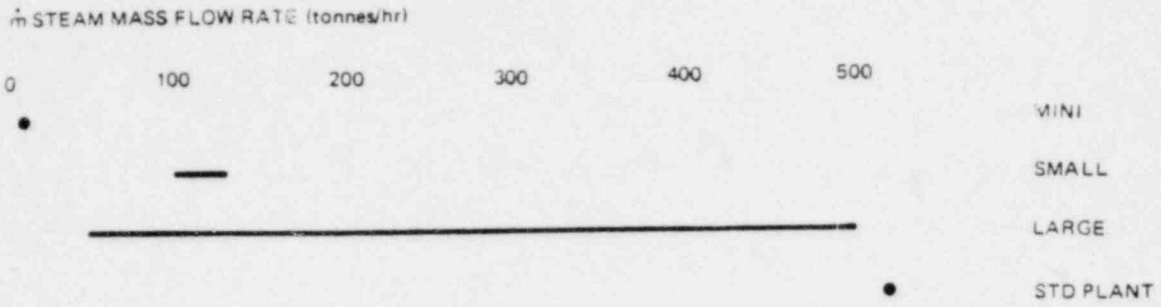


Figure A12.5-4. Page 2 of 4

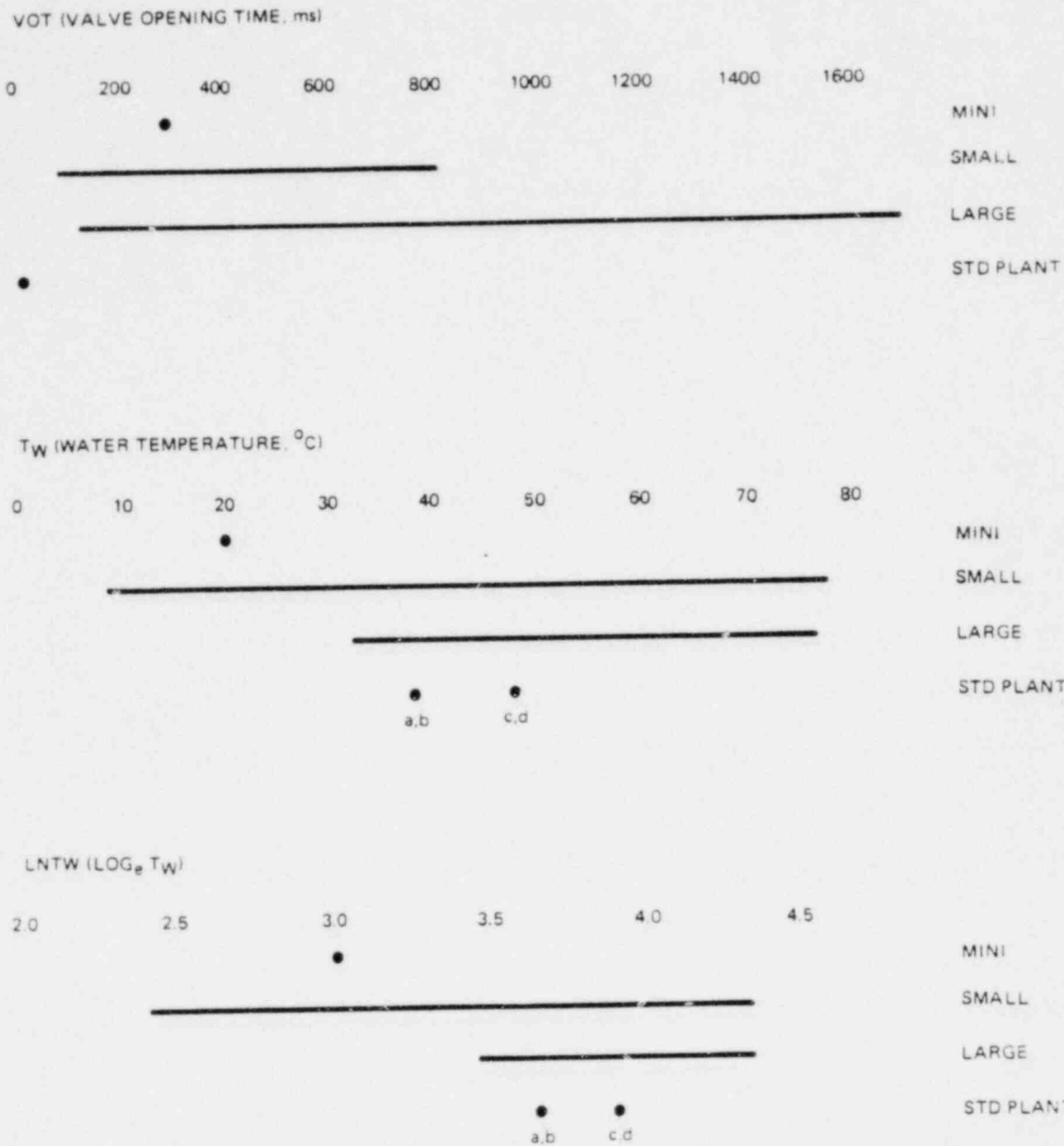
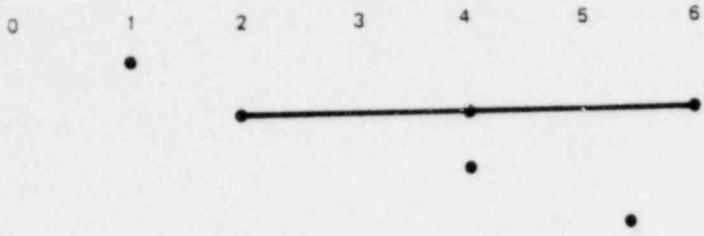


Figure A12.5-4. Page 3 of 4

WCL, WATER COLUMN LENGTH (m)



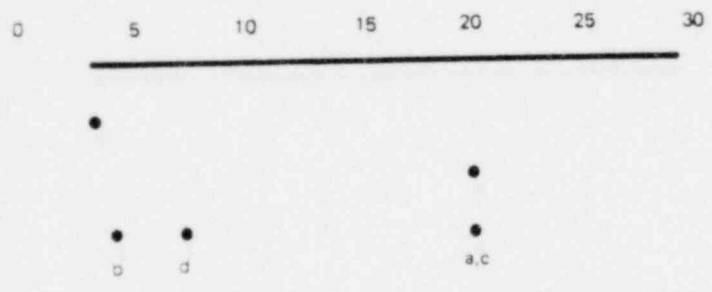
MINI
SMALL
LARGE
STD PLANT

A_W, m^2 (WATER SURFACE AREA)



MINI
SMALL
LARGE
STD PLANT

AWAQ (WATER SURFACE RATIO A_W/A_Q m^2/m^2)



MINI
SMALL
LARGE
STD PLANT

Figure A12.5-4. Page 4 of 4

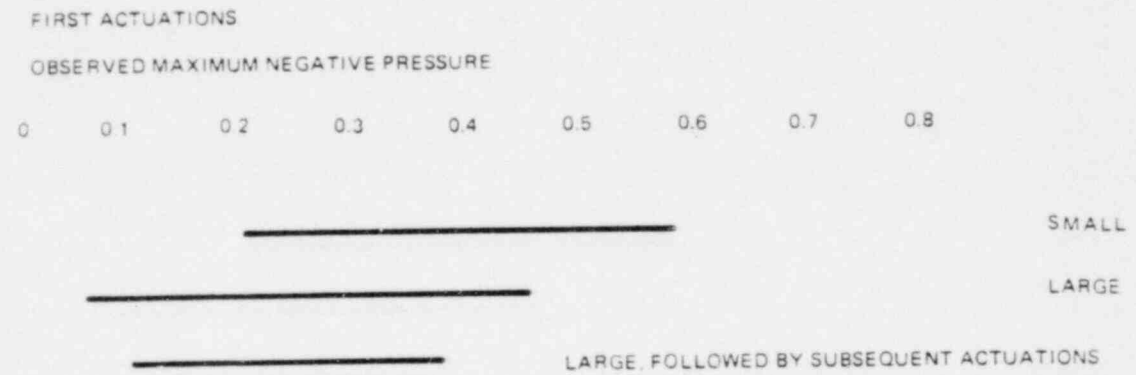
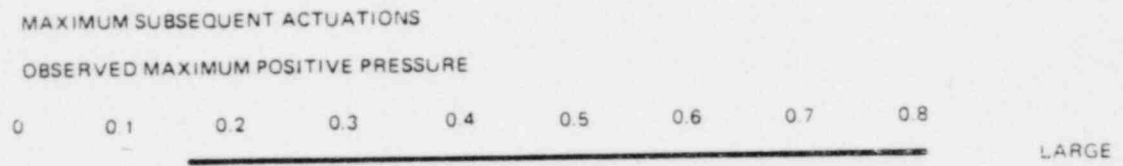
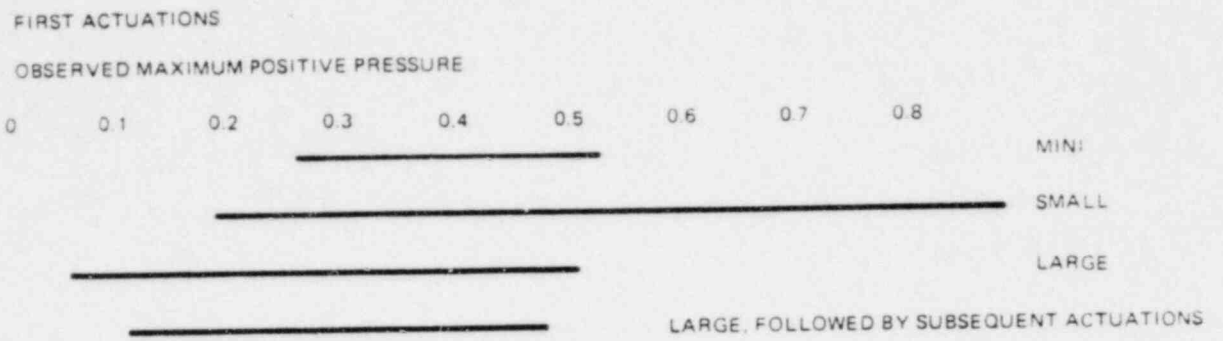


Figure A12.5-5. Ranges of Values; Dependent Variables

(GE COMPANY PROPRIETARY INFORMATION PROVIDED UNDER SEPARATE COVER)

Figure A12.5-6. Shell Residuals, VAAQ Omitted, and Effect of VAAQ Term on Prediction; Small Scale Data (Coefficient Estimated on These Data)

(GE COMPANY PROPRIETARY INFORMATION PROVIDED UNDER SEPARATE COVER)

Figure A12.5-7. Shell Residuals, MIAQ Omitted, and Effect of MIAQ Terms on Prediction; Large Scale Data (Coefficient Estimated on These Data)

(GE COMPANY PROPRIETARY INFORMATION PROVIDED UNDER SEPARATE COVER)

Figure A12.5-8. Shell Residuals, LNTW Omitted, and Effect of LNTW Term on Prediction; Large Scale Data (Coefficient Estimated on These Data)

(GE COMPANY PROPRIETARY INFORMATION PROVIDED UNDER SEPARATE COVER)

Figure A12.5-9. Shell Residuals, LNTW Omitted, and Effect of LNTW Term on Prediction; Small Scale Data (LNTW Coefficient Estimated from Large Scale)

22A4365
Rev. 2

(GE COMPANY PROPRIETARY INFORMATION PROVIDED UNDER SEPARATE COVER)

Figure A12.5-10. Shell Residuals, WCL Omitted, and Effect of WCL Terms on Prediction; Small Scale Data (Coefficients Estimated from These Data)

(GE COMPANY PROPRIETARY INFORMATION PROVIDED UNDER SEPARATE COVER)

Figure A12.5-11. Shell Residuals, VOT Omitted, and Effect of VOT Term on Prediction; Small Scale Data (Coefficient Estimated from These Data)

042178

(GE COMPANY PROPRIETARY INFORMATION PROVIDED UNDER SEPARATE COVER)

Figure A12.5-12. Shell Residuals, VOT Omitted, and Effect of VOT on Prediction, Large Scale Data (VOT Coefficient Estimated from Small Scale; not Significant in Large Scale)

(GE COMPANY PROPRIETARY INFORMATION PROVIDED UNDER SEPARATE COVER)

Figure A12.5-13. Shell Residuals, AWAQ Omitted, and Effect of AWAQ Terms on Prediction, Miniscale Data (Coefficients Estimated from These Data)

FIGURE A12.5-14a
STANDARD INTERCEPT FORM:
 $\tilde{Y} = A_0 + A_1 \dot{X}_1 + A_2 \dot{X}_2 + \dots$

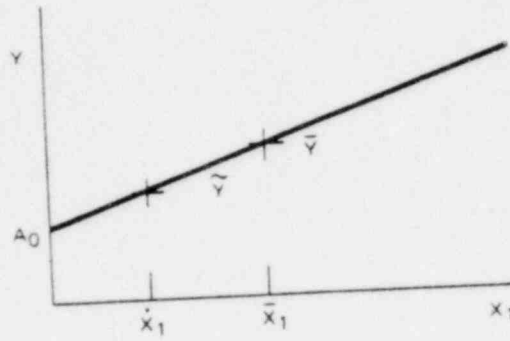


FIGURE A12.5-14b
MEAN ADJUSTED FORM:
 $\tilde{Y} = \bar{Y} + \Sigma \Delta \tilde{Y}_{14b} + \Sigma \Delta \tilde{Y}_{14c}$
 $\Sigma \Delta \tilde{Y}_{14b} = A_1 (\dot{X}_1 - \bar{X}_1)$
 $+ A_2 (\dot{X}_2 - \bar{X}_2)$
+

\bar{Y} FROM LARGE SCALE
 A_i 's ESTIMATED ON LARGE SCALE DATA

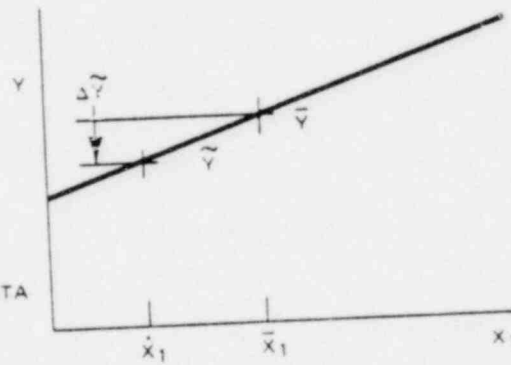


FIGURE A12.5-14c
REFERENCE ADJUSTED FORM:
 $\Sigma \Delta \tilde{Y}_{14c} = A_3 (\dot{X}_3 - X_{3 \text{ REF}})$
 $+ A_4 (\dot{X}_4 - X_{4 \text{ REF}})$
+

A_i 's ESTIMATED ON DATA OTHER
THAN LARGE SCALE

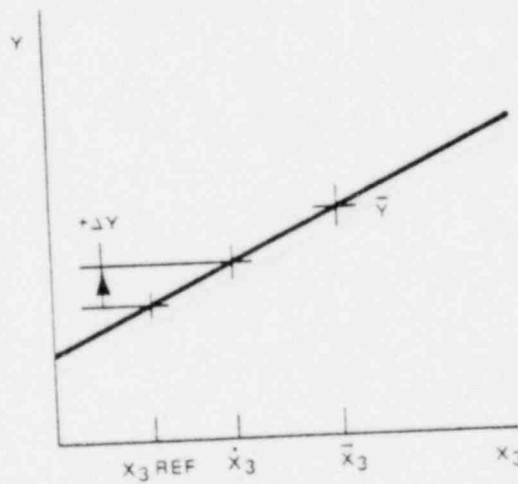


Figure A12.5-14. General Forms of Prediction Equations

(GE COMPANY PROPRIETARY INFORMATION PROVIDED UNDER SEPARATE COVER)

Figure A12.5-15. Observed MPPQ Maximum Subsequent Actuations, MPPQ Versus Predicted First Actuations, PRD1; Large Scale Data

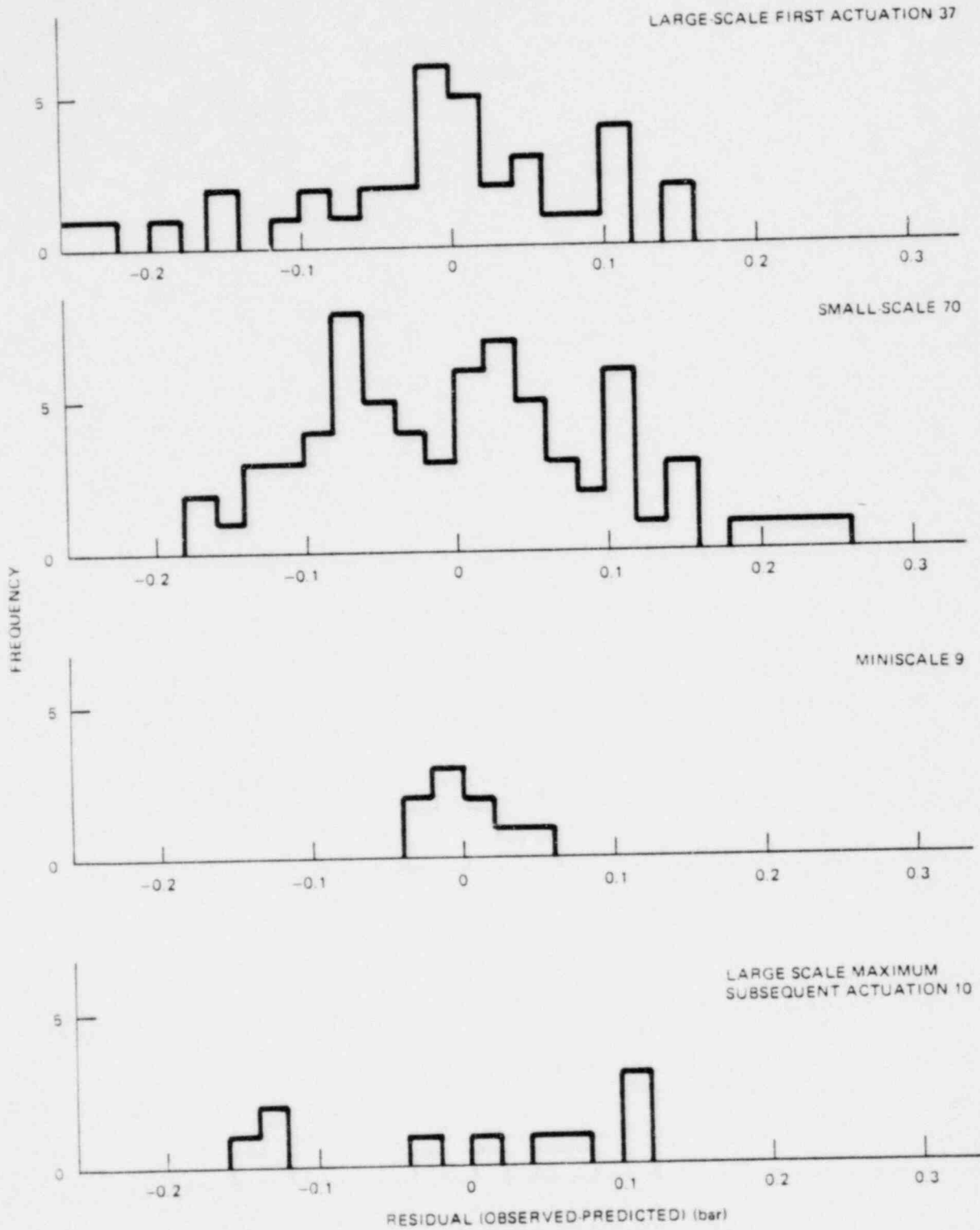


Figure A12.5-16. Frequency Distributing Showing Normality of Residuals

AN INDIVIDUAL FUTURE VALUE*

$$= \text{TRUE VALUE FOR PLANT} + \text{ERROR IN PREDICTED VALUE} + \text{ERROR IN INDIVIDUAL VALUE ABOUT PREDICTED VALUE}$$

DUE TO INDEPENDENCE OF ERRORS:

VARIANCE OF INDIVIDUAL FUTURE VALUE*

$$= 0 + \text{VARIANCE OF PREDICTED VALUE} + \text{VARIANCE OF RESIDUALS}$$

$$(VIFV = VPRD + VIND)$$

*VALUE OF FIRST OR MAXIMUM SUBSEQUENT ACTUATION MPP

Figure A12.5-17 Error Model

$$VVP1 = \frac{(\text{VAR RESID})_t = \text{LARGE SCALE}}{n = 37}$$

$$+ \sum_i (\bar{x}_i - \bar{x}_i) \text{Va}_i + 2 \sum_{\substack{i < j \\ i < j}} (\bar{x}_i - \bar{x}_i) (\bar{x}_j - \bar{x}_j) \text{COV} (a_i, a_j)$$

WHERE

$$\text{Va}_i = \text{VARIANCE OF ESTIMATED OF COEFFICIENT } a_i$$

$$= C_{ii} \text{VRESID}_{ti}$$

COV (a_i, a_j)

$$= C_{ij} (\text{VRESID}_{ti} \times \text{VRESID}_{tj})^{1/2}$$

WHERE t_i, t_j REFER TO THE SET OF TEST DATA ON WHICH THE COEFFICIENTS a_i AND a_j WERE ESTIMATED. AND C_{ii} AND C_{ij} REFER TO ELEMENTS IN THE C MATRIX. VALUES OF VRESID_t, AND C_{ii}, ETC., ARE TABULATED IN TABLE A12.5.7

THE EQUATION FOR VVP1 ABOVE IS FOR A PREDICTION EQUATION IN THE FORM OF THE EQUATION FOR \tilde{y} IN FIGURE A12.5.14b.

Figure A12.5-18 Variance of Predicted Value MPP, First Actuation Evaluated at x⁰ Values

VARIANCE OF SLOPE THROUGH ORIGIN

$$VVP1 = \frac{\text{VRESID MSA}}{\sum \text{PRD}_i^2} \quad (\text{ILLUSTRATED IN FIGURE A12.5.20})$$

$$= \frac{0.01188}{0.991}$$

$$= 0.01199$$

Figure A12.5-19. Variance of Coefficient (1.744) for Maximum Subsequent Actuation

(GE COMPANY PROPRIETARY INFORMATION PROVIDED UNDER SEPARATE COVER)

Figure A12.5-20. Proportionality of Average Absolute Residuals and Predicted Values, Maximum Subsequent Actuations

$$\text{AVERAGE ABSOLUTE DEVIATION} = \frac{\int_0^{\infty} z f(z) dz}{\int_0^{\infty} f(z) dz} = 0.5$$

$$\text{WHERE } f(z) = \frac{1}{\sqrt{2\pi}} e^{-z^2/2}$$

THE STANDARD NORMAL PROBABILITY DENSITY FUNCTION APPLIES TO NORMALLY DISTRIBUTED INDIVIDUAL VALUES USED IN THE EQUATION FOR $(VIND)^{1/2}$ IN FIGURE A12.5-20.

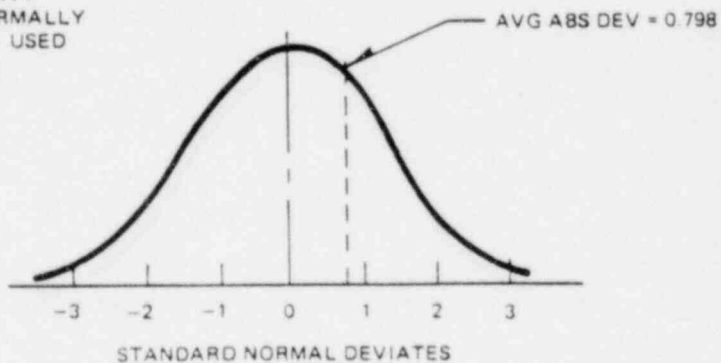


Figure A12.5-21. Derivation of Ratio of Average Absolute Deviation to Standard Deviation

(GE COMPANY PROPRIETARY INFORMATION PROVIDED UNDER SEPARATE COVER)

Figure A12.5-22. Residuals for MNP Large Scale Data

(GE COMPANY PROPRIETARY INFORMATION PROVIDED UNDER SEPARATE COVER)

Figure A12.5-23. Residuals for MNP Small Scale Data

22A4365
Rev. 2

(GE COMPANY PROPRIETARY INFORMATION PROVIDED UNDER SEPARATE COVER)

Figure A12.5-24. Observed vs Predicted Values, MPP (MPPI Versus PRDI or
MPQ Versus PRDQ)

042178

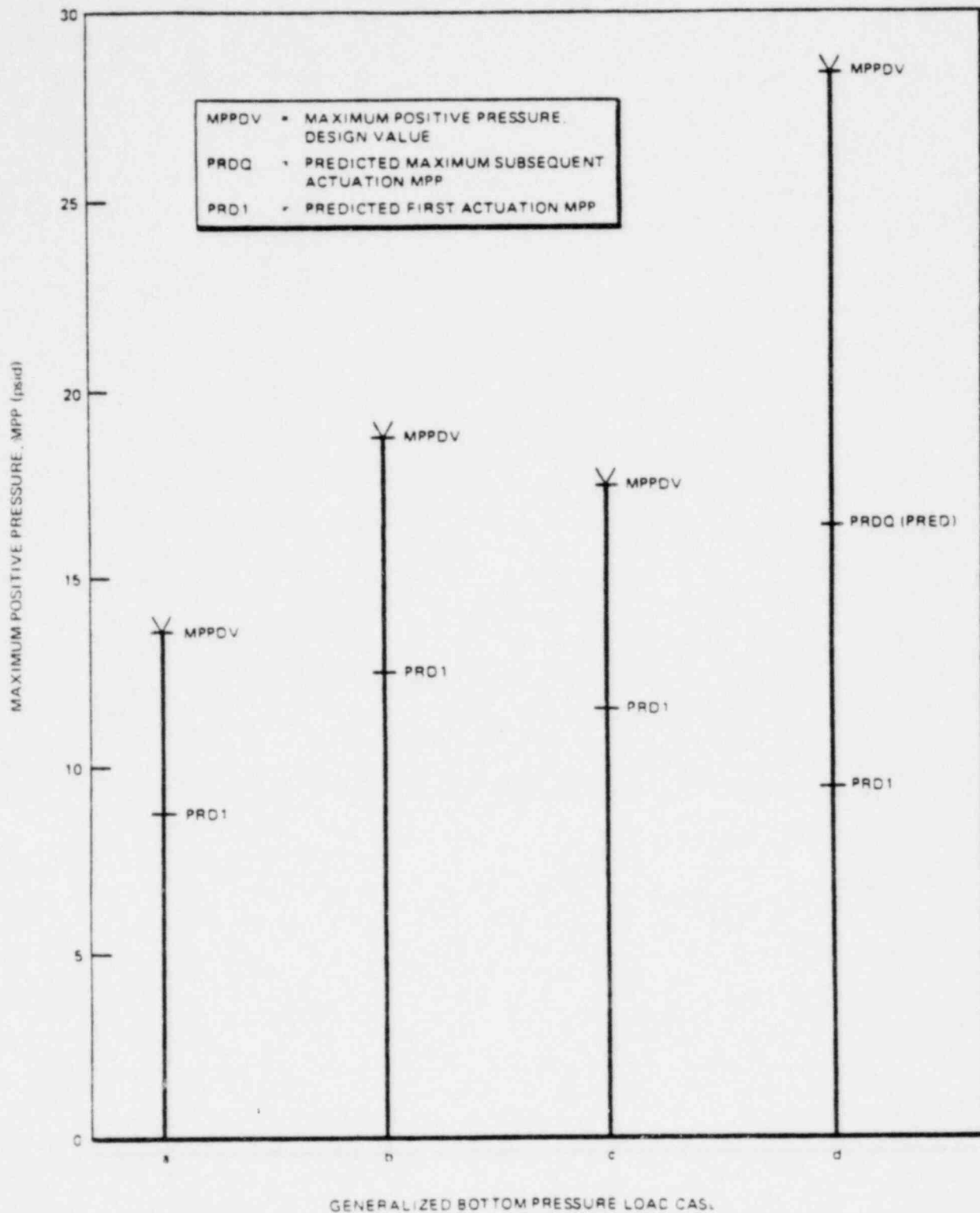


Figure A12.5-25. Generalized Bottom Pressure Load CAS. Predicted Values and Design Values of Maximum Positive Pressure from Table A12.5.6

A12.6 APPLICATION

The purpose of this section is to provide the designer with a simple and straightforward procedure for calculating the maximum positive and negative air-clearing pressures on the bottom of the suppression pool beneath the quencher. These pressures are to be used in the development of suppression pool boundary loads for the design of the containment. The development of boundary loads is discussed in Section A10.

A12.6.1 Procedure

All bottom pressures obtained by these procedures have a 95-95 confidence level, and are within $\pm 1.0\%$ of the values obtained by strict application of the techniques described in the previous chapter.

The first step in determining the bottom pressure is to calculate the predicted first actuation maximum positive pressure (PRD1). Since the quencher device is a fixed design (Area = 6.93 m^2), the maximum flow rate is 520 metric tons per hour, and the safety/relief valve opening time is at the minimum (20 msec). The equation for PRD1 in Table A12.5.1 can be reduced to:

$$\begin{aligned} \text{PRD1} &= 0.421 \\ &+ 2.58 (\text{VAAQ} - 0.1706) \\ &+ 0.1377 (\text{LNTW} - 3.83) \\ &+ 0.206 (\text{WCL} - 4) \\ &- 0.0176 (\text{WCL2} - 16) \\ &- 0.0336 (\text{AWAQ} - 20) \\ &+ 0.000761 (\text{AWQ2} - 400) \end{aligned}$$

where

PRD1 = mean first actuation peak positive pressure (bars);

VAAQ = air volume in the safety/relief valve discharge line (m^3) divided by the quencher area (m^2), where quencher area is defined as the area of a circle that circumscribes the quencher. (For the standard BWR/6 Mark III plant, the quencher area is $6.93 m^2$. If VAAQ is greater than 0.255, use VAAQ = 0.255.);

LNTW = Natural log of T_W , where T_W is the suppression pool temperature ($^{\circ}C$).

WCL = The actual length of the water leg from the centerline of the quencher arm to the air-water interface in the discharge pipe;

WCL2 = $(WCL)^2$;

AWAQ = The effective pool surface area per quencher divided by the quencher area, where quencher area, as the VAAQ, is $6.93 m^2$ (If AWAQ is greater than 20, use 20.); and

AWQ2 = $(AWAQ)^2$.

The above formula allows for the plant unique location of the quencher in the suppression pool and for plant unique routing of safety/relief valve discharge piping within the constraints identified in Section A.10 and, as stated above, is only applicable to the quencher design described in this attachment.

Using the value determined for PRD1, the corresponding maximum positive design pressure (MPPDV) is obtained from Figure A12.6-1 or A12.6-2. Using MPPDV, the negative design pressure (MNPDV) is obtained from the following equation:

$$MNPDV = P_{INF} \frac{MPPDV}{(P_{INF} + MPPDV)}$$

where

MPPDV = Design Positive Bottom Pressure (bars);

MNPDV = Design Negative Bottom Pressure (bars);

P_{INF} = Absolute Pressure at the Level of the centerline of the quencher arms (bars abs.)

To convert pressure from bars to psi, a conversion factor of 14.5 psi/bar is used.

A12.6.1.1 Development of Figures A12.6-1 and A12.6-2

The maximum positive bottom design pressure (MPPDV) is a function of PRD1. This functional relationship was described in A12.5 and can be summarized in the following form.

(GE COMPANY PROPRIETARY INFORMATION PROVIDED UNDER SEPARATE COVER)

A12.6.2 Examples

Given the following input, the design bottom pressures for the four cases described in Section A12.5.1.1 are calculated:

$$\text{Air Volume} = 1.59 \text{ m}^3$$

$$\begin{aligned} \text{Pool temperature} &= 37.8^\circ\text{C} (100^\circ\text{F}) \text{ for cases a and b} \\ &49.0^\circ\text{C} (120^\circ\text{F}) \text{ for cases c and d} \end{aligned}$$

Water Column Length = 5.42 m

Submergence to Centerline = 4.24 m

Effective Pool Area per Quencher = 548 m² for case a and c
27.2 m² for case b
54.8 m² for case d

A12.6.2.1 Calculation of Variables

$$VAAQ = \frac{1.59}{6.93} = 0.23$$

$$LNTV = \ln 37.8 = 3.63 \text{ for cases a and b}$$
$$\ln 49.0 = 3.89 \text{ for cases c and d}$$

$$WCL = 5.42$$

$$WCL2 = 29.38$$

$$AWAQ = \frac{548}{6.93} = 79.08. \text{ Therefore, 20 is used for cases a and d.}$$

$$\frac{27.2}{6.93} = 3.93 \text{ for case b}$$

$$\frac{54.8}{6.93} = 7.85 \text{ for case c}$$

$$AWQ2 = (20)^2 = 400 \text{ for case a and d}$$
$$(3.93)^2 = 15.44 \text{ for case b}$$
$$(7.85)^2 = 61.62 \text{ for case c}$$

$$P_{INF} = \frac{14.7}{14.5} + (0.098 \times 4.24) = 1.43 \text{ bar for case a, b and d}$$

$$\frac{19.7}{14.5} + (0.098 \times 4.24) = 1.77 \text{ bar for case c}$$

A12.6.2.2 Case a - First Actuation of One or Two Valves (100°F Pool Temperature)

PRD1 is calculated from the equation in Section A12.6.1.

$$\begin{aligned} PRD1 &= 0.421 \\ &+ 2.58 (0.23 - 0.1706) \\ &+ 0.1377 (3.63 - 3.83) \\ &+ 0.206 (5.42 - 4.0) \\ &- 0.0176 (29.38 - 16.0) \\ &- 0.0336 (20 - 20) \\ &+ 0.000761 (400 - 400) = 0.604 \text{ bars} \end{aligned}$$

From Figure A12.6-1, for PRD1 = 0.604, MPPDV = 0.93 bars. MNPDV is then calculated:

$$MNPDV = 1.43 \frac{0.93}{(1.43 + 0.93)} = 0.56 \text{ bars}$$

Converting to psi we get:

$$MPPDV = 0.93 \times 14.5 = 13.49 \text{ PSID}$$

$$MNPDV = 0.56 \times 14.5 = 8.12 \text{ PSID}$$

A12.6.2.3 Case b - First Actuation of All Valves (100°F Pool Temperature)

PRD1 is calculated from the equation in Section A12.6.1.

$$\begin{aligned} \text{PRD1} &= 0.421 \\ &+ 2.58 (0.23 - 0.1706) \\ &+ 0.1377 (3.63 - 3.83) \\ &+ 0.206 (5.42 - 4.00) \\ &- 0.0176 (29.38 - 16.00) \\ &- 0.0336 (3.93 - 20) \\ &+ 0.000761 (15.44 - 400) = 0.85 \text{ bars} \end{aligned}$$

From equation pg. 203 (top) when PRD1 = 0.85, MPPDV = 1.28 bars MNPDV is then calculated:

$$\text{MNPDV} = 1.43 \frac{1.28}{(1.28 + 1.43)} = 0.68 \text{ bars}$$

Converting to psi, we get:

$$\text{MPPDV} = 1.28 (14.5) = 18.56 \text{ psid}$$

$$\text{MNPDV} = 0.68 (14.5) = 9.86 \text{ psid}$$

A12.6.2.4 Case c - First Actuation of an ADS Valve (120°F Pool Temperature)

PRD1 is calculated from the equation in Section A12.6.1

$$\begin{aligned} \text{PRD1} &= 0.421 \\ &+ 2.58 (0.23 - 0.1706) \\ &+ 0.1377 (3.89 - 3.83) \\ &+ 0.206 (5.42 - 4.0) \\ &- 0.0176 (29.38 - 16.0) \\ &- 0.0336 (7.85 - 20) \\ &+ 0.000761 (61.62 - 400) = 0.79 \text{ bars} \end{aligned}$$

From Figure A12.6-1 for PRD1 = 0.79, MPPDV = 1.2 bars. MNPDV is then calculated:

$$\text{MNPDV} = 1.77 \frac{1.2}{(1.2 + 1.77)} = 0.72 \text{ bars}$$

Converting to psi, we get:

$$\text{MPPDV} = 1.2 (14.5) = 17.40 \text{ psid}$$

$$\text{MNPDV} = 0.72 (14.5) = 10.37 \text{ psid}$$

A12.6.2.5 Case d - Subsequent Actuation of a Single Valve (120°F Pool Temperature)

PRD1 is calculated from the equation in Section A12.6.1.

$$\begin{aligned} \text{PRD1} &= 0.421 \\ &+ 2.58 (0.23 - 0.1706) \\ &+ 0.1377 (3.89 - 3.83) \\ &+ 0.206 (5.42 - 4.0) \\ &- 0.0176 (29.38 - 16.0) \\ &- 0.0336 (20 - 20) \\ &+ 0.000761 (400 - 400) = 0.639 \text{ bars} \end{aligned}$$

From equation pg. 203 (top) when PRD1 = 0.64, MPPDV = 1.95 bars. MNPDV is then calculated:

$$\text{MNPDV} = 1.43 \frac{1.95}{(1.95 + 1.43)} = 0.825 \text{ bars}$$

22A4365

Rev. 2

Converting to psi, we get:

$$\text{MPPDV} = 1.95 (14.5) = 28.23 \text{ psid}$$

$$\text{MNPDV} = 0.825 (14.5) = 11.96 \text{ psid}$$

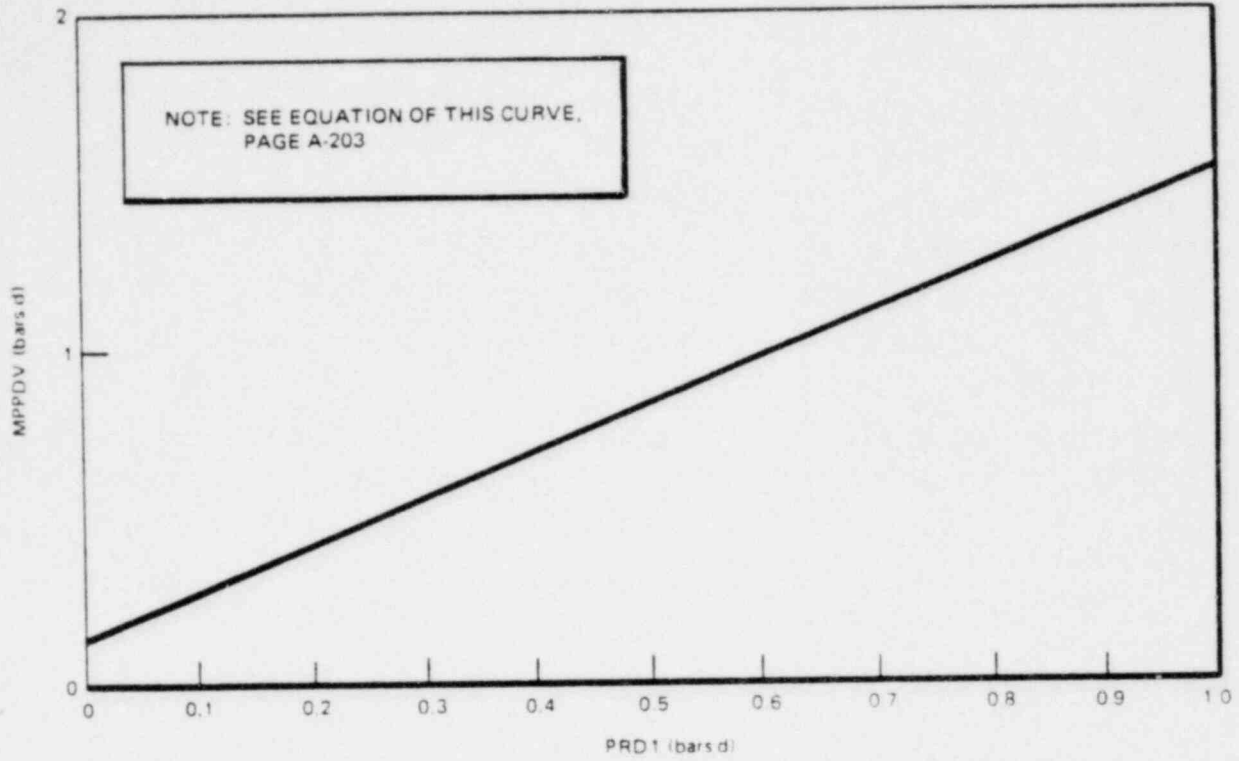


Figure A12.6-1. First Actuation Design Pressure Versus Predicted Pressure for First Actuation

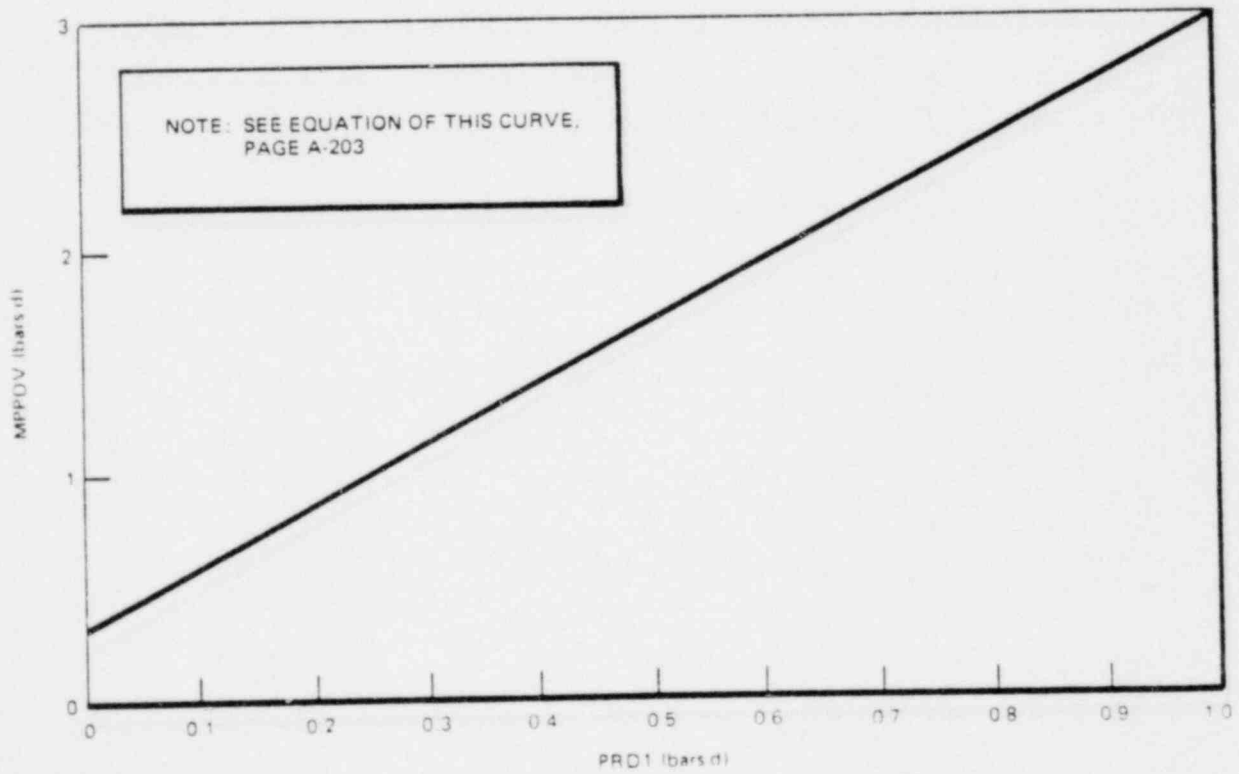


Figure A12.6-2. Subsequent Actuation Design Pressure Versus Predicted Pressure for First Actuation

A12.7 SRV LOAD REDUCTION MARK III STANDARD 238 PLANT

Evaluations of in-plant SRV discharge test results indicate that a significant conservatism exists in the Empirical Load Model upon which Mark III Load predictions are based. Test results are applicable to Mark III analysis since the same quencher and flow rates and comparable discharge lines are used in both designs. Statistical evaluations of the test data were performed typically at two levels of confidence and were compared to corresponding Empirical Load Model test predictions. Model predictions were based on test conditions of mass flow, pool temperature and valve opening times. The impact of the use of test conditions in the predictions is that the model data comparisons performed for this evaluation are on a comparable basis. For design application, bounding values of plant operating conditions are used to give design margin. The margin in the model itself is demonstrated in the Caorso Plant Model/data comparisons summary in Table 12.7-1. The Caorso data, documented in reference 4 and 5, support load reductions of 50% for single valve first actuations and subsequent actuations. Preliminary data from the second phase of Caorso testing suggests a comparable margin exists for multiple valve actuations.

For the Mark III Standard 238 Plant Design a smaller load reduction is recommended to cover differences in the Caorso and Mark III Standard 238 Plant configurations and to maintain an adequate conservative margin. Specifically, if load reduction is desired, a load reduction factor of 35% can be applied to design controlling loads for the SRV air bubble pressures as shown in Table A.4.5. The Attachment A methods for calculating loads are applicable. Load reduction factor is applied subsequent to the load calculation procedure.

Table A12.7-1
CAORSO MODEL/MEAN DATA COMPARISONS

<u>Prediction (psid)</u>	<u>Data (psid)</u>	<u>Potential Load Reduction Factor (Peak Pos./Peak Neg.)</u>
(SINGLE VALVE, FIRST ACTUATION)		
8.5/-6.2	4.3/-2.8	0.52
(SINGLE VALVE, SUBSEQUENT ACTUATION)		
14.9/-9.0	5.8/-3.1	0.63
(MULTIPLE VALVE ACTUATION - FOUR VALVES)		
11.2/-7.5	5.0/-3.4	0.55
(MULTIPLE VALVE ACTUATION - EIGHT VALVES)		
11.2/-7.5	5.6/-4.6	0.45

22A4365
Rev. 4

A12.8 REFERENCES

1. Test Results Employed by General Electric for BWR Containment and Vertical Vent Loads, Class III, October 1975 (NEDO-21078).
2. Safety-Relief Valve Discharge Analytical Models, May 1975, (NEDE-20942-P).
3. Comparison of Safety-Relief Valve Model Predictions With Test Data, July 1975 (NEDE-21062-P).
4. Caorso Phase I Test Data, NEDE-25100-P, dated May 1979.
5. Caorso Phase II Test Data, NEDE-24757-P, dated March 1980.

22A4365

Rev. 2

ATTACHMENT B

B1.0 SUPPRESSION POOL SEISMIC INDUCED LOADS (To be provided by A.E.)

B1.1 HYDROSTATIC PRESSURE

During both vertical and horizontal accelerations, the hydrostatic pressure distribution in the suppression pool undergoes distortions that lead to dynamic loads on the suppression pool boundary.

B1.2 VERTICAL ACCELERATION

The following methods can be used for design evaluation. For evaluating vertical accelerations, it may be assumed that the normal hydrostatic pressure increases by an amount that is directly dependent upon the magnitude of the vertical acceleration, i.e., at any point in the suppression pool the hydrostatic pressure P_H , is given by

$$P_H = \left(\frac{\rho H}{144} (1 + a/g) \right) \frac{\text{lb}}{\text{in.}^2}$$

where

ρ = specific weight of water, lb/ft^3

H = depth, ft

a = vertical acceleration, ft/sec^2

g = gravitation acceleration, ft/sec^2

B1.3 HORIZONTAL ACCELERATION

During horizontal accelerations there will be a non-symmetric modification of the hydrostatic pressure depending upon whether a particular surface is accelerating the mass adjacent to it or not. It is suggested that the normal hydrostatic pressure distribution be modified as follows.

For those structures which are providing this accelerating force, the hydrostatic pressure at any point, P_H , is given by

$$P_H = \left(\frac{\rho H}{144} + \rho \frac{W a/g}{144} \right) \frac{lb}{in.^2}$$

where

ρ = specific weight of water lb/ft³

W = width of suppression pool water that a particular point on the structure is accelerating, ft

a = horizontal acceleration, ft/sec²

g = gravitational acceleration, ft/sec²

On opposite surfaces, design adequacy is established assuming both normal hydrostatic pressure and no hydrostatic pressure on these surfaces.

22A4365

Rev. 2

ATTACHMENT C
WEIR ANNULUS BLOCKAGE

The following figure (C-1) indicates the effect of 0, 10, 20 and 30% blockage of the weir annulus on the drywell pressure. This figure was obtained using the analytical model presented in NEDO-20533 (Ref. 1) and was generated assuming that the annulus water associated with the blocked region still has to be accelerated during the vent clearing transient but that the corresponding vent flow area is not available. During vent clearing, the water in the blocked area was conservatively assigned to the unrestricted vent stacks.

Due to weir annulus flow blockage considerations horizontal pipe routings should be avoided in the region of 5 ft. above the top of the weir wall.

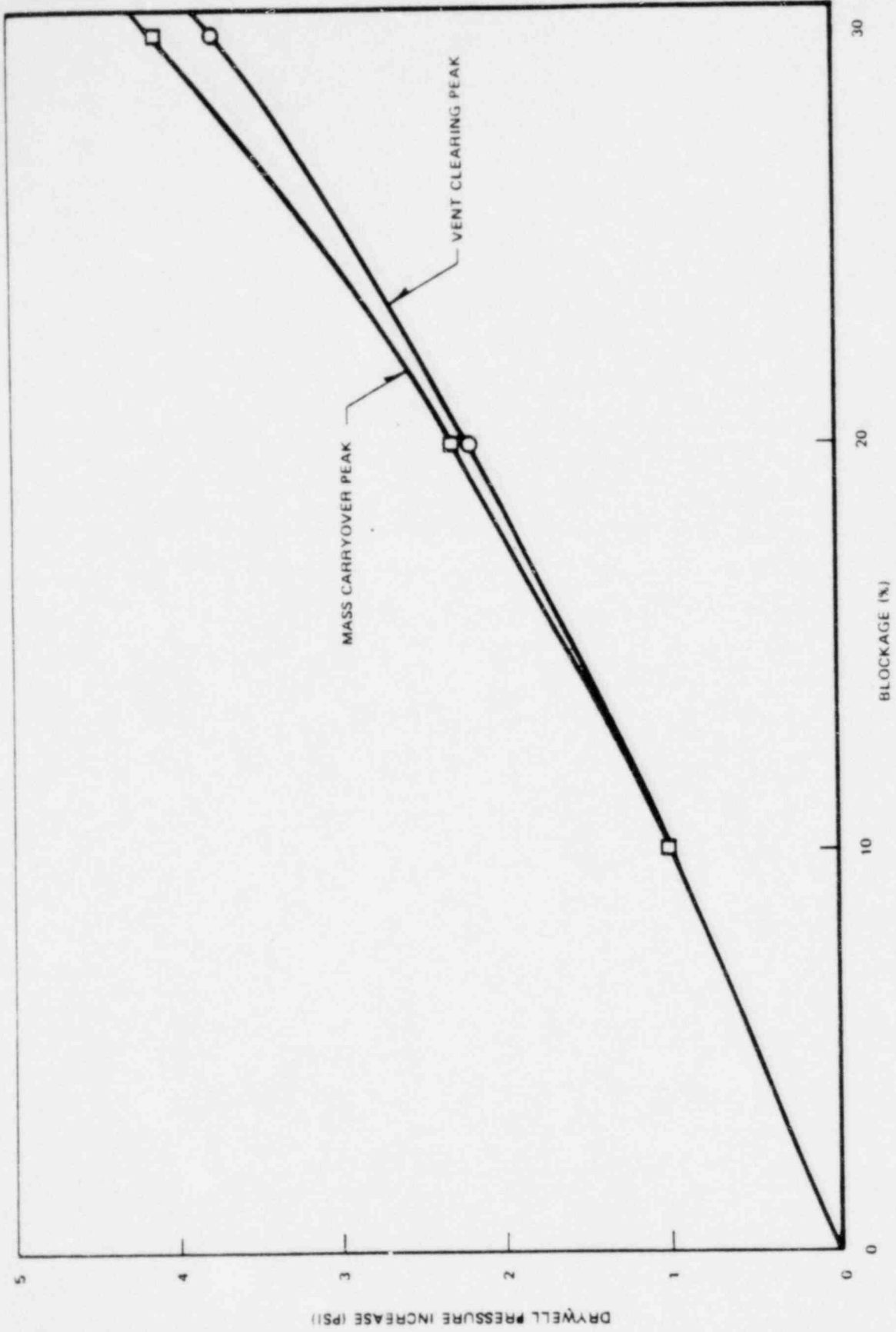


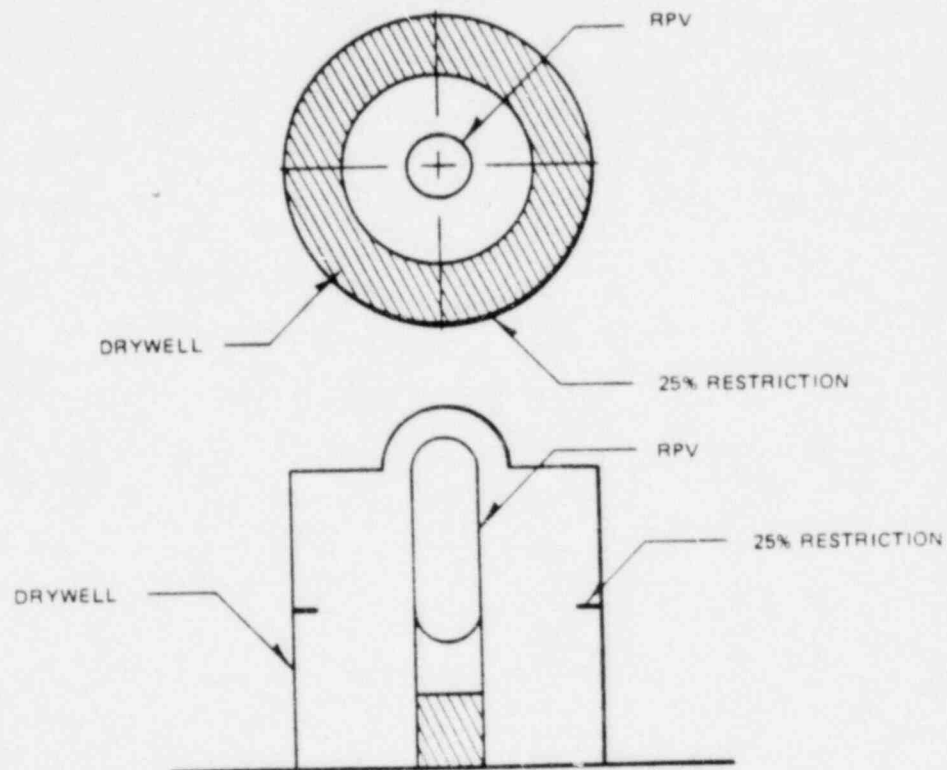
Figure C-1. Weir Annulus Blockage

22A4365
Rev. 2

ATTACHMENT D
DRYWELL PRESSURE DISTRIBUTION

INTRODUCTION

The purpose of this attachment is to show the resulting pressure differential across a given level with some flow restriction assuming a 25% restriction in the drywell.



The greatest pressure differential would occur during a steam break. The flow rate is:*

$$\begin{array}{ll}
 \text{at } t = 1 \text{ sec} & \dot{m}_f = 28,200 \frac{\text{lbm}}{\text{sec}} & h_f = 546 \frac{\text{Btu}}{\text{lbm}} \\
 & \dot{m}_g = 1,230 \frac{\text{lbm}}{\text{sec}} & h_g = 1,190.9 \frac{\text{Btu}}{\text{lbm}}
 \end{array}$$

*Data obtained from Table D.1

The quality of the break flow is:

$$X = \frac{m_{\text{gas}}}{m_{\text{total}}} = \frac{1,230}{29,430}$$

$$X = 0.0418$$

From the quality, the enthalpy of the break is:

$$h_o = (1 - X)h_f + Xh_g$$

$$h_o = (1 - 0.0418)(546.0) + 0.0418(1190.9)$$

$$h_o = 573.0 \frac{\text{Btu}}{\text{lbm}}$$

Assuming constant enthalpy process and a final pressure of 14.7 psia, the final quality can be calculated

$$h_o = h_g - (1 - X)h_{fg}$$

$$572.95 = 1150.5 - (1 - X)970.4$$

$$X = 0.405$$

Using this quality the final specific volume is

$$v = (1 - X)v_f + X v_g$$

$$= (1 - 0.405)0.016715 + 0.405(26.80)$$

$$v = 10.86 \text{ ft}^3/\text{lbm}$$

The differential pressure is then calculated using the following formula:

$$\Delta P = 1/2 K v^2 \text{ but } v^2 = \frac{\dot{m}^2}{\rho A^2}$$

Therefore

$$\Delta P = 1/2 K \frac{\dot{m}^2}{\rho A^2}$$

where the A is the remaining unrestricted area

$$A = A_{\text{Drywell}} 0.75$$

$$A = 0.75(3402.0)$$

$$A = 2551$$

and K is the loss coefficient. This is maximum for an orifice.

$$K = \frac{1}{0.6^2} = 2.778$$

Therefore we now have

$$\Delta P = 1/2(2.778) \frac{29,430^2(10.86)}{2551^2} \left[\frac{\frac{\text{lbm}^2}{\text{sec}^2} \times \frac{\text{Ft}^3}{\text{lbm}}}{\text{ft}^4} \right] \frac{\text{lb fsec}^2}{32.2 \text{ lbm ft}} \left[\times \frac{1}{144} \frac{\text{ft}^2}{\text{in.}^2} \right]$$

$$= \underline{0.433 \text{ psid}}$$

Table D.1
REACTOR PRIMARY SYSTEM BLOWDOWN FLOW RATES AND FLUID ENTHALPY
MAIN STEAM LINE BREAK

<u>Time</u> <u>(sec)</u>	<u>Liquid</u> <u>Flow</u> <u>(lbs/sec)</u>	<u>Liquid</u> <u>Enthalpy</u> <u>(Btu/lb)</u>	<u>Steam</u> <u>Flow</u> <u>(lbs/sec)</u>	<u>Steam</u> <u>Enthalpy</u> <u>(Btu/lb)</u>
0	0	551.6	11,540	1190.0
0.203	0	549.2	10,650	1190.7
0.204	0	549.2	9,960	1190.7
0.99	0	546.2	8,840	1191.4
1.0	28,200	546.2	1,230	1191.4
2.0	27,800	548.3	1,231	1190.9
3.0	27,450	549.8	1,390	1190.5
4.0	27,000	550.5	1,560	1190.3
5.0	22,660	550.5	1,454	1190.3
10	18,000	546.2	1,800	1191.4
15	15,400	533.2	2,220	1194.5
20	12,270	513.2	2,435	1198.7
25	9,030	485.7	2,387	1202.7
30	6,060	450.7	2,110	1205.3
35	4,150	410.0	1,590	1204.9
40	2,750	370.8	1,128	1201.4
45	2,082	333.0	750	1195.5
50	1,843	300.1	460	1188.2
55	1,736	274.7	280	1181.6
60	1,665	256.5	180	1176.3
65	1,635	246.3	126	1173.2
70	1,585	237.7	93	1170.5
75	1,545	231.4	70	1168.5
80	1,510	226.3	56	1166.8
85	1,472	222.7	45	1165.6
90	1,430	220.9	37	1165.0
95	1,390	217.0	30	1163.6
100	1,355	215.0	25	1163.0
105	1,330	212.9	21	1162.2
110	1,300	210.7	18	1161.5

Table D.1 (Continued)

At the end of blowdown these rates are as follows:

<u>Time (sec)</u>	<u>Primary System Liquid Flow (lb/sec)</u>	<u>Liquid Enthalpy (Btu/lb)</u>
399.98	2755	177.8
400.00	2755	177.8
800	2755	162.8
1400	2755	156.3
1799	1720	156.8
1800	1720	157.8
2400	1720	163.7
3500	1720	161.8
10,000	1720	152.7
2.1×10^4	1720	148.7
1.0×10^5	1720	126.4
2.5×10^5	1720	114.3
5.0×10^5	1720	106.9
7.5×10^5	1720	104.1
1.0×10^6	1720	102.2

22A4365

Rev. 3

ATTACHMENT E
 DRYWELL NEGATIVE PRESSURE CALCULATION

INTRODUCTION

The purpose of this attachment is to document the very conservative methods used to calculate the negative drywell pressure that could occur after the reflooding of the reactor vessel. It is a bounding end point calculation that leads to the maximum theoretically possible negative pressure.

CALCULATION

Somewhere between 100 and 600 sec the ECCS system will flood the vessel causing instantaneous condensation of steam in the drywell. At this time all the air initially in the drywell will have been purged into the containment. To evaluate the containment pressure at this time, the initial quantity of air in both the drywell and containment is needed.

Initial mass in D.W.

$$M_{DW} = \frac{(P - P_v) V_{DW}}{R_T}$$

where

P = Pressure in D.W. initially = 16.7 psia

P_v = Partial pressure of vapor = ϕP_{sat}

R = Temperature of D.W. = 135^oF

R = Gas constant = 53.34 $\frac{\text{ft-lbm}}{\text{lb}^{\circ}\text{R}}$

$$V_{DW} = \text{Volume D.W.} = 274,500 \text{ ft}^3$$

$$\phi = \text{Relative humidity} = 0.40$$

$$P_{\text{sat}} = P_{135} = \text{Sat. pressure at 135} = 2.5365 \text{ psia}$$

Therefore

$$M_{DW} = \frac{[16.7 - 0.4(2.5365)] (274,500)}{53.4(540)} 144 \frac{\text{in.}^2}{\text{ft}^2}$$

$$M_{DW} = 21,501 \text{ lbm of air}$$

Initial Mass in Containment

$$M_{\text{con}} = \frac{(P - P_v) V_{\text{cont}}}{RT}$$

where

$$P = \text{Pressure in containment initially} = 14.7 \text{ psia}$$

$$P_v = \text{Partial pressure vapor} = \phi P_{\text{sat}}$$

$$V_{\text{cont}} = \text{Volume of containment} = 1,138,750 \text{ ft}^3$$

$$R = \text{Gas constant} = 53.34 \frac{\text{ft-lbm}}{\text{lb}^\circ\text{R}}$$

$$T = \text{Initial temperature} = 80^\circ\text{F}$$

$$\phi = \text{Relative humidity} = 0.20$$

$$*P_{\text{sat}} = \text{Sat pressure} = 0.5067 \text{ psia}$$

22A4365
Rev. 2

$$M_{\text{cont}} = \frac{[14.7 - 0.2 (0.5067)] (1,138,750)}{53.34 (540)} 144 \frac{\text{in.}^2}{\text{ft}^2}$$

$$M_{\text{cont}} = 83,110 \text{ lbm of air}$$

From the above air masses the post blowdown containment pressure can be calculated.

$$P_{\text{cont}} = \frac{\Sigma M R T}{V_c} + \phi P_{\text{sat}}$$

ΣM = Summation of initial air mass in cont and
D.W. = 102,645 lbm air

R = Gas constant = $53.34 \frac{\text{lbm-ft}}{\text{lb}^\circ\text{R}}$

T = Final temperature = temperature of pool = 170°F

V_c = Containment volume = $1,138,750 \text{ ft}^3$

ϕ = Final relative humidity = 1.0

P_{sat} = Saturation pressure at 170 = 5.990

$$P_{\text{cont}} = \frac{102,645 (53.34) 630}{(1,138,750) 144 \frac{\text{in.}^2}{\text{ft}^2}} + 1.0 (5.990)$$
$$= 27.025 \text{ psia}$$

To evaluate the minimum drywell pressure at this time the following assumptions are made:

- (1) All steam in the drywell is condensed.
- (2) ECCS flow out of vessel is at temperature of 170°F.
- (3) Assume all the air has been purged out of drywell pressure.
- (4) No vacuum breakers.

Using these assumptions the final drywell pressure is equal to the saturation pressure at 170°F.

$$P_{\text{DW}} = P_{\text{sat}_{170}} = 5.990 \text{ psia}$$

Therefore the negative pressure load across the drywell wall is the difference in the final pressures of the containment and drywell.

$$P_{\text{D}} = P_{\text{DW}} - P_{\text{cont}}$$
$$= 5.990 - 27.025$$
$$= -21 \text{ psid}$$

SUMMARY

The above represents a very conservative bounding calculation of the maximum theoretical negative pressure.

The assumptions that noncondensibles return to the drywell via the vacuum relief system and that the steam temperature in the drywell instantaneously drops to the suppression pool temperature are both very conservative. In addition, the real estimate of relative humidity in containment is 50% rather than the 100% assumed.

An evaluation of the probable transient condition for this phase of the LOCA leads to the conclusion that the realistic negative pressure is less than 8 psi.

ATTACHMENT F
WETWELL ASYMMETRIC PRESSURES

INTRODUCTION

The purpose of this attachment is to determine the pressure gradient under the HCU floor during pool swell due to flow restriction at the HCU level.

CALCULATION

During pool swell the following conditions exist in the wetwell.

$$\Delta P_{\text{HCU}} = \text{HCU floor pressure differential} = 11 \text{ psi}$$

$$A_{\text{HCU}} = \text{Open area of HCU floor} = 1500 \text{ ft}^2$$

$$X_A = \text{X-Section area between Pool and HCU Floor} = 400 \text{ ft}^2 \\ \text{(Vertical plane)}$$

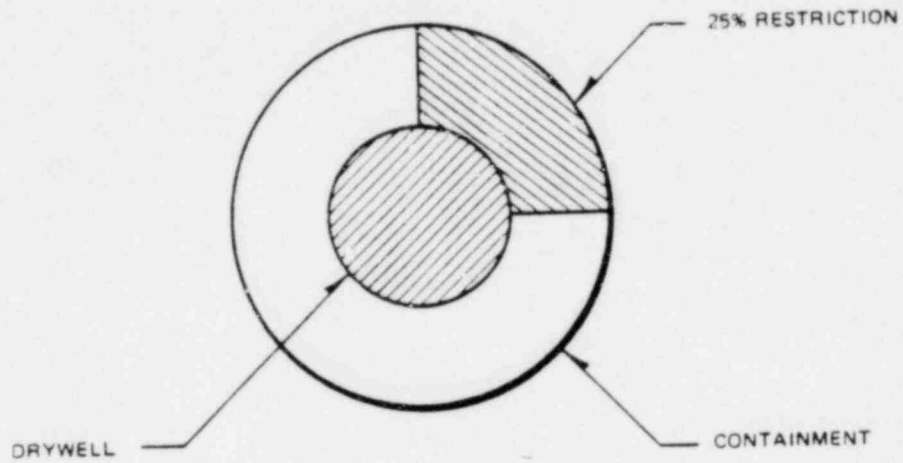
$$k = \text{loss coefficient through floor} = 5$$

$$\rho = \text{density of flow through floor} = 20 \frac{\text{lbm}}{\text{ft}^3}$$

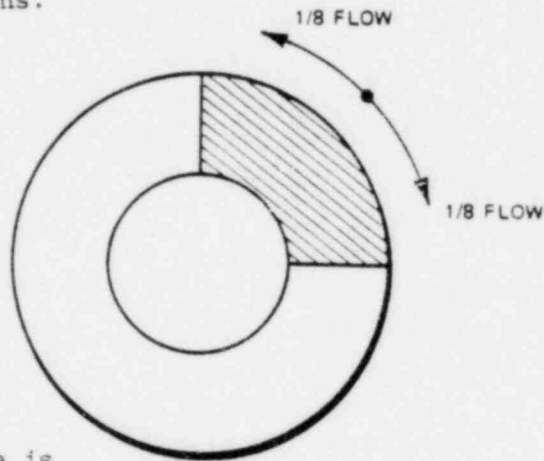
From this information the flow rate through the HCU floor can be calculated.

$$\begin{aligned} M_{\text{HCU}} &= \frac{A}{\sqrt{k}} \sqrt{2\rho\Delta P_{\text{HCU}}} \\ &= \frac{1500}{\sqrt{5}} \sqrt{2(20)(11) 144 \frac{\text{in}^2}{\text{ft}^2} \left(32.2 \frac{\text{lbm-ft}}{\text{lb-ft-sec}^2} \right)} \\ &= 958,968 \frac{\text{lbm}}{\text{sec}} \end{aligned}$$

In order to calculate a differential pressure under the HCU floor, assume a 25% restriction at the HCU level.



Using this 25% restriction then 1/8 of the flow will be horizontally diverted in both directions.



This horizontal flow rate is

$$\dot{V}_H = \frac{\dot{V}_{HCU}}{8}$$
$$= \frac{958,968}{8}$$

$$\dot{M}_H = 119,770 \frac{\text{lbm}}{\text{sec}}$$

Assuming the density is constant and using the above flow rate, the differential pressure under the HCU floor due to this restriction can now be calculated.

$$\Delta P = K \rho \frac{V^2}{2g} \quad \text{but } V^2 = \frac{\dot{M}^2}{\rho^2 A^2} \quad A = X_A$$

$$= \frac{K(\rho) \dot{M}^2}{2(g) \rho^2 (X_A^2)}$$

$$= \frac{1 (20) 119,770^2}{2 (32.2) 20^2 (400^2)} \frac{\text{ft}^2}{144 \text{ in}^2}$$

$$= \underline{0.483 \text{ psi}}$$

ATTACHMENT G
SUBMERGED STRUCTURE LOADS DUE TO LOCA AND SRV ACTUATIONS

TABLE OF CONTENTS

<u>Section</u>	<u>Title</u>	<u>Page</u>
G1.	INTRODUCTION	G-2
G2.	SUBMERGED STRUCTURE LOADS DUE TO LOCA	G-4
	G2.1 Compressive Wave Loading	G-4
	G2.2 LOCA Water Jet Loads	G-4
	G2.3 LOCA Bubble Loads	G-5
	G2.3.1 LOCA Bubble Loads - Sample Problem	G-17
	G2.4 Fall Back Loads	G-23
	G2.5 LOCA Condensation Oscillation Loads	G-24
	G2.5.1 LOCA Condensation Oscillation Loads - Sample Problems	G-25
	G2.6 LOCA Chugging Loads	G-27
	G2.6.1 LOCA Chugging Loads - Sample Problem	G-30
G3.	SUBMERGED STRUCTURE LOADS DUE TO SRV ACTUATIONS	G-33
	G3.1 Quencher Water Jet Load	G-33
	G3.2 Quencher Bubble Load	G-33
	G3.2.1 Quencher Bubble Load - Sample Problem	G-37
G4.	REFERENCES	G-42

G1. INTRODUCTION

In the following two sections, the flow induced loads on structures submerged in the suppression pool due to Loss-of-Coolant (LOCA) and Safety Relief Valve (SRV) actuations are discussed. During LOCA, steam rapidly escapes from the break and creates a compressive wave in the drywell air space. This wave is transmitted from the weir wall water surface to the suppression pool and finally to the submerged structure. This compressible wave loading is negligible (discussed in subsection G2.1). Following this compressive wave, the drywell is rapidly pressurized. The water in the weir annulus and drywell vents is expelled to the suppression pool. A highly localized induced flow field is created in the pool and a dynamic loading is then induced on submerged structures (discussed in subsection G2.2). After the water is expelled from the vent system, the air in the drywell air space, prior to the LOCA event, is forced from the top vents and forms expanding bubbles which create moderate dynamic loads on submerged structures (discussed in the subsection G2.3). These air bubbles cause the pool water surface to rise until they break through the pool water surface. The pool surface slug decelerates and falls back to the original pool level (fall back loads are discussed in subsection G2.4). At this point steam from the break fills the drywell space and is channeled to the pool via the vent system. Steam condensation oscillation starts and the vibratory nature of pool water motion causes an oscillatory load on submerged structures (discussed in subsection G2.5).

This condensation oscillation continues until pressure in the drywell decays. This is followed by a somewhat regular but less persistent vibration called chugging. During this chugging period, a high wave propagation spike is observed which causes an acoustic load on submerged structures (discussed in the subsection G2.6).

During SRV actuations, the dynamic process of the steam blowdown is quite similar to LOCA but the load is mitigated by the X-Quencher device attached at the end of each SRV discharge line. Two types of loads are important. One is due to the water jet formed at the confluence of the X-Quencher arm discharges (discussed in subsection G3.1) and another is due to the four air bubbles formed between the arms of the X-Quencher. These air bubbles are smaller in size than the LOCA air bubbles, reside longer in the pool, and oscillate as they rise to the surface of the pool. The load created by these bubbles are discussed in the subsection G3.2.

The material in Attachment G is organized as follows:

- (1) The specific analytical model is referenced, this is followed by
- (2) A load calculation procedure which is a summary of the engineering process. This is followed by
- (3) A sample problem which demonstrates the use of the procedures.

G2. SUBMERGED STRUCTURE LOADS DUE TO LOCA

G2.1 Compressive Wave Loading

As discussed in Section 6.1.1, the very rapid compression of the drywell air theoretically generates a compressive wave. But as pointed out in Sections 6.1.1 and 6.1.2, there were no loads recorded on the containment wall in PSTF for this phenomena. From this, it can be concluded that compression wave loads on structures in the suppression pool are significantly smaller than loads caused by the water jet, for structures close to drywell. For structures near the containment, neither compressive or jet loads are significant.

G2.2 LOCA Water Jet Load

During the initial phase of the DBA, the Drywell air space is pressurized and the water in the weir annulus vents is expelled to the pool and induces a flow field throughout the suppression pool. This induced flow field is not limited to direct jet contact and creates a dynamic load on structures submerged in the pool.

However, since none of the submerged structures in the Standard Plant are in the direct path of these jets, the dynamic load on these structures is less than the load induced by the LOCA air bubble which forms after the water is expelled. Examination of Reference G1 and G2 test data confirms this observation. Since the air bubble dynamic load is bounding, this load is conservatively used in place of the water jet load (for air bubble load, see paragraph G2.3.).

G2.3 LOCA Bubble Loads

During the initial phase of the DBA, pressurized drywell air is purged into the suppression pool through the submerged vents. After vent clearing, a single bubble is formed around each top vent. It is during the bubble growth period that unsteady fluid motion is created within the suppression pool. During this period all submerged structures below the pool surface will be exposed to transient hydrodynamic loads.

The bases of the flow model and load evaluation for the LOCA bubble-induced submerged structure load definition are derived from the model in Reference G4.3. The following procedure is recommended for calculating the loads on submerged structures.

1. Pool Dimensions and Bubble Data

Specific data that must be obtained are:

R_i : initial bubble radius, assumed to be the same as the vent radius, 1.146 ft.

P_o : Drywell transient pressure obtained from Figure 4.4 (page 4-12), in psia.

ρ_o : air density corresponding to drywell conditions when the drywell pressure is P_o , lb_m/ft^3 .

ρ : pool liquid density, $62.4 \text{ lb}_m/\text{ft}^3$.

P_c : containment air space pressure, assumed to be constant at 14.7 psia.

P_{∞} : initial pool pressure at the top vent centerline submergence, psia.

H: pool depth, 20 ft.

L: pool length, 18.5 ft

D: unit cell pool width (Figure G2.3.6c), 7.97 ft.

y_0 : initial bubble location from bottom of pool, same as the top vent centerline, 12.5 ft.

2. Duration of Loads

Loads on submerged structures due to LOCA air clearing begin when the air bubble forms at the vent exit immediately following air clearing and end when the bubble engulfs the structure, or when breakthrough occurs if the bubble does not engulf the structures.

3. Initial Bubble Location

Initially the bubble center (x_0, y_0, z_0) is assumed to be located on the vent axis at a distance equal to one vent radius from the vent exit.

4. Movement of Bubble Center

The bubble center movement is used only in the calculation of the bubble engulfment time. The effects of bubble movement on the predicted load are conservatively accounted for by a factor of 2 (see step 14).

5. Bubble Dynamics

The bubble dynamics equations given below can be solved for:

$R(t)$: the bubble radius at time t

$\dot{R}(t)$: the bubble growth rate at time t

$\ddot{R}(t)$: the rate of change of bubble growth rate at time t .

Bubble Dynamics Equations:

$$R = \frac{1}{\ddot{R}} \left[\frac{g_c}{\rho} (P_B - P_\infty) - \frac{3}{2} \dot{R}^2 \right] \quad (G2.3-1)$$

$$\dot{P}_B = 3k \left[\frac{1}{4\pi R^3} \frac{P_o \dot{m}_B}{\rho_o} - \frac{P_B \dot{R}}{R} \right] \quad (G2.3-2)$$

$$P_\infty = P_C + \rho(H - y_o) \quad (G2.3-3)$$

where

P_B = bubble pressure at time t , psia

\dot{m}_B = bubble charging rate, lb_m/sec (see eq. A46, Reference G4.3)

k = ratio of specific heats for air, 1.4

Initial Conditions

$$R(0) = R_i = \text{vent radius} = 1.146 \text{ ft}$$

$$\dot{R}(0) = V_i/4 = 13 \text{ ft/sec}$$

where V_i = top vent water jet velocity at vent clearing (from Figure G2.3.1) = 52 ft/sec

$$P_B(0) = P_o \text{ at top vent clearing} = 31.93 \text{ psia (from Figure 4.4)}$$

$$m_B(0) = \frac{4}{3} \pi R_i^3 \rho_o$$

A plot of bubble radius vs. time has been obtained from the bubble dynamics equations and is presented in Figure G2.3.2.

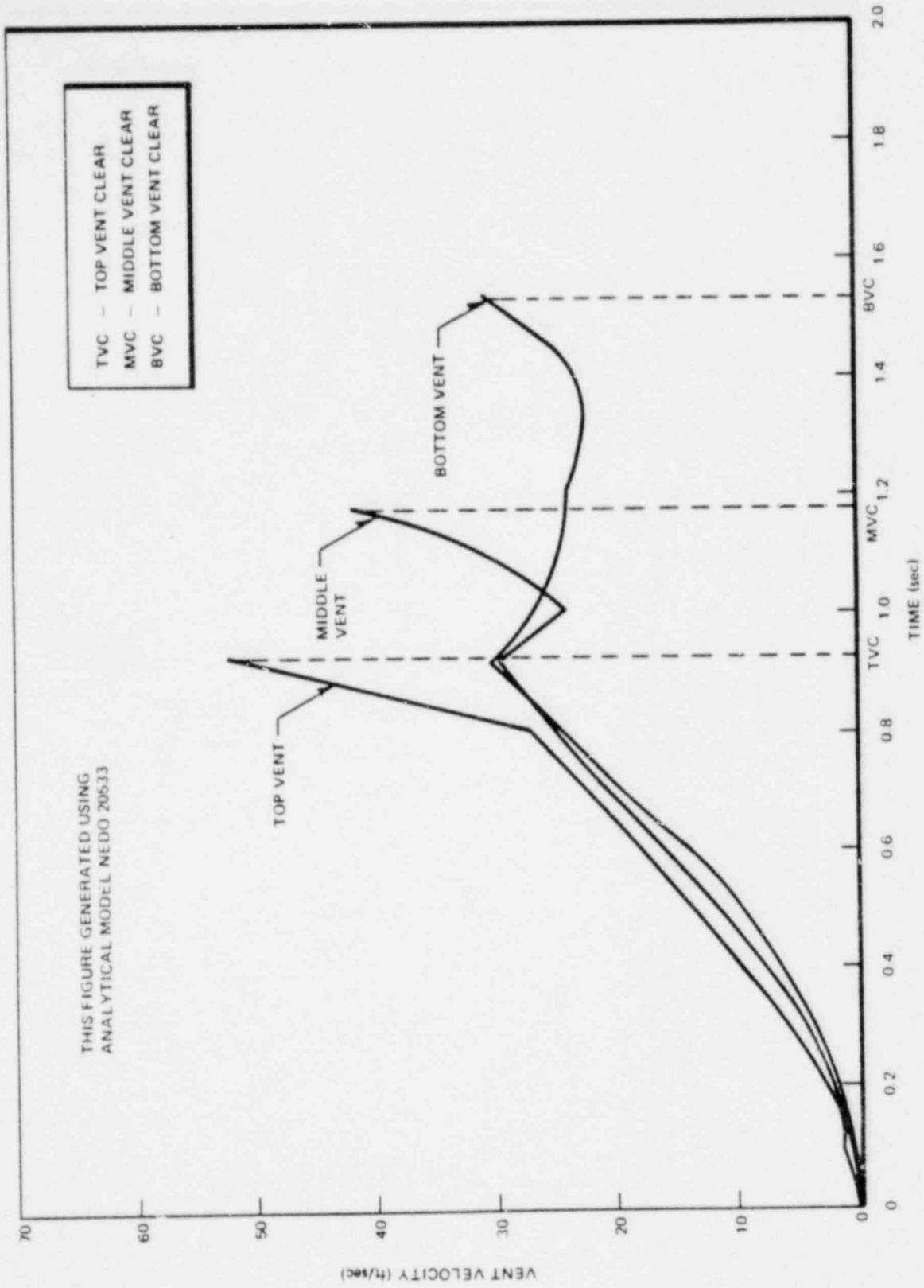


Figure G2.3.1. Mark III Horizontal Vent Water Jet Velocity

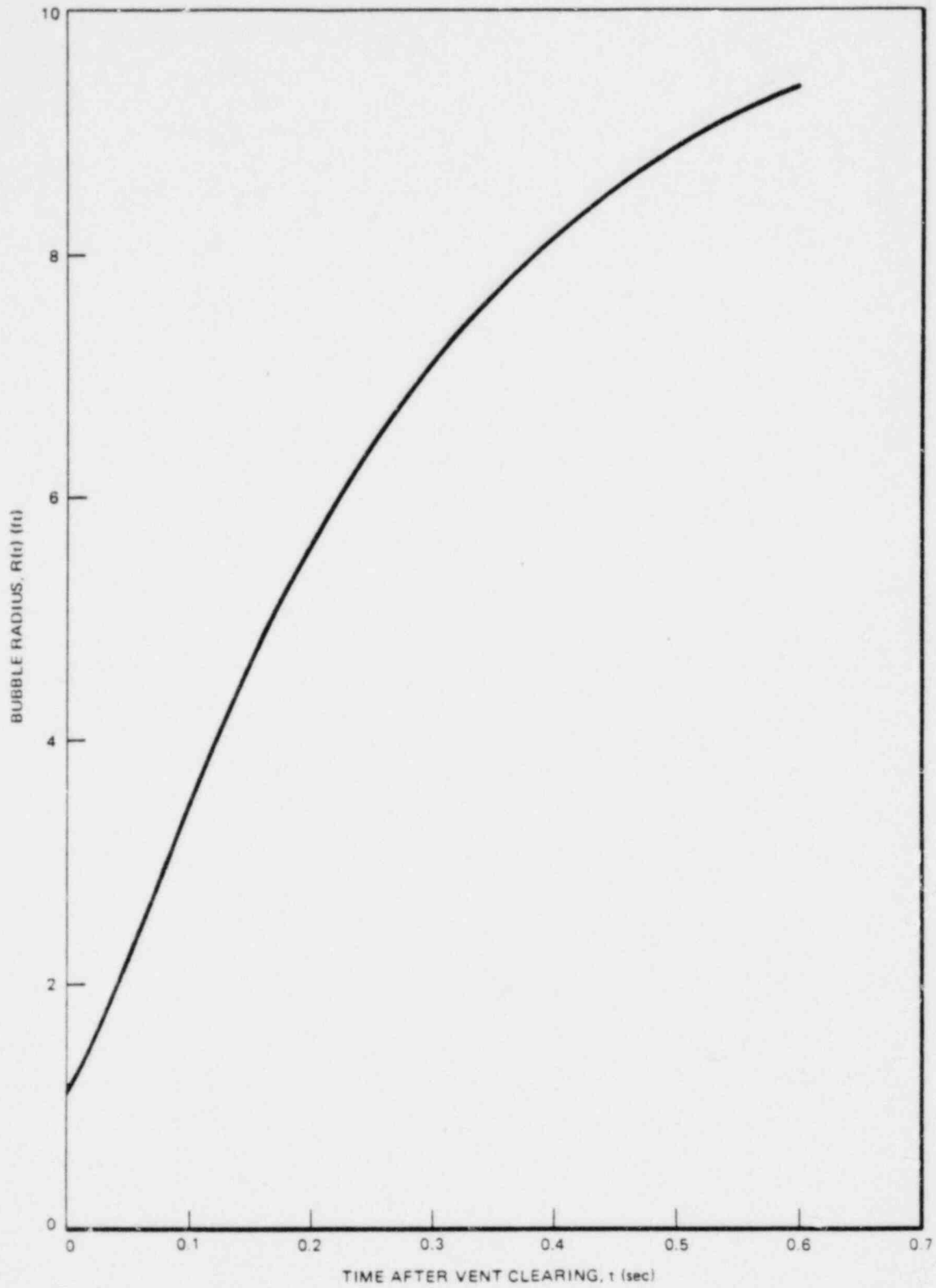


Figure G2.3.2. Bubble Radius, $R(t)$, vs. Time

6. Structure Data

Location of structure, including elevation, distance from the drywell wall, and distance from the containment wall.

Dimensions, shape, and orientation of structure. Long structures should be divided into smaller segments (with each segment approximately 2 ft long) for more precise evaluation.

7. Distance to Structure

Determine the following at time t

D_s : the cross-sectional dimension of structure or structure segment in the direction of the bubble center. (For this calculation, the bubble center is assumed to be displaced horizontally a distance equal to $R(t)$).

8. Check Structure/Bubble Contact

At anytime t using the value of bubble radius, $R(t)$, from Step 5 check if $R(t) \geq \sqrt{[x - R(t)]^2 + (y - y_0)^2 + (z - z_0)^2} - D_s/2$. If true, then loading calculations for the structure or structure segment under consideration end, because it is inside the bubble and the drag forces are zero. If not, proceed with Step 9 until the bubble breaks through the pool surface.

9. Pool Boundary Effects

To account for the effects of pool walls, floor and free surface, use the method of images as described in Section 4.10 of Reference G4.3. First determine r_{ijk} , which is the distance from the center of the structure or structure segment (x, y, z) to the source or sink image at (x_i, y_j, z_k) ,

$$r_{ijk} = \sqrt{(x - x_i)^2 + (y - y_j)^2 + (z - z_k)^2} \quad (G2.3-5)$$

Note that $r_{0,0,0}$ corresponds to the real source. Then evaluate the functions X, Y, Z as given by Equation A67 of Reference G4.3. Using the notations adopted here, these functions may be written as

$$X = K \sum_{k=-N}^N \sum_{j=-N}^N \sum_{i=-N}^N \frac{(-1)^j (x - x_i)}{r_{ijk}^3}$$

$$Y = K \sum_{k=-N}^N \sum_{j=-N}^N \sum_{i=-N}^N \frac{(-1)^j (y - y_j)}{r_{ijk}^3} \quad (G2.3-6)$$

$$Z = K \sum_{k=-N}^N \sum_{j=-N}^N \sum_{i=-N}^N \frac{(-1)^j (z - z_k)}{r_{ijk}^3}$$

where N is the total number of images considered, and K is a factor used for finite bubbles to satisfy the local pressure boundary condition at the real bubble surface, i.e., the pressure at the real bubble surface equals the independently calculated bubble pressure, P_B . The K factor is not a function of the structure's location in the pool. It is a function of bubble radius and the bubble image function. Values of K have been computed for the unit cell shown in Figure G2.3.6c and are provided as a function of time in Table G2.3.1.

10. Number of Images

The results of a sensitivity study show that 11 sets of images will provide adequate convergence. A typical arrangement of image sets in the vertical plane is shown in Figure G2.3.3. The K factors shown in Table G2.3.1 are based on 11 sets of images.

Table G2.3.1

K vs. Time

t (sec)	K						
0.50000E-02	0.51494E 00	0.24000E 00	0.16233E 00	0.48000E 00	0.12227E 00	0.48000E 00	0.12227E 00
0.10000E-01	0.49936E 00	0.24500E 00	0.16070E 00	0.48500E 00	0.12187E 00	0.48500E 00	0.12187E 00
0.15000E-01	0.48184E 00	0.25000E 00	0.15914E 00	0.49000E 00	0.12148E 00	0.49000E 00	0.12148E 00
0.20000E-01	0.46351E 00	0.25500E 00	0.15762E 00	0.49500E 00	0.12110E 00	0.49500E 00	0.12110E 00
0.25000E-01	0.44517E 00	0.26000E 00	0.15617E 00	0.50000E 00	0.12072E 00	0.50000E 00	0.12072E 00
0.30000E-01	0.42730E 00	0.26500E 00	0.15477E 00	0.50500E 00	0.12036E 00	0.50500E 00	0.12036E 00
0.35000E-01	0.41018E 00	0.27000E 00	0.15341E 00	0.51000E 00	0.11999E 00	0.51000E 00	0.11999E 00
0.40000E-01	0.39396E 00	0.27500E 00	0.15211E 00	0.51500E 00	0.11964E 00	0.51500E 00	0.11964E 00
0.45000E-01	0.37869E 00	0.28000E 00	0.15085E 00	0.52000E 00	0.11930E 00	0.52000E 00	0.11930E 00
0.50000E-01	0.36438E 00	0.28500E 00	0.14963E 00	0.52500E 00	0.11896E 00	0.52500E 00	0.11896E 00
0.55000E-01	0.35101E 00	0.29000E 00	0.14846E 00	0.53000E 00	0.11862E 00	0.53000E 00	0.11862E 00
0.60000E-01	0.33851E 00	0.29500E 00	0.14732E 00	0.53500E 00	0.11829E 00	0.53500E 00	0.11829E 00
0.65000E-01	0.32685E 00	0.30000E 00	0.14622E 00	0.54000E 00	0.11797E 00	0.54000E 00	0.11797E 00
0.70000E-01	0.31597E 00	0.30500E 00	0.14516E 00	0.54500E 00	0.11766E 00	0.54500E 00	0.11766E 00
0.75000E-01	0.30581E 00	0.31000E 00	0.14413E 00	0.55000E 00	0.11735E 00	0.55000E 00	0.11735E 00
0.80000E-01	0.29633E 00	0.31500E 00	0.14314E 00	0.55500E 00	0.11704E 00	0.55500E 00	0.11704E 00
0.85000E-01	0.28746E 00	0.32000E 00	0.14217E 00	0.56000E 00	0.11674E 00	0.56000E 00	0.11674E 00
0.90000E-01	0.27917E 00	0.32500E 00	0.14124E 00	0.56500E 00	0.11644E 00	0.56500E 00	0.11644E 00
0.95000E-01	0.27141E 00	0.33000E 00	0.14034E 00	0.57000E 00	0.11615E 00	0.57000E 00	0.11615E 00
0.10000E 00	0.26413E 00	0.33500E 00	0.13946E 00	0.57500E 00	0.11587E 00	0.57500E 00	0.11587E 00
0.10500E 00	0.25731E 00	0.34000E 00	0.13861E 00	0.58000E 00	0.11559E 00	0.58000E 00	0.11559E 00
0.11000E 00	0.25090E 00	0.34500E 00	0.13778E 00	0.58500E 00	0.11531E 00	0.58500E 00	0.11531E 00
0.11500E 00	0.24487E 00	0.35000E 00	0.13698E 00	0.59000E 00	0.11503E 00	0.59000E 00	0.11503E 00
0.12000E 00	0.23920E 00	0.35500E 00	0.13620E 00	0.59500E 00	0.11476E 00	0.59500E 00	0.11476E 00
0.12500E 00	0.23385E 00	0.36000E 00	0.13545E 00				
0.13000E 00	0.22881E 00	0.36500E 00	0.13472E 00				
0.13500E 00	0.22405E 00	0.37000E 00	0.13400E 00				
0.14000E 00	0.21955E 00	0.37500E 00	0.13331E 00				
0.14500E 00	0.21529E 00	0.38000E 00	0.13264E 00				
0.15000E 00	0.21126E 00	0.38500E 00	0.13198E 00				
0.15500E 00	0.20744E 00	0.39000E 00	0.13134E 00				
0.16000E 00	0.20380E 00	0.39500E 00	0.13072E 00				
0.16500E 00	0.20036E 00	0.40000E 00	0.13012E 00				
0.17000E 00	0.19708E 00	0.40500E 00	0.12953E 00				
0.17500E 00	0.19395E 00	0.41000E 00	0.12896E 00				
0.18000E 00	0.19098E 00	0.41500E 00	0.12840E 00				
0.18500E 00	0.18815E 00	0.42000E 00	0.12786E 00				
0.19000E 00	0.18544E 00	0.42500E 00	0.12733E 00				
0.19500E 00	0.18286E 00	0.43000E 00	0.12681E 00				
0.20000E 00	0.18039E 00	0.43500E 00	0.12631E 00				
0.20500E 00	0.17803E 00	0.44000E 00	0.12582E 00				
0.21000E 00	0.17576E 00	0.44500E 00	0.12534E 00				
0.21500E 00	0.17360E 00	0.45000E 00	0.12487E 00				
0.22000E 00	0.17152E 00	0.45500E 00	0.12441E 00				
0.22500E 00	0.16953E 00	0.46000E 00	0.12396E 00				
0.23000E 00	0.16762E 00	0.46500E 00	0.12353E 00				
0.23500E 00	0.16579E 00	0.47000E 00	0.12310E 00				
	0.16403E 00	0.47500E 00	0.12268E 00				

Note: t is time after vent clearing

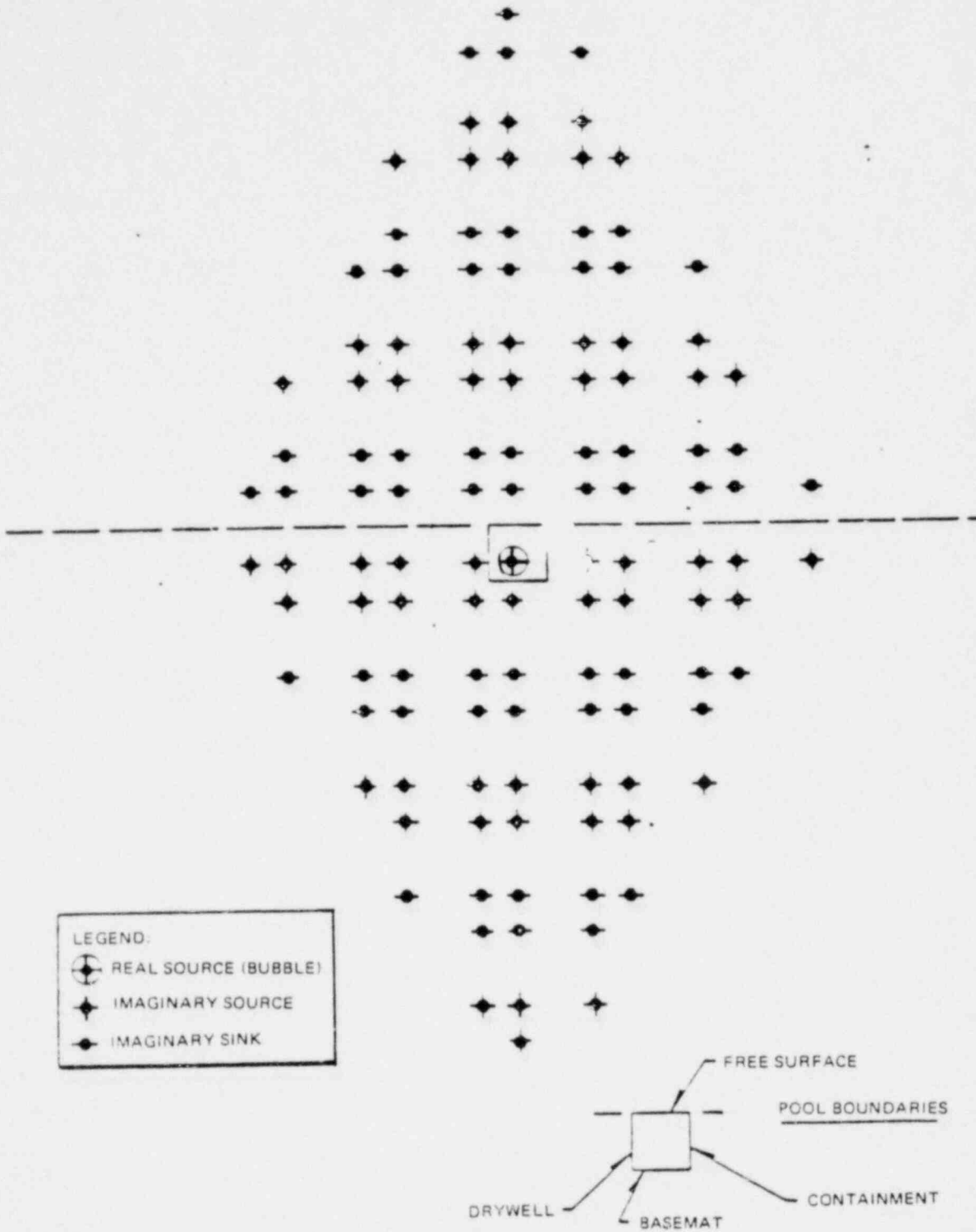


Figure G2.3.3. Arrangement of Images

11. Since the bubbles are symmetrically located in the circumferential direction, and are formed synchronously, the effects of multiple bubbles can be evaluated through image methods applied to a unit cell as shown in Figure G2.3.6c. A single pool segment is therefore modeled by means of a rectangular unit cell of equal size.

12. Direction of The Flow Field

The direction of the flow field at time t is determined by the unit vector, \vec{n} , where

$$\vec{n} = \frac{X \vec{n}_x + Y \vec{n}_y + Z \vec{n}_z}{\sqrt{X^2 + Y^2 + Z^2}} \quad (G2.3-8)$$

13. Acceleration and Velocity

Using the results from Steps 5 and 11, the equivalent uniform acceleration at time t at the structure location in a finite containment is

$$\dot{U}_\infty(t) = \left[R^2(t) \ddot{R}(t) + 2R(t) \dot{R}^2(t) \right] \sqrt{X^2 + Y^2 + Z^2} \quad (G2.3-9)$$

The corresponding velocity $U_\infty(t)$ may be obtained by numerically integrating $\dot{U}(t)$.

$$U_\infty(t) = R^2(t) \dot{R}(t) \sqrt{X^2 + Y^2 + Z^2} \quad (G2.3-10)$$

Characteristic $U_\infty(t)$ and $\dot{U}(t)$ plots

$$\left(\frac{U_\infty(t) K}{\sqrt{X^2 + Y^2 + Z^2}} ; \frac{\dot{U}_\infty(t) K}{\sqrt{X^2 + Y^2 + Z^2}} \right)$$

are presented in Figures G2.3.4 and G2.3.5 respectively.

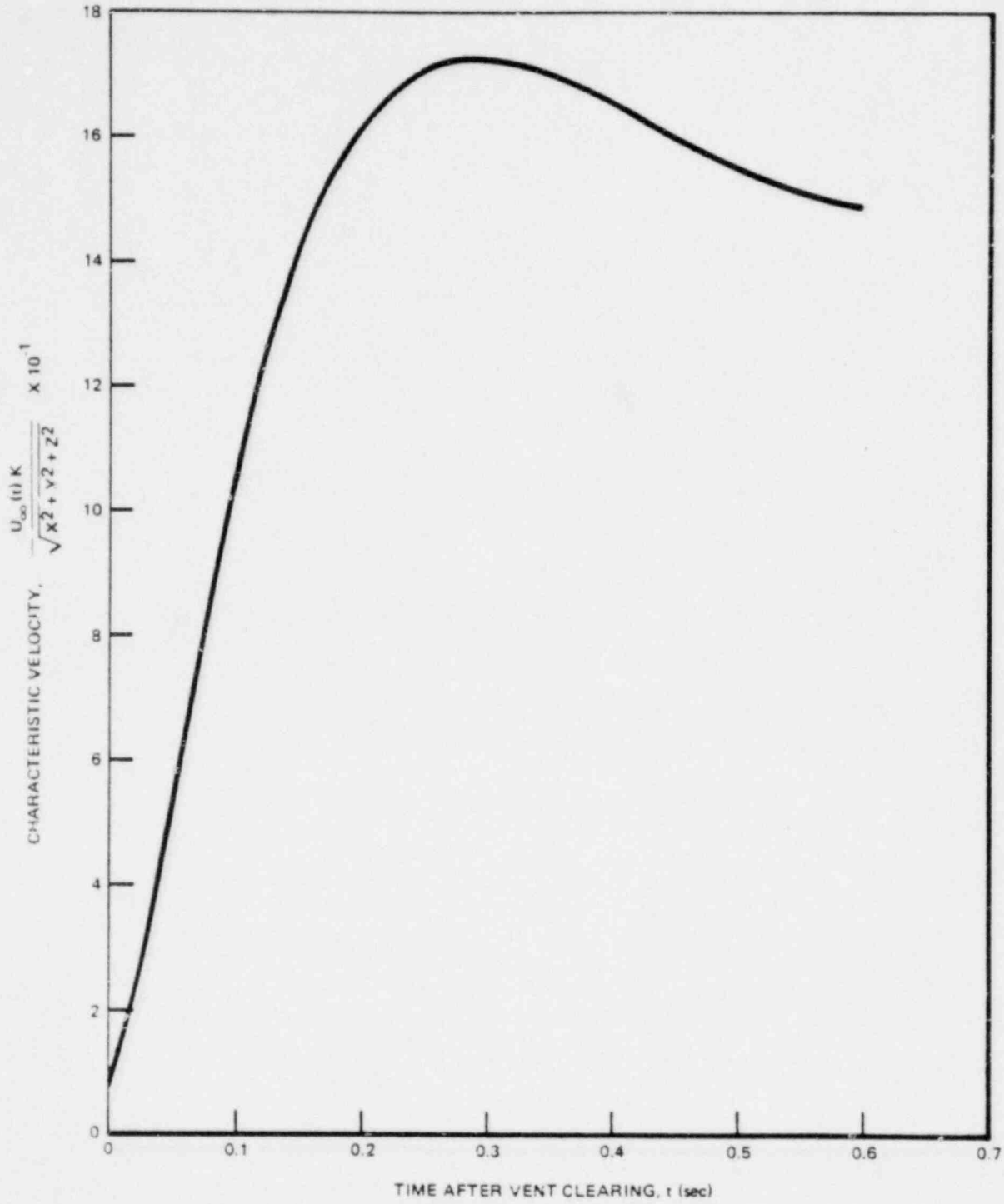


Figure G2.3.4. Characteristic Velocity vs. Time

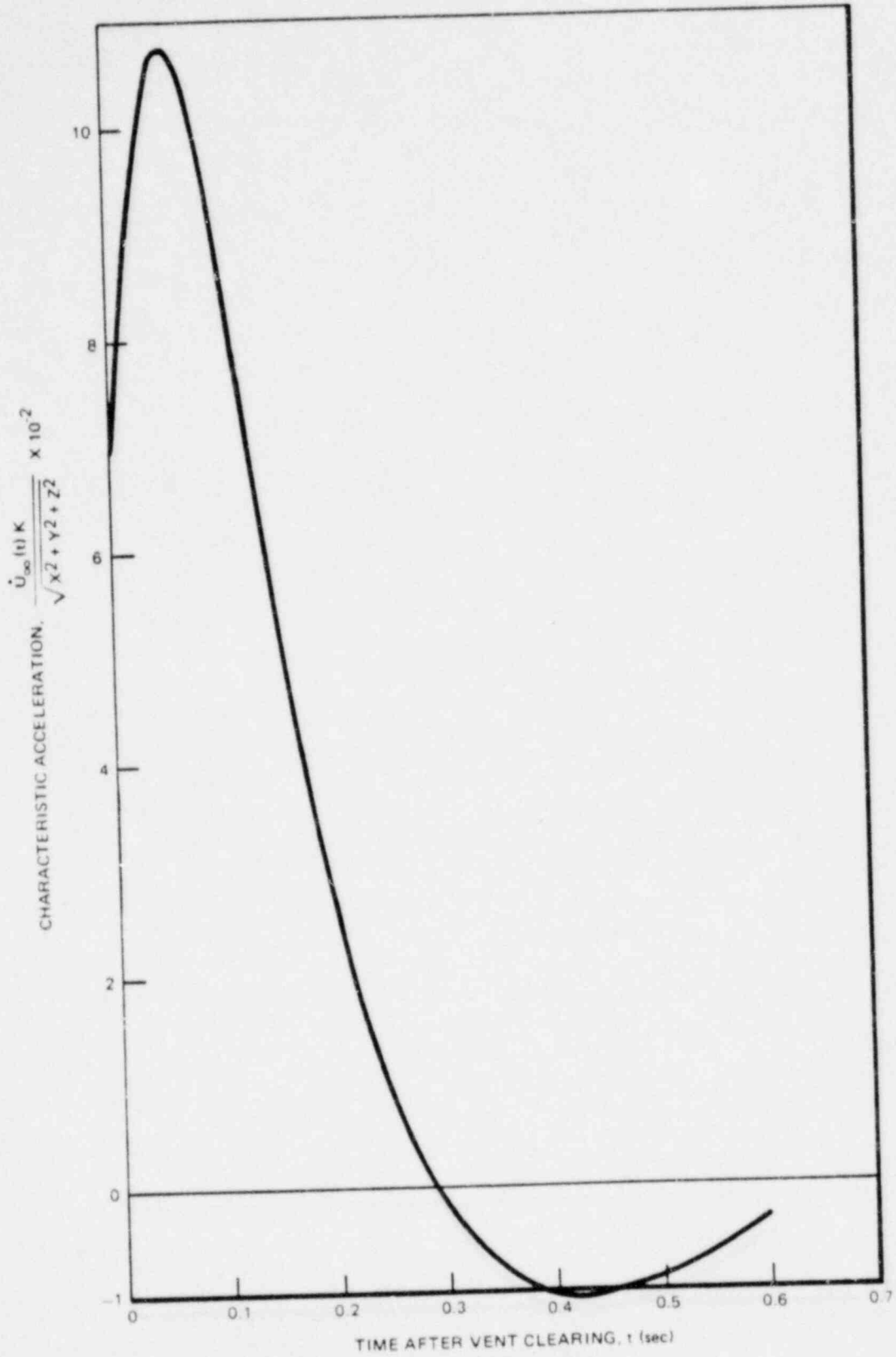


Figure G2.3.5. Characteristic Acceleration vs. Time

14. Drag Forces

The acceleration drag is calculated from

$$F_A(t) = \frac{\dot{U}_{\infty n}(t) V_A \rho}{g_c} \quad (G2.3-11)$$

where $\dot{U}_{\infty n}$ is the acceleration component normal to the structure and V_A is the acceleration drag volume (from Tables G2.3.2 and G2.3.3 for flow normal to the structure).

The standard drag force is calculated from

$$F_S(t) = C_D A_n \frac{\rho U_{\infty n}^2(t)}{2 g_c} \quad (G2.3-12)$$

where C_D is the drag coefficient for flow normal to the structure. A_n is the projected structure area normal to $U_{\infty n}(t)$.

Add F_A and F_S at any time t to get the total load on the structure segment.

The loads predicted by this procedure agree with the Mark III submerged structures test data (Reference G4.1). For additional conservatism, the final load should be multiplied by a factor of 2 to cover the effects of a moving source.

The direction of total drag is normal to the submerged structures.

Table G2.3.2
ACCELERATION DRAG VOLUMES FOR TWO-DIMENSIONAL
STRUCTURAL COMPONENTS
(LENGTH L FOR ALL STRUCTURES)

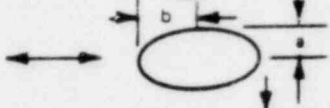
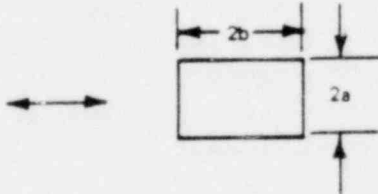
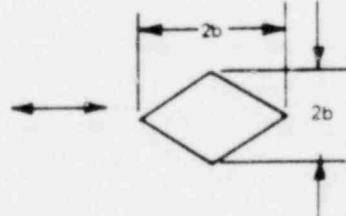
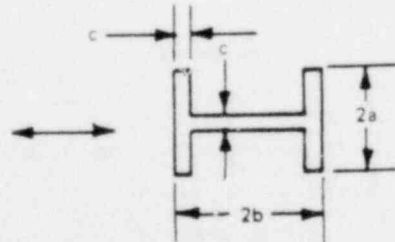
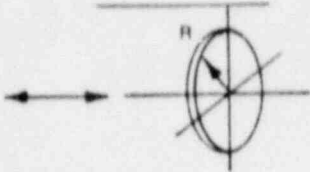
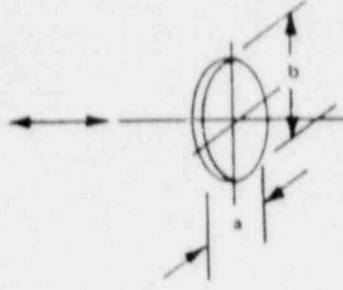
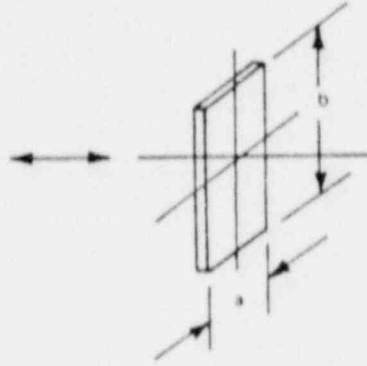
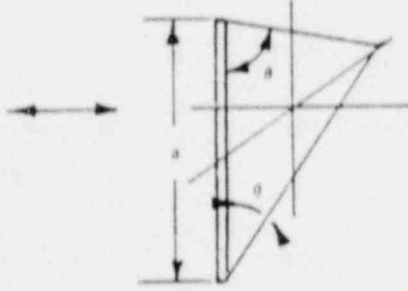
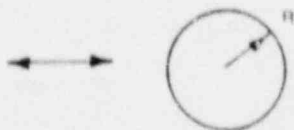
BODY	SECTION THROUGH BODY AND UNIFORM FLOW DIRECTION	HYDRODYNAMIC MASS	ACCELERATION DRAG VOLUME V_A	
CIRCLE		$\rho \pi R^2 L$	$2\pi R^2 L$	
ELLIPSE		$\rho \pi a^2 L$	$\pi a^2 a + bL$	
ELLIPSE		$\rho \pi b^2 L$	$\pi b^2 a + bL$	
PLATE		$\rho \pi a^2 L$	$\pi a^2 L$	
RECTANGLE		$\frac{a}{b}$ ∞	$\rho \pi a^2 L$	$aL(4b + \pi a)$
		10	$1.14 \rho \pi a^2 L$	$aL(4b + 1.14\pi a)$
		5	$1.21 \rho \pi a^2 L$	$aL(4b + 1.21\pi a)$
		2	$1.36 \rho \pi a^2 L$	$aL(4b + 1.36\pi a)$
		1	$1.51 \rho \pi a^2 L$	$aL(4b + 1.51\pi a)$
		1/2	$1.70 \rho \pi a^2 L$	$aL(4b + 1.70\pi a)$
		1/5	$1.98 \rho \pi a^2 L$	$aL(4b + 1.98\pi a)$
DIAMOND		$\frac{a}{b}$	$0.85 \rho \pi a^2 L$	$aL(2b + 0.85\pi a)$
		1	$0.76 \rho \pi a^2 L$	$aL(2b + 0.76\pi a)$
		1/2	$0.67 \rho \pi a^2 L$	$aL(2b + 0.67\pi a)$
		1/5	$0.61 \rho \pi a^2 L$	$aL(2b + 0.61\pi a)$
I BEAM		$\frac{a}{c}=2.6, \frac{b}{c}=3.6$	$2.11 \rho \pi a^2 L$	$[2.11\pi a^2 + 2c(2a + b - c)]L$

Table G2.3.3
ACCELERATION DRAG VOLUMES FOR THREE-DIMENSIONAL STRUCTURES

DESCRIPTION	BODY AND FLOW DIRECTION	HYDRODYNAMIC MASS	ACCELERATION DRAG VOLUME V_A	
CIRCULAR DISK		$\frac{8}{3} \rho R^3$	$\frac{8}{3} R^3$	
ELLIPTICAL DISK		$\frac{b}{a}$		
		∞	$\rho \pi/6 ba^2$	$\pi/6 ba^2$
		3	$0.9 \rho \pi/6 ba^2$	$0.9 \pi/6 ba^2$
		2	$0.826 \rho \pi/6 ba^2$	$0.826 \pi/6 ba^2$
		1.5	$0.748 \rho \pi/6 ba^2$	$0.748 \pi/6 ba^2$
1.0	$0.637 \rho \pi/6 ba^2$	$0.637 \pi/6 ba^2$		
RECTANGULAR PLATE		$\frac{b}{a}$		
		1	$0.478 \rho \pi/4 a^2b$	$0.478 \pi/4 a^2b$
		1.5	$0.680 \rho \pi/4 a^2b$	$0.680 \pi/4 a^2b$
		2	$0.840 \rho \pi/4 a^2b$	$0.840 \pi/4 a^2b$
		2.5	$0.953 \rho \pi/4 a^2b$	$0.953 \pi/4 a^2b$
		3	$\rho \pi/4 a^2b$	$\pi/4 a^2b$
		∞	$\rho \pi/4 a^2b$	$\pi/4 a^2b$
TRIANGULAR PLATE		$\frac{\rho a^3 (\tan \theta)^{3/2}}{\pi}$	$\frac{a^3 (\tan \theta)^{3/2}}{\pi}$	
SPHERE		$\frac{\rho 2}{3} \pi R^3$	$2\pi R^3$	

G2.3.1 LOCA Bubble Load - Sample Problem

As an example the drag force on a cylindrical structure induced by the LOCA bubble from one vent will be calculated, including the boundary effects. Figure G2.3.6 depicts the Mark III Containment and the submerged structure in question.

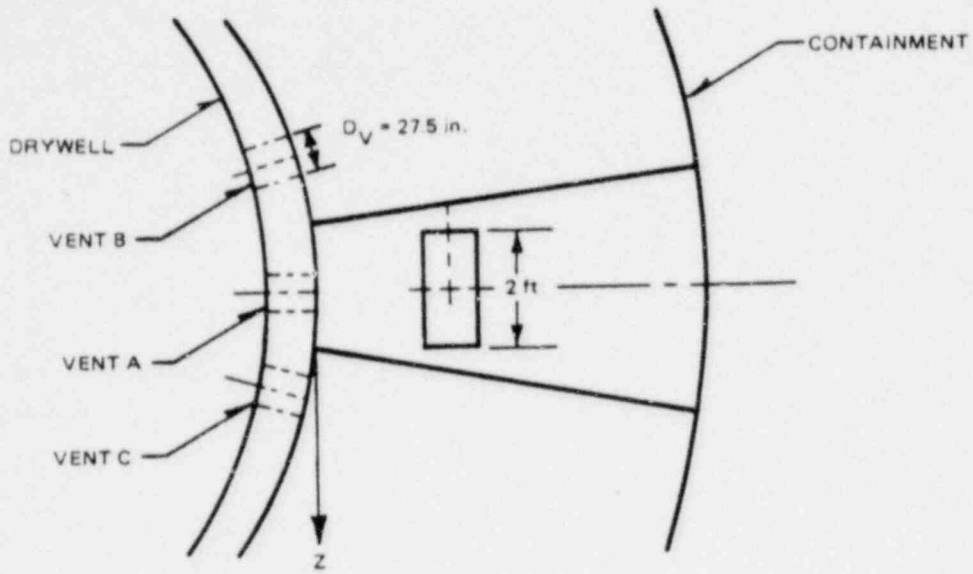
Step 1:

The following data were used in the sample calculation:

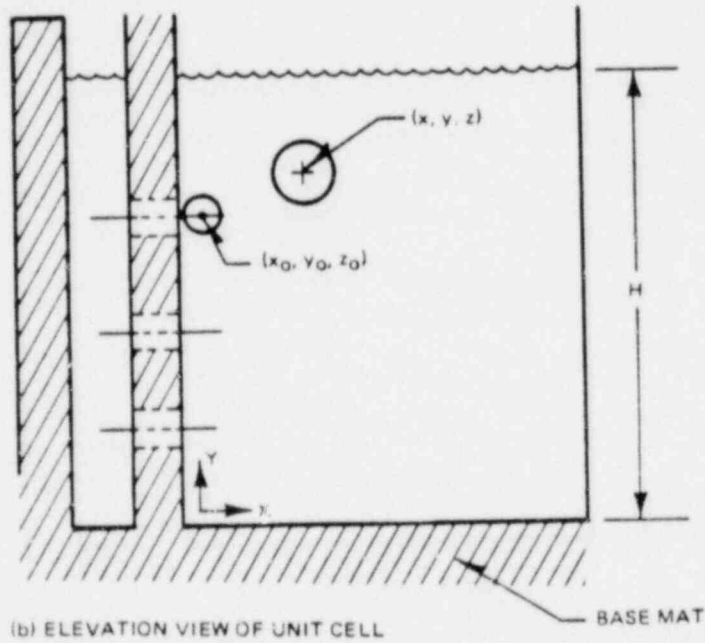
- (a) Initial bubble radius: $R_i = 1.146 \text{ ft}$
- (b) Initial bubble velocity: $v_i = 13 \text{ ft/sec}$
- (c) Initial bubble submergence: $H - y_o = 7.5 \text{ ft}$
- (d) Unit cell dimensions: $H = 20 \text{ ft}$, $L = 18.5 \text{ ft}$, $D = 7.97 \text{ ft}$
- (e) Containment air space pressure: $P_c = 14.7 \text{ psia}$
- (f) Pool liquid density: $\rho = 62.4 \text{ lbm/ft}^3$
- (g) Obtain drywell transient pressure from Figure 4.4 (Page 4-12)
- (h) Initial drywell temperature: 100°F
- (i) Vent friction factor is zero

Step 3

The initial bubble location is $X_o = 1.146 \text{ ft}$, $Y_o = 12.5 \text{ ft}$ and $Z_o = 3.986 \text{ ft}$.



(a) PLAN VIEW OF POOL SEGMENT



(b) ELEVATION VIEW OF UNIT CELL

Figure G2.3.6. Mark III Submerged Structure for Sample Calculation

5.92 ft

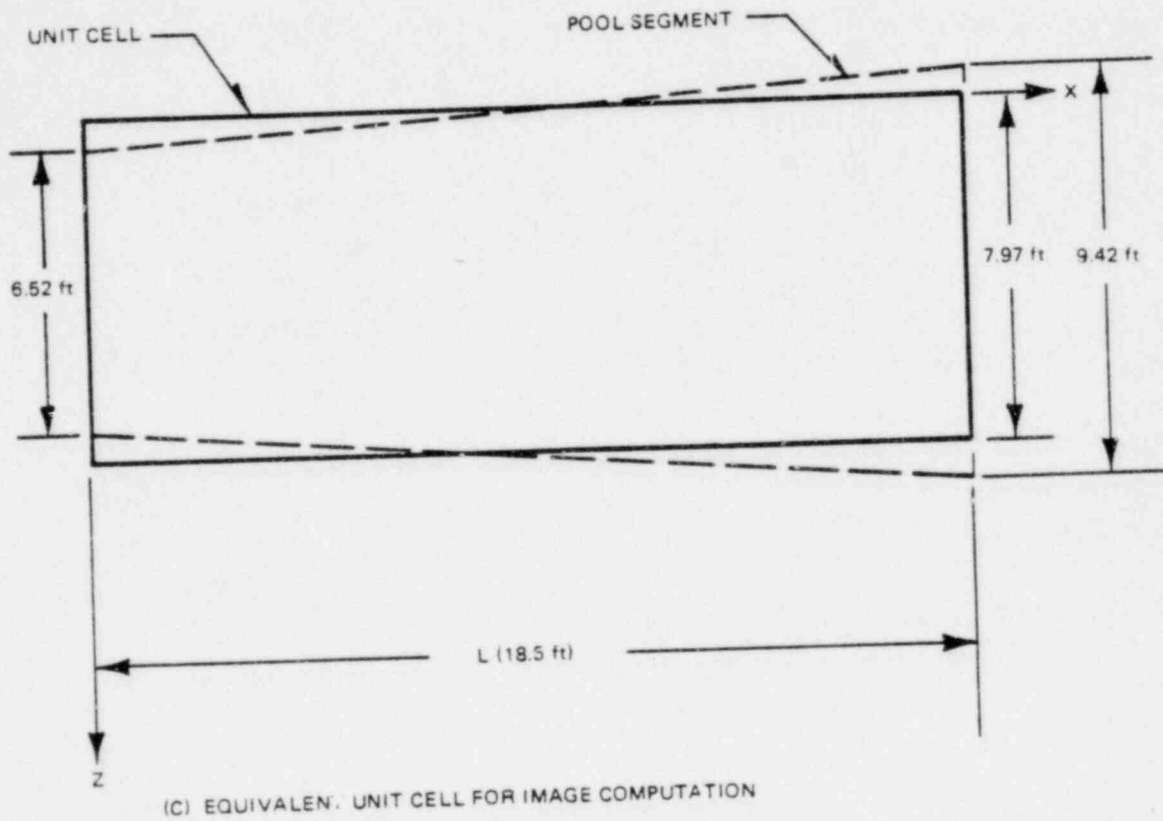


Figure G2.3.6. Mark III Submerged Structure for Sample Calculation
(Continued)

Step 5.

The bubble radius vs. time, $R(t)$, is obtained from Figure G2.3.2.

Step 6.

Structure center location is $x = 4.0$ ft, $y = 15.5$ ft, $z = 3.986$ ft. The structure length = 2.0 ft, diameter = 1.0 ft, projected area = 2.0 ft², acceleration drag volume = 3.14 ft³ (Table G2.3.2), and the standard drag coefficient = 1.2. The structure is assumed parallel to the Z axis (see Figure G2.3.6), and is considered as one segment.

Steps 7, 8.

$$\frac{D_s}{2} = 0.5 \text{ ft}; \quad R \geq \sqrt{[4 - R]^2 + (15.5 - 12.5)^2 + (0)^2} - \frac{1.0}{2}$$

and $R(t)$ for bubble engulfment = 2.4 ft. From Figure G2.3.2 for $R(t) = 2.4$ ft, $t = 55$ ms = bubble engulfment time.

Steps 9, 10, 11.

To account for the effects of pool walls, floor and free surface the method of images was used. A single pool segment is modeled by means of a rectangular unit cell of equal area (see Figure G2.3.6c). Equation (G2.3-6) is calculated for the function $\sqrt{X^2 + Y^2 + Z^2}$ which is the correction factor that accounts for boundaries and is applied to the velocity (Equation G2.3-10) and acceleration (Equation G2.3-9).

K values are obtained from Table G2.3.1 as a function of time. Values for X, Y, Z are computed and the results, for this sample problem, are $X/K = 0.07576$, $Y/K = 0.13101$, and $Z/K = 0.00$.

Steps 12, 13.

At time t obtain the characteristic velocity and characteristic acceleration from Figures G2.3.4 and G2.3.5 respectively. Combine these results with those from steps 9, 10, 11 as follows:

$$U_{\infty}(t)_x = \left(\frac{U_{\infty}(t) K}{\sqrt{X^2 + Y^2 + Z^2}} \right) \left(\frac{X}{K} \right)$$

$$U_{\infty}(t)_y = \left(\frac{U_{\infty}(t) K}{\sqrt{X^2 + Y^2 + Z^2}} \right) \left(\frac{Y}{K} \right)$$

$$U_{\infty}(t)_z = \left(\frac{U_{\infty}(t) K}{\sqrt{X^2 + Y^2 + Z^2}} \right) \left(\frac{Z}{K} \right)$$

$$\dot{U}_{\infty}(t)_x = \left(\frac{\dot{U}_{\infty}(t) K}{\sqrt{X^2 + Y^2 + Z^2}} \right) \left(\frac{X}{K} \right)$$

$$\dot{U}_{\infty}(t)_y = \left(\frac{\dot{U}_{\infty}(t) K}{\sqrt{X^2 + Y^2 + Z^2}} \right) \left(\frac{Y}{K} \right)$$

$$\dot{U}_{\infty}(t)_z = \left(\frac{\dot{U}_{\infty}(t) K}{\sqrt{X^2 + Y^2 + Z^2}} \right) \left(\frac{Z}{K} \right)$$

Results of these calculations, for this sample problem, are presented in Table G2.3.4.

Step 14.

The acceleration and standard drags are added together to give the total drag. The total x, y, and z components of drag, and the total resultant drag, calculated for this sample problem, are shown in Table G2.3.5. These results should be multiplied by a factor of 2 as previously stated.

Table G2.3.4

FLOW FIELD AT SUBMERGED STRUCTURE CENTER FOR SAMPLE PROBLEM

<u>t(sec)</u>	<u>Acceleration (ft/sec²)</u>			<u>Velocity (ft/sec)</u>		
	<u>x</u>	<u>y</u>	<u>z</u>	<u>x</u>	<u>y</u>	<u>z</u>
0.000	53.1	91.9	0.0	0.7	1.2	0.0
0.005	57.2	98.9	0.0	0.9	1.6	0.0
0.010	61.4	106.3	0.0	1.2	2.1	0.0
0.015	65.5	113.3	0.0	1.6	2.7	0.0
0.020	69.2	119.7	0.0	1.9	3.3	0.0
0.025	72.5	125.4	0.0	2.2	3.9	0.0
0.030	75.3	130.2	0.0	2.6	4.5	0.0
0.035	77.5	134.1	0.0	3.0	5.2	0.0
0.040	79.3	137.1	0.0	3.4	5.9	0.0
0.045	80.5	139.2	0.0	3.8	6.6	0.0
0.050	81.2	140.5	0.0	4.2	7.3	0.0
0.055	81.5	140.9	0.0	4.6	8.0	0.0

Table G2.3.5
TOTAL FORCES ON SUBMERGED STRUCTURE FOR SAMPLE PROBLEM

<u>t(sec)</u>	<u>x-Force(lbf)</u>	<u>y-Force(lbf)</u>	<u>z-Force(lbf)</u>	<u>Resultant Force(lbf)</u>
0.000	325.6	563.1	0.0	650.5
0.005	352.3	609.2	0.0	703.7
0.010	381.2	659.2	0.0	761.5
0.015	410.1	709.3	0.0	819.3
0.020	438.1	757.7	0.0	875.2
0.025	464.8	803.9	0.0	928.6
0.030	490.0	847.4	0.0	978.9
0.035	513.7	888.4	0.0	1026.2
0.040	535.9	926.9	0.0	1070.7
0.045	556.8	962.8	0.0	1112.2
0.050	576.2	996.5	0.0	1151.1
0.055	594.4	1027.9	0.0	1187.4

Note: Multiply these results by a factor of 2 to obtain the final answers.

G2.4 FALL BACK LOADS

There is no pressure increase in the suppression pool boundary during pool fall back as discussed in Section 4.1.6. Structures within the containment suppression pool that are above the bottom vent elevation will experience drag loads as the water level subsides to its initial level. For design purposes, it is assumed that these structures will experience drag forces associated with water flowing at 35 ft/sec; this is the terminal velocity for a 20 ft free fall and is a conservative, bounding number. Free fall height is limited by the HCU Floor. The Load computation procedure is the same as for calculating standard drag load in Step 14 of subsection G2.3 and will not be repeated here.

G2.5 LOCA CONDENSATION OSCILLATIONS LOADS

Steam condensation begins after the vent is cleared of water and the drywell air has been carried over into the wetwell. This condensation oscillation phase induces bulk water motion and therefore creates drag loads on structures submerged in the pool.

The basis of the flow model for condensation oscillation load definition is derived from the work in Reference G4.4. The following procedure is recommended for calculating the loads on submerged structures:

1. Note the dimension of the containment (L and H) as shown in Figure G2.3.6.
2. Note the location of the submerged structure (x, y, z).
3. Note the locations of the top vent exits (x_{oi} , y_{oi} , z_{oi}).
4. Determine $1/\bar{r}_{eff_i}^2$ for each vent. The parameter \bar{r}_{eff}^2 is defined in Appendix A of Reference G4.4 to account for the effects of pool boundaries and free surface by the method of images. Exclude those vents for which $1/\bar{r}_{eff}^2$ is small compared to the corresponding value for the vent nearest to the structure.
5. Calculate the acceleration field from

$$\dot{U}_{\infty} = \frac{\dot{S}}{L^2} \sum_{i=1}^N \frac{1}{\bar{r}_{eff_i}^2} \quad (G2.5-1)$$

where

$\dot{S} = 188 \text{ ft}^3/\text{sec}^2$ is source strength determined from Mark III $1/\sqrt{3}$ scale test data and N is the total number of vents considered.

6. Calculate the acceleration drag force from

$$F_A = \frac{\rho \dot{U}_\infty V_A}{g_c} \quad (Q2.5-2)$$

7. The forcing function may be approximated by a sine wave with an amplitude equal to F_A and a frequency range of 2 to 3.5 Hz.
8. The direction of the resultant force is approximately along the line joining the structure and its nearest vent.

G2.5.1 LOCA Condensation Oscillations Loads - Sample Problem

Step 1.

The submerged structure to be analyzed is that depicted in Figure G2.3.6. For simplicity, only three vents are considered here. The dimensions of the containment are:

$$L = 18.5 \text{ ft}$$

$$H = 20 \text{ ft}$$

Step 2.

The location of the submerged structure is

$$x = 4.0 \text{ ft}$$

$$y = 15.5 \text{ ft}$$

$$z = 0 \text{ ft}$$

Step 3.

The location of vents are:

<u>Vent</u>	<u>A</u>	<u>B</u>	<u>C</u>
X _{oi}	0	0	0
Y _{oi}	12.5	12.5	12.5
Z _{oi}	0	6.52	-6.52

Step 4.

$1/\bar{r}_{eff_i}^2$ for vents A, B and C are computed as before.

<u>Vent</u>	<u>A</u>	<u>B</u>	<u>C</u>
$\frac{1}{\bar{r}_{eff_i}^2}$	31	13	13

therefore

$$\sum \frac{1}{\bar{r}_{eff_i}^2} = 31 + 13 + 13 = 57$$

Step 5.

The acceleration field is (Equation G2.5-1)

$$\dot{U}_{\infty} = \frac{\dot{s}}{L^2} \sum \frac{1}{\bar{r}_{eff_i}^2} = \frac{188 \text{ (ft)}^3}{\text{sec}^2} \frac{1}{(18.5 \text{ ft})^2} \times (57) = 31.3 \text{ ft/sec}^2$$

Step 6.

The acceleration drag (Equation G2.5-2) per unit projected area is

$$F_A = 0.73 \text{ psi}$$

Steps 7, 8.

The direction of this force is along the line joining vent A centerline and the structure centerline. The forcing function is approximated by a sine wave with an amplitude equal to F_A and a frequency range of 2 to 3.5 Hz.

G2.6 LOCA CHUGGING LOADS

Chugging occurs after drywell air has been purged, and the vent mass flux falls below a critical value. Chugging then induces acoustic pressure loads on structures submerged in the pool.

The basis of the flow model for chugging load definition is derived from the work in Reference G4.4.

The loads on submerged structures due to chugging are calculated from the procedure described below.

1. Locate the bubble center at 2.0 ft above the top vent centerline.
2. Determine location of structure (x, y, z) relative to bubble center (see Figure G2.6.1).
3. Calculate distance r from chugging center to structure

$$r = \sqrt{x^2 + y^2 + z^2}$$

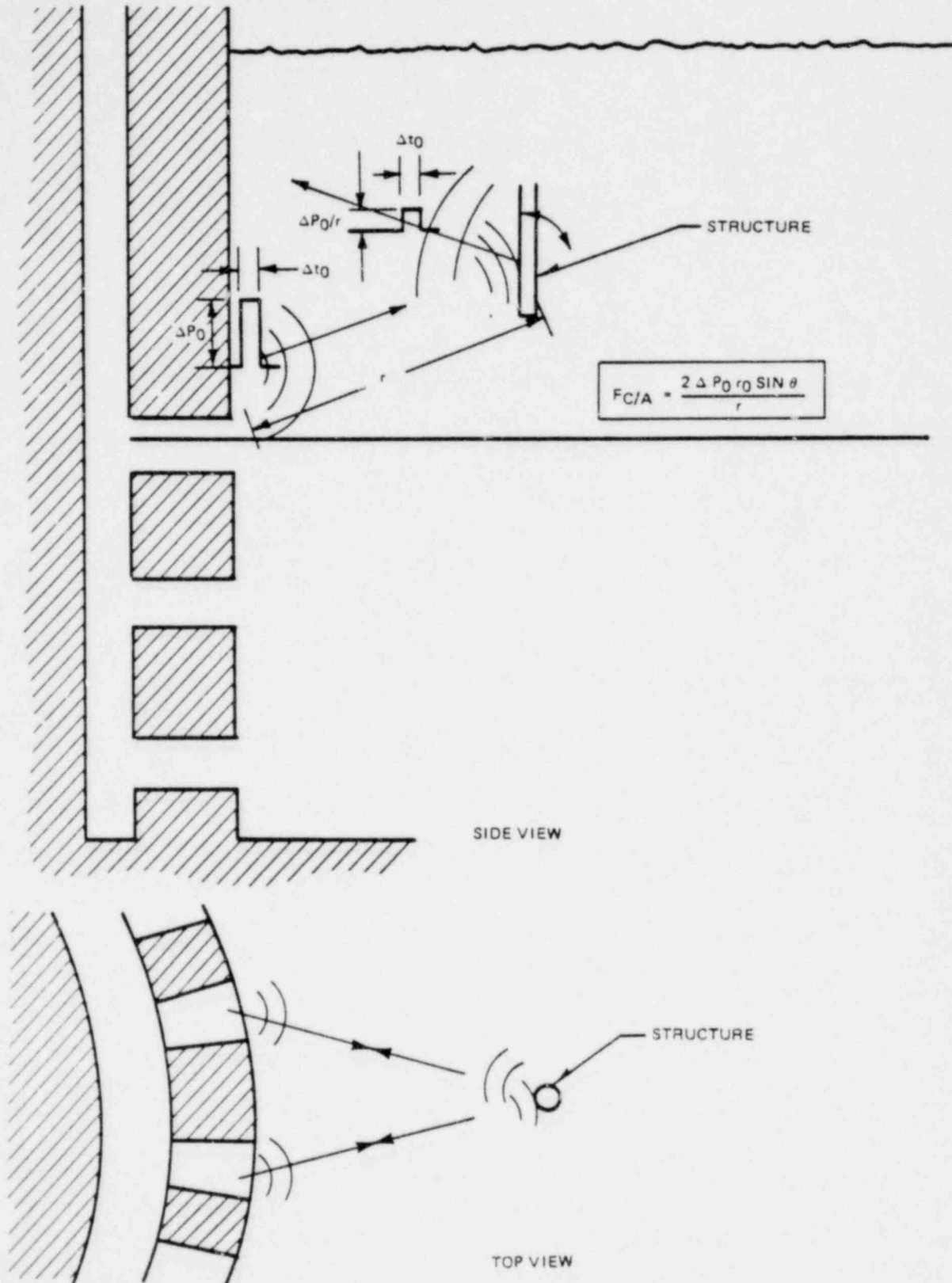


Figure G2.6.1. Mark III Horizontal Vent Chugging

4. Evaluate angle (θ) between structure axis and \vec{r} from

$$\cos \theta = \cos \alpha_s \cos \alpha_b + \cos \beta_s \cos \beta_b + \cos \gamma_s \cos \gamma_b$$

where $(\cos \alpha_s, \cos \beta_s, \cos \gamma_s)$ are the direction cosines of the structure axis, while $(\cos \alpha_b, \cos \beta_b, \cos \gamma_b)$ are the direction cosines of the vector \vec{r} from the hubble center of the structure.

5. Calculate chugging load from

$$F_C = \frac{A}{r} 2 (\Delta P_o r_o) \sin \theta = \frac{A}{r} 2(2.53) \sin \theta$$

where A is the projected area of the structure normal to its own axis, $\Delta P_o r_o = 2.53$ psi-ft as the pulse strength.

6. Include the effect of another vent by repeating Steps 1 through 5. The pulse width is 0.002 seconds. Include those vents for which the signal arrives at the submerged structure within 0.002 second of each other. Use 4000 ft/sec for the acoustic velocity in water.
7. Add the two forces linearly.
8. Obtain time history as follows:

load duration is 2 msec

period between individual chugs is 1 to 5 seconds

9. For long structures, break the structure into separate sections and calculate the load on each section as above.

G2.6.1 LOCA Chugging Loads - Sample Problem

Step 1.

The submerged structure to be analyzed is depicted in Figure G2.3.6.

Step 2.

Bubble location is X = 0 ft
 Y = 12.5 + 2.0 = 14.5 ft
 Z = 0 ft

Structure location is X = 4.0 ft
 Y = 15.5 ft
 Z = 0. ft

Step 3.

Distance r is calculated as

$$r = \sqrt{(4-0)^2 + (15.5 - 14.5)^2} = 4.12 \text{ ft for Vent A}$$

$$r = \sqrt{4^2 + 1^2 + 6.52^2} = 7.71 \text{ ft for Vent B or C}$$

Time for signal to arrive at submerged structure:

$$t = 4.12/4000 = 0.001 \text{ second, Vent A}$$

$$t = 7.71/4000 = 0.002 \text{ second, Vents B or C.}$$

Note that vents located further than B or C will have a signal that travels to the structure in more than 0.002 second.

Step 4.

The angle θ between the structure axis and the centerline of the bubble for the Vents A, B and C (see Figure G2.3.6) are:

<u>Vent</u>	<u>A</u>	<u>B</u>	<u>C</u>
θ	90°	22.3°	32.3°

Step 5.

The chugging load from each vent is calculated from

$$\frac{F_c}{A} = \frac{2.53 \sin \theta}{r}$$

thus for each vent

<u>Vent</u>	<u>A</u>	<u>B</u>	<u>C</u>
$\frac{F_c}{A}$	1.23	0.35	0.35

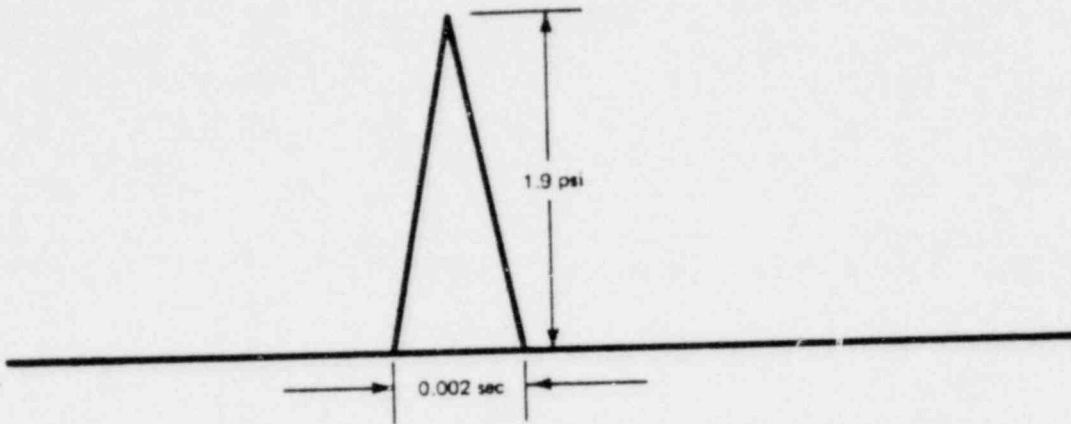
Step 7.

Add the three forces linearly, to obtain the total force per unit area

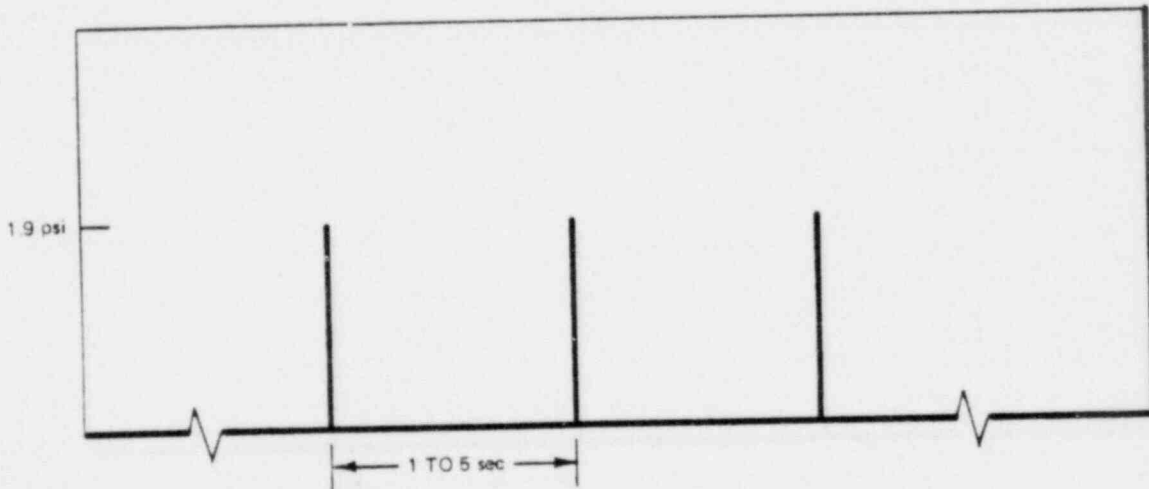
$$\frac{F_c}{A} = 1.9 \text{ psi}$$

Step 8.

The load duration is 2 msec, at 1.9 psi



The period between chugs is 1 to 5 sec. Hence the time history is



G3. SUBMERGED STRUCTURE LOADS DUE TO SRV ACTUATIONS

G3.1 Quencher Water Jet Load

Following the actuation of a safety relief valve (SRV), water is rapidly discharged through the X-Quencher device attached at the end of the SRV line. A highly localized water jet is formed around the X-Quencher arms. The load induced outside a sphere circumscribed around the quencher arms by the Quencher water jet is small. There are no submerged structures located within the sphere mentioned above in the standard Mark III arrangement. The induced load for submerged structures located outside a sphere circumscribed by the quencher arm is negligible and is ignored.

G3.2 Quencher Bubble Load

The analytical model for quencher air bubble loads on submerged structures is presented in Reference G4.3 and G4.5. The following procedure is recommended to apply the analytical model for calculating loads on submerged structures due to quencher air bubbles.

1. Determine the location, dimensions, shape and orientation of the submerged structure. For more precise evaluation long structures should be divided into smaller segments with each segment being approximately 2 ft long.
2. Determine the initial location of the four bubbles. Each bubble will be assumed to form at the intersection of hole pattern centerlines from adjacent arms (see Figure G3.1). If the presence of pool boundaries or other structures prevent bubble formation at the location thus determined, assume the bubble is located along the bisector between adjacent arms and is tangent to the boundaries or structures.

3. Obtain values of the following parameters from Table A4.4 and the specific plant documents:

P_{\max} : maximum bubble pressure, psia

P_{\min} : minimum bubble pressure, psia

T_{pool} : initial pool temperature, °R

H_q : quencher arm submergence, ft

V_i : initial air volume in the safety relief valve discharge line (SRVDL), ft³

P_i : initial air pressure in SRVDL, psia

T_i : initial air temperature in SRVDL, °R

P_c : containment air space pressure, psia

k : specific heat ratio of air

ρ : water density at T_{pool} , lb_m/ft³

4. Assume that the maximum volume of each bubble occurs when the pressure is at its minimum and the air in the bubble attains the surrounding pool water temperature and calculate the maximum bubble radius from

$$V_{\max} = \frac{V_i}{4} \frac{T_{\text{pool}}}{T_i} \frac{P_i}{P_{\min}}, \text{ ft}^3 \quad (\text{G3.2-1})$$

and

$$R_{\max} = \left(\frac{3}{4\pi} v_{\max} \right)^{1/3}, \text{ ft} \quad (\text{G3.2-2})$$

5. To account for the vertical motion of the bubbles, the bubble rise equation given below must be solved simultaneously with the bubble dynamics equations for $R(t)$, $\dot{R}(t)$, $\ddot{R}(t)$ and $Z_b(t)$, where

$R(t)$ = bubble radius at time t

$\dot{R}(t)$ = bubble growth rate at time t

$\ddot{R}(t)$ = rate of change of the bubble growth rate at time t

$Z_b(t)$ = submergence of bubble center at time t

Bubble Dynamics Equations

$$\ddot{R}(t) = \frac{1}{R} \left[\frac{g_c}{\rho} (P_B - P_\infty) - \frac{3}{2} \dot{R}^2 \right] \quad (\text{G3.2-3})$$

$$\dot{P}_B = -3 k P_B \dot{R}/R \quad (\text{G3.2-4})$$

$$P_\infty = P_C + \rho Z_b \quad (\text{G3.2-5})$$

Bubble Rise Equation

$$\ddot{Z}_b = \frac{\frac{1}{2} \pi \rho C_D R^2 \dot{Z}_b |\dot{Z}_b| - \frac{4}{3} \pi \rho g R^3 + m_B g}{m_B + \frac{2}{3} \pi \rho R^3} \quad (\text{G3.2-6})$$

$$m_B = \frac{1}{4} \frac{P_i V_i}{R_{air} T_i} = \text{bubble air mass} \quad (G3.2-7)$$

R_{air} = gas constant of air

Initial Conditions:

$$R(0) = R_{max}$$

$$\dot{R}(0) = 0$$

$$z_b(0) = H$$

$$\dot{z}_b(0) = 0$$

$$P_B(0) = P_{min}$$

6. Determine the location of images of the four source bubbles to account for the effects of pool walls, floor and free surface. Then calculate the parameters X, Y, and Z, which are defined by Equation (A67) of Reference G4.3
7. For multiple quenchers use Equation (A79) of Reference G4.3 to evaluate the parameters X, Y and Z. Note the Heaviside step functions $H(t-t_2)$ and $H(s_2-t)$ are introduced to account for phasing relations among the quenchers of interest.
8. Using the results from Steps 5 through 7 calculate the equivalent uniform acceleration, $\ddot{U}_\infty(t)$, at time t at the structure location from

$$U_\infty(t) = \left[R^2(t) \ddot{R}(t) + 2R(t) \dot{R}^2(t) \right] \sqrt{X^2 + Y^2 + Z^2} \quad (G3.2-8)$$

The corresponding velocity, $U_{\infty}(t)$, may be obtained by numerically integrating $\dot{U}(t)$. As a first approximation, $U_{\infty}(t)$ can also be evaluated from

$$U_{\infty}(t) = R^2(t) \dot{R}(t) \sqrt{X^2 + Y^2 + Z^2} \quad (G3.2-9)$$

9. The acceleration drag is calculated from

$$F_A(t) = \frac{\dot{U}_{\infty n}(t) V_A \rho}{g_c} \quad (G3.2-10)$$

where $\dot{U}_{\infty n}$ is the acceleration component normal to the structure and V_A is the acceleration drag volume for flow normal to the structure.

The standard drag force is calculated from

$$F_S(t) = C_D A_n \frac{\rho U_{\infty n}^2(t)}{2 g_c} \quad (G3.2-11)$$

where C_D is the drag coefficient for flow normal to the structure. A_n is the projected structure area normal to $U_{\infty n}(t)$. Add F_A and F_S at any time to t to get the total force on the structure or structure segment. The direction of the total force is normal to the submerged structure.

G3.2.1 Quencher Bubble Load - Sample Problem

Steps 1, 2, 3.

The following geometrical and bubble data were used in the sample calculation of the loads from one quencher to the structure shown in Figure G3.1.

(a) Maximum Bubble Pressure: $P_{max} = 39.3$ psia

(b) Minimum Bubble Pressure: $P_{min.} = 10.1$ psia

- (c) Initial Pool Temperature: $T_{pool} = 560^{\circ}R$
- (d) Quencher Arm Submergence: $Hg = 13.9 \text{ ft}$
- (e) Initial Air Volume in the Relief Valve Discharge Line (SRVDL)
 $V_i = 56.13 \text{ ft}^3$
- (f) Initial Air Temperature in SRVDL: $T_i = 560^{\circ}R$
- (g) Containment Air Space Pressure: $P_c = 14.7 \text{ psia}$
- (h) Initial Air Pressure in SRVDL: $P_a = 14.7 \text{ psia}$
- (i) Figure G3.1 shows the geometrical locations of the bubbles and the structure for which quencher bubble load will be calculated. The coordinate system is also shown in Figure G3.1.

Steps 4, 5.

The air leaving the quencher forms four independent and identical spherical bubbles which oscillate in phase while rising. The Bubble Dynamics equations (G3.2-3), (G3.2-4) and (G3.2-5) and Bubble Rise Equation (G3.2-6) were solved and shown below.

Time (sec)	Bubble Submergence (ft)	Bubble Radius (ft)	Bubble Radial Growth Rate (ft/sec)	Bubble Radial Acceleration (ft/sec ²)
0.	13.900	1.695	0	-467.021
0.050	13.822	1.691	-0.249	692.474
0.100	13.611	1.695	0.359	-441.970
0.150	13.314	1.692	-0.814	398.944
0.200	12.972	1.694	0.851	-282.412
0.250	12.608	1.694	-0.962	-175.039
.
.
.

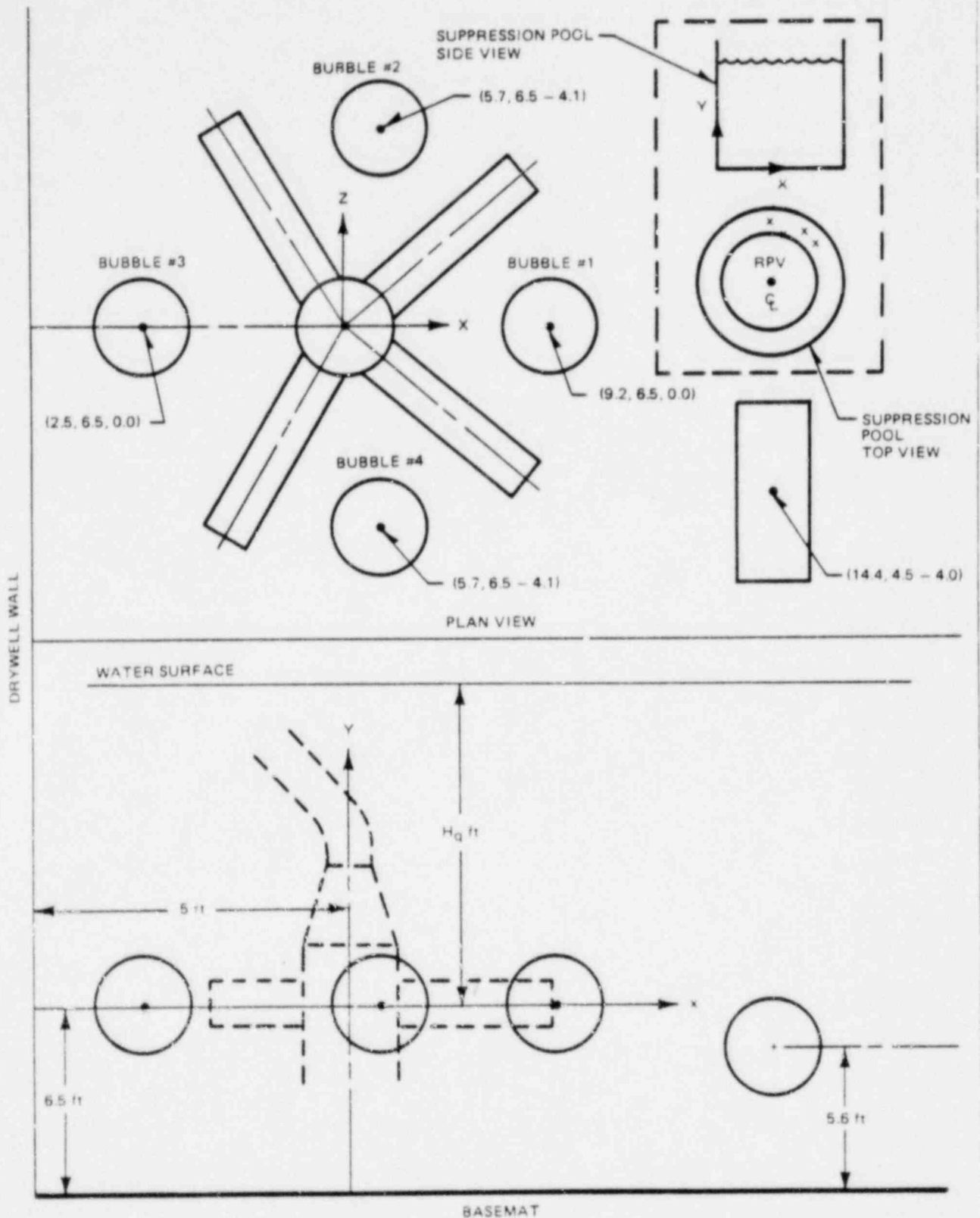


Figure G3.1. Four-Bubble Model for Quencher Air Discharge

Steps 6, 7.

To account for the effects of pool walls, floor and fill surface, the method of images given in (A62) of Reference G4.3 was used. For simplicity, the correction factor K of (A84) of Reference G4.3 is assumed to be one. The resulting parameters of X, Y and Z are shown as below.

<u>t</u>	<u>X</u>	<u>Y</u>	<u>Z</u>
0.	0.0364	0.0170	-0.0311
0.05	0.0361	0.0163	-0.0310
0.10	0.0356	0.0146	-0.0305
0.15	0.0346	0.0134	-0.0298
0.20	0.0334	0.0097	-0.0289
0.25	0.0320	0.0072	-0.0279
.	.	.	.
.	.	.	.
.	.	.	.

Step 8.

Using Equations G3.2-8 and G3.2-9, U_{∞} and \dot{U}_{∞} are calculated as follows:

<u>t</u>	<u>U_{∞}</u>	<u>\dot{U}_{∞}</u>
0.	0.	-68.162
0.05	-0.0339	94.264
0.10	0.0483	-59.420
0.15	-0.1064	52.240
0.20	0.1077	-35.642
0.25	-0.1172	-21.182
.	.	.
.	.	.
.	.	.

Step 9.

The normal acceleration and velocity components to the submerged structure are calculated and their associate acceleration and standard drag are also computed and shown as below.

<u>t</u>	<u>U_{∞n}</u>	<u>U_{∞m}</u>	<u>Standard Drag</u> (x 10 ⁻⁸ psi)	<u>Acceleration Drag</u> (x 10 ⁻² psi)
0.	0.	-53.780	0.	-22.74
0.05	-0.0282	78.522	-0.642	33.20
0.10	0.0396	-48.724	1.266	-20.60
0.15	-0.0865	42.471	-6.042	17.96
0.20	-0.0849	-28.086	5.821	-11.88
0.25	-0.0906	-16.374	-6.68	-6.92
.
.
.

The direction of the force is normal to the submerged structure and is given as

$$\frac{X \vec{n}_X + Y \vec{n}_Y}{\sqrt{X^2 + Y^2 + Z^2}}$$

(Refer to Steps 6, 7.)

G4. REFERENCES

1. Mark III Confirmatory Test Program - Full Scale Condensation and Stratification Phenomena - Test Series 5707, NEDE-21853-P, August, 1978 (Proprietary Report).
2. T. H. Chuang, Mark III One-Third Areas Scale Submerged Structure Tests, NEDE-21606P, October, 1977.
3. F. J. Moody, Analytical Model for Estimating Drag Forces on Rigid Submerged Structures Caused by LOCA and Safety Relief Valve Ramshead Air Discharges, NEDE-21471; revised by L. C. Chow and L. E. Lasher, September, 1977.
4. L. E. Lasher, Analytical Model for Estimating Drag Forces on Rigid Submerged Structures Caused by Steam Condensation and Chugging, NEDO-25153, July, 1979.
5. T. H. Chuang, L. C. Chow, and L. E. Lasher, Analytical Model for Estimating Drag Forces on Rigid Submerged Structures Caused by LOCA and Safety Relief Valve Ramshead Air Discharges, NEDO-21471, supplement 1; June, 1978.

ATTACHMENT H

SUBJECT: WEIR WALL LOADS DURING DRYWELL DEPRESSURIZATION

METHOD

The calculations of the velocity of the water in the vent system during the negative drywell containment differential pressure are conservatively calculated using the network shown in Figure H-1. The explanation of this network is given in Table H-1. The particular values used to determine the velocity as well as the unknowns are given in Table H-2. Neglecting inertial terms the equation for each loop is obtained by using the formula,

$$\Sigma \Delta P = \frac{\rho}{2g_c} \left[\Sigma K \left(\frac{Q}{A} \right)^2 \right]$$

The equations for the three paths are

$$21.0 = -3.25 + \frac{62.4}{2(32.2)(144)} \left[0.5 \left(\frac{am}{4.12} \right)^2 + (6.35a^2 + 1.5a - 0.75) \left(\frac{m}{12.0} \right)^2 + \left(\frac{m}{12.0} \right)^2 \right] + 5.71$$

$$21.0 = -3.20 + \frac{62.4}{2(32.2)(144)} \left[0.5 \left(\frac{bm}{4.12} \right)^2 + \left(6.35 \left(\frac{b}{1-a} \right)^2 + 1.5 \left(\frac{b}{1-a} \right) - 0.75 \right) \left(\frac{(1-a)m}{12} \right)^2 + (1.55a - a^2) \left(\frac{m}{12.0} \right)^2 + \left(\frac{m}{12.0} \right)^2 \right] + 5.71 + 1.95$$

$$21.0 = -7.15 + \frac{62.4}{2(32.2)(144)} \left[0.5 \left(\frac{(1-a-b)m}{4.12} \right)^2 + 7.10 \left(\frac{(1-a-b)m}{12.0} \right)^2 + \left(1.55 \left(\frac{b}{1-a} \right) - \left(\frac{b}{1-a} \right)^2 \right) \left(\frac{(1-a)m}{12.0} \right)^2 + (1.55a - a^2) \left(\frac{m}{12.0} \right)^2 + \left(\frac{m}{12.0} \right)^2 \right] + 5.71 + 1.95 + 1.95$$

These three equations are solved simultaneously for the quantities a, b and m. The velocity in the vents can be calculated using the equation

$$V_{\text{top}} = \frac{am}{4.12}$$

$$V_{\text{mi}} = \frac{bm}{4.12}$$

$$V_{\text{bot}} = \frac{(1-a-b)m}{4.12}$$

The impingement force on the weir wall (behind the individual vents) can be calculated using the equation for momentum loss;

$$F = \frac{\rho V^2 A}{gc}$$

Results:

$$V_{\text{top}} = 37.91 \approx 40 \frac{\text{ft}}{\text{sec}}$$

$$V_{\text{mid}} = 32.09 \approx 35 \frac{\text{ft}}{\text{sec}}$$

$$V_{\text{bot}} = 26.65 \approx 30 \frac{\text{ft}}{\text{sec}}$$

$$F_{\text{top}} = 12800 \text{ lbf}$$

$$F_{\text{mid}} = 9800 \text{ lbf}$$

$$F_{\text{bot}} = 7200 \text{ lbf}$$

Table H-1

- 1 Pressure due to top vent submergence
- 2 Pressure due to mid vent submergence
- 3 Pressure due to bottom vent submergence
- 4 Loss at entrance
- 5 Friction loss
- 6 Loss at Tee junction
- 7 Loss at entrance
- 8 Friction loss
- 9 Loss at Tee junction
- 10 Loss at entrance
- 11 Friction loss
- 12 Loss at Tee junction
- 13 Pressure loss due to elevation difference between bottom and mid vents
- 14 Friction loss
- 15 Loss in Tee junction
- 16 Pressure loss due to elevation difference between mid and top vents
- 17 Friction loss
- 18 Loss in Tee junction
- 19 Pressure loss due to elevation difference between top vent and top of wier wall
- 20 Friction loss
- 21 Loss at Exit

Table H-2

	ΔP	A	Q	K
1	-3.25	-	aM	-
2	-5.20	-	bM	-
3	-7.15	-	(1-a-b)M	-
4	-	4.12	aM	0.5
5	-	-	aM	0.0
6	-	12.00	M	$6.35a^2 + 1.5a - 0.75$
7	-	4.12	bM	0.5
8	-	-	bM	0.0
9	-	12.00	(1-a)M	$6.35 \left(\frac{b}{1-a}\right)^2 + 1.5 \left(\frac{b}{1-a}\right) - 0.75$
10	-	4.12	(1-a-b)M	0.5
11	-	-	(1-a-b)M	0.0
12	-	12.00	(1-a-b)M	7.10
13	1.95	-	(1-a-b)M	-
14	-	-	(1-a-b)M	0.0
15	-	12.00	(1-a)M	$1.55 \left(\frac{b}{1-a}\right) - \left(\frac{b}{1-a}\right)^2$
16	1.95	-	(1-a)M	-
17	-	-	(1-a)M	0.0
18	-	12.00	M	$1.55a - a^2$
19	5.70556	-	M	-
20	-	-	M	0.0
21	-	12.00	M	1.0

ΔP - Pressure Drop due to static head

A - Flow Area

Q - Volume Flow Rate

K - Loss Coefficient (from Idel Chik)

$$\Delta P = K \frac{\rho V^2}{2gc} = \frac{\rho}{2gc} \left(\sum K \left(\frac{Q}{A} \right)^2 \right)$$

a - % of volume flow rate through top vent

b - % of volume flow rate through middle vent

M - Total volume flow rate through the entire vent system

- SURFACE AREA - WIER ANN. = 480 ft²
- NUMBER OF VENTS = 120
- SURFACE AREA PER 3 VENTS = 12 ft²
- DIAMETER OF VENTS = 27.5"
- AREA OF VENT CROSS SECTION = 4.12 ft²
- WIER WALL HEIGHT = 26'1"
- HWL HEIGHT = 20'5"
- ℄ TOP VENT HEIGHT = 12'11"
- ℄ MID VENT HEIGHT = 8'5"
- ℄ BOTTOM VENT HEIGHT = 3'11"
- $P_C - P_{DW}$ = 21 psi

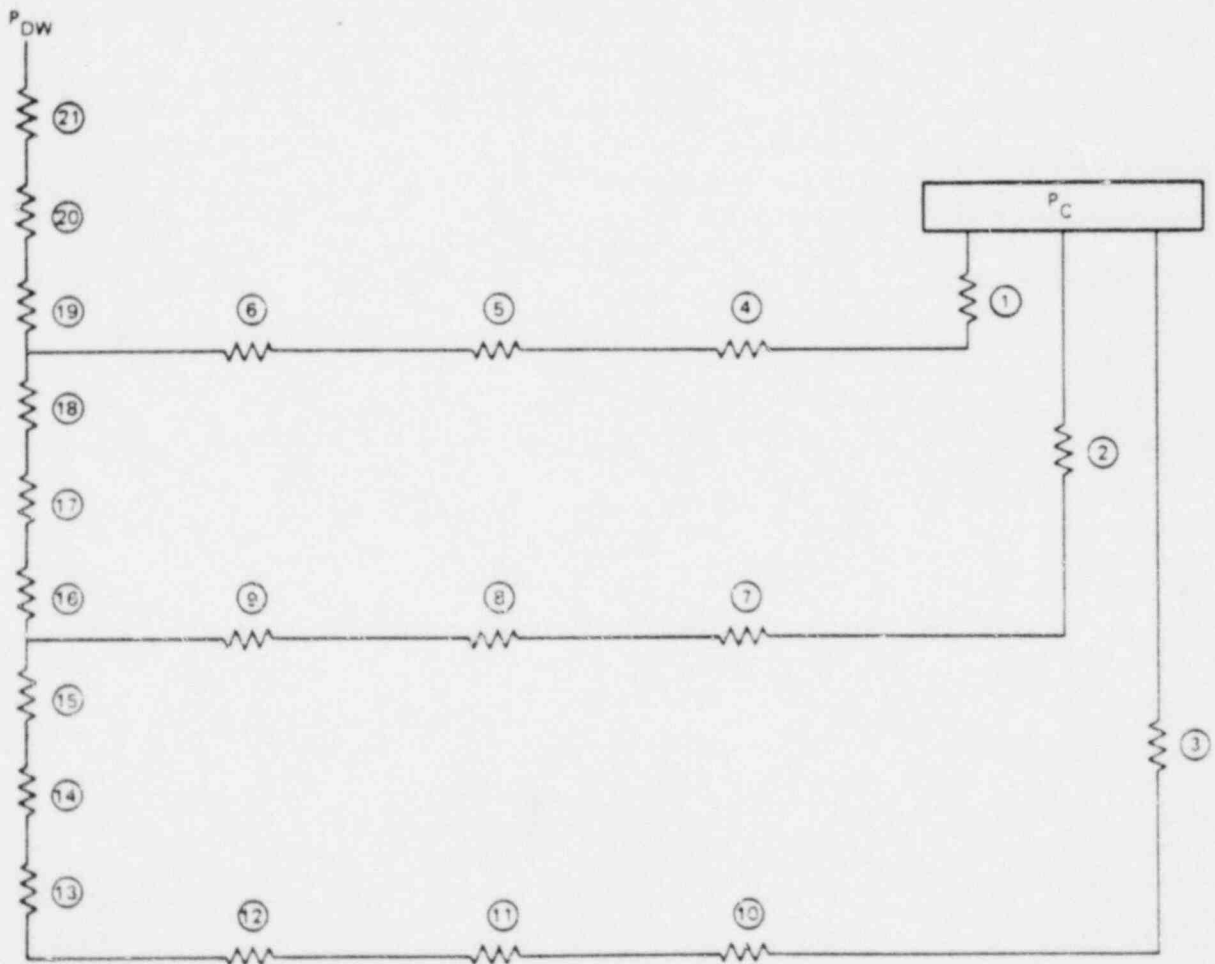
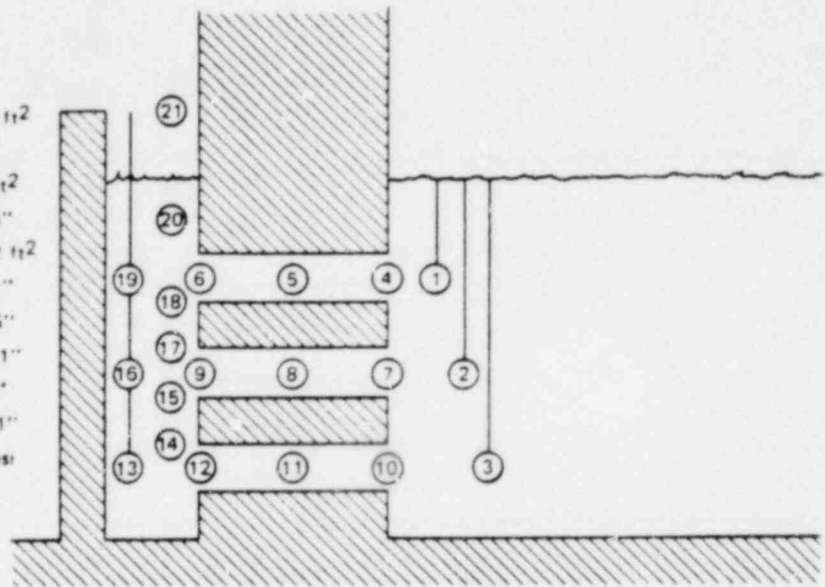


Figure H-1. Mark III Vent System Network

ATTACHMENT I
POOL SWELL VELOCITY

Early in the Mark III program it became necessary to establish an upper bound pool swell velocity. This was accomplished by conservatively assuming that during the pool swell transient the top two rows of vents are open with air only flowing in each (air test data shows that breakthrough occurs just as the second vent opens - See NEDO-20550 Ref. 7). The pool surface velocity was then calculated using a simple volumetric flow rate calculation.

The following is a summary of the calculations:

Using the 238 reference design, the total venting area between the drywell and containment is 481 ft^2 , thus the area for two rows of vents is 320 ft^2 . Assuming that during the majority of the pool swell transient the drywell pressure is typically 35 psia and the pressure of the air in the submerged bubble is typically 18 psia (atmosphere pressure plus 3 psi hydrostatic pressure) then the pressure ratio across the vent system is 0.52.

Under these circumstances, classical compressible flow theory for flow in ducts with friction will give an inlet Mach number of 0.35 for a duct with a total loss coefficient of 3.5 (this is the Mark III value used in SAR calculations) with drywell stagnation conditions of 35 psia and 300°F (adiabatically compressed from 135°F initial conditions), this gives an air mass flux of 54 (lb/sec)/ft^2 or a total flow rate of 17,300 lbm/sec. Assuming that the temperature of the air in the bubble is equal to the pool temperature and using a pool surface area of 5900 ft^2 gives a pool surface velocity of 34 ft/sec. For design purposes, this was rounded off to 40 ft/sec to cover such uncertainties as bubble temperature and pressure.

22A4365
Rev. 3

J-1 through J-52

ATTACHMENT J
SCALING ANALYSES AND SMALL STRUCTURE
POOL SWELL DYNAMIC LOADS

ATTACHMENT J is PROPRIETARY and is provided under separate cover.

090779

22A4365
Rev. 4

K-1

ATTACHMENT K
RESPONSES TO NRC QUESTIONS

This attachment has been deleted
Pages K-2 through K-46 removed

L1.0 Containment Asymmetric Loads

This attachment discusses the potential for circumferential variations in the LOCA dynamic loads and relief valve loads. The asymmetric loads are identified and the data being used for containment design evaluation is presented. Table L-1 is a tabulation of the postulated phenomena which could cause loading asymmetries. The table either provides a reference for the asymmetric loads that are significant and should be considered, or provides a reference that justifies the assumption that a particular phenomenon does not lead to asymmetric loads of significance.

L2.0 Asymmetric Pool Swell

As discussed in section 6, the maximum containment pressure increase associated with the bubble formation that follows vent clearing is specified as 10 psi. The basis for this specification is data from the large scale air blowdown tests that were conducted as part of the Mark III test program. Circumferential variations in this relatively small pressure increase could result from either seismically induced submergence variations or variations in the vent flow composition (i.e., air/steam mixture variations). Increased submergence could lead to an increase in the load. However, PSTF data shows a very weak relationship between submergence and the containment pressure increase caused by bubble formation. The survey of the PSTF data shown in Figure 6.6 shows that for tests having the same drywell pressure at vent clearing, variations of up to 6 ft in submergence lead to variations in the bubble load of 2 to 3 psi; it is concluded that variations in suppression pool depth due to seismically induced waves will not lead to significant asymmetric containment bubble loads.

The bubble loading specification of 10 psi being used for Mark III design was derived from an air test and is thus the most conservative in terms of vent flow composition. Any steam in the vent flow would be condensed and this would lead to a less rapid pool acceleration and thus a reduced pressure load on the containment wall. It should be noted that PSTF data shows that the high degree of turbulent mixing in the drywell during a LOCA leads to a uniform mixture of air and steam in the vent flow. This condition will also exist in the full scale Mark III and this uniform vent flow composition will preclude any

Table L-1

<u>Phenomena</u>	Is there the potential for significant asymmetric containment loads	<u>Asymmetric Loads Being Used for Design Evaluation</u>	<u>Comments</u>
1. Seismic induced pool surface waves	No	See Attachment B	
2. Seismic induced changes in the pool hydrostatic pressure	Yes	See Attachment B	
3. Relief valve actuation	Yes	See Attachment A	
4. Jet Loads during vent cleaning	No	0	Loads are of negligible magnitude (see 6.1.2)
5. Sonic and compressive waves	No	Both 0	Loads are of negligible magnitude (see 4.1.1 and 6.1.1)
6. Bubble pressure load	Yes	0-10 psi	See following discussion.
7. HCU floor flow pressure differential	No	0	See Attachment F
8. Fall back	No	0	Loads on the containment are of negligible magnitude (see 6.1.7).

22A4365
Rev. 2

042178

L-2

Table L-1 (Continued)

<u>Phenomena</u>	Is there the potential for significant asymmetric containment loads	Asymmetric Loads Being Used for Design Evaluation	<u>Comments</u>
9. Post LOCA waves	No	0	Loads on the containment are of negligible magnitude (see 6.1.8)
10. Containment pressurization	No	0	This is a relatively slow charging process. See Figure 4.4.
11. Condensation oscillations	No	0	Loads are small (see 6.1.9)
12. Chugging	No	0	See following discussion.
13. Pool Swell loads with seismic induced waves present	No	0	See Section 10.1 and following discussion.

22A4365
Rev. 2

significant circumferential variations in the containment bubble formation loads. In addition, Attachment D shows no significant circumferential variations in drywell pressure that could lead to variations in vent flow rates and thus pool swell. Despite strong evidence that circumferential variation in the containment bubble load will not occur, an arbitrary loading combination of 0 psid on one side of the containment with a simultaneous 10 psid load on the other side should be considered to account for any uncertainties about asymmetric loading conditions. The conservative asymmetric condition assumes that all air is vented on half of the drywell periphery and steam is vented on the other half.

The large scale PSTF test data is the basis for specifying the maximum asymmetric load of 10 psi. Figure 6-6 is a summary of all the peak containment wall pressures observed in PSTF tests during the bubble formation phase of the blowdown. Figure 6-4 shows a typical transient. A maximum increase of 10 psi on the containment wall was observed in the PSTF at the Mark III drywell peak calculated pressure of 36.5 psia; Figure 6-6 shows the maximum increase close to zero. Thus, use of a 10 psi asymmetric pressure condition applied in a worst case distribution as a bounding specification will be used for containment evaluation.

L3.0 Asymmetric Chugging

An analysis was performed to determine the possible asymmetric chugging effects. It was assumed that all of the vents chugged simultaneously, but all vents on one half of the drywell were at a maximum 90-90% tolerance limit pressure while the other half of the vents in the opposite 180° sector were at a minimum 90-90% tolerance limit pressure. The resulting differential forces were then applied to the pool boundaries and weir annulus. Overturning moments were calculated and compared to the currently specified asymmetric pool swell load (Sections 4.1.9 and 6.1.3). The current specification loads (from asymmetric pool swell) result in moments twice as large as the asymmetric chugging moments. Since the current asymmetric pool swell specification bounds the conservatively calculated asymmetric chugging results by a large margin, asymmetric chugging is not a design basis load.

ATTACHMENT M
MULTIPLE SAFETY/RELIEF VALVE ACTUATION
FORCING FUNCTION METHODS

TABLE OF CONTENTS

<u>SECTION</u>	<u>TITLE</u>	<u>PAGE</u>
M1.0	INTRODUCTION	M-5
M2.0	RANDOM PARAMETERS	M-6
M2.1	Reactor Vessel Pressure Rise Rate	M-6
M2.2	Valve Setpoint	M-6
M2.3	Valve Opening Time	M-7
M2.4	Quencher Bubble Frequency Distribution	M-7
M3.0	MONTE CARLO TRIAL SIMULATIONS	M-13
M3.1	Approach	M-13
M3.2	Bubble Arrival Time	M-14
M3.2.1	Calculation of Reference Arrival Time	M-14
M3.2.2	Adjustment of Bubble Arrival Time for Valve Setpoint Variations	M-14
M3.2.3	Adjustment of Bubble Arrival Time for Valve Opening Time Variations	M-14
M3.3	Quencher Bubble Frequency Variations	M-15
M3.3.1	Adjustment of Quencher Bubble Frequency for Discharge Line Volume	M-15
M3.3.2	Adjustment of Quencher Bubble Time History for Selected Frequency	M-15

TABLE OF CONTENTS (Continued)

<u>SECTION</u>	<u>TITLE</u>	<u>PAGE</u>
M4.0	FACTORS AFFECTING PRESSURE DISTRIBUTION ON THE SUPPRESSION POOL BOUNDARY	M-15
M4.1	Bubble Pressure Attenuation	M-16
M4.2	Line-of-Sight Influence	M-16
M4.3	Combination of Multiple SRV Pressure Time Histories	M-16
M5.0	FORCING FUNCTIONS FOR NSSS EQUIPMENT EVALUATIONS	M-16
M5.1	Time Sequencing	M-16
M5.2	Pressure Time Histories	M-17
M5.3	Vertical Basemat Force and Overturning Moment	M-17
M5.4	Fourier Spectra	M-17
M6.0	STRUCTURAL RESPONSE ANALYSIS	M-18

LIST OF ILLUSTRATIONS

<u>FIGURE</u>	<u>TITLE</u>	<u>PAGE</u>
M2-1	Probability Density Function vs Pressure Rise Rate	M-8
M2-2	Probability Density Function vs Valve Group Setpoint Variation	M-9
M2-3	Probability Density Function vs Valve Opening Time Variation	M-10
M2-4	Probability Density Function vs Bubble Frequency	M-11
M2-5	Quencher Bubble Pressure Time History	M-12
MA-1	Basemat Load vs Time	MA-5
MA-2	Fourier Spectrum of Basemat Force	MA-6
MA-3	Fourier Spectra of Vertical Basemat Force	MA-7

M1.0 INTRODUCTION

This attachment describes the procedure for determining the safety/relief valve (SRV) discharge 95-95 percent confidence level forcing functions that are imposed on the containment structure to obtain structural responses which are used as input for the evaluation of equipment located within the containment. The procedure utilizes the random nature of several parameters that significantly influence the phase relationship of the individual air bubbles formed in the suppression pool during multiple SRV discharge events. The random variables that are utilized in this procedure are 1) SRV Setpoint Tolerance, 2) Valve Opening Time, 3) Reactor Vessel Pressure Rise Rate, and 4) Quencher Bubble Frequency. Other parameters that influence the phase relationship are being studied for future application.

The maximum positive and negative bubble pressures for each individual discharge location are determined by using the method described in Section A12.6 of Attachment A. It should be noted that test data indicated randomness in the peak pressure amplitude which could also be used for determining structural response. This is also being studied for future application.

Of the SRV cases identified for consideration in containment structural design (Table A4.4 of Attachment A), the expected bounding vertical response at equipment locations is based on the all valve case. The expected bounding horizontal response is based on either the single valve subsequent actuation, two adjacent valves, or the all valve case. The ADS case is also evaluated. From each of these four cases, the Fourier Spectra of the forcing functions for 59 Monte Carlo simulations of the event are plotted. A bounding forcing function is then selected in each of the frequency ranges of interest for use in developing the dynamic responses at a selected location on the containment structure (i.e., basemat, drywell, and containment). These dynamic responses are then employed for NSSS and BOP equipment evaluations. A dynamic time history analysis is performed to determine the acceleration time histories, response spectra, and displacements needed. Dynamic responses for equipment evaluations are made by

enveloping the results from the selected trial cases with the largest Fourier spectra magnitude in each frequency interval. For clarification, an example is presented in Appendix M.A to this attachment.

M2.0 RANDOM PARAMETERS

M2.1 Reactor Vessel Pressure Rise Rate (PRR)

The pressure rise rate distribution for BWR/6 plants is shown in Figure M2-1. The distribution is determined from an evaluation of BWR/6 transient events. The figure represents the probability density function for pressure rise rates for events opening $> 2/3$ of the SRV's, weighted by the relative occurrence of the events and averaged over all reactor conditions anticipated during the last 40% of an operating cycle. The lower limit of 40 psi/sec is the minimum pressure rise rate expected to open $2/3$ of the SRV's. The upper limit of 140 psi/sec has a high probability of not being exceeded for any operating condition.

It should be noted that the PRR variable is only used in the all valve case Monte Carlo event simulations.

M2.2 Valve Setpoint

The setpoints for SRV's on BWR/6 are arranged in three groups with redundant logic trains consisting of a pressure transducer and three pressure switches. The logic for the 238 BWR/6 design consists of one pressure switch set at 1103 psi, nine on a pressure switch set at 1113 psi, and the remaining nine on a pressure switch at 1123 psi. A testability feature is also included which utilizes pressure trip instrumentation. The tolerance on the pressure switch setpoints with this testability feature is based on a normal (Gaussian) distribution with a standard deviation of 2 psi as shown in Figure M2-2. For the grouped arrangement, the standard deviation is applied to the group setpoints; thus, the valves within the group will have the same adjustment.

The SRV arrangement and pressure setpoints for the Mark III standard plants are identified in Figures A4-3 through A4-9 of Attachment A. The actual location of the quenchers in the suppression pool is defined by the purchaser.

M2.3 Valve Opening Time (VOT)

Test data indicates that there is a normal distribution for the VOT with a standard deviation of 0.009 seconds as shown in Figure M2-3.

M2.4 Quencher Bubble Frequency Distribution (QBF)

A typical forcing function for a quencher SRV bubble with a frequency of 8 Hz is shown in Figure A5.11 of Attachment A. The bubble lasts effectively 0.75 seconds in the suppression pool. In the 8 Hz bubble, the pressure decays to one-third of the peak value over 5 cycles and a complete pressure cycle oscillation period lasts 0.125 seconds, 0.05 seconds for the positive pulse and 0.075 seconds for the negative pulse. For other frequencies, the same damping definition applies, i.e., two-third decay over 5 cycles, or 0.133 decay per cycle.

The quencher bubble pressure time history in Figure A5.11 of Attachment A is an idealized bubble model. For the purposes of this procedure a pressure time history curve is constructed by assigning half sine waves to both the positive and negative portions as shown in Figure M2-5. The P_{\max} and P_{\min} ratios and the positive and negative pulse duration periods are maintained. This provides a time history that is more representative of the test observations and allows for computer simulation.

Quencher test data shows that the frequency of the air bubble is a function of the SRV discharge line air volume. The distribution of bubble frequencies for a discharge line air volume of 50 ft.³ is shown in Figure M2-4 and is used as the reference for this procedure. This reference value is the SRV line volume from the operating plants from which the Quencher bubble frequency data was obtained. The normal distribution for the curve has a mean frequency of 8.1 Hz with a standard deviation of 1.7 Hz. It is truncated at the minimum and maximum bounds of 5 and 12 Hz.

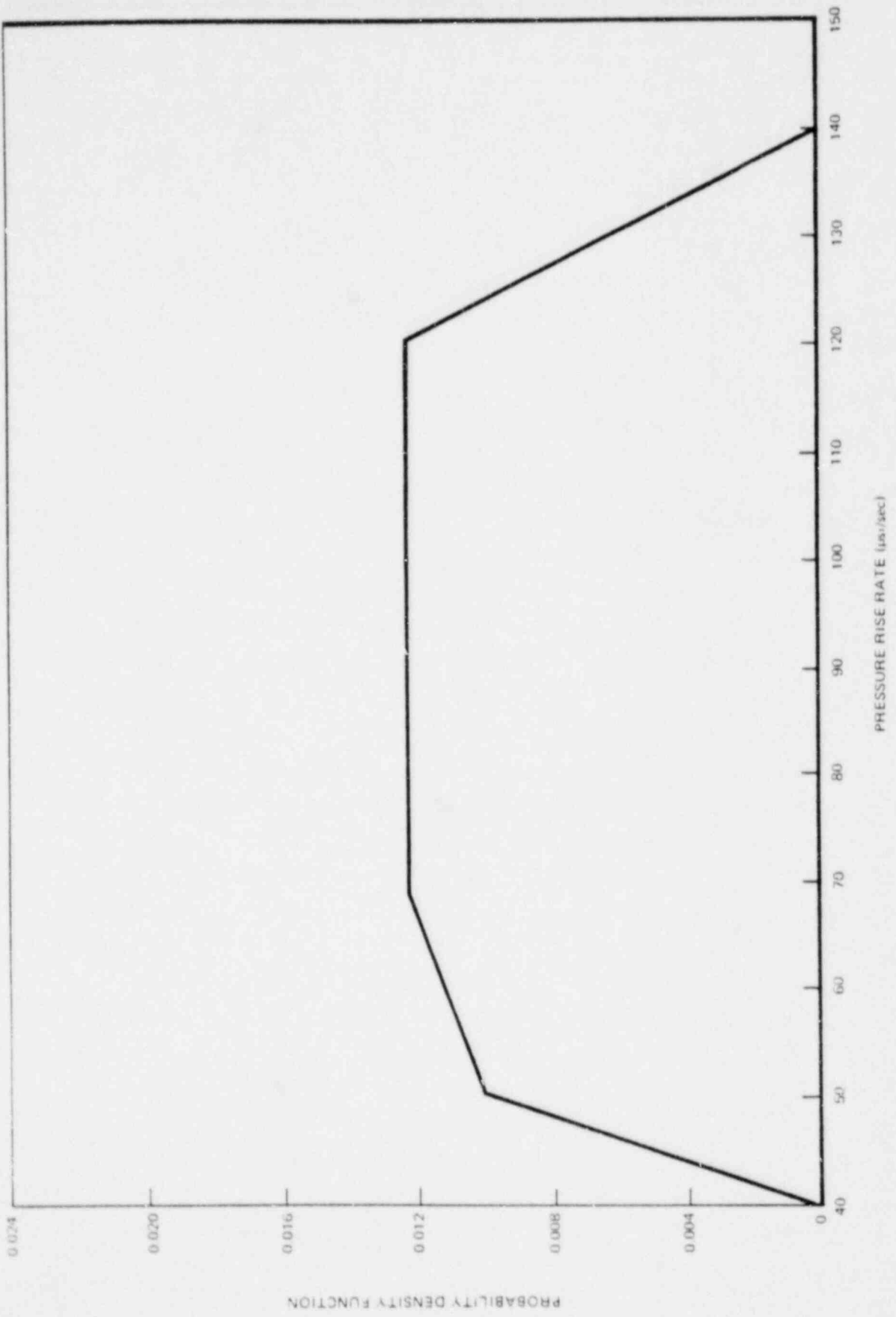


Figure M2-1. Probability Density Function vs. Pressure Rise Rate

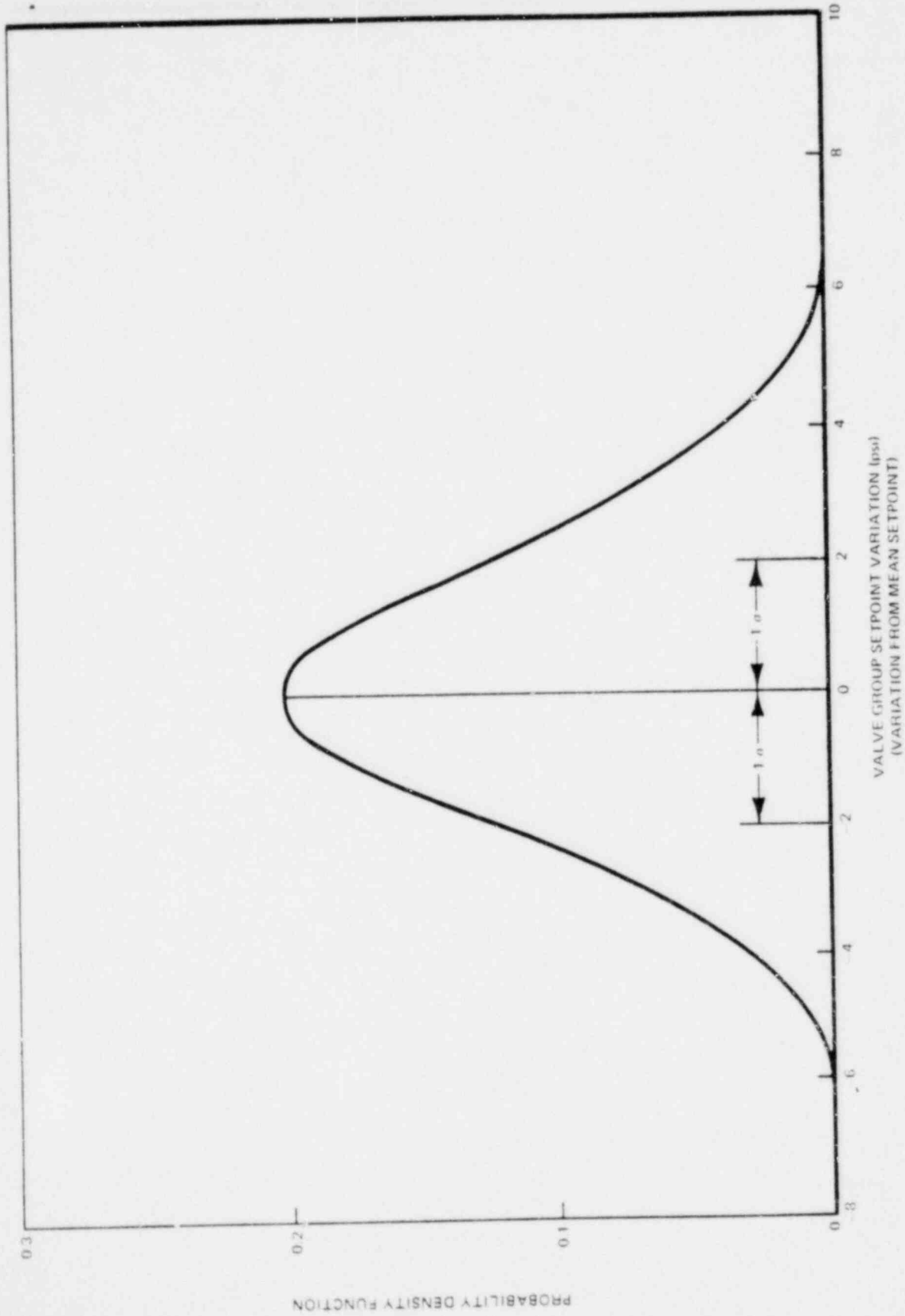


Figure M2-2. Probability Density Function vs. Valve Group Setpoint Variation

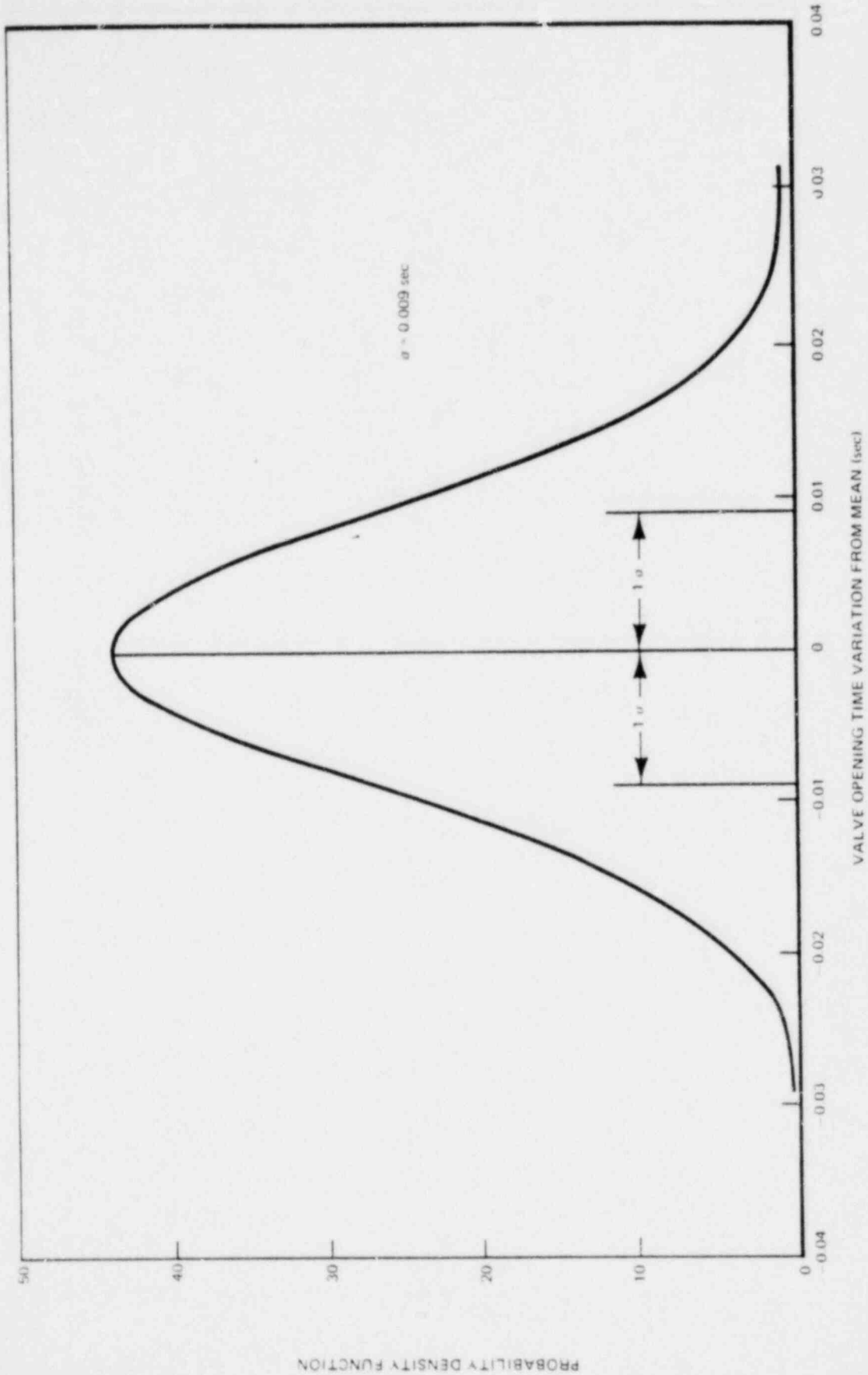


Figure M2-3. Probability Density Function vs. Valve Opening Time Variation
(for Crosby and Dikkers Valves)

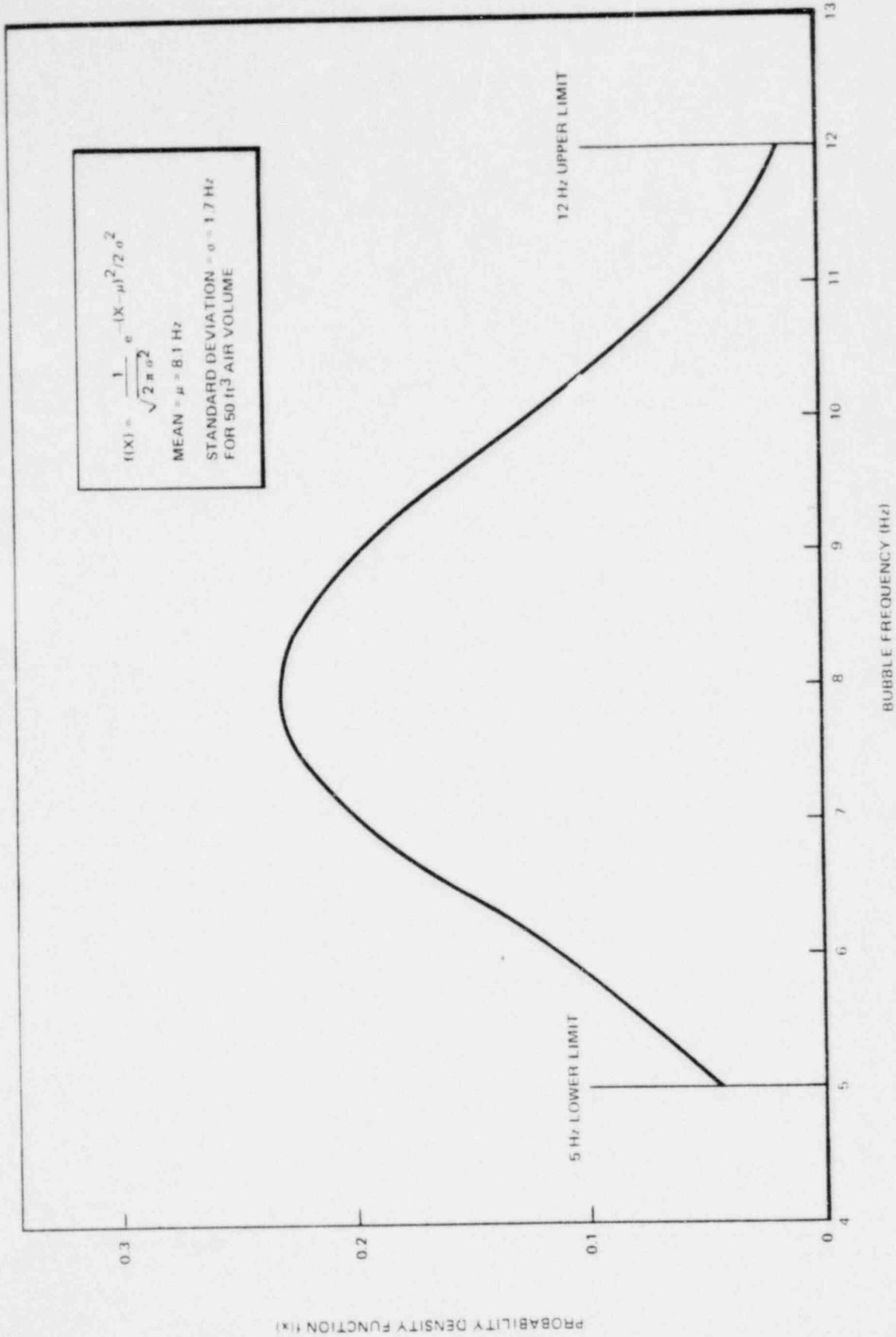


Figure M2-4. Probability Density Function vs. Bubble Frequency

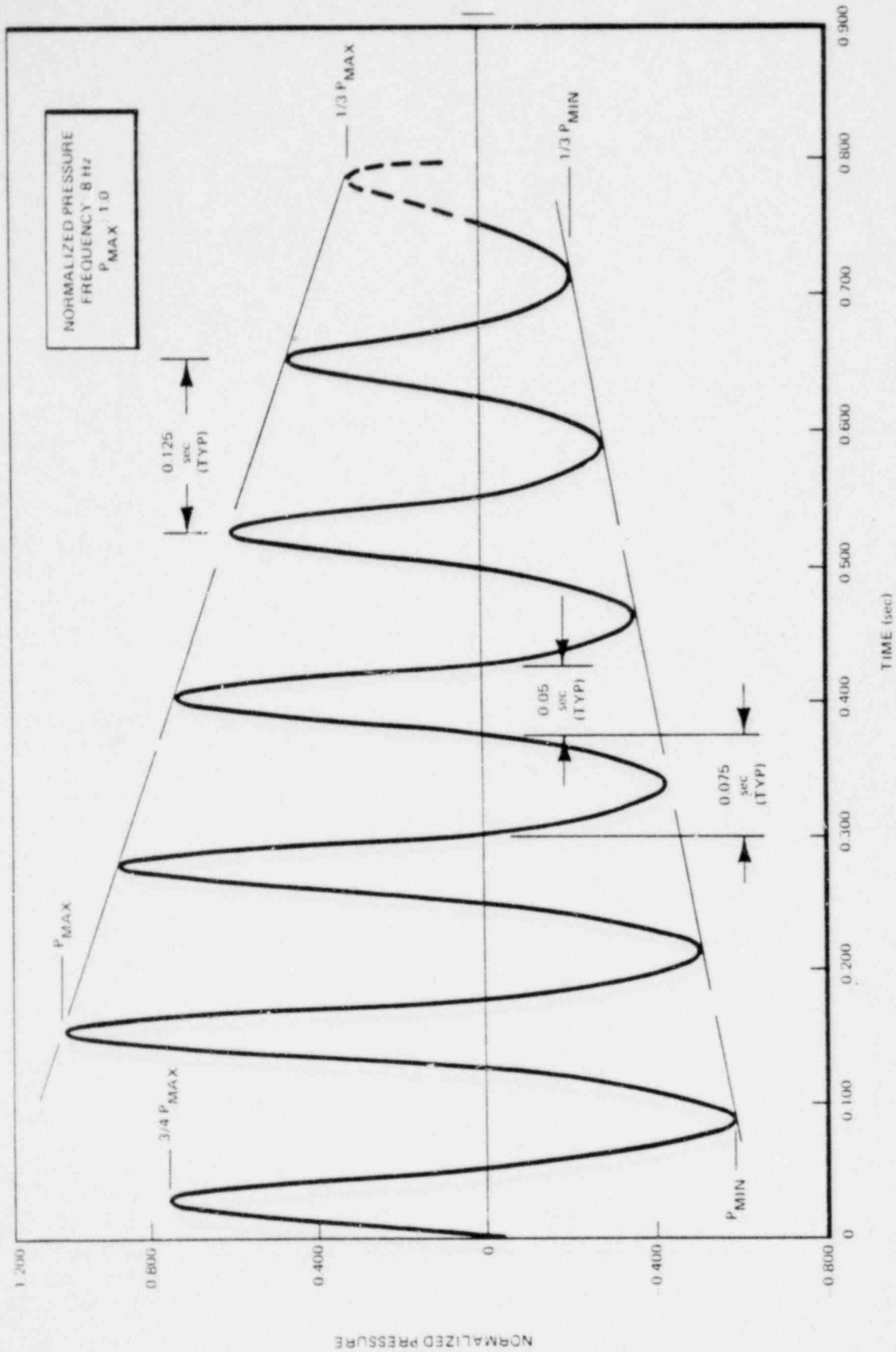


Figure M2-5. Quencher Bubble Pressure Time History

M3.0 MONTE CARLO TRIAL SIMULATIONS

M3.1 Approach

There are four SRV cases that are considered to get bounding forcing functions for the equipment evaluations. They are:

- Single Valve subsequent actuation
- Two adjacent valves
- ADS valves
- All valves

In each of these cases, 59 Monte Carlo trials are performed in which appropriate random variable adjustments are selected for the parameters listed in Section M2.0. For the single valve subsequent actuation case only the quencher bubble frequency is varied. For the ADS and two adjacent valves cases, the valve set point tolerance and pressure rise rate considerations are not incorporated for obtaining the forcing function because the entire group of ADS valves is simultaneously activated by a single signal. For all valve case all variables are considered.

The all valve trials each consist of selecting a random pressure rise rate from Figure M2-1 and a random pressure switch setpoint for each group of SRVs using Figure M2-2. This information is used to compute the bubble arrival time difference or separation between each group of valves. These bubble arrival times are adjusted for each individual valve by randomly selecting a time variation due to valve opening time (VOT) using Figure M2-3.

Once the bubbles are in the suppression pool, each bubble frequency is randomly varied by selecting a frequency from a unique distribution for the discharge line volume involved. See Figure M2-4 for typical distribution for discharge line with an air volume of 50ft³. The bubble time history for each valve location

is then used to determine the forcing function on the suppression pool boundary by utilizing the methods described in Section A10.3.1 of Attachment A.

For the ADS and two adjacent valve cases, each trial assumed that all valves are actuated together and then bubble phasing is adjusted by randomly selecting a time variation due to VOT for each valve. Each bubble frequency is then randomly selected as for the multiple valve trials. For the single valve case only the bubble frequency is varied.

M3.2 Bubble Arrival Time

M3.2.1 Calculation of Reference Arrival Time

The arrival time for each air bubble in the suppression pool relative to the lowest set SRV is a function of the SRV setpoint arrangement and the reactor pressure rise rate. Assuming no tolerance on setpoints, no variation in valve opening time (VOT), and randomly selecting a pressure rise rate (PRR), the arrival times of the bubbles in the suppression pool are computed by dividing the nominal setpoint differences (i.e., $\Delta p = 10$ and 20 psi for BWR-6) by the PRR. It should be noted that SRV discharge line lengths are not considered. For BWR-6 with nominal setpoints at 1103, 1113, and 1123 psi the time separation is 0.077 and 0.154 seconds, based upon $PRR = 130$ psi/sec.

M3.2.2 Adjustment of Bubble Arrival Time for Pressure Setpoint Variations

Each all valve Monte Carlo trial will include an adjustment of the bubble arrival times as calculated in Section M3.2.1 by slightly increasing or decreasing the valve setpoint for each group of valves. This is done by using a random number generator code to select valve setpoint variation from the distribution shown in Figure M2-2.

M3.2.3 Adjustment of Bubble Arrival Time for Valve Opening Time Variations

Each Monte Carlo trial will include an adjustment of the bubble arrival time as calculated in Section M3.2.2 by slightly increasing or decreasing the VOT

for each valve. This is done by using a random number generator code to select VOT variation from the distribution shown in Figure M2-3.

M3.3 Quencher Bubble Frequency Variation

M3.3.1 Adjustment of Bubble Frequency for Discharge Line Air Volume

As indicated in Section M2.4 the frequency of the quencher bubble is a function of the SRV discharge line air volume. A reference line air volume of 50 ft³ has been selected to generate the bubble pressure time history shown in Figure M2-5. For each SRV discharge line volume a unique frequency distribution is generated by adjusting all of the characteristics (mean, standard deviation, lower bound, upper bound) of the reference distribution curve by multiplying by the cube root of the ratio of 50 ft³ to the actual air volume in the SRV discharge line. For example, the adjustment of frequency for a 100 ft³ line volume is:

$$8.1 \text{ Hz} \times \sqrt[3]{\frac{50}{100}} = 8.1 \times 0.79 = 6.4 \text{ Hz}$$

Examples for the other characteristics:

<u>Volume</u> (ft ³)	<u>Mean</u> (Hz)	<u>Std. Dev.</u> (Hz)	<u>Lower Bound</u> (Hz)	<u>Upper Bound</u> (Hz)
50	8.1	1.7	5	12
100	6.4	1.3	4	9.5

M3.3.2 Adjustment of Quencher Bubble Time History for Selected Frequency

In each Monte Carlo trial, a random number generator code is used to select a frequency from each of the frequency distribution curves generated in Section M3.3.1. For each frequency selected, a time history of the Quencher bubble pressure oscillation is generated by adjusting the reference time history (8.0 Hz). This is accomplished by maintaining the ratio of negative to positive pulse period constant. The pressure cycle period, positive pressure pulse time and negative pressure pulse time are adjusted by multiplying each by the ratio of the reference frequency (8 Hz) to the selected frequency. For example, for 6 Hz:

$$\text{Pressure cycle period} = 0.125 \text{ sec.} \frac{8 \text{ Hz}}{6 \text{ Hz}} = 0.167 \text{ sec.}$$

$$\text{Positive pressure pulse time} = 0.05 \text{ sec.} \frac{8 \text{ Hz}}{6 \text{ Hz}} = 0.067 \text{ sec.}$$

$$\text{Negative pressure pulse time} = 0.075 \text{ sec.} \frac{8 \text{ Hz}}{6 \text{ Hz}} = 0.100 \text{ sec.}$$

$$\text{Number of cycles per } 0.75 \text{ sec. duration} = \frac{\text{Bubble duration}}{\text{Pressure cycle period}} = \frac{0.75 \text{ sec.}}{0.167 \text{ sec/cycle}} = 4.5 \text{ cycles}$$

M4.0 FACTORS AFFECTING PRESSURE DISTRIBUTION ON THE SUPPRESSION POOL BOUNDARY

M4.1 BUBBLE PRESSURE ATTENUATION

The attenuation of the bubble pressure with distance r from the quencher is $2r_0/r$ where r_0 - radius of the quencher - (4.87 ft) and $r \geq 2r_0$ (see Section A.10.3.1 of Appendix 3B). r = true spatial distance from the quencher center to the node.

M4.2 LINE-OF-SIGHT INFLUENCE

The line-of-sight criterion for the bubble pressure states that points which cannot be seen through a direct line from the outer radius of the quencher arms to the location in question will not be affected by the pressure from that quencher (see Section A.10.3.2.1 of Appendix 3B).

M4.3 COMBINATION OF MULTIPLE SRV PRESSURE TIME HISTORIES

The time sequencing application provides a given phase relationship between quencher bubbles. The pressure at each node point and time step is calculated by combining the contribution from each valve (in the line of sight) using algebraic summation. At each node where the total calculated pressure at any time step exceeds the maximum pressure (positive or negative) from any of the contributing valves, the calculated pressure at the specific time step is set equal to the maximum bubble pressure at the same instant in time.

M5.0 FORCING FUNCTIONS FOR NSSS EQUIPMENT EVALUATION

M5.1 TIME SEQUENCING

Time sequencing with random parameters is used to arrive at the forcing function for the multiple SRV air-clearing events referenced in Section M3.1.

A Monte Carlo technique is used to generate the building forcing function for equipment evaluations. The bounding forcing function from 59 trials will result in a 95% confidence level that 95% of the time the actual forcing function will be less than the forcing function determined by the Monte Carlo technique.

M5.2 PRESSURE TIME HISTORIES

Fifty-nine (59) cases of pressure distribution on the pool boundary are calculated using the random parameters delineated in Section M2.0.

M5.3 VERTICAL BASEMAT FORCE AND OVERTURNING MOMENT

The total basemat force is calculated as a function of time by integrating the node pressures over the suppression pool basemat incremental areas. The overturning moments (about two perpendicular horizontal axes through the basemat center upper surface) are calculated, as a function of time, by integrating the product (node pressure x the incremental area moment arm x the incremental area) over the suppression pool boundary (containment, basemat, and drywell wall).

M5.4 FOURIER SPECTRA

Fourier spectra* of the vertical basemat force and overturning moment for the 59 cases are developed for selecting the cases used to determine dynamic responses for equipment evaluations. The significant frequency range is divided into three frequency intervals as determined below:

-
- *Reference 1: Cooley, J.W., & Tukey, J.W., (1965), "An Algorithm for the Machine Calculation of Complex Fourier Series," *Mathematics of Computation*, Vol. 19, No. 90, pp 297-301.
2. Shingleton, Richard C., "On Computing the Fast Fourier Transform," *Communication of Applied Computation Mathematics*, (10(10) 1967, pp 647-654.

- Step 1. Adjust the mean frequency of each safety/relief valve discharge line for air volume differences, see Sub-section M3.3.1.
- Step 2. Calculate the mean frequency (f_m) for all applicable safety relief valve discharge lines.
- Step 3. Establish the frequency intervals based on 0.5 f_m to 1.5 f_m , 1.5 f_m to 2.5 f_m , and 2.5 f_m to 3.5 f_m .

$$\text{where } f_m = \frac{1}{N} \sum f_i ; \quad i = 1, \dots, N$$

$N = \text{total no. of valves actuated}$

The basemat loading cases with the largest spectral value within each frequency interval (from the 59 cases) are selected for determination of equipment responses.

M6.0 STRUCTURAL RESPONSE ANALYSIS

Forcing functions corresponding to the case selected in each frequency range (selected in Section M5.4) are used as input to the structural analysis. Structural dynamic analysis is then performed for these selected cases. The resulting dynamic responses are then enveloped for NSSS and BOP equipment evaluations.

APPENDIX MA

EXAMPLE OF TYPICAL TIME SEQUENCING APPLICATION

This example is provided to clarify the time sequencing procedures provided in this attachment. Typical random parameter values are used to outline the steps required to determine the bounding vertical basemat force. Examination of the Fourier spectra for the vertical basemat force and overturning moments permits calculation of bounding equipment responses. Guidelines for selecting the bounding responses for equipment evaluations are included.

MA. RANDOM PARAMETERS

The following random parameters are used: pressure setpoints, valve opening time, and vessel pressure rise rate. The random parameter values used in this example problem are:

- (1) Pressure rise rate distribution per Subsection M2.1.
- (2) Pressure setpoints variation per Subsection M2.2.

<u>Valves</u> *	<u>Mean</u> * <u>Setpoint</u> <u>(psi)</u>	<u>Standard</u> <u>Deviation</u> <u>(psi)</u>
1	1103	2
9	1113	2
9	1123	2

- (3) Valve opening time variations per Subsection M2.3

Standard deviation = 0.009 sec.

Step 1

An 80 psi/sec vessel pressure rise rate was randomly selected from Figure M2-1.

*Note that this example is for the 238 BWR/6 Mark III standard plant with a ganged valve arrangement.

Step 2

The valve pressure setpoints are randomly selected from a random number generator code using the distribution given in Figure M2-2. The valve pressure setpoints from a typical random selection are 1104.5 psi, 1114.3 psi, and 1124.6 psi.

Step 3

The relative valve opening time for each of the two groups of 9 valves is calculated:

$$T_i \text{ (sec)} = \frac{\text{Valve setpoint}_{(i)} \text{ (psi)} - \text{Valve setpoint}_{(1)} \text{ (psi)}}{\text{Pressure rise rate (psi/sec)}}$$

where

- i = 2, 3 (the number of subsequent valve groups), and
- 1 = the reference valve.

Hence, for i = 2, the valve opening time for the first group of 9 valves is:

$$T_2 = \frac{1114.3 - 1104.5}{80} = 0.1225 \text{ sec}$$

Step 4

The bubble arrival time is calculated by adding the group valve opening time and a randomly selected delta time for each valve using the valve opening time distribution shown in Figure M2-3. Therefore, for each quencher the bubble arrival time = $T_{(group)} + \text{individual valve opening time (IVOT)}$.

For this sample problem, the typical set of randomly selected IVOT's for the distribution values stated above are:

<u>Valve No.</u>	<u>IVOT (sec)</u>	<u>Valve No.</u>	<u>IVOT (sec)</u>	<u>Valve No.</u>	<u>IVOT (sec)</u>
1	0.067	7	0.067	13	0.056
2	0.069	8	0.051	14	0.061
3	0.065	9	0.062	15	0.056
4	0.059	10	0.065	16	0.065
5	0.063	11	0.058	17	0.057
6	0.038	12	0.057	18	0.071
				19	0.069

Note that a mean value of 0.057 sec is included in the above numbers. Adding these values to the group T_1 calculated in Step 3 and normalizing to have the first bubble arrive at zero time results in the following bubble arrival times:

<u>Valve No.</u>	<u>Arrival Time (sec)</u>	<u>Valve No.</u>	<u>Arrival Time (sec)</u>	<u>Valve No.</u>	<u>Arrival Time (sec)</u>
1	0.125	7	0.125	13	0.243
2	0.256	8	0.238	14	0.127
3	0.123	9	0.120	15	0.243
4	0.247	10	0.0	16	0.124
5	0.122	11	0.246	17	0.245
6	0.225	12	0.116	18	0.129
				19	0.256

M.3 BUBBLE FREQUENCIES

Bubble frequencies for individual quenchers are randomly selected from a random number generator code using the distribution shown in Figure M2-4. Typical random bubble frequency values for the 19 quenchers are:

<u>Valve No.</u>	<u>Frequency (Hz)</u>	<u>Valve No.</u>	<u>Frequency (Hz)</u>
1	6.56	11	7.22
2	9.77	12	5.39
3	9.15	13	5.68
4	5.01	14	8.60
5	9.33	15	9.86
6	6.88	16	7.04
7	9.41	17	11.08
8	9.10	18	8.68
9	7.92	19	8.52
10	11.14		

NOTE: For this example, all lines are considered as uniform in length and frequencies are randomly selected from one Quencher Bubble Frequency (QBF) distribution curve (Figure M2-4). In this example, mean = 8.23 Hz and $\sigma = 1.80$ Hz. With nonuniform line lengths, Subsection M3.2.1 is used to develop unique QBF distribution curves from which a frequency is randomly selected for each line.

M.C The forcing function is calculated by computing the pressure distribution around the pool boundary using the criteria defined in Section M4.0 which are:

- (1) $2r_0/r$ attenuation, r_0 = quencher radius and $r \geq 2r_0$.
- (2) Line-of-sight influence.
- (3) Algebraic summation at each time step of the individual pressure waves.
- (4) Truncation of the total calculated pressure to the maximum bubble pressure of any of the pressure waves in the pool at each time step.

The basemat force vs time shown in Figure MA-1 is computed for a typical trial case.

The Fourier spectrum of this basemat force (Section M5.0) is calculated in Figure MA-2.

M.D A Monte Carlo technique is used to generate 59 forcing functions. This gives 95% confidence and 95% probability that these loads will not be exceeded. The significant frequency range for building and equipment evaluation is then divided into several frequency intervals. Out of these 59 trials, the maximum trial case is selected for each frequency interval based on the peak Fourier amplitudes of the integrated vertical basemat forces or overturning moment, in that frequency interval. Figure MA-3 shows an example of this selection procedure. Structural dynamic analyses are performed for these potential critical cases. The resulting dynamic responses are then enveloped for NSSS and BOP equipment evaluation.

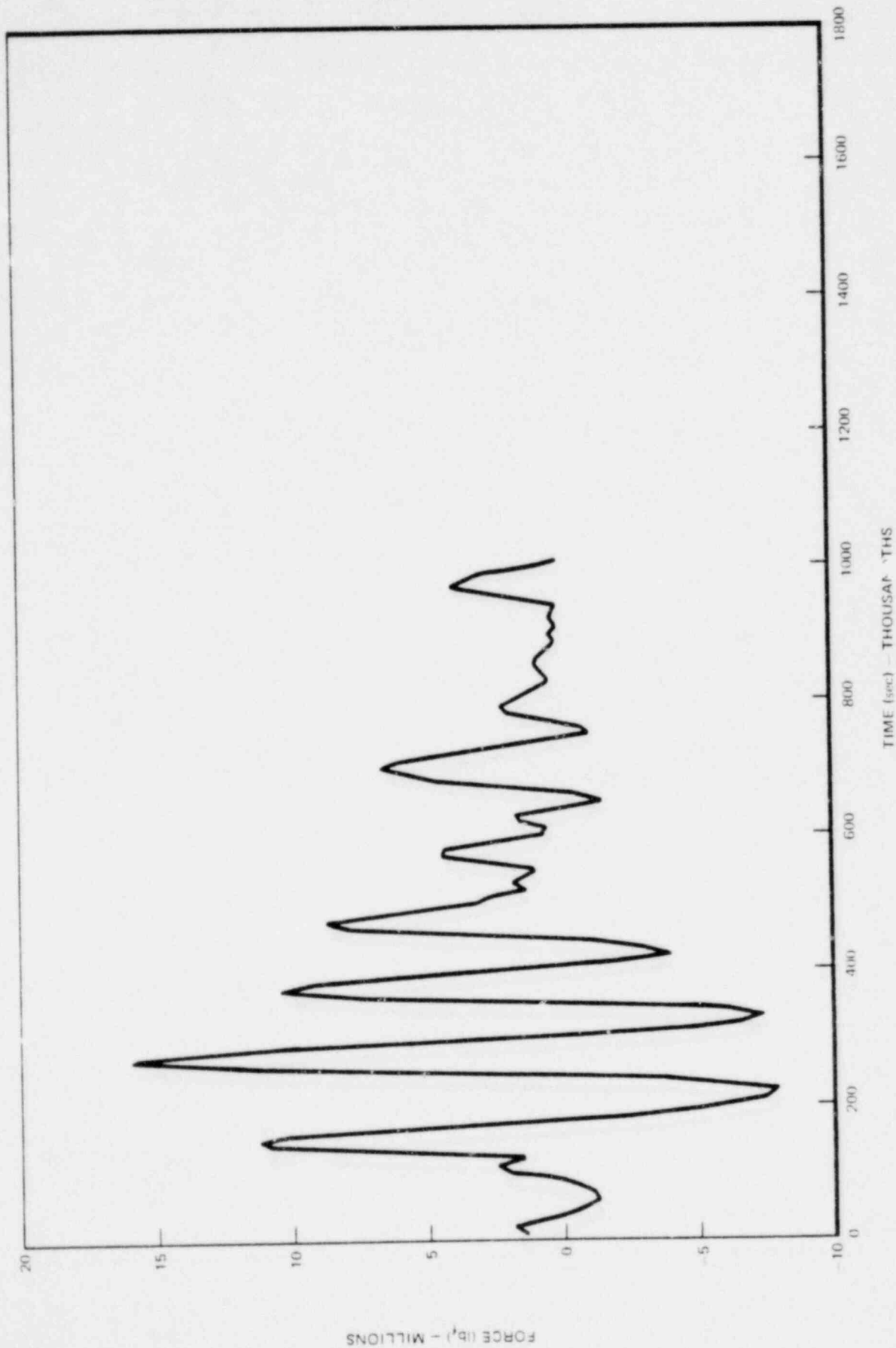


Figure MA-1. Basemat Load vs. Time

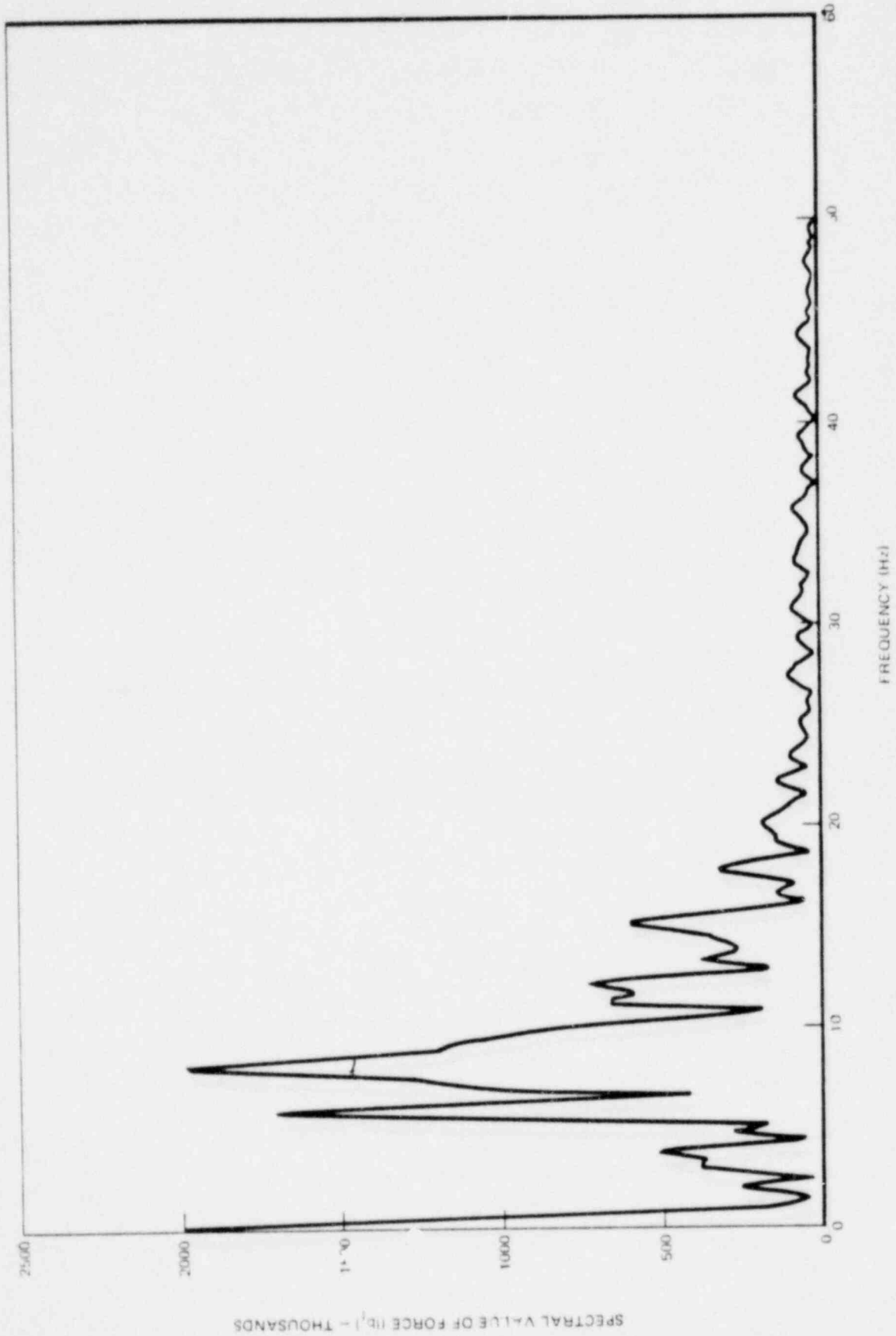


Figure MA-2. Fourier Spectrum of Basemat Force

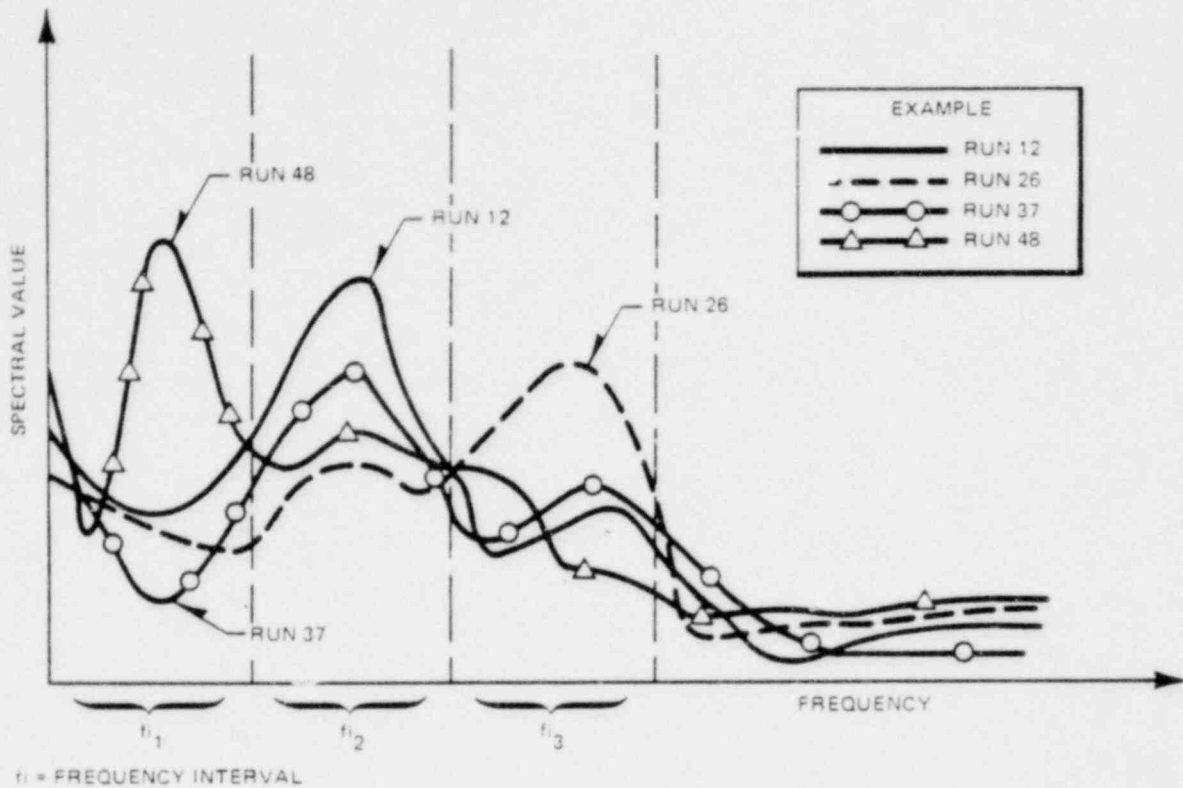


Figure MA-3. Fourier Spectra of Forcing Functions

NOTES:

1. Fourier Spectra of forcing function for all 59 Monte Carlo runs are plotted.
2. The above example shows maximum forcing functions in the three selected frequency intervals.
 - ° Run 48 is max. for frequency interval, f_{i1}
 - ° Run 12 is max. for frequency interval, f_{i2}
 - ° Run 26 is max. for frequency interval, f_{i3}
3. Run 37 is a typical non-maximum case.
4. The time histories for Runs 48, 12, and 26 are used in developing dynamic responses.
5. The dynamic responses that result from these forcing functions are then enveloped for NSSS & BOP equipment evaluations.

ATTACHMENT N SUPPRESSION POOL THERMAL STRATIFICATION

N1.0 INTRODUCTION

During the period of steam condensation in the suppression pool, from a postulated LOCA, the pool water in the immediate vicinity of the vents is heated because of the energy release. For the Mark III suppression pool configuration, most of the mass and energy is released to the pool through the top vents. As a result, the top portion of the pool is heated more than the lower portion. By natural convection the hot water rises and the cold water is displaced toward the bottom portion of the pool. The vertical temperature gradient resulting from these effects is known as thermal stratification.

N1.2 REVIEW OF TEST DATA

During the LOCA blowdown, the pool vertical temperature profile varies not only with time but also with the distance from the vent exit. Figures N-1 and N-2 present the typical temperature profiles for a large break liquid blowdown. In Figure N-1, which shows the profiles measured for the half pool near the drywell wall, the temperature peaks at the elevation of the top vent during the initial stages of the blowdown ($t \leq 25$ sec), indicating concentrated energy discharge through the top vent. As blowdown proceeds ($t \geq 25$ sec), the temperature profile smooths out due to thermal mixing, turbulence, and pool agitation by chugging. In the other half of the pool away from the drywell wall, the temperature profile, as shown in Figure N-2 is not as steep as that of Figure N-1 at the early stages of the blowdown. However, toward the end of the blowdown the temperature profiles are nearly the same throughout the entire pool.

In general, the steam blowdowns in PSTF give less stratification than liquid blowdowns of the same break size. This is attributed to the smaller total energy release associated with the steam blowdowns. For the full scale plant the energy from either break is equal. Thermal stratification is also dependent on the break size for the same blowdown fluid type. Large breaks create more stratification than small breaks because energy deposition in the pool is more

rapid. Since the specific heat of water is essentially constant within the temperature range from 70°F to 200°F, the temperature rise of the pool is independent of the initial pool temperature for a given amount of energy input. As a result, the initial pool temperature has little effect on thermal stratification.

Ni-3 APPLICATION

To determine the maximum temperature profile for structural evaluation, it is assumed that the energy deposition distribution as a function of submergence is the same for the 1/3 area scale (Test Series 5807, Ref. 15) as for the full scale plant. Dividing the pool depth into five equal segments, the percentage energy deposition distribution for the maximum stratification expected is established as follows:

Segment No. (i) From Pool Top	Height of Segment i in % of Total Pool Depth (H_i/H)	% of Total Energy Deposition (E_i)
1	20	23
2	20	23
3	20	22
4	20	20
5	20	12

To obtain the temperature profile for a prescribed initial pool temperature (T_o) and total blowdown energy, the bulk pool temperature (T) from energy balance at the end of the blowdown was calculated, then the mean temperature (T_i) for each pool segment was determined from:

$$T_i = E_i(\bar{T} - T_o) \frac{H}{H_i} + T_o$$

where H is the total pool depth, H_i is the height of the i^{th} segment, and E_i is the fraction of total energy deposited in the i^{th} segment. Assuming the mean temperature of each segment occurs in the middle of the segment, the temperature profile is readily plotted. Note the above table is valid only for a top vent initial submergence of 7.5 ft.

N1-3.1 Stratification During Large Break Accident

For design evaluation of the large break accident, a total energy discharge of 4×10^8 Btu into a 100°F pool with 8×10^6 lb_m of water was assumed. The mean pool temperature after energy release is:

$$\bar{T} = 100 + \frac{4 \times 10^8}{8 \times 10^6 \times 1} = 100 + 50 = 150^\circ\text{F}$$

$$T_1 = T_2 = 0.23(150-100) (5) + 100 = 157.5^\circ\text{F}$$

$$T_3 = 0.22(150-100) (5) + 100 = 155^\circ\text{F}$$

$$T_4 = 0.2(150-100) (5) + 100 = 150^\circ\text{F}$$

$$T_5 = 0.12(150-100) (5) + 100 = 130^\circ\text{F}$$

Figure N-3 shows the resulting pool temperature profile. Note that, although the temperature difference from top to bottom is almost 30°F , the peak temperature is only 7.5°F above the mean.

N1-3.2 Stratification During Intermediate and Small Break Accidents

Figure N-4 shows the localized nature of the energy addition as observed in the PSTF Full Scale Tests (Reference 16). The localized energy addition (through the top vent) from the full scale tests is more representative of the smaller accident breaks. Test results show that, for a very limited blowdown (about 2 minutes) with much less energy added to the pool than prototypical, the temperature in the lower pool region (26 feet) was essentially unchanged and the upper pool region was uniformly heated. This thermal stratification profile will not persist in actual conditions, since ECCS suction and return will promote pool mixing. The long term profile will essentially be as shown in Figure N-3.

Since Figure N-3 from $1/\sqrt{3}$ PSTF results shows a thermal gradient near the bottom of the pool, and full scale tests (Reference 16) show the gradient at higher locations, it is conservatively recommended for design evaluations that the maximum temperature gradient shown in Figure N-3 be applied from the lower pool region up to the top vent centerline. For the upper parts of the pool (above top vent centerline) the temperature profile, from full scale and $1/\sqrt{3}$ scale tests, shows uniform heating (Reference Figure N-3).

This figure is PROPRIETARY and is provided under separate cover.

Figure N-1. Typical Transient Temperature Profiles Near Drywell Wall,
Run 22

This figure is PROPRIETARY and is provided under separate cover.

Figure N-2. Typical Transient Temperature Profiles Near Containment Wall,
Run 22

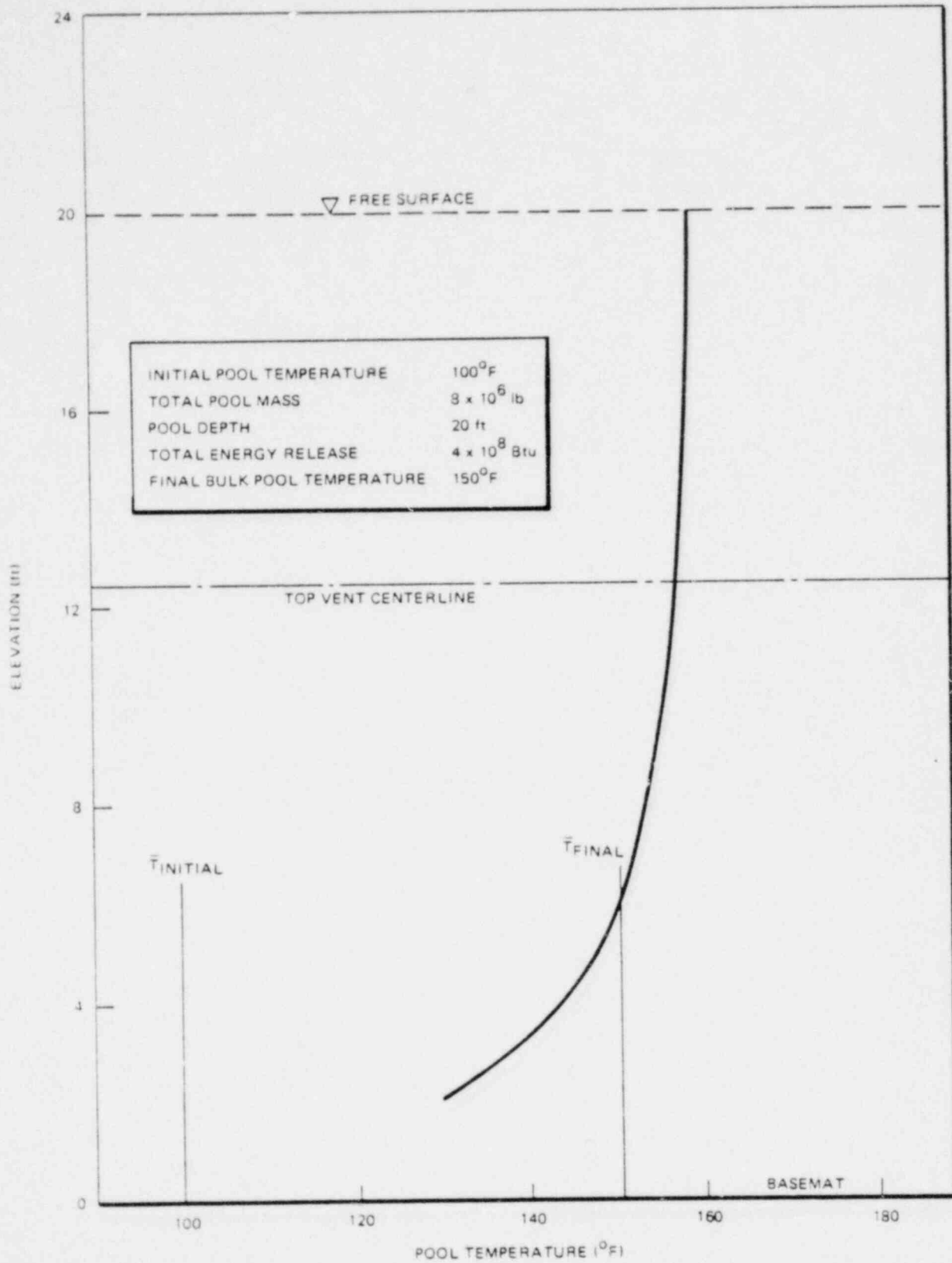


Figure N-3. Suppression Pool Temperature Profile for Large Breaks

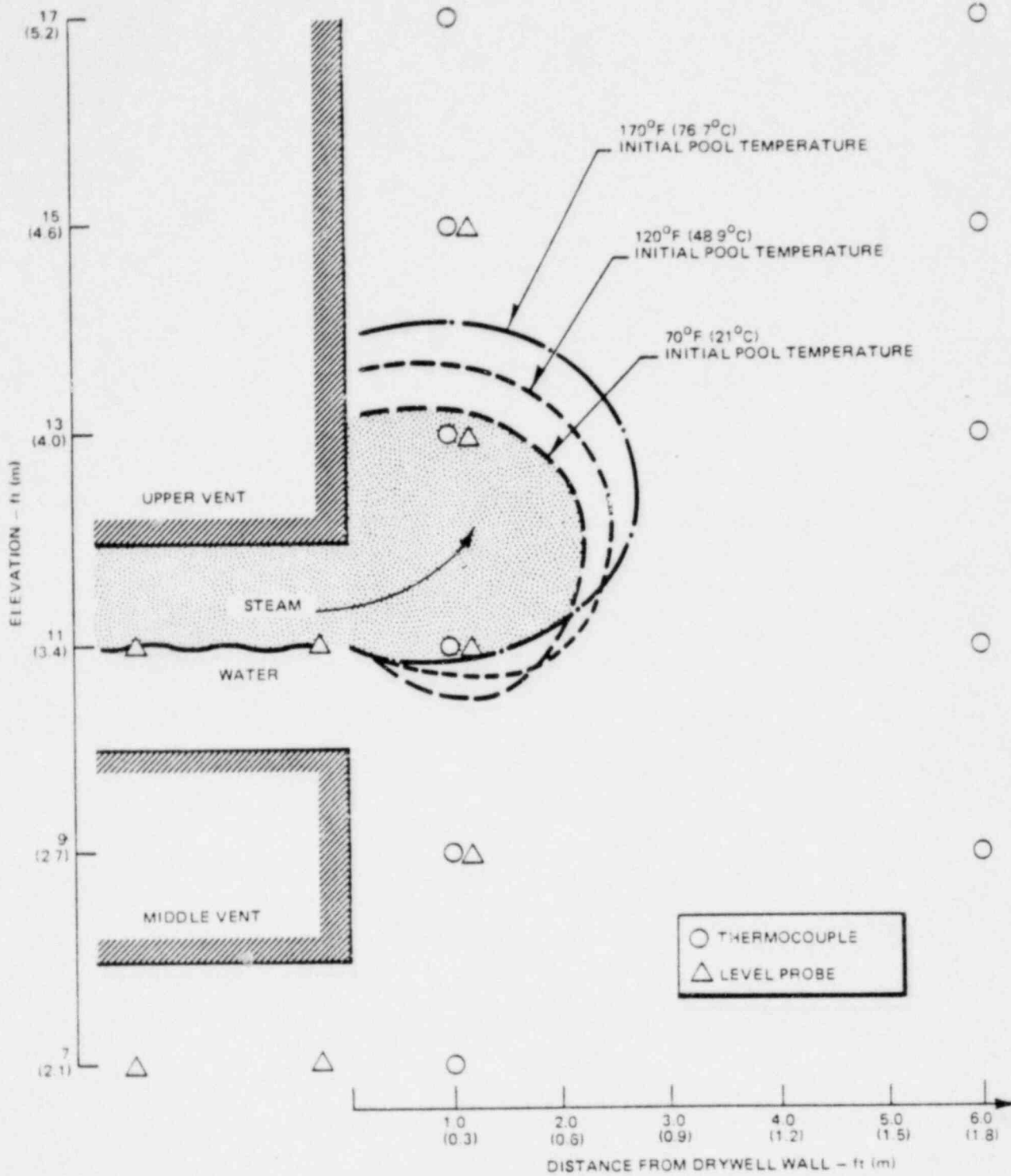


Figure N-4. Postulated Maximum Steam Bubble Travel As a Function of Pool Temperature (Reference Test 5707)

22A4365
Rev. 2

ATTACHMENT 0

DIGITIZATION OF FORCING FUNCTION
FOR
CONDENSATION OSCILLATION

ATTACHMENT O

Mark III Condensation Oscillation Forcing Function for t = 3.0 to 30.0 Second

TIME (SEC)	PRESSURE (PSID)										
3.000	0.	3.513	4.3476	3.997	0.0000	4.462	-3.9782	4.911	0.	5.347	3.6337
3.010	2.8550	3.522	4.5573	4.007	0.1085	4.471	-3.8659	4.920	2.3142	5.355	3.8089
3.021	5.2012	3.532	4.5921	4.016	-0.0129	4.480	-4.0321	4.928	4.2160	5.364	3.8380
3.031	6.6810	3.542	4.2596	4.026	-0.5001	4.489	-4.5403	4.937	5.4155	5.373	3.5601
3.041	7.1869	3.552	3.5169	4.035	-1.3391	4.498	-5.2716	4.946	5.8256	5.381	2.9394
3.052	6.8755	3.562	2.4865	4.044	-2.3703	4.507	-5.9475	4.955	5.5732	5.390	2.0782
3.062	6.0942	3.572	1.4047	4.054	-3.3525	4.517	-6.2168	4.963	4.9399	5.398	1.1740
3.072	5.2487	3.581	0.5246	4.063	-4.0605	4.526	-5.7791	4.972	4.2546	5.407	0.4384
3.083	4.6613	3.591	0.0135	4.073	-4.3774	4.535	-4.4990	4.981	3.7784	5.416	0.0113
3.093	4.4692	3.601	-0.1138	4.082	-4.3442	4.544	-2.4694	4.990	3.6226	5.424	-0.0951
3.104	4.5990	3.611	0.0000	4.092	-4.1443	4.553	0.	4.998	3.7279	5.433	0.0000
3.114	4.8208	3.621	0.1138	4.101	-4.0273	4.562	2.3846	5.007	3.9077	5.441	0.0951
3.124	4.8576	3.631	-0.0135	4.111	-4.2005	4.571	4.3443	5.016	3.9375	5.450	-0.0113
3.135	4.5059	3.641	-0.5246	4.120	-4.7299	4.580	5.5803	5.025	3.6524	5.459	-0.4385
3.145	3.7203	3.650	-1.4048	4.130	-5.4918	4.589	6.0028	5.033	3.0156	5.467	-1.1741
3.155	2.6302	3.660	-2.4866	4.139	-6.1958	4.598	5.7427	5.042	2.1320	5.476	-2.0782
3.166	1.4859	3.670	-3.5170	4.149	-6.4764	4.607	5.0902	5.051	1.2044	5.484	-2.9394
3.176	0.5549	3.680	-4.2597	4.158	-6.0205	4.616	4.3840	5.060	0.4498	5.493	-3.5602
3.186	0.0143	3.690	-4.5921	4.167	-4.6869	4.625	3.8933	5.068	0.0116	5.502	-3.8380
3.197	-0.1204	3.700	-4.5573	4.177	-2.5725	4.634	3.7328	5.077	-0.0976	5.510	-3.8089
3.207	0.0000	3.709	-4.3476	4.186	0.	4.643	3.8413	5.086	0.0000	5.519	-3.6336
3.217	0.1204	3.719	-4.2249	4.196	2.4696	4.652	4.0266	5.095	0.0976	5.527	-3.5311
3.228	-0.0143	3.729	-4.4065	4.205	4.4991	4.660	4.0573	5.103	-0.0116	5.536	-3.6829
3.238	-0.5550	3.739	-4.9619	4.214	5.7792	4.669	3.7635	5.112	-0.4498	5.545	-4.1471
3.248	-1.4860	3.749	-5.7612	4.223	6.2168	4.678	3.1073	5.121	-1.2045	5.553	-4.8151
3.259	-2.6304	3.759	-6.4997	4.232	5.9474	4.687	2.1969	5.130	-2.1321	5.562	-5.4324
3.269	-3.7203	3.768	-6.7941	4.241	5.2716	4.696	1.2411	5.138	-3.0157	5.570	-5.6784
3.280	-4.5060	3.778	-6.3157	4.251	4.5402	4.705	0.4635	5.147	-3.6525	5.579	-5.2786
3.290	-4.8576	3.788	-4.9167	4.260	4.0321	4.714	0.0119	5.156	-3.9375	5.588	-4.1093
3.300	-4.8208	3.798	-2.6987	4.269	3.8659	4.723	-0.1006	5.165	-3.9077	5.596	-2.2555
3.311	-4.5990	3.808	0.	4.278	3.9782	4.732	0.0000	5.173	-3.7279	5.605	0.
3.321	-4.4692	3.817	2.5727	4.287	4.1701	4.741	0.1006	5.182	-3.6226	5.613	2.2071
3.331	-4.6613	3.827	4.6870	4.296	4.2019	4.750	-0.0119	5.191	-3.7784	5.622	4.0209
3.342	-5.2488	3.836	6.0205	4.306	3.8977	4.759	-0.4635	5.200	-4.2546	5.630	5.1649
3.352	-6.0943	3.846	6.4764	4.315	3.2181	4.768	-1.2412	5.208	-4.9399	5.639	5.5560
3.362	-6.8756	3.855	6.1958	4.324	2.2752	4.777	-2.1970	5.217	-5.5732	5.647	5.3153
3.373	-7.1869	3.865	5.4917	4.333	1.2853	4.786	-3.1074	5.226	-5.8256	5.656	4.7113
3.383	-6.6809	3.874	4.7299	4.342	0.4800	4.795	-3.7636	5.235	-5.4155	5.664	4.0577
3.393	-5.2010	3.884	4.2005	4.351	0.0123	4.804	-4.0573	5.243	-4.2159	5.672	3.6035
3.404	-2.8547	3.893	4.0273	4.361	-0.1041	4.812	-4.0266	5.252	-2.3140	5.681	3.4550
3.414	0.	3.902	4.1443	4.370	0.0000	4.821	-3.8413	5.261	0.	5.690	3.5554
3.424	2.6989	3.912	4.3442	4.379	0.1041	4.830	-3.7328	5.269	2.2557	5.698	3.7269
3.434	4.9169	3.921	4.3774	4.388	-0.0124	4.839	-3.8933	5.278	4.1095	5.706	3.7553
3.444	6.3158	3.931	4.0605	4.397	-0.4800	4.848	-4.3941	5.287	5.2787	5.715	3.4834
3.453	6.7941	3.940	3.3525	4.407	-1.2854	4.857	-5.0902	5.295	5.6784	5.723	2.8760
3.463	6.4997	3.950	2.3702	4.416	-2.2753	4.866	-5.7428	5.304	5.4323	5.732	2.0334
3.473	5.7611	3.959	1.3390	4.425	-3.2181	4.875	-6.0028	5.312	4.8150	5.740	1.1487
3.483	4.9618	3.969	0.5000	4.434	-3.8977	4.884	-5.5902	5.321	4.1470	5.749	0.4290
3.493	4.4065	3.978	0.0129	4.443	-4.2019	4.893	-4.3441	5.330	3.6829	5.757	0.0110
3.503	4.2249	3.988	-0.1085	4.452	-4.1701	4.902	-2.3844	5.338	3.5311	5.766	-0.0931

TIME (SEC)	PRESSURE (PSID)										
5.774	0.0000	6.195	-3.4905	6.610	0.	7.019	3.3579	7.425	0.0000	7.828	-3.3085
5.783	0.0931	6.203	-3.3919	6.618	2.1064	7.027	3.5199	7.433	0.0872	7.837	-3.2151
5.791	-0.0111	6.211	-3.5378	6.626	3.8375	7.035	3.5467	7.441	-0.0104	7.845	-3.3533
5.800	-0.4290	6.220	-3.9837	6.634	4.9294	7.044	3.2899	7.450	-0.4018	7.853	-3.7760
5.808	-1.1488	6.228	-4.6253	6.642	5.3026	7.052	2.7163	7.458	-1.0759	7.861	-4.3842
5.817	-2.0335	6.237	-5.2183	6.651	5.0729	7.060	1.9204	7.466	-1.9045	7.869	-4.9462
5.825	-2.8761	6.245	-5.4546	6.659	4.4964	7.068	1.0349	7.474	-2.6938	7.877	-5.1702
5.834	-3.4835	6.253	-5.0706	6.667	3.8726	7.076	0.4051	7.482	-3.2626	7.885	-4.8062
5.842	-3.7553	6.262	-3.9474	6.675	3.4392	7.084	0.0104	7.490	-3.5172	7.893	-3.7416
5.850	-3.7269	6.270	-2.1666	6.683	3.2974	7.092	-0.0879	7.498	-3.4906	7.901	-2.0537
5.859	-3.5554	6.278	0.	6.692	3.3932	7.101	0.0000	7.506	-3.3300	7.909	0.
5.867	-3.4550	6.287	2.1336	6.700	3.5569	7.109	0.0879	7.514	-3.2359	7.917	2.0441
5.876	-3.6035	6.295	3.8870	6.708	3.5840	7.117	-0.0104	7.522	-3.3751	7.925	3.7239
5.884	-4.0577	6.303	4.9929	6.716	3.3245	7.125	-0.4052	7.530	-3.8005	7.933	4.7833
5.893	-4.7113	6.311	5.3710	6.724	2.7449	7.133	-1.0850	7.539	-4.4126	7.941	5.1455
5.901	-5.3153	6.320	5.1383	6.733	1.9406	7.141	-1.9205	7.547	-4.9783	7.949	4.9226
5.910	-5.5560	6.328	4.5544	6.741	1.0963	7.149	-2.7164	7.555	-5.2038	7.957	4.3632
5.918	-5.1649	6.336	3.9225	6.749	0.4094	7.158	-3.2900	7.563	-4.8374	7.965	3.7579
5.927	-4.0208	6.345	3.4835	6.757	0.0105	7.166	-3.5467	7.571	-3.7659	7.973	3.3373
5.935	-2.2069	6.353	3.3399	6.765	-0.0888	7.174	-3.5199	7.579	-2.0670	7.981	3.1997
5.944	0.	6.361	3.4370	6.774	0.0000	7.182	-3.3579	7.587	0.	7.989	3.2927
5.952	2.1668	6.369	3.6027	6.782	0.0888	7.190	-3.2631	7.595	2.0539	7.997	3.4515
5.960	3.9475	6.378	3.6302	6.790	-0.0106	7.198	-3.4034	7.603	3.7417	8.005	3.4779
5.969	5.0707	6.386	3.3674	6.798	-0.4095	7.206	-3.8324	7.611	4.8063	8.013	3.2261
5.977	5.4546	6.394	2.7802	6.806	-1.0964	7.215	-4.4497	7.619	5.1702	8.021	2.6635
5.986	5.2183	6.403	1.9657	6.815	-1.9407	7.223	-5.0201	7.627	4.9462	8.029	1.8831
5.994	4.6253	6.411	1.1104	6.823	-2.7449	7.231	-5.2474	7.635	4.3841	8.037	1.0638
6.002	3.9836	6.419	0.4147	6.831	-3.3246	7.239	-4.8780	7.643	3.7759	8.045	0.3973
6.011	3.5377	6.427	0.0107	6.839	-3.5840	7.247	-3.7975	7.651	3.3533	8.053	0.0102
6.019	3.3919	6.436	-0.0900	6.847	-3.5569	7.255	-2.0843	7.659	3.2151	8.061	-0.0862
6.027	3.4905	6.444	0.0000	6.856	-3.3932	7.263	0.	7.668	3.3085	8.069	0.0000
6.036	3.6588	6.452	0.0900	6.864	-3.2974	7.272	2.0672	7.676	3.4681	8.077	0.0862
6.044	3.6868	6.460	-0.0107	6.872	-3.4392	7.280	3.7660	7.684	3.4945	8.085	-0.0102
6.052	3.4198	6.469	-0.4147	6.880	-3.8727	7.288	4.8375	7.692	3.2415	8.093	-0.3973
6.061	2.8235	6.477	-1.1105	6.888	-4.4965	7.296	5.2038	7.700	2.6763	8.101	-1.0639
6.069	1.9963	6.485	-1.9657	6.897	-5.0729	7.304	4.9783	7.708	1.8922	8.109	-1.8832
6.078	1.1277	6.494	-2.7803	6.905	-5.3026	7.312	4.4126	7.716	1.0689	8.117	-2.6636
6.086	0.4211	6.502	-3.3674	6.913	-4.9293	7.320	3.8004	7.724	0.3992	8.125	-3.2261
6.094	0.0108	6.510	-3.6302	6.921	-3.8374	7.328	3.3751	7.732	0.0103	8.133	-3.4779
6.103	-0.0914	6.518	-3.6027	6.930	-2.1063	7.336	3.2359	7.740	-0.0866	8.141	-3.4515
6.111	0.0000	6.527	-3.4369	6.938	0.	7.344	3.3300	7.748	0.0000	8.149	-3.2927
6.119	0.0914	6.535	-3.3399	6.946	2.0845	7.352	3.4906	7.756	0.0866	8.157	-3.1997
6.128	-0.0109	6.543	-3.4835	6.954	3.7976	7.361	3.5172	7.764	-0.0103	8.165	-3.3373
6.136	-0.4212	6.552	-3.9226	6.962	4.8781	7.369	3.2626	7.772	-0.3992	8.173	-3.7579
6.144	-1.1278	6.560	-4.5544	6.970	5.2474	7.377	2.6937	7.780	-1.0690	8.181	-4.3632
6.153	-1.9963	6.568	-5.1383	6.978	5.0201	7.385	1.9045	7.788	-1.8923	8.189	-4.9226
6.161	-2.8236	6.576	-5.3710	6.987	4.4496	7.393	1.0759	7.796	-2.6764	8.197	-5.1455
6.170	-3.4199	6.585	-4.9928	6.995	3.8323	7.401	0.4018	7.804	-3.2416	8.205	-4.7833
6.178	-3.6868	6.593	-3.8869	7.003	3.4034	7.409	0.0103	7.812	-3.4945	8.213	-3.7237
6.186	-3.6588	6.601	-2.1334	7.011	3.2631	7.417	-0.0872	7.820	-3.4681	8.221	-2.0439

101678

22-A-365
Rev. 2

0-2

TIME (SEC)	PRESSURE (PSID)										
8.229	0.	8.628	3.2757	9.026	0.0000	9.422	-3.2748	9.818	0.	10.213	3.2972
8.237	2.0374	8.636	3.4337	9.034	0.0857	9.430	-3.1824	9.826	2.0405	10.221	3.4562
8.245	3.7117	8.644	3.4599	9.042	-0.0102	9.438	-3.3192	9.834	3.7174	10.229	3.4826
8.253	4.7577	8.652	3.2094	9.049	-0.3950	9.446	-3.7376	9.842	4.7751	10.237	3.2305
8.261	5.1287	8.660	2.6498	9.057	-1.0577	9.454	-4.3396	9.849	5.1366	10.245	2.6672
8.269	4.9065	8.668	1.8734	9.065	-1.8722	9.462	-4.8960	9.857	4.9141	10.253	1.8857
8.277	4.3490	8.676	1.0583	9.073	-2.6481	9.470	-5.1176	9.865	4.3557	10.260	1.0653
8.285	3.7456	8.684	0.3952	9.081	-3.2073	9.478	-4.7574	9.873	3.7514	10.268	0.3978
8.293	3.3264	8.692	0.0102	9.089	-3.4576	9.485	-3.7036	9.881	3.3315	10.276	0.0102
8.301	3.1893	8.700	-0.0858	9.097	-3.4314	9.493	-2.0328	9.889	3.1942	10.284	-0.0863
8.309	3.2820	8.708	0.0000	9.105	-3.2735	9.501	0.	9.897	3.2870	10.292	0.0000
8.317	3.4403	8.716	0.0858	9.113	-3.1811	9.509	2.0358	9.905	3.4456	10.300	0.0863
8.325	3.4665	8.724	-0.0102	9.121	-3.3178	9.517	3.7089	9.913	3.4719	10.308	-0.0103
8.333	3.2155	8.732	-0.3953	9.129	-3.7360	9.525	4.7641	9.921	3.2205	10.316	-0.3979
8.341	2.6549	8.740	-1.0584	9.137	-4.3378	9.533	5.1249	9.928	2.6589	10.324	-1.0654
8.349	1.8770	8.748	-1.8735	9.145	-4.8939	9.541	4.9028	9.936	1.8799	10.332	-1.8858
8.357	1.0604	8.755	-2.6499	9.153	-5.1155	9.549	4.3457	9.944	1.0620	10.339	-2.6673
8.365	0.3960	8.763	-3.2094	9.161	-4.7554	9.557	3.7428	9.952	0.3966	10.347	-3.2305
8.373	0.0102	8.771	-3.4599	9.169	-3.7020	9.565	3.3239	9.960	0.0102	10.355	-3.4826
8.381	-0.0859	8.779	-3.4337	9.176	-2.0319	9.573	3.1869	9.968	-0.0860	10.363	-3.4562
8.389	0.0000	8.787	-3.2757	9.184	0.	9.580	3.2795	9.976	0.0000	10.371	-3.2972
8.397	0.0859	8.795	-3.1832	9.192	2.0330	9.588	3.4377	9.984	0.0860	10.379	-3.2041
8.405	-0.0102	8.803	-3.3201	9.200	3.7037	9.596	3.4639	9.992	-0.0102	10.387	-3.3419
8.413	-0.3960	8.811	-3.7386	9.208	4.7574	9.604	3.2131	10.000	-0.3966	10.395	-3.7631
8.421	-1.0604	8.819	-4.3407	9.216	5.1176	9.612	2.6528	10.008	-1.0621	10.403	-4.3692
8.429	-1.8771	8.827	-4.8972	9.224	4.8959	9.620	1.8756	10.015	-1.8800	10.411	-4.9294
8.437	-2.6549	8.835	-5.1190	9.232	4.3396	9.628	1.0596	10.023	-2.6590	10.418	-5.1526
8.445	-3.2156	8.843	-4.7586	9.240	3.7375	9.636	0.3957	10.031	-3.2205	10.426	-4.7898
8.453	-3.4665	8.851	-3.7045	9.248	3.3192	9.644	0.0102	10.039	-3.4719	10.434	-3.7288
8.461	-3.4402	8.859	-2.0333	9.256	3.1824	9.652	-0.0859	10.047	-3.4455	10.442	-2.0467
8.469	-3.2819	8.867	0.	9.264	3.2749	9.660	0.0000	10.055	-3.2870	10.450	0.
8.477	-3.1893	8.875	2.0321	9.272	3.4328	9.667	0.0859	10.063	-3.1942	10.458	2.0547
8.485	-3.3264	8.883	3.7021	9.279	3.4590	9.675	-0.0102	10.071	-3.3315	10.466	3.7432
8.493	-3.7457	8.891	4.7554	9.287	3.2086	9.683	-0.3957	10.079	-3.7515	10.474	4.8082
8.501	-4.3490	8.899	5.1155	9.295	2.6491	9.691	-1.0596	10.087	-4.3557	10.482	5.1722
8.509	-4.9066	8.907	4.8939	9.303	1.8729	9.699	-1.8757	10.094	-4.9141	10.490	4.9481
8.517	-5.1287	8.915	4.3377	9.311	1.0581	9.707	-2.6529	10.102	-5.1366	10.497	4.3858
8.525	-4.7677	8.922	3.7360	9.319	0.3951	9.715	-3.2131	10.110	-4.7750	10.505	3.7774
8.533	-3.7116	8.930	3.3178	9.327	0.0102	9.723	-3.4639	10.118	-3.7173	10.513	3.3546
8.541	-2.0372	8.938	3.1811	9.335	-0.0857	9.731	-3.4376	10.126	-2.0403	10.521	3.2163
8.549	0.	8.946	3.2735	9.343	0.0000	9.739	-3.2795	10.134	0.	10.529	3.3098
8.557	2.0335	8.954	3.4314	9.351	0.0857	9.747	-3.1869	10.142	2.0468	10.537	3.4694
8.565	3.7046	8.962	3.4576	9.359	-0.0102	9.755	-3.3239	10.150	3.7290	10.545	3.4959
8.572	4.7587	8.970	3.2072	9.367	-0.3952	9.762	-3.7428	10.158	4.7899	10.553	3.2428
8.580	5.1190	8.978	2.6480	9.375	-1.0581	9.770	-4.3457	10.166	5.1526	10.561	2.6774
8.588	4.8972	8.986	1.8722	9.382	-1.8730	9.778	-4.9029	10.174	4.9293	10.569	1.8929
8.596	4.3407	8.994	1.0576	9.390	-2.6492	9.786	-5.1249	10.181	4.3692	10.576	1.0694
8.604	3.7385	9.002	0.3950	9.398	-3.2086	9.794	-4.7641	10.189	3.7630	10.584	0.3993
8.612	3.3201	9.010	0.0102	9.406	-3.4590	9.802	-3.7088	10.197	3.3418	10.592	0.0103
8.620	3.1832	9.018	0.857	9.414	-3.4328	9.810	-2.0357	10.205	3.2041	10.600	-0.0866

101678

22A4365
Rev. 2

TIME (SEC)	PRESSURE (PSID)										
10.608	0.0000	11.003	-3.3245	11.399	0.	11.794	3.3801	12.191	0.0000	12.588	-3.4249
10.616	0.0466	11.011	-3.2307	11.406	2.0858	11.802	3.5431	12.199	0.0891	12.596	-3.3282
10.624	-0.0133	11.019	-3.3696	11.414	3.7998	11.810	3.5702	12.207	-0.0106	12.604	-3.4713
10.632	-0.3994	11.027	-3.7943	11.422	4.8809	11.818	3.3117	12.215	-0.4105	12.612	-3.9088
10.640	-1.0694	11.035	-4.4055	11.430	5.2505	11.826	2.7342	12.223	-1.0992	12.620	-4.5394
10.648	-1.8930	11.043	-4.9703	11.438	5.0230	11.834	1.9331	12.230	-1.9456	12.628	-5.1203
10.656	-2.6774	11.051	-5.1953	11.446	4.4522	11.842	1.0921	12.238	-2.7519	12.636	-5.3521
10.663	-3.2428	11.059	-4.8296	11.454	3.8346	11.850	0.4078	12.246	-3.3330	12.644	-4.9753
10.671	-3.4959	11.066	-3.7598	11.462	3.4054	11.858	0.0105	12.254	-3.5931	12.652	-3.8732
10.679	-3.4694	11.074	-2.0636	11.470	3.2650	11.866	-0.0895	12.262	-3.5659	12.660	-2.1259
10.687	-3.3098	11.082	0.	11.478	3.3599	11.874	0.0000	12.270	-3.4018	12.667	0.
10.695	-3.2163	11.090	2.0742	11.486	3.5219	11.882	0.0895	12.278	-3.3058	12.675	2.1412
10.703	-3.3546	11.098	3.7788	11.494	3.5488	11.889	-0.0105	12.286	-3.4479	12.683	3.9009
10.711	-3.7774	11.106	4.8540	11.501	3.2919	11.897	-0.4079	12.294	-3.8825	12.691	5.0108
10.719	-4.3859	11.114	5.2215	11.509	2.7179	11.905	-1.0921	12.302	-4.5078	12.699	5.3902
10.727	-4.9482	11.122	4.9953	11.517	1.9216	11.913	-1.9332	12.310	-5.0857	12.707	5.1567
10.735	-5.1722	11.130	4.4276	11.525	1.0855	11.921	-2.7343	12.318	-5.3160	12.715	4.5707
10.742	-4.8081	11.138	3.8134	11.533	0.4054	11.929	-3.3117	12.326	-4.9418	12.723	3.9366
10.750	-3.7431	11.146	3.3865	11.541	0.0104	11.937	-3.5702	12.334	-3.8471	12.731	3.4960
10.758	-2.0545	11.153	3.2470	11.549	-0.0880	11.945	-3.5431	12.342	-2.1116	12.739	3.3519
10.766	0.	11.161	3.3413	11.557	0.0000	11.953	-3.3801	12.350	0.	12.747	3.4493
10.774	2.0638	11.169	3.5025	11.565	0.0880	11.961	-3.2846	12.357	2.1261	12.755	3.6156
10.782	3.7599	11.177	3.5292	11.573	-0.0104	11.969	-3.4259	12.365	3.8734	12.763	3.6432
10.790	4.8296	11.185	3.2737	11.581	-0.4054	11.977	-3.8577	12.373	4.9754	12.771	3.3795
10.798	5.1953	11.193	2.7029	11.589	-1.0856	11.985	-4.4791	12.381	5.3521	12.779	2.7902
10.806	4.9702	11.201	1.9109	11.596	-1.9216	11.992	-5.0533	12.389	5.1202	12.787	1.9727
10.814	4.4054	11.209	1.0795	11.604	-2.7180	12.000	-5.2821	12.397	4.5384	12.795	1.1144
10.821	3.7942	11.217	0.4031	11.612	-3.2919	12.008	-4.9102	12.405	3.9088	12.803	0.4162
10.829	3.3696	11.225	0.0104	11.620	-3.5488	12.016	-3.8226	12.413	3.4713	12.811	0.0107
10.837	3.2307	11.232	-0.0875	11.628	-3.5219	12.024	-2.0981	12.421	3.3282	12.819	-0.0903
10.845	3.3246	11.240	0.0000	11.636	-3.3599	12.032	0.	12.429	3.4249	12.827	0.0000
10.853	3.4849	11.248	0.0875	11.644	-3.2650	12.040	2.1118	12.437	3.5901	12.835	0.0903
10.861	3.5115	11.256	-0.0104	11.652	-3.4054	12.048	3.8473	12.445	3.6175	12.843	-0.0107
10.869	3.2573	11.264	-0.4032	11.660	-3.8346	12.056	4.9418	12.453	3.3556	12.851	-0.4162
10.877	2.6893	11.272	-1.0796	11.668	-4.4523	12.064	5.3160	12.461	2.7705	12.859	-1.1145
10.885	1.9014	11.280	-1.9110	11.676	-5.0230	12.072	5.0857	12.469	1.9588	12.867	-1.9728
10.893	1.0741	11.288	-2.7029	11.683	-5.2505	12.080	4.5078	12.477	1.1065	12.875	-2.7903
10.900	0.4011	11.296	-3.2737	11.691	-4.8809	12.088	3.8924	12.485	0.4132	12.883	-3.3795
10.908	0.0103	11.304	-3.5292	11.699	-3.7997	12.096	3.4479	12.493	0.0106	12.890	-3.6432
10.916	-0.0870	11.312	-3.5025	11.707	-2.0856	12.104	3.3058	12.501	-0.0897	12.898	-3.6156
10.924	0.0000	11.319	-3.3413	11.715	0.	12.111	3.4018	12.509	0.0000	12.906	-3.4493
10.932	0.0870	11.327	-3.2470	11.723	2.0983	12.119	3.5659	12.516	0.0897	12.914	-3.3519
10.940	-0.0103	11.335	-3.3866	11.731	3.8227	12.127	3.5931	12.524	-0.0107	12.922	-3.4960
10.948	-0.4012	11.343	-3.8134	11.739	4.9103	12.135	3.3329	12.532	-0.4133	12.930	-3.9366
10.956	-1.0742	11.351	-4.4277	11.747	5.2821	12.143	2.7518	12.540	-1.1066	12.938	-4.5707
10.964	-1.9014	11.359	-4.9953	11.755	5.0532	12.151	1.9455	12.548	-1.9588	12.946	-5.1567
10.972	-2.6894	11.367	-5.2215	11.763	4.4790	12.159	1.0991	12.556	-2.7706	12.954	-5.3902
10.979	-3.2573	11.375	-4.8539	11.771	3.8576	12.167	0.4104	12.564	-3.3556	12.962	-5.0107
10.987	-3.5115	11.383	-3.7787	11.779	3.4258	12.175	0.0106	12.572	-3.6175	12.970	-3.9008
10.995	-3.4849	11.391	-2.0740	11.786	3.2846	12.183	-0.0891	12.580	-3.5901		

TIME (SEC)	PRESSURE (PSID)										
12.985	0.	13.385	3.5014	13.786	0.0000	14.187	-3.5574	14.590	0.	14.995	3.6474
12.994	2.1571	13.393	3.6703	13.794	0.0924	14.195	-3.4569	14.599	2.2452	15.003	3.8233
13.002	3.9298	13.401	3.6983	13.802	-0.0110	14.203	-3.6056	14.607	4.0903	15.011	3.8525
13.010	5.0479	13.409	3.4305	13.810	-0.4258	14.211	-4.0690	14.615	5.2540	15.020	3.5736
13.018	5.4301	13.417	2.8324	13.819	-1.1402	14.220	-4.7140	14.623	5.6518	15.028	2.9505
13.026	5.1948	13.425	2.0025	13.826	-2.0183	14.228	-5.3193	14.631	5.4069	15.036	2.0860
13.034	4.6045	13.433	1.1313	13.834	-2.8547	14.236	-5.5592	14.639	4.7925	15.044	1.1784
13.042	3.9657	13.441	0.4225	13.842	-3.4576	14.244	-5.1678	14.647	4.1277	15.052	0.4401
13.050	3.5218	13.449	0.0109	13.850	-3.7274	14.252	-4.0231	14.655	3.6657	15.060	0.0113
13.058	3.3767	13.457	-0.0917	13.858	-3.6991	14.260	-2.2082	14.663	3.5146	15.068	-0.0955
13.066	3.4748	13.465	0.0000	13.866	-3.5289	14.268	0.	14.671	3.6167	15.076	0.0000
13.074	3.6424	13.473	0.0917	13.874	-3.4293	14.276	2.2265	14.679	3.7911	15.084	0.0955
13.082	3.6702	13.481	-0.0109	13.882	-3.5767	14.284	4.0563	14.687	3.8201	15.093	-0.0113
13.090	3.4045	13.489	-0.4225	13.890	-4.0276	14.292	5.2104	14.696	3.5435	15.101	-0.4401
13.098	2.8108	13.497	-1.1313	13.898	-4.6763	14.300	5.6049	14.704	2.9256	15.109	-1.1785
13.106	1.9873	13.505	-2.0026	13.906	-5.2758	14.308	5.3521	14.712	2.0684	15.117	-2.0861
13.114	1.1227	13.513	-2.8324	13.914	-5.5147	14.316	4.7527	14.720	1.1685	15.125	-2.9505
13.122	0.4192	13.521	-3.4305	13.922	-5.1265	14.324	4.0934	14.728	0.4364	15.133	-3.5736
13.130	0.0108	13.529	-3.6983	13.930	-3.9909	14.332	3.6352	14.736	0.0112	15.141	-3.8525
13.138	-0.0910	13.537	-3.6703	13.938	-2.1905	14.340	3.4954	14.744	-0.0947	15.149	-3.8233
13.146	0.0000	13.545	-3.5014	13.946	0.	14.348	3.5467	14.752	0.0000	15.158	-3.6474
13.154	0.0910	13.553	-3.4025	13.954	2.2084	14.357	3.7597	14.760	0.0947	15.166	-3.5444
13.162	-0.0108	13.561	-3.5488	13.962	4.0232	14.365	3.7884	14.768	-0.0112	15.174	-3.6968
13.170	-0.4193	13.569	-3.9961	13.970	5.1679	14.373	3.5141	14.776	-0.4364	15.182	-4.1628
13.178	-1.1227	13.577	-4.6398	13.978	5.5592	14.381	2.9013	14.785	-1.1686	15.190	-4.8333
13.186	-1.9874	13.585	-5.2346	13.986	5.3183	14.389	2.0513	14.793	-2.0685	15.198	-5.4529
13.194	-2.8109	13.593	-5.4716	13.994	4.7139	14.397	1.1588	14.801	-2.9257	15.206	-5.6998
13.202	-3.4045	13.601	-5.0864	14.002	4.0600	14.405	0.4327	14.809	-3.5435	15.214	-5.2985
13.210	-3.6702	13.609	-3.9597	14.010	3.6056	14.413	0.0111	14.817	-3.8201	15.222	-4.1249
13.218	-3.6424	13.617	-2.1734	14.018	3.4569	14.421	-0.0939	14.825	-3.7911	15.231	-2.2640
13.226	-3.4748	13.625	0.	14.027	3.5574	14.429	0.0000	14.833	-3.6167	15.239	0.
13.233	-3.3767	13.633	2.1907	14.035	3.7290	14.437	0.0939	14.841	-3.5146	15.247	2.2837
13.241	-3.5219	13.641	3.9910	14.043	3.7574	14.445	-0.0112	14.849	-3.6657	15.255	4.1605
13.249	-3.9658	13.649	5.1265	14.051	3.4854	14.453	-0.4328	14.857	-4.1277	15.263	5.3442
13.257	-4.6046	13.657	5.5147	14.059	2.8777	14.461	-1.1589	14.865	-4.7926	15.271	5.7489
13.265	-5.1949	13.665	5.2758	14.067	2.0345	14.469	-2.0514	14.874	-5.4070	15.279	5.4997
13.273	-5.4301	13.673	4.6762	14.075	1.1493	14.477	-2.9014	14.882	-5.6518	15.288	4.8748
13.281	-5.0478	13.681	4.0275	14.083	0.4292	14.486	-3.5141	14.890	-5.2539	15.296	4.1985
13.289	-3.9297	13.689	3.5767	14.091	0.0110	14.494	-3.7884	14.898	-4.0901	15.304	3.7285
13.297	-2.1569	13.697	3.4293	14.099	-0.0931	14.502	-3.7596	14.906	-2.2450	15.312	3.5749
13.305	0.	13.706	3.5289	14.107	0.0000	14.510	-3.5866	14.914	0.	15.320	3.6787
13.313	2.1736	13.714	3.6992	14.115	0.0931	14.518	-3.4454	14.922	2.2642	15.328	3.8562
13.321	3.9599	13.722	3.7274	14.123	-0.0111	14.526	-3.6353	14.930	4.1250	15.336	3.8856
13.329	5.0865	13.730	3.4575	14.131	-0.4293	14.534	-4.0934	14.938	5.2986	15.345	3.6043
13.337	5.4716	13.738	2.8546	14.139	-1.1494	14.542	-4.7528	14.946	5.6998	15.353	2.9758
13.345	5.2346	13.746	2.0183	14.147	-2.0346	14.550	-5.3521	14.955	5.4529	15.361	2.1039
13.353	4.6397	13.754	1.1402	14.155	-2.8777	14.558	-5.6049	14.963	4.8332	15.369	1.1886
13.361	3.9961	13.762	0.4258	14.163	-3.4854	14.566	-5.2103	14.971	4.1627	15.377	0.4439
13.369	3.5408	13.770	0.0110	14.171	-3.7574	14.574	-4.0562	14.979	3.6968	15.385	0.0114
13.377	3.4025	13.778	-0.0924	14.179	-3.7290	14.582	-2.2263	14.987	3.5444	15.393	-0.0963

22A4365
Rev. 2

TIME (SEC)	PRESSURE (PSID)										
15.402	0.0000	15.810	-3.7106	16.220	0.	16.632	3.8094	17.046	0.0000	17.462	-3.8773
15.410	0.0963	15.818	-3.6059	16.228	2.3441	16.640	3.9932	17.054	0.1006	17.470	-3.7679
15.418	-0.0114	15.826	-3.7609	16.236	4.2705	16.648	4.0236	17.062	-0.0120	17.479	-3.9299
15.426	-0.4439	15.834	-4.2350	16.244	5.4855	16.656	3.7323	17.071	-0.4638	17.487	-4.4252
15.434	-1.1886	15.842	-4.9171	16.252	5.9009	16.665	3.0915	17.079	-1.2418	17.495	-5.1380
15.442	-2.1040	15.851	-5.5475	16.261	5.6452	16.673	2.1787	17.087	-2.1981	17.504	-5.7967
15.450	-2.9759	15.859	-5.7987	16.269	5.0037	16.681	1.2308	17.095	-3.1089	17.512	-6.0591
15.459	-3.6043	15.867	-5.3904	16.277	4.3095	16.689	0.4596	17.104	-3.7655	17.520	-5.6326
15.467	-3.8856	15.875	-4.1964	16.285	3.8272	16.698	0.0118	17.112	-4.0593	17.529	-4.3849
15.475	-3.8562	15.883	-2.3033	16.294	3.6694	16.706	-0.0997	17.120	-4.0286	17.537	-2.4068
15.483	-3.6787	15.891	0.	16.302	3.7760	16.714	0.0000	17.129	-3.8432	17.545	0.
15.491	-3.5749	15.900	2.3237	16.310	3.9582	16.723	0.0997	17.137	-3.7347	17.554	2.4284
15.499	-3.7286	15.908	4.2333	16.318	3.9884	16.731	-0.0118	17.145	-3.8953	17.562	4.4240
15.507	-4.1985	15.916	5.4377	16.327	3.6996	16.739	-0.4597	17.154	-4.3862	17.570	5.6827
15.516	-4.8748	15.924	5.8494	16.335	3.0545	16.747	-1.2309	17.162	-5.0927	17.579	6.1130
15.524	-5.4998	15.932	5.5960	16.343	2.1596	16.756	-2.1788	17.170	-5.7456	17.587	5.8482
15.532	-5.7488	15.941	4.9601	16.351	1.2200	16.764	-3.0816	17.179	-6.0058	17.595	5.1835
15.540	-5.3441	15.949	4.2719	16.360	0.4556	16.772	-3.7324	17.187	-5.5830	17.604	4.4645
15.548	-4.1603	15.957	3.7938	16.368	0.0117	16.780	-3.0237	17.195	-4.3463	17.612	3.9648
15.556	-2.2835	15.965	3.6374	16.376	-0.0988	16.789	-3.9931	17.203	-2.3856	17.621	3.8014
15.564	0.	15.973	3.7431	16.384	0.0000	16.797	-3.8094	17.212	0.	17.629	3.9118
15.573	2.3035	15.982	3.9237	16.392	0.0989	16.805	-3.7019	17.220	2.4070	17.637	4.1005
15.581	4.1966	15.990	3.9536	16.401	-0.0117	16.813	-3.8610	17.228	4.3851	17.646	4.1318
15.589	5.3905	15.998	3.6673	16.409	-0.4557	16.822	-4.3477	17.237	5.6327	17.654	3.8326
15.597	5.7987	16.006	3.0279	16.417	-1.2201	16.830	-5.0480	17.245	6.0591	17.662	3.1644
15.605	5.5474	16.014	2.1407	16.425	-2.1597	16.838	-5.6951	17.253	5.7965	17.671	2.2372
15.613	4.9171	16.023	1.2094	16.434	-3.0546	16.847	-5.9530	17.262	5.1379	17.679	1.2639
15.622	4.2349	16.031	0.4516	16.442	-3.6997	16.855	-5.5339	17.270	4.4251	17.688	0.4720
15.630	3.7609	16.039	0.0116	16.450	-3.9884	16.863	-4.3081	17.278	3.9298	17.696	0.0121
15.639	3.6059	16.047	-0.0980	16.458	-3.9582	16.871	-2.3546	17.287	3.7679	17.704	-0.1024
15.646	3.7107	16.055	0.0000	16.467	-3.7760	16.880	0.	17.295	3.6773	17.713	0.0000
15.654	3.8896	16.064	0.0980	16.475	-3.6694	16.888	2.3358	17.303	4.0644	17.721	0.1024
15.663	3.9193	16.072	-0.0116	16.483	-3.8272	16.896	4.3464	17.312	4.0954	17.729	-0.0122
15.671	3.6356	16.080	-0.4517	16.491	-4.3096	16.905	5.5831	17.320	3.7989	17.738	-0.4720
15.679	3.0016	16.088	-1.2094	16.500	-5.0038	16.913	6.0058	17.328	3.1365	17.746	-1.2639
15.687	2.1222	16.096	-2.1408	16.508	-5.6452	16.921	5.7456	17.337	2.8175	17.755	-2.2373
15.695	1.1989	16.105	-3.0280	16.516	-5.9009	16.929	5.0927	17.345	1.2527	17.763	-3.1644
15.703	0.4477	16.113	-3.6674	16.524	-5.4854	16.938	4.3862	17.353	0.4678	17.771	-3.8327
15.712	0.0115	16.121	-3.9536	16.532	-4.2703	16.946	3.8952	17.362	0.0120	17.780	-4.1319
15.720	-0.0971	16.129	-3.9236	16.541	-2.3439	16.954	3.7347	17.370	-0.1015	17.788	-4.1005
15.728	0.0000	16.137	-3.7431	16.549	0.	16.963	3.8432	17.378	0.0000	17.796	-3.9118
15.736	0.0971	16.146	-3.6374	16.557	2.3648	16.971	4.0286	17.387	0.1015	17.805	-3.8014
15.744	-0.0115	16.154	-3.7938	16.565	4.3082	16.979	4.0593	17.395	-0.0121	17.813	-3.9649
15.752	-0.4478	16.162	-4.2720	16.574	5.5340	16.988	3.7654	17.403	-0.4679	17.822	-4.4645
15.761	-1.1990	16.170	-4.9601	16.582	5.9530	16.996	3.1089	17.412	-1.2528	17.830	-5.1837
15.769	-2.1223	16.179	-5.5960	16.590	5.6951	17.004	2.1940	17.420	-2.2176	17.838	-5.8482
15.777	-3.0017	16.187	-5.8494	16.599	5.0479	17.012	1.2417	17.428	-3.1366	17.847	-6.1130
15.785	-3.6356	16.195	-5.4376	16.607	4.3476	17.021	0.4637	17.437	-3.7939	17.855	-5.6826
15.793	-3.9193	16.203	-4.2331	16.615	3.8610	17.029	0.0119	17.445	-4.0954	17.863	-4.4239
15.801	-3.8896	16.211	-2.3235	16.623	3.7019	17.037	-0.1006	17.454	-4.0643		

22A365
Rev. 2

TIME (SEC)	PRESSURE (PSID)												
17.889	0.	18.301	3.9816	18.725	0.0000	19.150	-4.0524	19.579	0.	20.010	4.1599		
17.889	2.4500	18.310	4.1737	18.733	0.1052	19.159	-3.9380	19.597	2.5601	20.019	4.3606		
17.897	4.4634	18.318	4.2055	18.742	-0.0125	19.167	-4.1073	19.596	4.6639	20.027	4.3939		
17.905	5.7332	18.327	3.9010	18.750	-0.4847	19.176	-4.6250	19.605	5.9909	20.036	4.0757		
17.914	6.1673	18.335	3.2208	18.758	-1.2979	19.184	-5.3695	19.613	6.4445	20.045	3.3651		
17.922	5.9001	18.343	2.2771	18.767	-2.2974	19.193	-6.0584	19.622	6.1653	20.053	2.3791		
17.931	5.2297	18.352	1.2864	18.775	-3.2494	19.202	-6.3327	19.630	5.4647	20.062	1.3440		
17.939	4.5041	18.360	0.4804	18.784	-3.9356	19.210	-5.8869	19.639	4.7066	20.071	0.5019		
17.947	4.0000	18.369	0.0124	18.792	-4.2428	19.219	-4.5829	19.648	4.1798	20.079	0.0129		
17.956	3.8351	18.377	-0.1042	18.801	-4.2106	19.227	-2.5154	19.656	4.0075	20.088	-0.1089		
17.964	3.9466	18.386	0.0000	18.809	-4.0169	19.236	0.	19.665	4.1239	20.097	0.0000		
17.973	4.1369	18.394	0.1042	18.818	-3.9035	19.244	2.5378	19.674	4.3228	20.105	0.1089		
17.981	4.1685	18.403	-0.0124	18.826	-4.0713	19.253	4.6234	19.682	4.3558	20.114	-0.0129		
17.990	3.8667	18.411	-0.4805	18.835	-4.5845	19.261	5.9388	19.691	4.0405	20.123	-0.5020		
17.998	3.1925	18.419	-1.2865	18.843	-5.3229	19.270	6.3885	19.699	3.3359	20.131	-1.3441		
18.006	2.2571	18.428	-2.2772	18.852	-6.0053	19.279	6.1117	19.708	2.3585	20.140	-2.3792		
18.015	1.2751	18.436	-3.2209	18.860	-6.2772	19.287	5.4172	19.717	1.3324	20.149	-3.3652		
18.023	0.4762	18.445	-3.9011	18.869	-5.8353	19.296	4.6656	19.725	0.4976	20.157	-4.0758		
18.032	0.0122	18.453	-4.2055	18.877	-4.5427	19.304	4.1434	19.734	0.0128	20.166	-4.3939		
18.040	-0.1033	18.462	-4.1736	18.886	-2.4934	19.313	3.9726	19.742	-0.1080	20.175	-4.3606		
18.048	0.0000	18.470	-3.9816	18.894	0.	19.321	4.0981	19.751	0.0000	20.183	-4.1599		
18.057	0.1033	18.479	-3.8692	18.903	2.5157	19.330	4.2853	19.760	0.1080	20.192	-4.0425		
18.065	-0.0123	18.487	-4.0356	18.911	4.5830	19.339	4.3180	19.769	-0.0128	20.201	-4.2163		
18.074	-0.4762	18.496	-4.5442	18.920	5.8870	19.347	4.0053	19.777	-0.4976	20.209	-4.7477		
18.082	-1.2752	18.504	-1.2762	18.928	6.3327	19.356	3.3069	19.786	-1.3325	20.218	-5.5125		
18.090	-2.2572	18.512	-5.9526	18.937	6.0583	19.364	2.3380	19.794	-2.3586	20.227	-6.2191		
18.099	-3.1926	18.521	-6.2221	18.946	5.3699	19.373	1.3208	19.803	-3.3360	20.235	-6.5007		
18.107	-3.8667	18.529	-5.7841	18.954	4.6249	19.381	0.4932	19.811	-4.0405	20.244	-6.0431		
18.116	-4.1685	18.538	-4.5028	18.963	4.1073	19.390	0.0127	19.820	-4.3558	20.253	-4.7045		
18.124	-4.1369	18.546	-2.4715	18.971	3.9380	19.399	-0.1070	19.829	-4.3228	20.261	-2.5822		
18.133	-3.9466	18.555	0.	18.980	4.0524	19.407	0.0000	19.837	-4.1239	20.270	0.		
18.141	-3.8351	18.563	2.4936	18.988	4.2479	19.416	0.1070	19.846	-4.0075	20.279	2.6048		
18.149	-4.0000	18.572	4.5429	18.997	4.2803	19.424	-0.0127	19.855	-4.1798	20.288	4.7455		
18.158	-4.5042	18.580	5.8354	19.005	3.9704	19.433	-0.4933	19.863	-4.7066	20.296	6.0957		
18.166	-5.2297	18.589	6.2772	19.014	3.2781	19.441	-1.3209	19.872	-5.4647	20.305	6.5572		
18.175	-5.9002	18.597	6.0053	19.022	2.3176	19.450	-2.3181	19.880	-6.1653	20.314	6.2731		
18.183	-6.1673	18.606	5.3228	19.031	1.3093	19.459	-3.3070	19.889	-6.4445	20.322	5.5602		
18.191	-5.7332	18.614	4.5844	19.039	0.4889	19.467	-4.0054	19.898	-5.9908	20.331	4.7889		
18.200	-4.4632	18.623	4.0713	19.048	0.0126	19.476	-4.3180	19.906	-4.6638	20.340	4.2529		
18.208	-2.4498	18.631	3.9035	19.056	-0.1061	19.484	-4.2852	19.915	-2.5598	20.349	4.0776		
18.217	0.	18.640	4.0169	19.065	0.0000	19.493	-4.0881	19.924	0.	20.357	4.1961		
18.225	2.4717	18.648	4.2106	19.074	0.1061	19.502	-3.9726	19.932	2.5824	20.366	4.3984		
18.234	4.5030	18.657	4.2428	19.082	-0.0126	19.510	-4.1435	19.941	4.7046	20.375	4.4320		
18.242	5.7841	18.665	3.9356	19.091	-0.4890	19.519	-4.6657	19.950	6.0432	20.383	4.1111		
18.250	6.2221	18.674	3.2494	19.099	-1.3094	19.527	-5.4172	19.958	6.5008	20.392	3.3943		
18.259	5.9525	18.682	2.2973	19.108	-2.3177	19.536	-6.1117	19.967	6.2191	20.401	2.3998		
18.267	5.2761	18.691	1.2978	19.116	-3.2782	19.544	-6.3885	19.976	5.5124	20.410	1.3557		
18.276	4.5441	18.699	0.4847	19.125	-3.9704	19.553	-5.9387	19.984	4.7476	20.418	0.5063		
18.284	4.0355	18.708	0.0125	19.133	-4.2803	19.562	-4.6232	19.993	4.2162	20.427	0.0130		
18.293	3.8692	18.716	-0.1052	19.142	-4.2478	19.570	-2.5376	20.001	4.0425	20.436	-0.1098		

22A4365
Rev. 2

0-7

TIME (SEC)	PRESSURE (PSID)										
20.444	0.0000	20.881	-4.2323	21.321	0.	21.765	4.3414	22.212	0.0000	22.662	-4.4144
20.453	0.1098	20.890	-4.1128	21.330	2.6725	21.774	4.5508	22.221	0.3146	22.671	-4.2898
20.462	-0.0131	20.899	-4.2896	21.339	4.8687	21.783	4.5856	22.230	-0.0136	22.680	-4.4743
20.471	-0.5063	20.908	-4.8303	21.348	6.2539	21.792	4.2536	22.239	-0.5283	22.689	-5.0382
20.479	-1.3558	20.916	-5.6083	21.357	6.7275	21.801	3.5119	22.248	-1.4146	22.698	-5.8497
20.488	-2.3999	20.925	-6.3273	21.366	6.4360	21.810	2.4829	22.256	-2.5039	22.707	-6.5997
20.497	-3.3944	20.934	-6.6138	21.375	5.7046	21.818	1.4027	22.265	-3.5415	22.716	-6.8985
20.505	-4.1112	20.943	-6.1482	21.383	4.9132	21.827	0.5238	22.274	-4.2894	22.725	-6.4128
20.514	-4.4320	20.952	-4.7863	21.392	4.3633	21.836	0.0135	22.283	-4.6241	22.734	-4.9923
20.523	-4.3984	20.960	-2.6271	21.401	4.1834	21.845	-0.1137	22.292	-4.5891	22.743	-2.7402
20.531	-4.1960	20.969	0.	21.410	4.3050	21.854	0.0000	22.301	-4.3779	22.752	0.
20.540	-4.0776	20.978	2.6499	21.419	4.5126	21.863	0.1137	22.310	-4.2543	22.761	2.7631
20.549	-4.2529	20.987	4.8276	21.428	4.5471	21.872	-0.0135	22.319	-4.4372	22.770	5.0339
20.558	-4.7889	20.995	6.2011	21.437	4.2179	21.881	-0.5239	22.328	-4.9965	22.779	6.4660
20.566	-5.5603	21.004	6.6706	21.445	3.4824	21.890	-1.4028	22.337	-5.8013	22.788	6.9556
20.575	-6.2731	21.013	6.3816	21.454	2.4621	21.899	-2.4830	22.346	-6.5451	22.797	6.6542
20.584	-6.5572	21.022	5.6564	21.463	1.3909	21.908	-3.5120	22.355	-6.8414	22.806	5.8981
20.592	-6.0956	21.031	4.8717	21.472	0.5194	21.916	-4.2536	22.364	-6.3598	22.815	5.0798
20.601	-4.7453	21.040	4.3264	21.481	0.0134	21.925	-4.5856	22.373	-4.9510	22.824	4.5112
20.610	-2.6046	21.048	4.1481	21.490	-0.1127	21.934	-4.5508	22.382	-2.7175	22.834	4.3253
20.619	0.	21.057	4.2686	21.499	0.0000	21.943	-4.3414	22.391	0.	22.843	4.4510
20.627	2.6273	21.066	4.4745	21.507	0.1127	21.952	-4.2169	22.400	2.7404	22.852	4.6657
20.636	4.7865	21.075	4.5086	21.516	-0.0134	21.961	-4.4003	22.409	4.9925	22.861	4.7013
20.645	6.1483	21.084	4.1822	21.525	-0.5195	21.970	-4.9549	22.418	6.4129	22.870	4.3609
20.654	6.6138	21.092	3.4530	21.534	-1.3910	21.979	-5.7530	22.427	6.8985	22.879	3.6005
20.662	6.3273	21.101	2.4413	21.543	-2.4622	21.988	-6.4905	22.436	6.5996	22.888	2.5456
20.671	5.6083	21.110	1.3791	21.552	-3.4825	21.997	-6.7844	22.445	5.8496	22.897	1.4381
20.680	4.8302	21.119	0.5150	21.561	-4.2179	22.006	-6.3068	22.454	5.0381	22.906	0.5370
20.689	4.2896	21.128	0.0132	21.570	-4.5471	22.015	-4.9098	22.463	4.4742	22.915	0.0138
20.697	4.1128	21.136	-0.1117	21.578	-4.5126	22.023	-2.6949	22.472	4.2898	22.924	-0.1165
20.706	4.2323	21.145	0.0000	21.587	-4.3050	22.032	0.	22.481	4.4145	22.933	0.0000
20.715	4.4364	21.154	0.1117	21.596	-4.1834	22.041	2.7177	22.490	4.6274	22.942	0.1165
20.724	4.4703	21.163	-0.0133	21.605	-4.3633	22.050	4.9512	22.499	4.6627	22.952	-0.0138
20.733	4.1466	21.172	-0.5151	21.614	-4.9133	22.059	6.3599	22.508	4.3251	22.961	-0.5371
20.741	3.4236	21.180	-1.3792	21.623	-5.7047	22.068	6.8414	22.517	3.5710	22.970	-1.4382
20.750	2.4205	21.189	-2.4414	21.632	-6.4360	22.077	6.5450	22.526	2.5247	22.979	-2.5457
20.759	1.3674	21.198	-3.4531	21.640	-6.7274	22.086	5.8013	22.535	1.4263	22.988	-3.6006
20.768	0.5106	21.207	-4.1823	21.649	-6.2538	22.095	4.9964	22.544	0.5326	22.997	-4.3609
20.776	0.0131	21.216	-4.5087	21.658	-4.8685	22.104	4.4372	22.553	0.0137	23.006	-4.7013
20.785	-0.1108	21.225	-4.4745	21.667	-2.6722	22.113	4.2543	22.562	-0.1156	23.015	-4.6657
20.794	0.0000	21.233	-4.2686	21.676	0.	22.122	4.3779	22.571	0.0000	23.024	-4.4510
20.803	0.1108	21.242	-4.1481	21.685	2.6951	23.131	4.5891	22.580	0.1156	23.033	-4.3253
20.811	-0.0132	21.251	-4.3264	21.694	4.9099	22.140	4.6241	22.589	-0.0137	23.042	-4.5113
20.820	-0.5107	21.260	-4.8717	21.703	6.3069	22.149	4.2893	22.598	-0.5327	23.051	-5.0799
20.829	-1.3675	21.269	-5.6565	21.711	6.7844	22.158	3.5414	22.607	-1.4264	23.060	-5.8981
20.838	-2.4206	21.277	-6.3816	21.720	6.4905	22.167	2.5036	22.617	-2.5248	23.070	-6.6543
20.846	-3.4237	21.286	-6.6706	21.729	5.7529	22.176	1.4145	22.626	-3.5710	23.079	-6.9556
20.855	-4.1467	21.295	-6.2010	21.738	4.9548	22.185	0.5282	22.635	-4.3252	23.088	-6.4659
20.864	-4.4703	21.304	-4.8274	21.747	4.4002	22.194	0.0136	22.644	-4.6627	23.097	-5.0330
20.873	-4.4364	21.313	-2.6496	21.756	4.2189	22.203	-0.1146	22.653	-4.6274		

22A4365
Rev. 2

C-8

101678

TIME (SEC)	PRESSURE (PSID)										
23.115	0.	23.572	4.5240	24.033	0.0000	24.498	-4.5970	24.967	0.	25.440	4.7060
23.124	2.7858	23.582	4.7422	24.043	0.1194	24.507	-4.4672	24.976	2.8989	25.449	4.9330
23.133	5.0751	23.591	4.7784	24.052	-0.0142	24.517	-4.6592	24.985	5.2812	25.459	4.9707
23.142	6.5191	23.600	4.4325	24.061	-0.5503	24.526	-5.2465	24.995	6.7838	25.468	4.6108
23.151	7.0127	23.609	3.6596	24.070	-1.4735	24.535	-6.0916	25.004	7.2974	25.478	3.8068
23.161	6.7088	23.618	2.5874	24.080	-2.6083	24.545	-6.8725	25.014	6.9813	25.487	2.6915
23.170	5.9465	23.627	1.4617	24.089	-3.6892	24.554	-7.1837	25.023	6.1879	25.497	1.5205
23.179	5.1215	23.637	0.5458	24.098	-4.4683	24.563	-6.6780	25.033	5.3295	25.506	0.5678
23.188	4.5483	23.646	0.0140	24.107	-4.8170	24.573	-5.1987	25.042	4.7330	25.516	0.0146
23.197	4.3608	23.655	-0.1184	24.117	-4.7805	24.582	-2.8535	25.052	4.5379	25.525	-0.1232
23.206	4.4875	23.664	0.0000	24.126	-4.5605	24.591	0.	25.061	4.6697	25.535	0.0000
23.215	4.7040	23.673	0.1184	24.135	-4.4317	24.601	2.8763	25.070	4.8950	25.544	0.1232
23.225	4.7399	23.683	-0.0141	24.144	-4.6223	24.610	5.2401	25.080	4.9323	25.554	-0.0146
23.234	4.3967	23.692	-0.5459	24.154	-5.2049	24.619	6.7310	25.089	4.5752	25.563	-0.5679
23.243	3.6301	23.701	-1.4618	24.163	-6.0433	24.629	7.2406	25.099	3.7775	25.573	-1.5206
23.252	2.5665	23.710	-2.5875	24.172	-6.8180	24.638	6.9269	25.108	2.6707	25.582	-2.6916
23.261	1.4499	23.719	-3.6597	24.181	-7.1267	24.648	6.1398	25.118	1.5087	25.592	-3.8069
23.270	0.5414	23.729	-4.4325	24.191	-6.6250	24.657	5.2880	25.127	0.5634	25.602	-4.6108
23.279	0.0139	23.738	-4.7784	24.200	-5.1575	24.666	4.6961	25.137	0.0145	25.611	-4.9707
23.289	-0.1175	23.747	-4.7422	24.209	-2.8308	24.676	4.5026	25.146	-0.1222	25.621	-4.9330
23.298	0.0000	23.756	-4.5240	24.218	0.	24.685	4.6334	25.156	0.0000	25.630	-4.7060
23.307	0.1175	23.765	-4.3963	24.228	2.8537	24.694	4.8569	25.165	0.1222	25.640	-4.5732
23.316	-0.0140	23.775	-4.5853	24.237	5.1989	24.704	4.8939	25.174	-0.0145	25.649	-4.7698
23.325	-0.5415	23.784	-5.1632	24.246	6.6781	24.713	4.5396	25.184	-0.5635	25.659	-5.3710
23.334	-1.4500	23.793	-5.9949	24.256	7.1837	24.723	3.7481	25.193	-1.5088	25.668	-6.2361
23.343	-2.5666	23.802	-6.7635	24.265	6.8725	24.732	2.6499	25.203	-2.6708	25.678	-7.0356
23.352	-3.6301	23.811	-7.0697	24.274	6.0915	24.741	1.4970	25.212	-3.7776	25.687	-7.3541
23.362	-4.3967	23.821	-6.5720	24.284	5.2464	24.751	0.5590	25.222	-4.5753	25.697	-6.8364
23.371	-4.7399	23.830	-5.1162	24.293	4.6592	24.760	0.0144	25.231	-4.9323	25.706	-5.3221
23.380	-4.7039	23.839	-2.8082	24.302	4.4672	24.769	-0.1213	25.241	-4.8950	25.716	-2.9212
23.389	-4.4875	23.848	0.	24.312	4.5970	24.779	0.0000	25.250	-4.6697	25.725	0.
23.398	-4.3608	23.857	2.8311	24.321	4.8187	24.788	0.1213	25.259	-4.5379	25.735	2.9439
23.407	-4.5483	23.867	5.1577	24.330	4.8555	24.798	-0.0144	25.269	-4.7330	25.744	5.3632
23.416	-5.1216	23.876	6.6251	24.340	4.5039	24.807	-0.5591	25.278	-5.3295	25.754	6.8891
23.426	-5.9465	23.885	7.1268	24.349	3.7186	24.816	-1.4971	25.288	-6.1880	25.764	7.4107
23.435	-6.7089	23.894	6.8180	24.358	2.6291	24.826	-2.6500	25.297	-6.9813	25.773	7.0897
23.444	-7.0127	23.904	6.0432	24.368	1.4852	24.835	-3.7482	25.307	-7.2974	25.783	6.2840
23.453	-6.5190	23.913	5.2048	24.377	0.5546	24.845	-4.5397	25.316	-6.7837	25.792	5.4122
23.462	-5.0749	23.922	4.6223	24.386	0.0143	24.854	-4.8939	25.326	-5.2810	25.802	4.8064
23.471	-2.7855	23.931	4.4317	24.395	-0.1203	24.863	-4.8569	25.335	-2.8986	25.812	4.6083
23.480	0.	23.941	4.5605	24.405	0.0000	24.873	-4.6334	25.345	0.	25.821	4.7422
23.490	2.8084	23.950	4.7805	24.414	0.1203	24.882	-4.5026	25.354	2.9214	25.831	4.9710
23.499	5.1164	23.959	4.8170	24.423	-0.0143	24.891	-4.6962	25.364	5.3223	25.840	5.0089
23.508	6.5721	23.969	4.4682	24.433	-0.5547	24.901	-5.2881	25.373	6.8365	25.850	4.6463
23.517	7.0697	23.978	3.6891	24.442	-1.4853	24.910	-6.1398	25.383	7.3541	25.859	3.8361
23.526	6.7634	23.987	2.6082	24.451	-2.6292	24.920	-6.9270	25.392	7.0355	25.869	2.7122
23.536	5.9948	23.996	1.4734	24.461	-3.7187	24.929	-7.2406	25.402	6.2360	25.879	1.5322
23.545	5.1632	24.006	0.5502	24.470	-4.5040	24.938	-6.7309	25.411	5.3709	25.888	0.5722
23.554	4.5853	24.015	0.0142	24.479	-4.8555	24.948	-5.2399	25.421	4.7697	25.898	0.0147
23.563	4.3963	24.024	-0.1194	24.489	-4.8197	24.957	-2.8761	25.430	4.5732	25.907	-0.1241

TIME (SEC)	PRESSURE (PSID)										
25.917	0.0000	26.399	-4.7784	26.884	0.	27.376	4.8462	27.872	0.0000	28.373	-4.9575
25.927	0.1241	26.408	-4.6435	26.894	3.0110	27.386	5.1219	27.882	0.1288	28.383	-4.8175
25.936	-0.0147	26.418	-4.8431	26.904	5.4855	27.396	5.1610	27.892	-0.0153	28.393	-5.0247
25.946	-0.5722	26.428	-5.4535	26.914	7.0462	27.405	4.7873	27.902	-0.5939	28.403	-5.6580
25.955	-1.5323	26.437	-6.3320	26.924	7.5797	27.415	3.9526	27.912	-1.5903	28.413	-6.5693
25.965	-2.7123	26.447	-7.1137	26.934	7.2513	27.425	2.7945	27.922	-2.8150	28.423	-7.4115
25.975	-3.8362	26.457	-7.4672	26.943	6.4273	27.435	1.5787	27.932	-3.9816	28.433	-7.7471
25.984	-4.6463	26.466	-6.9415	26.953	5.5356	27.445	0.5895	27.941	-4.8223	28.443	-7.2017
25.994	-5.0089	26.476	-5.4039	26.963	4.9160	27.455	0.0152	27.951	-5.1987	28.453	-5.6065
26.003	-4.9710	26.486	-2.9661	26.973	4.7134	27.465	-0.1279	27.961	-5.1593	28.463	-3.0773
26.013	-4.7422	26.495	0.	26.983	4.8504	27.475	0.0000	27.971	-4.9219	28.473	0.
26.022	-4.6083	26.505	2.9887	26.992	5.0843	27.485	0.1279	27.981	-4.7829	28.483	3.0995
26.032	-4.8065	26.515	5.4448	27.002	5.1231	27.494	-0.0152	27.991	-4.9886	28.493	5.6468
26.042	-5.4123	26.524	6.9940	27.012	4.7522	27.504	-0.5896	28.001	-5.6173	28.503	7.2533
26.051	-6.2841	26.534	7.5235	27.022	3.9236	27.514	-1.5788	28.011	-6.5222	28.514	7.8025
26.061	-7.0897	26.544	7.1976	27.032	2.7740	27.524	-2.7946	28.021	-7.3583	28.524	7.4645
26.070	-7.4107	26.554	6.3796	27.041	1.5671	27.534	-3.9527	28.031	-7.6915	28.534	6.6162
26.080	-6.8890	26.563	5.4946	27.051	0.5852	27.544	-4.7873	28.041	-7.1500	28.544	5.6984
26.090	-5.3630	26.573	4.8795	27.061	0.0151	27.554	-5.1610	28.051	-5.5662	28.554	5.0606
26.099	-2.9436	26.583	4.6785	27.071	-0.1270	27.564	-5.1219	28.061	-3.0552	28.564	4.8520
26.109	0.	26.592	4.8144	27.081	0.0000	27.573	-4.8862	28.071	0.	28.574	4.9930
26.118	2.9663	26.602	5.0466	27.090	0.1270	27.583	-4.7482	28.081	3.0775	28.584	5.2338
26.128	5.4041	26.612	5.0852	27.100	-0.0151	27.593	-4.9524	28.091	5.6067	28.595	5.2737
26.138	6.9416	26.622	4.7170	27.110	-0.5853	27.603	-5.5766	28.101	7.2018	28.605	4.8919
26.147	7.4672	26.631	3.8945	27.120	-1.5672	27.613	-6.4748	28.111	7.7471	28.615	4.0389
26.157	7.1437	26.641	2.7534	27.130	-2.7741	27.623	-7.3049	28.121	7.4115	28.625	2.8556
26.167	6.3319	26.651	1.5555	27.140	-3.9237	27.633	-7.6357	28.131	6.5693	28.635	1.6132
26.176	5.4535	26.661	0.5809	27.149	-4.7522	27.643	-7.0981	28.141	5.6579	28.645	0.6024
26.186	4.8431	26.670	0.0149	27.159	-5.1231	27.653	-5.5258	28.151	5.0246	28.655	0.0155
26.196	4.6435	26.680	-0.1260	27.169	-5.0843	27.662	-3.0330	28.162	4.8175	28.666	-0.1307
26.205	4.7784	26.690	0.0000	27.179	-4.8503	27.672	0.	28.172	4.9575	28.676	0.0000
26.215	5.0089	26.700	0.1260	27.189	-4.7134	27.682	3.0554	28.182	5.1966	28.686	0.1307
26.225	5.0471	26.709	-0.0150	27.198	-4.9161	27.692	5.5664	28.192	5.2363	28.696	-0.0155
26.234	4.6817	26.719	-0.5810	27.208	-5.5357	27.702	7.1501	28.202	4.8572	28.706	-0.6025
26.244	3.8653	26.729	-1.5556	27.218	-6.4274	27.712	7.6915	28.212	4.0102	28.716	-1.6133
26.254	2.7328	26.738	-2.7536	27.228	-7.2513	27.722	7.3582	28.222	2.8353	28.726	-2.8557
26.263	1.5438	26.748	-3.8946	27.238	-7.5797	27.732	6.5221	28.232	1.6017	28.737	-4.0390
26.273	0.5765	26.758	-4.7170	27.247	-7.0461	27.742	5.6173	28.242	0.5981	28.747	-4.8920
26.283	0.0148	26.768	-5.0852	27.257	-5.4853	27.752	4.9885	28.252	0.0154	28.757	-5.2737
26.292	-0.1251	26.777	-5.0466	27.267	-3.0108	27.762	4.7829	28.262	-0.1298	28.767	-5.2338
26.302	0.0000	26.787	-4.8144	27.277	0.	27.772	4.9219	28.272	0.0000	28.777	-4.9929
26.312	0.1251	26.797	-4.6785	27.287	3.0333	27.782	5.1593	28.282	0.1298	28.787	-4.8520
26.321	-0.0149	26.807	-4.8796	27.297	5.5260	27.792	5.1987	28.292	-0.0154	28.797	-5.0606
26.331	-0.5766	26.816	-5.4947	27.307	7.0982	27.802	4.8223	28.302	-0.5982	28.807	-5.6984
26.341	-1.5439	26.826	-6.3797	27.316	7.6357	27.812	3.9815	28.312	-1.6018	28.818	-6.6163
26.350	-2.7329	26.836	-7.1976	27.326	7.3049	27.822	2.8149	28.322	-2.8354	28.828	-7.4645
26.360	-3.8654	26.846	-7.5235	27.336	6.4748	27.832	1.5902	28.332	-4.0103	28.838	-7.8025
26.370	-4.6817	26.855	-6.9939	27.346	5.5765	27.842	0.5938	28.342	-4.8572	28.848	-7.2532
26.379	-5.0471	26.865	-5.4446	27.356	4.9523	27.852	0.0153	28.352	-5.2363	28.858	-5.6466
26.389	-5.0088	26.875	-2.9884	27.366	4.7482	27.862	-0.1288	28.363	-5.1966	28.868	-3.0993

TIME (SEC)	PRESSURE (PSID)	TIME (SEC)	PRESSURE (PSID)	TIME (SEC)	PRESSURE (PSID)
28.878	0.	29.320	5.0635	29.908	0.0000
28.889	3.1215	29.401	5.3077	29.918	0.1335
28.899	5.6867	29.411	5.3482	29.929	-0.0159
28.909	7.3047	29.421	4.9610	29.939	-0.6152
28.919	7.8577	29.432	4.0960	29.950	-1.6474
28.930	7.5173	29.442	2.8959	29.960	-2.9160
28.940	6.6631	29.452	1.6359	29.970	-4.1244
28.950	5.7387	29.463	0.6109	29.981	-4.9954
28.960	5.0964	29.473	0.0157	29.991	-5.3852
28.970	4.8863	29.483	-0.1326		
28.981	5.0283	29.494	0.0000		
28.991	5.2708	29.504	0.1326		
29.001	5.3111	29.514	-0.0157		
29.011	-4.9265	29.525	-0.6110		
29.022	4.0675	29.535	-1.6361		
29.032	2.8758	29.545	-2.8960		
29.042	1.6246	29.555	-4.0961		
29.052	0.6067	29.566	-4.9610		
29.062	0.0156	29.576	-5.3482		
29.073	-0.1316	29.586	-5.3077		
29.083	0.0000	29.597	-5.0635		
29.093	0.1316	29.607	-4.9205		
29.103	-0.0156	29.617	-5.1321		
29.114	-0.6067	29.628	-5.7789		
29.124	-1.6247	29.638	-6.7098		
29.134	-2.8759	29.648	-7.5700		
29.144	-4.0676	29.659	-7.9127		
29.154	-4.9266	29.669	-7.3557		
29.165	-5.3111	29.679	-5.7263		
29.175	-5.2708	29.690	-3.1430		
29.185	-5.0283	29.700	0.		
29.195	-4.8863	29.710	3.1651		
29.206	-5.0964	29.721	5.7661		
29.216	-5.7388	29.731	7.4067		
29.226	-6.6631	29.741	7.9675		
29.236	-7.5174	29.752	7.6223		
29.246	-7.8577	29.762	6.7561		
29.257	-7.3046	29.773	5.8188		
29.267	-5.6865	29.783	5.1675		
29.277	-3.1212	29.793	4.9546		
29.287	0.	29.804	5.0985		
29.298	3.1433	29.814	5.3444		
29.308	5.7265	29.825	5.3852		
29.318	7.3558	29.835	4.9953		
29.329	7.9127	29.846	4.1243		
29.339	7.5699	29.856	2.9159		
29.349	6.7097	29.866	1.6473		
29.360	5.7788	29.877	0.6152		
29.370	5.1320	29.887	0.0158		
29.380	4.9205	29.898	-0.1335		

22A4365
Rev. 2

0-11

101678